Quantifying Nutrient Dynamics through a Lowland Karst Network

By

Ted McCormack B.Eng., MSc., PG Dip. Stat.

A Thesis submitted to the University of Dublin for the degree of

Doctor of Philosophy

Department of Civil, Structural and Environmental Engineering

University of Dublin

Trinity College

Dublin

Declaration

I hereby declare that the work contained in this thesis is my own work, and has not been submitted as an exercise for a degree at this or any other university.

I also give the library permission to lend or copy this thesis, upon request, for academic purposes. This permission covers only single copies made for study purposes, subject to normal conditions of acknowledgment.

_____

Ted McCormack April 2014

Summary

In this thesis, hydrochemical methods are used in combination with hydrologic analysis to characterise and model the Gort Lowlands catchment in western Galway, specifically focussing on an interlinked chain of ephemeral lakes (known as turloughs). The Gort Lowlands is a relatively unique karstic system, both hydrologically and hydrochemically, and lies within the pure Carboniferous lowlands of western Ireland. The primary source of water to the catchment is derived from the largely impermeable Devonian sandstone catchment found on the Slieve Aughty Mountains. Three rivers draining from these mountains (the Owenshree, Ballycahalan and Beagh Rivers) discharge down into the karst lowlands allogenically, imparting the catchment with a distinct hydrochemical flux.

The Gort Lowlands catchment has been monitored and sampled for over three years, focussing on five turloughs in particular, Blackrock, Coy, Coole, Garryland and Caherglassaun. These turloughs form an interlinked chain, joined by subterranean conduits which ultimately drain at a series of intertidal springs at Kinvara. The turloughs are known to act as surcharge tanks, filling with excess water when the underground conduit network has reached capacity. Over the study period, these turloughs as well as rivers, groundwater and outlet springs were sampled monthly in an effort to characterise the hydrochemical behaviour of the entire catchment. The hydrologic behaviour of the karst lowlands was found to be dominated by an active conduit network. This network is fed by the Beagh, Owenshree and Ballycahalan Rivers which contribute 55.3%, 24% and 20.7% of the total flow respectively. The flow through this conduit network is supplemented by input from the epikarst system which surrounds it. Hydrochemical and modelling studies found this epikarstic contribution to add approximately 10-17% extra flow to the system.

With this improved hydrological understanding of the catchment, the numerical model of Gill et al. (2013a) could be recalibrated for better accuracy. Based on the findings of physical modelling and a sensitivity analysis, the re-calibrated model could be used for a range of studies and analytical purposes. One such study involved the prediction of likely future flooding patterns based on the most recent climate change projections. This found that turlough flooding patterns are likely to become more extreme in the future, displaying dryer summers and more severe flooding in the winters. For instance, IPCC (2007) scenario A2 predicts that by 2080, a typical winter flood will reach the levels of the 1-in-500 year floods of November 2009.

The alkalinity of the turloughs was found to be closely related to the alkalinity of the allogenic rivers feeding the catchment. The upper two turloughs in the network, Blackrock and Coy, showed very similar concentrations to their feeding river whereas the lower three turloughs displayed higher alkalinity concentrations, most likely due to the contribution of high alkalinity water from the epikarst as water moved through the system. Using alkalinity and EC measurements, the contrasting water retention behaviour of the turloughs was investigated. Blackrock and Coole turloughs both exhibit flow-through behaviour whereas Coy and Caherglassaun present surcharge tank behaviour. The behaviour of Garryland changes depending on water level; at lower water levels, it acts as a surcharge tank and at higher water levels, it hydraulically joins with Coole and acts more like a flow-through system. Alkalinity measurements also showed an influx of diffuse groundwater into the turloughs over the flooding season, particularly during a recession period. The volume of water entering the turloughs amounted to between 1 and 10% of the entire volume that drained from a turlough during a recession period.

Analysis of nutrient concentrations (nitrogen, N, and phosphorus, P) within the catchment found that as water moves through the conduit network, it gains N and loses P. The gain in N is due to contribution from the N-enriched epikarst. As a result of this enrichment, the N load at the tidal spring at Kinvara was shown to be approximately 17% higher than that of the combined river input into the system. This load is lower than would be expected (based on model results) due to N losses within the turloughs. It was postulated that the primary mechanism of N loss within the turloughs was denitrification. Unlike N, P loads decrease as water moves through the system. The P load discharging at Kinvara was found to be approximately 8% lower than the combined input from the rivers. This reduction was due to the minimal contribution of P from the epikarst and P losses from the turloughs. The primary mechanism of P loss within the turloughs was deemed to be sedimentation. Overall, the turloughs appear to act as nutrient sinks over flooded periods, particularly the surcharge tank turloughs. Blackrock and Coy turloughs, however, were found to be nutrient sources, primarily due to the presence of an abattoir at Blackrock (enhancing N and P) and a high degree of grazing during dry periods (enhancing P).

Finally, isotopic analysis of the catchment revealed that the $^{18}\delta$ signature of water becomes slightly enriched as it moves through the catchment due to frequent interaction with the atmosphere (causing slight evaporative effects). Overall however, the effect of evaporation within the catchment is quite minor. Within the turloughs, evaporation tends to only takes place during the summer when the turlough water levels are low. Thus the evaporative effect on turlough water volumes was negligible.

Acknowledgments

Firstly, I would like to express my thanks to Dr. Laurence Gill for supervising me throughout this thesis. Laurence has been there throughout my PhD research to offer valuable advice and constructive suggestions, whether it came to numerical modelling advice or chain-sawing tree stumps out of rivers, Laurence's hands-on approach to project supervision was extremely helpful and often entertaining.

Thank you to my co-supervisor Professor Paul Johnston for his guidance over the course of this project and the effort he put into acquiring my project funding.

I wish to acknowledge the AXA Research Fund for providing the funding that enabled me to undertake this research project.

I wish to thank Owen Naughton for being smarter than me about all things karst, and to Pat Veale for his help with fieldwork and laboratory testing.

I would like to thank my fellow Pearse Street office dwellers, Aisling, Andy, Davie, Francesco, John, Mairead, Seanie and the Commissioner. Four years in Pearse Street has been a true experience and a stunning performance. I fear I shall never again be part of an office of such high calibre nonsense.

I would also like to thank all those who helped me with site work over the years. In particular, I wish to thank Laura, Maurice and Maeve for their contribution.

I would like to thank Aisling, for putting up with me both in the office and out of it. I look forward to the chocolate biscuit cake you have promised me when this is all over.

Finally, I wish to thank my family for all their support along the way and it is to them that I dedicate this thesis. I would like to offer my special thanks to my mom, Wyn, for all her encouragement and diligent proof-reading.

Table of Contents

List of Figures

List of Tables

Abbreviations

^{18}O	Oxygen 18 isotope
^{2}H	Deuterium isotope
ANC	Acid Neutralisation Capacity
CDC	Combined Discrete-Continuum Approach
CIFR	Conduit-Influenced Flow Regime
DC	Double Continuum Approach
DCN	Discrete Channel Network Approach
DFN	Discrete Fracture Network approach
DIP	Dissolved Inorganic Phosphorous
DO	Dissolved Oxygen
DOP	Dissolved Organic Phosphorous
EC	Electrical Conductivity
EMMA	End Member Mixing Analysis
EPA	Environmental Protection Agency
EPM	Equivalent Porous Medium Approach
ERT	Electrical resistivity tomography
GCM	Global Climate Model
GMWL	Global Meteoric Water Line
GNIP	Global Network of Isotopes in Precipitation
GPR	Ground Penetrating Radar
IAEA	International Atomic Energy Agency
IPCC	Intergovernmental Panel on Climate Change
KE	Kinvara East
KW	Kinvara West
LMWL	Local Meteoric Water Line
LT	Lower Turlough (physical modelling section)
mAOD	Meters Above Ordinance Datum
mbgl	Meters Below Ground Level
MRFR	Matrix-Restrained Flow Regime
MWA	Mean Weighted Average
N	Nitrogen
NPWS	National Parks and Wildlife Service
NRA	National Roads Authority

OPW	Office of Public Works
P	Phosphorous
PP	Particulate Phosphorous
SAC	Special Area of Conservation
SPA	Special Protected Area
SRP	Soluble Reactive Phosphorous
TDP	Total Dissolved Phosphorous
TN	Total Nitrogen
TON	Total Oxidised Nitrogen
TP	Total Phosphorous
UT	Upper Turlough (physical modelling section)
VSMOW	Vienna Standard Mean Ocean Water
ZOC	Zone of Contribution
δ^{18}	Oxygen 18 isotope
δ^{2}	Deuterium isotope

Chapter 1

Introduction

1 INTRODUCTION

1.1 Background

In this thesis, hydrochemical methods are used in combination with hydrologic analysis to characterise and model the Gort Lowlands catchment in western Galway.

The Gort Lowlands catchment is a relatively unique karstic system, both hydrologically and hydrochemically. The catchment lies within the pure Carboniferous lowlands of western Ireland. This lowland nature of the catchment provides a somewhat different hydrologic setting to many other karst regions. Most of the catchment is located less than 30m above sea level, and as a result, there is significant interaction between groundwater and surface water. The other defining feature of the Gort Lowlands is that half of the catchment is underlain by largely impermeable non-calcareous rocks. These non-calcareous rocks are primarily Devonian sandstone and are found on the Slieve Aughty Mountains to the east. These mountains are the primary source of water to western Lowlands, and feed the karst catchment via three main rivers. This allogenic recharge nature of the karst lowlands offers the catchment a distinctive hydrochemical flux. Parameters such as alkalinity and electrical conductivity can be used to great effect to exploit this hydrochemical flux and identify the source of water within the catchment.

The low lying nature of this karst landscape and the resultant groundwater-surface water interaction promotes the development of turloughs, a virtually unique feature of the Irish karst landscape. Turloughs are depressions in karst, which are intermittently flooded on an annual cycle via groundwater sources and have substrate and/or ecological communities characteristic of wetlands. Turloughs in Ireland have been the focus of research for many years, with the main interest being twofold. Firstly, they often contain unique flora and fauna and are protected areas as a result. Under Annex 1 of the EU Habitats Directive (92/43/EEC) (EEC, 1992), turloughs are designated as Priority Habitats and many are further designated as Special Areas of Conservation (SAC). Also, under the EU Water Framework Directive, turloughs are considered as Groundwater Dependent Terrestrial Ecosystems (GWDTE). The most comprehensive study to date on turlough eco-hydrology was that of the *Conservation Status of Turloughs Project*. This multidisciplinary study was funded by the National Parks and Wildlife Service (NPWS) and was carried out in order to provide a robust scientific foundation for assessing the conservation status of turloughs, integrating hydrology, land-use and catchment management. The final report from this project is yet to be

published. The second reason for research interest in the Gort Lowlands is due to the risk of localised flooding. The Gort Lowlands area experienced four major flood events within six years between 1989 and 1995. The damage caused by these floods combined with ecological importance of the area prompted the commissioning of an extensive investigation known as the Gort Flood Studies Report (Southern Water Global, 1998). At the time, the report was considered the largest regional interdisciplinary investigation of a karstic environment carried out worldwide. Further flooding within the region occurred in November 2009, causing widespread damage.

For this thesis, the Gort Lowlands catchment has been monitored and sampled for over three years, focussing on five turloughs in particular, Blackrock, Coy, Coole, Garryland and Caherglassaun. These turloughs form an interlinked chain, joined by subterranean conduits which ultimately drain at a series of intertidal springs at Kinvara. The turloughs are known to act as surcharge tanks, filling with excess water when the underground conduit network has reached capacity. Over the study period, these turloughs were sampled and monitored for a range of hydrochemical parameters. Other catchment features such as rivers, groundwater and the outlet springs at Kinvara were also sampled in an effort to characterise the hydrochemical behaviour of the entire catchment. Hydrochemical analysis of karstic aquifers is a commonly used method to provide insight into the functioning of karst aquifer systems. Hydrochemical studies typically use chemical compounds as natural tracers, providing information on the dynamics of a karst aquifer. Alternatively, hydrochemistry can be used to analyse contaminant transport through a karst aquifer.

1.2 Aims and objectives

The overall aim of this thesis is to characterise the hydrology and hydrochemistry of the Gort Lowlands and of the individual turloughs within the Gort Lowlands; in particular, the transport of and fate of nutrients through the conduit network.

This has been achieved through the following objectives:

HYDROLOGICAL

- To monitor the hydrological behaviour of the catchment over a 3-4 year period. This was carried out using rain gauges and depth gauges located in rivers, turloughs, boreholes and wells.

- To improve upon the rating curves of the three rivers feeding the catchment. In particular, the collection of stage-discharge data for high flow situations.

- To successfully apply a reservoir routing methodology between the inflow and outflow of Lough Cutra.

MODELLING

- To improve to accuracy of the hydrological model constructed by Gill et al. (2013a). This recalibration shall be aided by the application of a sensitivity analysis and construction of a physical model.

- To use this recalibrated model for analysis purposes such as prediction of future flooding patterns based on projected rainfall patterns according to the latest climate change models.

HYDROCHEMICAL

- To investigate the hydrochemical relationship between turloughs and the rivers feeding them.

- To investigate the contribution of diffuse/epikarst water into the active conduit network and the turloughs.

- To investigate the hydrochemical processes occurring within the turloughs over the course of a flooded period.

- To further develop the conceptual model of turloughs as flow-through systems and as surcharge tanks.

- To use the hydrological model in an effort to compare conservative nutrient flow behaviour (as required for the model) against the observed nutrient behaviour within the catchment.

- To carry out an isotopic study of the catchment in order to compare against the findings of other hydrochemistry methods as well as to investigate the significance of evaporation within the catchment.

Chapter 2

Literature Review

2 LITERATURE REVIEW

2.1 Overview of Karst Hydrology

Karst can be defined as terrain comprising of distinctive hydrology and landforms that arise from a combination of high rock solubility and well developed secondary (fracture) porosity (Ford and Williams, 2007). Karst aquifers are characterised primarily by open conduits which provide low resistance pathways for groundwater flow and which often short-circuit the granular or fracture permeability of the aquifer (White, 2002). An estimated 20% of the Earth's land surface is covered by karst terrains (Figure 2.1) and the aquifers in karst rocks act as a water resource for approximately 25% of the world's population (Ford and Williams, 2007).

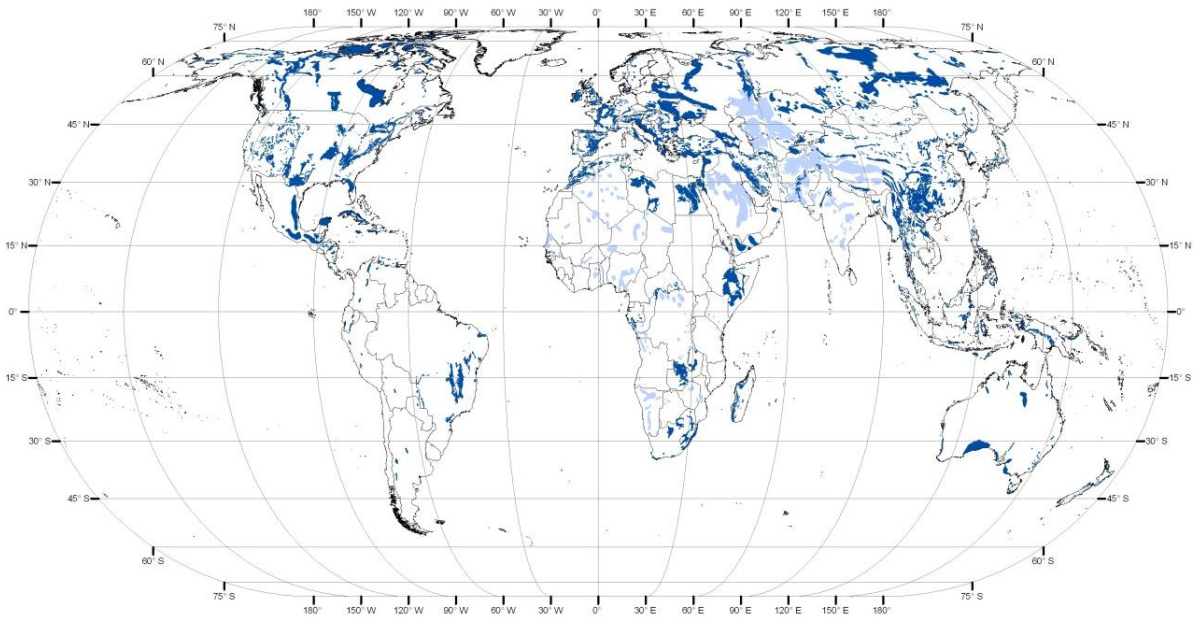

Figure 2.1: Global distribution of major outcrops of carbonate rocks (dark blue: pure, continuous, light blue: impure, discontinuous) (Williams and Ford, 2006)

Research on the topic of karstic geology and geomorphology has been carried out for over a century. However early publications such as those by Grund (1914) and Cvijic (1924) were more closely related to geomorphology than to hydrology. Geomorphology remained the focus of research for decades. During the 1970s the emphasis then shifted to the hydrology of karst landforms as indicated by Monroe (1970), Herak and Stringfield (1972) and Jennings (1972). Interest in the study of hydrology of karst had been encouraged by actions of the International

Hydrological Decade, particularly in the Mediterranean region and in the United States. Further studies have also been promoted by The International Association of Hydrogeologists (LeGrand and Stringfield, 1973).

The disciplines of hydrology and speleology have been the major contributors to the understanding of karst hydrology although historically there have been major differences in the way the two disciplines view the carbonate aquifers that they study. Speleologists have traditionally been primarily concerned with the formation of caves and presumed karst aquifers were dominated by conduit flow (Sasowsky, 2000). Hydrologists on the other hand were more concerned with finding water and assumed that the aquifer behaved equivalently to a porous medium and considered the conduits insignificant, being viewed as water filled cavities separate to the flow field (Thrailkill, 1968). Technological advances in the fields of hydrology and speleology the 1970s and 1980s such as cave exploration, tracer studies and physical and chemical studies of karst springs have led to a more combined approach between the views. The combined viewpoint meant researchers were now talking about conduit flow, fracture flow, matrix flow and the relationship between them (Quinn et al., 2006). Karst hydrology also combines both surface water and groundwater hydrology concepts as conduit flow has more in common with surface water and engineered hydraulic networks then it does with the classical study of groundwater.

2.2 Karst Aquifers

All aquifers evolve over time (on the scale of hundreds of thousands of years), as rivers downcut into lower base levels, tectonic forces shift elevations and soils thicken or are eroded away. The permeability of silicate rock aquifers, for example, changes slowly with dissolution or precipitation of minerals within the pore spaces or along the fractures. In contrast, the permeability of karst aquifers is due primarily to the enlargement of joints and bedding plane partings as circulating groundwater removes the carbonate bedrock. Due to this, the evolution of karst aquifers is a very rapid process occurring over periods of (only) thousands of years (White, 2002).

The main characteristic of karst aquifers is the existence of irregular networks of pores, fissures, fractures and conduits of various size and forms. Such structure with a significant physical and geometrical heterogeneity causes complex hydraulic conditions and spatial and temporal variability of the hydraulic parameters (Denić-Jukić and Jukić, 2003). Karst areas are indicated by a general absence of permanent surface streams and the presence of swallow holes or enclosed depressions. The water is usually all underground in solutionally enlarged channels, some of which

are large enough to be termed caves (Karst Working Group, 2000). Due to the complexity of karst aquifers, it is difficult to explain them easily but attempts have been made in the past such as White (1969) and LeGrand and Stringfield (1971).

In both classifications, three types of karst aquifer have been recognised due to their varying permeability development. White (1969) classified the aquifers in three ways: diffused flow, free flow or confined flow (see Table 2.1). Another method which corresponded closely to that of White (1969) was proposed by LeGrand and Stringfield (1971) who classified aquifers as: fine textured systems, coarse textured systems and reactivated systems. More recently, the classification of karst aquifers has been refined into the triple permeability concept which describes a karst aquifer as being comprised of three independent permeability components: matrix, fracture and conduit. This concept will be discussed in more detail in Section 2.2.2.

The conceptual model of a karst aquifer can be drawn in various forms but the essential features remain the same. White (2002) provided the conceptual model shown below in Figure 2.2. The features of this model shall be discussed in the subsections that follow.

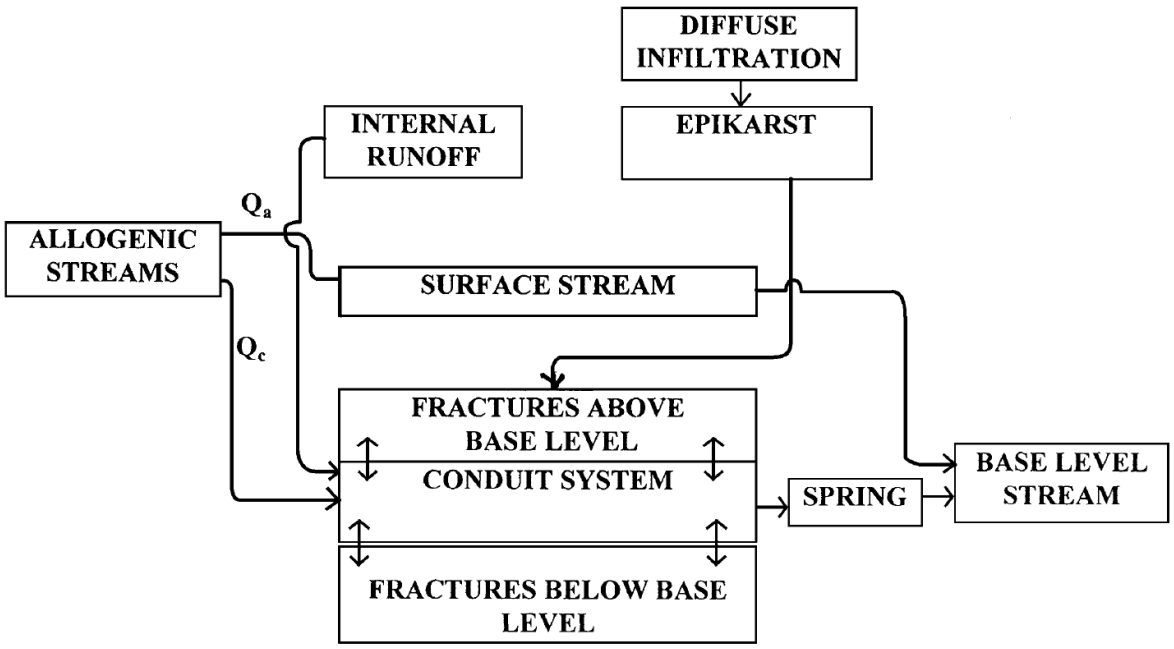

Figure 2.2: Conceptual model for a carbonate aquifer (White, 2002)

Table 2.1: Hydraulic classification of carbonate aquifers (White, 1969)

Flow Type	Hydrological Control	Associated Cave Type
Diffuse Flow	Gross Lithology. Shaley limestones; crystalline dolomites; high permeability porosity	Caves rare, small, have irregular patterns
Free Flow	Thick, massive soluble rocks.	Integrated conduit cave systems
Perched	Karst system underlain by impervious rocks near or above base level	Cave streams perched – often have free air surface
Open	Soluble rocks extend upward to level surface	Sinkhole inputs: heavy sediment load; short channel morphology caves
Capped	Aquifer overlain by impervious rock	Vertical shaft inputs; lateral flow under capping beds; long integrated caves
Deep	Karst system extends to considerable depth below base level	Flow is through submerged conduits
Open	Soluble rocks extend to land surface	Short tubular abandoned caves likely to be sediment-choked
Capped	Aquifer overlain by impervious rocks	Long, integrated conduits under caprock. Active level of system inundated
Confined Flow	Structural and stratigraphic controls.	
Artesian	Impervious beds which force flow below regional base level	Inclined 3-D network caves
Sandwich	Thin beds of soluble rock between impervious beds	Horizontal 2-D network caves.

2.2.1 Recharge

A characterisation of hydrology in karst lands is high infiltration and low surface runoff. For instance, in the Parnasos-Ghiona area in Greece, infiltration into the limestone aquifer has been calculated to be 45.2% while surface runoff is only 3.6% (Burdon and Papakis, 1961). This infiltration from rainfall can be divided into two components: allogenic recharge and autogenic recharge.

Allogenic recharge occurs when runoff from the neighbouring or overlying non-karst rocks drain into the karst aquifer through *swallets (*or swallow holes). Allogenic recharge can be considered to occur as concentrated point-inputs to the karst aquifer. Two main types of swallets exist: vertical inputs from perforated overlying beds and lateral point inputs from adjacent impervious rocks (Ford and Williams, 2007).

Autogenic recharge is the recharge that enters the aquifer directly from the overlying soil. It can be separated, as suggested by Gunn (1983), into two components: *Diffuse Infiltration* and *Internal Runoff*. Diffuse infiltration can be considered as comparable to any other hydrological setting. The initial precipitation is absorbed by the soil until the soil becomes saturated at which point the water percolates down through the matrix porosity or along fractures in the bedrock until it reaches the water table (Shaw, 2011). It should be noted however that in karst, the infiltration rate is much higher than in other hydrological settings due to the high permeability of rock and the fact that flow mainly crosses soil vertically rather than horizontally. Internal runoff is storm flow and is equivalent to overland flow in the usual hydrological cycle. Storm flow runoff flows into closed depressions (dolines) where the storm water enters the aquifer quickly through sinkhole drains (White, 2002).

Autogenic and allogenic recharge styles differ in terms of recharge per unit area and water chemistry with considerable consequences on the scale and distribution of the development of secondary permeability (Ford and Williams, 2007). The differences between autogenic and allogenic recharge are presented in Figure 2.3.

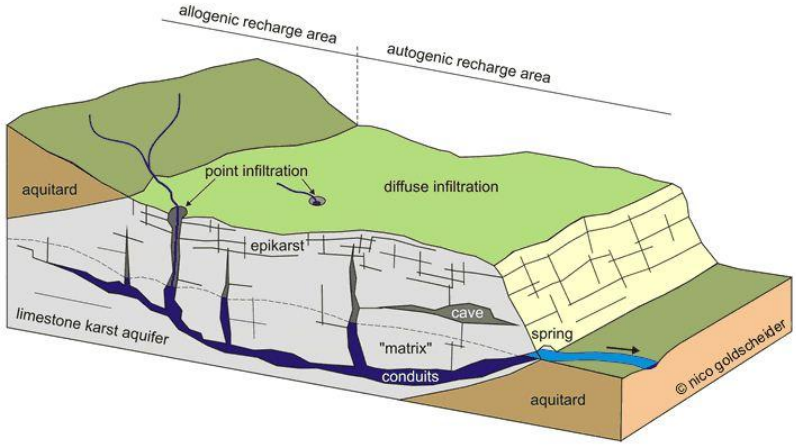

Figure 2.3: Illustration displaying duality of recharge (allogenic vs. autogenic) and infiltration (point vs. diffuse) (Goldscheider and Drew, 2007).

One component of karst aquifers that differs from typical aquifers is the existence of an epikarst (or subcutaneous zone) in which the soil-carbonate rock interface is very sharp with the weathered rock zone (or C-horizon) often missing. The karst soil tends to be very well leeched with little carbonate material surviving and the bedrock is often highly irregular with deep crevices dissolved

along fractures ('grikes' or 'cutters'). Water can be forced to move laterally for considerable distances before being able to descend into the bedrock. Thus the epikarst provides a temporary storage with water requiring days or weeks to reach the groundwater system (Williams, 1983).

The volume of recharge entering the karst aquifer is regulated by the capacity of the input passages or *catchment control* (Palmer, 1984). If the inflow from surface streams is too great then the system will start to back up and ponding will occur, giving rise to surface streams or surface flooding. If the carrying capacity is not sufficient to carry even the minimum surface flow, this will result in a permanent surface stream. Localised flooding may also occur if the infiltration capacity of a swallow-hole is not sufficient due to a constriction or obstruction at the input point.

2.2.2 Flow Systems

Water in a karst aquifer moves down-gradient through the aquifer using a combination of three distinct types of porosity (triple permeability) models (White and White, 2005):

- Matrix permeability: The intergranular permeability of the unfractured bedrock.
- Fracture permeability: Mechanical joints, joint swarms and bedding plane partings, all of these possibly enlarged by solution.
- Conduit permeability: Pipe-like openings with apertures ranging from 1 cm to a few tens of meters.

These three elements of permeability carry different roles within the karst aquifer, with differing aperture sizes, distributions and flow mechanisms defined for each type. See Table 2.2 for a summary of their essential characteristics.

Table 2.2: Essential characteristics of triple permeability model (White and White, 2005)

Permeability	Aperture	Travel Time	Flow Mechanism	Distribution
Matrix	µm to mm	Long	Darcian flow field. Laminar	Continuous medium
Fracture	10 µm to 10 mm	Intermediate	Cube Law. Mostly laminar; may be non-linear components	Localised but statistically distributed
Conduit	10 mm to 10m	Short	Darcy-Weisbach. Open channel and pipe flow. Turbulent.	Localised

MATRIX

Matrix flow through a karst aquifer is not fundamentally different from ground water flow in any other aquifer. The guiding equation is Darcy's Law (Darcy, 1856). However the hydraulic conductivity of the rock (for use with Darcy's law) is difficult to ascertain as the usual technique, pump tests on wells, is dominated by the fracture flow component (White and White, 2005). Though matrix porosity (2-11%) is shown to be much larger than the sum of fracture and conduit porosities (0.5 and 0.2%), its contribution to the hydraulic conductivity is practically negligible (Zuber and Motyka, 1998). As a result, matrix flow is often ignored. Matrix flow is assumed to follow in a lognormal distribution (Ford and Williams, 2007).

FRACTURES

The term 'fracture' (or 'fissure') is used to encompass single joints, joint swarms and bedding plane partings. Fracture apertures normally range between 50 - 500 μm. When fractures reach a width of 1cm, they are deemed as conduits (White, 2002). Under the assumptions of parallel walls and uniform aperture, fracture permeability can be modelled using the cubic law (derived from the Navier-Stokes equations) (White and White, 2005) which states that:

$$Q = \frac{w\rho g b^3}{12\mu} . \frac{dh}{dl} \qquad \textit{Equation 2.1}$$

and,

$$K = \frac{\rho g b^3}{12\mu} \qquad \textit{Equation 2.2}$$

where b is the full aperture of fracture, μ is the dynamic viscosity of water, w is the fracture width, dh/dl is the hydraulic gradient and K is the hydraulic conductivity. Fracture apertures are also assumed to follow a lognormal distribution.

CONDUITS

Conduits are solutionally enlarged pathways through the carbonate aquifer. Water flow through conduits is predominantly turbulent (non-Darcian behaviour occurring when the aperture exceeds 1cm). As much as 80% of the flow through a karst aquifer occurs in the conduit network (Palmer, 1991). When a conduit is large enough for human exploration it is deemed to be a cave. The minimum size of conduit is 0.01m and minimum size of conduit needed for direct exploration is approximately 0.5m. This leaves any conduit within the range of 0.01 - 0.5m out of reach of direct

investigation. However spring hydrochemistry and tracer tests (as discussed in Section 2.4) can prove their presence. Conduits are typically elliptical in shape since corrosion is equal in all directions but concentrates along the guiding bedding planes (Ford and Williams, 2007).

Conduit flow in a single conduit with radius r in the laminar regime can be described by the Hagen-Poiseuille equation:

$$Q = \frac{\pi \rho g r^4}{8\mu} \cdot \frac{dh}{dl} \qquad \textit{Equation 2.3}$$

When the flow regime is turbulent, the Darcy-Weisbach equation can be used (assuming circular cross section). This gives:

$$Q = 2\pi \left(\frac{g}{f}\right)^{\frac{1}{2}} r^{\frac{5}{2}} \left(\frac{dh}{dl}\right)^{\frac{1}{2}} \qquad \textit{Equation 2.4}$$

However the use of this equation relies on a value for the Darcy-Weisbach friction factor, f, which must be determined empirically. It can be determined either by directly investigating the wall roughness of the conduit in question or can be back-calculated when all other parameters in the equation are known.

Friction factors have been calculated for numerous karst aquifers by different investigations such as Gale (1984), Atkinson et al. (1983) and Jeannin (2001) among others. The friction factors obtained cover a large range (0.039-340). Some studies such as Atkinson et al. (1983) and Lauritzen et al. (1985) calculated f by both approaches (investigation of conduit and back-calculation) and found that back-calculation tends to give dramatically higher results of f. However, as the friction factor is square rooted in the Darcy-Weisbach equation, the effect of different values is dampened. The study carried out by Lauritzen et al. (1985) was on an active phreatic conduit in Norway. The study found that the Darcy-Weisbach friction factor, f, decreases dramatically as discharge increases but levels out when discharge reaches 10 m^3/s.

A number of studies have been carried out investigating storage and flow in karst aquifers. Einsiedl (2005) carried out one such study using environmental and chemical tracers on the Böhming spring catchment in south Germany. This study found that only 6% of the total water volume is stored in the soil zone and epikarst and that storage capacity of the conduits was negligible. The author concluded that the rock matrix (phreatic zone) represented the major storage system zone of the karst aquifer with a porosity of 5.5%. Other studies on karst aquifers in Kentucky (Worthington et

al., 2000b), Canada, England and Mexico (Ford and Williams, 2007) have found similar results with approximately 95% of storage within the rock matrix. It should be noted however that some aquifers have a relatively small phreatic zone compared to the epikarst and vadose zones. In these aquifers, the storage in the epikarst and vadose zones can be significant, possibly more than in the phreatic zone (Perrin et al., 2003)

2.2.3 Discharge

Groundwater from karst aquifers is usually discharged back to surface routes through large springs. In fact most of the largest springs in the world are from karst aquifers. They represent the end of underground river systems and mark the point at which surface processes become more dominant (Ford and Williams, 2007). The largest spring in the world is the Tobio spring in Papua New Guinea with a mean flow of between 85-115 m^3/s (Maire, 1981). White (2002) categorised springs into 5 types:

i. Open conduit gravity springs where water emerges from an open cave mouth.
ii. Alluviated conduit springs where water emerges from a rise pool formed by a blockage of glacial or alluvial material.
iii. Rise pools discharging water from shallow flooded conduits.
iv. Artesian springs where water rises from considerable depths.
v. Springs that discharge from solutionally widened fracture swarms.

There is great variety in the physical forms and rates of discharge from different springs. Sometimes spring clusters can form where the discharges from multiple drainage basins can have springs in the same general area. Over the last decade, useful information on spring discharge systems has been provided by cave divers particularly for spring types (iii) and (iv) (White, 2002).

The type (v) spring has historically been known as a *diffuse flow* spring, being labelled as such by Shuster and White (1971). This is because these springs have a constant temperature and chemical composition seemingly independent to surface storms compared with *conduit flow* springs where water varies in temperature and chemical composition. More recently, the distinction has been changed to *underflow* springs carrying the baseflow from groundwater basins and *overflow* springs which only carry part of the discharge or become active only during storm flow (Worthington, 1991). In some cases, springs can reverse and act as sink points or 'estavelles' as is the case with the turloughs that form the basis of this thesis (as shown in Figure 2.4).

The flow behaviour, turbidity and chemistry of springs are considered to strongly reflect the aquifer from which the spring is draining and, as a result, are extensively used as gauging points, sampling points and monitoring points for karst aquifers.

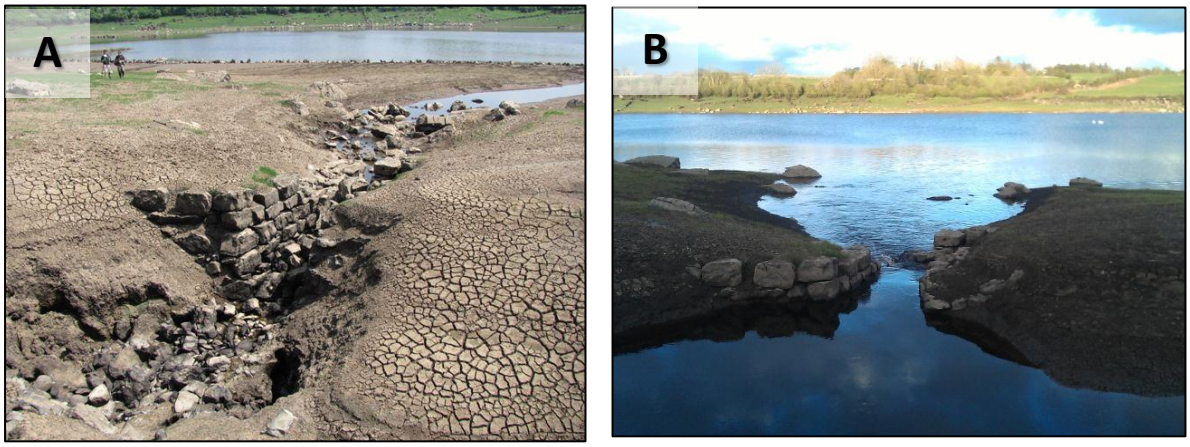

Figure 2.4: Estavelle at Coy Turlough. Acting as sink in summer (a) and a spring in winter (b)

2.2.4 Chemistry

The chemistry of the dissolution of calcite and dolomite reached an advanced formulation in the 1980s with the publication of reliable values for equilibrium constants (Plummer and Busenberg, 1982). This study identified the pertinent complexes and their role in the chemistry and established useful parameters such as hardness, saturation index and calculated carbon dioxide partial pressure. These chemical calculations can now be carried out using several speciation and reaction path computer programs such as WATEQ4F, MINTEQA2 and PHREEQE (available from the US Geological Survey and the US Environmental Protection Agency) (Langmuir, 1997).

The development of a karst aquifer is mostly a matter of the dissolution reactions rather than the final equilibrium state of these reactions. A paper by Plummer et al. (1978), was the first to attempt to classify the different chemical reactions. The individual rates of these reactions are summed to provide an overall dissolution rate for calcite. The reactions are set out below:

$$CaCO_3 + H^+ \rightarrow Ca^{2+} + HCO_3^- \quad \textit{Equation 2.5}$$

$$CaCO_3 + H_2CO_3 \rightarrow Ca^{2+} + 2HCO_3^- \quad \textit{Equation 2.6}$$

$$CaCO_3 + H_2O \rightarrow Ca^{2+} + HCO_3^- + OH^- \quad \textit{Equation 2.7}$$

Each reaction is described for a forward reaction term in the rate equation:

$$Rate = k_1 a_{H^+} + k_2 a_{H_2CO_3} + k_3 a_{H_2O} - k_4 a_{Ca^{2+}} a_{HCO_3^-} \qquad \textit{Equation 2.8}$$

This rate equation is known as the PWP equation (after Plummer, Wigley and Parkhurst (1978)). The first term is mass transfer-controlled but the second and third terms are reaction rate-controlled so that, in the pH range common to karst ground waters, the dissolution rate is only slightly dependent on flow regime.

Further investigations of reaction rates (Dreybrodt and Buhmann, 1991) have made use of a generic rate equation:

$$Rate = \frac{A}{V}\frac{dC}{dt} = k\left(1 - \frac{C}{C_s}\right)^n \qquad \textit{Equation 2.9}$$

where, A = area, V = volume of solution, k = reaction rate constant, C = concentration of dissolved carbonate, C_s = equilibrium saturation concentration for the dissolved carbonate and n = reaction order.

The reaction order can be determined empirically and shows that there is a break in the reaction rate at about 85% saturation (White, 2002). It was found that when the water is less than 85% saturated with $CaCO_3$ the reaction is approximately first order causing rapid dissolution but approaches a slower fourth order reaction rate as saturation reaches 85% (Svensson and Dreybrodt, 1992). This break is very significant in the development of conduit permeability as it stops the water from becoming overly saturated which would prevent further conduit development.

Further investigations (Liu and Dreybrodt, 1997, Svensson and Dreybrodt, 1992) of dissolution kinetics under turbulent flow and near equilibrium conditions have revealed additional controls.

- The hydration reaction of aqueous CO_2 to H_2CO_3 is shown to be rate-controlling when the A/V ratios are high and under some conditions of turbulent flow.
- Adsorption of ions on the reactive surface becomes rate-controlling under near-saturation conditions.
- A diffusion boundary layer becomes important under conditions of turbulent flow.

2.3 Karst Network Development

Significant changes to a karst aquifer in terms of flow paths and conduit network can take place over thousands of years which, on a geologic timescale, makes it a very rapid process. The fractures are solutionally enlarged by flow under laminar flow conditions into conduits where turbulent flow conditions prevail (Ford and Williams, 2007).

2.3.1 Energy Supply

The development of a flow network in a carbonate aquifer depends on the energy supply available and its spatial distribution. Ford and Williams (2007) describe how this is mainly from:

i. The throughput volume of water.
ii. The difference in elevation between the recharge and discharge areas (i.e. hydraulic gradient).
iii. The spatial distribution of recharge, i.e. on whether it is evenly distributed (autogenic recharge) or is focused (allogenic point recharge).
iv. The chemical aggressivity of the recharging waters.

If the aquifer is close to a volcanic or hot spring region, the geothermal heat flux may also be important. Dissolution is a key factor in the development of a karst aquifer (and is directly related to the amount of rainfall) but in addition to this chemical energy, the primary forms of fluid energy are *potential*, *kinetic* and *internal* energy.

Most of the *potential* energy is realised as kinetic energy as water descends down through the vadose zone where a large amount of mechanical work can be done by fluvial processes.

The velocity of water (*kinetic energy*) in karst aquifers varies substantially both between and within aquifers. Within an aquifer the velocity can vary over several orders of magnitude between the matrix, fractures and conduits as indicated by hydraulic conductivity values ranging from $1x10^{-10}$ for matrix to $4x10^{-1}$ in a conduit system (Worthington, 1999). Water velocity can also vary considerably within conduits in different aquifers. A study by Worthington et al. (2000a) of 2877 tracer tests in different conduit systems shows a variance of greater than four orders of magnitude and a global average channel flow velocity of $0.022ms^{-1}$. Another form of kinetic energy within the conduits can be caused during recharge when a recharge pulse from heavy rain reaches a sink. The

pulse travels down the cave passage as a kinematic wave until the saturated zone is reached and a pressure pulse is forced through the phreatic conduits giving a hydrograph peak at the spring. This is known as piston flow (Ford and Williams, 2007).

Internal energy, best represented by rock and water temperature, is another significant form of energy in an aquifer. Temperature is important because of the effect it has on the dynamic (and kinematic) viscosity of water which is more than twice as viscous at 0°C as at 30°C. Thus the lower viscosity at higher temperatures allows greater discharge through capillary tubes (Poiseuille's law) and increases hydraulic conductivity. This influence of temperature is therefore a good explanation for the differences between karst in cool temperate and more tropical zones.

2.3.2 Fracture Enlargement

Carbonate aquifers are not the only type to experience fracture flow. For example, there are fractured quartzites, granites and basalts, all of which can be effective aquifers. The difference between these types and carbonate aquifers is that, in carbonate aquifers, the fractures enlarge much quicker with time and ground water circulation. Once water has entered the aquifer, the various forms of energy mentioned above are used up in the enlargement of primary pores and fractures into secondary conduit networks. White (2002) has described how, in the early stages of this process, there are three thresholds that appear when the aperture exceeds about 0.01m, these are: hydraulic, kinetic and transport.

HYDRAULIC THRESHOLD

The hydraulic threshold permits the breakdown of laminar flow and the onset of turbulent flow. In principle it is quite straightforward. Flow in the fractures will be laminar and follows Darcy's Law until the Reynolds number reaches the range of approximately 500 and turbulent flow starts to take over.

KINETIC THRESHOLD

This threshold marks the shift in dissolution rate from fourth order kinetics to linear kinetics. When unsaturated water enters a fracture, there is a rapid reaction and uptake of dissolved carbonate. If the kinetics are linear, the water will quickly become saturated, dissolution will cease and there will be no dissolutional enlargement of fractures deep within the aquifer. However, as the rate shifts from first order to fourth order at 85% saturation, the rate of dissolution slows down significantly (Svensson and Dreybrodt, 1992). This allows the dissolution to continue as slow (unsaturated)

laminar flow penetrates deep into the aquifer. This water continues to slowly dissolve its way through the aquifer until 'break-through' occurs. This is the point at which an aperture/pathway has enlarged enough to allow water with less than 85% saturation to penetrate the entire aquifer. When this occurs, the kinetics shift from fourth order back to first order and the rate of dissolution dramatically increases causing a runaway process which allows the chosen pathway to enlarge rapidly. This threshold explains why the number of fully developed conduits is usually much smaller than the number of fractures.

TRANSPORT THRESHOLD

The transport threshold enables flow velocities to be sufficient for the transport of clastic material. These particles can range in size from colloids to boulders either as bed load or suspended load. Transport of these particles is not completely understood but it is known that the critical velocities for sediment movement are very similar to the velocities at the onset of turbulence. Thus the transport threshold occurs at near the same aperture as the other thresholds.

The coincidence of these three thresholds at 0.01m provides a natural division between fractures and conduits as well as separating the process of conduit development into an initiation phase where fractures grow to critical threshold and an enlargement phase as the conduit then expands to the size of a typical cave passage.

2.3.3 Development of Vadose Zone and Epikarst

Unkarstified crystalline carbonate rocks typically have very low primary porosity (≈2%). Thus when fresh water first meets the rock, the standing water level in the rock is close to the surface. Porosity and permeability of the karst increases over time and consequently more void space becomes available to store and transmit groundwater. As a result, the water level gradually falls and so the aerated zone becomes deeper. As this is happening the surface level also drops due to denudation which means the resultant thickness of the vadose zone depends on its upper (surface) and lower (water table) boundaries. The vadose zone in well-karstified rock can extend to as much as 2 km below the surface (Ford and Williams, 2007).

The epikarst (or subcutaneous zone) is located at the top of the vadose zone. It usually consists of a weathered zone of limestone that lies immediately at the top of the bedrock, gradually merging into the main body of the vadose zone comprising mostly unweathered bedrock. It is typically 3-10m deep. Williams (1983) describes how the subcutaneous weathering pattern is a result of solutional

erosion. With percolation water available, solution is greatest near the surface because of the relative abundance of carbon dioxide and thus carbonic acid in the soil. As the water percolates downwards, there is less CO_2 available to the solution and thus the capacity for continued corrosion is diminished as the solution approaches equilibrium. This is illustrated in Figure 2.5. The amount and depth of solution varies with rainfall, time, lithology, soil composition, soil thickness, the partial pressure of CO_2 and the nature of the solution system (i.e. 'open' or 'closed').

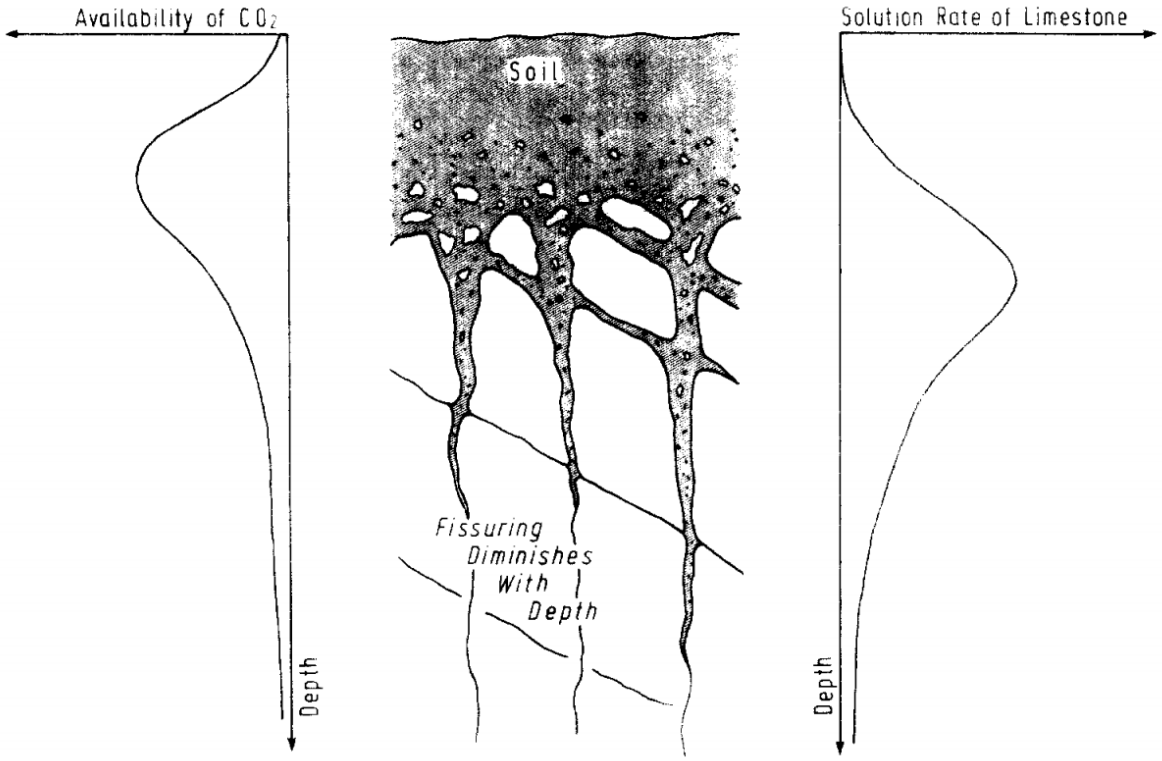

Figure 2.5: Relationship between soil CO_2, rate of limestone solution and fissuring beneath the soil. (Williams, 1983)

Due of the diminishing corrosive capacity with depth, the extent and frequency of the fissures through which the percolation water passes diminishes with depth. As a result, permeability also diminishes with depth. Porosity in the epikarst is typically > 20% and the unweathered rock beneath is commonly < 2% (Ford and Williams, 2007). As a consequence, water tends to accumulate at the base of the epikarst because it cannot drain as freely as it arrived. Some fissures do remain however and it is through these that the water can eventually pass downwards into the vadose zone. Water stored in the epikarst (i.e. an epikarst aquifer) has a significant influence on the overall karst hydrology. By detaining recharge, it moderates floods and attenuates discharge. The water stored in the epikarst provides a habitat for aquatic fauna and a store of water that sustains

percolation into cave systems over dry periods. These aquifers are also used as water supplies with many epikarstic springs being used to supply local water-schemes, especially in China (Williams, 2008). An excellent example of epikarst is the Burren in County Clare as the bare, crystalline, carboniferous hills have been stripped of protective cover during the Pleistocene to reveal a glacially-polished limestone surface containing solutionally enlarged fissures (or 'grikes').

Unlike the majority of karst aquifers found around the globe, the karst aquifers found in Ireland (such as in the catchment under study in this thesis) are predominantly lowland regions. As such, the vadose zone in Irish karsts can be relatively shallow which often results in epikarst occurring within the phreatic or epiphreatic zone. Due to this, a significant quantity of diffuse flow through an Irish karstic aquifer can be flowing through the epikarstic zone, i.e. horizontal flow occurring within epikarst rather than (the more typical) vertical flow.

2.3.4 Conduit Network Development

INITIATION

The main concept for the initiation of conduit permeability is that of an initial pathway connecting the recharge area to the (future) drainage area by means of joints, joint swarms and bedding plane partings. Water is driven through the sequence of fractures due to the head difference between inlet and outlet. As mentioned above, the apertures increase slowly under fourth order kinetics until they become wide enough to allow the total penetration of under-saturated water from entry to exit. After the relatively short time of 5000-10,000 years, turbulent flow may be first encountered. This is known as 'breakthrough' (Dreybrodt, 1990). Groves and Howard (1994b) concluded that, due to the sensitivity of breakthrough time to the initial aperture, breakthrough would not occur in apertures below a few hundred micrometres and thus, conduits would not form.

One significant result from modelling of this initiation phase is the special case of wide initial fractures with short path lengths and high hydraulic gradients. In these cases, breakthrough can occur in as little as 100 years (Dreybrodt, 1992) which is significant as this is within the design life of dams and related hydraulic structures. Previously, it had been assumed that dissolution rates are too slow to impact the bedrock beneath or around a dam over the lifetime of the structure but Dreybrodt's calculations now imply that leaks due to dissolutional enlargement are possible. Such leaks around dams on gypsum terrains have already been documented (White, 2002).

With models constructed for single fractures, the next step is to extend the calculations to multiple fractures which make up a flow path in an aquifer. Groves and Howard (1994a) developed a model which started on a hypothetical grid of fractures at very wide spacings. Siemers and Dreybrodt (1998) then developed a model with smaller fracture spacing which introduced a probability that any given fracture segment on the grid could be connected to other fractures and thus could contribute to the flow path. Many of these modelling attempts assume a simple geometry of plane parallel fractures, fixed apertures and uniform cross-section. As a result, the flow through the fracture is proportional to the cube of the aperture. However, in reality a correction to the cube law is required as fractures have rough walls, and variable aperture sizes (Oron and Berkowitz, 1998). These models validate what is seen in nature that karst networks developing very few large conduit channels with diffuse flow through numerous small fractures.

CONDUIT ENLARGEMENT AND INTEGRATION

When the optimum flow path has been determined and the aperture size has reached the value of approximately 0.01m, the under-saturated water now traverses the entire width of the aquifer and the dissolution kinetics shift into a more or less linear regime. Palmer (1991), showed that the rate of retreat of conduit wall depended only on the degree of saturation and is described by equation 2.10:

$$S = \frac{31.56k_1\left(1-\frac{C}{C_s}\right)^n}{\rho_R} \qquad \textit{Equation 2.10}$$

where S = rate of wall retreat (cm/yr), k_1 = 1st order reaction rate constant, C = concentration of dissolved carbonate, C_s = saturation concentration of dissolved carbonate, n = reaction order and ρ_R = density of bedrock.

Values of k_1 and n have been determined experimentally by Palmer (1991). It has been found that the maximum rate of wall retreat is from 0.01 to 0.1 cm/yr. At this dissolution rate, an active conduit can enlarge from a threshold conduit (0.01m) to the diameter of a meter within a few thousand years.

There has been little success in trying to model the actual pattern of the conduit system. Howard and Groves (1995) determined that the enlargement phase is marked by fairly uniform conduit growth. However the distinction between single conduit, branchwork caves, network maze caves etc. must be derived from the geological constraints and the arrangement of recharge and discharge areas.

2.4 Investigative Techniques

As discussed previously in Section 2.1, karst aquifers are extremely heterogeneous and complex groundwater flow systems. For this reason, they can be difficult to characterise or model with accuracy. An important and simplifying aspect of a karst aquifer is the fact that most of the groundwater resurfaces at a single or limited group of springs. White (2002) thus describes karst springs 'like a perfectly placed well in other aquifers' which carry an imprint of everything upstream within the aquifer. Due to this, springs are a key component amongst the wide variety of characterisation techniques that can be applied to karst aquifers. The use of an individual technique on its own reveals a limited amount of information about a karst aquifer. It is the combination of several methods being used on the same aquifer that can provide a wealth of information. For example, separate studies on the lowland karst of western Ireland by Southern Water Global (1998) and Hickey (2010) both used at least five separate techniques to establish a conceptual model of the region. These characterisation methods are discussed below but for a more detailed description see Goldscheider and Drew (2007) and Ford and Williams (2007).

2.4.1 Geomorphology and Speleology

When studying karst groundwater systems, an understanding of their geology and geomorphology is essential. It would be impossible to characterise a karst aquifer without considering the lithology, stratigraphy, fracturing and faulting as well as topography and landscape history (Goldscheider and Andreo, 2007).

The evaluation of karst features in the context of their geologic setting can aid in the understanding of groundwater flow in karst aquifers (Sasowsky, 2000). The most reliable indicators of the presence of a karst aquifer are landforms related to point recharge and discharge (swallow holes, estavelles and large springs). These landforms indicate an active conduit network exists. However, these surface features give no indication of any deeper or confined karst aquifers and may be misleading if karst landforms have formed in the geological past (paleokarst) and are no longer connected to the active conduit system (Goldscheider and Andreo, 2007).

Geomorphological mapping is a useful aid in the hydrological modelling of karst flow systems. Zibret and Simunic (1976) used mapping on a local scale to delineate zones of groundwater flow within a polje basin using the presence and location of active karst features. On a much larger scale, a study by Butscher and Huggenberger (2007) of the Gempen plateau in northern Switzerland used mapping of aquifers, aquitards and fault lines to generate a 3D geological model which was then

used to develop a hydrological model. This hydrological model was then used to delineate spring catchment areas and determine dominant flow processes.

On a smaller scale, a conduit that is large enough for human exploration can be observed directly allowing for measurement and sampling of major flow paths. The shape of the conduit can help determine whether the cave was formed in the phreatic of vadose zone. Also, the cross-sections of dissolution scallops have been used to estimate discharge and velocities in conduits (Gale, 1984).

The mapping of an individual cave system is mainly carried out by amateur speleologists using a combination of GPS, underwater compass and tape, dive computers and digital depth gauges. These studies contribute greatly to the understanding of conduit flow networks in karst catchments by mapping out the actual pathway that the groundwater takes. For example, the University of Bristol Spelæological Society has carried out mapping of the cave systems in the Galway karst region including those under study in this thesis. These studies (catalogued by Mullan (2003)) are discussed further in Section 3.3.

2.4.2 Boreholes and Test Wells

For most aquifer types, drilling test wells is a standard technique. For karst aquifers it is less useful and often pointless due to the highly heterogeneous nature of karst groundwater flow. It is highly unlikely that a test well will penetrate the main conduit unless there has been extreme care and good luck in its placement. A study by Worthington et al. (2000b) carried out on the central Kentucky karst found the chances of a borehole penetrating the main conduit system to be 0.4 to 4%. A borehole that has penetrated a conduit can be used to install instrumentation to monitor temperature and specific conductance etc. The application of a transducer can allow a borehole to be used as a piezometer to measure pressure head in the conduit under flood flow conditions (White, 2002). Wells drilled on fractures and fracture intersections can be pump-tested to provide the hydraulic conductivity of the fracture system. Packer and slug tests can provide additional information but data must be interpreted with caution. Borehole tests such as these are discussed in greater detail by Kresic (2007).

In some cases, if surface karstic landforms are deemed inadequate to characterise an aquifer, an investigation into the underground karst via boreholes and piezometers may be appropriate. Bonacci and Roje-Bonacci (2000) used such techniques in a study of the Dinaric karst in Croatia whereby the groundwater levels were monitored in four catchments over varying lengths of time

(up to 16 years) and evidence of salt water intrusion was observed and the direction of groundwater flow estimated. However, the authors concluded that this method of field sampling is not an accurate spatial or time representation of a karst aquifer and thus should not be used for modelling.

A study carried out by Mace and Hovorka (2000) used several different techniques to characterise porosity and permeability of the Edwards karstic aquifer in Texas and demonstrated the strengths and weaknesses of the techniques. Seven methods were used and their results compared and contrasted. These techniques included using core and outcrop plug samples, geophysical logs and a three dimensional geocellular model amongst other methods. The authors concluded core plugs are useful for defining the relationship between matrix porosity and permeability to stratigraphy and geophysical log response. Outcrop measurements were seen to be useful for estimating secondary porosity due to fractures and dissolution features although they tend to be biased towards higher values due to unloading effects and weathering, but were still felt to be better than estimates based on core plugs or poor resolution geophysical logs. Another study assessing the usefulness of borehole logs found them to be beneficial for providing *representative* data on the development of karst so long as several conditions are met such as sufficient number of logs, adequate length of logs and similar amount of data from each examined section of a vertical profile (Urban and Rzonca, 2009).

2.4.3 Geophysical Methods

Due to the heterogeneous nature of karst aquifers and their flow paths, it is difficult to predict what features may lie underground within an aquifer. Geophysical methods are a way of helping with this problem. It is the science of 'seeing' into the earth without digging or drilling (Bechtel et al., 2007). Applications commonly involve helping the siting of boreholes, determination of soil thickness and the detection and characterisation of water bearing fractures or conduits. Geophysical methods can be broken into 3 distinct groups: seismic, gravimetric and electrical/electromagnetic.

SEISMIC

Seismic techniques involve an array of listening devices or geophones that measure the travel time of seismic energy from 'shots' (e.g. a weight drop) through the subsurface. The seismic wave is reflected and refracted off a distinct density contrast underground and both the reflection and refraction waves can be detected separately (the waves return to surface level at different times). Each wave has its advantages; reflection is more suited for deep karst targets whereas refraction is

more useful for shallow karstic zones. The use of both waves combined can be even more beneficial as seen by Šumanovac and Weisser (2001) who combined reflection and refraction to determine faulted and fractured zones at surface level and at greater depths.

GRAVIMETRIC

This method (microgravity) is based on the principle that the Earth is not a homogenous sphere and thus gravitational acceleration is not constant at various locations. This is of use for investigations in karst as voids or conduits will exert a relatively lower gravity pull than the surrounding more dense material. Therefore theoretically the mapping out of karst features is straightforward with the right instrumentation. The maps created by this process are known as *Bouguer anomaly* maps (Rodriguez, 1995). Many studies use this technique in conjunction with another (resistivity, GPR etc.) to locate well defined targets or anomalous zones such as dolines (Mochales et al., 2008, McGrath et al., 2002).

ELECTRICAL/ELECRTOMAGNETIC

There is a wide variety of electrical and electromagnetic methods which may differ in terms of operational principle but are all based on their sensitivity to the electrical properties of the subsurface (porosity, degree of saturation etc.) (Bechtel et al., 2007). Two common applications of this principle are Ground Penetrating Radar (GPR) and Electrical Resistivity Tomography (ERT).

- GPR is similar to seismic methods but uses an electromagnetic rather than an acoustic signal. It has been strongly developed in recent years and provides probably the most direct information about subsoil geometry (Mochales et al., 2008).

- ERT measurement employs an artificial electrical field created by driving a known electrical current between two electrodes. It can be used to find the location of cavities and water filled bodies underground. When multiple parallel profiles are carried out, it is possible to see the approximate path of an underground conduit. Such a study has been implemented on Caherglassaun turlough (which is under observation in this thesis) by O'Connell et al. (2012). Using ERT, O'Connell identified two prominent conduits, of approx. 25-30m in diameter, coming in from the west which appeared to join up on the eastern side of the turlough (Figure 2.6). A similar ERT study was carried out on Blackrock turlough and is discussed in Section 7.2.3.1

Each geophysical technique has its merits but the best practice is an integrated geophysical approach using multiple methods which enables the building of an accurate 3-D hydrological model. Rodriguez (1995) suggests the best procedure is a strategic reconnaissance stage first involving a microgravity study and a resistivity survey followed by a second stage or 'tactic exploration' by means of high resolution seismic method. Care should be taken to select the appropriate geophysical technique that is sensitive to the expected physical property of the feature of interest and its contrast with surrounding features. Also, the method must be insensitive to local sources of interference (Bechtel et al., 2007).

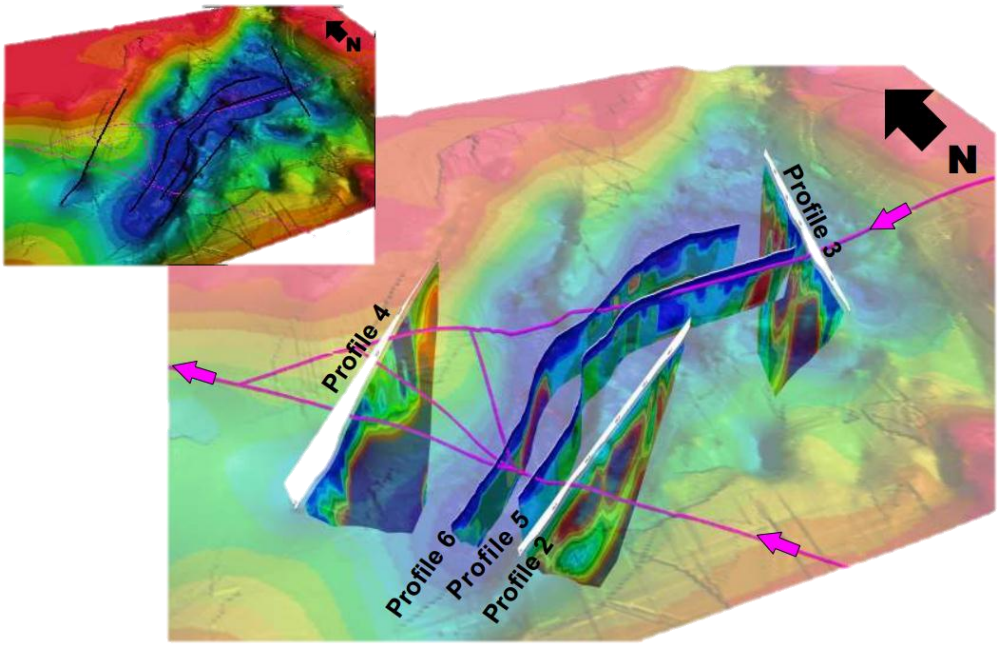

Figure 2.6: Resistivity study of Caherglassaun turlough (overlaid with topography plot), (O'Connell et al., 2012).

Some surface geophysical methods have been adapted for use with boreholes by placing a signal receiver at depth. This down-borehole technique has extended the scope of geophysical methods into areas inaccessible by humans. This technique aids the mapping of subsurface features and can be used to estimate the physical characteristics of subsurface karst systems. Borehole cameras can now also be used to get real time images of a fracture or conduit system as seen in a study by Worthington et al. (2000b).

It should be noted that while geophysical methods are not used as part of this thesis, they are well suited to the lowland catchment under study. The catchment is characterised by shallow large

conduits which are relatively easy to detect. In more typical upland karst catchments, geophysical methods are more limited in determining the presence, position and characteristics of karst conduits.

2.4.4 Artificial Tracers

Tracer tests can be used in all types of hydrological environments to obtain information about water movement and contaminant transport but are most commonly used in karst where groundwater flow paths are not obvious (Goldscheider et al., 2008). It is a powerful technique which can delineate the catchment areas and identify hydraulic connections within a karst aquifer.

The first known tracer study was carried out more than 100 years ago using uranine. Since then the search for additional dye tracers has been on-going (Leibundgut et al., 2009). For a tracer to be suitable, it must be conservative and exactly mimic the water movement (Goldscheider et al., 2008). A tracer is deemed appropriate if it satisfies the following criteria: it must be unreactive, absent but ready soluble in water, easy to detect, non-toxic, invisible, inexpensive and easy to handle (Benischke et al., 2007, Käss, 1998). Within the past few decades, many new tracer techniques have been introduced resulting in both improved sensitivity and reliability and fluorescent tracers have emerged as the most popular and widely used of all tracers (White, 2002).

Tracing involves injecting a conservative substance into a known upstream point and measuring the presence and/or concentration at the output points, usually springs. Qualitative tracing simply involves trying to establish a hydrologic connection between input and output points, i.e. the tracer is injected and its presence is detected (or not detected). Quantitative tests involve monitoring the varying concentration of tracer through a system to allow for more detailed information to be obtained. This process is made easier by technological advances such as auto samplers and in-situ fluorometers allowing for detailed dye breakthrough curves to be produced. Smart (1988) is an example of a quantitative test. In this test rhodamine $_{WT}$ was used to estimate the conduit storage of the Maligne karst in Alberta, Canada. Many studies use both quantitative and qualitative tests at the same time such as Baedke and Krothe (2000) who used rhodamine $_{WT}$ and Ionic Bromide to estimate a conduit velocity in the Beech Creek karst aquifer in Indiana where a velocity of 286 m/hr was recorded.

There is a wide variety of artificial tracers available and most operate by being dissolved into the water body being studied. These dyes include: fluorescent dyes, salt dyes, radioactive tracers (e.g.

tritium (^3H)), activatable tracers (e.g. bromide) and advanced tracers such as the gases or heavy water. Some comparison studies have been carried out (Harden et al., 2003, Atkinson et al., 1973) to compare the merits of different tracers. Fluorescent tracers generally come out as favourites and are the tracer of choice for hydrologists. This is because of their relatively easy handling, simple analysis, high sensitivity of the analysis, low detection limit and consequently, the small quantity of tracer needed for an experiment (Benischke et al., 2007). They are also (mostly) ecotoxicologically safe (Behrens et al., 2001). Although it should be noted that fluorescent tracers do have drawbacks such as sorption onto particles and photolytic decay (uranine has a half-life of approximately 11 hours when exposed to light (Leibundgut et al., 2009). Due to these dependencies, care should be taken in considering what fluorescent tracer to use for a particular study. For example if the water channel being traced is exposed to sunlight, uranine should not be considered; a rhodamine dye would be better suited. Typically, the goal of a tracer study is to build a time-concentration breakthrough curve which represents the behaviour of the injected tracer in the flow route. For example, Barnes (1999) used tracer breakthrough curves in the cretaceous chalk aquifer in Northern Ireland to characterise the aquifer. The study used uranine (or fluorescein) to calculate water velocities of up to 2838 meters per day and thus concluded flow to be through a conduit system rather than through fractures. Einsiedl (2005) and Morales et al. (2007) provide examples of similar studies using breakthrough curves on European karstic aquifers. See Figure 2.7 for an illustration of the use of uranine dye.

Figure 2.7: Injection of uranine dye into a small stream.

Another group of artificial tracer, known as drifting particles operate differently to soluble tracers as discussed above. These tracers are engineered micro-organisms that are used for special applications particularly hygiene related issues such as the flow patterns of micro-organisms in surface water systems (Leibundgut et al., 2009). Tracers that have been used include lycopodium spores (Atkinson et al., 1973) and bacteriophages (Maurice et al., 2010, Drew et al., 1997). As these tracers do not dissolve into the water body being studied, they do not allow for the creation of a tracer breakthrough curve and thus only semi-quantitative analysis is possible.

For large studies with many objectives, it is necessary to use more than one tracer to avoid interferences. These studies must be well planned, with the most conservative and easily detected tracers being assigned the longest and most diluted trajectory (Benischke et al., 2007). For instance, Einsiedl (2005) used a combination of tritium (^3H), uranine, bromide and strontium to characterise slow and preferential water flow in a karst aquifer of the Franconian Alb, Germany. The use of multiple tracers allowed for the determination of flow velocities in two flow paths (100 and 91 m/h) and for the estimation of mean transit time (57-67 years). A multi-tracer experiment has also been carried out in the catchment under study by this thesis (the Gort Lowlands). Eighteen tracer experiments were carried out using the tracers rhodamine $_{WT}$, uranine, leucophore, salt and bacteriophage (types Psf2, T7, H6, H4 and H40). This study established a number of groundwater flow routes (Figure 2.8) and revealed the rapid speed at which water moved through the catchment (Southern Water Global, 1998). This study is described further in Section 3.5.1.1.

A tracer study may be enhanced by the use of activated charcoal bags. These bags can be placed into a water body to absorb the tracer. The tracer will subsequently be extracted from the bags in a laboratory. This technique can only be used qualitatively or semi-quantitatively as there is no strong correlation between volume of water and adsorption onto the charcoal (Leibundgut et al., 2009). Charcoal bags have several advantages: they are efficient, cheap, immune to vandalism and, importantly, can amplify the ambient signal by up to ten times (Smart and Simpson, 2002). For example, Farmer and Blew (2010) used charcoal bags effectively in a tracer study in the Malad Gorge State Park, Idaho. Fluorescent dyes were released into a domestic well with the objective of detecting them at a gorge 900m away. Charcoal bags were placed at springs along the gorge and a two phased tracer test carried out. In the first phase, uranine was injected first and the charcoal bags were used to delineate the spatial distribution of the dye cloud. The second phase used rhodamine $_{WT}$ and additional charcoal bags to increase the resolution of the first test. The average linear water velocity between the well and gorge was calculated as 800 feet per day.

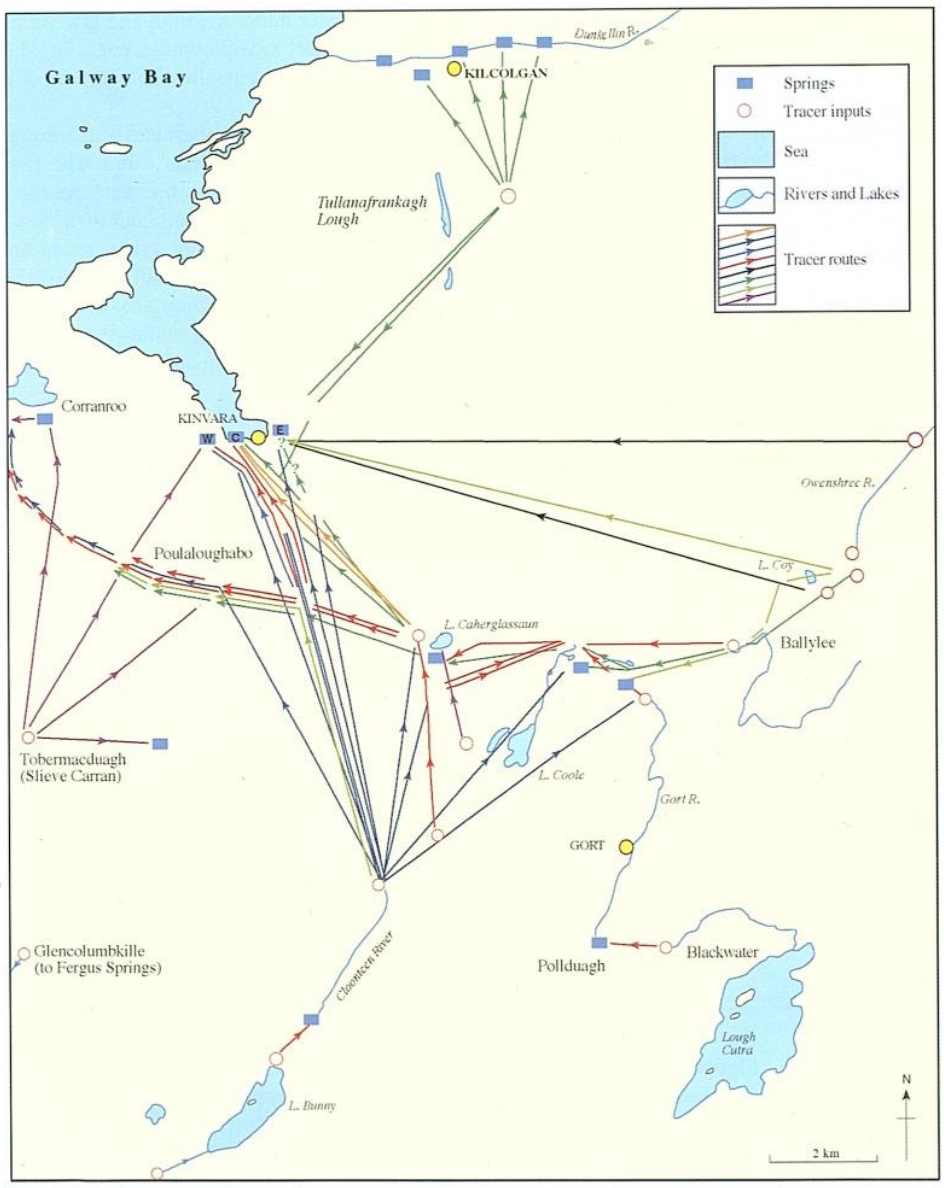

Figure 2.8: Tracer tests in the Gort Lowlands catchment carried out as part of the Gort Flood Studies Report (Drew, 2003).

2.4.5 Environmental Tracers (Isotopes)

With the development of mass spectrometers in the 1950s and the improvements in accuracy and efficiency since then, isotopic measurements have become commonplace and are a critical tool in current groundwater studies (Sanford et al., 2011). These environmental tracers are defined as the properties or constituents of water that have not been induced as a result of an intended experiment and which can provide qualitative or quantitative information about the hydrological system (Leibundgut et al., 2009).

Isotopes of an element have the same atomic number but different atomic weights due to variance in the number of neutrons within the nucleus. For example, most oxygen has 8 protons and 8 neutrons giving an atomic mass of 16 (^{16}O). However 0.035% of oxygen has 9 neutrons (^{17}O) and 0.2% has 10 (^{18}O). The range of variance is limited by the instability created by having too many or too few neutrons (Clark and Fritz, 1997). Some isotopes will be *stable* and others will be *unstable* (or radioactive) and will decay over time. *Stable Isotopes* (e.g. ^{18}O, ^{2}H, ^{34}S) can be used as tracers of water and *Radioactive Isotopes* (e.g. ^{3}H, ^{14}C, ^{36}Cl) offer the possibility to determine water age due to their decay. The most commonly studied isotopes are the stable isotopes of water (^{18}O, and ^{2}H). The principles behind the use of stable isotopes in hydrology are discussed further in Chapter 8.

The International Atomic Energy Agency (IAEA) has played a crucial role in isotope hydrology since its inception in the 1950s. One of the most important duties it carries out is the Global Network for Isotopes in Precipitation (GNIP). This is a network of currently 185 stations in 53 countries that contribute monthly samples to be tested for ^{18}O and ^{2}H as well as tritium (Aggarwal et al., 2011). This data is invaluable to isotope studies worldwide including the studies in this thesis which make use of GNIP data from Valentia weather station in Kerry.

Environmental tracers can be of great use in karst studies just as artificial tracers have been proven to be (and even greater advantage if both are used together (Einsiedl, 2005)). Stable isotopes were used in a study by Perrin et al. (2003) to conceptualise the epikarstic storage of a karst aquifer in Switzerland. The system was sampled weekly over a period of two and a half years and tested for ^{18}O and ^{2}H. The results indicated the importance of the epikarst as a storage element which separates water into either a base flow component or a quick flow component depending on recharge. Long and Putnam (2004) used ^{18}O to model the distinct responses and relative proportions of the conduit, intermediate and diffuse flow components in karst aquifers. Conduit flow was described by linear system methods whereas diffuse flow was described by mass-balance methods. The results of this study could also be used to indicate relative proximity of a well to a main conduit flow-path and to help predict the movement and residence times of potential contaminants. A general finding of O and H isotopic studies is that most karst waters are derived from local meteoric water, with the spatial and temporal variations in these parent meteoric waters being inherited but imperfectly homogenised in the karst reservoir (Criss et al., 2007).

Lakes are well suited to isotope analysis, the only prerequisite being that isotopic variations can occur as a result of natural processes within the water bodies (Gonfiantini, 1986). The investigations most frequently carried out on lakes deal with water dynamics and with the water balance. To

carry out a water balance study, it is crucial to understand if the lake under observation is *steady* or *non-steady*. A steady state system is one in which there is little variability of the lakes properties (depth, temperature, salinity etc.). If the lake is deemed steady state, the water balance can be relatively simply carried out using the mass balance equation below (see Figure 2.9):

$$\frac{dV_L}{dt} = I_S + I_G + P - O_S - O_G - E \qquad \textit{Equation 2.11}$$

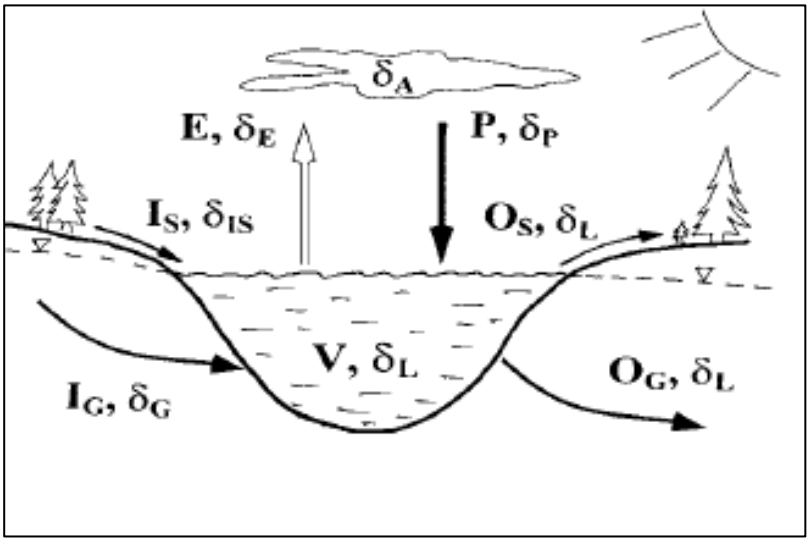

Figure 2.9: Hydrological and isotopic budget of a lake system (Mook, 2001)

Such studies using this mass balance principle have been carried out on Lake Edward in Uganda-Congo (Russell and Johnson, 2006), Lake Garda in Italy (Longinelli et al., 2008) and Lake Titicaca in Peru-Bolivia (Fontes et al., 1979).

In situations where the system is evolving in time, both hydrologically and isotopically, the lake is non-steady and the steady state version of the mass balance equations cannot be used. Ephemeral lakes such as turloughs are examples of non-steady state systems. To carry out a water balance on a non-steady state lake ($dV/dt \neq 0$), Equation 2.11 can still be used so long as all other variables are known. Non-steady mass balance methods have been carried out on alpine lakes (Gurrieri and Furniss, 2004), shallow arctic lakes (Gibson, 2002) and the hypersaline, Owen's Lake in California (Phillips et al., 1986). However, uncertainty is a problem with this method, with best fit models having an accuracy of ±30% (Gonfiantini, 1986, Zimmerman, 1979).

A small number of isotopic studies have been carried out on lakes and surface waters in Ireland. Deifendorf and Patterson (2005) sampled 144 lake and river locations in Ireland over a three week period to give a snapshot of stable isotope values for one season. Surface water δ^{18} values ranged from -7.4 to -2.4‰, averaging -5.4‰, and δ^{2} values ranged from -53 to -17, averaging -37‰. Turloughs were not sampled in this study as they were dry during the sampling period. However in a study on sea-water/groundwater interaction by Einsiedl (2012), a turlough was incorporated and values of -3.5‰ and -26‰ were recorded for δ^{18} and δ^{2} respectively. Similar isotopic values of surface waters were found in a study of the British Isles (Darling et al., 2003). The most relevant study for this thesis is that of Bowen and Williams (1973) who carried out an isotopic study on the Gort Lowlands and the adjoining River Fergus catchment using ^{18}O and tritium (^{3}H). In this study, 28 sites were sampled on two occasions and the results used to broadly determine the groundwater circulation from an isotopic perspective. Bowen and Williams concluded that due to the substantial amounts of tritium found within the catchment, the groundwater undergoes relatively rapid circulation. Also, the ^{18}O results showed how the groundwater variability and its isotopic signature are determined by the rapidity of water throughput and the season of recharge. These conclusions are in accordance with what would be expected from a karstic region such as the Gort Lowlands.

2.4.6 Spring Hydrographs

The temporal variation in spring discharge, as expressed by the spring hydrograph, can provide great insight into the storage and transport characteristics of a karst aquifer. The spring hydrograph can provide information about internal structure and geometry of karst aquifers, storage volumes of different aquifer components and transfer times (Groves, 2007). In this manner, the karst conduit network can be thought of as a transfer function, transforming the input function (precipitation) into an output function observed in the form of a spring hydrograph.

A number of factors affect the response time of a karst aquifer and thus the spring hydrograph. These factors include the contribution of allogenic recharge and internal runoff, the carrying capacity and internal structure of the conduit system, and the catchment area of the spring (White, 2002). Depending on these factors, spring hydrographs vary in sensitivity, some showing individual storm pulses while others only displaying seasonal trends. An aquifer with a fast response time shows individual storm pulses similar to a surface stream hydrograph. This indicates a system with a well-developed conduit network dominated by allogenic recharge. A slower response time may indicate that the aquifer is recharged by diffuse infiltration rather than sinking streams or internal runoff (White, 1988). It should be noted however that a slow response

catchment can give a misleadingly fast response hydrograph if there is a sinking stream located close to the spring (Quinlan et al., 1991).

Boussinesq (1904) and Maillet (1905) were the first to apply quantitative analysis to hydrograph recessions. They proposed that the discharge of a spring is a function of the volume of water held in storage (Ford and Williams, 2007). Maillet put forward a simple exponential relationship to describe the recession limbs of a hydrograph:

$$Q_t = Q_0 e^{-\alpha t} \qquad \textit{Equation 2.12}$$

where Q_t is the discharge at time t, Q_o, is the initial discharge at time zero and t is the time elapsed. This relationship implies that a semi-log plot of time versus spring discharge for the recession period yields a single straight line with slope α. However, springs often diverge from this exponential behaviour and display two or more straight line segments (for an example, see Figure 2.10). One line represents the portion of the aquifer that drains quickly and the other line displays a more slowly draining portion. Atkinson (1977) referred to these portions as 'quickflow' and 'slowflow', where 'quickflow' represents the portion of the catchment draining quickly via conduit flow and 'slowflow' represents the purely Darican response of the drainage from the fractures into the conduit system. However, more recent studies such as Kovacs et al. (2005) have found this 'quickflow' and 'slowflow' hypothesis to be an over simplification. Instead, Kovacs et al. (2005) suggest that spring flow can be described in terms of matrix-restrained flow regime (MRFR) and conduit-influenced flow regime (CIFR).

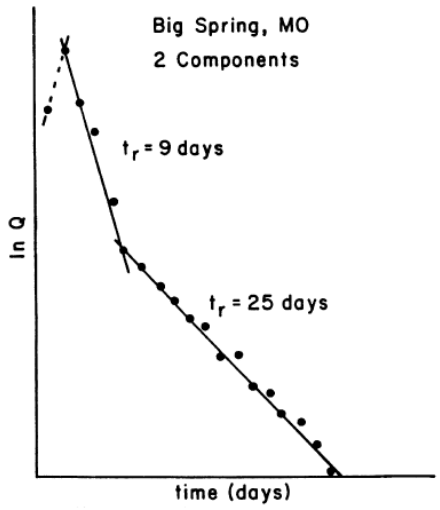

Figure 2.10: Storm hydrograph from Big Spring MO, showing quickflow and slowflow components (From White (1993)).

The analysis of spring hydrographs has been developed further to provide a method of estimating hydraulic and geometric parameters of karst systems. For example, Bonacci (1993), used the recession coefficient, α, from Equation 2.12 to derive storage and transportation characteristics of an aquifer. Kovács and Perrochet (2008) describe the use of two dimensional analytical solutions for diffusive flux from symmetric and asymmetric rectangular blocks. These solutions are used to analytically simulate spring hydrographs of shallow karst systems for constant recharge conditions. This method enabled the estimation of hydraulic parameters and conduit network geometry of karst aquifers.

A good example of a study using spring hydrographs to solve a hydrological problem is that of Fiorillo (2009). In this study, hydrographs were used to provide a forecast for an oncoming drought in Southern Italy. Hydrographs with no peak (or flat spring hydrographs) signify insufficient recharge due to poor annual rainfall. This results in deep aquifer emptying and is considered an indicator of drought for an entire karst system. Using a flat hydrograph, the author determined that, if cumulative rainfall exceeds the threshold value of 740 mm, no drought will occur. This conclusion is an important tool for water management in the region with more frequent droughts likely to occur due to global warming.

2.4.7 Spring Water Chemistry (Hydrochemistry)

While some features of karst aquifers can be determined from hydrographs (retention times, volumes etc.), these methods yield no information concerning the actual transit or residence time and on location of storage (epikarst, unsaturated or saturated zone). Hydrochemical methods can provide answers to these questions if enough parameters are measured (Hunkeler and Mudry, 2007) In carbonate aquifers, the chemical composition is usually dominated by products from dissolution of carbonate minerals such as calcite, aragonite and dolomite. Minor amounts of Fe- or Mn-carbonates may also be present. Throughout European carbonate aquifers, trace element concentrations in groundwater are generally low (Hunkeler and Mudry, 2007, Kilchmann et al., 2004).

The most obvious chemical effect on the behaviour of a carbonate aquifer is carbonate dissolution as it controls groundwater flow. Hardness (the amount of divalent cations Ca^{2+} and Mg^{2+}), temperature and calcite saturation index are some of the most commonly used hydrochemical indicators as they fluctuate seasonally and respond to storm water inputs into the catchment. For example, Shuster and White (1971) used variation in hardness to classify springs as diffuse-flow

feeder system types or conduit feeder system types. It was concluded that a high coefficient of variation was an indication that the spring was draining into an open conduit system. This is because a conduit flow system would be more affected by a surge of low-hardness storm water, thus diluting the overall hardness of the spring. Springs with low coefficients of variation are usually close to saturation with respect to calcite or dolomite and are thus believed to come from interangular porosity reflecting the long residence time in the rock. Worthington et al. (1992) however, points out that a low coefficient of variation does not imply an absence of conduits, only that the recharge is mainly from diffuse infiltration rather than allogenic recharge or internal runoff. Similar to hardness, variations in specific conductance of a spring is a good indicator of the proportion of allogenic and internal runoff water compared with the proportion of diffuse infiltrations (White, 2002). A study on the cretaceous chalk aquifer in Northern Ireland used these principles (as well as a tracer test) to characterise the aquifer. Measurements of conductivity, temperature and total hardness were recorded and due to the high variability of these parameters, it was concluded that the springs met conduit flow criteria (Barnes, 1999). López-Chicano et al. (2001) however warns that hydrochemical variability on its own is not enough for the structural characteristics (diffuse or conduit) of a karst aquifer to be established. The hydrodynamic aspects of the aquifer must also be considered.

Another way of using these parameters is a more focused approach that targets individual storm events. If done correctly, this method can provide information about the arrival of different water types at a spring and the mixing between them. During the initial phase of flood, the concentration of limestone-dissolution related parameters can stay constant or even increase indicating that highly mineralised water is pushed out of the system (piston effect). This piston-flow water may have spent long residence time in contact with the limestone and thus have high concentrations of ions. After time, the concentration of limestone-dissolution related parameters decreases due to the mixing of pre-event water with storm derived water (Hunkeler and Mudry, 2007). If concentrations of dissolved ions Ca^{2+}, Mg^{2+}, and HCO_3 are continuously monitored at a spring, they can be used to separate the pre-event water from the storm water based on the premise that there is a significant difference in ionic concentration of old and new water. An example of such a study is that of Ryan and Meiman (1996) which was carried out on the Big Spring basin in the south-central Kentucky karst. In this study, it takes a full day after a storm event for the piston flow water (with its limestone-dissolution related parameters) to move through the system to be replaced with low-hardness storm water. A dye-trace was used also in this test to successfully back up hydrochemical data. Dreiss (1989) carried out a similar piston flow experiment in south-eastern Missouri. See Figure 2.11 for an example of piston flow observed at Coy turlough estavelle (taken from an

electrical conductivity survey of Blackrock and Coy turloughs, see Section 7.2.3 for more information). In this figure, the black line represents the turlough stage and the blue line represents the electro-conductivity (EC) recorded at the turloughs spring. The EC can be seen to peak and then dip as the turlough starts to fill before recovering to its normal concentration.

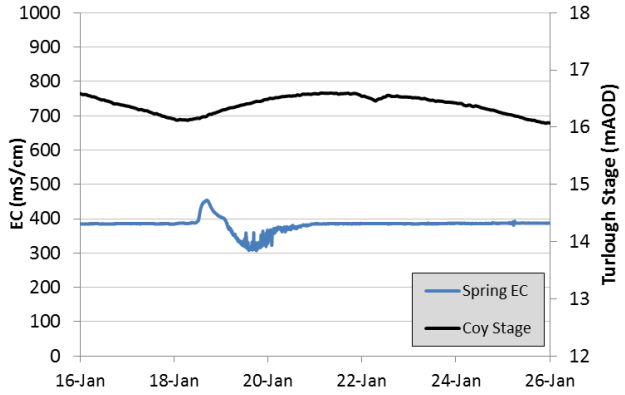

Figure 2.11: Piston flow behaviour in Coy turlough, January 2013. Blue line is EC, Black line is Stage.

A study by Valdes et al. (2006) in the Haute-Normandie region of France observed the response of conductivity and turbidity at 5 outlets (2 wells and 3 springs) after rainfall events to separate out slow and fast flow. Autocorrelation functions and turbidity conductivity (T-ΔC) hysteresis curves were used to analyse the responses. The results display how the memory effect of conductivity can indicate whether water was stored in the system or not based on the principle that stored water will deposit its suspended solids. The (T-ΔC) curves also demonstrated the difference between transport of dissolved solids and suspended solids, as suspended solids can undergo suspension and deposition.

Some studies use a technique known as Principal Component Analysis (PCA) in conjunction with hydrochemical data to estimate mixing proportions of water among different sources within a karst system. PCA is a multivariate statistical technique used to reduce the complexity of and decipher patterns within large data sets by determining a small number of principal components that account for the greatest variance in all the original variables (Wold et al., 1987). It can be used to identify which of the measured components provide the greatest variation in the composition of the water. For example, a study by Moore et al. (2009) compared variations in surface/ground water chemistry to physical conditions (stage, precipitation, evapotranspiration) and used PCA to determine where the water was sourced. PCA suggested that mixing of two shallow sources (diffuse and allogenic recharge) and one upwelling deep-water source explained 91% of the

chemical variation in the sink rise system. The author noted however, that even in a system dominated by allogenic recharge and conduit flow, the deep source provided most of Na^+, Mg^{2+}, K^+, Cl^- and SO_4^{2-} to the system and thus is the primary influence on major-element chemistry. Another study by Doctor et al. (2006) used PCA combined with End Member Mixing Analysis (EMMA) to estimate mixing proportions among three sources, allogenic, autogenic and epikarst in the classical karst (kras) region of Italy/Solvenia. Using this PCA/EMMA model, it was determined that a component derived from shallow vadose-zone storage is expressed immediately following intense rainfall, and is gradually replaced by a second epikarst water component influenced by anthropogenic activities.

An interesting study by Perrin et al. (2007) in the Swiss Jura describes the impact of tributary mixing on chemical variations at a karst spring. A simple transient flow and transport numerical model was created which could reproduce chemographs and hydrographs observed at a spring. This model was then subject to a sensitivity analysis which showed that it is possible to produce chemical variations at the spring even if all tributaries have constant (but different for each) solute concentrations. This process is known as tributary mixing. This study led to two important conclusions concerning transport of chemicals in the phreatic zone: (1) transport is mainly non-reactive, even during flood events and (2) no significant mixing component with water stored in the low permeability volumes occurs in the phreatic zone.

Acid Neutralization Capacity (ANC) is a parameter sometimes used for hydrograph splitting of rivers. It is useful because it is easily measured, behaves conservatively on groundwater-soil-water mixing and provides a clear marker between soil and groundwater zone. ANC decreases with increased flow in a river due to the dilution with water of low base cation concentration (Neal et al., 1997, Robson and Neal, 1990). In karst catchments, it can be assumed that the contribution of weak organic acids, phosphates, silicates, borates etc. to the ANC of the system is minimal, thus reducing ANC to a function of the carbonate system:

$$\mathrm{ANC} \approx [HCO_3^-] + 2[CO_3^{2-}] + [OH^-] - [H^+] \qquad \textit{Equation 2.13}$$

This corresponds to the definition of alkalinity and therefore the study of alkalinity can be reasonably represented by ANC. Chandler and Bisogni Jr (1999) used alkalinity in this way to calculate contact time of water with a limestone aquifer. The responses of the alkalinity saturation ratio and the runoff depth to increasing rainfall depth were used to affirm the hypothesis that epikarst infilling and changing soil structure creates throttles to percolation and infiltration.

2.5 Modelling Karst Aquifers

Mathematical models of groundwater flow have existed since the late 1800s and have evolved rapidly during the second half of the 20th century. The development of computer technology since the 1960s facilitated the creation of complex numerical models which could solve detailed hydrogeological problems (Kovacs, 2003). However, due to the highly heterogeneous nature of karst groundwater flow, specially adapted modelling methodologies are required for modelling of karst aquifers. Teutsch and Sauter (1998) describe how the most appropriate modelling approach for karst aquifers depends on whether the inputs to the aquifer are point or diffuse and whether the observation point is point (e.g. a well) or diffuse (e.g. a spring). Scanlon et al. (2003) lists another four important factors in choosing a particular modelling approach:

- **Degree of karstification**: A predominantly diffuse aquifer can be successfully modelled as an equivalent porous medium. A similar approach can be used for a conduit dominated system if the conduits are uniformly distributed and well interconnected (although Kovacs (2003) disputes this). A poorly distributed but well understood conduit system can be modelled by a discrete channel network model such as that of Gill et al. (2013a) and Peterson and Wicks (2006).

- **Objective of the modelling study:** The objective will dictate the conceptual structure of the model. Examples of objectives include evaluation of groundwater flow for water management, analysis of contaminant transport and assessment of aquifer vulnerability to contamination.

- **Data availability:** The more data you have, the better the chance of achieving an accurate calibration for a model. Some models are based on spring discharge alone compared to other models which may have detailed information on the flow system such as water levels, flow velocities, tracer results, spring temperature and chemistry.

- **Availability of codes:** The relevant numerical codes are imperative to a good simulation. For example, a karst model must include numerical codes for turbulent flow which are not included in regional scale models even for karst systems.

Developing an appropriate conceptual model is the most important part of the entire modelling process (Ford and Williams, 2007). The conceptual model is the theoretical representation of a real

system and consists of representative parameters such as flow-describing differential equations, geometry of the aquifer, a set of flow parameters, initial conditions and boundary conditions (Kovacs and Sauter, 2007). A good conceptual model of a karst system includes the heterogeneity and interlinked nature of the flow processes such as infiltration, storage, groundwater flow and discharge processes. An aquifer can be conceptually broken into three zones in the vertical direction. These zones are typically: soil and epikarst, unsaturated or vadose zone and phreatic zone. An early example of a conceptual model of a karst system is that of Drogue (1980) (see Figure 2.12) which consisted of fissured blocks separated by high-permeability low storage units. This system contained 3 main porosity systems:

(A) A highly permeable upper zone (epikarst) with closely spaced fissure.
(B) Largely unweathered blocks with low-permeability cracks that permit slow flow.
(C) High-permeability conduits that permit rapid flow.

Overall, two distinct approaches of mathematical modelling have been developed for karst hydrological systems, global models and distributive models. Global models (or lumped parameter models / spatially lumped models) derive a relationship between input and output. When using a global model, the karst system is being considered as a transducer that transforms input signals (recharge) into output signals (discharge). Distributive models, on the other hand, use theoretical concepts such as aquifer structure and hydrodynamic flow equations to simulate the hydraulic behaviour of a karst aquifer (Ford and Williams, 2007).

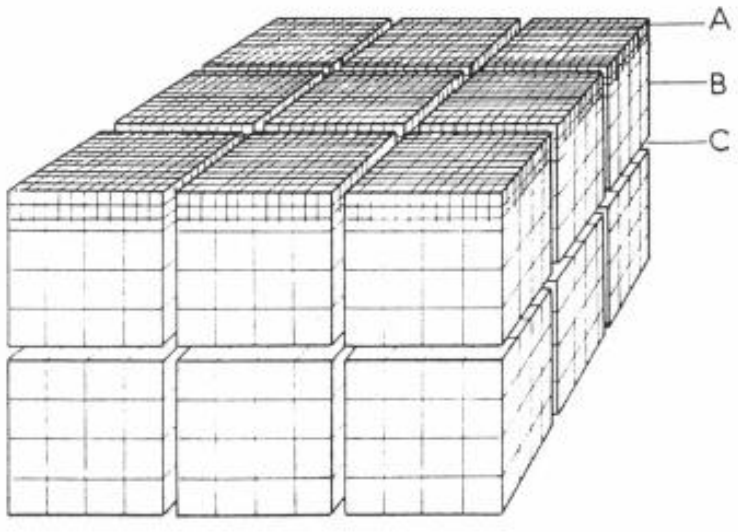

Figure 2.12: Double fissured porosity system (Drogue, 1980)

2.5.1 Global Models

Global models transform an input signal (generally rainfall or allogenic recharge) into a spring hydrograph signal by representing the karst aquifer as a transfer function. Thus the monitoring of spring discharge from a karst aquifer makes the characterisation of the hydraulic behaviour of the entire system possible. As these lumped parameter models are based on physical phenomena, they can supply significant information regarding the global functioning of the karst system. However they lack spatial predictive power as they do not consider spatial heterogeneity of the aquifers (Kovacs, 2003). Global models can be used for example, to make predictions about the spring water quality based on recharge and spring data. They are not capable however, of assessing the spatial distribution of the water quality (Ghasemizadeh et al., 2012). Two distinct types of transfer function analysis methods can be distinguished, single event methods and time series analyses. Single event methods deal with the global hydraulic response of the aquifer to a single rainfall event and time series analyses deal with the global hydraulic response of the karst system to a succession of rainfall events (Kovacs, 2003). Time series analysis is also known as 'black-box modelling' as it does not rely on the specification of the size, shape or location of the internal structure of the aquifer whereas single event modelling is often based on simple or sometimes more complex reservoir systems and involve physical phenomena which makes it appropriate to call them 'grey-box models' rather than 'black-box models' (Kovacs and Sauter, 2007).

The transfer function of a lumped parameter model can be represented by a single mathematical function or a time series although usually there is no simple method to derive the transfer function used to model an individual storm event or more long-term series. To identify transfer functions, two distinct methods can be distinguished. The first is to determine parametric transfer functions (e.g. an instantaneous unit hydrograph determined from a conceptual model) and then optimise the parameters to fit the data. The second method uses numerous different numerical methods for the determination of non-parametric transfer functions which include Fourier transforms, least squares approaches and statistical method (Denić-Jukić and Jukić, 2003).

If a system is assumed to be linear and time invariant, the relationship between input and output is represented by the convolution equation:

$$y(t) = \int_0^t h(t - t')x(t')dt' \qquad \textit{Equation 2.14}$$

where y(t) is the output time series, h(t-t') is the transfer function, x(t') is the system input time series and (t-t') represents the delay between input and output (Long and Derickson, 1999). So if the input x(t') and output y(t) functions are known, the transfer function h(t-t') can be derived using deconvolution methods such as linear programming (Neuman and De Marsily, 1976). It should be noted however that the assumption of a karst system being linear and time invariant is an erroneous one. As such, transfer function models of karst systems are always very approximative. The shape of the transfer functions can be characterised by the known physical structure of the karstic system. A delay in response can be due to delay in the non-karstic soil and sub-soil during surface infiltration and runoff or due to exchange of water between micro and macro fissure systems (Gill, 2010).

Irregularities in transfer functions are common due to the unavoidable errors in input and output time series and the simplifications made by assuming the system is linear and time-invariant. These irregularities, which cause unstable oscillatory functions, are pronounced in the tail of the transfer functions. As a consequence, the transfer function is not suitable for simulating the recession part of a karst spring hydrograph and should only be used on the quick-flow component (Denić-Jukić and Jukić, 2003, Dreiss, 1982). A new form of transfer function for karst aquifers, known as a Composite Transfer Function (CTF), has been developed to avoid this irregularity. These functions use the superposition of two transfer functions adapted for the quick flow and slow flow hydrograph components (Denić-Jukić and Jukić, 2003). Jukic and Denic-Jukic (2005) also derived a kernel function for karst aquifers from the time-invariant and non-anticipatory Volterra series. Another method was presented by Padilla and Pulido-Bosch (2008) whereby the karst Tocal de Antequera aquifer in Spain is divided into three zones: surface zone, unsaturated zone and saturated zone. Each of these zones being described by its own transfer function that determines the water supplied from the overlying zone.

Global models based on a set of linked reservoirs have also been developed such as the empirical reservoir model developed for the Fontaine de Vacluse aquifer in southern France which used three reservoirs to simulate the high and low spring discharge rates (Figure 2.13). The first soil reservoir simulates the infiltration through the soil using effective rainfall and a transfer function. This infiltration is then split between two parallel reservoirs, one representing slow flow (fracture flow) and the other representing rapid flow (conduit flow). The slow flow reservoir transfer function was determined by hydrodynamic analysis of the spring hydrograph while the rapid flow reservoir was a fitted parameter. The discharge from each reservoir was proportional to the water level within the reservoir (Fleury et al., 2007).

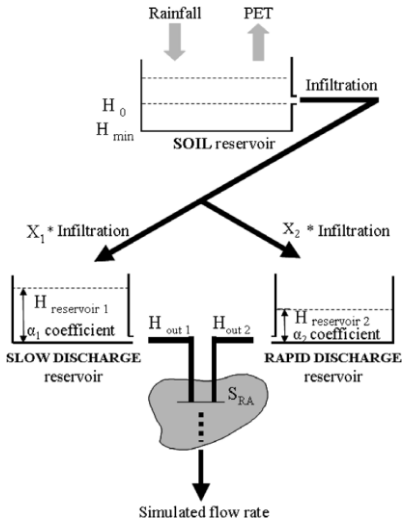

Figure 2.13: Conceptual model of Fontaine de Vacluse system (Fleury et al., 2007)

2.5.2 Distributive Models

Distributive models of a karst aquifer split the hydrogeological system into homogeneous sub-units in which groundwater flow can be described by basic physical laws (Kovacs and Sauter, 2007). These models may consider both spatial and temporal variations in recharge, hydraulic parameters and in the discharge and thus can represent the complete quantitative characterisation of the flow systems in karst aquifers (Kovacs, 2003). These models are preferable if groundwater quality parameters are to be assessed at many different locations within the aquifer, such as the simulating the development of a contaminant distribution (Ghasemizadeh et al., 2012). Distributive models however may require detailed information on aquifer geometry, hydraulic parameter fields and recharge conditions, details of which are often difficult to ascertain.

Distributed models can be partitioned into two principal concepts: a single continuum representing the effective overall parameters of the aquifer or a discrete set of fractures and conduits with flow only considered within those discrete flow paths. Kovacs (2003) combine these two concepts into five distinct modelling approaches (based of earlier classifications by Teutsch and Sauter (1998)). These approaches are the following:

- Discrete Fracture Network approach (DFN)
- Discrete Channel Network Approach (DCN)
- Equivalent Porous Medium Approach (EPM)
- Double Continuum Approach (DC)
- Combined Discrete-Continuum Approach (CDC).

Each method has its advantages and disadvantages, and the selection of an appropriate modelling approach is crucial with respect to the desired output of the model. The approaches are displayed visually below in Figure 2.14.

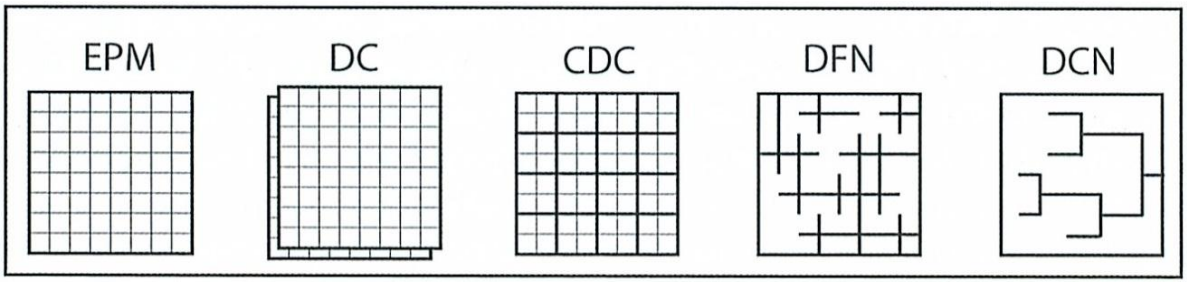

Figure 2.14: Classification of distributive karst modelling methods (Kovacs and Sauter, 2007)

The terminology for these modelling approaches varies across the literature. Ghasemizadeh et al. (2012) created a useful table for comparing these model names as can be seen below in Table 2.3.

Table 2.3: Varied terminology for modelling approaches found in the literature (Ghasemizadeh et al., 2012)

Modelling approach	Other names	Type
Equivalent porous medium approach (EPM)	Single continuum porous equivalent approach (SCPE) Heterogeneous continuum approach Distributed parameter approach Smeared conduit approach Single continuum approach	Distributed
Double porosity model (DPM)	**Double continuum approach (DC)** Double Continuum porous equivalent approach (DCPE)	Distributed
Discrete fracture network approach (DFN)	Parallel plate model Two types: Discrete singular fracture set approach (DSFS) Discrete multiple fracture set approach (DMFS)	Distributed
Discrete channel network approach (DCN)	**Discrete channel network approach (DCN)**	Distributed
Hybrid model (HM)	**Combined discrete-continuum approach (CDC)** Combined single continuum–discrete fracture set approach (SCPE-DSFS)	Distributed
Hydrograph-chemograph analyses	Single event methods	Lumped
Linear storage models	Rainfall-discharge models Time series analyses Box models	Lumped
Soft computing methods	Computationally intelligence methods	Lumped

2.5.2.1 Discrete Fracture and Conduit Network approaches (DFN and DCN)

Discrete fracture (or conduit) models describe flow within individual fractures or conduits but ignore matrix characteristics by assuming negligible permeability. Flow within the fractures and conduits is modelled using hydraulic equations that govern laminar and turbulent flow (Hagen-Poiseuille and Darcy-Weisbach laws). It should be noted that these models are of limited use at the scale of an aquifer due to the computational power needed to account for every fracture or conduit but this limitation is disappearing with improvements in technology and the use of supercomputers (Ford and Williams, 2007).

DISCRETE FRACTURE NETWORK (DFN)

The DFN approach considers only certain sets of fractures within an aquifer to be permeable. It simplifies a fissured system into a network of two dimensional, and sometimes three dimensional (Long et al., 1985), fracture planes. Fracture networks are generated stochastically by applying a Monte Carlo process. According to this process, probability density functions are fitted to field data describing the spacing, length, direction and aperture of fracture sets identified on stereonets. Parameters are then sampled from these statistical distributions and assigned to individual fractures in the model (Kovacs and Sauter, 2007). The major advantage of DFN models is the capacity to model the compartmentalisation phenomenon of some karst aquifers whereby compartments of adjacent rock can have significant differences in hydraulic heads (Sawada et al., 2000).

DISCRETE CONDUIT NETWORK (DCN)

The DCN approach simulates flow in networks of pipes that represent karst conduits. The first documented successful attempt at a pipe-network approach was by Thrailkill (1974) for an aquifer in Kentucky. Since then, many aquifers have been modelled in this way with the more recent models being called 'discrete' models and containing an explicit conduit system based on actual exploration or by estimation as to where the conduits should be (Mohrlok and Sauter, 1997, White, 2002, Jeannin, 2001). A good example of a DCN study was carried out by Jeannin (2001) in Europe's longest cave, the 185 km Hölloch cave network in Switzerland. This model accurately simulated the turbulent flow in the variably saturated, conduit flow-dominated karst system (see Figure 2.15).

Springer (2004) developed a one-dimensional closed conduit model of a discrete cave segment of Buckeye Creek Cave, West Virginia, using Bernoulli's energy equation and the assumption that energy losses in the segment are generated by large-scale flow separation associated with expansions and bends. The study used paleostage indicators and passage geometry to estimate the

total head loss across the 1.6 km conduit. Channel roughness was estimated using pipe-based equations and a skin friction factor was also estimated. Discharge was then varied until calculated head loss matched observed head loss. Using this information, the discharge from Buckeye Creek cave was able to be estimated. Another aspect of this study was the estimation of a conduit friction factor (f) of 0.4-0.7 which Springer found reasonable as it lay between f values for large uniform passages from Norway (f = 0.116) (Lauritzen et al., 1985) and significantly obstructed passages (f = 24-340) (Atkinson, 1977). The choice of friction factor is important in constructing a pipe flow model and care should be taken due to the wide range of derived friction (0.039-340) factors found by various researchers as seen previously in Section 2.2.2. Some numerical models use Manning's equation as part of the calculation for flow rate in conduits. For this reason, the Manning's roughness coefficient (n) is sometimes needed to be estimated. Typical values for this roughness parameter are 0.035 (Peterson and Wicks, 2006) and 0.04 (Thrailkill et al., 1991).

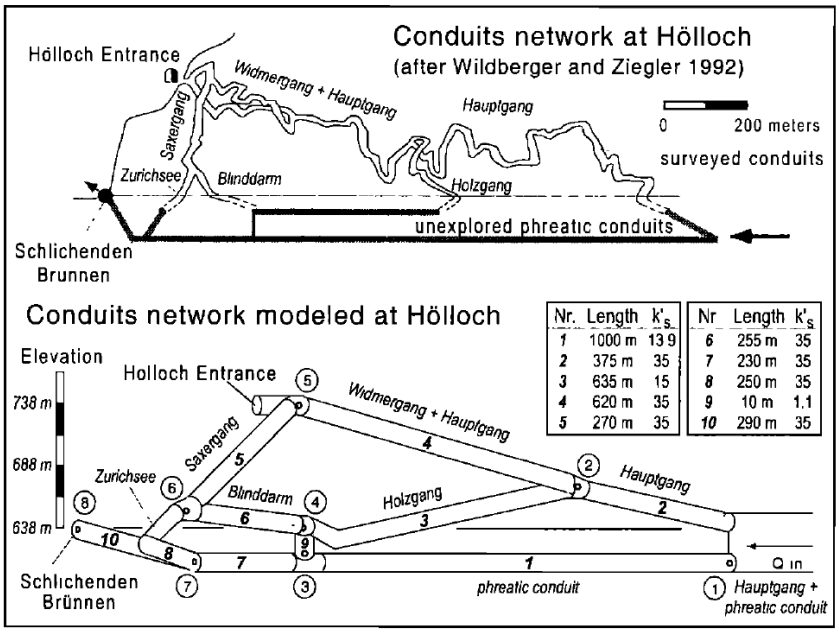

Figure 2.15: DCN model of downstream part of Hölloch cave (Jeannin, 2001)

Peterson and Wicks (2006) carried out a study on the sensitivity of a pipe network model using the U.S. Environmental Protection Agency's Storm Water Management Model (SWMM) software. The model was applied to the Devil's Icebox-Connor's Cave System in central Missouri. The study found that 10% changes in the length or width of the conduits produced statistically different outflows in the calibrated baseline model. The model was also extremely sensitive to changes in Mannings n but was relatively insensitive to changes in slope and infiltration rates.

The most relevant DCN study to this thesis is the conduit network model created for the Gort Lowlands turlough system (Gill et al., 2013a). This model simulated the behaviour of turloughs along a major conduit flow system using a conduit network with surcharged tanks. The diffuse contribution from the epikarst was included in the model by using a series of Darcian soil stores draining into permeable pipes. This recharge was then fed via these pipes into the main conduit network (discussed further in Chapter 6).

2.5.2.2 Equivalent Porous Medium Approach (EPM)

Equivalent porous medium models largely ignore conduit flow within an aquifer and assume Darcian flow conditions on the basis that, at a large enough scale, the aquifer behaves as an isotropic, homogeneous medium. This modelling technique is only appropriate for well-connected porous media or fractured systems at a fairly large scale (Ford and Williams, 2007) and as a result has generally only been applied to aquifers characterised as predominantly diffuse (Teutsch, 1993). Such an approach obviously does not adequately represent the complex flow patterns in well karstified aquifers and has been shown to produce fundamentally different temporal and hydraulic behaviour from karst media (Kovacs et al., 2005). Consequently, the use of EPM models is limited and is inadequate for modelling karst systems over a large range of applications.

EPM models can use either single continuum or double continuum approaches. The single continuum approach has proved adequate for simulating regional groundwater flow in lesser karstified aquifers (Scanlon et al., 2003, Greene et al., 1999, Keeler and Zhang, 1997). For more karstified aquifers a dual continuum approach can also be used whereby one continuum represents a diffuse zone of low conductivity and another zone represents a high conductivity, highly karstified zone (Teutsch, 1993). Flow in both zones is assumed to be laminar.

A study by Scanlon et al. (2003) carried out in the Barton Springs Edwards karstic aquifer in Texas compared two different EPM approaches: lumped and distributed parameter. The lumped parameter model described five connected reservoirs, each representing a major river in the study area and was calibrated using spring discharge. The distributed parameter model used MODFLOW modelling software and comprised of 14,400 cells, each cell representing all types of flow (conduit, fracture and matrix). Both models resulted in fairly accurate simulations of spring discharge which led Scanlon to conclude that either approach would be adequate for this purpose. However for detailed evaluation on a more local scale, a distributed parameter model is recommended.

In 2000, the misuse of the EPM technique contributed to a pollution incident in Walkerton, Canada. After the water supply became contaminated with E. coli, MODFLOW was used to delineate a 30-day capture zone, outside of which water would be safe to drink. However, the MODFLOW assumes Darcian flow and ignores the rapid movement of water through fractures/conduits in a karst aquifer. Subsequent tracer tests demonstrated travel times of less than a day to pass the supposed 30-day capture zone. Seven people died and 2300 became ill as a result of the miscalculation (Goldscheider and Drew, 2007).

2.5.2.3 Double Continuum Approach (DC)

The double continuum approach is currently the most useful modelling technique for simulating observed aquifer conditions in karst (Ford and Williams, 2007). As mentioned previously in Section 2.5.2.2, the double continuum approach separates an aquifer into two zones: a diffuse zone of low conductivity and high storativity and more karstified zone with high conductivity and low storativity. It is best applied to karst aquifers that can be considered adequately represented by dual matrix-fissure, matrix-conduit or fissure-conduit groundwater systems. The two zones are treated as two separate overlapping continua, each with its own hydraulic and geometric parameters and flow equations (Ford and Williams, 2007). The two continua are joined by a source-link term in each equation and exchange of flow is governed by local differences in potentials.

DC models have been shown to simulate spring discharges adequately when compared to field observations (Mohrlok and Sauter, 1997) and have been used successfully in real world applications such as studies in the Swabian Alb in southern Germany (Teutsch, 1993, Sauter, 1992). A disadvantage of DC models is the inability to model the temporal delay of diffuse infiltration since both subsystems are coupled directly at each node. In order to incorporate diffuse infiltration, a retention function is necessary (Kovacs and Sauter, 2007). DC models provide meaningful results from a functional point of view, but as of yet no study has successfully demonstrated that they adequately describe the structural and spatial behaviour of a real karst system (case studies have all been carried out in regions where the conduit networks are mostly or completely unknown).

The next logical step from the DC approach is a triple porosity model incorporating matrix, fracture and conduit systems. Such a model has not yet been developed due to difficulties in model calibration, availability of required data and computing capability. The development of a realistic triple porosity model for a karst aquifer represents the frontier in karst hydrogeological modelling (Ford and Williams, 2007).

2.5.2.4 Combined Discrete-Continuum Approach (CDC)

The CDC approach is a method that is capable of handling the discontinuities that exist at all scales in a karst system (fractures, fault zones, karst channels etc.) by representing them as networks of different orders of magnitude embedded in each other (Kovacs, 2003, Kiraly, 1975). This method uses the finite element discretion method and allows the use of one, two or three-dimensional elements. High conductivity karst conduits can be simulated by one dimensional finite elements, which are set in a low permeability matrix represented by three dimensional elements. Also, the use of two dimensional elements can make the simulation of fractures and fault zones possible (Kovacs and Sauter, 2007). This approach enables the testing of conceptual models of karst systems as it facilitates the direct application of observed hydraulic parameters from an aquifer.

The SHETRAN physically-based distributed hydrological model has been used to model karstic groundwater movement as a combined system (Adams and Parkin, 2001), coupling surface and subsurface processes together into an integrated 3-D model of water flow and transport (Ewen et al., 2000). Flow in the sub-horizontal cave network in the saturated zone was modelled using the VSS-NET component of the model, originally developed to simulate groundwater rebound in abandoned mines (Adams and Younger, 2001). Also, recently MODFLOW software has been upgraded to include different conduit processes into its modelling suite. This upgrade enables the modelling of conduit flow and matrix flow in the single MODFLOW software package.

CDC models are the most appropriate models for simulating the actual physical processes of interacting matrix and conduit flow. However, due to the large data requirements, modelling efforts and computational costs of this approach, its use is limited (Ghasemizadeh et al., 2012).

2.6 Summary

In this chapter a literature review was conducted to provide an overview of karst systems and to review the studies conducted on these landscapes to date. This review discussed the fundamental elements of karst hydrology (recharge, chemistry etc.) and karst network development. This chapter also introduced typical 'investigative techniques' employed in the monitoring and analysis of these systems and discussed the various modelling techniques (global and distributive) which have been applied to karst systems globally.

This literature review highlighted that the research conducted in this thesis into the hydrological behaviour of a lowland karst system would provide a valuable insight into a scarce form of karst

hydrology for the global karst hydrological knowledgebase. Several 'investigative techniques' discussed in this chapter were identified as suitable methods for carrying out research as part of this thesis. These techniques and their contribution to knowledge include:

- Offering an overview of the geological and speleological background of a lowland karst catchment. In particular, the most recent speleological investigations have been described and detailed in Section 3.3.

- The use of environmental tracers and general hydrochemistry techniques are fundamental to the findings of this thesis. This research offers the first published isotopic study of a turlough system and one of the most detailed hydrochemical studies of a lowland karst system (the hydrochemical work of the Gort Flood Studies Report was wider in scope but took much fewer measurements from each turlough).

This thesis describes the application of a discrete channel network model to a lowland karst system. Such lowland systems are rarely modelled (or investigated in general) and as such, the model provides a relatively important contribution to global karst modelling literature. Furthermore, the numerical model is combined with hydrochemical measurements in order to characterise the transport and fate of nutrients as they travel through the system.

Chapter 3

Background and Site Description

3 BACKGROUND AND SITE DESCRIPTION

3.1 Irish Karst

Carboniferous limestone is the most common rock type in Ireland. It underlies almost half the land surface in Ireland (making it the primary aquifer in the country) and is often heavily karstified. Consequently, karst landforms and karst features are a significant aspect of the Irish landscape. Karst features such as dolines, bare rock exposures, collapsed conduits, springs and turloughs have been documented in 80-85% of limestone outcrops indicating that most and possibly all carboniferous limestones in Ireland have some degree of karstification (Drew et al., 1996).

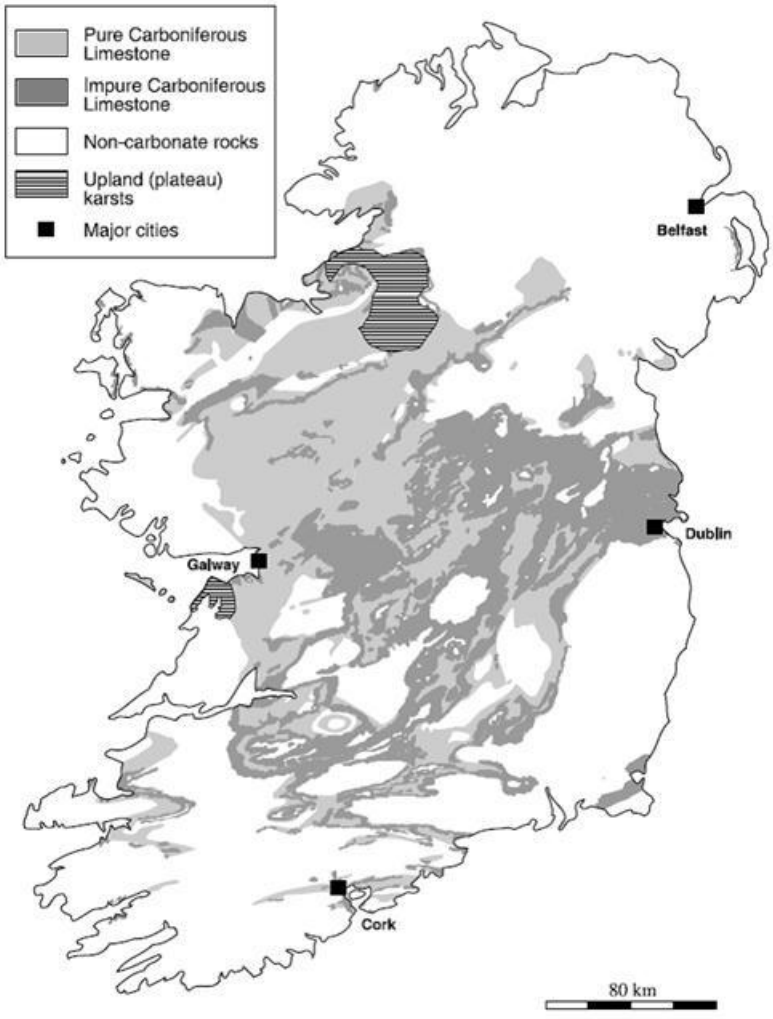

Figure 3.1: Distribution of carboniferous limestone in Ireland (Drew, 2008).

With very few exceptions, Irish limestones belong to two periods of geological history: the Carboniferous (approx. 300-340 million years ago) and the Cretaceous (70-120 million years ago) (Karst Working Group, 2000). More recently, karstification has taken place in the Holecene (10 ka to present) which has resulted in the development of a weathered zone of limestone near the soil-carbonate rock interface known as epikarst (Section 2.3.3) as well as active karst features such as stream caves in the Burren (Drew and Jones, 2000). The degree of karstification on limestones in Ireland is spatially inconsistent as it depends on the purity of the limestone. In the east and midlands of the country, the limestone is impure and large areas of limestone can be found absent of any karst features. In these areas, there is little interaction with the underlying karst aquifer and normal surface drainage systems are present. The purest limestones are found west of the River Shannon with extensive areas such as eastern Co. Galway, south Co. Mayo and Co. Roscommon completely devoid of any surface drainage systems. The distribution of limestones and their purity is displayed Figure 3.1.

The unusual aspect of Irish karst is that, unlike the situation in the remainder of Europe, Irish karst terrain is primarily lowland. Over 90% of the limestones are below 150m above sea level (asl) and much of it less than 100 masl. Due to the lowland nature of the karst, it often underlies some of the most productive agricultural land in the country as well as some major centres of population (Drew, 2008). Upland karst is only found in the Burren, Co. Clare and the north-west of Ireland.

Lowland karst is characterised by considerable interaction between ground and surface waters. The exchange of water between these two systems is made evident by certain karstic features including losing and gaining streams, swallow holes, estavelles, springs and turloughs. These complex interactions between surface and groundwater boundaries make it difficult to delineate boundaries of contributing areas or accurately quantify recharge for karst aquifers. Lowland karst in Ireland has relatively low hydraulic gradients, estimated at 0.01-0.001, and groundwater flow velocities recorded between 5 and 250 m/h. Upland karst tends to have hydraulic gradients an order of magnitude higher but velocities of 20-300 m/h similar to lowland karst (Drew, 2008).

As mentioned in Section 2.3.3, due to the lowland nature of Irish karsts, the vadose zones of these aquifers are relatively shallow which results in epikarst occurring within the phreatic or epiphreatic zones. As such, a significant quantity of diffuse flow through an Irish karstic aquifer can flow through the epikarstic zone. Thus in aquifers such as these, diffuse flow and epikarst flow can be thought of as roughly equivalent. Thus in terms of the Gort lowlands catchment, the terms diffuse

flow and epikarstic flow are often interchangeable and shall be treated as such throughout this thesis.

3.2 The Gort Lowlands: Geology and Hydrogeology

The subject area of this research is the Gort Lowlands region, a 500 km² catchment located in south Galway (see Figure 3.2). The area is bounded to the east by the low lying Slieve Aughty Mountains and to the west by the northern edge of the Burren (one of the largest karst landscapes in Europe) and drains north-west from the mountains across the Gort Lowlands to the sea at Kinvara. The catchment is a good example of low lying karst limestone in Ireland but has one differing feature; approximately half of the catchment is underlain by largely impermeable non-calcareous rocks. These non-calcareous rocks are primarily Devonian sandstones and underlay the Slieve Aughty Mountains to the east. The western side of the catchment is mostly flat and underlain by pure carboniferous limestone. As a result, the three primary surface rivers which drain the mountains run along an impermeable substrate surface until they reach the western karst region where they sink underground providing allogenic recharge to the karst aquifer.

This significant contribution of allogenic recharge to the low lying karst plain provides the catchment with unique hydrological and ecological characteristics. Furthermore, the catchment has seen relatively little human impact on the natural drainage system giving the region and its karst features an important conservation status. Consequently, the area has historically been the subject of intense research by hydrologists and ecologists (e.g. Kinahan (1865), Praeger (1932) and Williams (1964)). Since the 1980's, the area has also become a popular location for speleologists due to its well-developed karst conduit network offering many kilometres of unexplored underwater cave systems. In fact, the Gort Lowlands may be one of the longest underground cave networks in Europe (Siggins, 2010).

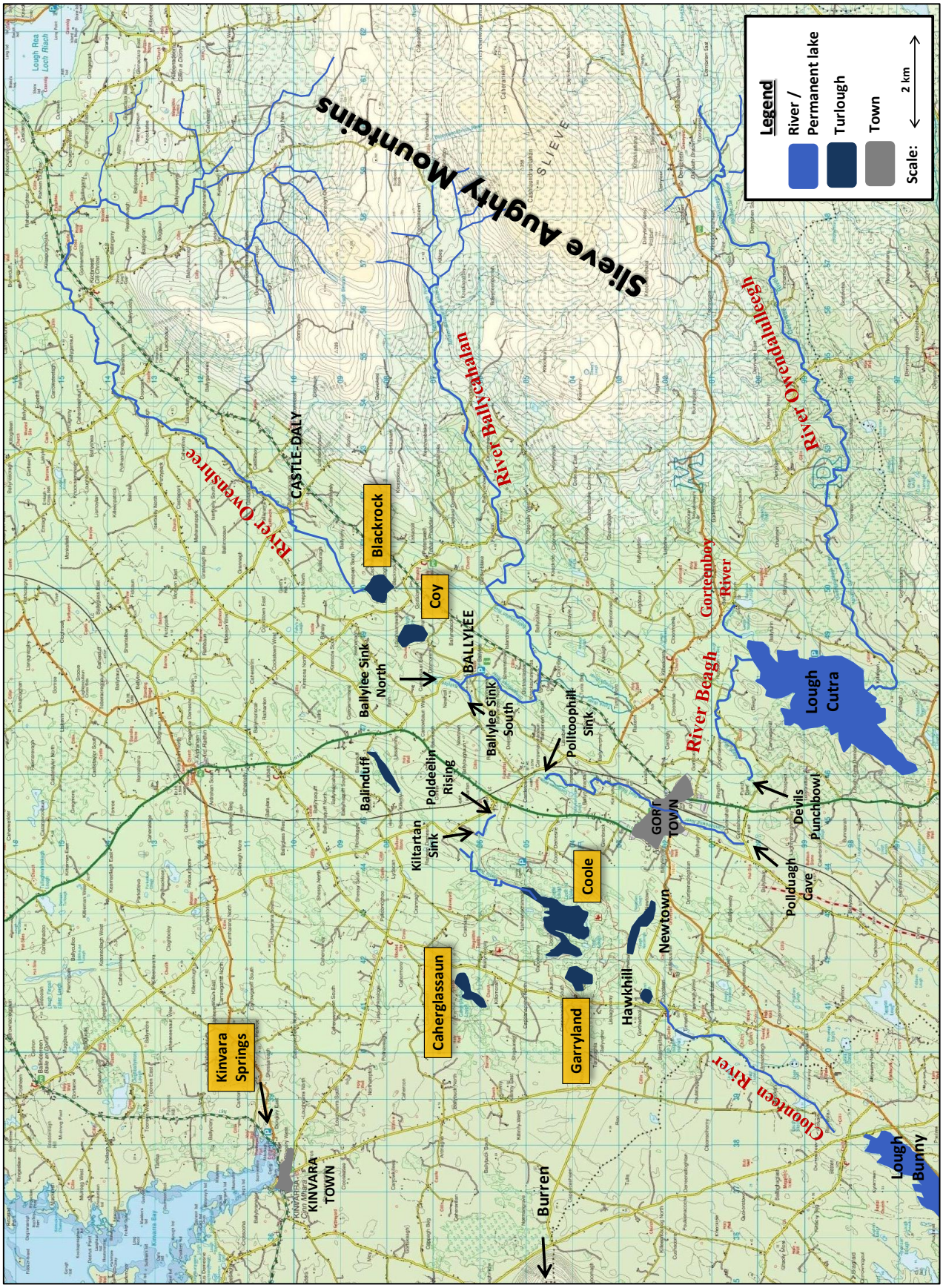

Figure 3.2: Map of Gort lowlands showing the locations of turloughs, rivers, lakes, springs, swallow holes and towns.

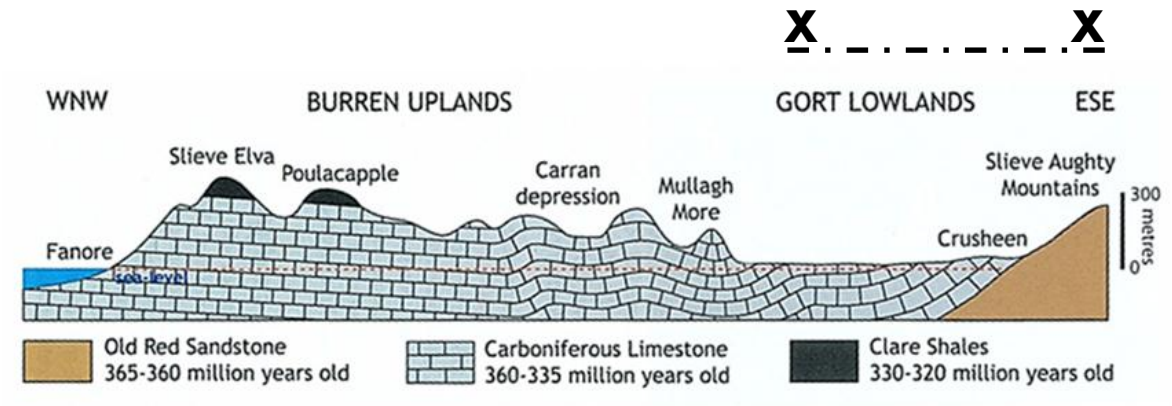

Figure 3.3: East-West sketch section through the Burren and Gort Lowlands (Simms, 2001). The location of the section X-X can be seen in Figure 3.4

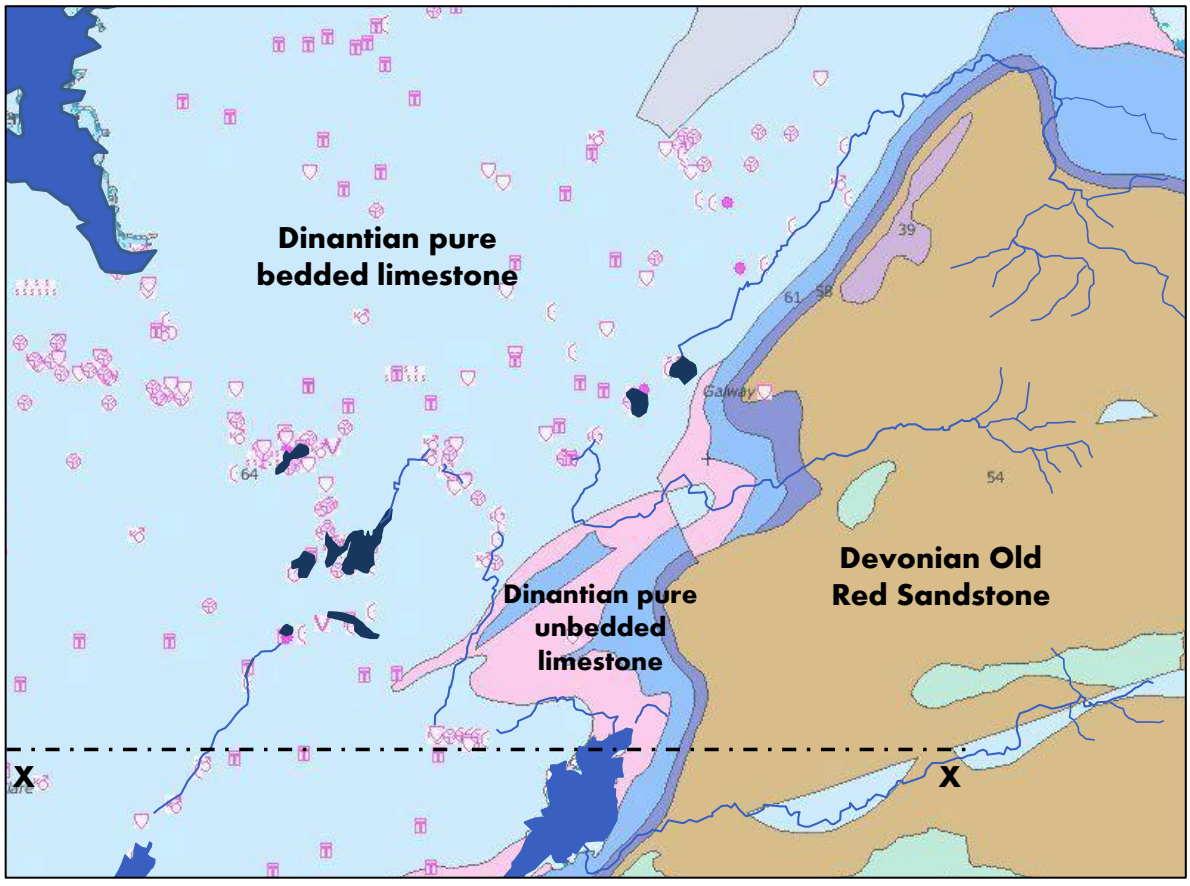

Figure 3.4: Bedrock geology of the Gort Lowlands

(Karst features on the GSI database are shown as pink symbols).

The Slieve Aughty uplands extend over some 640 square kilometers spread over County Galway and County Clare. They consist of two ridges rising to 300-360 meters separated by the Owendalulleegh River and are covered by bogs and some forested areas. Due to the lack of tree cover, lack of cultivation and poor drainage provided by the Devonian Sandstone, the area has substantial bog coverage. The region suffers from erosion problems which are exacerbated at present by extensive plantations of coniferous trees which accelerate the rate of run-off (Nugent, 2006). Three main rivers run down from the mountains and into the carboniferous lowlands: the Owenshree, the Ballycahalan (or Ballylee/Boleyneedonish) and the Owendalulleegh (or Derrywee).

These three rivers supply chemically-aggressive waters derived from non-carbonate catchment areas into the lowlands: the Owenshree to the north-east, the Ballycahalan to the east and the Owendalulleegh to the south-east. The allogenic recharge supplied by these rivers has rapidly influenced karst development in the region, whereby the relatively acidic waters (mean pH: 7.2) derived from the peaty catchment of the Slieve Aughty Mountains has contributed to the development of a complex network of sinking streams, conduits and turloughs (carbonate aquifers typically have pH's closer to 7.9, Chapman (1996)). A further two rivers drain the extremities of the Gort Lowlands, the Cloonteen River to the south and the Aggard Stream to the north (Figure 3.14). The Cloonteen River system originates in Lough Bunny and flows northwards until it sinks underground in all but high flow conditions which occur during the winter (Southern Water Global, 1998). During such periods the river continues northwards, flowing into Hawkhill Turlough on the southern boundary of the Coole-Garryland complex. The Aggard Stream rises in sandy till on the northern boundary of the Gort Lowlands and flows into the Dunkellin River (Figure 3.14) arterial drainage scheme, and so is not thought to contribute significantly to the hydrology in the Gort area. The conceptual operation of the three rivers and their conduit linkages are described below (see Figures 3.2 and 3.6 for reference maps).

OWENSHREE RIVER – BLACKROCK TURLOUGH – COY TURLOUGH – BALLYLEE

The Owenshree River drains the northern extremity of the Slieve Aughty Mountains, flowing north-west initially before turning south-west towards the limestone plain. The majority of the river continues to flow overland along the carboniferous limestone plain for approximately 13 km until it reaches Blackrock turlough, whereupon it sinks underground. The water then moves south, either surcharging into Lough Coy turlough or bypassing it completely along its path towards Ballylee. At Ballylee, the path of the river water is determined by the prevailing flood conditions. In dry weather, flow remains underground and it is presumed to join up with water from the Ballycahalan River after it has sank at Ballylee sink south (Figure 3.2). In wet weather conditions (when the levels

of the turloughs exceed the level of Ballylee), flow from the Owenshree re-emerges at the estavelle known as Ballylee sink north and continues overland, joining up with water from the Ballycahalan before entering the subterranean system via the southern sink.

It should also be noted that a series of swallow holes exist along the river bed of the Owenshree. These swallow holes drain a proportion of river water either transmitting the flow underground towards Blackrock turlough or via a separate deep karst conduit link directly towards Kinvara. This separate conduit system is known as the northern flow route (Southern Water Global, 1998).

BALLYCAHALAN RIVER - BALLYLEE

The Ballycahalan River flows down from the western flank of the Slieve Aughty Mountains until it reaches Ballylee, to the south of Lough Coy, where it splits into two branches. The southern branch conveys the majority of the river discharge towards a swallow hole (Ballylee sink south), while the northern branch links to Ballylee sink north. At the Ballylee sinks, the Ballycahalan River starts to interact with the Owenshree. During dry periods Ballycahalan River drains into both the northern and southern sinks, merging underground with discharge from the Owenshree. During wet periods, the entirety of the Ballycahalan (along with a contribution from the Owenshree from the northern estavelle) drains into the southern sink. From here, the collective flow from both rivers travels through an underground conduit towards Polldeelin rising. The conduit runs for an estimated 3.5-4 km, making it, one of if not the longest, underwater caves in Britain and Ireland (Kozlowski and Warny, 2009). Tracer studies have also shown evidence of a second flow path from Ballylee sink south whereby water bypasses Polldeelin, instead flowing directly towards Caherglassaun turlough to the west (Southern Water Global, 1998). See Figure 3.5 below for photos of Ballylee sink north discharging (A) and empty (B) (note: for (B), water sinking into estavelle out of view).

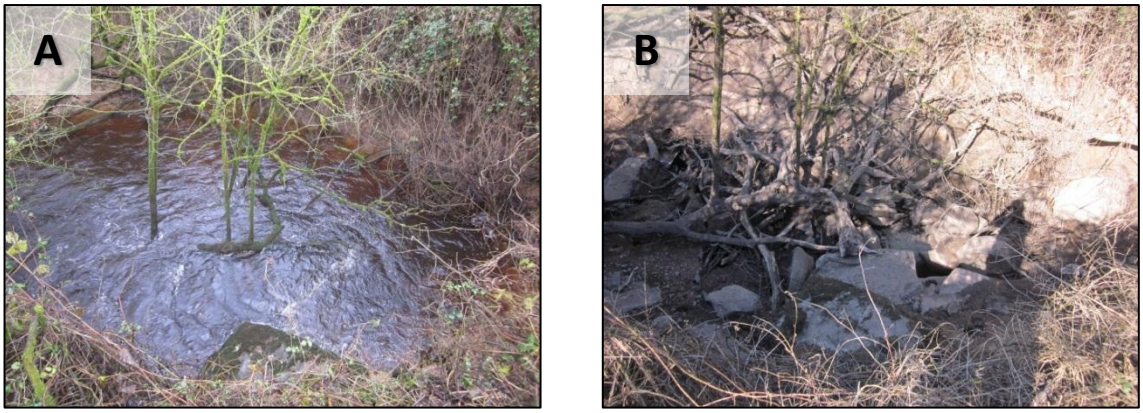

Figure 3.5: Ballylee sink north discharging *(A)* and empty *(B)*.

OWENDALULLEEGH RIVER – LOUGH CUTRA – DEVIL'S PUNCHBOWL – POLLDUAGH RISING – GORT TOWN – POLLATOOPHIL SINK

The largest river feeding the Gort Lowlands, the Owendalulleegh River, rises in Derrybrien East approximately 15 km due east of Gort town. The Owendalulleegh flows westward towards Lough Cutra, fed by a dendritic network of surface channels on the southern slopes of the Slieve Aughty Mountains. The Owendalulleegh discharges into Lough Cutra, where it combines with further flow from a smaller river, the Gorteenboy, which drains a sub-catchment on the south-western side of the Slieve Aughty Mountains. Lough Cutra acts significantly to attenuate the Owendalulleegh flows, dampening peak discharges of the river as it exits the lake in the north-west corner as the Beagh River.

From Lough Cutra the river flows westwards before sinking first at the Devil's Punchbowl, temporarily emerging as a 200m stretch known as the Blackwater (Figure 3.7), before rising from Pollduagh Cave. From here the river flows northwards through Gort for approximately 6 km until it sinks again at Polltoophill (Castletown) sink. From here, the river flows towards Polldeelin rising via a 2.4 km long underground conduit, sinking 62m below ground level before re-emerging at the spring to the west of the N18 at Kiltartan along with the combined flow from the Owenshree and Ballycahalan Rivers. From here, flow is over-ground for around 500m before sinking at the Kiltartan sink (Tommy Murray's sink), only to rise again 400m to the west as the Coole River.

COOLE RIVER – COOLE-GARRYLAND COMPLEX – CAHERGLASSAUN – KINVARA/CORRANROO

The majority of the Coole River flows into Coole turlough, the largest turlough in the Gort Lowlands system and part of the Coole-Garryland complex Special Area of Conservation (SAC). This SAC is made up of Coole and a number of other surrounding turloughs including Garryland, Doo (not shown on map), Newtown and Hawkhill. These turloughs are grouped together as one SAC based on their similar ecological behaviour rather than their hydrologic behaviour which is more varied.

The northernmost turloughs (Coole, Doo and Garryland) are fed predominantly by water from the Coole River. During low to mid-range water levels, the southern turloughs (Newtown and Hawkhill) are chiefly fed from the Cloonteen River to the south which keeps them hydrologically (and hydrochemically) separate from the northern turloughs (Southern Water Global, 1998). However, during high water level periods, a shallow epikarst system connects the northern and

southern turlough systems. In extreme flood events, overland connections are established between the two systems causing extensive flooding which can last several months.

As the water drains from the Coole-Garryland complex, it flows northwest towards Kinvara via Caherglassaun turlough (Figure 3.6). This turlough is the last in the Gort Lowlands chain of turloughs and has no surface water inputs (except during extreme flood events). The most significant feature of Caherglassaun turlough is that, due of its proximity to sea-level, it is subject to tidal effects. The drainage area between Caherglassaun turlough and Kinvara Bay is completely subterranean. The landscape is flat and featureless and completely devoid of surface water. The most distinctive landforms are a series of large enclosed depressions which are a result of collapses into a major water filled karst conduit (up to 25m in diameter). The collapses follow a line from Caherglassaun Turlough to Corranroo (an inlet approximately 4 km west of Kinvara). Corranroo is the ancient outlet for the conduits, which most of the modern drainage now short-circuits, flowing instead towards a series of intertidal springs in Kinvara. Kinvara is thus the focal point for the underground drainage system with a total catchment area of 483.41 km^2 (Environmental Protection Agency, 2011) where two major (and some more minor) intertidal springs on the coastline discharge water at flows typically between 5-20 m^3/s. Studies by Drew (2003), Cave and Henry (2011) and Jennings O'Donovan & Partners (2011) have suggested maximum flows of up to 80-100 m^3/s.

The two springs at Kinvara (Kinvara East and Kinvara West) discharge chemically contrasting water. It is understood that Kinvara West is the main outlet for the Gort lowland conduit system whereas Kinvara East discharges water from more diffuse epikarst-type sources within the catchment (discussed in more detail later in Sections 7.1.3 and 7.2.4). The Kinvara springs are part of a chain of intertidal springs along the south Galway Bay coast. Ballyvaughan, Bellharbour, Corranroo and Kinvara are all funnel shaped sea inlets with springs located at the head of each bay. These inlets are possibly the result of glacial erosion from the last ice age but also may be due to preferential solution of the limestone. The mixing of fresh and saline waters produces subsaturated water which is known to accelerate enlargement of the karstic fissures causing subsequent collapse of overlying strata a headward migration of the spring (Drew, 1990).

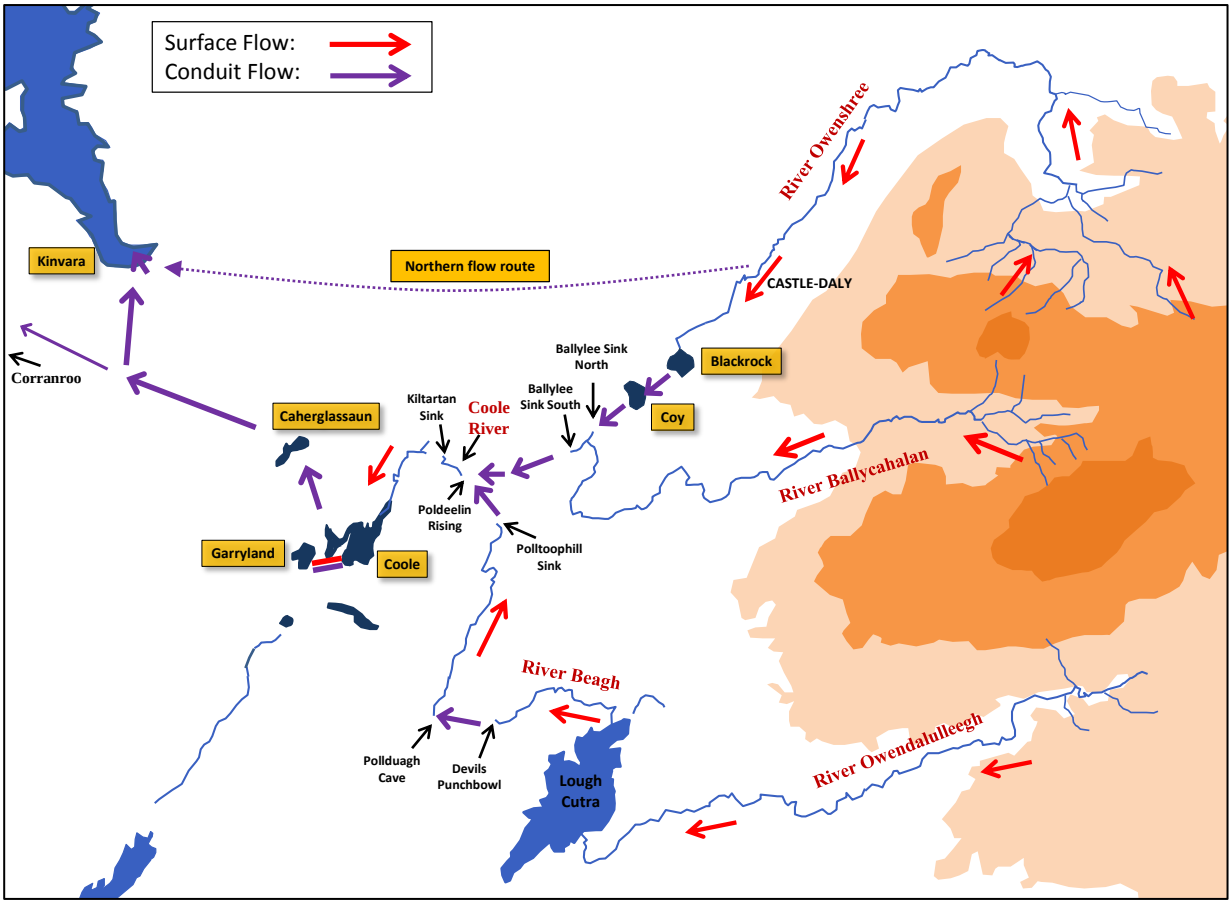

Figure 3.6: Schematic map displaying the distribution of flow within the Gort Lowlands.

Superficial deposits in the catchment vary in thickness from nothing (bare rock) up to possibly tens of meters, but they play a relatively minor role in the overall hydrological response of the catchment. They could however be locally important in providing groundwater storage and slowing the runoff rate. Depending on the character of the deposits, the effect could be to confine the limestone aquifer, or, at the other extreme, to function as an interangular aquifer with high storage feeding water into the highly transmissive limestone aquifer beneath (Drew, 2008).

3.3 Speleological Investigations

The Gort Lowlands has been an area of intense speleological investigation for many years due to its well-developed conduit network system. In contrast to the Burren with its elevated karst and dry cave passages, the Gort Lowlands lie much closer to sea level with the majority of cave passages being phreatic. Many of the explorable cave passages are still part of an active hydrological conduit system and consequently are only accessible to experienced cave divers.

Cave diving in the region started in the early 1980s but it was not until the Dark Shamrock Expeditions of 1991-1994 that the potential of the region was truly explored. These expeditions targeted the western cave system between Gort and Kinvara with up to 3 km of passages successfully being traversed (Kozlowski and Warny, 2009). Since the Dark Shamrock expeditions, the region has continued to be explored with existing traverses being expanded upon and a number of major hydrological linkages being established such as that of Polltoophill to Polldeelin in 2010 (see Figure 3.7).

The region is a popular destination for cave divers due to the sheer length of underwater passages and the technical difficulty involved in exploring them. The cave passages are amongst the longest explored cave systems in Britain and Ireland with possibly one of the longest siphons in Europe (Siggins, 2010). The region also offers some rare technical challenges such as tidal influence (up to 8 km inland), strong currents and poor visibility within the conduits.

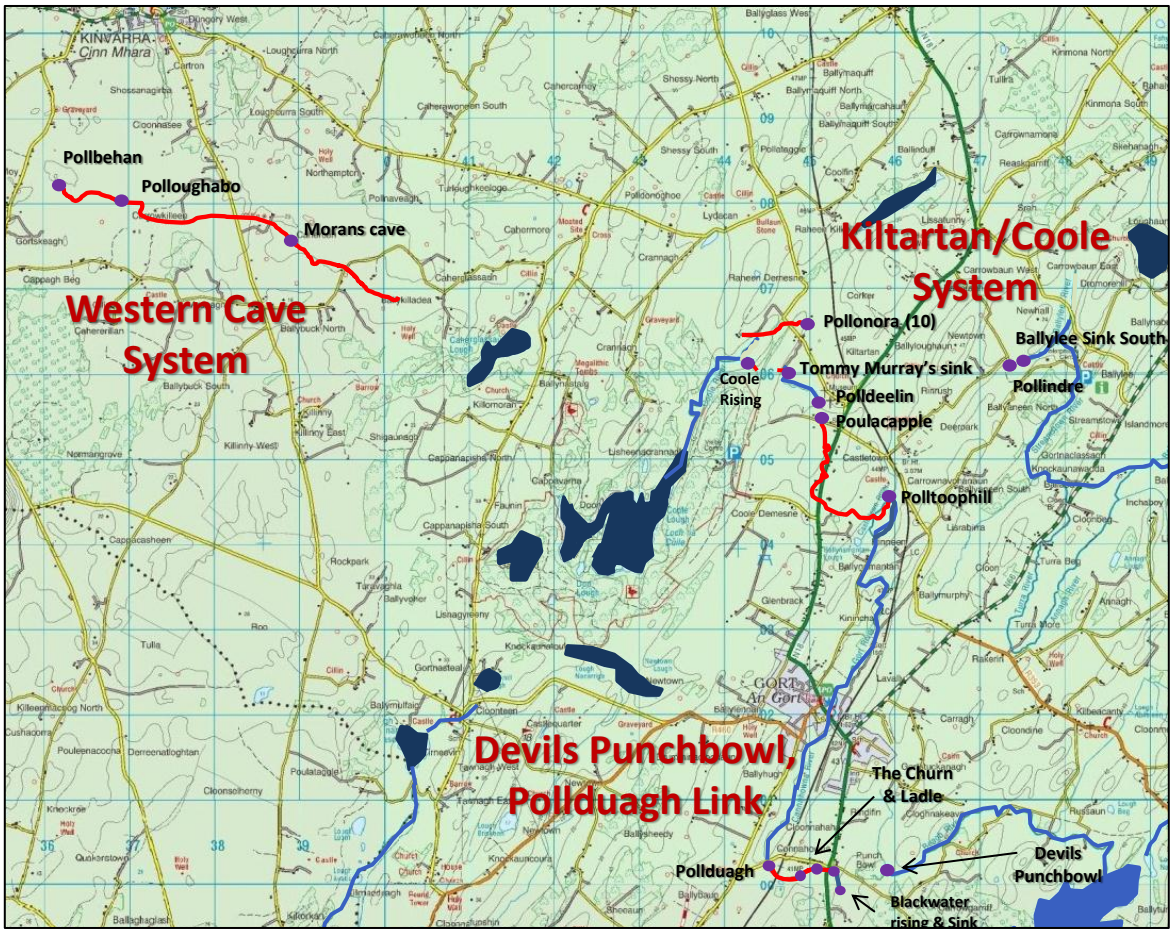

Figure 3.7: Map displaying locations of speleological sites of interest and explored cave systems (red lines).

The explored underground cave network of the Gort Lowlands can be described in terms of three broad systems: the *Devil's-Punchbowl to Pollduagh linkage*, the *Kiltartan/Coole system* and the *Western Cave system*. Each of these systems contain an important water carrying conduit for the Gort Lowland hydrological network and is described in some detail below:

DEVIL'S-PUNCHBOWL TO POLLDUAGH LINKAGE

The Devil's Punchbowl is a major sink characterised by a steep sided gorge cut into a thick layer of boulder clay. As mentioned in Section 3.2 the Beagh River sinks into the Punchbowl, re-emerging a short distance later as the Blackwater River only to sink again and rise at Pollduagh (Cannahowna Cave).

In 1982, the connection between Pollduagh and the Blackwater was the first cave passage to be explored within the Gort Lowlands. Numerous advances were made over the following years with connections to two karst collapse features, the Churn and the Ladle, being established until the complete 1062m Pollduagh-Blackwater traverse was made in 2009. The connection between the Devil's Punchbowl and the Blackwater has not been explored due to the dangerously high flow volumes passing through the passage.

KILTARTAN/COOLE SYSTEM

Kiltartan is the focus point of the three main rivers within the Gort Lowlands. Water from the three rivers arrives at Kiltartan via two large conduits, both emerging at Polldeelin before flowing east towards Coole turlough. Both upstream passages of Polldeelin have been explored to some extent, primarily by the late Polish cave diving enthusiast, Artur Kozlowski. Polltoophill-Polldeelin was successfully connected in 2010 while Polldeelin-Pollindre has yet to be established. The Polltoophill-Polldeelin linkage was first explored during the 1990's but it was not until 2008 that it was intensively dived. After two years, the connection was finally made by diving from both upstream and downstream ends. However no through trip has yet been made. The 2400m passage conveys the entire Gort River towards Kiltartan, dropping to a depth of 62m en route. The other inflow into Polldeelin rising derives from the combined flow of the Owenshree and Ballycahalan Rivers. The passage can be accessed from the downstream end via Polldeelin or a nearby collapse feature known as Pollacapple. By 2009, the passage had been traversed up to 1.5 km reaching a depth of 71m (Kozlowski and Warny, 2009). In 2010, an upstream access point to this passage had been found near Ballylee sink south. This new access point, given the name Pollindre, was explored up to 1 km downstream (towards Polldeelin) reaching a maximum depth of 82 m. Currently the passage, estimated to be over 4 km long (Boycott et al., 2011), remains unconnected. There have

been no recorded explorations upstream of Pollindre cave. It should be noted that near the entrances of Pollindre and Pollacapple caves, conduit constrictions (or boulder-chokes) have been observed. Aside from hindering cave exploration, these constrictions validate the concept of a conduit *throttle* which is a key component of the hydrological pipe-network model as discussed in Chapter 6.

Downstream of Polldeelin, the river travels for a few hundred meters before entering another major sink at the foot of a drumlin known as Tommy Murray's sink. The water re-appears less than 300m downstream at Coole River rising (or Lug Na Cumar). This passage has been explored approximately 150m from both ends but no connection has been reported.

Some other features in the area include the dry Coole cave and the mostly dry Pollonora holes. The Pollonora holes are a series of nine interconnected depressions, lying north of the Coole River, probably formed by collapse into an underlying cave passage (Mullan, 2003). It is quite conceivable that the cave passage was formed by the Gort (Beagh) River, as before the present east-west underground connection was established, the Gort River would have been forced by a drift hill to flow northwards (Williams, 1964). Tracer studies have shown these caves to be linked to Caherglassaun, bypassing Coole turlough entirely (Kozlowski and Warny, 2009). In 2008, a tenth Pollonora hole was discovered and explored up to a distance over 800m and a depth of 52 m. Interestingly, unlike the brown peaty waters of the Slieve Aughtys, the cave consists of clear water until approximately 700m inside the passage when the waters turn peaty suggesting a linkage into the active conduit network. During winter high water levels, the peaty water has been seen at the cave entrance. These findings suggest that the Pollonora holes were once part of an active conduit system fed by the Gort River that did not link with Coole turlough. The system has since become an inactive paleokarst system but still retains a link to the active conduits. This link enables the paleokarst system to become back flooded with Slieve Aughty water during wet periods.

WESTERN CAVE SYSTEM

The Western Cave system encapsulates a number of cave and access points, all of which are associated with the main active conduit between Caherglassaun turlough and the intertidal springs at Kinvara. The system was first explored during the Dark Shamrock expedition which established the linkage between Pollbehan and Pollaloughabo caves. This phreatic passage known as 'the Dark Shamrock Traverse' is heavily influenced by tide and should only be traversed during suitable tidal periods. It is along the passage between Pollbehan and Pollaloughabo that the main flow path changes direction from the ancient outlet at Corranroo towards Kinvara (Drew, 2003). Downstream

of Pollbehan, the explorable route comes to an end when the passage reduces to low wide bedding caves with huge quantities of silt (Mullan, 2003). Upstream of Pollaloughabo, the passage continues 2870m towards Moran's Cave (connected in 2010) with conduits recorded at up to 18m wide. The passage has been explored a further 1.5 km upstream of Moran's cave but no connection has yet been made to the upstream end near Caherglassaun.

3.4 Turloughs

3.4.1 Definition and Origin

Turloughs are a virtually unique feature of the Irish karst landscape. They are ephemeral lakes that typically flood in winter and empty in summer. Their flooding results from a combination of high rainfall and consequently high groundwater levels in topographic depressions in karst. Turloughs are described by the Working Group on Groundwater (Environmental Protection Agency, 2004) as topographic depressions in karst which are intermittently inundated on an annual basis, mainly from groundwater, and which have substrate and/or ecological communities characteristic of wetlands. Turloughs usually flood through underground conduits and springs in autumn when rainfall exceeds evapotranspiration, form a lake for several months in winter and empty underground through swallow holes or estavella in the springtime (Sheehy Skeffington et al., 2006). There may be occasional flooding at other times in response to high rainfall with a turlough filling by up to 9m in 48 hours (Johnston and Peach, 1998). Coxon (1987b) defined what constituted a turlough based on these hydrological criteria:

- The area must flood seasonally, i.e. it must consist of open water to a minimum depth of 0.5m for part of the year, and must be dry (except for any small residual pools occupying a small % of the area) for part of the year.

- There must be evidence of emptying to groundwater, which generally means that there must be no surface water outlet.

The origin of turloughs is still not firmly understood. They were originally considered hollows in glacial till with underlying karst drainage systems (Williams, 1964) but alternatively, Drew (1976) insisted that turloughs in fact lie within bedrock hollows. There are two main theories of how these hollows formed: they are glacial in origin (Williams, 1964) or that they are pre-glacial developing as a result of Tertiary dissolutional processes (Coxon, 1986). Since not enough time has passed since

the last glaciation for a well-developed network of karst depressions to develop, it is likely that the turloughs are pre-glacial (Coxon et al., 2005). Coxon (1986) suggested that while glacial deposition may have an influence on the area and slope of turloughs, solutional rather than glacial processes may be the determining factor in turlough formation. This concept of pre-glacial influence on turlough origin is supported by evidence found in the Pollnahallia townland, Co. Galway, where dating of organic sediments in both shallow and deep depressions to the late Pliocene implied a limestone land surface of Pliocene or pre-Pliocene age (Coxon et al., 2005). The lines of high permeability associated with turloughs may thus represent the re-use of remnants of karst drainage systems created during Tertiary dissolution but partially blocked by glacial drift, rather than post-glacial dissolutional pathways (Naughton, 2011)

Post glaciation, it is thought that most turloughs have not always acted as ephemeral lakes. Coxon (1986) carried out a study of 90 sites and found at least 51% contained calcareous marl or lacustrine chalk indicating that at one point, they were permanent lakes (marl deposition indicates a permanent water body). It is not fully understood why a permanent water body would change to a seasonal lake. However Sheehy Skeffington et al. (2006) suggest a combination of factors: silting up of the depression or increased karstification in postglacial times, resulting in the development of swallow holes and a zone of higher permeability.

A study by Coxon and Coxon (1994b) surveyed the deposits in the turloughs relevant to this research project and concluded that Blackrock and Coole had no marl deposits while Coy, Garryland and Caherglassaun contained significant amounts. This indicates that Blackrock and Coole have always been turloughs. This is unsurprising in the case of Blackrock, but for Coole (which is closer to sea level and normally slow to empty), this indicates that it was at one time not hydraulically connected to Caherglassaun. This finding lines up with the speleological evidence from the Pollonora holes which indicate an old conduit system that used to transmit Slieve Aughty river water directly towards Caherglassaun without passing through Coole. Tracer studies carried out as part of the Gort Flood studies report indicate that a portion of this Coole bypass system is still active with bacteriophage tracer injected at Ballylee reaching Caherglassaun but not Coole (Southern Water Global, 1998).

3.4.2 Distribution

Turloughs are a rare karstic feature as they require a moist climate and low-lying karst limestone which is not commonly found (Drew, 1990). They are often thought to be a uniquely Irish feature

although examples of similar karst features have been reported in Wales, Slovenia, Spain and Canada (Sheehy Skeffington and Scott, 2008, Blackstock et al., 1993). The GSI database records more than 400 turloughs in Ireland although not all have been verified (GSI, 2011). The greatest density of turloughs is in the West of Ireland with highest concentrations in Galway, Clare, Mayo and Roscommon (see Figure 3.8). The largest recorded turlough in Ireland was Turloughmore in Co Galway which was approximately 400 ha in area until it was drained in 1847 (D'Arcy, 1983). The largest surviving turlough is Rahasane in Co. Galway which measures 260ha at maximum inundation (Sheehy Skeffington et al., 2006).

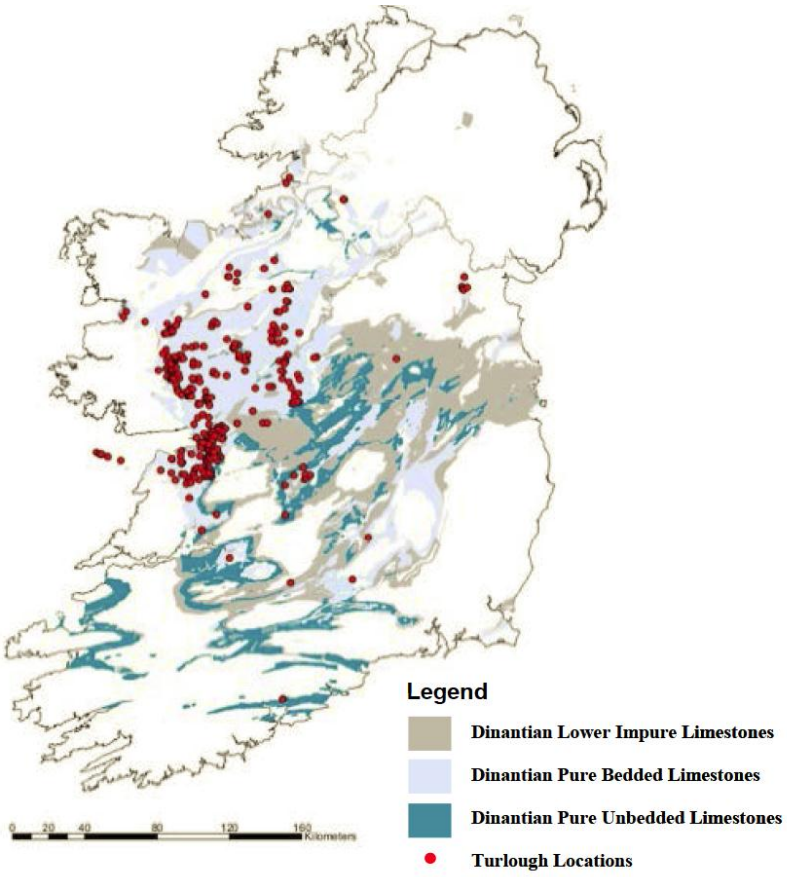

Figure 3.8: Turlough distribution in Ireland (Sheehy Skeffington et al., 2006).

The most comprehensive work on the pattern of turlough distribution was carried out by (Coxon, 1986) who explored the distribution of turloughs based on geology, topography and drift cover. 90 sites of area greater than 10 ha were located using primarily the 1:10560 Ordnance Survey maps of areas underlain by carboniferous limestone. At the time there was no consistent bedrock mapping available for the area in which turloughs are located and so Coxon could only conclude that the majority of turloughs occur on well-bedded, pure grey calcarenite lithologically but not necessarily

stratigraphically similar to the Burren limestone. Since then, work carried out to facilitate the implementation of groundwater body delineation for the Water Framework Directive has reduced the 1200 Irish geological formations to 27 Rock Unit Groups based on hydrogeological criteria (Working Group on Groundwater, 2005) and when these new classifications were applied to Coxon's 90 sites, all but two were found to lie on Rock Unit Group 11: Dinantian pure bedded limestone. This is thought to be due to the greater purity of this rock type rendering it more soluble and susceptible to a greater degree of karstification (Tynan et al., 2007).

3.4.3 Turlough Hydrology

As discussed previously, turloughs are linked hydrologically to groundwater via swallow holes or estavella that typically flood in autumn and empty in spring. Coxon (1986) identified swallow holes in 80 out of the 90 sites studied. Most of which were located around the outskirts of the basin where bedrock is close to ground surface. In some cases, swallow holes occur in the centre of the turlough or are scattered over the base of the turlough in the form of depressions or collapses (Sheehy Skeffington et al., 2006, Coxon, 1987b). In most cases, turloughs are exclusively groundwater fed, but some are fed primarily by surface water streams. For example, Blackrock turlough is fed by the Owenshree River. In dry periods the entire flow of this river sinks into the riverbed several kilometres upstream of the turlough and there will be no turlough input via surface or groundwater. After a rainfall event, the river reaches the turlough and sink straight into the swallow hole ('A' in Figure 3.9). After persistent surface water input the swallow hole starts to backup and fill the turlough ('B' in Figure 3.9). Direct precipitation and surface run-off also contribute to turlough flooding.

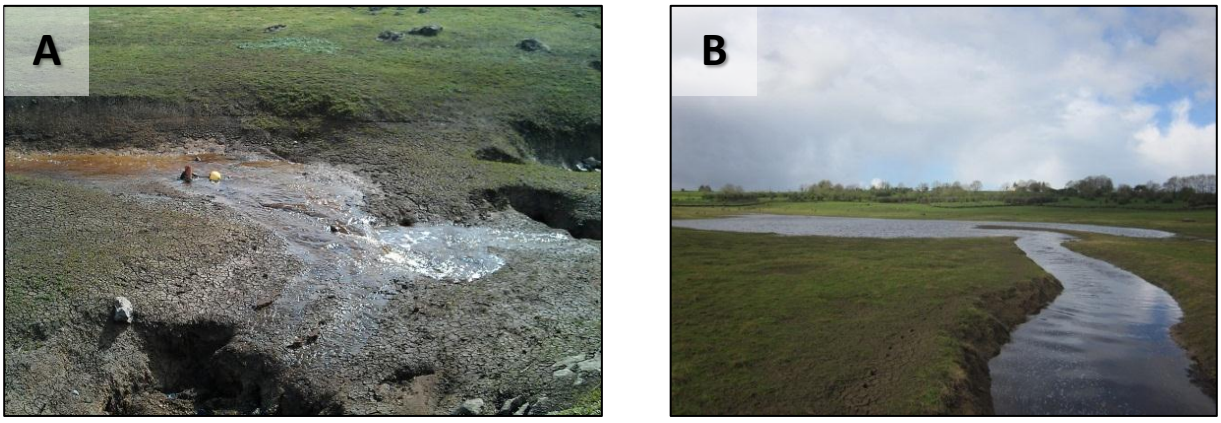

Figure 3.9: Blackrock turlough surface input variations. A: sinking straight into spring, B: turlough starts to back up.

The flooding of a turlough is a function of the climactic regime and of the hydrological functioning of the turlough (Tynan et al., 2007). The west of Ireland, where the majority of turloughs occur, receives high levels of rainfall (approximately 1000 mm per annum) with a seasonal pattern. This pattern of rainfall is strongly emulated in the pattern of flooding within the turloughs which typically flood in autumn and empty in spring. Although, due to differences in the hydrological functioning of individual turloughs, flooding patterns of turloughs within the same climactic environment can be vastly different. These differences in turlough flooding patterns reflect the nature of the karst aquifer beneath the turloughs and the resulting flow system. A *shallow epikarst flow system* has little storage and supports low volumes of flow. As a result a turlough on this system reacts slowly, showing long duration flood events with an extended recession limb within each hydrological year. This is due to the low storage capacity of the receiving system which impedes outflow. A *conduit flow system* with its discrete flow and interconnected pathways has high storage and supports large volumes of flow. This large storage capacity allows for rapid discharge from turloughs once the hydraulic head has dropped in response to dropping water levels in the conduit system (Tynan et al., 2007). The Gort Lowlands chain of turloughs lies within a conduit type flow system and as a result, the turloughs react rapidly to rainfall and transfer large quantities of water. This is reflected in a study by Naughton et al. (2012) in which 21 turloughs were selected which represented a broad hydrological spectrum. Of these 21 turloughs, the 4 turloughs with highest flood depths were all part of the Gort Lowlands system. The highest depth recorded was by Blackrock which reached 15.4m within the monitoring period. In fact changes in water level at Blackrock have been observed at up to 9m in 48 hour (Johnston and Peach, 1998). These values are dramatically higher than the average turlough flood depth of 0.5 - 6m with median 1.5m (Coxon, 1987b).

One of the most important factors in determining how a turlough operates is its *hydraulic functioning*. This concept is a key aspect of a turloughs hydrological and hydrochemical behaviour and is discussed throughout this thesis. The two conceptual models for the hydraulic functioning of turloughs, as described by Naughton et al. (2012) are the *flow-through system* and the *surcharge tank*. In the flow-through model, both inflow and outflow occur simultaneously and largely independently within the turlough basin. Groundwater flow through the turlough would be constant resulting in lower residence time than the surcharged tank model. Flow-through systems can be further broken into *diffuse flow through* and *river flow-through* systems (as discussed later in Chapter 7). In the surcharged tank model, the turlough can be viewed as a pressure release point along an underground pipe network. It provides overflow storage for the excess groundwater that cannot be accommodated due to insufficient capacity. In this instance, there is no outflow from the

turlough during filling periods. These conceptualisations are presented graphically in Figure 3.10 and are discussed further in chapter 7. The Gort Lowlands system appears to support the surcharged tank model (as well as the *river flow-through* model) and has been successfully modelled predominantly as such (Gill et al., 2013a).

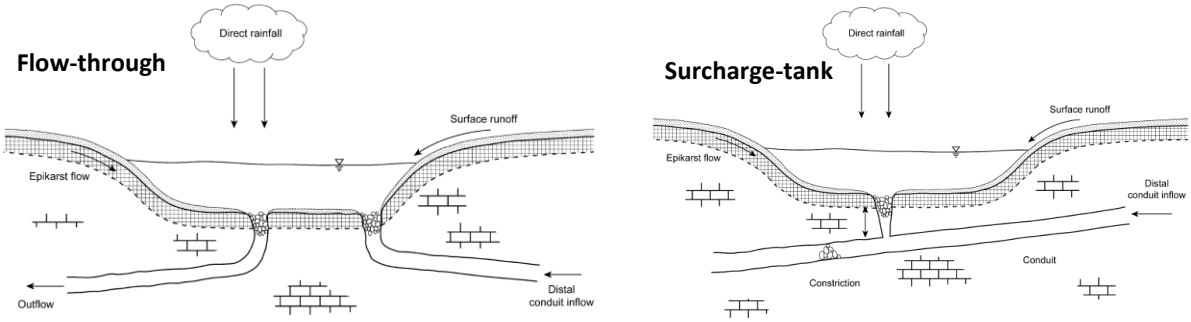

Figure 3.10: Flow-through and surcharge tank conceptualisations of turloughs (Naughton, 2011).

Hydrologically, turloughs are often compared to poljes as both are periodically flooded karst basins displaying interior drainage and lacustrine sediment deposition. However, in terms of geomorphology, the two karst features vary considerably (Coxon, 1986). Poljes are a more obvious karstic feature than turloughs as they are larger and show a distinct topographic boundary between area of inundation and the sides of the polje whereas turloughs tend to be more gently sloping. Turloughs are influenced by glaciation and solutional processes whereas poljes are more clearly influenced by tectonic movement. As such, turloughs are only found in areas of glacial deposits while poljes exist in a wide range of climactic zones, including the tropics (Gunn, 2006). Possibly the most well researched turlough-polje comparison is that of the Slovenian poljes (Coxon, 1986, Sheehy Skeffington and Scott, 2008). These studies have concluded the larger poljes are considerably different to turloughs. However the smaller temporary and seasonally flooded lakes found in the Pivka valley can be likened to turloughs (although they differ in terms of flooding duration, land use and plant communities) (Cunha Pereira, 2011, Sheehy Skeffington and Scott, 2008).

3.4.4 Turlough Ecology

Turloughs are unique wetland ecosystems that provide a habitat for many protected flora and fauna species of national and international importance. Wetlands such as these are increasingly rare across Europe due to land drainage and intensification of land use (Sheehy Skeffington et al., 2006). As a result, turloughs have been designated a Priority Habitat in Annex 1 of the EU Habitats

Directive (92/43/EEC) (EEC, 1992). A proportion of these turloughs have also been designated as Special Areas of Conservation (SACs). Additionally, the Water Framework Directive (WFD) (EC, 2000) designates turloughs as Groundwater Dependant Terrestrial Ecosystems (GWDTE). Both of these EU directives require monitoring and management of these habitats to ensure a favourable conservation and groundwater status is achieved. The Water Framework Directive in particular requires a good understanding of the hydrological linkage and interactions between the turlough wetland, its ecological functioning and the connected groundwater body (Kimberley and Coxon, 2013, Naughton et al., 2012).

The largest turlough-ecology study ever undertaken was that of the *Turlough Conservation Project*. This study was carried out by a multidisciplinary project team from Trinity College Dublin and was commissioned by the National Parks and Wildlife Service (NPWS). By investigating several aspects of turlough ecology such as aquatic invertebrates, hydrochemistry, vegetation, hydrology, soils and land-use, the study aimed to provide a robust scientific foundation for assessing the conservation status of turloughs. The project included four PhD projects and one Post-Doctoral sub-project, each project dealing with a particular aspect of turlough hydro-ecology. One of the primary themes of this project was the use of 'hydrological indicators'. These 'indicators' were a set of hydrological factors which could be related to ecological parameters within the turloughs (e.g. vegetation distribution, soil nutrients, trophic status etc.). The indicators chosen were:

- **Flood duration:** The duration of turlough inundation, typically represented using flood-duration curves (described in Section 6.4.4).

- **Hydroperiod:** A single variable used to characterise the flooding duration for each turlough, its interpretation varied depending on which ecological dataset it was applied to. Generally, a turlough with a short hydroperiod showed relatively quick (flashy) flooding and emptying behaviour (e.g. Blackrock).

- **Flood Frequency:** The number of times a given water level was equalled or exceeded over a given interval.

Numerous journal articles, reports and theses have been published as part of this project e.g. Kimberley and Coxon (2013), Naughton et al. (2012), Cunha Pereira et al. (2011), Porst et al. (2012).

Results from these publications are discussed throughout this chapter, and this thesis. The final report from the project is yet to be published (National Parks and Wildlife, in review).

3.4.4.1 Flora and Fauna

FLORA

Due to the unpredictable nature of turlough flooding, only a relatively low number of species have adapted to grow within them. A number of species grow from the edge of the turlough to near its base while other are less tolerant to variable flooding patterns and are restricted to definite zones (Goodwillie, 2003). Rare wetland species that grow in turloughs include the fen violet *Viola persicifolia* and the shrubby cinquefoil *Potentilla fruticosa* which are common on some upper margins and the annual northern yellowcress *Rorippa islandica* which is found on the bare mud of late drying turloughs (Sheehy Skeffington et al., 2006). As far as is known, no plant species are restricted to Irish turloughs but some species are more common in turloughs than elsewhere (Goodwillie, 2003). The species can be separated into two groups: amphibious species that can withstand flooding in situ and species that are able to colonise the land quickly after the flood waters have retreated.

A number of factors affect the distribution of plant species across a turlough. These factors include flood regime, nutrients and soil, grazing and other threats. The effect of flood regime (particularly flood duration rather than flood depth) has historically received the most attention with studies dating back to the 1930s. The flooding affects plants by interrupting the gaseous exchange and thus forcing the plants to develop adaptations needed to survive the conditions. Plants that have adapted in this way are termed wetland species. Adaptations include morphological/physiological changes and timing of important life cycle events (Tynan et al., 2007, Lynn and Waldren, 2001). Praeger (1932) was among the first to describe the gradual change from dry species on the edge of a turlough to wetland species in the centre. Most turloughs display this pattern with plant communities encircling the basin in roughly concentric zones according to duration of inundation. Typically, aquatic or semi-aquatic species such as *Polygonum amphibium* and *Mentha aquatic* extend away from the sink hole gradually giving way to grassland where *Potentilla anserina* and sedges such as *Carex panacea* can be found (Reynolds, 1996). At the upper limits of a turlough, shrubs such as *Frangula alnu*s and *Potentilla fruticosa* may occur, otherwise vegetation will closely resemble the adjacent grassland pasture as it is rarely flooded for long periods (Goodwillie, 1992). Some turloughs such as Coole and Garryland are surrounded by woodland. Woody plants such as *Rhamus catahritca* and *Frangula alnus* surround the turlough but die out closer to the upper limits of

the turlough. In years of high flood levels, summer growth may be delayed due to the susceptibility of tree roots to oxygen depletion.

A good indicator of turlough flood regime is the black moss *Cinclidotus fontinaloides* which gathers on rocks and surrounding shrubs. The moss itself is an indicator of maximum water level but, more usefully, the competition between *Cinclidotus* and more vigorous aquatic mosses such as *Fontinalis antopyretica* can reveal details regarding flood duration. Most turloughs contain an upper zone dominated by *Cinclidotus* and a lower zone dominated by *Fontinalis*. However when *Cinclidotus* is found near the base of the turlough, it indicates short flood duration and frequent filling and emptying (Sheehy Skeffington et al., 2006). This indicator was used by Coxon (1987b) in her study of 90 turloughs to deduce maximum water depths and flood durations (35% of the 90 sites contained *Cinclidotus* at the base of the turlough).

Tynan et al. (2007) carried out a study of turloughs using hydrological indicators (in the same fashion as the NPWS Turlough Conservation Project). The indicators were related to ecological parameters such as vegetation distribution and wetness index. Dominant vegetation types (e.g. grass, sedge or aquatic dominated) within turloughs were broken into six categories in order of decreasing wetness and compared to turlough recession constant. Aside from two anomalous turloughs (Termon and Caherglassaun), a significant relationship was found ($R^2 = 0.8$) whereby as the recession constant decreases (turlough rate of emptying decreases), the vegetation tends towards being dominated by wet plant species. The two anomalous turloughs showed wetter vegetation than expected and it was concluded that the reason for this was the presence of marl which impeded drainage and held onto water later into the dry season than other substrates (Tynan et al., 2007).

FAUNA

Turloughs are home to a variety of invertebrate and vertebrate species whose development and distribution depends on the same factors that affect vegetation. These factors include depth, temperature and flooding regime. Due to the irregularity of flooding patterns in turloughs, aquatic invertebrate communities are unpredictable and sparse in many of the oligotrophic turlough sites. These aquatic fauna are also highly spatially variable in terms of species diversity and abundance (Sheehy Skeffington et al., 2006). Porst et al. (2012) describes turloughs as 'disturbed habitats' with flooding characterised by pronounced irregularities resulting in the adaptation of aquatic species to the comparatively short turlough wet seasons. The temporal pattern of these communities follow the turlough flooding patterns with intermittent shocks to the system caused by rapid changes in

water level. Despite these adversities, many aquatic species regularly occur in turloughs. Groups such as flatworms, gastropod molluscs, mayfly nymphs and beetles are common. These species are not unique to turloughs but have adapted well to the temporary nature of turloughs (Reynolds, 1982). Terrestrial invertebrate species characteristic of turloughs include ground beetles, flies and butterflies. Some of these species are very rare such as the ground beetles *Platynus livens*, *Badister meridionalis* and *Badister peltatus* which are found exclusively in Ireland in the Coole-Garryland complex. Some species of fly (Diptera) are also exclusive to the Coole-Garryland complex although it is hard to say whether this is due to the turlough or surrounding woodland (Sheehy Skeffington et al., 2006).

Fish are uncommon in turloughs as they are long-lived fully aquatic organisms. However, occasionally they may be washed into a turlough from surface waters (Reynolds and Marnell, 1999). Three-spined sticklebacks *Gasterosteus aculeatus* and small pike *Esox lucius* have been recorded (Reynolds, 1997) and have also been observed during fieldwork for this thesis in Coy and Garryland turloughs. Amphibians are more common in turloughs. Frogs and newts are often seen with newts taking advantage of fish-free ponds for breeding and being the top predators during the early part of the year.

Turloughs offer particularly good feeding grounds for wildfowl as they are shallow and wide with gently sloping margins and a basin floor covered in vegetation (Madden and Heery, 1997). Moderately flooded turloughs provide feeding and roosting opportunities with both water and exposed marginal grassland attracting bird populations. As turlough water levels increase in winter, the water covers most of the marginal grassland and curtails feeding of species such as dabbling ducks and waders. At which point the wildfowl will move off towards a new site (Southern Water Global, 1998). Many turloughs are designated special protection areas for birds (SPAs) under the EU birds directive (EU, 1979).

3.4.4.2 Turlough Trophic Status

Tynan et al. (2007) presented a classification of turloughs based on the relationship between karstic flow systems (as discussed previously in Section 3.4.3) and turlough trophic status. The measurement of trophic status was based on Ellenberg N indicator values for plants, the N value relating to the occurrence of plants which are indicative of the general fertility of the site. Turloughs were classified as having either high medium or low trophic sensitivity. It should be noted however that the trophic range used to describe turloughs in this study is distorted compared to other

ecosystems trophic ranges (a relatively eutrophic turlough would be classed as mesotrophic in a different eco-system). A significant relationship between trophic status and flow system was found with turloughs of low trophic status (ultra-oligotrophic) being associated with shallow epikarst flow systems and turloughs of high trophic status (relatively eutrophic) being associated with conduit type flow systems. Tynan et al. (2007) concluded that this relationship was due to the size of storage system and ability to transmit water associated with a given karstic flow system. A conduit type flow system has high volumes of water potentially moving at high velocities which results in high cumulative mass loading of nutrients to the turlough, resulting in a relatively high trophic status. Alternatively, shallow epikarst systems have low storage and low flow volumes. Turloughs in these systems have small catchment areas which provide relatively little opportunity to accumulate nutrient load resulting in a low trophic status. This study classified all the Gort lowland network of turloughs (Blackrock, Coy, Coole, Garryland and Caherglassaun) to be relatively eutrophic. Tynan et al. (2007) went on to use this relationship to classify five main types of 'natural' turloughs and a sixth anthropogenically impacted type:

- *Type 1*: Conduit/conduit type flow system turloughs, with relatively high trophic status.
- *Type 2*: Shallow epikarst type flow system turloughs, with low trophic status.
- *Type 3*: Combined conduit/conduit type, shallow epikarst type flow system turloughs, with relatively high trophic status.
- *Type 4*: Turloughs with riverine input, with high trophic status.
- *Type 5*: Turloughs receiving distributed flow from certain types of sediment.
- *Type 6*: Turloughs with anthropogenic inputs.

Another study by Cunha Pereira et al. (2010) compared the trophic status of turloughs to that of permanent lakes in Ireland. Trophic status was calculated by applying the OECD (1982) lake trophic classification to turloughs which used mean values of Total Phosphorus (TP) and Chlorophyll *a* (Chl *a*) to determine trophic status. The study determined that of the 22 turloughs under investigation, 2 were eutrophic, 8 mesotrophic, 4 oligotrophic and 8 were ambiguous (mean TP values indicated different trophic statuses to mean Chl *a* values). The Gort Lowlands network of turloughs were found to be eutrophic or mesotrophic. Cunha Pereira's study concluded that, when full, turloughs are productive water bodies with levels of nutrients directly comparable to those of permanent lakes. Cunha Pereira also suggests that phosphorus (P) concentrations rather than nitrogen (N) concentrations determine the trophic status of most turloughs. However, again, the Gort lowland turlough system proved to be an exception. This is due to the large contribution of

allogenic (non-limestone) waters to these turloughs compared to the limestone-derived waters of other turloughs, giving them higher soluble reactive phosphorus (SRP) values.

3.4.4.3 Turlough Threats and Conservation

As is the case with most karstic features, turloughs are sensitive to changes in catchment dynamics. Threats can have sources within the basin itself and/or from the wider catchment. Turloughs fed by conduit type flow systems are susceptible to threats from great distances whereas epikarst systems are more locally based. The most significant threats to turloughs are those of drainage, nutrient input and grazing (Sheehy Skeffington et al., 2006). Historically, the most significant threat to turloughs has been from drainage but more recently, land use has had an increasing role to play.

DRAINAGE

Drainage of wetlands has been a feature of Ireland since the famine. Up to 40,000 people were employed following the drainage act of 1842 which resulted in the rapid drainage of 100,000 ha of land (Reynolds, 1996, Baldock, 1984). During this period, many of the great turloughs of East Galway were eliminated including Turloughmore (Section 3.4.2). Large-scale drainage projects such as this have now ceased but have left a permanent impact with the loss of at least 50% of flooded turlough area (Goodwillie, 2001). Coxon (1986) estimated that one third of turloughs over 10 hectares have been irreversibly damaged by drainage and due to the complex nature of karst hydrology, restoration is unlikely. Changes in flood regime due to drainage causes changes to the composition and distribution of turlough biological communities particularly impacting the rarer communities (Sheehy Skeffington et al., 2006). Decreasing flow volumes entering a turlough may also increase the loading of pollutants/nutrients into the system due to decreased dilution and dispersion (Tynan et al., 2007). Similarly to drainage, climate change has an impact on the flood regime of turloughs. Climate change has led to more intense rainfall events and increased winter rainfall in Western Ireland (Environmental Protection Agency, 2008) which floods the turloughs in excess of their natural levels.

NUTRIENT INPUT

As mentioned previously, turloughs are generally phosphate limited systems with some exceptions (such as the Gort Lowlands system). Any changes in nutrient input affects the composition and productivity of flora and fauna species and may change the overall trophic status of the turlough (Tynan et al., 2007). The primary source of nutrients into a turlough system is thought to be catchment water (Sheehy Skeffington et al., 2006). The quality of this water is dependent on land

use practices within the catchment. Practices such as agricultural fertiliser spreading, farmyard run-off, forestry and septic tank discharges influence the nutrient input and can have a detrimental effect on a turlough. The effects caused by nutrient input and land-use are dealt with further in Sections 7.1.2 and 7.3.

GRAZING

During summer months, turloughs are mostly empty which facilitates the use of the land for marginal grazing. Fields often radiate from a central commonage area, resulting in a mosaic of land parcels under different grazing regimes (Sheehy Skeffington and Gormally, 2007). The grazing of turloughs by cattle, sheep or horses (Figure 3.11) is a major ecological factor which limits shrub growth, removes more palatable plant species and most importantly, it is a source of nutrients via manure. The National Parks and Wildlife Service recommends a stocking density of 1.5 livestock units per hectare ($LUha^{-1}$) although agricultural practices seem to indicate an upper limit of 1 $LUha^{-1}$. Large variations exist in times and rates of stocking between turloughs and also within individual turloughs (Ní Bhriain et al., 2003).

Figure 3.11: Horses grazing at Coy turlough.

A study by Kimberley et al. (2012) on the influence of flood duration on soil type and grazing management found that turloughs with mineral soils are more associated with shorter flood durations and higher grazing intensities. These findings indicate how turlough management practices are influenced by the soil properties. However, even with this information, it is still

uncertain whether the till subsoils are the 'cause' or a 'result' of relatively shorter turlough flood durations (Kimberley et al., 2012, Coxon, 1987b). Kimberly also found that soil TP concentrations were significantly higher under a grazed regime than an ungrazed regime, whereas the opposite was true for TN. This indicates that grazing animals are a source of TP to turloughs but a sink of TN.

Grazing is an important aspect of turlough biodiversity and as turloughs are considered marginal land, the cessation of grazing would likely do more harm than good (Sheehy Skeffington et al., 2006). Certain patterns and intensities of grazing have a positive impact on plant species and diversity and as such, these practices should be well managed to preserve turlough biodiversity. A worrying trend is that of high intensity agriculture which is leading to land abandonment at some turloughs leaving many turlough land parcels ungrazed (Visser et al., 2007).

3.5 Previous Hydrological Studies in the Gort Lowlands

The large-scale and recurring floods that originate from turloughs are the primary form of groundwater flooding in Ireland. The Gort lowland system has historically been prone to severe flooding events on a relatively infrequent basis (approximately 1 in 30 years). However at the start of the 1990's, four major flood events caused by exceptional rainfall occurred within six years (1989-1995). The damage caused by these floods combined with ecological importance of the area prompted the commissioning of an extensive investigation. This investigation, known as the Gort Flood Studies, was carried out by *Southern Water Global* and *Jennings O'Donovan & Partners* and at the time (1998), was considered the largest regional interdisciplinary investigation of a karstic environment carried out worldwide (Southern Water Global, 1998). The study included drilling, surface geophysics, tracer studies, geological and topographic modelling and the creation of a hydrologic model which was then used to model various flood alleviation scheme options.

In November 2009, record amounts of rainfall fell in Western Ireland causing another major flood event (see Figure 3.12, further images can be seen in Appendix B). A monthly total of 329.4 mm of rain fell, representing 286% of average November rainfall for the period between 1961-1990 and a peak daily rainfall of 60.8 mm was recorded at NUI Galway on the 17th Nov (Jennings O'Donovan & Partners, 2011). Walsh (2010) estimated the 25-day return period for the rainfall quantities over November 2009 to be greater than 500 years. This major flooding event prompted further investigations and a review of the recommendations provided by the Gort Flood Studies report.

This review was broken into 3 separate reports which were published in winter 2010/2011. Both the original Gort Flood Studies report and the review report are discussed in more detail below.

Figure 3.12: Flooding at Kiltartan, November 2009 (Jennings O'Donovan & Partners, 2011).

3.5.1 Gort Flood Studies

The objectives of the Gort Flood Studies were to define the current flooding problem and hydrological processes, assess the effects of climate change, define the flood hazard and propose engineering solutions while keeping in mind the environmental significance of the region. The main elements of the study included field-work, modelling and engineering solutions.

3.5.1.1 Field-work

TRACING STUDIES

As mentioned previously in Section 2.3.4, a detailed tracing study was carried out to establish point to point flow routes within the study area. The study was likely the most detailed tracing study ever carried out in Ireland at the time. A variety of tracers were used such as fluorescent dyes (rhodamine $_{WT}$, leucophore and fluorescein), salt and bacteriophages. Eighteen tracer experiments were carried out with sampling from 38 detection locations, the results of these tests are summarised in Figure 2.8. The tracer study helped to identify major water carrying conduits and revealed how groundwater flow rates are very rapid and increase with increasing stage. Mean flow

rates in the vicinity of Coole turlough was calculated to be around 4-5 m^3/s but up to 15 m^3/s in winter with ranging velocities from 60 to 1000 m/h. The bacteriophage tracers (types T7, Psf2, H6/1, H40/1 and H4/4) were used successfully in an attempt to determine the existence of a deep karst layer (>40 mbgl) near Kinvara. The study in fact found three layers of karst, a shallow layer (15-25 mbgl), an intermediate (40-50 mbgl) and a deep layer (70-80 mbgl). The shallower two layers appeared to transmit rapid throughflow waters at high groundwater levels whereas the deeper karst layer appeared to be paleo-karst containing old groundwater (Smyth, 1996).

MONITORING NETWORK

A network of river flow gauges, rain gauges and turlough depth gauges were installed across the study area. Spot gauging was carried out on various water courses in an effort to develop rating curves in order to establish losses from the Owenshree River and flows on the Coole River. Attempts were also made to quantify the flow at the Kinvara Springs. However this proved unsuccessful due to density effects of saline and fresh water and also the short time available between high tides. This monitoring network was first installed in 1996 and is still in place. It plays an important role for providing data for this thesis.

BOREHOLE WATER LEVEL MONITORING

Twenty three newly drilled boreholes were monitored within the catchment. These wells along with twenty seven domestic wells were used to establish regional flow direction and gradients. With these measurements, a groundwater contour map was drawn for March and April 1997 (Figure 3.13).These maps indicated high heads to the east, north and south surrounding a relatively lower central area which extends from Coy turlough through Ballylee towards Coole turlough, then widens to encompass the Low Burren, some limestone pavement areas and Kinvara. This pattern was found to remain the same for high and low water levels.

A groundwater fluctuation map was also created which highlighted areas with rapid response to recharge events. These rapid responses imply low storage and high transmissivity Areas with fluctuation greater than 3m were considered to transmit water from the three large rivers draining the Slieve Aughty Mountains. This pattern echoed the findings of the other studies and maps. However an additional northern flow route was also identified flowing from Castle-Daly towards Kinvara (Figure 3.6) which was confirmed with tracing studies. Areas of tidal influence were also identified from this study (a version of this groundwater fluctuation map can be seen in Chapter 5, Figure 5.23).

It should be noted that water level maps such as these are highly approximate and should only be used for an overview. These maps ignore the highly heterogeneous hydrological environment and thus groundwater flow paths cannot be determined reliably.

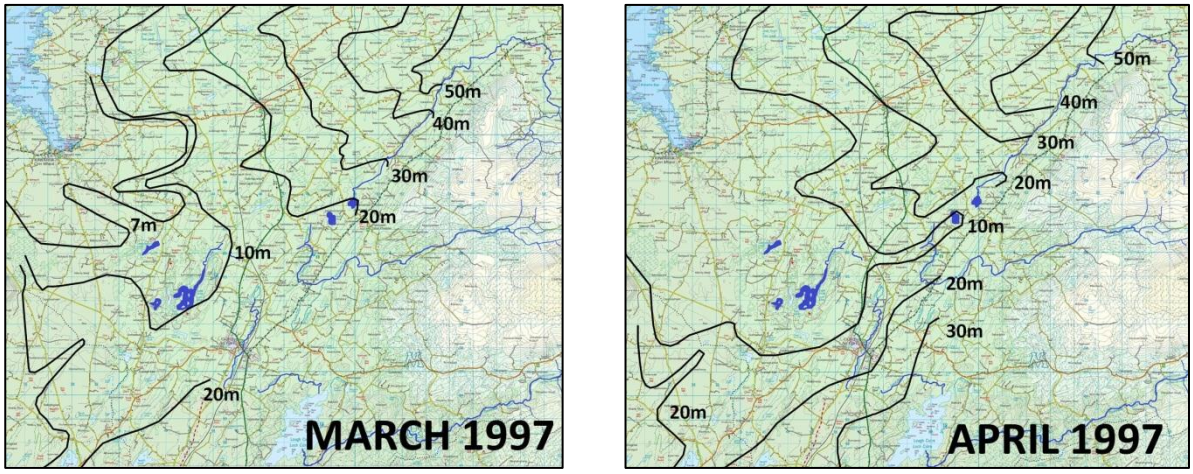

Figure 3.13: Groundwater level contour maps showing the hydraulic gradient of the catchment during March and April 1997 (based on the maps of Southern Water Global (1998))

HYDROCHEMISTRY

Extensive sampling and hydrochemistry was carried out as part of the study. Water was divided into seven different 'types' based on alkalinity and iron concentrations. Recharge from rivers draining the Slieve Aughtys was found to have low alkalinity and high iron concentration whereas water from other catchments (such as the Cloonteen catchment to the south) was found to have higher alkalinity and lower iron concentrations. Using this principle, the contribution of water from other catchments could be identified. The seven types of water are displayed in Table 3.1.

Hydrochemical analysis of Coole, Garryland, Caherglassaun and Hawkhill (turlough within Cloonteen catchment to the south) found rapid changes in concentrations with time, particularly alkalinity and iron. When these chemistries were compared with turlough water levels, it was found that flow direction of water between the turloughs can reverse. Typically, water levels in the Gort Lowlands network of turloughs rise faster than in Hawkhill, and Slieve Aughty waters dominate their hydrochemistry. When the turloughs empty, Hawkhill turlough drops slower than the others and thus flows into them resulting in rapidly elevated alkalinities and iron concentrations.

Table 3.1: Water types identified in the Study Area (Southern Water Global, 1998).

Type	Alkalinity (mg/l $CaCO_3$)	Iron (mg/l)	Other	Description
Ia	< 75	> 0.3		• Surface water or rapid conduit flow
Ib	100-150	< 0.03		• Direct recharge having undergone rapid surface water/groundwater flow. • Restricted to the rapid epikarstic flows of the Cloonteen catchment
Ic	75-125	> 0.3		• Indirect River recharge • e.g. Owenshree River, Blackrock and Coy
Id	> 150	< 0.03	Cl < 30 mg/l	• Direct recharge, slow moving groundwater
II	50-150	0.1-0.3		• Mixtures of type I waters, either mixes of rapid groundwater throughflow (e.g. Garryland) or of direct and indirect recharge
III	> 150		Cl > 30 mg/l	• Waters affected by the marine environment (saline intrusion)
C	> 155		NO_3 > 8 mg/l-NO_3	• Sample contaminated by anthropogenic pollution

3.5.1.2 Hydraulic Model

A key objective of the Gort Flood Studies was the building of a numerical model. This model, constructed with the aid of collected field data, could be used test the hypotheses of system response and evaluate management options. Due to the highly heterogeneous nature of the Gort Lowlands catchment, it was decided that an equivalent porous media model would not be suitable. The best approach would be to use a network model that could adequately simulate confined groundwater conditions. Such a model is provided by the sewer network analysis software *Hydroworks* (Wallingford Software).

This model uses a network of links to represent conduits and nodes which can represent storage (or turloughs). These links and nodes are connected together to model the entire catchment. The individual links were based on a hydraulic resistance derived from real hydrological response from field work data. In this manner, a single link could represent a single conduit or an active fracture system operating under a pressure head (Johnston and Peach, 1999). The model input came from net rainfall and surface water inflows from the three rivers draining the Slieve Aughty Mountains. The outlet was controlled by a cyclical tidal head rather than a discharge as the intertidal nature of the Kinvara springs made discharge measurement impractical.

The conduit network model allowed for the prediction of turlough behaviour based on known surface water inputs into the system but an additional model was required to predict these surface water inputs based on known rainfall data. For this purpose, the IHACRES (Institute of Hydrology) rainfall-runoff model was chosen which provided a continuous simulation of runoff and thus a suitable discrete input into the conduit network model at the three stream gauging points. Rainfall data from five installed rain gauges was reduced to areal rainfall using Thiessen polygons and combined with the discharge data from the gauging stations.

The completed model provided better than hoped for accuracy when compared to the measured elevations from the 1994/1995 season. Some inaccuracies remained such as:

- Insufficient groundwater/conduit storage, particularly in the Blackrock/Coy area.
- Poor river flow accuracy at high flow levels due to measurement difficulty.
- Poor definition of the Cloonteen catchment.
- Poor turlough water level recession curve accuracy, particularly for Blackrock and Coy turlough.
- Poor modelling of antecedent conditions in *Hydroworks*.

Despite these issues, the overall performance of the model was deemed acceptable because of the high level of accuracy in the central area Coole, through which the majority of flows pass.

The completed model was then used to determine the hydrological effects of various proposed engineering solutions. The proposals included: control structures (embankment dams with concrete spillways) to control flooding, diversion channels to divert excess flood water and drain it into a neighbouring catchment and river channel clearances. The most significant proposal was the construction of a major overland channel transmitting water from Coole to Kinvara via Caherglassaun. All proposals but one (a drainage channel for Termon Lough) were deemed economically unjustifiable and so no work was carried out other than some road protection works and the abandonment of the worst affected properties.

3.5.2 Review of Gort Flood Studies and Proposed Engineering Works

In July 2010, Jennings O'Donovan & Partners were appointed by the OPW to review the recommendations of the Gort Flood Studies Report. This review was divided into three topics each

with an individual publication. Firstly, a report on Kiltiernan and Ballinderreen maintenance works. Secondly, a report on Mannin Cross, Kilchreest and Termon flood alleviation schemes, and thirdly, a report discussing various engineering proposals (see Figure 3.14 for locations of proposed engineering works).

3.5.2.1 Kiltiernan and Ballinderreen

The first publication, (Jennings O'Donovan & Partners, 2010a) is an assessment of the existing Kiltiernan/Ballinderreen Flood relief scheme. During emergency flood relief works in 1995, two emergency drainage channels were privately constructed. However they have since fallen into disrepair. This report assesses the conditions of these channels and proposes a range of maintenance works with a view to restoring natural flow conditions. These drainage schemes do not affect the Gort Lowlands active conduit network.

3.5.2.2 Mannin Cross, Kilchreest and Termon

The second publication, (Jennings O'Donovan & Partners, 2010b), deals with the recommendations and conclusions of the Mannin Cross, Kilchreest and Termon Flood alleviation scheme as refined under the Design Review Reports carried out in 2000 and 2003. This report details two separate flood alleviation schemes: a proposal to upgrade drainage channels for Termon north and south turloughs and a joint flood alleviation scheme for Mannin Cross and Kilchreest (see Figure 3.14). The latter scheme is of relevance to the Gort Lowlands active conduit system.

The Mannin Cross and Kilchreest works describe two sub-schemes. Firstly, the construction of a flood alleviation channel to transmit water from Mannin Cross to the Dunkellin River via the Aggard stream. Secondly and of greater relevance to the Gort Lowlands conduit network, the report proposes the construction of a river diversion near Kilchreest which would divert excess flood water from the Owenshree river towards the Dunkellin river via the Aggard stream. An open channel (of up to 10m in width at certain locations) was deemed financially and technically viable although the potential impacts to the Dunkellin River system were not assessed. In addition to the impact on the Dunkellin River, the mixing of different catchment water could have harmful ecological impacts on Rahasane turlough (SAC) which is located in the Dunkellin catchment. The report does not mention the potential impacts of this scheme on Blackrock and Coy turloughs (SACs) which are directly fed from the Owenshree River. Ultimately, the report proposes that the potential impacts mentioned above be assessed prior to any construction.

3.5.2.3 Engineering Proposals

The final and most detailed report describes the engineering proposals for reinstatement of existing culverts, the provision of new culverts and the feasibility of an overland channel from Coole to Kinvara (Jennings O'Donovan & Partners, 2011).

Firstly the report details the repair of existing culverts along the N18 Gort-Galway road. For example, a culvert at Kiltartan became blocked during the 2009 floods, emergency works were carried out to unblock it but, in the process, caused some damage reducing the flow capacity from 30 to 20 m^3/s. This culvert is to be restored to its maximum capacity along with similar culverts along the N18. In addition to this, new culverts are to be installed on the main Kiltartan-Kinvara route.

The original Gort Flood Studies Report proposed the construction of an overland flood channel between Coole and Kinvara. However, the cost of such a scheme was deemed prohibitive and consequently the scheme was not developed any further. Under the 2011 review report, the route was refined based on site surveys, aerial photographs and information from the Irish Farmers Association Flood Committee. The route is split into two sections: Coole to Caherglassaun and Caherglassaun to Kinvara (see Figure 3.14). The Coole-Caherglassaun section would be 580m long, 3m wide at the base and up to 1.25m deep. The Caherglassaun-Kinvara section would involve a 5150m long channel, 3m wide at the base and up to 7.5m deep. While the first channel was deemed acceptable in scale, the second channel was judged to be excessive both financially and in terms of environmental impact. Consequently, a smaller-scale alternative to this channel was considered which involved identifying existing natural channels and improving drainage by replacing stone walls and hedges with post and wire fences and adding culverts. This solution was found to be of positive benefit under a cost-benefit analysis. It should be noted that the maximum design flow upon which these engineering proposals were based (83.9 m^3/s) was calculated using the *Crudepix Method* (simple calculation based on surface area daily rainfall) rather than observed river flow data due to the lack of rating curves.

A survey of key swallow holes was also conducted in January 2011. This survey found the area surrounding typical swallow holes to be overgrown and in some cases, debris and pieces of wood could be found floating in the swallow holes. In particular, Polltoophill sink (Figure 3.7), was found to be containing a significant amount of waste. The report recommends the clearing of vegetation around swallow holes to prevent further blockages.

Finally, the report details the future extension of the N18 Gort to Tuam motorway. Construction was expected to begin in the first quarter of 2011 although no work has begun as of yet (September 2013). The road is of significance as it runs perpendicularly across a major flow route near Kiltartan. Particular care must be taken so as to avoid any flow restrictions cause by settlement of collapses. Two routes, an eastern and a western were considered and the western route (west of Kiltartan along Coole ridge) was found to have least likelihood of collapse with less severe consequences. Accordingly, the western route was chosen as the preferred option.

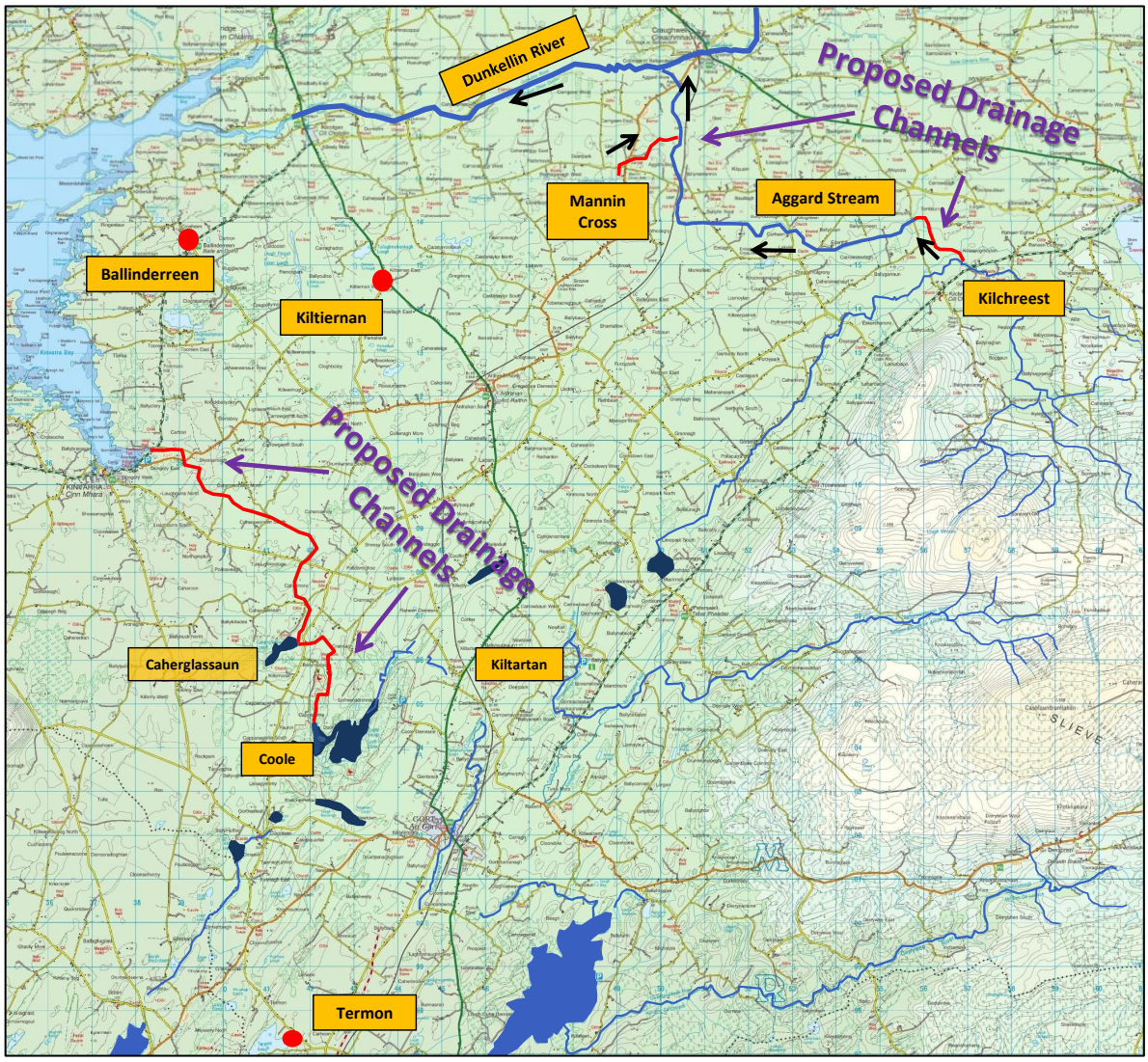

Figure 3.14: Locations of proposed engineering works as part of the Gort Flood Studies Review (Jennings O'Donovan & Partners, 2011).

3.6 Gort Lowland Turlough Network

As mentioned previously, the Gort Lowlands network of turloughs is exceptional as the turloughs are fed predominantly by allogenic river water draining from the Slieve Aughty Mountains. This water mostly sinks underground into a well-developed conduit network providing high flows with little storage. Consequently, all 5 turloughs within the network are relatively eutrophic in comparison to other turloughs (discussed previously in Section 3.4.4.2). The turloughs are deeper and more coloured than typical turloughs (Cunha Pereira, 2011) and are underlain by non-alluvial mineral soil types (of relatively low $CaCO_3$ concentration) compared to the organic and marly soil types generally associated with turloughs of longer hydroperiods. The following sub-sections detail some of the hydrological parameters and ecological factors pertaining to each individual turlough. Aerial photographs contrasting the typical summer and winter water levels are shown for each turlough in Figures 3.15, 3.16, 3.17, 3.18 and 3.19. Numerous other turloughs are present within the Gort Lowlands such as Hawkhill, Newtown are Ballinduff (as seen in Figure 3.2) however these turloughs are not part of the active conduit network, and as such, they are not discussed in this section. However these turloughs and their influence on the active conduit network (particularly in terms of hydrochemistry) are discussed throughout this thesis.

3.6.1 Blackrock turlough

Blackrock turlough (also known as Peterswell turlough) is the first turlough in the Gort Lowlands chain of turloughs. It is surrounded by gently rolling and drift covered land with a steep wooded slope on the south-eastern edge. Scattered rocks and boulders are present on the sides of the turlough and also within the basin floor. It is fed by the Owenshree River from the north which sinks within the turlough (Figure 3.9). The turlough is protected as a Special Area of Conservation (SAC) as it is an example of a 'unique untouched turlough high up in a catchment that has never been effectively drained' (National Parks and Wildlife, 2001a).

Naughton et al. (2012) found Blackrock to be the deepest (max depth:15.4 m, average depth 6.8 m) and largest in terms of volume (4.008×10^6 m^3) of the 21 turloughs that he studied, although the turlough ranked only fifth in terms of max area recorded (59.3 ha). The most striking parameter is the average daily inflow to the turlough of 10.25 m^3/s. This is over four times higher than the next highest ranked turlough and approximately eight times higher than the neighbouring turlough, Coy. In fact, Blackrock has a greater increase in volume per day than the maximum volume recorded at most other studied sites. The reason for this is the contribution of the predominantly allogenic Owenshree River. At high flow rates, the capacity of the conduit system underneath

Blackrock and Coy is exceeded, causing the river to discharge directly into Blackrock turlough. Consequently, Blackrock absorbs the excess flood water causing rapid volume increase whereas Coy does not. During the floods of November 2009, Blackrock peaked at a depth of approximately 18.5m but, as the depth exceeded the maximum surveyed level, no accurate volume information is available for that period.

Figure 3.15: Blackrock turlough, summer vs. winter.

Presently, the turlough is grazed by cattle and horses during dry periods but there is little evidence of any ecological damage being caused (National Parks and Wildlife, 2001a). A possible threat to the turlough comes from a nearby abattoir which should not cause nutrient loading. However, as Blackrock is a relatively eutrophic turlough, the impact is not as discernible as it would be on a turlough with lower trophic status (Tynan et al., 2007).

3.6.2 Coy turlough

Coy turlough (or Lough Coy) consists of a small permanent lake in the middle of an oval shaped depression with regular sloping sides. The site contains considerable depths of drift deposits and some visible bedrock outcrops along the northern boundary. The turlough floods and empties through a swallow hole on the west slope of the basin which is situated slightly above the basin floor and as a result, the turlough never empties completely as the remaining water below the swallow hole is undrained. Coy is protected as a SAC as it is a great example of a riverine (fed

indirectly by Owenshree River) eutrophic turlough in excellent ecological condition (National Parks and Wildlife, 2005). The SAC is split into two areas, the turlough itself and the southern Ballylee section which drains into a turlough at the very south of the site. In high winter floods, these two sections join together to form one water body.

Figure 3.16: Coy turlough, summer vs. winter.

Naughton et al. (2012) found the maximum depth to be 10.6m and average depth to be 5.9m over the monitoring period. The max volume, max area and average daily inflow recorded were 1.479×10^6 m^3, 25.3 ha and 1.33 m^3/s respectively. Interestingly, during the 2009 floods, Coy only reached a max depth of 10.8m which is only 20 cm greater than the previous 3 year maximum. This is significantly smaller than Blackrock which rose to over 3m higher than the previous 3 year max. This contrast highlights the difference between the turlough input mechanisms, Blackrock is river fed and can rise unrestricted whereas Coy is regulated by the conduit system feeding it from below limiting the flood levels.

The permanent water body left during dry summers takes up 9% of the total SAC site area and can be as shallow as 60 cm. Similarly to Blackrock, the land is grazed by cattle and horses during dry periods. However Coy is especially important to birds as it contains a safe roosting area in the form of permanent water all year round. Using a score system based on a turloughs plant and wildlife,

the Gort Flood Studies deemed Blackrock and Coy turloughs to be of 'national importance' (Southern Water Global, 1998).

3.6.3 Coole turlough

Coole turlough (or Coole Lough) is the largest turlough in the Gort Lowlands system and is part of the SAC known as the *Coole-Garryland complex*. This SAC is made up of Coole and a number of surrounding turloughs including Garryland, Doo, Newtown, Hawkhill and Lydacan. The turloughs within this complex differ hydrologically as they are fed by water from different catchments but, despite this, they are grouped together based on their close association with the surrounding woodland. The juxtaposition of these two distinct habitats (turlough and woodland) has led to the development of uncommon communities and rare species of plants and insects. For this reason, the complex is considered to be the most ecologically diverse in the country and is of prime importance for conservation. Indeed the Gort Flood studies ranks Coole and Garryland turloughs as sites of 'world importance' and 'European importance' respectively. The complex is also listed as a Special Protected Area (SPA) as it is an important habitat for protected bird species, particularly the Whooper Swan.

Figure 3.17: Coole turlough, summer vs. winter.

Coole turlough is fed by Coole River from the north which holds the combined water from the three Slieve Aughty Rivers (including water from Blackrock and Coy turloughs). The turlough is drained by a single swallow hole on the western bank of the turlough and has an average depth of approximately 4.1m (Gill, 2010). The maximum observed water level in Coole occurred during the 2009 floods when the turlough rose to an estimated 12.5m (value estimated due to equipment failure). This depth corresponds to a turlough volume of approximately $12.6x10^6$ m^3 and a surface area of 198 ha. At this depth, many of the turloughs within the Coole-Garryland complex joined together to form one surface water body. The site is not grazed but is used as a popular amenity area. However visitor access is controlled meaning little threat is posed to the sensitive habitat.

The turlough is closely related, hydrologically, to the other two nearby turloughs; Garryland and Caherglassaun. These three turloughs show very similar profiles with little lag indicating relatively unconstrained hydraulic connections between them (Gill, 2010). Tynan et al. (2007) describe the three turloughs as deep epikarst flow systems with overland flow at high stages. The three turloughs are also influenced by tidal effects, particularly at shallow depths.

3.6.4 Garryland turlough

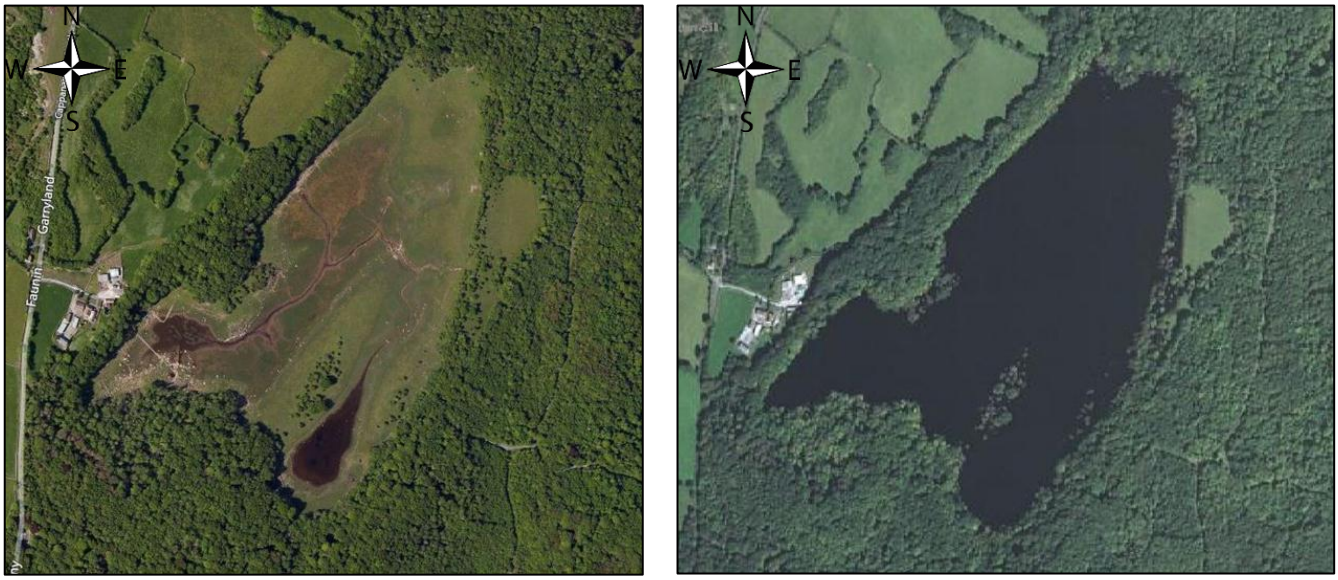

Figure 3.18: Garryland turlough, summer vs. winter.

Garryland turlough, part of the *Coole-Garryland complex* (SAC), is a medium sized horse-shoe shaped turlough situated approximately 1.5 km south-west of the main body of Coole. The turlough is fed by a single swallow hole on the south-west bank and empties completely most

summers. The maximum and average depths as seen by Naughton et al. (2012) are 10.9 and 5.5 m. The max volume, max area and average daily inflow recorded were 2.33×10^6 m^3, 42.1 ha and 1.83 m^3/s respectively. The turlough is lightly grazed by sheep and horses during the dry summer months.

Garryland and Coole turloughs are fed primarily by Slieve Aughty water. However during periods of recession, the turloughs have been seen to take water from the Cloonteen catchment to the south (Section 3.5.1.1) (Southern Water Global, 1998). Also, both Garryland and Coole have been seen to react to tidal influence at very low water levels (Gill, 2010).

3.6.5 Caherglassaun turlough

Figure 3.19: Caherglassaun turlough, summer vs. winter.

Caherglassaun is the final turlough in the Gort Lowlands conduit chain. It is situated in a natural depression comprising of a permanent lake at its core while the rest of the basin functions as a turlough. The site also comprises of open grassland, mixed deciduous woodland and exposed limestone. Beyond Caherglassaun, groundwater does not reach the surface until it is discharged at Kinvara. The turlough is thought to be filled through a single swallow hole known as 'Polldalagha' on the north bank of the turlough, although during periods of heavy flooding, a series of nearby collapse features also act as swallow holes. Caherglassaun is protected as an SAC and was rated as the sixth most important turlough in the country (National Parks and Wildlife, 2001b) and a site of 'European importance' (Southern Water Global, 1998). The site is important as it shows two key features atypical of turloughs. Firstly, it has a relatively deep permanent lake at its base which is

home to some aquatic fauna. Secondly, due to its proximity to sea-level, the lake is subject to tidal effects. In fact, the lake fluctuates by approximately 30cm in sync with tidal period although at a significant delay (National Parks and Wildlife, 2001b). This tidal relationship was further explored by Gill et al. (2013b) who determined the mean lag between tidal and turlough peaks to be 3 h and 53 minutes with a mean attenuation in amplitude (tidal efficiency) of 0.072. The turlough-tide relationship between September and October 2007 is shown in Figure 3.20

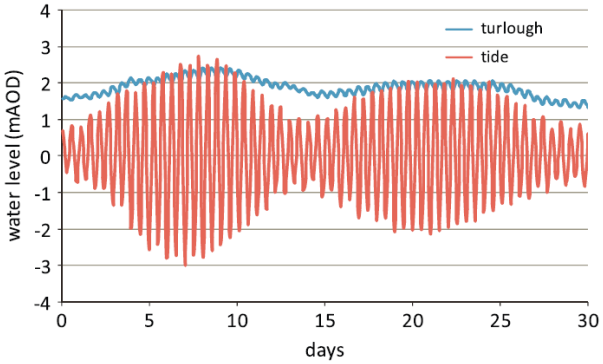

Figure 3.20: Caherglassaun turlough water levels and Kinvara tidal variation (Gill et al., 2013b).

Maximum and average water levels of Caherglassaun were recorded at 9.4 and 4.8m respectively by Naughton et al. (2012) (although the water level was observed reaching over at 11.7m during the heavy flooding of winter 2009). The max volume and max area of the turlough were 2.99×10^6 m^3 and 62.6 ha. Due to the position of Caherglassaun at the end of the chain of turloughs, it has the largest catchment area and thus the largest average daily inflow of any turloughs (without surface water input) at 2.496 m^3/s (Naughton et al., 2012). It also has the largest average daily outflow of the groundwater-only turloughs at 1.192 m^3/s. This high outflow value indicates a relatively unconstrained path between the turlough and Kinvara.

As mentioned earlier, Caherglassaun does not completely drain and has a permanent lake at its base. However, interestingly, Williams (1964) observed that at periods of low flow in the Gort (Coole) River, Caherglassaun was 'often completely drained'. This suggests that in the near 50 years since the study by Williams, the hydrological behaviour of Caherglassaun turlough has changed. Another curious observation is the fact that Caherglassaun does not receive any saltwater or brackish water from Kinvara. Yet in a study by Praeger (1932), salt water was detected in the turlough using silver nitrate solution. Again, this suggests a change in hydrological behaviour of the turlough within the last 80 years. Perhaps this change could be due to a collapse at some point along the Caherglassaun-Kinvara linkage restricting its ability to drain but also restricting the

passage of saltwater back towards the turlough. Cave-divers exploring this region (the western cave system), have observed evidence of such collapses within the conduit describing 'huge terrifying slabs fallen from the roof' (Kozlowski and Warny, 2009).

3.7 Summary

In this chapter, an overview was presented of the Gort Lowlands, turloughs and previous hydrological studies within the catchment. The main elements of this chapter which will be further developed throughout this thesis are the following:

- The hydrological functioning of a turlough (i.e. surcharge tank or flow-though) is an integral concept to this thesis. The hydrological functioning of the five turloughs under study shall be investigated using modelling and hydrochemical techniques.

- The trophic status of the five turloughs under study shall be re-evaluated based on the measurements taken over the course of this study.

- The nutrient behaviours of each turlough shall be explored in terms of inputs, outputs and behaviour during flooded periods. The findings of this study are predominantly linked with the hydrological functioning of the turloughs.

- The findings of the Gort Flood Studies shall be further investigated via the use of a hydrological model and hydrochemical analysis.

Chapter 4

Instrumentation and Data Collection

4 INSTRUMENTATION AND DATA COLLECTION

4.1 Introduction

The collection of field-data was a critical aspect of this project. A variety of data types were collected over a three year period between 2010 and 2013. These data types included continuously monitored parameters such as rainfall, river flows and water levels in turloughs and boreholes. In addition, hydrochemical data was obtained via monthly sampling of rivers, turloughs, boreholes and springs.

4.2 Continuous Monitoring

Some parameters, such as turlough water levels, were of such importance to this study that they required the use of long lasting, durable and expensive continuous monitoring equipment to allow for year round data collection at set time intervals.

The equipment chosen for the majority of field situations were submersible, barometric dataloggers called *divers* (Schlumberger Water Services). Divers use built-in pressure transducers to measure the total pressure above them. If the diver is not submerged in water, it measures atmospheric pressure just like a barometer. When the diver is submerged, the atmospheric pressure is supplemented by water pressure so the higher the water column, the higher the measured pressure. In order to get an accurate reading of water column height, the diver must be compensated for the variation in prevailing air pressure. This is done by installing a separate diver at surface level known as a *barodiver*. The barodiver measurement is simply subtracted from the diver measurement to give the height of the water column. One centrally located barodiver was deemed necessary for the Gort Lowland catchment due to the proximity of the turloughs as well as the little difference in elevation between them.

Divers are available in different sizes and depth ranges. The most commonly used divers for this study were mini-divers (DI501 and DI502). The DI501 has a range of 10m of water, an accuracy of 0.5cm and resolution of 0.2cm. The DI502 has a range of 20m of water, an accuracy of 1cm and resolution of 0.4cm. The barodiver (DI500) was designed only to be used out of water and thus had a much lower range of 1.5m (water pressure head) but higher accuracy and resolution: 0.5cm and 0.1cm respectively. Divers also record the water temperature for each timestep and automatically

provide a correction to the water level measurement. The divers have a 10 year battery and an internal datalogger capable of storing or 48,000 measurements (or 24,000 in the case of older divers). So a diver set to record once an hour has over 5 years' worth of memory whereas a diver recording once a minute only has approximately 1 months' worth of memory. Another class of diver, known as a *CTD-Diver* (DI271), is a specialised diver which is capable of measuring the conductivity of water as well as pressure and temperature. CTD-divers have ceramic casings (as opposed to stainless steel) as they are designed to be suitable for salt water applications. Divers were programmed and downloaded using specific software and a reading unit. The diver was inserted into the optical reading unit which is connected to a laptop. It was then programmed or downloaded via the software (Diver-Office) which imports the data into an Excel spreadsheet format. See Figure 4.1 below for a map of continuous monitoring locations.

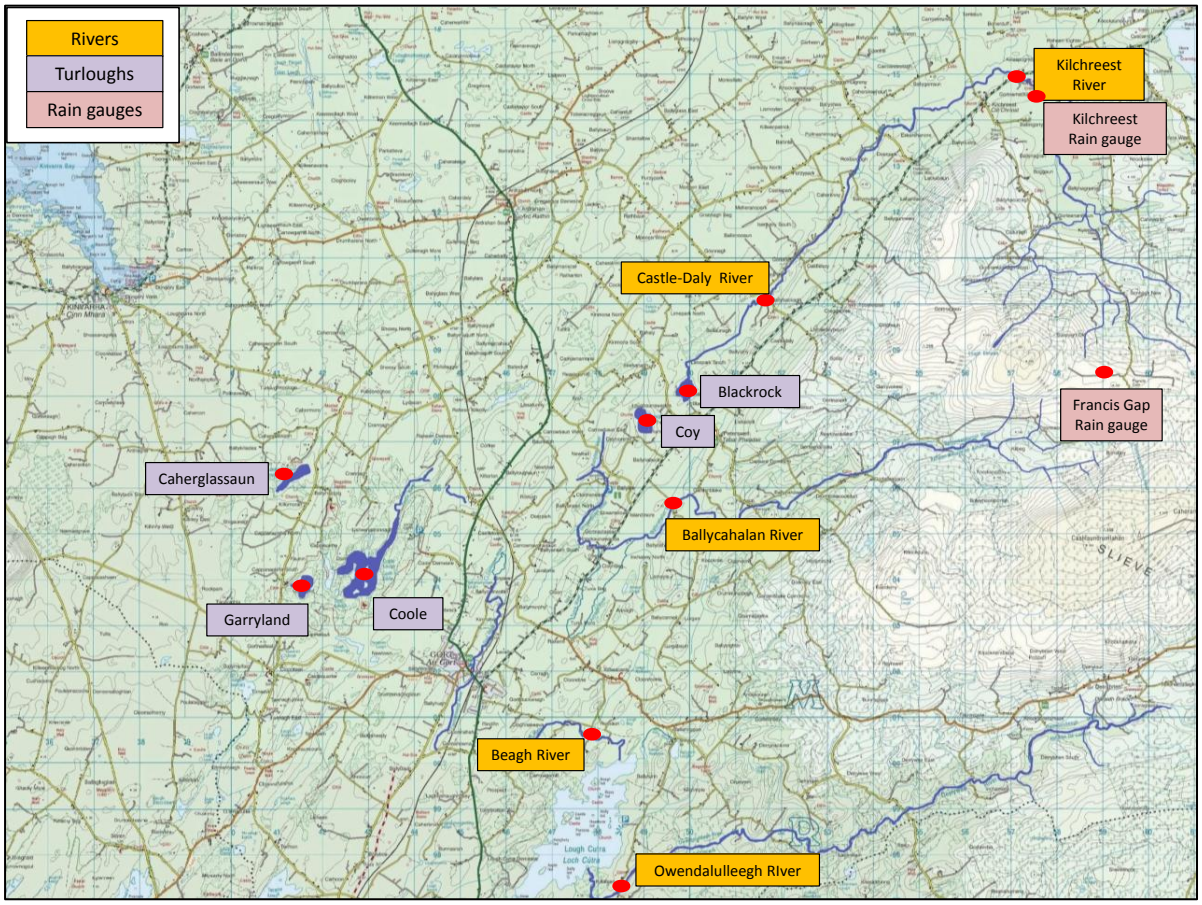

Figure 4.1: Monitoring locations (measuring water depth or rainfall).

4.2.1 Turlough Water Levels

The water levels in all turloughs were monitored using divers. The divers were placed at the lowest point in each turlough during the summer when the turloughs were dry. A concrete platform was

constructed in order to house the diver while submerged. A sturdy platform was important as grazing animals could cause damage during the dry summer months. The platform was connected to a buoy on the surface via a rope which marked its position and provided access to the diver when the turlough was flooded (Figure 4.2). 20m divers were necessary for turloughs as winter water levels often exceed 10m and one hour timesteps were deemed adequate as the turloughs are relatively slow moving systems. The locations of the diver platforms were surveyed via GPS which allowed the water depth readings to be referenced against Ordnance Datum. This meant all the turloughs had a fixed 0m and all other data was adjusted to this reference.

The divers were usually downloaded during the summer when access was easy although in some cases, it was necessary to download them in winter. Winter downloads bore an element of risk however, as once the diver platform was lifted, it was difficult to place down again in the same location. In some instances, this difficulty led to lost data as the platform was placed too high resulting in no data for low turlough water levels.

Figure 4.2: Diver platform, site laptop, diver download cable and various diver models.

4.2.2 Groundwater Levels

A variety of groundwater access points are present within the catchment. The majority of access points are individual boreholes for domestic drinking water. In recent years however, these individual wells have been superseded in favour of regional group schemes. Also present within the catchment are a number of NRA (National Roads Authority) test wells (put in place as part of

the temporary works for the N18 Gort to Tuam motorway extension) and some historic stone wells (Figure 4.3(d)). Each type of borehole/well was monitored at some point during the study period.

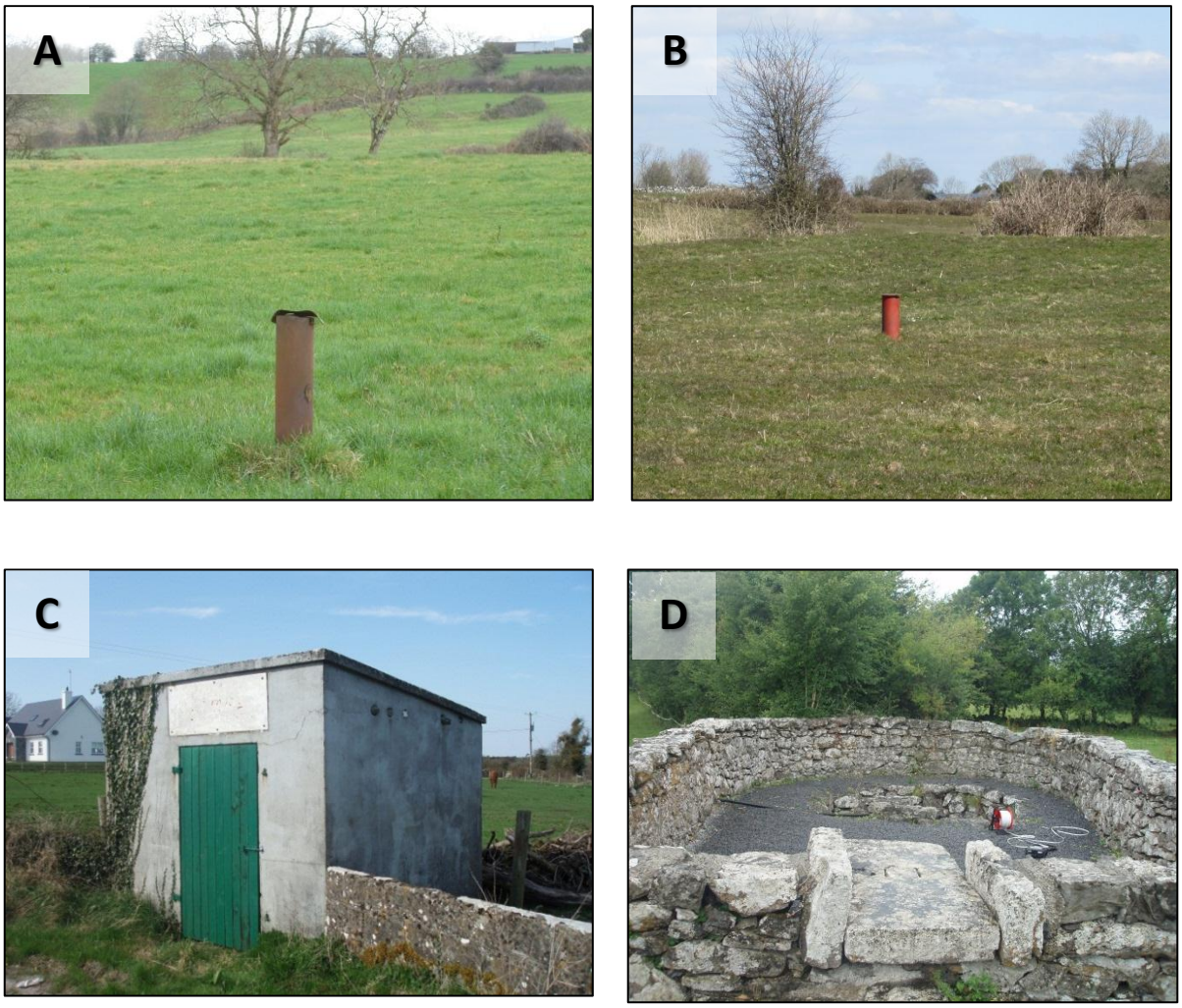

Figure 4.3: Various groundwater access points within the catchment.

The water level in wells and boreholes was monitored using divers. The divers were suspended from the surface by a cable and dropped into the borehole to a depth below the minimum water level. The divers were set at 15 minute timesteps as they were easily accessible and could be downloaded more often. The range of diver chosen depended on the variability of groundwater within the well. In most cases 10m divers were sufficient. In the case of old stone wells, the well was large and shallow enough to place a diver platform at the base rather than suspend a diver from the top. The wells used for groundwater monitoring were part of the water sampling network (Section 4.3) and their locations are displayed later in Figure 4.10. The location of each

borehole/well was recorded by GPS in order to convert diver depth readings into water level AOD (above ordinance datum).

4.2.3 Rainfall

Two tipping bucket ARG100 rain gauges (Environmental Measurement Ltd.) were installed at the upper end of the catchment. They were installed at Kilchreest (70 mAOD) and Francis Gap (250 mAOD) as can be seen in Figure 4.1. The gauges were set level and placed in an open area away from any interference from trees, walls etc. They were enclosed in a small fence which provided protection from roaming livestock (Figure 4.4). The internal dataloggers were set at 15 minute timesteps which recorded the amount of tips within that timestep, each tip consisting of 0.2 mm of rainfall. The gauges were downloaded every 2-3 months and cleaned regularly to avoid blockages.

Figure 4.4: Francis Gap rain gauge.

4.2.4 River Gauging

River gauging stations were present on the three primary rivers draining off the Slieve Aughty Mountains. There were five monitoring points, four of these permanent gauges operated by the Office of Public Works and one station a temporary gauge put in place for this study. The OPW gauges were located on the three main rivers, the Owenshree, Ballycahalan and Owendalulleegh, with an additional station in place on the Beagh River near the outlet of Lough Cutra. This additional station allowed for the investigation of flood routing of the Owendalulleegh River across Lough Cutra. The OPW gauges consisted of a pressure transducer embedded into the river referenced against an accompanying staff gauge (Figure 4.5). The fifth gauge, consisting of a mini-

diver fixed to river bank, was positioned on the Owenshree River at Castle-Daly, approximately 12 km downstream of the OPW gauge at Kilchreest. Having these two gauges on the one river allowed an investigation into the effect on the river of passing over 12 km of karst bedrock. A comparison of these river flows was used to determine the addition or possible loss of water from the underlying karst.

The dataloggers were set at 15 minute timesteps and downloaded on average once every six months. As these gauges only recorded water depth and not flow, the development of a stage-discharge relationship (rating curve) for each monitoring point was necessary.

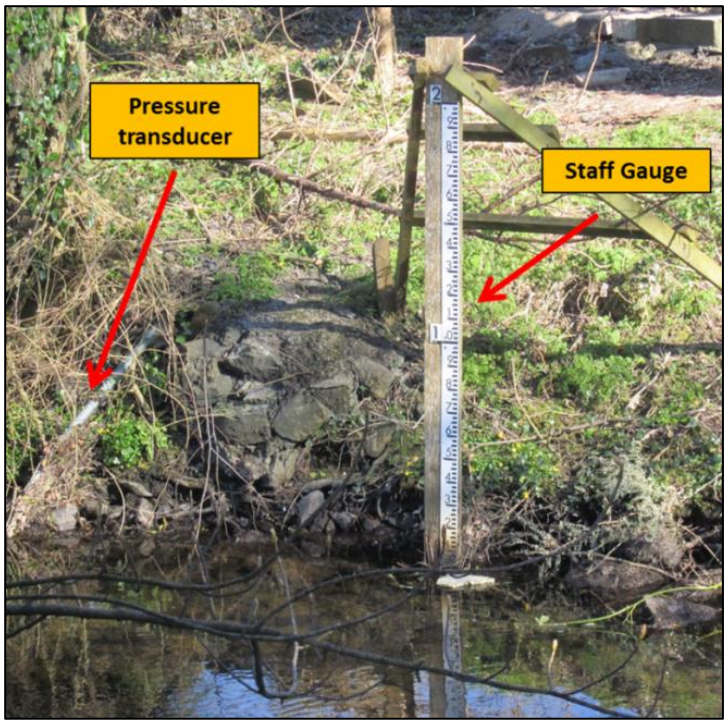

Figure 4.5: OPW River gauging station showing pressure transducer and staff gauge.

4.2.4.1 Determination of Rating Curves.

Rating curves were needed for each of the five gauging stations on the rivers. A rating curve is a relationship between stage and discharge and is constructed by determining the flow at different stages for a particular section of river. When enough measurements have been observed for all levels of flow, a rating curve can be used to calculate flow based on a known stage. In the case of the Gort Lowlands, the construction of rating curves involved numerous visits to the catchment to measure flows between the years 2009 and 2012.

Flows were measured on the rivers using the mid-section velocity depth surveying method. This method involves measuring the river velocity and depth at several points across the river to calculate the discharge (Figure 4.6). For a particular river cross section to be chosen, it had to satisfy the following hydrological parameters: straight length of channel, regular cross-section and consistent bed gradient. As well as this, the sections should not have any still areas or eddy currents. In many cases, the most suitable cross sections were found underneath bridges. The number and position of vertical measuring points was chosen according to the European/International Standard (EN ISO 748, 2007).

Velocity measurements were taken using an acoustic digital ultrasonic current meter (OTT ADC) (Figure 4.7). This meter is capable of measuring velocity and depth and automatically calculates flow for the user eliminating the need for hand calculations. The velocity measuring range is -0.2 to 2.5 m/s with a resolution of 0.001 m/s and accuracy of 1%. The depth measurement range was 0 to 5m with accuracy of 1%.

Figure 4.6: Measuring river flow.

Figure 4.7: ADC meter used to measure flow.

The greatest issue with the construction of rating curves for these five monitoring sites was the inclusion of high flows. High flow measurements present two main problems:

- High flows occur after a heavy rainfall event. Such events often happen with little warning and the resulting peak flow will occur as soon as 8 hours after the rain has started to fall due to the fast runoff from the Old Red Sandstone Slieve Aughty Mountains. This led to a practical problem in terms of gathering equipment and reaching the rivers in time to catch the peak flows.

- As flow increases, it becomes increasingly difficult to remain in the river to carry out the measurement. Typically, flows above 4 m^3/s were too dangerous making it necessary to measure the river velocity by another means. A solution was found by dropping the velocity meter from a bridge using an extended pole and cable (Figure 4.9).

The highest flow successfully recorded was calculated as 60 m^3/s. This occurred on 8th June 2012 on the Owendalulleegh River after 30 mm of rain had fallen in the preceding 24 hours (see Figure 4.8).

Figure 4.8: Low flow and high flow (8/6/2012) comparison at Owendalulleegh River.

Figure 4.9: Measuring high flows on Ballycahalan River (8/612).

During the investigations for the Gort Flood Studies Report, a number of other discharge monitoring points were established or attempted to be established within the catchment. The two most relevant attempts (to this thesis) were at the Coole River and the spring discharge at Kinvara. Gauging Coole River proved unsuccessful due to difficulty in entering the river at high stage and the frequency at which the river burst its banks. Attempts were also made to gauge the flow at the

springs at Kinvara. Two surveys were attempted at low tide conditions but the data was not used due to problems with the density effects of the saline and freshwater. At high tide the saline water intrudes a great distance into the aquifer and as a result the springs take several hours to flow with freshwater. Due to this, it could not be determined whether the flow being measured was salt water released from the aquifer or freshwater discharge. For these reasons, neither Coole River nor Kinvara springs were included or attempted to be gauged as part of this thesis. Attempts were made however to estimate flows at Kinvara using hydrochemical methods as discussed in Section 7.2.4.

4.3 Monthly Sampling

From March 2010 until March 2013, monthly sampling was carried out at key locations within the catchment. Over 30 sampling locations were identified and sampled from over the course of the 3 year campaign with 20-25 locations being regularly sampled. Samples were collected from 8 river sites, 18 boreholes/wells, 5 turloughs, and the two springs at Kinvara. These locations are displayed in Figure 4.10. In total, approximately 680 individual visits were made to the sites with up to 7 sample bottles been taken at each site. These samples were collected and tested for a range of hydrochemical parameters such as alkalinity, pH, specific conductivity, nutrients and stable isotopes. Details on hydrochemical the analysis techniques can be found in Section 4.5.

Rivers were sampled to characterise the water feeding into the catchment. Samples were collected from the three rivers feeding the catchment at two locations (upper and lower) on each. Two more samples were also taken of peat and forestry runoff from the Slieve Aughty Mountains. Samples were recovered at depth from the centre of the rivers by grab sample or use of a bucket. See Table 4.1 for details on the river sampling locations.

Table 4.1: River Sampling locations and site ID names.

Site ID:	Location	Comment
OR-U	Owenshree River – Upper	
OR-L	Owenshree River – Lower	
BR-U	Ballycahalan River –Upper	
BR-L	Ballycahalan River – Lower	
DR-U	Derrywee River –Upper	(Owendalulleegh River)
DR-L	Derrywee River – Lower	(Owendalulleegh River)
F	Forest area of Slieve Aughtys	Forestry runoff
P	Peat area of Slieve Aughtys	Peat runoff

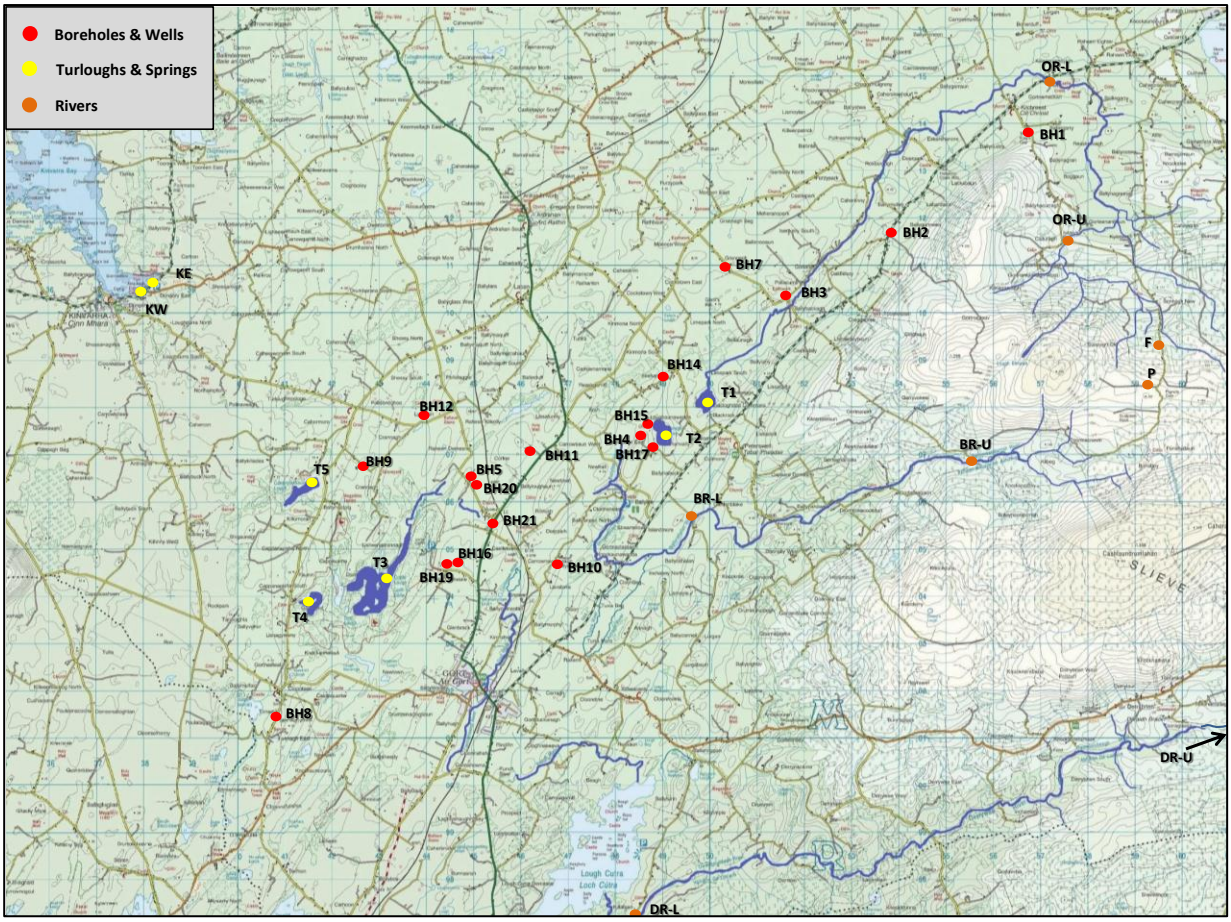

Figure 4.10: Plot of sampling network displaying site type (colour) and name.

Boreholes and wells were sampled to collect groundwater from within the carboniferous aquifer surrounding the turlough network. Samples were recovered from open wells by grab sample or using bailers after being purged by removing three times their stored volume. Samples from pumped wells were collected from a tap before the water reached the treatment system. The range of boreholes/wells being sampled varied over the three year sampling period due to loss of access and the discovery of new wells as research progressed. Access to private boreholes was provided by permission of the landowner and in three cases, access was lost resulting in the discontinuation of sampling at that location. See Table 4.2 for details on borehole/well sampling locations.

Table 4.2: Borehole and well sampling locations.

Site ID:	Location	Details
BH1	Kilchreest	• Well owned by Kilchreest group water scheme. • Extremely deep high capacity well. • Pumping water from Old Red Sandstone rather than Carboniferous aquifer.
BH2	Ballygunneen	• Private household well
BH3	Pollacurra	• Open Borehole installed for housing development but development abandoned due flooding problems. • See Figure 4.3(a).
BH4	Near Coy turlough	• 70m deep private household well located on hill above Coy turlough.
BH5	Kiltartan	• Private agricultural well.
BH7	Grannagh	• Private household well.
BH8	Cloonteen	• Private household well within southern Cloonteen catchment. • Dropped from sampling due to difficulty in collecting untreated sample.
BH9	Caherglassaun	• Private household well located on hill above Caherglassaun turlough
BH10	Ballyaneen South	• Private household well. • Sample collected from untreated kitchen sink tap.
BH11	Bunragh	• Private agricultural well.
BH12	Crannagh	• Former Crannagh group scheme well. • Figure 4.3(c).
BH14	Skehanagh	• Old stone well. • Figure 4.3(d).
BH15	Near Coy turlough	• Old stone well on hillside next to Coy turlough.
BH16	Near Coole	• Coole group water scheme.
BH17	Near Coy turlough	• Abandoned household well next to Coy turlough.
BH19	Near Coole (nra)	• NRA monitoring well nearby BH16.
BH20	Kiltartan (nra)	• NRA monitoring well nearby BH5.
BH21	Kiltartan (along N18)	• Former Gort Flood Studies monitoring well.

The turloughs were assumed to be well mixed water bodies and consequently, only one sample taken from the main body of the turlough at a depth of 1m was deemed necessary to give a

representative measurement. This assumption is based on studies carried out by Gill (2010) and Cunha Pereira (2011) (further details on these studies can be seen in Section 7.1.1). The sample was collected from the main body of the turlough using a kayak, this method prevented contamination of the samples from the build-up of filamentous green algae at the banks of the turloughs. Typically fewer samples were able to be collected in summer due to the turloughs emptying. Samples were collected from the two Kinvara springs (east and west) at low tide. See Table 4.3 for sampling locations.

Table 4.3: Turlough and Spring sampling locations

Site ID:	Details
T1	Blackrock
T2	Coy
T3	Coole
T4	Garryland
T5	Caherglassaun
KW	Kinvara West
KE	Kinvara East

4.4 External Data

To develop a full hydrological model of the catchment (see chapter 6), various additional hydrological datasets were required. Many of these datasets were not collected as part of this research as they were available from various state-run organisations. External data such as this included:

TIDAL DATA

The Irish Marine Institute provided water level data from a tidal gauge installed in Galway Port. This gauge is the closest available gauge to the catchment outfall at Kinvara. However a 72 minute delay was detected between tide peaks at Kinvara and Galway Port. This delay was applied to the tidal data before it was inputted into the hydrological model.

RAINFALL AND EVAPOTRANSPIRATION

The Irish meteorological service, Met Éireann, possesses a vast array of weather stations and rain gauges across the country. Hourly rainfall and evapotranspiration data was received from climactic weather stations in Birr, Gurteen and Shannon Airport. In addition to this, daily rainfall amounts

were recorded by a number of rain gauges surrounding the catchment. Daily rainfall data from gauges in Ardrahan, Ballyvaughan, Carron, Gort and Loughrea was received.

RIVER FLOW DATA

As mentioned previously, most of the river flow data for this project was obtained from fixed river monitoring points run by the Office of Public Works (OPW). The OPW record water depths at 4 monitoring points (ref no's: 29020, 29021, 29023 and 29009) in 15 minute timesteps. This water level data was then converted to flow data using rating curves.

4.5 Chemical Analysis

Water samples were tested in the laboratory as soon as possible after collection and within 24 hours of sampling. The samples were stored in a cool box during transportation. The testing methods are described below:

4.5.1 General Chemistry

Samples were tested for alkalinity based on Standard Methods (APHA, 1999). This involved taking 50 ml of sample, injecting an indicator dye into it and titrating the sample with 0.02N H_2SO_4 until the dyed sample changes colour due to change of pH. The titration is made up of two steps using two indicator dyes. The first step involves titrating the sample until the pH is lowered to 8.3 at which point, the *phenolphthalein* indicator turns from pink to colourless. This step is used for samples containing carbonate and bicarbonate alkalinity which have a pH of > 8.3 and usually less than 11. The second phase of the titration uses *bromcresol green* to mark when the pH has dropped to 4.5. At this point the indicator changes from blue to yellow. This step is used for samples containing only bicarbonate alkalinity which have a pH of 8.3 or less. The pH levels within the Gort Lowlands were rarely above 8.3 and as such, only the second titration phase was carried out.

Samples were also tested for specific-conductivity (conductivity corrected to 25°C) using an electrical conductivity (EC) meter (WTW® Cond.197i) and pH was recorded using a pH meter (Eutech Instruments ph6+).

4.5.2 Nutrients

A range of nutrient tests were carried out to determine total nutrient quantity and the quantity of their most common forms. Total nitrogen (TN) tests were carried out using test kits capable of detecting low concentrations. Two varieties of test kits were used for TN, *Merck total nitrogen cell test kit (1.00613.0001)* with range 0.5-15 mg/l and *Dr. Lange 138 cell test kit* with range 1-16 mg/l. For nitrate (NO_3), *Merck test kit (1.09713.0001)* was used which had a range of 0.1-25 mg. Quality control (QC) was carried out for TN and NO_3 using Merck Combicheck standards (*1.14695.0001* for TN and *1.14675.0001* for NO_3). In the early stages of sampling, ammonium (*1.14752.0002*, 0.02-1.3 mg/l) and nitrite (*1.09713.0001*, 0.1-25 mg/l) test kits were also used. However concentrations were found to be too low to warrant the continuation of testing.

Phosphorus (P) was measured in two forms: total phosphorus (TP) and total dissolved phosphorus (TDP). 25 ml of water was collected and put into its own dedicated bottle to avoid contamination. For TP, 25 ml of sample was measured in a graduated cylinder and poured into the sample bottle on site. For TDP, the sample was filtered through a 45 micron filter *(Puradisc 25 PP, 515-1434)* before being poured into the sample bottle. The procedure for lab analysis was as follows:

- Standards made up for 0, 0.05 and 0.1 mg/l and a quality control standard of 0.05 mg/l was also used.
- Digestion reagent was added to each sample. The reagent was made up of 6g $K_2S_2O_8$, and 10 ml of 3.6N H_2SO_4 mixed into ultrapure water to fill a 100 ml volumetric flask.
- Samples were digested in an autoclave at 121°C for 1 hour.
- After digestion, 5 ml of sample was pipetted into a test tube and 1 ml of mixed reagent was added. This reagent contained 13.5 ml 3.6N H_2SO_4, 25 ml antimony stock, 25 ml molybdate stock and 0.2g ascorbic acid which was made up to 100 ml using ultrapure water.
- After 10 minutes, samples are inserted into a spectrometer and their absorbance measured (882nm).

QC was carried out for P by running a QC sample with each batch of P analyses. This solution was prepared to a specific concentration (0.025 mg/l TP) at the onset of laboratory testing and kept in individual bottles in a freezer. Duplicate samples were also collected and tested rule out sampling error.

4.5.3 Stable Isotopes

Separate samples were collected for stable isotope analysis. These samples were flooded before sealing under water to ensure no air was trapped in the bottle which could alter the isotope signature via fractionation. Samples were transferred to a cool box before being stored in a fridge until ready for analysis by mass spectrometry.

^{18}O

The analysis of the samples to yield the $^{18}O/^{16}O$ ratio was carried out using a gas bench mass spectrometer. Samples were collected in the field and stored for a period of up to six months before testing in bulk. The sample preparation to find the $\delta^{18}O$ of water by equilibration was as follows.

- 0.5 mL of water was pipetted into a 12 mL exetainer which is capped with a rubber septum.
- The exetainer was flushed with a 0.3% CO_2 in helium for 800 seconds.
- The exetainer was allowed to equilibrate in the sample block for >20 hours. Two equilibrations occur:

  (1) $CO_2(g) <=> CO_2 (aq)$

  where CO_2 is exchanged between the gaseous and aqueous phase.

  (2) $CO_2 (aq) + H_2O <=> H_2CO_3$

  where dissolved CO_2 reacts with water to form carbonic acid.

- Samples were run with the standard method (5 reference CO_2 peaks, 10 sample peaks and 2 reference CO_2 peaks). The middle 8 sample peaks were then averaged to give the $\delta^{18}O$ value.

Corrections to the standard were made and the Standard Deviation was reported as 1SD for all standards run with unknowns.

^{18}O AND ^{2}H

Samples to be analysed for both ^{18}O and ^{2}H were sent to the Stable Isotope Facility in Queens University Belfast for testing. A portion of sample was transferred from the 100 ml HDPE sample bottles into 2 ml glass vials and posted to the laboratory.

4.6 Problems Encountered

During the course of monitoring the catchment over a period of 3 years, a number of issues were encountered that hampered data collection. These issues had to be dealt with urgently so as to have reliable data for analysis later on. Such issues included:

Diver unreliability

The reliability of the diver instrumentation was of key importance to the collection of field data. On a number of occasions the divers broke down as they were recording data on site resulting in lost data. The sites most at risk for this are the turloughs as they are downloaded so seldom. This occurred at Garryland turlough twice during the monitoring period resulting in many months of lost data. Another problem was caused by frost damage. In one instance the diver in Blackrock turlough showed increased pressure when the turlough was known to be empty. It was later determined that the elevated pressure was due to frost build-up which impacted upon the pressure transducer. Similar frost effects were found with the OPW river data.

Obstructions

An issue that arose at gauging stations was that of blockages by fallen trees. This problem arose on two occasions during the study period whereby a fallen tree had caused a blockage between bridge piers just downstream of a gauging station. The blockages caused significant backwater effects which artificially raised the stage of the river resulting in erroneous data. The blockages were removed and the data from these periods was used with caution.

Erroneous data

As mentioned before, a large amount of data was obtained from external institutions. This external data often had a number of errors or omissions in it. Tidal data often had gaps of many hours where no data was provided and some timesteps were repeated within the dataset. To correct the missing tidal data, previous tidal cycles of similar amplitude were used to fill in the gaps where needed. For missing river flow data, the rainfall-runoff model *NAM* was used to estimate flows based on rainfall. More details on the NAM rainfall-runoff modelling process are discussed in Section 5.4.2.

Interference with equipment

Installing equipment in the field brings with it the risk of vandalism or interference from members of the public. This was an issue for the diver installed on the Owenshree River at Castle-Daly. The diver placed inside a pipe casing and mounted on a stone wall beneath the water line. Upon

detailed inspection of the data, the diver baseline datum appeared to move at various points suggesting the diver had been lifted out of the water and placed back incorrectly. As the site is often used by locals for fishing, it is quite likely that the diver could have been tampered with. As a result, the data from the diver was of limited use due to the uncertainty in water level readings.

Other issues

Other problems encountered during site work included divers becoming lodged down boreholes and in one instance, the rope and buoy attached to a diver platform getting sucked down an estavelle.

Chapter 5

Hydrology

5 HYDROLOGY

5.1 Introduction

In this chapter, the continuously monitored hydrological field data is presented and discussed. This includes: turlough water levels, weather data, river flow data and groundwater levels. Additionally, a number of parameters such as turlough stage-volume relationships and river rating curves have been improved upon those used in the previous study by Gill (2010).

5.2 Turloughs

The water depths of the five turloughs: Blackrock, Coy, Coole, Garryland and Caherglassaun between October 2009 and April 2013 are displayed on Figure 5.1. From this graph the four flooding seasons can be observed:

- The extreme flooding of 2009 is visible with all turloughs experiencing excessively high water levels, particularly Blackrock which reached over 18m in depth.

- Winter 2010/2011 was characterised by an irregular flooding pattern. Four distinct flooding events are discernible between July 2010 and April 2011.

- Winter 2011/2012 was a more "typical" flooding season with one large filling event starting in October 2011 and ending in April 2012.

- The 2012/2013 flood season started early with four of the five turloughs filling in May 2012 and not emptying again until March 2013.

It should be noted that the straight lines shown for turloughs at low levels are due to the diver being above the water level, not necessarily that the turlough is empty. However, in these cases, the turloughs are low enough so that their volume is negligible. For example, in March 2012, the diver in Blackrock was relocated from the main body of the turlough to within the main estavelle. This resulted in a drop of approximately 1m in diver level but no loss of accuracy as at these depths, the drop only resulted in a calculated volume differential of approximately 80 m^3.

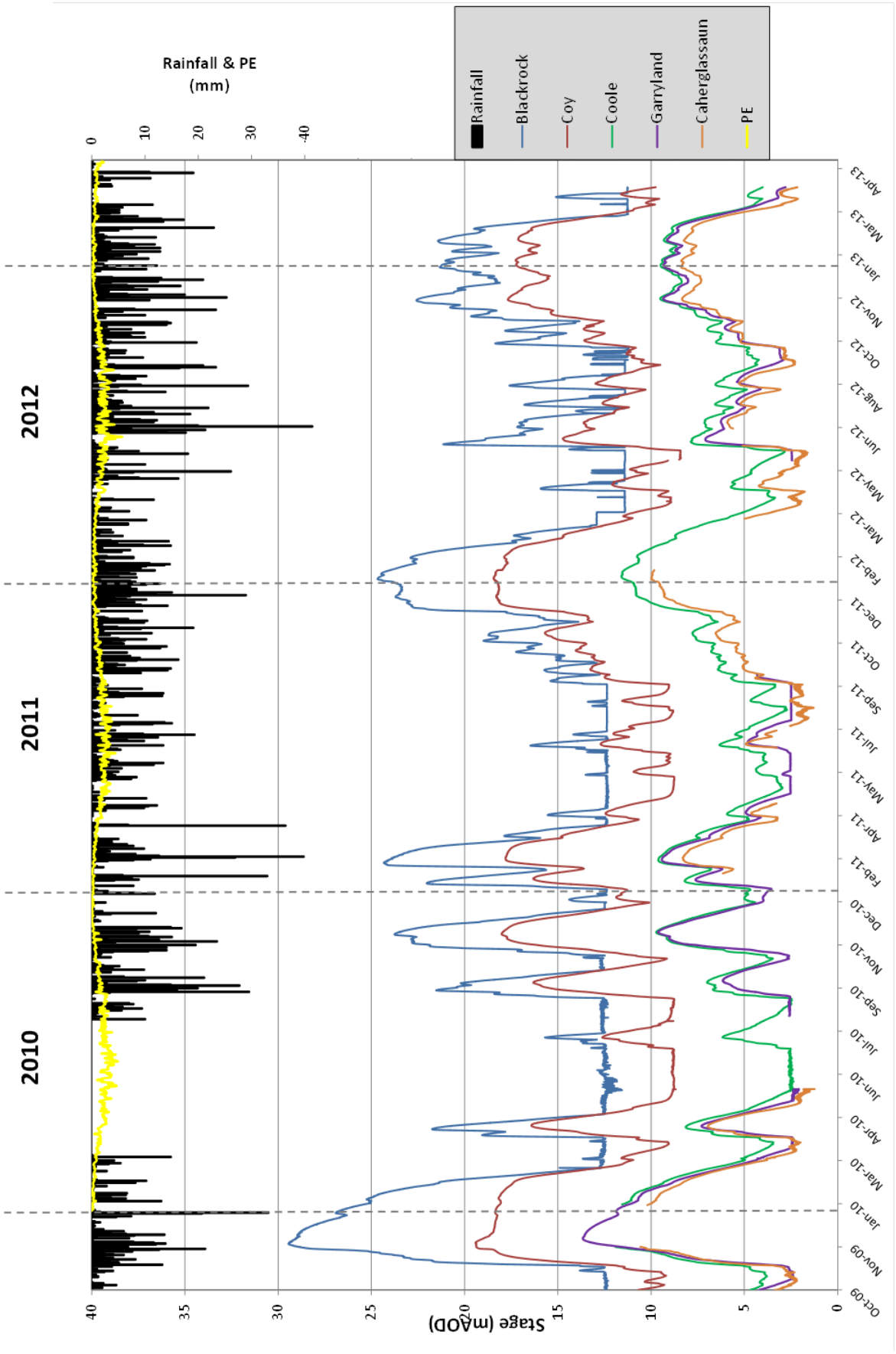

Figure 5.1: Turlough water levels (stage) for all turloughs, daily rainfall from Francis Gap rain gauge and PE from Shannon Met Éireann synoptic station.

Also displayed in Figure 5.1 is daily rainfall from Kilchreest rain gauge and potential evapotranspiration data from the Met Éireann synoptic station at Shannon Airport. Unfortunately no rainfall data was recorded during summer 2010 due to a faulty datalogger.

Overall, the turloughs display similar patterns to those observed between 2006-2009 by Gill (2010) with three of the four flooding seasons experiencing one major flooding event. The irregular flooding pattern of winter 2010/2011 was caused by periods of light rainfall, particularly December 2010 where only 46 mm of rain fell compared to 170 mm and 141 mm for December 2011 and 2012 respectively. The turloughs can be split into two groups: Blackrock and Coy as the upper turlough group and Coole, Garryland and Caherglassaun as the lower turlough group.

UPPER TURLOUGHS (BLACKROCK AND COY)

Blackrock is the uppermost turlough in the system and is fed on the surface by the Owenshree River. As a result, it shows a very sharp response to rainfall with many flashy filling and emptying events over the study period. It floods the deepest of the five turloughs (Table 5.1) but also spends the most amount of time completely empty due to its rapid recession rate. Coy on the other hand, is a damped version of Blackrock. It does not flood as deep (rarely flooding above 17 mAOD) and experiences slower filling and a longer recession curve. The primary reason for the differences between the turloughs is the fact that Blackrock is predominantly river fed whereas Coy is fed by groundwater via an estavelle. A river fed turlough has no restrictions on its inflow whereas a turlough fed by an estavelle (acting essentially a surcharge tank) is limited by conditions underground.

Table 5.1 Statistics on turlough inundation 2009 - 2013.

	Apr 2009-Apr 2010		Apr 2010-Apr 2011		Apr 2011-Apr 2012		Apr 2012-Apr 2013	
	Days empty (no.(%))	Max (mean) water depth (m)	Days empty (no.(%))	Max (mean) water depth (m)	Days empty (no.(%))	Max (mean) water depth (m)	Days empty (no.(%))	Max (mean) water depth (m)
Blackrock	111 (30%)	18.5 (6.6)	110 (30%)	13.3 (4.9)	130 (36%)	13.7 (4.8)	111 (31%)	11.6 (4.7)
Coy	3 (1%)	10.9 (5.3)	65 (18%)	9.5 (4.2)	24 (6)	10 (4.4)	11 (3%)	9.2 (4.6)
Coole	0 (0%)	11.3 (*)	1 (0.2%)	9.1 (5.1)	0 (0%)	11 (5.9)	0 (0%)	8.9 (5.9)
Garryland	37 (10%)	11.8 (*)	*	7.7 (*)	*	*	*	7.5 (*)
Caherglassaun	0 (0%)	11.7 (*)	*	7.8 (*)	*	9.5 (*)	*	7.9 (*)

* data not available due to equipment failure

LOWER TURLOUGHS (COOLE, GARRYLAND, CAHERGLASSAUN)

The lower three turloughs behave similarly to the upper two turloughs but appear more dampened with slower flooding and receding. The turloughs are slower to fill due to the origin of the water supplying them. The majority of the water has come from the Owendalulleegh River catchment which has been significantly attenuated as it passed through Lough Cutra (see Section 5.4.3.1). The remainder of the water comes from the Rivers Ballycahalan and Owenshree (which has been attenuated by Blackrock and Coy turloughs which act as a form of header tank to damp the linked hydraulic network). The turloughs are then also slow to empty as they are restricted by the capacity of the underground conduit network and the lack of hydraulic gradient between the turloughs and the ultimate destination of the water at Kinvara.

Comparing the lower three turloughs to each other, they show very similar profiles with little lag which indicates relatively unconstrained hydraulic connections between them. There is also evidence of some hydraulic connections that become active only when the turloughs have reached certain depths. For instance, at low-medium flood levels Garryland and Caherglassaun have very similar depths while Coole tends to be approximately 1m higher. As flooding increases above 7-8 mAOD, Garryland will start to mirror Coole rather than Caherglassaun. This suggests a possible epiphreatic zone or epikarst/fracture linkage between the Coole and Garryland turloughs at 7-8m. At approximately 10 mAOD, a surface channel will emerge between the two turloughs and their water levels will equalise.

5.2.1 Updating Turlough Surveys

For the modelling and analysis of the turloughs and their water volumes, accurate surveys of the turloughs are required. The Gort Lowland turloughs were originally surveyed during the summers of 2006-2009 by Gill (2010) and Naughton (2011). The surveys were carried out using a Trimble 4700 GPS system which enabled accuracies of 0.02m in both the horizontal and vertical directions. The GPS data (Easting, Northing and elevation) was downloaded to an Excel .csv file and exported to Surfer® version 8.6 software which computed the land surface and produced contour maps (Figure 5.2). Using these contour maps, depth-area and depth-volume relationships were computed at 0.02m depth intervals for each turlough. The specific depths (measured by the divers) could then be converted to volumes using the depth-volume relationships.

The survey data was extremely accurate at low depths but at higher depths, precision was more difficult. Some of the problems encountered by Gill and Naughton included:

- At higher levels, surveying became problematic due to increased vegetation density. Vegetation not only made the terrain difficult to traverse but also interfered with GPS signal. As a result, topographic points were sparser in vegetated areas resulting in lost accuracy. This was an issue particularly in the *Coole-Garryland Complex* which is known for the close proximity of its forest to the turlough.
- The maximum levels taken by the surveys did not encompass the highest levels that the turloughs reached in November 2009. As a result, any water that reached above the maximum surveyed level could not be quantified.
- Some turloughs (e.g. Coole) never completely emptied during any of the surveying trips. This meant that the lowest levels could not be known and had to be estimated.

An aerial LIDAR survey of the region, commissioned by the OPW, was carried out in the summer of 2012. This survey provided detailed terrain maps of the turloughs with an accuracy of typically less than 20cm. As the turloughs flooded early in 2012, many of the turloughs were not empty when the fly-over was carried out and as a result the lowest turlough levels could not be surveyed. However, using a combination of low level GPS data with higher level LIDAR data, turlough stage-volume relationships could be determined to a great degree of accuracy (thus improving upon the current surveys of Gill (2010) and Naughton et al. (2012)). See Figures 5.2 & 5.3 for a comparison between the original survey and the LIDAR updated survey for Blackrock turlough. In this case, the updated survey takes into account the significant low lying area to the north-east which floods during extreme high water levels in Blackrock.

This improvement that the updated survey has on the stage discharge relationships of Blackrock turlough is shown in Figure 5.4. The stage-volume relationship is unchanged until the water level reaches 22m at which point the volume increase per change in elevation is dramatically increased. Although Blackrock turlough is the most dramatic alteration, all 5 turloughs showed changes in stage-volume relationships as can be seen in Appendix A. These changes have a significant impact on the running of the hydrological model.

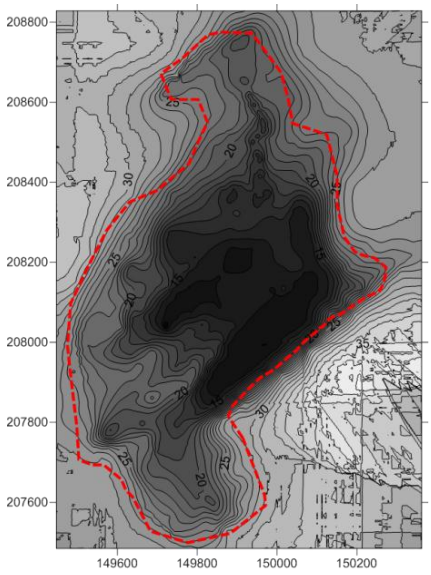

Figure 5.2: Blackrock turlough original survey.

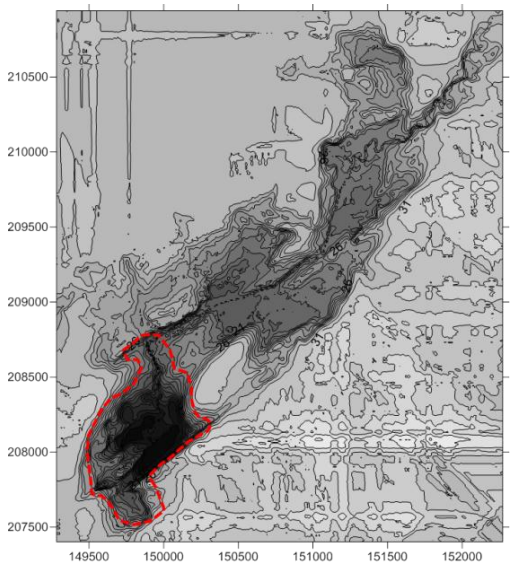

Figure 5.3: Blackrock turlough LIDAR updated survey.

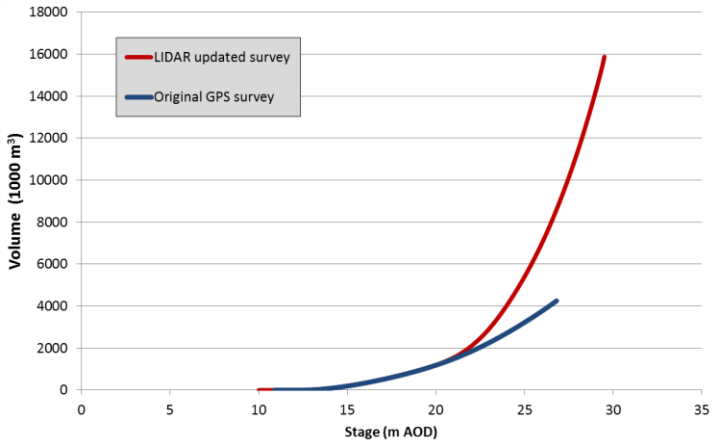

Figure 5.4: Upgraded stage-volume curve for Blackrock turlough.

5.3 Rainfall & Evapotranspiration

5.3.1 Rainfall

Rainfall was measured using two tipping bucket gauges at Kilchreest and Francis Gap which recorded rainfall every 15 minutes. A correlation between the two gauges (Figure 5.5) based on daily rainfall (Sep 2010 – Apr 2013) shows a reasonable correlation (R^2=0.84) with Francis Gap recording approximately 35% more rainfall than Kilchreest over that period. The additional rainfall at Francis Gap is expected due to its position high up the Slieve Aughty Mountains.

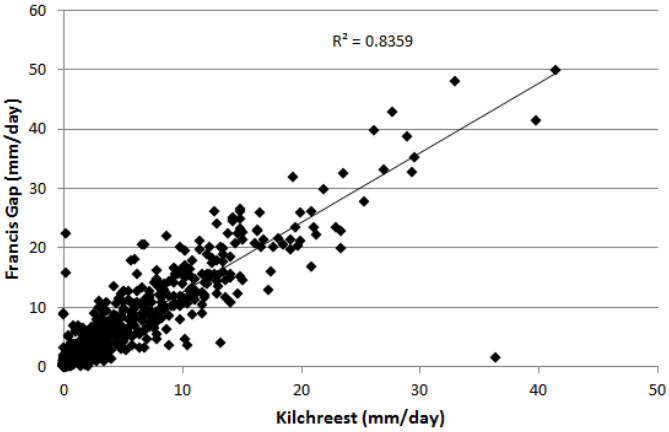

Figure 5.5: Daily rainfall correlation between Kilchreest and Francis Gap (Sep 2010-April 2013).

Walsh (2010) describes the average annual reference rainfall (1981-2010) across the Gort area ranging from over 1500 mm on the high ground of the Slieve Aughty Mountains and the Burren plateau, down to approximately 1100 mm in low-lying areas around Gort Town. The lowest monthly average rainfall generally occurs in April, followed by a gradual rise in average rainfall to the highest values between October and January. Data from 2010-2013 broadly conforms to this trend with a number of notable exceptions (>200 mm rainfall in March 2010 and June 2012). See Figure 5.6 below for a plot of monthly rainfall values between January 2010 and March 2013.

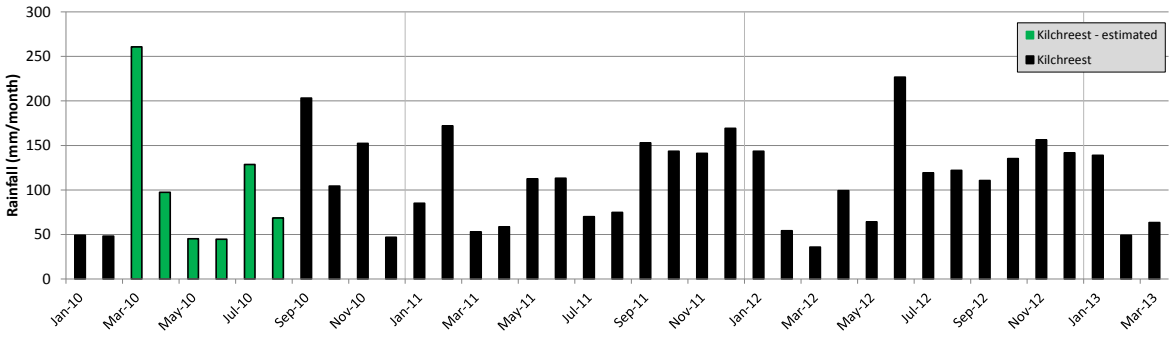

Figure 5.6: Monthly rainfall for Kilchreest rain gauge (2010-2013).

Unfortunately, equipment failure during summer 2010 caused the loss of 6 months of rainfall data from both Kilchreest and Francis Gap rain gauges (green bars on Figure 5.6). This loss of data is not catastrophic as there are a number of Met Éireann operated rain gauges in the region that can record daily rainfall. However, for use as an input into the hydrological model, hourly Slieve Aughty rainfall is required. To obtain an approximation of hourly rainfall, the hourly data from the nearest operational synoptic station at Shannon was used and weighted against daily rainfall values

at the Derrybrien/Gort rain gauge (Met Éireann). This method provided a reasonable estimation of hourly rainfall for modelling purposes. See Table 5.1 for yearly rainfall statistics for a number of relevant rain gauges.

Table 5.2: Yearly rainfall amounts (mm) for rain gauges within/nearby catchment.

	Hourly rainfall stations				Daily rainfall stations (Met Éireann)			
	Kilchreest	Francis Gap	Shannon (Met Éireann)	Galway (NUIG)	Ballyvaughan	Carron	Derrybrien (Gort)	Loughrea
2010	*	*	845	*	1109.3	1305	1153	959
2011	1345	1821	1012	1490	*	1824	1553	*
2012	1408	1953	1046	1417	*	*	*	*

*full dataset unavailable, **some notable stations omitted (e.g. Ardrahan) due to lack of continuous dataset.

Using the network of rain gauges within the region, a rainfall contour map can be produced which clearly displays the different rainfall quantities between the upland and lowland portions of the catchment (Figure 5.7).

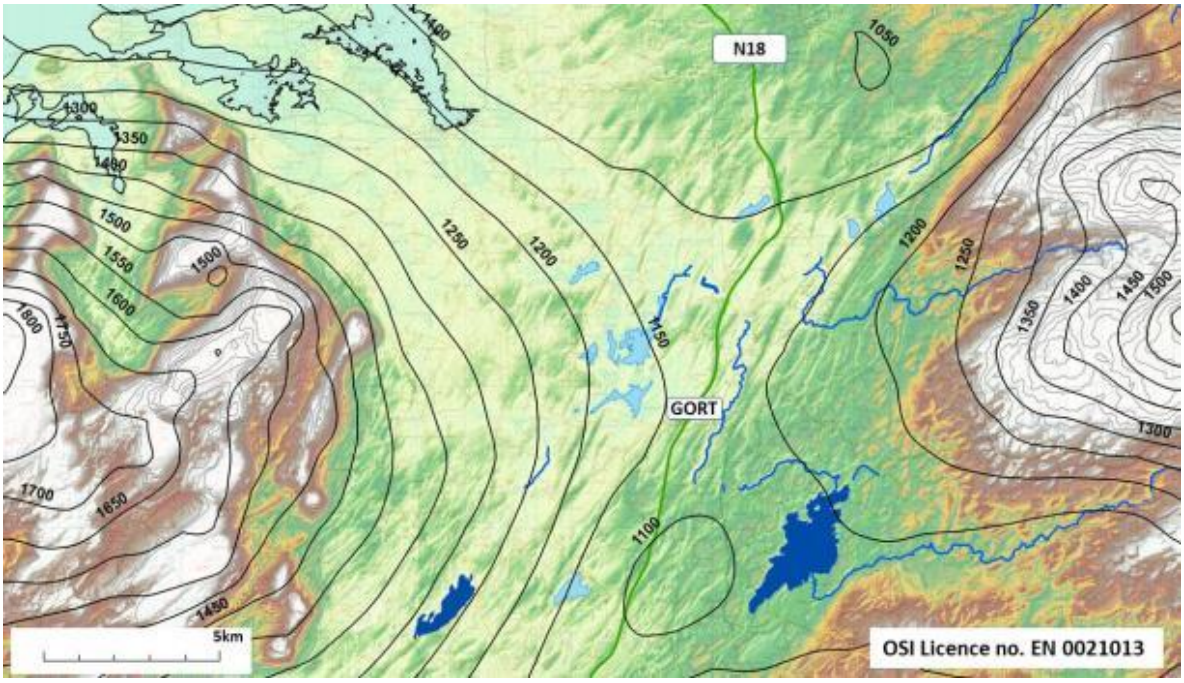

Figure 5.7: Rainfall contour map for the Gort Lowlands (Office of Public Works, 2013).

5.3.2 Evapotranspiration

Potential evapotranspiration (PE) measurements were only available from Met Éireann synoptic weather stations. Most of these stations calculate evaporation using the Penman-Monteith equation and report values on a daily basis. The two closest stations to the Gort Lowlands, Shannon and Gurteen, share a close relationship with an R^2 value of 0.896. As the catchment lies between these two stations, the average daily value between the two was taken as the input into the network model. In June 2012, a new Met Éireann synoptic station came online at Athenry. This station lies quite close to the catchment and thus the data from this station was used after 28 June 2012 (the R^2 value between Athenry data and the Shannon-Gurteen average was 0.881). See Figure 5.8 for a plot of PE between 2010 and 2013. In terms of modelling the turlough network, PE measurements are required but hold little influence over the turlough dynamics. The turlough levels are not very sensitive to PE levels as when turlough are highest in winter, the PE is low. In summer, when PE is high, many of the turloughs are empty or low enough for PE to make little difference in terms of turlough volume.

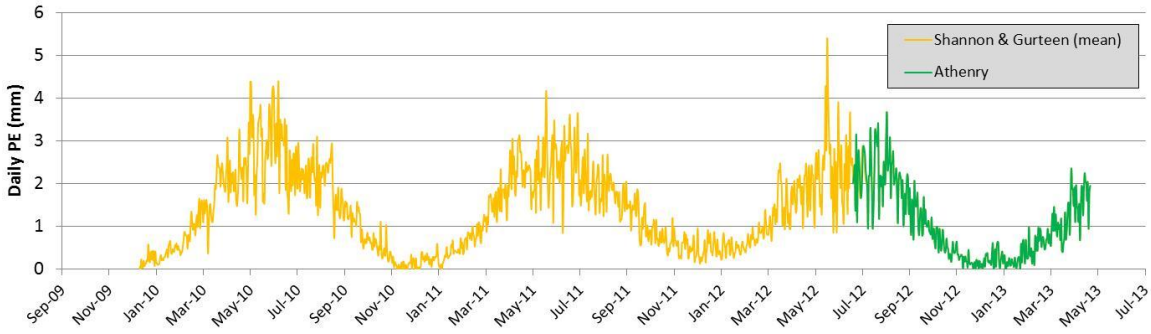

Figure 5.8: PE data used for the Gort Lowlands.

5.4 Rivers

As mention in Section 4.2.4**,** the three primary rivers (Owenshree, Ballycahalan, Beagh) feeding the catchment are monitored by the OPW. The Owendalulleegh River was also monitored by the OPW and the Owenshree River was monitored at a second location (Castle-Daly) as part of this research project. The river gauging stations all measured water depth but not flow and thus needed to be rated. In this section, the design of rating curves for the rivers is discussed as well as the estimation of river flows for periods of equipment failure at the river monitoring stations. See Figure 5.9 for an example of raw OPW water depth readings (with approximately 20% of the data missing).

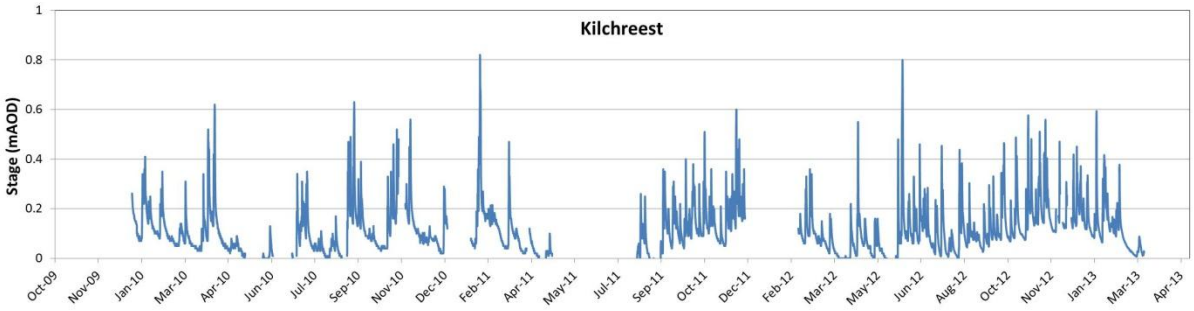

Figure 5.9: OPW water depth data for Kilchreest monitoring station (Owenshree).

5.4.1 Rating Curves

Rating curves have already been established for the rivers under study in this thesis (McCormack, 2009) and put to use with the hydrological model (Gill, 2010). However, these rating curves suffered from a lack of river flow measurements for high flow events. An extrapolation using the Velocity-Area method had to be used in order to estimate flows at high water levels. As a result of this extrapolation, there was a large degree of uncertainty with predictions of high flow events.

During 2012, five site visits were carried out with the sole purpose of collecting additional high flow data. In many cases, not all rivers were gauged as the peak flow had been missed. The measured flows are presented in Table 5.3. For ease of interpretation, the two gauging stations on the Owenshree River have been denoted as 'Kilchreest' (OPW station) and 'Castle-Daly'.

The updated rating curves for all rivers except Beagh River are shown in figures 5.10-5.13. For Kilchreest River, the Velocity-Area Method extrapolation was again used to get a better fitting rating curve. This extrapolation method was chosen over other methods such as Steven's Method and the Manning Formula due to their unlikely assumptions that the roughness coefficients would remain constant at higher discharges. The logarithmic method was also examined but the extrapolation was beyond the recommended limit of 20% higher than the highest gauged discharge. In Figure 5.10, error bounds are displayed in order to represent the typical range of error which could occur due to flow measurement error or natural variation of river flows (similar error bounds apply to all rivers but are not plotted in each graph). For each river, a best fit trend-line was applied to the data and its characteristic equation was used to convert stage measurements to flow.

Table 5.3: Additional river gauging measurments carried out as part of this thesis.

Date& time	River	Mean depth (m)	Mean Velocity (m/s)	Area (m^2)	Flow (m^3/s)	Stage (m)	OPW stage (m)
26/01/12 11.45	Ballycahalan	0.594	0.545	4.981	2.69	0.69	0.68
26/01/12 13.40	Owendalulleegh	0.856	0.615	9.419	5.80	1.29	1.29
26/01/12 13.40	Beagh	1.238	0.975	10.46	10.42	-	1.27
08/06/12 11.30	Kilchreest	0.85	2.21	8.83	19.5	0.8	-
08/06/12 12.45	Castle-Daly	1.375	1.42	6.753	7.01	-	-
08/06/12 14.00	Ballycahalan	1.4	1.58	11.62	2.746	1.60	1.55
08/06/12 16.00	Owendalulleegh	2.59	2.03	30.8	60.46	3.04	2.95
08/06/12 15.00	Beagh	1.5	1.11	15.15	16.46	1.22	1.22
15/06/12 15.45	Ballycahalan	0.55	0.601	4.564	2.746	0.70	0.71
15/06/12 12.00	Owendalulleegh	0.669	0.6	7.36	4.42	1.14	1.15
15/06/12 13.00	Beagh	0.947	0.873	8.273	7.294	0.70	1.15
16/08/12 15.00	Beagh	1.25	0.87	10.935	9.525	0.82	0.824
2/10/12 10.45	Kilchreest	0.597	0.749	5.97	4.47	0.325	0.314
2/10/12 11.30	Castle-Daly	1.022	0.88	5.02	4.46	-	-
2/10/12 14.15	Owendalulleegh	1.021	1.173	12.251	14.37	1.53	1.47

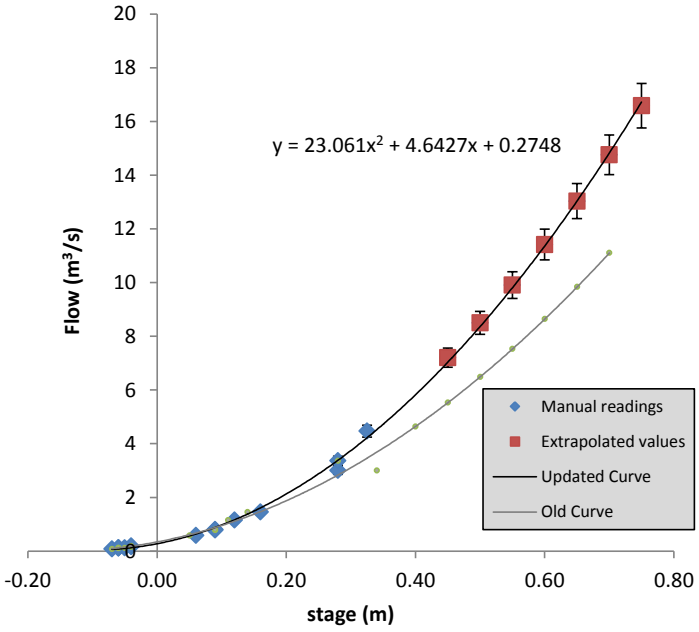

Figure 5.10: Owenshree River (Kilchreest) rating curve featuring ±5% error bounds.

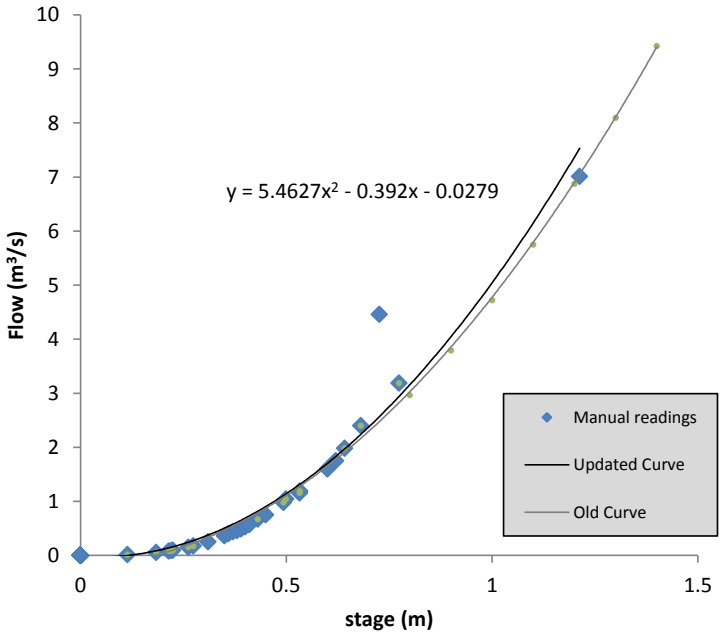

Figure 5.11: Owenshree River (Castle-Daly) rating curve.

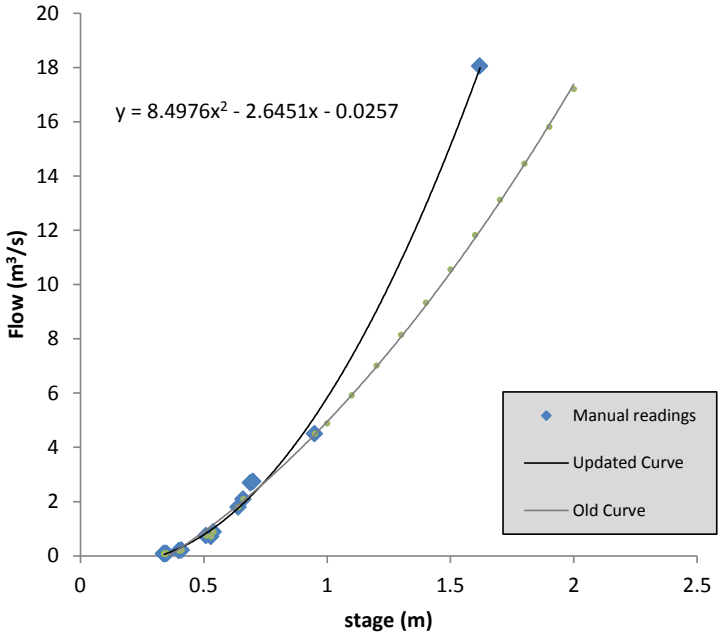

Figure 5.12: Ballycahalan rating curve.

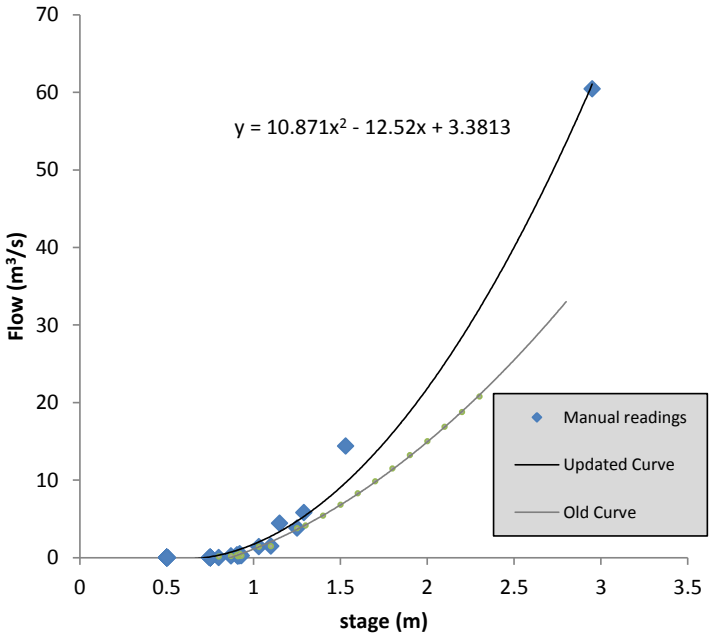

Figure 5.13: Owendalulleegh River rating curve.

From the above plots, it is clear to see that the updated stage-discharge curves are considerably different to the original curve (Grey line) in three of the four monitoring locations. In all cases, the flow has been increased for a given stage value. This has important consequences for the hydrological model which needs to be re-calibrated based on the increased flow volumes. It should be noted that the negative stage values depicted in Figure 5.10 are due the position of the datum lying above the river-bed.

The Beagh River monitoring station is the only station within the study that has been rated previously. Manual measurements of flow have been recorded by the OPW since the 1970's to construct a robust rating curve. This rating curve was chosen to be used in preference to the manual measurements recorded and used previously. See Figure 5.14 for the Beagh River rating curve as designed by the OPW (The green point represents a manual measurement taken in June 2012 which validates the OPW rating curve). This updated rating curve is significantly different to the original curve. Mid-range flows become approximately a third higher while high flow values are almost double those of the original curve.

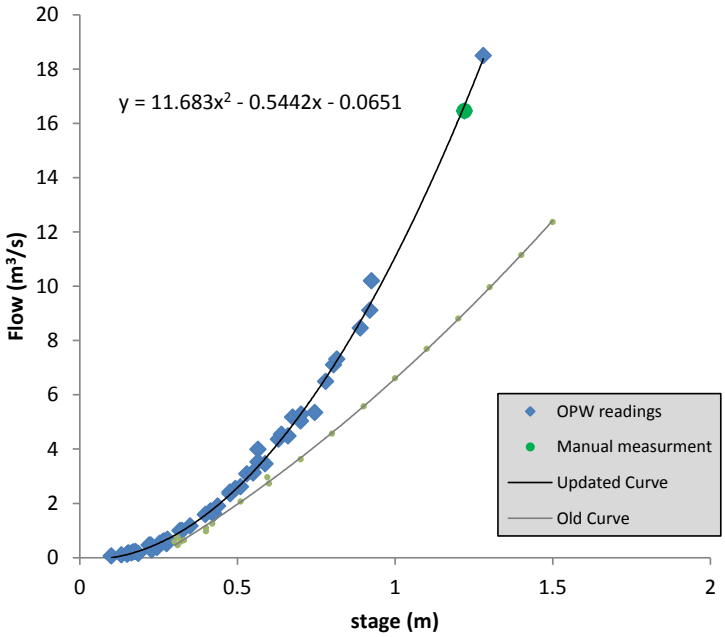

Figure 5.14: Beagh River rating curve.

5.4.2 Rainfall-Runoff Modelling

As seen in Figure 5.9, Kilchreest, Ballycahalan and Owendalulleegh monitoring stations suffered from equipment failure during the study period resulting in gaps in the dataset. As the hydrological model requires complete datasets from the rivers Owenshree, Ballycahalan and Beagh, the gaps in these datasets needed to be estimated using a rainfall runoff model. Between Kilchreest and Ballycahalan monitoring stations, over 11 months' worth of missing data needed to be estimated. The rainfall-runoff modelling software chosen to model the rivers was MIKE11-NAM (DHI Software).

MIKE11-NAM

MIKE11-NAM is a single-catchment watershed lumped-parameter model for simulating rainfall-runoff and the hydrological cycle. Developed in 1973 by the Department of Hydrodynamics and Water Resources at the Technical University of Denmark (Nielsen and Hansen, 1973), the model simulates the various hydrograph components using a moisture budgeting approach for different storages (O'Brien et al., 2013). The form of model structure applied to this catchment involved four storages: snow storage (which was omitted), upper (surface), middle (rootzone) and lower (groundwater) storages with the lower storage being split into two storages, one for shallow and one for deep groundwater. Overland flow and interflow were modelled as discharges from the

uppermost storage. The middle storage monitored soil moisture deficit in the catchment and acted as a control for overland flow, interflow and recharge occurrence. The structure of the NAM model is shown below in Figure 5.15.

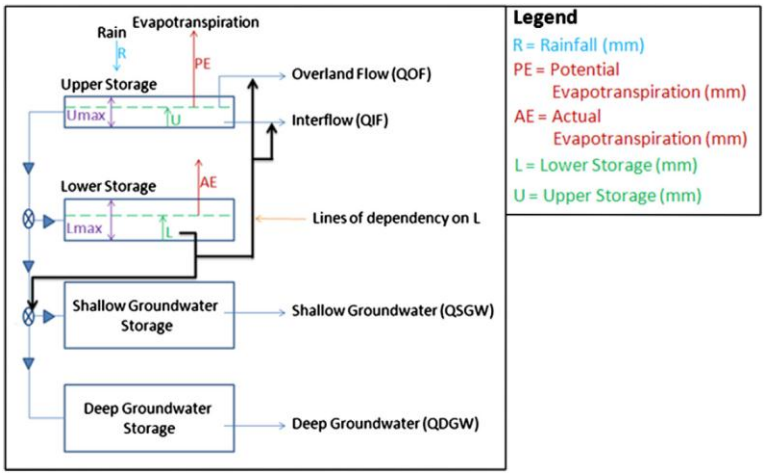

Figure 5.15: NAM conceptual structure (from O'Brien et al. (2013)).

A NAM modelling run calculation is based on nine hydrological parameters representing the surface zone, root zone and groundwater storages. Additional parameters can be used to account for snow melt, irrigation schemes and special cases (e.g. ground water storage influenced by river level variations). However, these provisions were unnecessary for modelling the Gort Lowlands. The hydrological parameters consist of the following (as described by the NAM users-manual):

Surface-rootzone parameters:

- **Maximum water content in surface storage (Umax)** – represents the cumulative total water content of the interception storage, surface depression storage and storage in the uppermost layers of the soil.
- **Maximum water content in the root zone storage (Lmax)** – represents the maximum soil moisture content in the root zone, which is available for transpiration by vegetation.
- **Overland flow runoff coefficient (CQOF)** – determines the division of excess rainfall between overland flow and infiltration.
- **Time constant for interflow (CKIF)** – determines the amount of interflow, which decreases with larger time constants.
- **Time constants for routing overland flow (CK1,2)** – Determines the shape of hydrograph peaks. High, sharp peaks are simulated with small time constants whereas low, longer peaks are simulated using large values of these parameters.

- **Root zone threshold value for overland flow (TOF) –** Determines the relative value of moisture content in the root zone (L/Lmax) above which overland flow is generated.
- **Root zone threshold value for inter flow (TIF) –** determines the relative value of moisture content in the root zone (L/Lmax) above which interflows is generated.

Groundwater parameters:

- **Time constant for routing baseflow (CKBF) –** determined from the hydrograph recession in dry periods.
- **Root zone threshold value for ground water recharge (Tg) –** determines the relative value of moisture content in the root zone (L/Lmax) above which ground water recharge is generated.

The following input data was required to carry out a NAM model calculation:

- **Setup parameters –** catchment area, soil properties etc.
- **Model Parameters –** as described previously.
- **Meteorological data –** precipitation and potential evapotranspiration. Data from multiple weather stations/rain gauges could be inputted and the percentage contribution from each specified.
- **Initial conditions -** initial values for surface, rootzone and groundwater model parameters.
- **Observed discharge data for model calibration**.

To calibrate the model, an auto-calibration function is available. After the required data has been input and model parameters estimated, the model is run for a single catchment. The autocalibration function calculated best fit values for the nine hydrological parameters based on the inputted observed discharge data. See Table 5.4 below for calibrated model parameters for Owenshree and Ballycahalan Rivers and Figure 5.16 for an example of observed and predicted runoff.

Table 5.4: List of optamised NAM hydrological parameters.

Catchment	Area (km^2)	Umax	Lmax	CQOF	CKIF	CK1	CK2	TOF	TIF	TG	CKBF	% Rainfall contribution
Owenshree	34.5	15.1	40.5	0.661	275.1	5.9	13.7	0.145	0.394	0.632	744	10% Kilchreest, 90% Francis Gap
Ballycahalan	47.7	26	979	0..772	795.1	12.2	5.5	0.0012	0.364	0.98	3987	0% Kilchreest, 100% Francis Gap

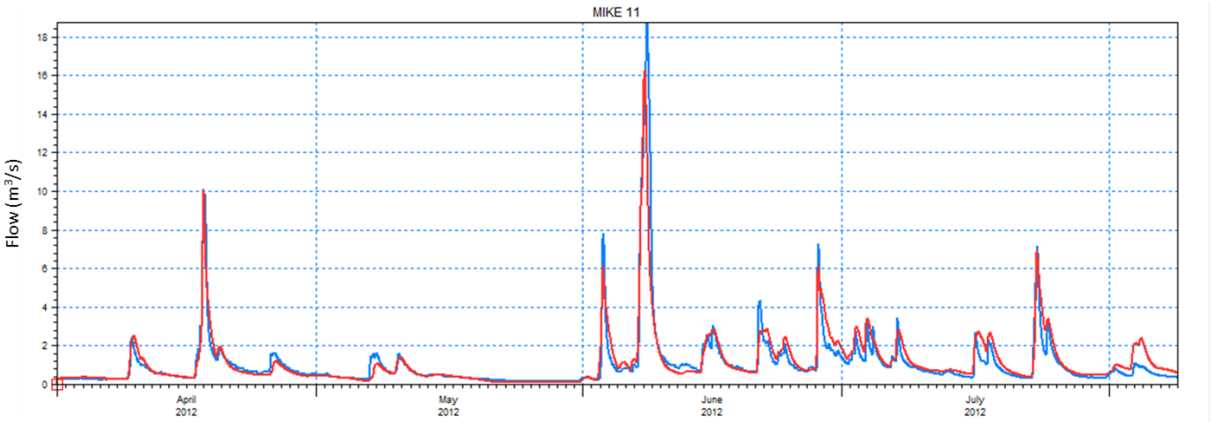

Figure 5.16: Example of observed (blue) & predicted (red) runoff for Kilchreest River (Summer 2012).

The two main performance statistics for goodness of fit are model efficiency (or R^2 – i.e. the Nash-Sutcliffe criterion) and bias. R^2 is calculated according to Equation 5.1:

$$R^2 = 1 - \frac{\sum(Q_o - Q_{sim})^2}{\sum(Q_o - \bar{Q}_o)^2} \qquad \textit{Equation 5.1}$$

where Q_o is the observed flow and Q_m is the modelled flow at each timestep (Lee and Singh, 1999). Bias is the overall error in volume (in mm/year) and is calculated as:

$$bias = \frac{\sum(Q_o - Q_{sim})}{n} \qquad \textit{Equation 5.2}$$

The results of the statistical goodness of fit tests are shown below in Table 5.5:

Table 5.5: Goodness of fit parametes for NAM results.

	Efficiency	Bias
Owenshree	0.871	0.000053
Ballycahalan	0.917	-0.1569

As can be seen from Table 5.5, the efficiency of the Ballycahalan NAM calibration is very good while the Owenshree calibration is marginally less accurate. Bias (the overall error in volume in mm/year) is negligible for both rivers. Using the calibrated NAM models for Owenshree and Ballycahalan rivers, the missing data could now be substituted with NAM predicted flow data to obtain full datasets (Figure 5.17).

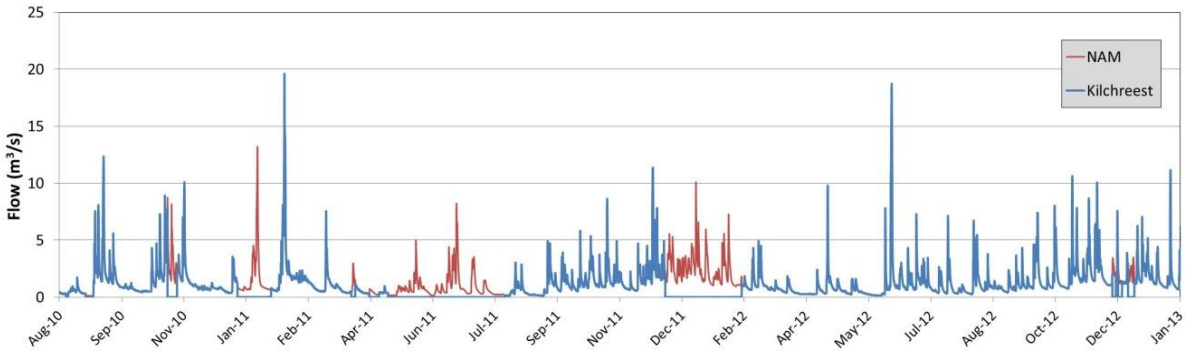

Figure 5.17: Owenshree River hydrograph with NAM flow estimations.

Attempts were made to calibrate NAM for the Owendalulleegh River catchment but these proved unsuccessful. The model was unable to simulate the rapid occurrence of peak flow in the river, the likely cause of which was unsuitable rainfall input data. The closest rain gauge available for calibration was the Francis Gap rain gauge. However this rain gauge was located beyond the north-most extremity of the catchment. In future studies, a rain gauge located within the Owendalulleegh catchment will be necessary for accurate rainfall-runoff modelling.

5.4.3 Analysis

5.4.3.1 Quantifying Flow Volumes

A quantitative comparison was carried out to determine the relative contribution of each river to the hydrological regime of the Gort Lowlands. Cumulative discharge time series were calculated for the year 2010. From Figure 5.18 it can be seen that Beagh River is the greatest contributor of autogenic recharge to the Gort area, supplying 55.3% of the cumulative discharge over 2010 with the Owenshree and Ballycahalan Rivers supplying 24% and 20.7% respectively. Owendalulleegh River was not included in this cumulative analysis as it transmits the same water as the Beagh River. It should also be noted that the majority of the flow in these rivers can be attributed to overland flow and interflow (lateral subsurface flow in soils and subsoil) with very little deep groundwater flow (O'Brien et al., 2013).

The average flows, peak flows and catchment sizes for the Owenshree, Ballycahalan, Beagh and Owendalulleegh Rivers for the years 2010-2012 are shown in Table 5.6. As expected, the River Beagh carries the largest average flow of 3.67 m^3/s compared to the Owenshree and Ballycahalan with 1.32 m^3/s and 1.26 m^3/s respectively. The Owendalulleegh River's average flow was not

calculated due to the extent of missing data although it can be assumed to be similar but slightly smaller than the Beagh River flow due to the contribution of the smaller Gorteenboy River (with catchment size: 8.2 km²) in the north east corner of Lough Cutra (Figure 5.19).

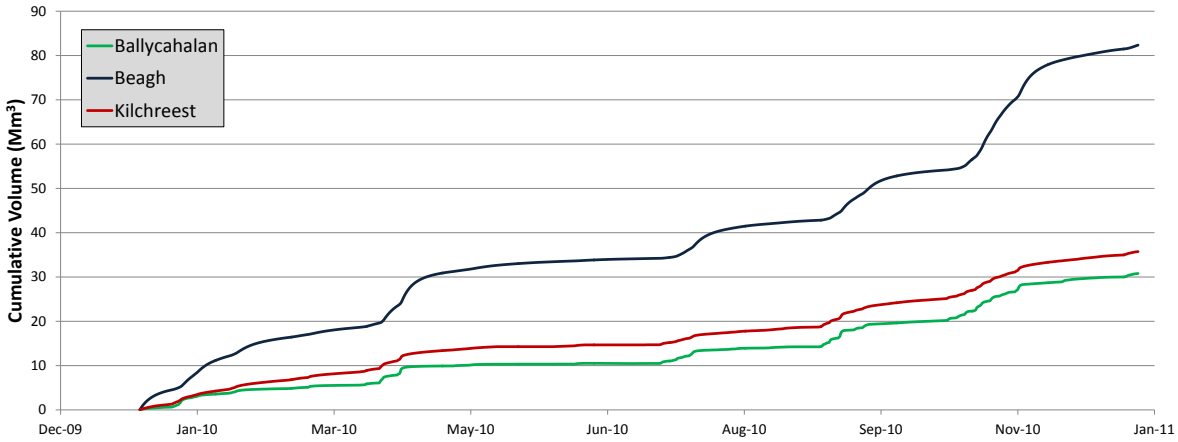

Figure 5.18: Cumulative flow for Owenshree, Ballycahalan and Beagh Rivers for the year 2010.

Table 5.6: Average and Peak flows for rivers (2010-2012).

River	Average Flow (m^3/s)	Peak Flow (m^3/s)	Catchment size (km^2)
Owenshree	1.32	19.6	34.5
Ballycahalan	1.26	44.3	47.7
Beagh	3.67	22.2	123.8
Owendalulleegh	*	72	89.3

* could not be calculated due to lack of full dataset.

The peak flows of the rivers are somewhat proportional to the size of catchment feeding them with the larger catchments providing greater amounts of rapid surface runoff. The River Beagh is an exception however due to attenuation and lagged response caused by Lough Cutra (3.9 km²), as can be seen in Figure 5.20. This lagged response is reflected by the flooding of the turloughs as the lower three turloughs, fed mostly (55%) by the River Beagh, flood and empty slower than the upper two turloughs which only receive water from the River Owenshree. The attenuation affect caused by Lough Cutra was analysed using the reservoir (or level-pool) routing method in Section 6.3.4.1.

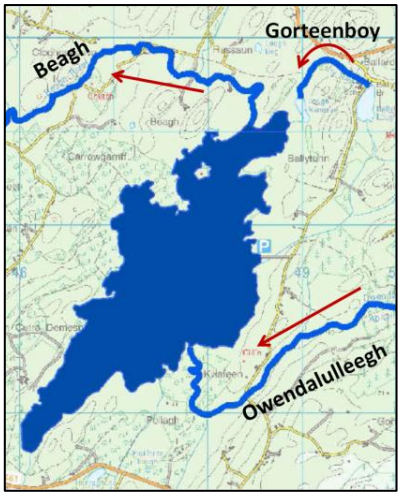

Figure 5.19: Lough Cutra and its feeding/receiving rivers.

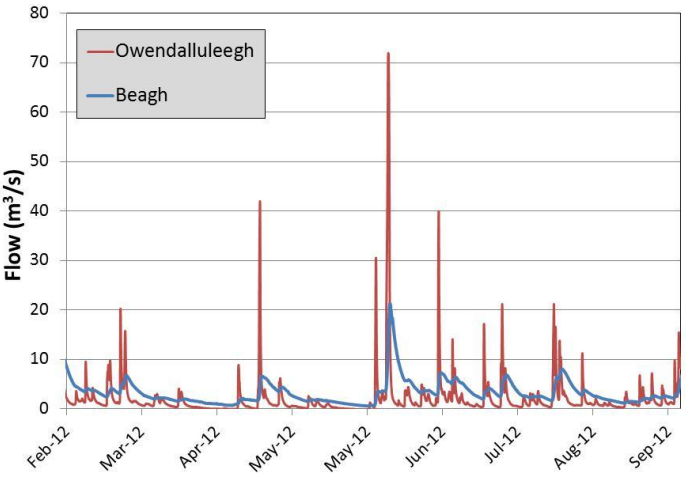

Figure 5.20: Owendalulleegh inflow and Beagh outflow from Lough Cutra.

5.4.3.2 Inflow to Blackrock Turlough

In March 2012, the Blackrock turlough diver was moved from a low point within the body of the turlough to the base of the largest estavelle. The reason for the change in location was to observe the dynamics of the estavelle at low flood levels. At low levels, the estavelle is known to behave as a sinking stream before the underground conduit network has reached its capacity and the estavelle starts to back up and flood the turlough. The flow required in the river for the underground network to reach its capacity is relevant for modelling purposes.

Comparing flows measured at Kilchreest gauging station to Blackrock turlough flood levels, the minimum flow required to begin flooding the turlough could be calculated. Between March 2012 and April 2013, during the periods when Blackrock turlough was dry, the Owenshree River experienced 19 river flow peaks of varying strength. On 14 of these occasions, the river peak exceeded 1.23 m^3/s and resulted in flooding of the turlough. As a consequence, it could be concluded that 1.23 m^3/s is the maximum flow allowed by the Owenshree River before the underground capacity has been reached. Figure 5.21 provides an illustration of this with flows exceeding 1.23 m^3/s being highlighted by red circles and flows below 1.23 m^3/s highlighted by purple circles.

Over the analysis period, one exception could be found where a flow peak of 1.23 m^3/s did not result in the flooding of the turlough (not shown in Figure 5.21). This was due to the fact that the

turlough had only emptied 12 hours previous to the flooding event. The 12 hours between floods was evidently not a long enough period for the conduit network to restore its capacity.

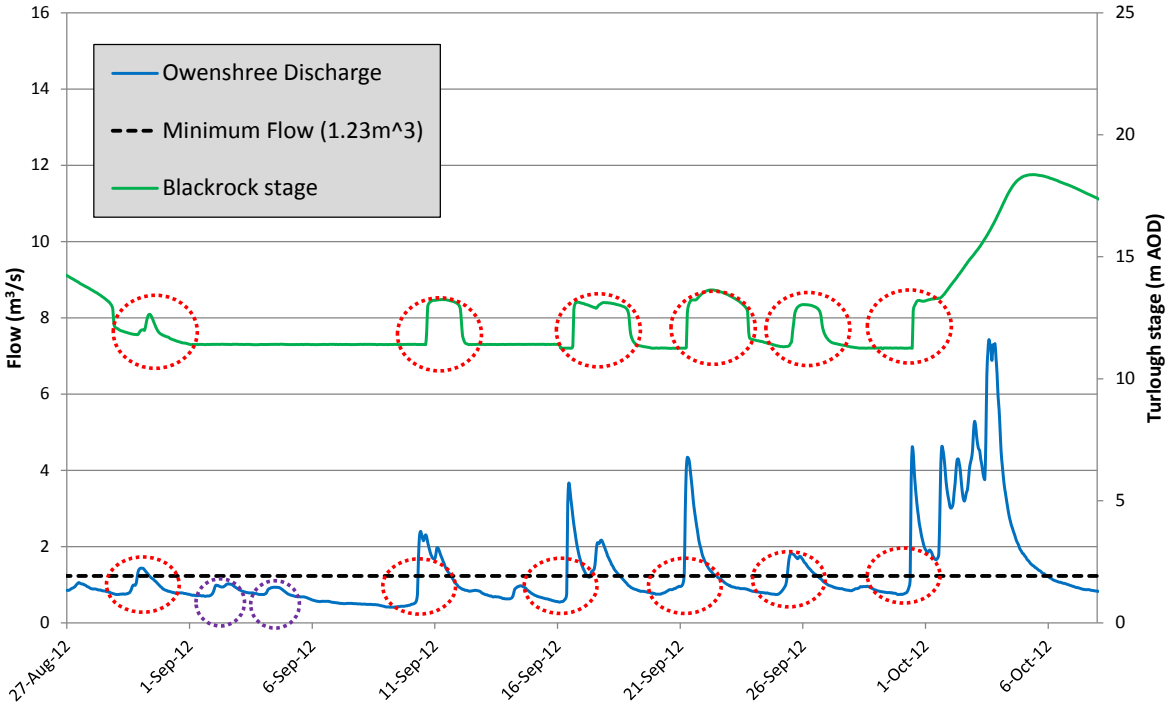

Figure 5.21: Owenshree flow & Blackrock turlough level (August-October 2012). Red circles indicate periods when flow exceeds 1.23m³/h and thus causes a response from the turlough.

5.5 Groundwater

Groundwater levels within the catchment were monitored using a range of boreholes and wells. Of the 18 boreholes/wells studied, 12 were accessible for observing groundwater level using a dipper and 7 of these 12 wells were instrumented with divers for continuous measurements at some point during the study period. The data shows a wide range of water level fluctuations between boreholes, no matter the distance between them. This is a typical characteristic of highly karstified areas (Ford and Williams, 2007). See Figure 5.22 for an example of two extremes of water level fluctuation within the catchment (from boreholes 2.5 km apart). Note: continuous lines indicate diver data, dashed lines with points indicate monthly dipped levels.

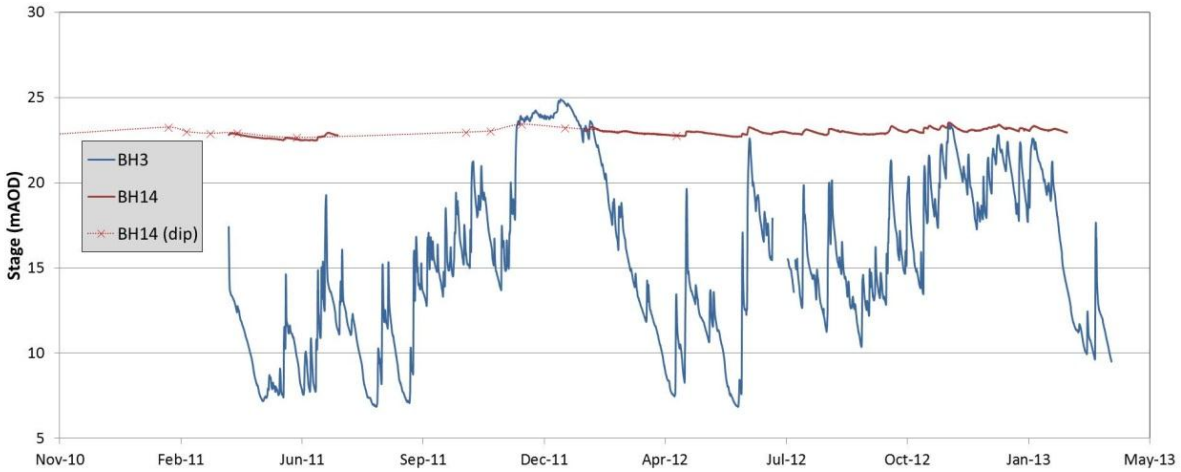

Figure 5.22: Various degrees of borehole water level fluctuation within the catchment. Solid line represents continuous monitoring using a diver. Points and dotted line represent point measurements and interpolation.

In this section, hydrographs and groundwater fluctuations are to be interpreted in terms of their hydrological significance to the conceptual model of the groundwater regime. It should be noted that there are a number of limitations in interpreting this data, due to either lack of information or monitoring constraints. These limitations include:

- Domestic wells of unknown depth and construction.
- Domestic wells are intermittently pumped which could affect the recorded water level.
- Borehole may penetrate different geological formations (including drift), each with potentially differing water levels.
- Monthly dipped data may miss rapid recharge events.

Water level fluctuation within the catchment was monitored previously as part of the fieldwork for the Gort Flood Studies Report during the 1990s. In this report, groundwater level fluctuations were mapped out in terms of three degrees of fluctuation: less than 3m, greater than 3m and tidally influenced. This map (along with the locations of boreholes monitored in this thesis) is presented in Figure 5.23. From the map, the preferential flow pathways are clear to see with areas of high fluctuation following the known conduit paths, implying low storage and high transmissivity. Also visible in the map is the possible northern flow route as suggested by tracing studies carried out during the Gort Flood Studies.

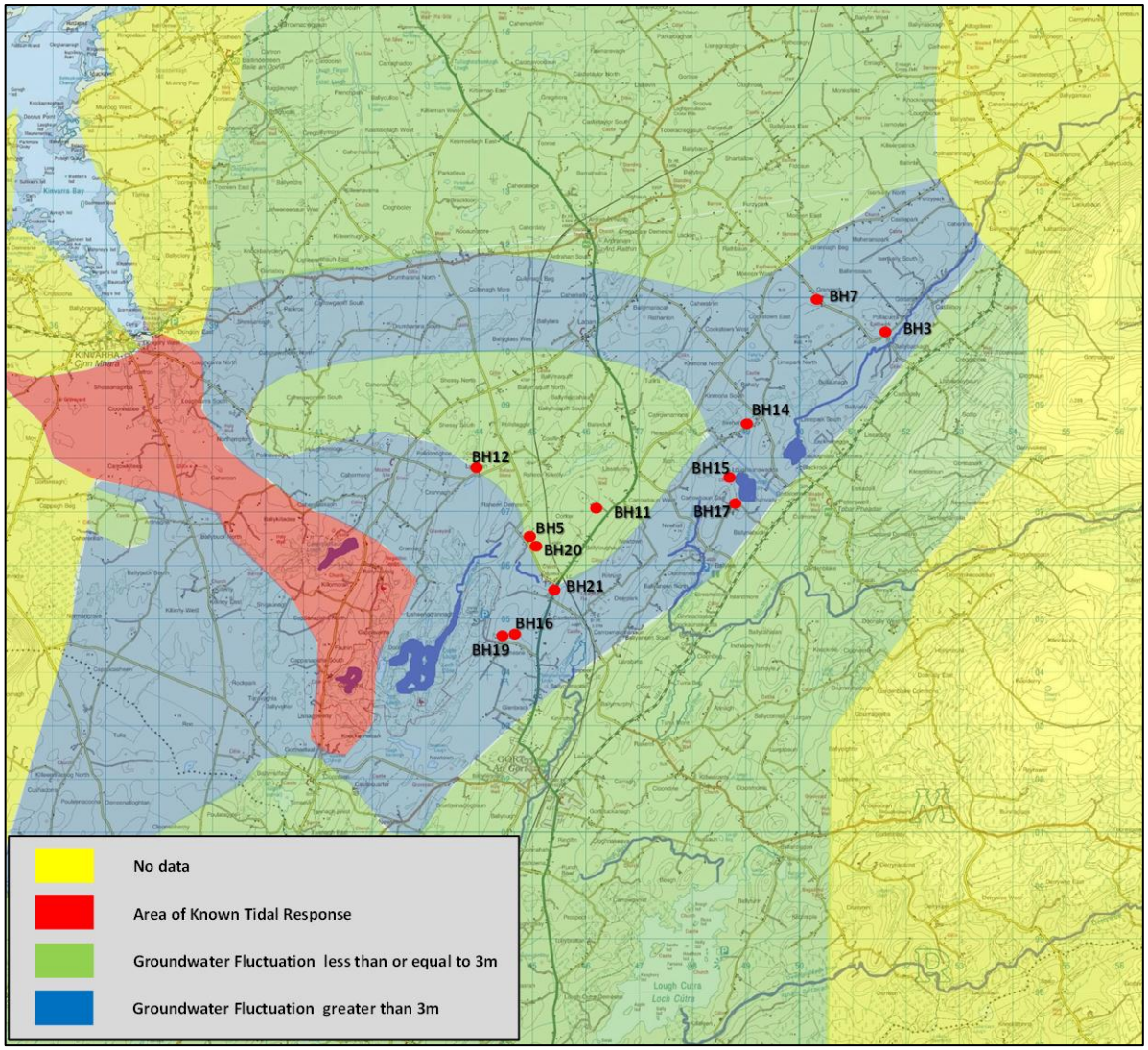

Figure 5.23: Borehole locations in this study superimposed upon groundwater level fluctuations as mapped out by the Gort Flood Studies (Southern Water Global, 1998).

Based on water level fluctuation, the boreholes in this thesis can be described as either responsive or non-responsive. Responsive boreholes are those that vary in water level by greater than 3m or show a high degree of conformity with the conduit network. Non-responsive boreholes are those that showed little variation indicating that they were separate from the conduit network, instead fed by the more diffuse epikarst portion of the catchment.

RESPONSIVE

BH3

BH3 is located along the Owenshree River approximately 3 km north-east of Blackrock turlough. The borehole was instrumented with a diver between April 2011 and March 2013 and showed a high degree of correspondence with Blackrock turlough (Figure 5.24). This correspondence suggests that the borehole has accessed a fracture layer hydraulically connected to an underground conduit feeding Blackrock turlough. Evidence of this suspected underground conduit has already been witnessed during dry periods when the Owenshree River has been seen sinking into its riverbed.

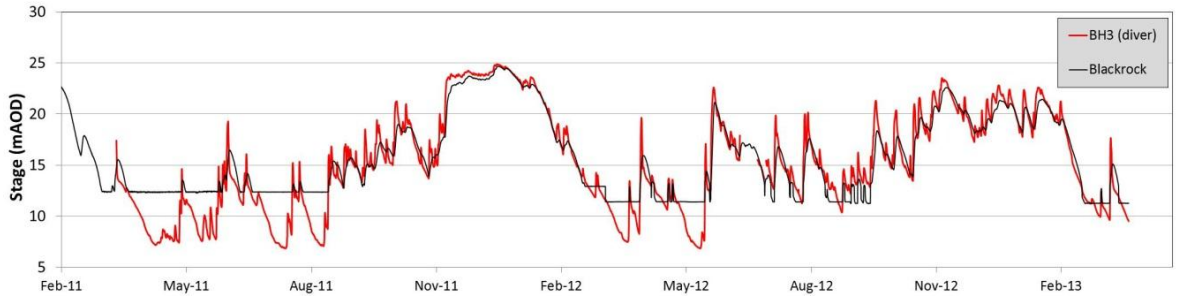

Figure 5.24: BH3 & Blackrock turlough water levels (Feb 2011-Mar 2013).

The speed of response of BH3 is striking. Its long term trend follows that of Blackrock turlough but in the short term, it responds rapidly to river flows in the nearby Owenshree River (250m away) with the borehole capable of rising up to 10m in 30 hours following a river surge. See Figure 5.25 below for a comparison of river flow and borehole level (note: river flow data is from the Castle-Daly gauging station. As such, its accuracy is uncertain).

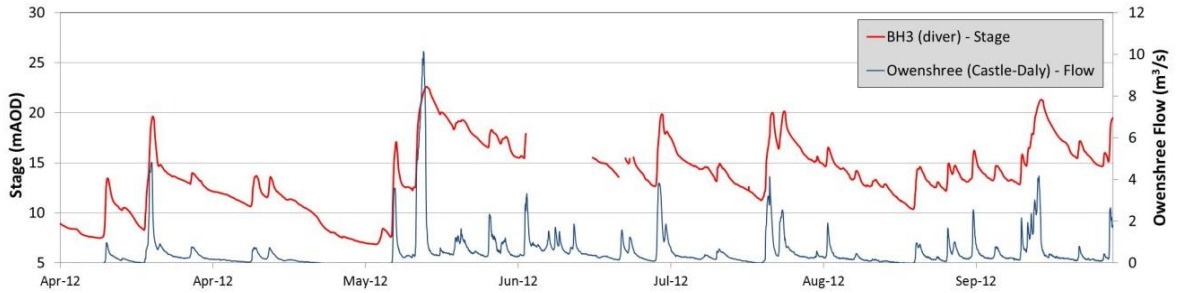

Figure 5.25 BH3 water level & Owenshree flow (Apr-Sept 2012).

BH7

Similarly to BH3, BH7 follows the pattern of Blackrock turlough closely. However the pattern is slightly more damped than that of BH3 with high water levels not reaching the heights of Blackrock

Figure 5.26. Yet the pattern is still significant considering that the borehole is approximately 1.4 km from the Owenshree River. Perhaps the borehole lies close to the northern flow route transmitting flow from Castle-Daly towards Kinvara.

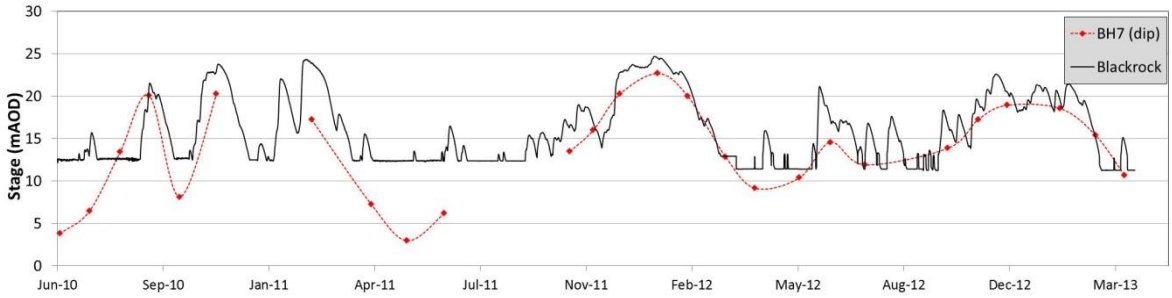

Figure 5.26: BH7 & Blackrock turlough water levels (Jun 2010-Mar 2013).

BH17

BH17 is a domestic well for a property located beside Coy turlough. At high flood levels, the well could be less than 50m from the water's edge. As a result, the water level in the well almost matches the water level in Coy turlough. This shows evidence of a highly fractured epikarst layer surrounding the turlough (or suggests that BH17 lies very near to the conduit feeding Coy).

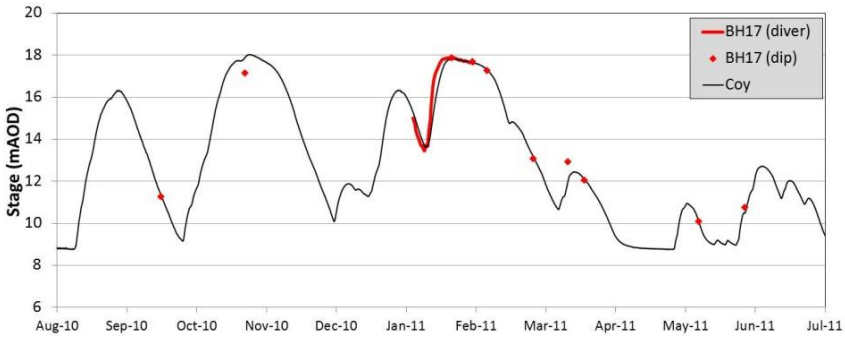

Figure 5.27: BH17 & Coy turlough water levels (Aug 2010-Jun 2011).

BH12

BH12 is an abandoned public water scheme for the Crannagh town-land approximately 2.5 km north of Coole and Caherglassaun turloughs. The location is not thought to be connected to the primary Gort Lowlands conduit network but does lie next to a separate turlough known as Lydacan. This turlough acts more like an epikarst, diffuse fed turlough with slow floods and recessions and hydrochemically different water supplying it. This slower flooding and receding pattern is echoed by the water level observed in BH17. See Figure 5.28 for a graph of this (Note: Lydacan turlough was not gauged so Coole turlough is used in this graph for illustrative purposes).

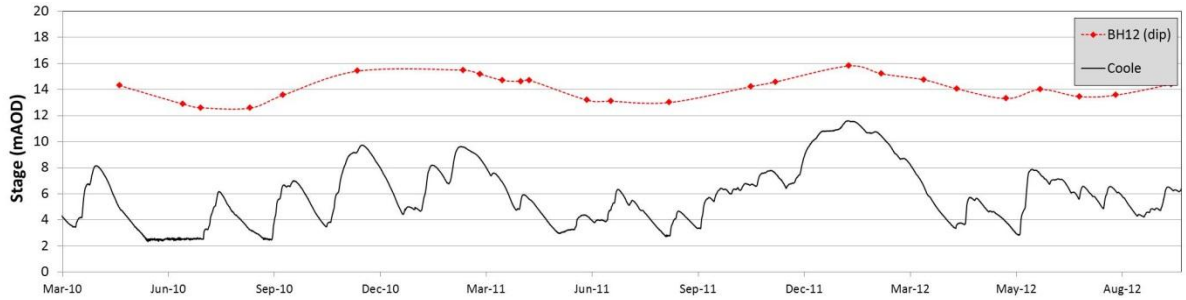

Figure 5.28: BH12 & Coole turlough water levels (May 2010–Aug 2012).

Boreholes BH5 and BH16 also showed variation exceeding 3m and are likely to be responsive boreholes but were not shown here as regular abstraction from these wells made them little use for analysis purposes (see Appendix C).

NON-RESPONSIVE

As can be seen in Figure 5.29 below, a number of wells showed very little fluctuation over time. These wells (BH11, BH14, BH15, BH19, and BH21) remain relatively still irrespective of the dominant hydrological conditions at the time. This suggests the wells have been dug into a slow moving epikarst layer with little or no interaction with the active conduit network.

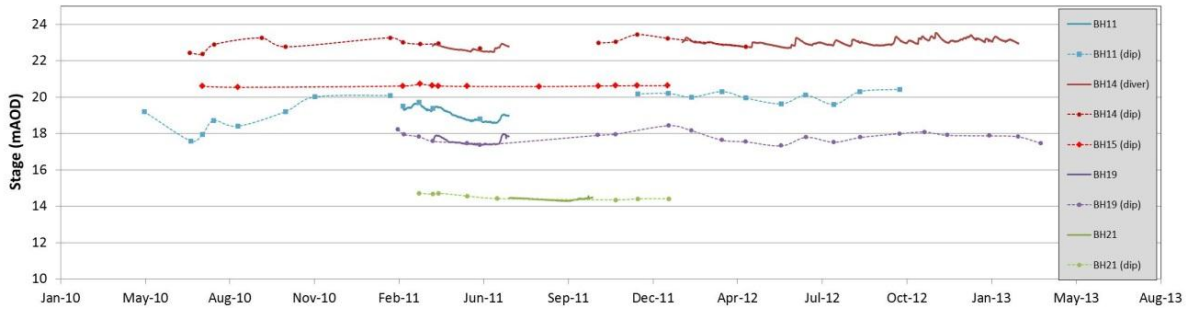

Figure 5.29: Non-Responsive boreholes/wells water levels (Jan 2010 – May 2013).

Upon closer inspection of BH14, an old stone well approximately 1 km north of Coy, the well turns out to actually be linked to the active system but with only minimal impact. For example, in early June 2012, Blackrock turlough flooded 9m in three days. In the same period, BH14 rose just under 50cm (Figure 5.30). This suggests that the well is linked very distantly to the active conduit system by a network of very fine fractures. During periods of extreme flooding however, the well is known by the local population to become suddenly active and flood the locality. This occurred during the

floods of November 2009 causing widespread flood damage to nearby homes. This suggests that once a certain underground water level has been reached, a higher level connection is established between the active conduit network and the well. The higher level connection is likely to have wider fractures than the lower level judging by the rapid flooding caused in November 2009.

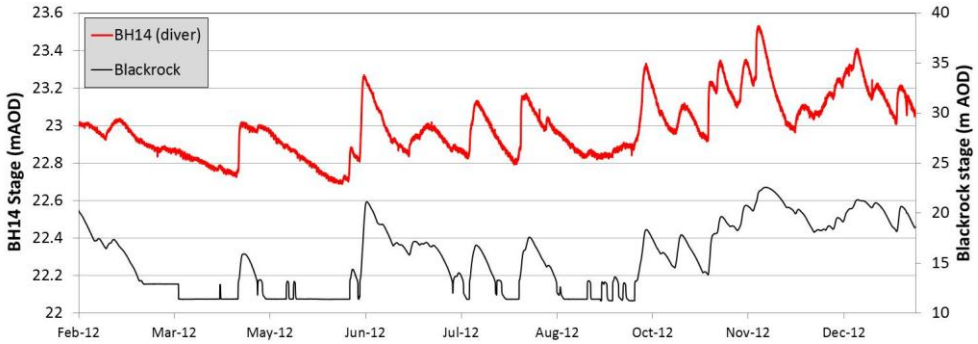

Figure 5.30: BH14 (small scale) and Blackrock turlough comparison.

Another example of a well that becomes hydrologically active only during high water level periods is BH20. The water level in the well typically varies between 10 and 11 mAOD but doing winter 2011/2012 when the nearby Coole turlough rose above 10 m, the well rose up to 12.5m in response (Figure 5.31).

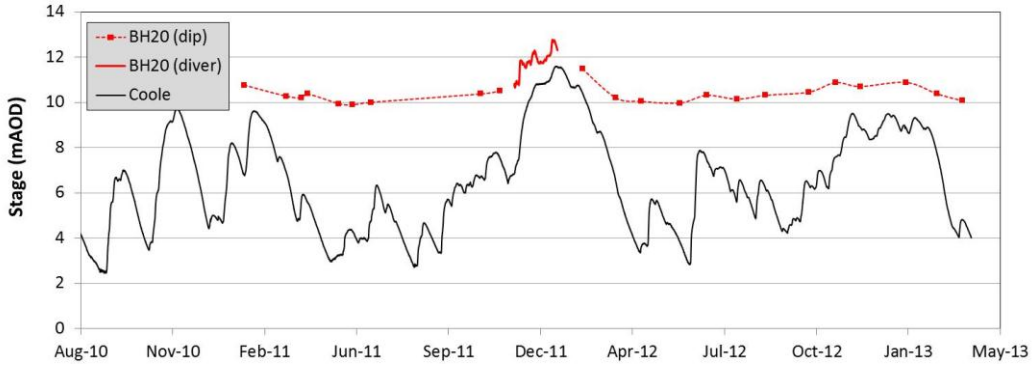

Figure 5.31: BH20 and Coole turlough water levels (August 2010 – May 2013).

In some examples, the lack of hydrological connection to the turloughs can be striking. BH15 is a stone well located within 100m of the edge of Coy turlough. The water level in this well remains constant year round, irrespective of the water level in the nearby turlough. This indicates an elevated water table surrounding Coy which remains higher than Coy at all times throughout the year. As such, a hydraulic gradient exists between Coy and its surrounding epikarst catchment and this gradient increases with reductions in Coy water level. A similar situation was found with

Coole turlough and the nearby borehole, BH19. These hydraulic gradients between the turloughs and their surrounding epikarst catchments are relevant as hydrochemical results indicate seepage from this epikarst into the turloughs, particularly during recession periods (Section 7.2).

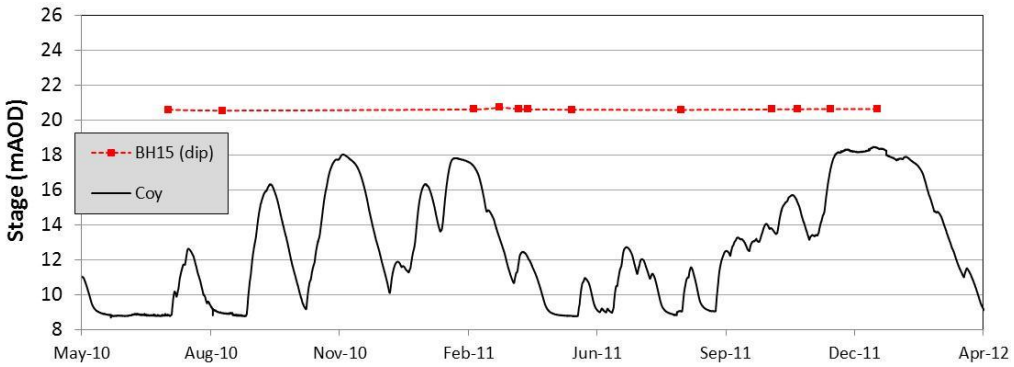

Figure 5.32: BH15 and Coy turlough water levels (May 2010 – April 2012).

5.6 Tide

Accurate tidal data is of key importance when it comes to the running of the hydrological model. As the system outlet is inter-tidal, the total outflow is very sensitive to tidal level. As mentioned in Section 4.4, tidal data was obtained from the Marine Institute for a gauge located in Galway Port. In previous studies using the hydrological model, the tide data from Galway Port was inputted into the model directly. However during 2012, a series of studies of Kinvara Bay were carried out involving CTD divers being placed at various locations around the bay. These divers recorded tidal depth at 15 minute intervals over two months and found a delay of 72 minutes between Galway Port tidal peak and Kinvara tidal peak (Figure 5.33).

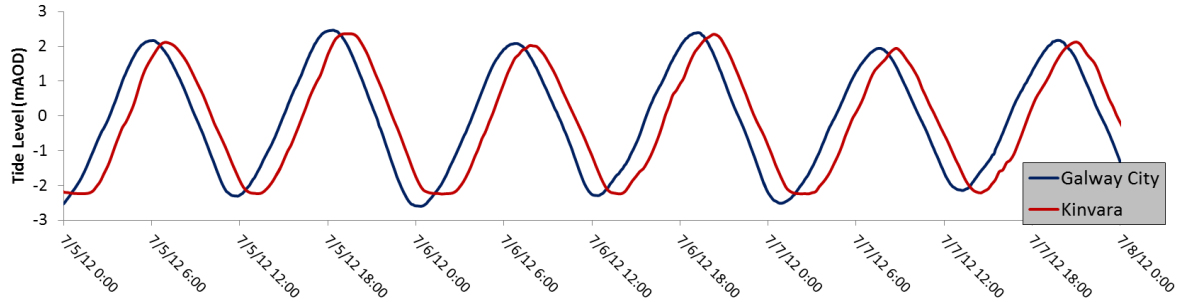

Figure 5.33: Tidal data for Galway city and Kinvara. Note the 72 minute offset between the two locations.

An offset of 72 minutes is quite significant for Kinvara Bay and Galway City which are only 16 km apart; especially considering that Inishmore tidal gauge located on the Aran Islands approximately

50 km away appears to have no offset from Galway City (Gill, 2010). The reason for the offset could be put down to the constriction caused by the shape of the Bay. A similar effect is also found at the nearby Bell Harbour Bay which lies 5 km west of Kinvara. A study by NUIG found the similarly sized bay to have a 45 minute offset from Galway Port (Perriquet et al., 2012).

Chapter 6

Pipe Network Modelling

6 PIPE NETWORK MODELLING

6.1 Introduction

The Gort Lowlands chain of turloughs was first modelled as part of the Gort Flood Studies Report during the 1990's. Due to the highly heterogeneous nature of the Gort Lowlands catchment, it was decided that an equivalent porous media model would not be suitable. Instead, the sewer network analysis model, *Hydroworks* (Wallingford Software) was used as it could adequately simulate the confined groundwater conditions found in the Gort Lowlands catchment. Despite a number of issues (mentioned in Section 3.5.1.2) the model performed reasonably well. For an illustration of the layout of the Gort Flood Studies model, see Figure A.16 in Appendix A.

The next attempt of modelling the Gort Lowlands was that of Gill (2010) who combined the pipe network approach with a groundwater infiltration module in an effort to account for the epikarst contribution to the hydrological regime. The hydraulic model was built using *Infoworks CS* version 8.5 (Wallingford Software) which incorporates the *Hydroworks* modelling engine. This software enabled the modelling of diffuse/epikarst recharge using a network of subcatchments and porous pipes which could simulate lateral inflow. This model also benefited from several years of accurate turlough water level data and accurate GPS surveying. An updated version of the model, recalibrated for better accuracy, was published by Gill et al. (2013a).

In this chapter, the model of Gill et al. (2013a) is subject to a sensitivity analysis and following some re-adjustment and re-calibration, the model is used for analysis. However first, the results of a physical model study of Blackrock and Coy turloughs will be presented.

6.2 Physical Model:

In an effort to understand the hydrodynamics of the turloughs, a simple physical model was constructed consisting of two tanks and a network of pipes. The tanks represented two turloughs (an upper and a lower) and the pipes represent the underground conduit network connecting the turloughs. As the model was to be used for illustrative purposes and not detailed analysis, it was not designed as an exact scaled version of any turloughs. It was however broadly based on the conceptualisation of Blackrock (upper) and Coy (lower) from Gill (2010) (see Figure 6.1). Some alterations to Gill's conceptualisation were made such as the addition of a surface input and removal of the upper bypass.

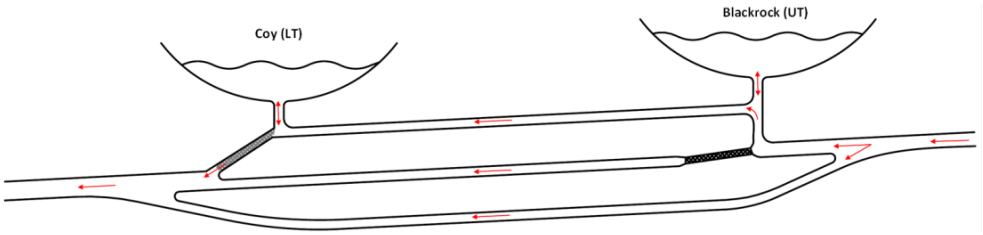

Figure 6.1: Blackrock-Coy conceptualisation from Gill (2010).

The layout of the model can be seen in Figures 6.2 and 6.3. It consisted of:

- An inlet pipe fed by a constant head tank with a flow meter attached. (*Micronics Portaflow 330* with accuracy of ±3%)
- Two model input sources representing surface and conduit inputs.
- Two 20 L tanks representing turloughs with depths monitored by two Linear Variable Differential Transformers (LDVT) linked to a datalogger.
- A network of ¾″ and ½″ plastic pipes representing the underground conduit network. The ½″ pipes were used for the bypass and the surface input with the ¾″ pipes used for the rest of the system.
- Seven tap valves used to control flow at different locations within the system. The valves could be used to activate/deactivate different model components such as the bypass and surface inlet or could be used to constrict flow at certain locations representing underground throttles.

From this point onwards, the two tanks will be described as 'Upper Turlough' or 'UT' and 'Lower Turlough' or 'LT'. A full schematic of the model components and their titles is shown in Figure 6.3.

Figure 6.2: Photo of physical model.

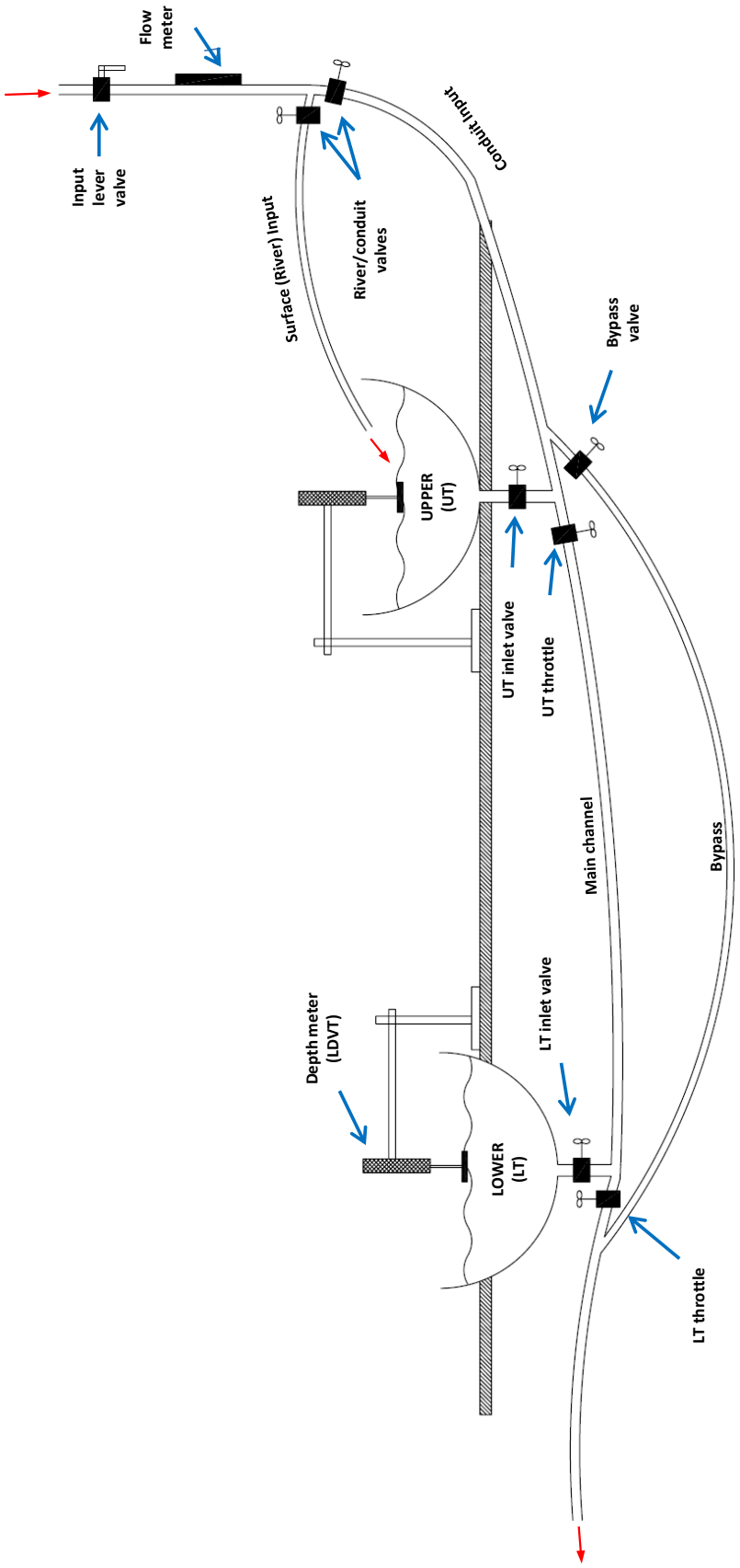

Figure 6.3: Physical model schematic.

6.2.1 Results

6.2.1.1 Preliminary Investigations

The first stage of physical modelling involved a series of initial tests carried out in order to understand the boundaries of the system (e.g. maximum flows, time taken to fill tanks etc.).

MAXIMUM FLOWS

The model was equipped with two separate sources of flow input, the surface (river) input and the conduit input. The relative contribution of each input into the system could be altered by adjusting the relevant tap valves (throttles) and fine-tuning the flow with the aid of the flow gauge. The maximum flows possible for each input were the following:

- Conduit alone: 21 L/m
- River alone: 15 L/m
- River and Conduit combined: 30.6 L/m

Although these input flows could be reached, they could not be maintained as the tanks and the sink would overflow. For this reason, flows chosen for testing were kept much below the maximum.

IMPACT OF VALVES

Tap valves were used to control flow within the system. However their impact on flow was not directly observable. To gauge the effect caused by constricting a valve, a number of simple tests were run whereby the effect caused by one valve was measured. Valve adjustments were recorded in terms of the number of turns used. Each valve could be turned 3 ¾ times from open to closed. The results of adjusting the conduit inlet valve (with river inlet closed) are shown below:

- Fully open: 21 L/s
- One turn closed: 20.4 L/s
- Two turns closed: 20.4 L/s
- Three turns closed: 19.8 L/s
- 3¼ turns closed: 11.4 L/s

It is clear to see from the above results that the valves only caused a significant impact to the flow with greater than three turns applied to them. This test was also carried out on the river input with similar results. See Figure 6.4 for a photo of the throttles installed under the upper tank (UT).

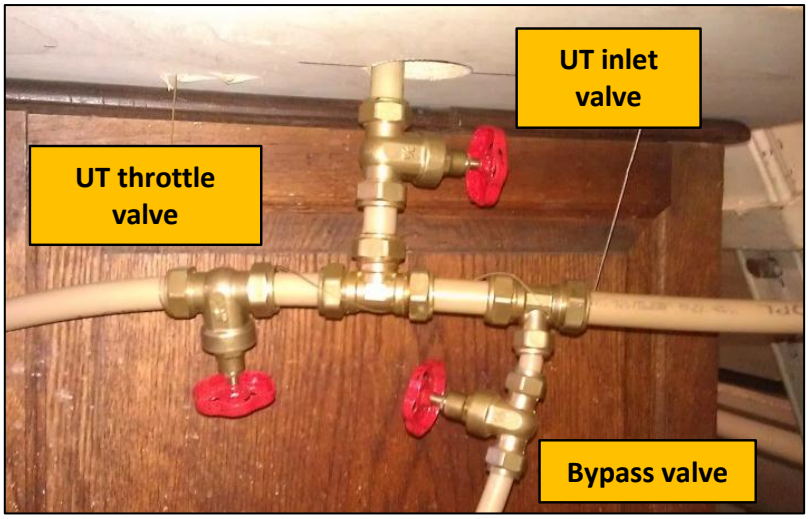

Figure 6.4: Tap valves underneath the Upper Turlough (UT).

CHOICE OF SYSTEM INPUT

In order to carry out testing efficiently, an input signal needed to be chosen that could be replicated multiple times for a range of tests. A comparison between two input signals was carried out to determine the practicality and efficiency of each. The first signal (Figure 6.5) consisted of a rising flow input and a recession built with short time-steps. The second signal (Figure 6.6) consisted of only two flow stages with no recession.

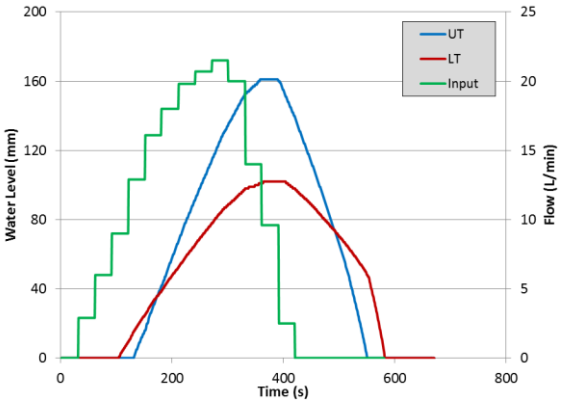

Figure 6.5: Input signal 1.

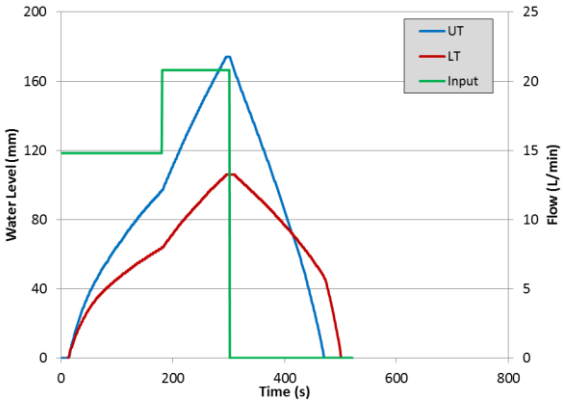

Figure 6.6: Input signal 2.

From the figures above, little difference (in terms of the goals of this study) can be seen between the tank water levels resulting from each input. Considering this and the fact that two inputs is easier to replicate than multiple inputs, a two flow input signal was chosen.

6.2.2 Effect of Bypass

The effect of the bypass was demonstrated by two tests - with the bypass closed and with the bypass open. For these tests, the input signal was a flow of 14.8L/m (2 ¾ turns closed) for 3 minutes followed by 20.8L/m (2 ¼ turns closed) for two minutes being transmitted through the lower conduit input. All non-relevant throttles were left open. The results of the tests are shown below in Figures 6.7 and 6.8.

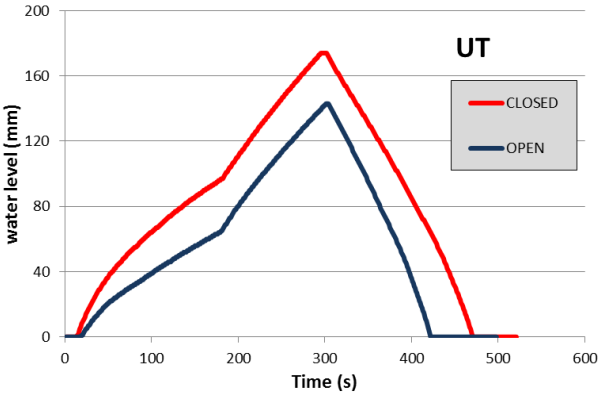

Figure 6.7: Effect of bypass: UT.

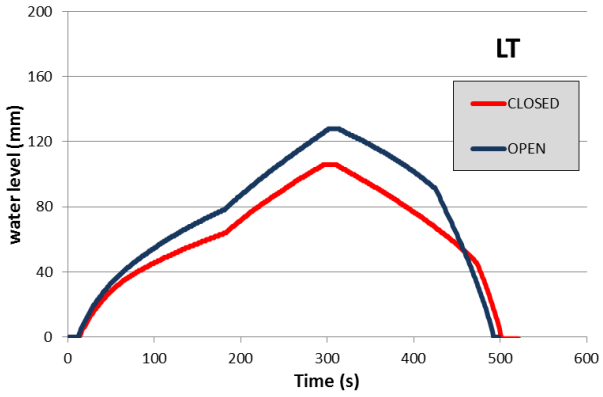

Figure 6.8: Effect of bypass: LT.

As can be seen from the figures above, the presence of a bypass reduces peak height and recession of UT while LT increases peak height but hastens its recession.

6.2.3 Effect of Inlet Constriction

Both tanks were fitted with tap valves along their inlet pipe. These valves could be constricted to observe the effect of narrowing the width of the inlet feeding/draining the tanks. For these tests, the bypass was left open and only the conduit inlet was used.

The effect of constricting UT inlet is shown in Figures 6.9 and 6.10. From these figures, it can be seen that constricting the inlet to UT reduces its peak and lengthens its recession. For LT, the constriction on UT's inlet increases peak height and speeds up recession. The changes in peak heights are due to the fact that the inlet constriction allows more water to reach LT rather than UT, thus reducing UT's peak and increasing LT's peak. Then in recession, there is more 'room' for flows out of LT relative to UT because UT's contribution to the pipe network is less. As a result, the recession of LT is sped up while UT's recession slows down as it has a reduced drainage capacity.

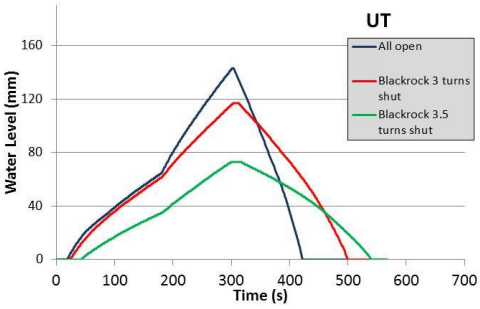

Figure 6.9: Constricting UT inlet (UT).

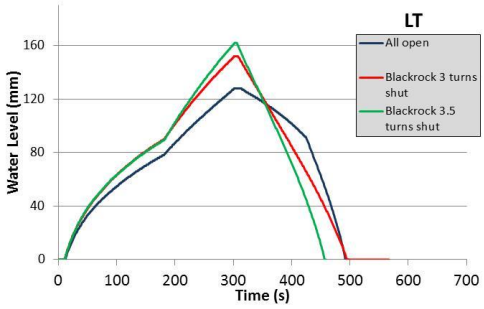

Figure 6.10: Constricting UT inlet (LT).

In Figures 6.11 and 6.12, the effect of constricting LT's inlet can be observed. UT peak increases with little change in recession while LT reduces in level and increases recession length. This increased peak/volume of UT is due to the slight backing-up affect caused by the constriction of LT's inlet. The reduction in peak/volume of LT is due to less water filling the tank but once the water has entered the tank, it is harder for it to drain away, thus the recession is lengthened.

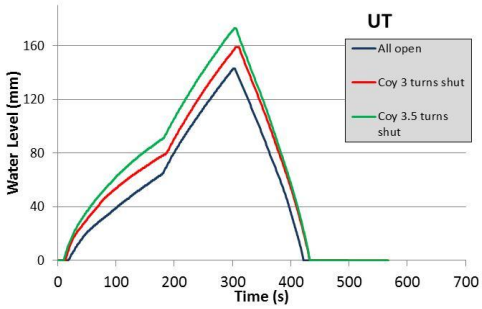

Figure 6.11: Constricting LT inlet (UT).

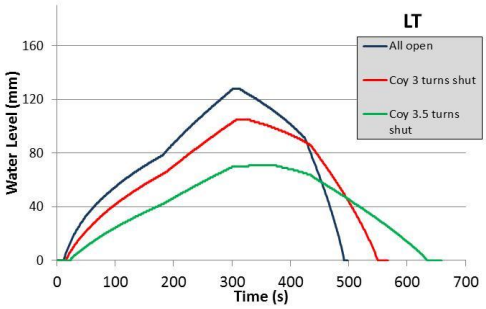

Figure 6.12: Constricting LT inlet (LT).

Constricting both inlets leads to a reduced peak and increased recession for both tanks (Figures 6.13 and 6.14)

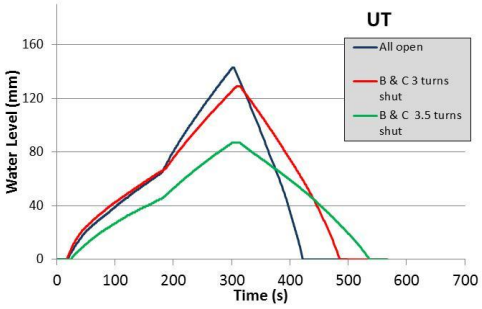

Figure 6.13: Constricting both inlets (UT).

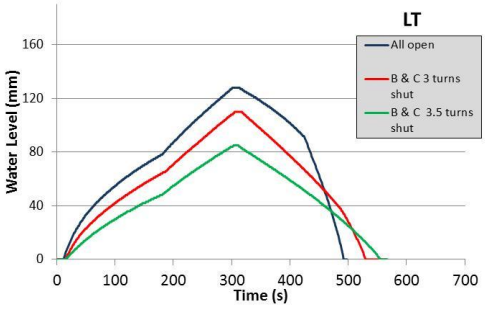

Figure 6.14: Constricting both inlets (LT).

6.2.4 Effect of Throttles

A range of tests were carried out on the throttle valves (the valves located just downstream of the tanks). Valves were set as either: open, two turns closed and three turns closed. All valve combinations were tested for both bypass open and bypass closed scenarios.

When a strong throttling effect was applied to a tank, the water level rose rapidly. As a result, the input signal for the tests had to be altered in order to prevent the tanks overflowing. The input signal was shortened to a flow of 14.8 L/min for only two minutes. The effect of UT and LT throttles (with bypass closed initially) is displayed in the sections below:

UPPER TURLOUGH (UT) THROTTLE

As can be seen from Figures 6.15 and 6.16 below, both tanks are impacted significantly by UT throttle. The more constricted the UT throttle, the higher UT gets and the lower LT gets. In essence, when UT is throttled, storage capacity from LT is transferred to UT. At three throttle turns, LT does not receive water at all with all storage going into UT.

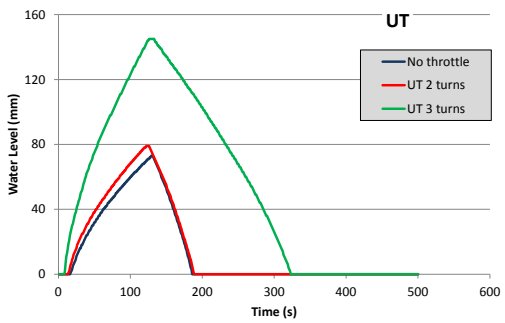

Figure 6.15: Constricting UT throttle (UT).

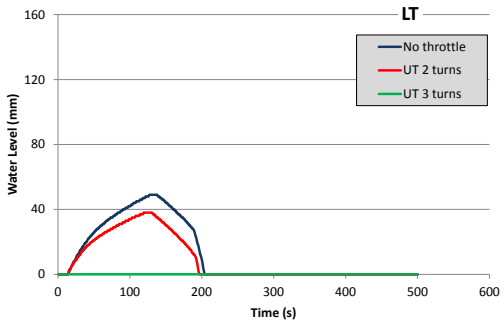

Figure 6.16: Constricting UT throttle (LT).

LOWER TURLOUGH (LT) THROTTLE

The effect of constricting LT throttle is shown in Figures 6.17 and 6.18. In this scenario, both tanks rise higher although LT is significantly more affected than UT. LT almost doubles in depth while UT is raised only a few centimetres higher. A noticeable effect can be observed when LT is throttled by 3 turns; the tank continues to rise after the input has been stopped (at 120 seconds). This result shows that after the input signal has stopped, LT is filled further by the water draining from UT tank (due to the head difference between them).

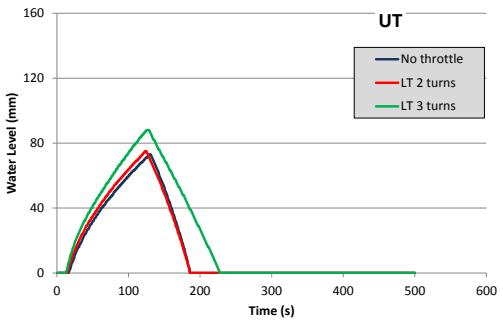

Figure 6.17: Constricting LT throttle (UT).

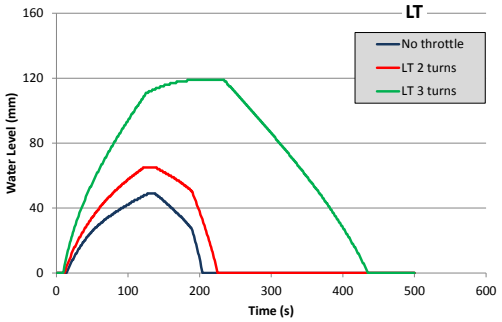

Figure 6.18: Constricting LT throttle (LT).

THROTTLE COMBINATIONS

As would be expected, if both throttles are constricted, both tanks are significantly impacted. UT rises higher and is full for longer than if just UT throttle was constricted. LT does not rise as high as if LT alone was throttled because UT is not releasing water to it as fast. However, its recession is elongated considerably due to the constriction hampering drainage (Figures 6.19 and 6.20).

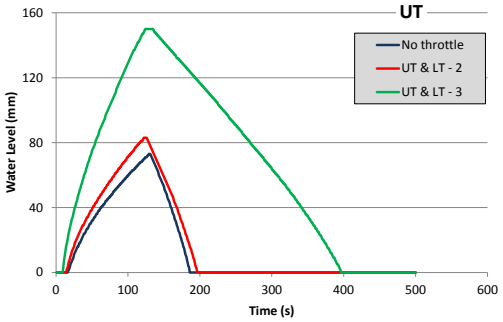

Figure 6.19: Constricting both throttles (UT).

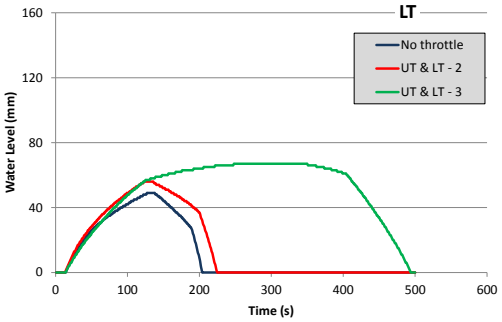

Figure 6.20: Constricting both throttles (LT).

BYPASS

In this test, the effect of opening the bypass while LT throttle is constricted (3 turns) is examined. As seen is Section 6.2.2, the bypass tends to reduce peak height and recession in UT while increasing peak height of LT and speeding its recession (when no throttles are applied). As can be seen in Figures 6.21 and 6.22, UT behaves similarly to an un-throttled scenario but LT's flooding pattern is altered with the peak reducing rather than increasing. The reduction in peak is due to the bypass offering a new flow path which can transmit water past the throttle unrestricted resulting in less water discharging into LT.

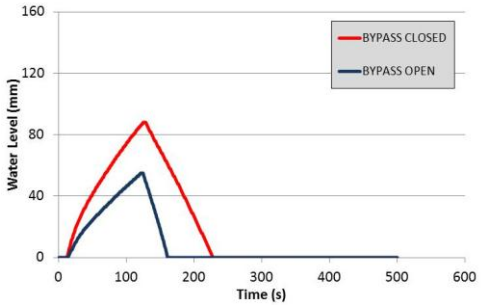

Figure 6.21: Coy bypass and throttle combination (UT).

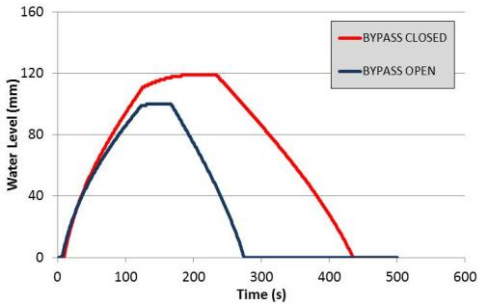

Figure 6.22: Coy bypass and throttle combination (LT).

In summary, both throttles offer a method of controlling water levels in the tanks but behave differently. UT throttle can be used to control the tanks *separately*, i.e. constricting UT throttle increases flooding in UT and reduces it in LT. LT throttle on the other hand can be used to control the tanks *together*, i.e. constricting LT increases the water level in both tanks, albeit with LT filling to a greater extent. This contrast between throttles proved very useful when calibrating the full scale *Infoworks* model, particularly in controlling the shape of recession curves.

6.2.5 Effect of River Input

To assess the different effects caused by the two inlet options (the river and the conduit), a series of tests were carried out in which the proportion of flow from each input was altered. Keeping the flow constant using the input lever valve (Figure 6.3), five different input setups were conceived ranging from entirely river fed to entirely conduit fed. The relative contribution of each input was controlled using the river/conduit control valves. The five input setups are shown below. It should be noted that precise flow contributions could not be known due to lack of precision using the tap valves (flow meter can be used to fine-tune total flow but not individual river or conduit flows):

- River only.
- Predominantly river input.
- Flow evenly split.
- Predominantly conduit input.
- Conduit only.

As the experiment required the same flow for all tests and the maximum sustainable flow from the river input was 9.3 L/m, all tests were carried out with a relatively low flow of 9.3L/m. See Figure 6.23 for a table of results.

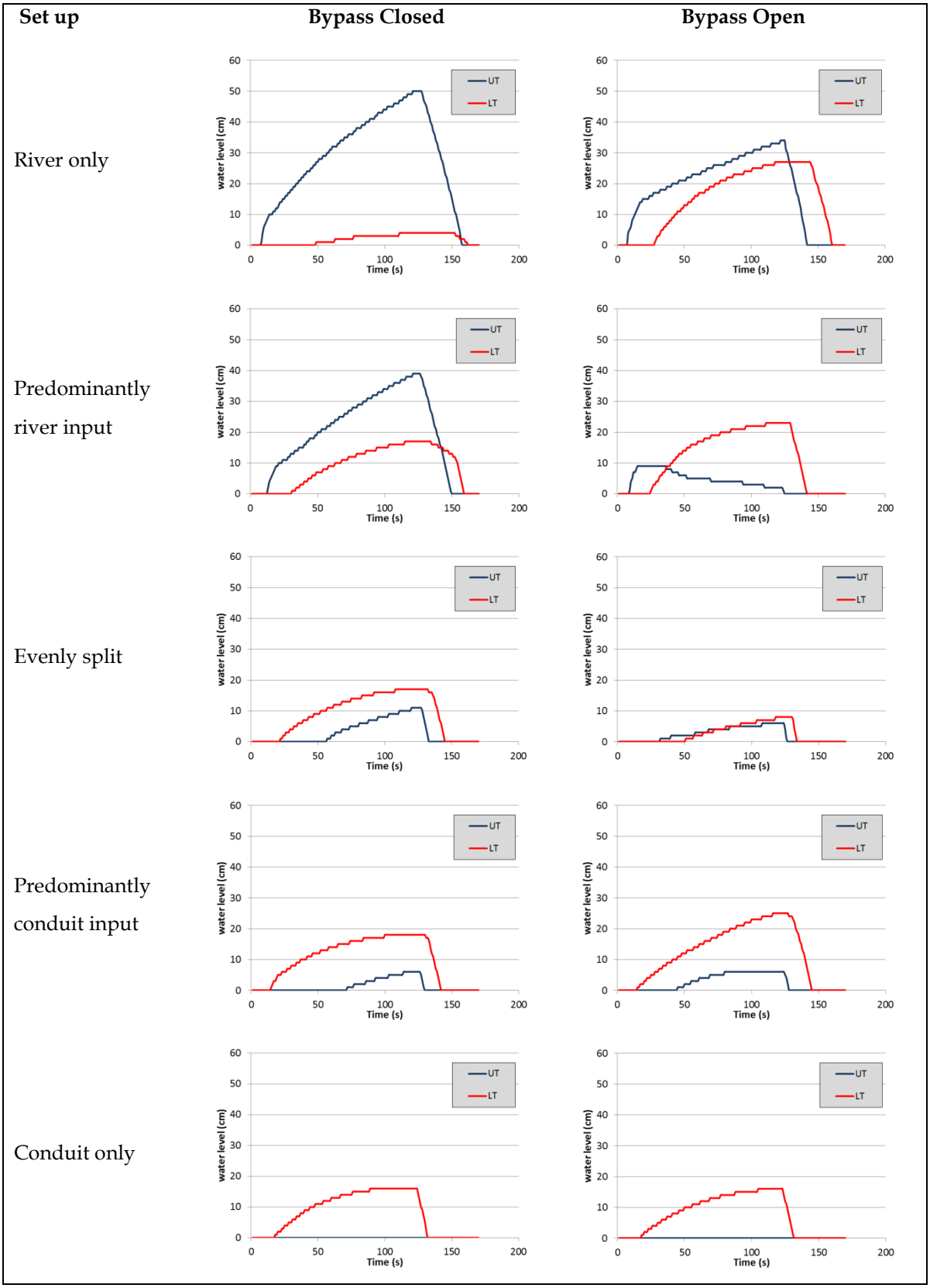

Figure 6.23: River-Conduit test results.

As can be seen in Figure 6.23, changing the relative input contributions of the river and conduit can cause significant changes in the tank water levels. In the closed bypass scenario, as the relative contribution of conduit input rises, UT's water level drops while LT's water level rises. By the time the input contributions are evenly split, LT is filling more than UT. After that point, LT stabilises while UT continues to drop until it does not fill at all.

In the open bypass scenario, a similar trend is visible with the more river-fed tests being greatly affected by the bypass whereas the more conduit-fed tests experience little change. For the river fed tests, the bypass reduces the peak of UT and increases the peak of LT. When only a small contribution of conduit flow is applied, the level of UT plummets while LT is relatively unchanged. For the more conduit fed scenarios, the bypass has little effect although this is likely due to the low flow (9.3 L/m) which is not strong enough to surcharge UT tank.

The results of these tests display the importance of using the correct input ratio when setting up the full scale *Infoworks* model.

6.2.6 Tracer Studies

In the previous tests, the physical model has provided details about the alteration of pipe model elements and their impact on the water levels of both tanks. In this section, the findings of the previous studies are combined with the use of an artificial tracer to test the mixing characteristics of the tanks.

For these tests, 10.08 mg (8 μL in solution) of the fluorescent tracer fluorescein was injected into the conduit system just upstream of the river/conduit divide. The injection was performed using a syringe which injected 0.4 ml of 1-in-50 fluorescein solution as an instantaneous shot (Figure 6.24). The injection took place as soon as possible (within a few seconds) after the flow was applied to the system. The resulting tracer concentration in the tanks (Figure 6.25) was sampled at 10 second intervals using 10 ml plastic cuvettes which were inserted into a handheld *Turner Aquafluor* fluorometer.

Figure 6.24: Fluorescein injection using syringe.

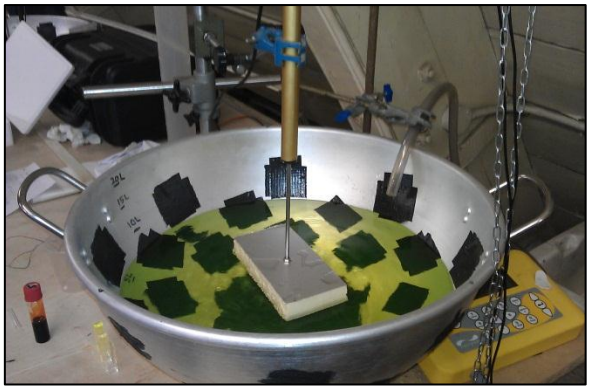

Figure 6.25: Tank containing fluorescein.

Two model elements were tested using the tracer, the *river/conduit contribution* (river tests) and the *application of a throttle*:

RIVER TESTS

Firstly, the effect of input type on water distribution was studied. The system was flooded using just the river input (Figure 6.26) and just conduit input (Figure 6.27). The tests were carried out with an input signal of 9.3 L/m for 2 minutes as this was the maximum flow possible from the river channel.

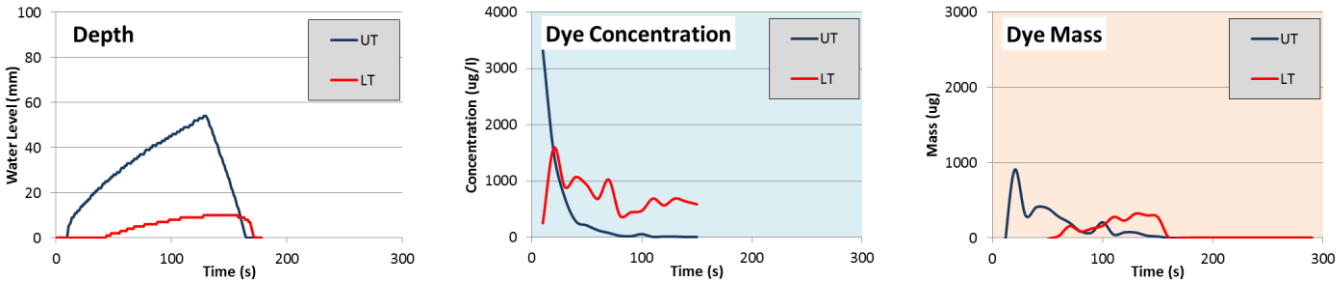

Figure 6.26: Tracer test – River input.

A river fed system results in UT peaking in tracer concentration early and slowly declining while LT slowly increases in concentration until it experiences a rapid recession. The decline in UT tracer mass over time suggests that the tank was draining through its conduit inlet while it was being filled by the river input. For LT, the fact that tracer mass slowly increases indicates that some of the tracer draining from UT was surcharging into LT.

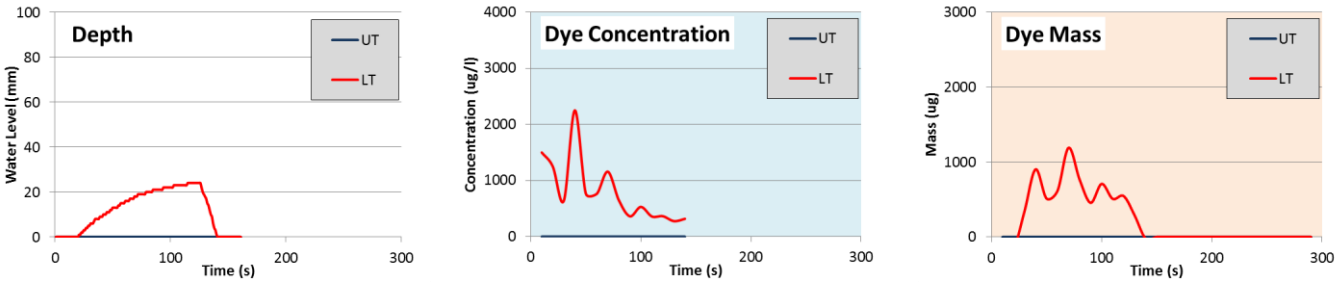

Figure 6.27: Tracer test – Conduit input.

The conduit fed system test was not as successful as the flow of 9.3L/m proved too low to surcharge UT. However, what can be seen is that, as LT fills, the tracer mass rises to a certain level and stays relatively constant within the tank before dropping as the tank recedes. This indicates that a burst of tracer entered LT and remained there being diluted by additional water until recession.

For further tests of full conduit and split river/conduit inputs flow (and the effect of the bypass on each), the input flow was increased to 14.8 L/m so as to fill UT as well as LT. See Figure 6.28 below for the conduit-fed tracer test with closed bypass and Figure 6.29 for an open bypass. With a closed bypass both tanks surcharged with a large concentration of tracer until approximately 50 seconds when the mass plateaued. UT filled with 17% of the tracer input (17% of the total mass of injected tracer) while LT filled with 11.5%. So 28.5% of the tracer enters the tanks and remained there until recession while over 70% of the tracer bypasses the tanks completely (tracer mass within the tanks was assumed to be fully mixed).

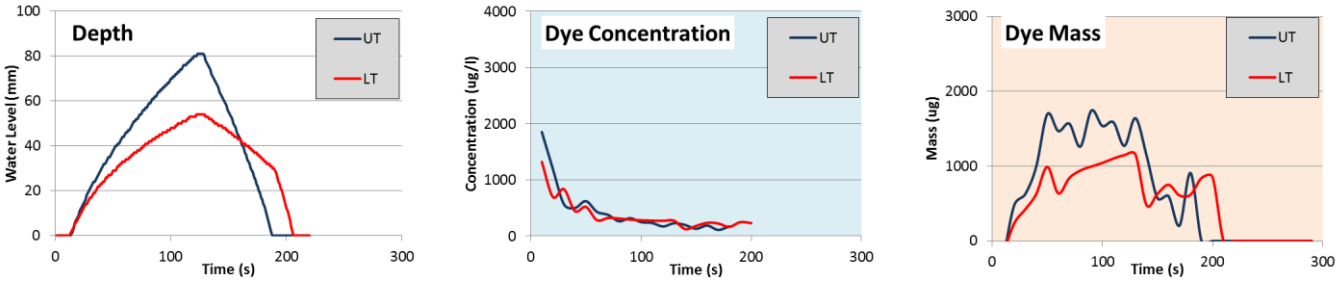

Figure 6.28: Tracer test – Conduit input, bypass closed.

When the bypass was opened, the tracer concentrations plummet within the tanks with only 2.5% tracer mass in UT and 1.8% in LT. So the bypass increased the quantity of water bypassing the tanks from 70% to 95% (Figure 6.29).

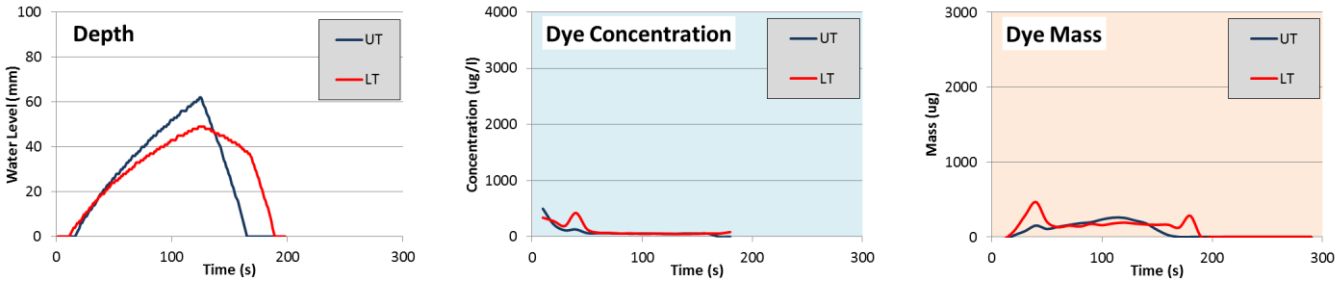

Figure 6.29: Tracer test – Conduit input, bypass open.

Combined river/conduit flow tests were then carried out with flow split evenly between the river and conduit inputs. Both bypass closed (Figure 6.30) and bypass open (Figure 6.31) scenarios produce similar results with UT tracer mass peaking early then slowly declining while LT tracer mass slowly increases until recession. Similar to the river-only tracer test, these tests show evidence of UT draining as it is filling with some tracer mass transferring from UT into LT. For the bypass closed scenario, UT peaks with 9% of total tracer mass initially and steadily drops while LT slowly increases to 4% tracer mass. When the bypass is opened, less tracer reaches UT with a peak of 6.3% while LT receives more tracer with 4.5%. In both cases, over 90% of the tracer bypasses the tanks completely.

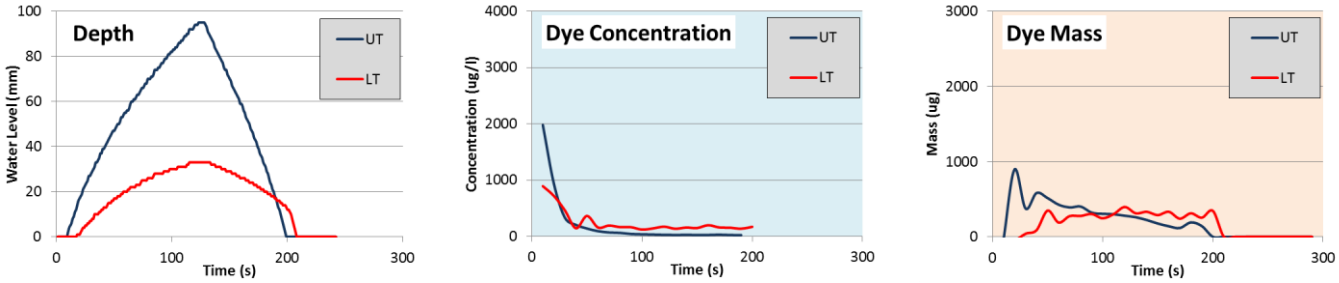

Figure 6.30: Tracer test – Split river/conduit input, bypass closed.

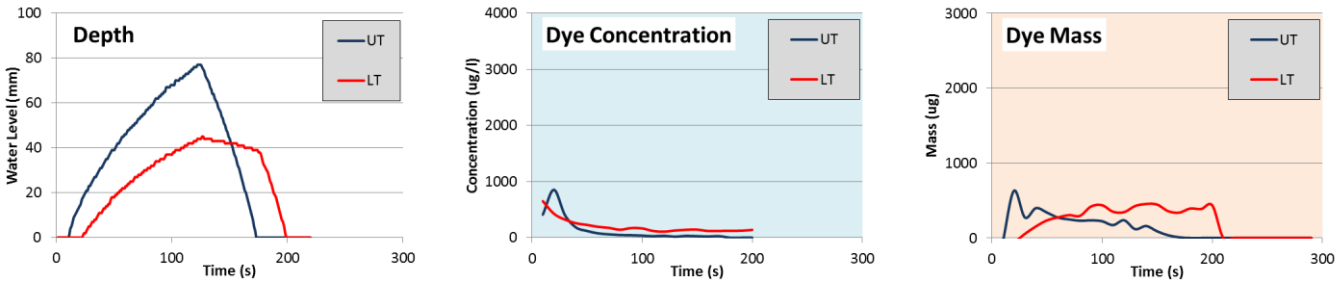

Figure 6.31: Tracer test – Split river/conduit input, bypass open.

APPLICATION OF THROTTLE

To assess the impact of throttling the tanks to the mixing characteristics, two tests were carried out whereby both UT and LT throttles were constricted to three turns (with an evenly split river-flow input). Constricting the throttles should result in more realistic water distribution with a greater proportion of water entering the tanks rather than bypassing them. As the throttles increased the rate of filling, the flow had to be dropped to 9.3 m^3/s to avoid overfilling.

See Figure 6.32 below for the results of the bypass closed scenario. The quantity of tracer in UT increased significantly when compared to the previous similar but un-throttled test (Figure 6.30). The application of the throttle increased the initial tracer peak in UT from 9% to 18% although the flow was reduced so a direct comparison cannot be made. Tracer concentrations in LT were extremely low with a maximum concentration of 2% just before emptying.

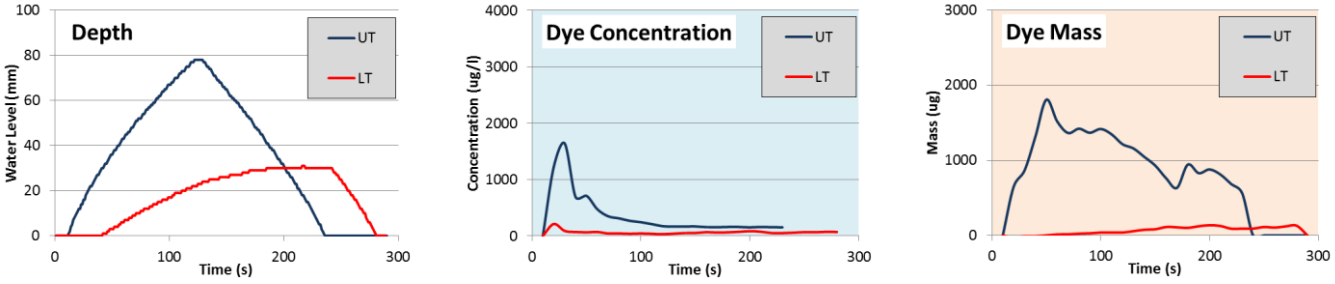

Figure 6.32: Tracer test – Split river/conduit input, throttles applied, bypass closed.

See Figure 6.33 below for results of the bypass open scenario. While the initial burst of tracer concentration remained high, the tracer mass in the tanks was considerably reduced as the tank water levels were much lower. The bypass transmitted a significant amount of water with approximately 95% of the tracer bypassing the tanks compared to 82% with the bypass closed.

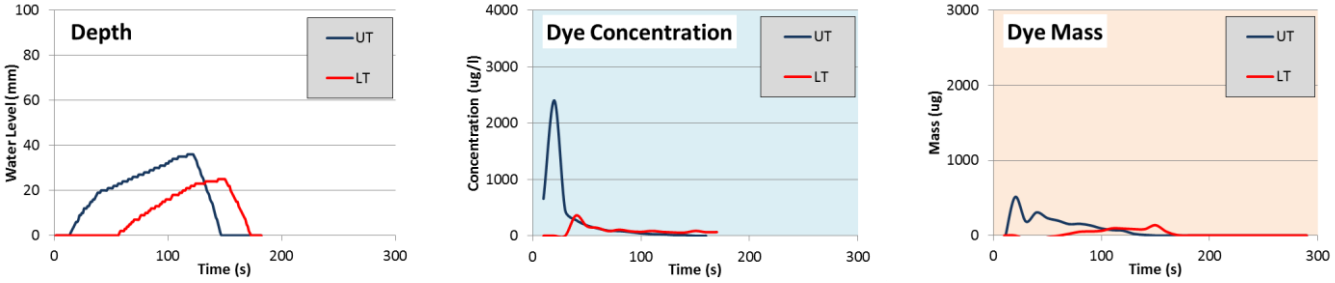

Figure 6.33: Tracer test – Split river/conduit input, throttles applied, bypass open.

6.2.7 Physical Model Conclusions

The physical model proved an insightful tool for the understanding of the turlough water level dynamics linked by underground conduit network and in particular the type of configuration thought to link Blackrock and Coy turloughs in the Gort Lowlands. Several conclusions that could be drawn are:

- The bypass channel has a significant impact on the levels of the turloughs affecting both turloughs in separate ways. When the bypass is opened, the upper turlough reduces in size whereas the lower turlough increases. *Note, this bypass setup was changed for the Infoworks model so the physical model conclusions did not apply.*

- Constricting the turlough inlets impacts filling and drainage in both turloughs resulting in lower water levels and longer recessions.

- The downstream turlough throttles are powerful tools in controlling turlough flooding. They provide highly sensitive elements in the pipe network enabling accurate calibration. The upper turlough throttle can be used to tune the turloughs separately while the downstream turlough throttle provides a combined effect for both turloughs.

- Altering the ratio of river to conduit input for the system has a considerable effect on the upper turlough with higher water levels for increased river flow. The effect on the lower turlough is less pronounced. Unfortunately these tests could only be carried out at low flow conditions.

- The tracer studies enabled the distribution of water between the turloughs to be observed and served as a useful preliminary study for a planned full-scale tracer test of Blackrock and Coy turloughs (unfortunately, this tracer study could not be carried out due to lack of suitable hydrological conditions during the study period).
    - For scenarios with either full or partial river input, some of the water draining from the upper turlough can be seen transferring into the lower lake. As the real Blackrock-Coy system is predominantly river fed, this finding should be observable using hydrochemistry (see Chapter 7)
    - The tests showed a larger than anticipated proportion of the flow completely bypassing the turloughs with a maximum of only 30% of total tracer mass being picked up in the turloughs.

6.3 Gort Lowlands Infoworks Model

6.3.1 Infoworks CS

The hydraulic model of the Gort Lowlands was built using *Infoworks CS* version 8.5 (Wallingford Software). This software package is designed for management of urban drainage networks and incorporates the *Hydroworks* modelling engine. The model simulates the hydraulic behaviour of a pipe network under varying conditions of rainfall, land use, population, inflows etc. As the model is capable of modelling the hydraulic conditions in both open channel and pressurised flow channels, it is highly suitable for modelling a well-developed karst conduit network such as that of the Gort Lowlands.

An Infoworks model is built up using a variety of different elements such as conduits, nodes, ponds, outfalls etc. If these elements are linked together to form a coherent network with no missing values, errors or inconsistencies, the model will be validated and ready for simulation. The model inputs include rainfall, river inflow data and boundary conditions such as tidal level at an outfall. After a successful simulation, the model can output a range of data such as flow, water level, water volume, surcharge state etc. for each element of the network.

The governing model equations are the Saint-Venant equations which are a pair of conservation equations of mass and momentum:

$$\frac{\delta A}{\delta D} + \frac{\delta Q}{\delta x} = 0 \qquad \textit{Equation 6.1}$$

$$\frac{\delta Q}{\delta t}\frac{\delta}{\delta x}\left(\frac{Q^2}{A}\right) + gA\left(cos\theta\frac{\delta y}{\delta x} - S_o + \frac{Q|Q|}{K^2}\right) = 0 \qquad \textit{Equation 6.2}$$

where Q = discharge (m^3/s), S_o = bed slope, K = conveyance, A = cross-sectional area (m^2) and θ = angle of bed to horizontal (°).

The conveyance function is based either on the Colebrook-White or Manning expressions. For the Gort Lowlands model, the Colebrook-White equation is used.

Pressurised pipe flow is modelled in one of two ways:

- Retaining the Saint-Venant equations but introducing a suitably narrow slot known as the Preissmann slot, into the pipe soffit level. This slot enables a smooth transition between free surface and surcharged conditions by offering an abrupt change in surface width derivative and wave celerity in the transition to pressurised conditions. The slot width is defined such that the wave celerity in the slot is ten times that at half the conduit height, resulting in a slot width that is 2% of the conduit width. The model equations for pressurised flow differ in that the free surface width is replaced conceptually by the term:

$$B = \frac{gA_f}{C_P^2} \qquad \textit{Equation 6.3}$$

where B = free surface width (m), A_f = pipe full area (m^2) and C_P = pipe full velocity of pressure wave (m/s).

- In some instances such as rising mains or inverted siphons, the pressurised pipe model can be used instead of the full Saint-Venant solution. The model equations for pressurised pipe flow are:

$$\frac{\delta Q}{\delta x} = 0 \qquad \textit{Equation 6.4}$$

$$\frac{\delta Q}{\delta t} + gA\left(\frac{\delta h}{\delta x} - S_o + \frac{Q|Q|}{K^2}\right) = 0 \qquad \textit{Equation 6.5}$$

where A = full pipe area (m^2) and K = pipe full conveyance.

A comparison between these two pressurised pipe flow modelling methods was carried out by (Gill, 2010) using the Gort Lowlands pipe network model. The comparison showed no difference between the two methods.

6.3.2 Gort Lowlands Model

The conceptual model upon which the Infoworks model was based is shown in Figure 6.34. This model, designed by Gill et al. (2013a) consists of three river inputs transferring water through a pipe and node network which feeds five storage nodes (or ponds) before discharging at the outfall.

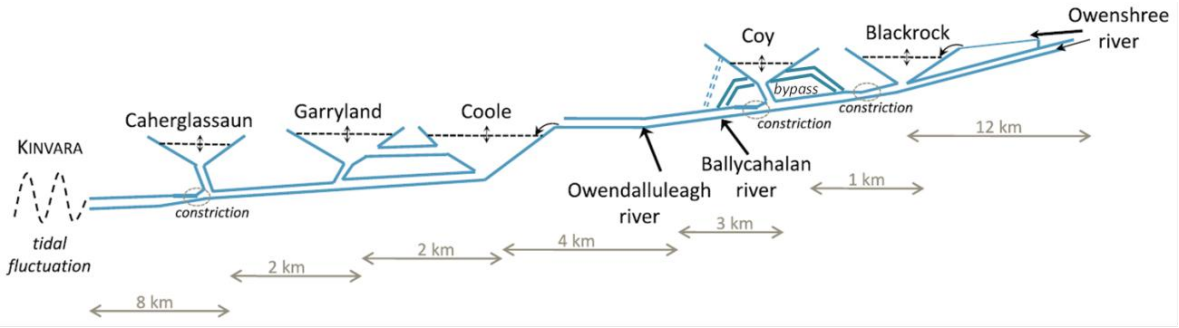

Figure 6.34: Conceptual model of the Gort Lowlands (Gill et al., 2013a, Gill et al., 2013b).

The contribution of rainfall falling on the lowland karst limestone area that infiltrates into the epikarst and fracture network was also incorporated into the model. This was achieved using a combination of runoff-routing model, groundwater infiltration module (GIM) and use of SUDS (sustainable urban drainage) applications in the Infoworks modelling suite. The rainfall hitting the subcatchment was first subjected to evapotranspiration losses and initial wetting and storage losses. The water was then routed down through the soil into the conceptual epikarst fracture system which was represented by pipes with permeable characteristics (with flow calculated via Darcy's Law), which then link to the main open conduits (Gill et al., 2013a). The subcatchments and their relative positions in the network can be seen below in Figure 6.35.

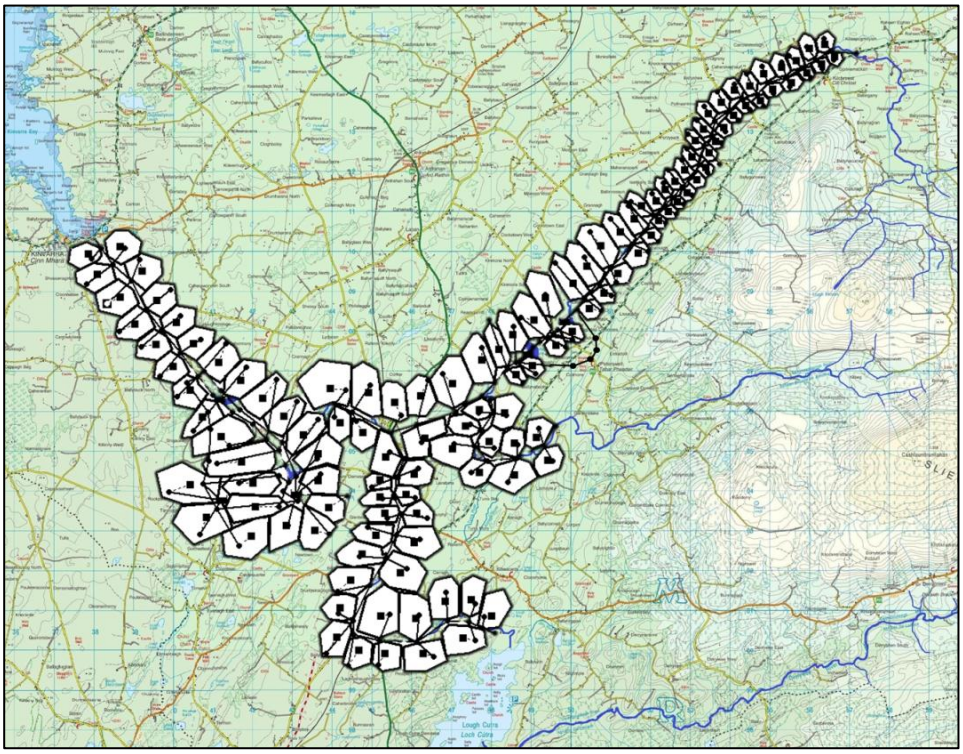

Figure 6.35: Model Layout overlaid on topographical map.

The Groundwater Infiltration Module (GIM) has been developed for Infoworks to provide a highly attenuated response to rainfall to represent the below-ground processes of infiltration through the soil into a pipe network and also the contribution from a high water table. This allows two additional mechanisms for water to get into the conduit network via the soil storage reservoir and/or the ground store reservoir. A conceptual model of the GIM is shown in Figure 6.36.

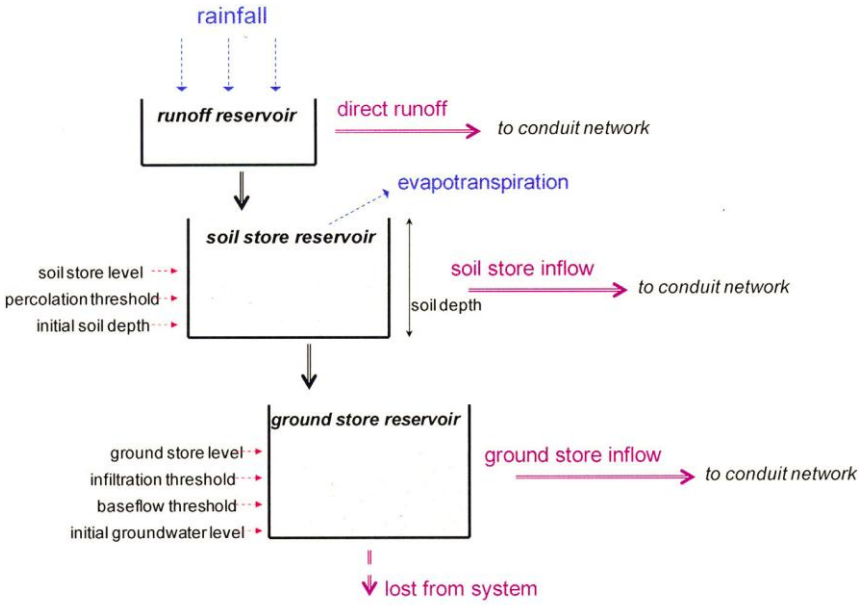

Figure 6.36: Conceptual model of the runoff model, soil storage reservoir and groundwater store reservoir (Gill et al., 2013a).

Sub-catchments were delineated across the catchment in order to provide diffuse infiltration into the main conduit network. These subcatchments vary in area between 35 to 150 ha and are connected to the main conduit network through permeable pipe conduits extending from the network into the catchment, typically at 750m intervals. These conduits were modelled as rectangular pipes filled with porous media which allowed the flow through the pipes to be calculated using Darcy's Law (equation 6.6) which is an appropriate flow regime for flow through fractures and epikarst (White and White, 2005). The subcatchment runoff slope was defined by mean topography of each subcatchment area and a soil class 3 was used in the modelling denoting a *wet* soil.

$$Q = -KA\left(\frac{\Delta h}{L}\right) \qquad \textit{Equation 6.6}$$

where K= hydraulic conductivity, A= Cross-sectional area of permeable formation and Δh= difference in head.

The flow rate through these permeable pipes, and therefore the rate of diffuse inflow to the conduit network, is controlled by two parameters: media conductivity and porosity. These parameters, along with the runoff parameters presented in Figure 6.36, were calibrated through a study of the Owenshree River. The two gauging stations along the river are separated by 13 km of river running across limestone bedrock. The difference between the flows at the two positions was thus used to quantify the typical amount of diffuse infiltration draining into the network from the karst. The final calibration parameters from this study were then set for all subcatchments in the final model (Gill et al., 2013a).

Overall, the model is made up of 229 conduits, 218 nodes, 124 subcatchments, 5 storage nodes (ponds) and one outfall. See Figure 6.37 for the major element locations labelled on an Infoworks schematic. To run a successful simulation, the model required a full set of hydrological input data. This input data consisted of the following:

- Hourly river flow data from the Owenshree, Ballycahalan and Beagh Rivers.
- Hourly rainfall data from Kilchreest rain gauge.
- Daily PET data from Shannon and Athenry synoptic stations.
- Hourly tidal data for Kinvara (based on Galway Port tidal data).

After a successful simulation, a large range of output data was available such as flow, velocity, water level, surcharge state, hydraulic gradient, Froude number etc. for any node or link in the network.

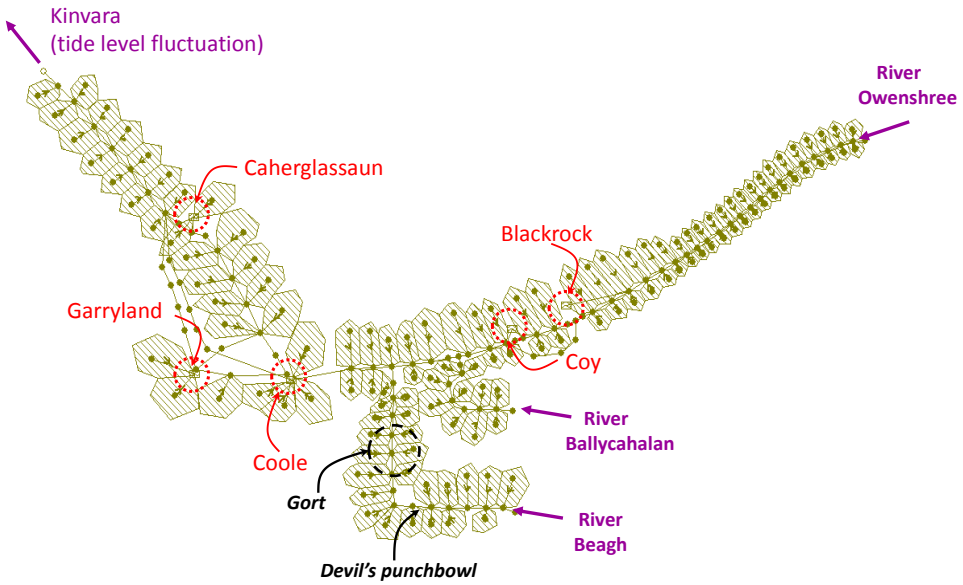

Figure 6.37: Schematic of Gort Lowlands model as seen in Infoworks.

The model was initially calibrated over a period of relatively rapid fluctuation, 1st August 2008 – 10th October 2008. As outflow from Kinvara could not be quantified, the calibration was based on matching predicted and observed turlough water levels. Conduit diameters and lengths were then iteratively adjusted to balance the system. The subcatchments were kept at the same proportions and used the same coefficients as was defined in the calibration of diffuse flows. The trickiest part of the model to calibrate proved to be Blackrock and Coy turloughs (as was the case for the Gort Flood Studies model). A number of different pipe network combinations were tested out in order to correctly mimic the filling and recession characteristics of Blackrock and Coy turloughs. The chosen combination is shown in Figure 6.39 and the results of are shown in Figure 6.38 for the 2007-2008 flooding season.

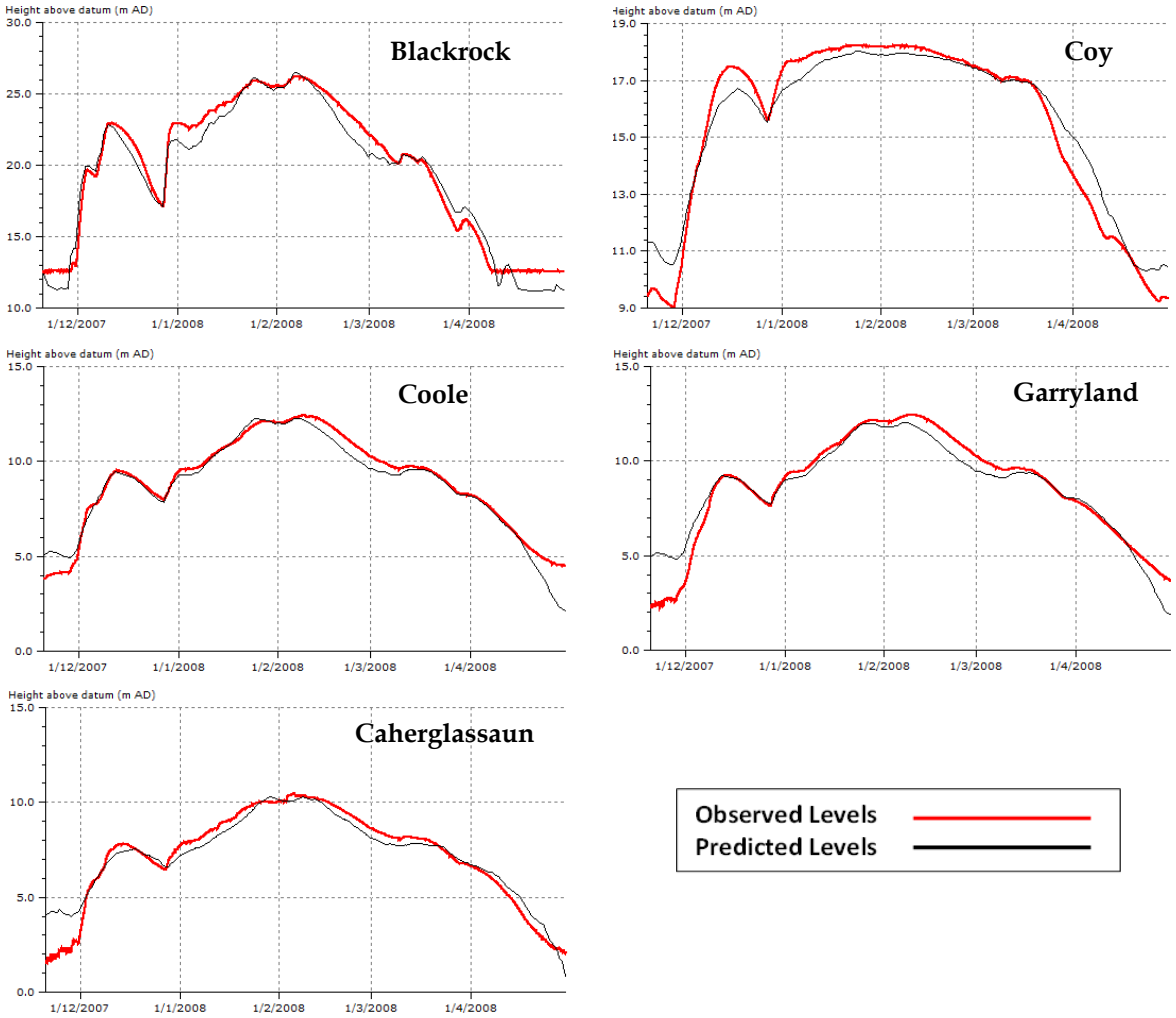

Figure 6.38: Blackrock and Coy results (2007-2008) from Gill et al. (2013a) model.

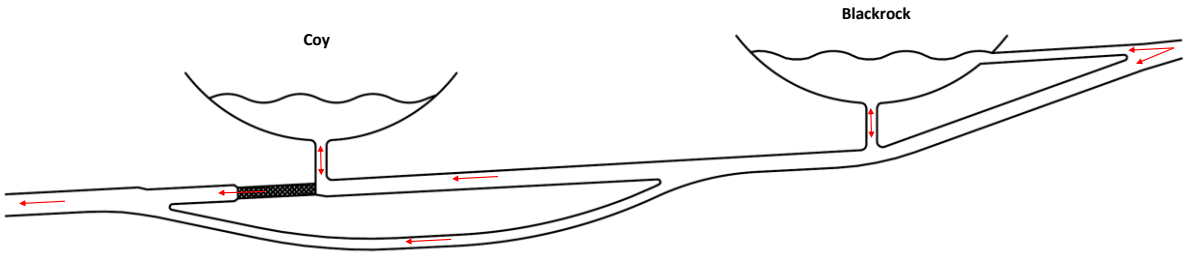

Figure 6.39: Blackrock-Coy configuration from (Gill, 2010).

These results, though clearly quite accurate, are however calibrated based on an outdated rating curve for the Beagh River (Section 5.4.1). This rating curve underestimates flow by approximately 30% for mid-range flows and up to 50% for high flows. This inaccuracy was accounted for in the model by Gill et al. (2013a) in two ways:

- The older turlough stage-volume areas (Section 1.2.1) tended to underestimate the turlough volumes. The effect on water levels of the lower Beagh River flow would thus be offset by the underestimated stage-volume curves resulting in better accuracy.

- The conduit dimensions were calibrated for the lower flows.

For the purposes of Gill et al. (2013a), the primary aim of the model was to predict turlough water levels. For this thesis however, the model is intended to be used for a wider range of purposes, many of which require accurate turlough volume results (e.g. nutrient concentrations and mass in turloughs) and so the model needed to be corrected with the more accurate Beagh flow data.

When the corrected OPW rating curve was applied to the original model, water levels increased and recessions lengthened, especially for the lower three turloughs. See Figure 6.40 for an illustration of the effect of correcting the Beagh rating curve on Coole turlough. The green line represents the flooding pattern in the turlough when using the updated rating curve which increases flow volumes. Not only is the peak increased but it also reaches beyond the maximum surveyed level of the turlough (resulting in the horizontal line at 13 mAOD). In order to correct the model, the turlough stage-volume curves and conduit dimensions needed to be re-adjusted.

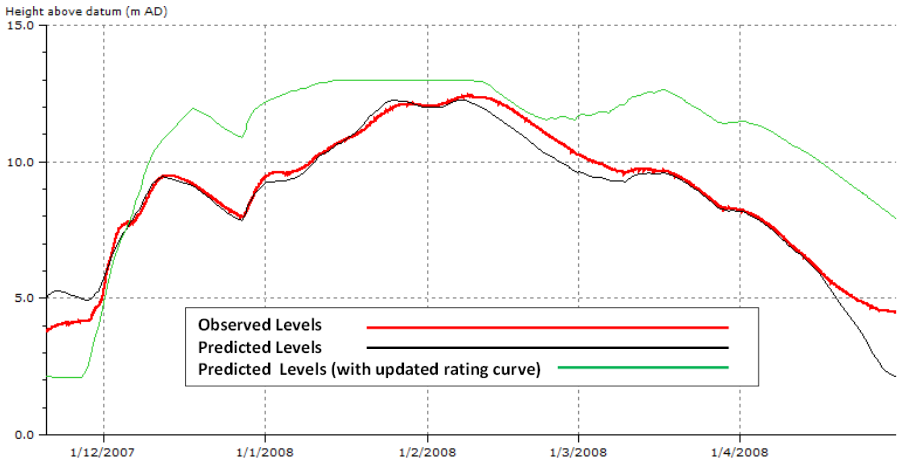

Figure 6.40: Coole turlough water levels for observed, modelled and updated model (rating curve) scenarios.

6.3.2.1 Turlough Stage-Volume Relationships

The survey data for each of the five turloughs was updated using LIDAR data to develop new stage-volume relationships (discussed in Section 5.2.1). These new relationships provided increased volume to store the increased flow from Beagh River. Coy, Garryland and Caherglassaun were altered minimally whereas the volumes of Blackrock and Coole turloughs were significantly increased at mid-high levels (Appendix A).

In an attempt to take account of the significant storage provided by Newtown and Hawkhill turloughs to the south of Coole (Figure 6.41), an additional storage node (pond) was added to the network. These turloughs are known to receive the majority of their water from the southern Cloonteen catchment (not included in this model) but at typical winter water levels, an overland connection is established with Coole turlough which provides a considerable additional storage volume for Coole. The new storage node (pond) was given a stage-volume relationship based on LIDAR data and connected to Coole via a wide overland open channel. The channel was flat and connected to both turloughs at 7 mAOD (the elevation at which overland flow is known to occur). A drainage node was also added to the Newton storage unit at its base which joined into the main conduit network between Coole and Caherglassaun turloughs. Ultimately, the Newtown node did more to hinder than to help the model calibration.

As the underground connections between Newtown, Hawkhill and Coole are not well understood, a suitable conduit link could not be hypothesised. As the turloughs emptied, Newtown slowly released its stored water into Coole storage node which lengthened the recession to an inaccurate

degree. The fact that Coole turlough performed better without Newtown storage node could indicate that the majority of Newtown and Hawkhill turloughs are drained through a separate conduit network. This lines up with the conceptual model of the catchment as proposed by the Gort Flood Studies which included a major conduit running from Newtown and Hawkhill north westwards (Figure A.16 in appendix A), linking up with the western cave system before draining to Kinvara.

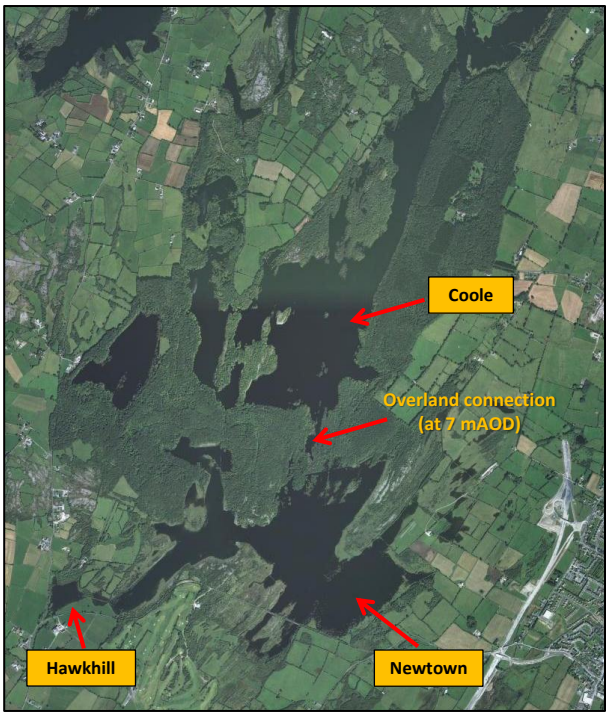

Figure 6.41: Newtown and Hawkhill turlough connection with Coole.

6.3.3 Recalibration

The first stage in recalibrating the conduit network was to carry out a sensitivity analysis of the system to decipher which conduits play the most important role in controlling flow through the network. Using the results of this analysis, the conduit network was re-adjusted in a more targeted manner.

6.3.3.1 Sensitivity Analysis

This analysis was carried out to determine which conduits could play the greatest role in re-calibrating the system. As a result, the analysis was only carried out for the underground conduit segments of the network (see Figure 6.42). The open channel segments (except Blackrock River

input) were ignored as they were based on river channels of known geometry and had less impact overall than the surcharged conduit elements. The analysis consisted of running a simulation for a range of different diameter sizes for each conduit and observing the consequent change in turlough water levels for each simulation.

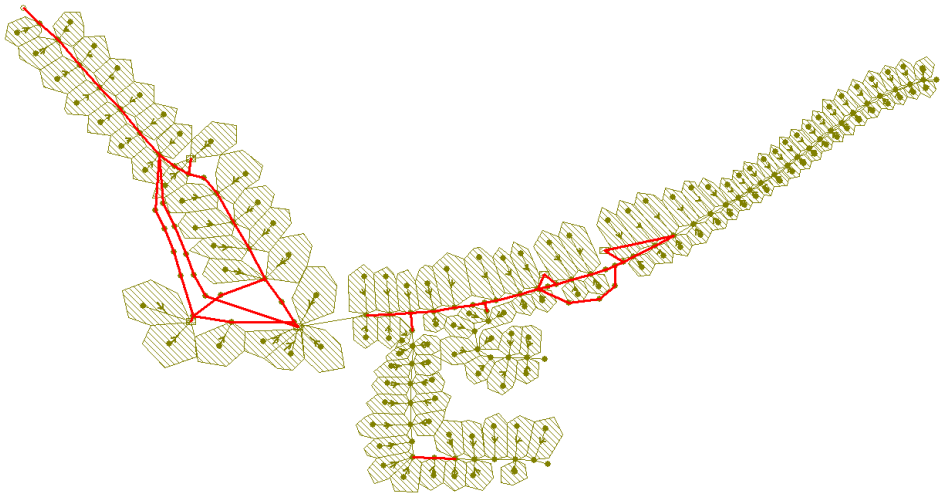

Figure 6.42: Underground conduits targeted for sensitivity analysis.

The period used for analysis was 3rd September 2010 to 20th October 2010. This period was chosen as it contained a number of heavy rainfall events followed by a long dry spell resulting in typical turlough flooding pattern over a period of only two months (as shown in Figure 6.43). The short period was necessary for practical reasons as there would be multiple simulations run and the shorter the period chosen, the faster the simulation time.

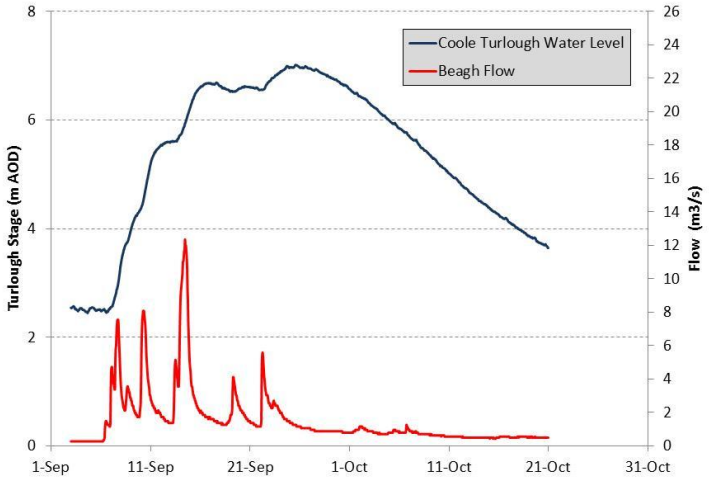

Figure 6.43: Sensitivity analysis test period (Sept – Oct 2010).

There were 66 underground conduits in the network. A set of simulations was run for each conduit whereby that conduit had its diameter altered by ± (5, 10, 25, 50, 75)% and +100% with all other conduits remaining the same. So each of the 66 conduits had 12 simulations (1 original run and 11 altered runs) giving a total of 780 runs. Each simulation took over 8 minutes to run so running all 780 simulations took over 4 days. Infoworks does not provide the tools to run such an analysis and so a MATLAB routine was written which could run models consecutively, automatically altering the parameters in series.

As Infoworks is not open-source code, it could not be run through MATLAB. However, the free pipe network modelling software SWMM 5.0 (USEPA) is open-source and capable of integrating with MATLAB. SWMM is similar software to Infoworks: a pipe network is setup, inputs applied to it, a simulation carried out and results generated. In SWMM, when a network is built and the relevant inputs have been stipulated, the network is saved as an input (.inp) file. A simulation is carried out and two files are produced, a report file (.rpt) and an output file (.out). The report file contains a brief review of the simulation providing maximum and minimum values for each network element whereas the output file contains the entire suite of results for each element of the system. For this analysis, only the report file was of interest as it provided the maximum volumes reached by each storage node. The key aspect to SWMM is that the files (.inp, .rpt, .out) can be accessed and altered manually as text files (.txt) allowing them to be manipulated using MATLAB. The procedure was as follows:

- Template .inp file created.
- MATLAB opens template file, inserts altered data and saves as new .inp file.
- MATLAB runs SWMM simulation using new .inp file.
- MATLAB opens .rpt file and extracts the relevant results (i.e. storage tank max volumes). These results are pasted into a separate results file.
- MATLAB opens template file again, inserting new altered data and saves over previous .inp file.
- Process repeated (779 times) with all results being pasted into the same results file.

The first step of this process was determining whether the SWMM modelling engine was suitable for modelling the Infoworks network. The governing equations of the SWMM modelling engine (Saint-Venant flow equations) are the same as Infoworks but there are a number of differences. These differences include:

- The infiltration model in SWMM is less advanced than for Infoworks with only three runoff routing methods available: Horton, Green-Ampt and Curve number. As the chosen runoff routing method for the Infoworks model, the Wallingford method, was not available, the Horton method was applied. As a result, the dynamics of the Groundwater Infiltration module change between SWMM and Infoworks models.
- SWMM does not support the use of porous pipes, an important element of the Infoworks model. The porous pipe conduits are modelled as simple hollow conduits in SWMM.
- SWMM uses Manning's equation for the conveyance function rather than the Colebrook-White formula. As such the Colebrook-White roughness factor (ks) is converted to a Manning's n value using the formula: $n = 0.038ks^{\frac{1}{6}}$.

Due to the differences between the SWMM and Infoworks modelling engines, the outputs from the models differ. The main differences encountered were regarding the infiltration module. However, as the predominant source of water in the network is from the river inputs rather than rainfall, the effect of an inaccurate infiltration module is relatively minor. Also, as the purpose of this analysis was to observe if the turlough volumes change with altering conduit dimensions, the qualitative effects caused (whether a turlough rises or falls) still hold true even if each simulation is not perfect. See Figure 6.44 below for a comparison of SWMM and Infoworks over the test period for Blackrock turlough.

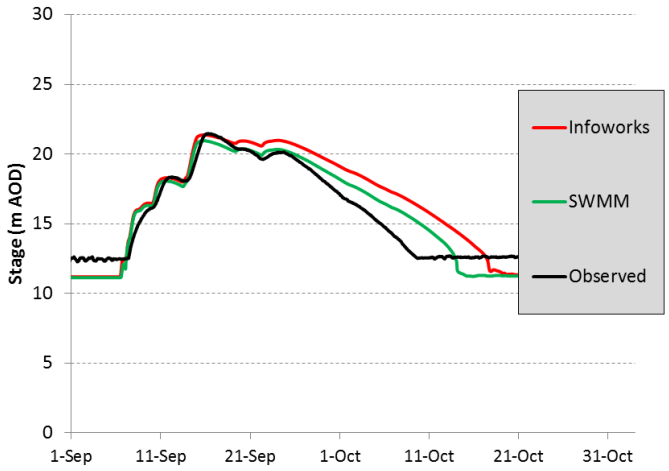

Figure 6.44: Comparison of SWMM and Infoworks simulations (with observed water level) for the analysis period (Blackrock turlough).

The parameters of interest in this study were the peak volumes of each turlough. Modifying the size of any underground conduit within the conduit network proved to alter these peak volumes (by a

large or small amount) depending on the changes applied. Inevitably, most conduits proved to be more influential on certain turloughs rather than on others. For this reason, the results of this analysis are presented in terms of an individual turlough and how changes to each conduit influence the volume of that specific turlough. In many cases, the effect of altering a conduit would impart a similar change to one or more turloughs. For instance, constricting any conduit between Caherglassaun and Kinvara leads to increased peak volumes in all five turloughs. In other cases, the alteration of a conduit could cause contrasting behaviour between two turloughs. An example of this effect can be seen when the primary conduit between Blackrock and Coy turloughs is narrowed. This causes Blackrock to increase due to reduced drainage capacity and Coy to reduce due to slower influx of water.

So for each turlough, the change in volume of that turlough caused by altering the size of each conduit by ± (5, 10, 25, 50, 75)% and +100% was quantified. The results of the analysis for Coole turlough are shown in Figures 6.45 and 6.46 (see Appendix D for results from other turloughs). These plots show bar charts with each bar representing a conduit. The shading of the bars indicates the incremental change applied to that conduit (e.g. +10%, +25% etc.). Figure 6.45 shows the impact on Coole turloughs volume if conduits were expanded while Figure 6.46 shows the impact of narrowing these conduits (See Figure D.1 in appendix D for conduit name and locations).

These results can also be presented using a map (such as those shown in Figures 6.47 and 6.48). These figures show the effect caused to a specific turlough from one particular degree of alteration (e.g. 100%) which has been applied to an individual conduit. This alteration was then applied to all other conduits (individually) and the amalgamation of these results is shown on the maps. The degree to which this alteration (of an individual conduit) influences a specific turlough is then illustrated by the size and colour of the conduit on the map. A blue conduit indicates a reduction in peak volume of the specific turlough and a red conduit indicates an increase. The thickness and shade of the conduit indicate degree of volume change occurring in the turlough (as can be seen in the maps legend). So in Figure 6.47, the effect that each conduit has on Coole when their diameters are increased by 100% (i.e. the conduit diameters were doubled) can be seen. For instance, Caherglassaun throttle (conduit 48.2) is shown to reduce the volume of Coole turlough by between 40-60% (of the original volume) when its diameter is doubled. Figure 6.48 on the other hand shows the effect of reducing the size of individual conduits by 50% (i.e. conduit diameters are halved). In this example, the constriction of Caherglassaun's throttle (conduit 48.2) results in Coole's volume increasing by between 100-150% (i.e. the new volume is greater than double the original volume).

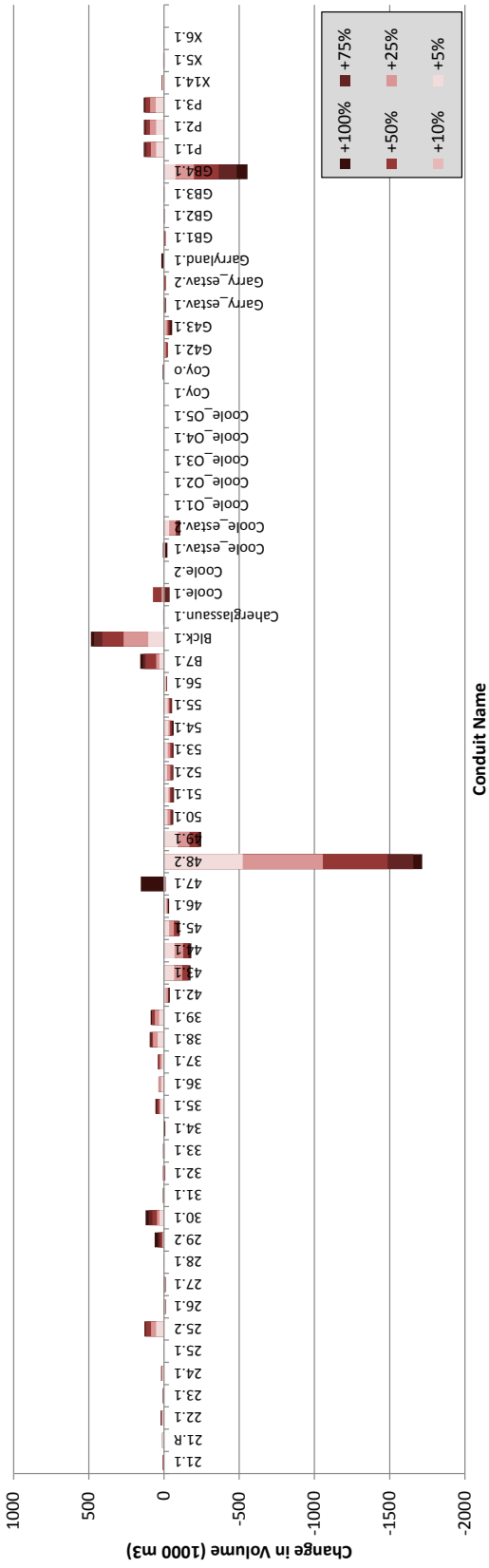

Figure 6.45: Sensitivity Analysis results: Volume change in Coole with conduits expanded.

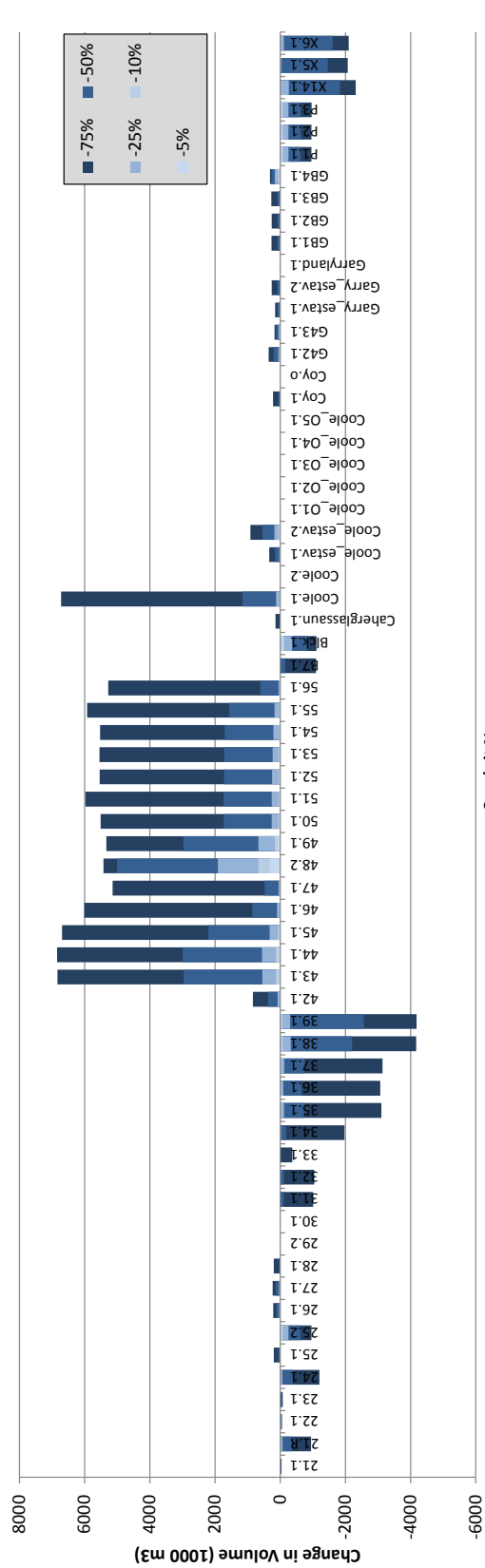

Figure 6.46: Sensitivity Analysis results: Volume change in Coole with conduits narrowed.

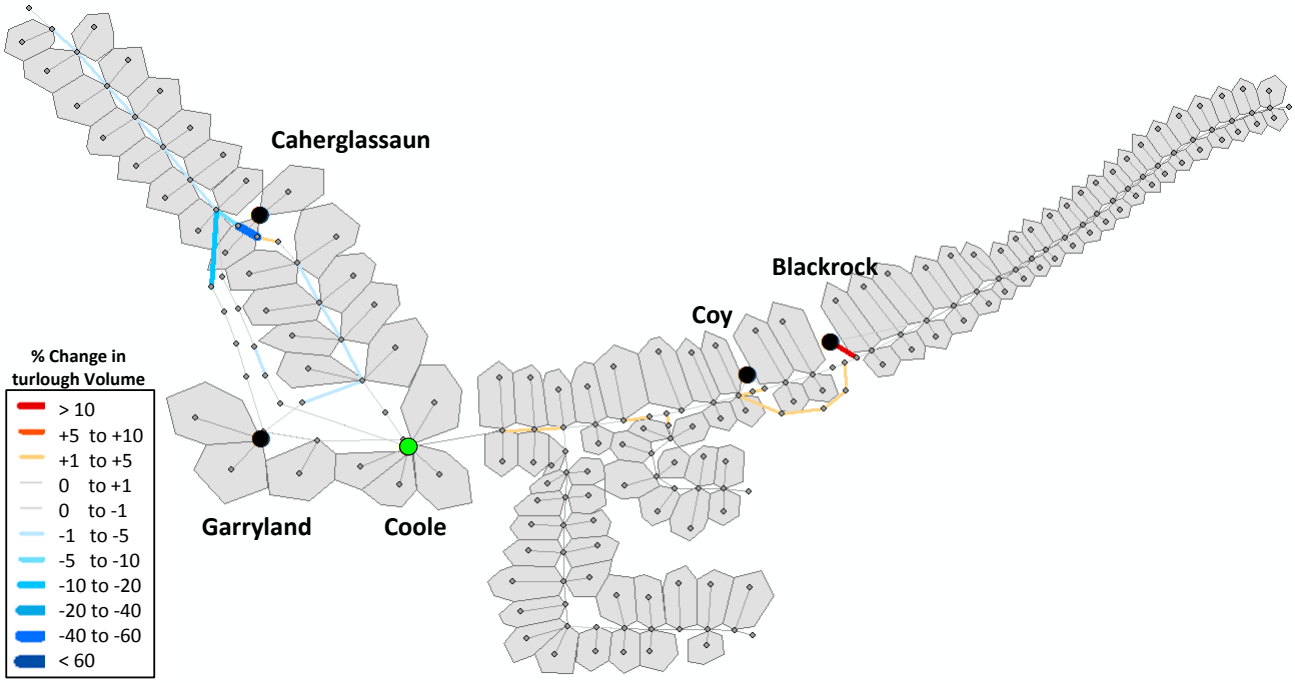

Figure 6.47: Percentage change in volume of Coole turlough from increasing size of individual conduits by 100%.

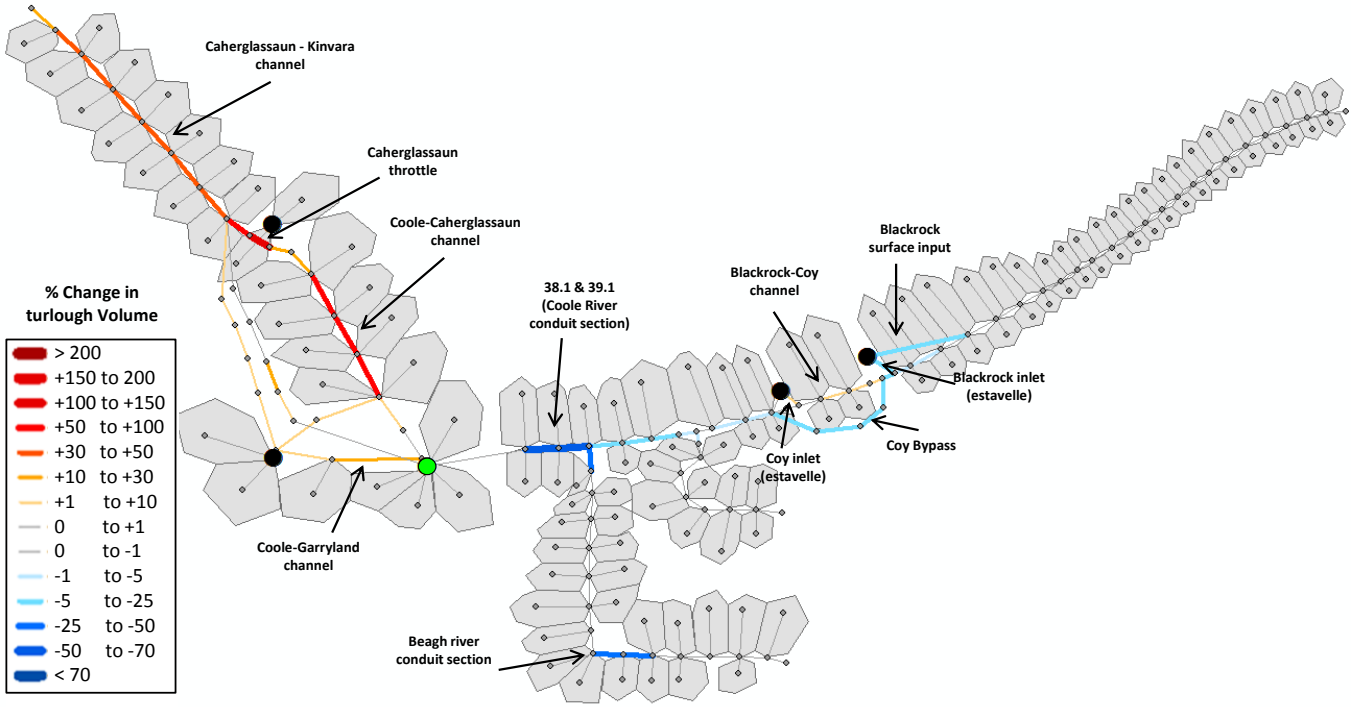

Figure 6.48: Percentage change in volume of Coole turlough from decreasing size of individual conduit by 50%.

Table 6.1: Sensitivity Analysis results summary.

	Blackrock	Coy	Coole	Garryland	Caherglassaun
To **increase** turlough volume, constrict:	• Blackrock inlet • Coy Bypass • Blackrock-Coy channel • Coole River conduit	• Coy Bypass • Coole River conduit	• Coole-Caherglassaun channel • Caherglassaun throttle • Caherglassaun-Kinvara channel	• Coole-Caherglassaun channel • Caherglassaun throttle • Caherglassaun-Kinvara channel	• Caherglassaun throttle • Caherglassaun-Kinvara channel
To **reduce** turlough volume, constrict:	• Blackrock surface input	• Brock surface input • Blackrock-Coy channel • Coy inlet	• Coole River conduit • Beagh River conduit • Coy Bypass • Blackrock surface input	• Coole River conduit • Beagh River conduit • Coy Bypass • Blackrock surface input • Coole-Gland inlet conduit • (Anything upstream of Coole)	• Coole River conduit • Beagh River conduit • Coy Bypass • Blackrock surface inlet • Coole-Gland inlet conduit • Coole-Caherglassaun channel • (anything upstream of Coole)

*in the case of expanding conduit diameters, the results are inversed.

The overall results of the sensitivity analysis for constricting conduit dimensions are summarised in Table 6.1. The results of expanding conduit diameters are not presented as they are essentially the inverse of the constriction results (i.e. while constricting a conduit increases a turlough's volume, expanding the conduit reduces the volume). The general theme of the analysis is that *constricting* conduits downstream of a turlough increases its water level because the drainage capacity of the conduit has been reduced. Constricting a conduit upstream of a turlough slows down the input of water to that turlough and so the peak water level (volume) is reduced. When a conduit is *expanded*, its drainage capacity is increased and so a turlough upstream of the expanded conduit drains faster, reducing the peak while a turlough downstream of the conduit fills faster, increasing its peak. Using the results of this sensitivity analysis, the re-calibration of the model could be carried out in a targeted fashion knowing which conduits have the most influence on the turloughs.

6.3.3.2 Readjusting the Conduit Network

Readjusting the model was an iterative process. Each alteration made had consequences on all five turloughs either increasing or reducing accuracy to a high or low degree. As a result, the readjustment process was largely trial and error. In the end, over 680 various alterations were simulated before the optimum calibrated model was achieved. Most changes involved re-sizing pre-existing conduits. However a number of new conduit linkages were added to the model. These additional linkages will be described briefly below.

BLACKROCK RIVER-CONDUIT LINKS

Approximately 2 km upstream of Blackrock, an underground conduit section splits off the Owenshree River channel. As the Owenshree River is known to sink into the riverbed, two conduits were added to take account for this river conduit interaction (shown as red links in Figure 6.50). In Figure 6.49, the effect caused by the addition the two conduits is shown. The addition of the two conduits speeds up the recession curve to a more accurate shape (red: observed, green: original, black: conduits added).

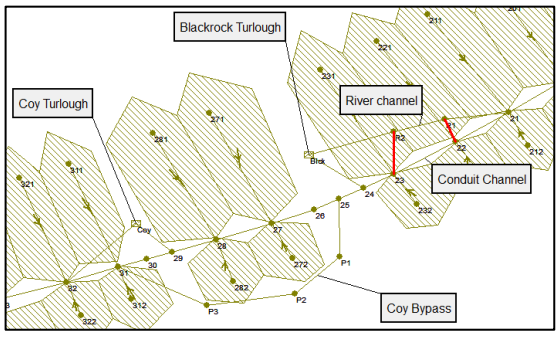

Figure 6.50: Model schematic (new links in red)

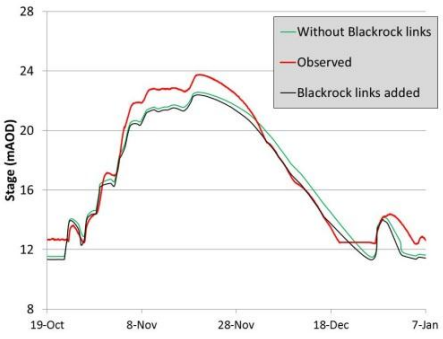

Figure 6.49: Flooding patterns (Blackrock).

COOLE BYPASS

Tracer studies carried out as part of the Gort Flood Study suggest the existence of a conduit link bringing water directly from the Gort River sink (Polltoophill) towards Caherglassaun bypassing Coole. The precise dynamics of this conduit are unknown but, in an effort to make the model more representative of the real system, the bypass link was added (Figure 6.51). After a number of simulations using various conduit diameters, the link proved to make little to no difference to the turlough flooding patterns. However, as the link did not reduce model accuracy, it was left in place (diameter: 0.5 m).

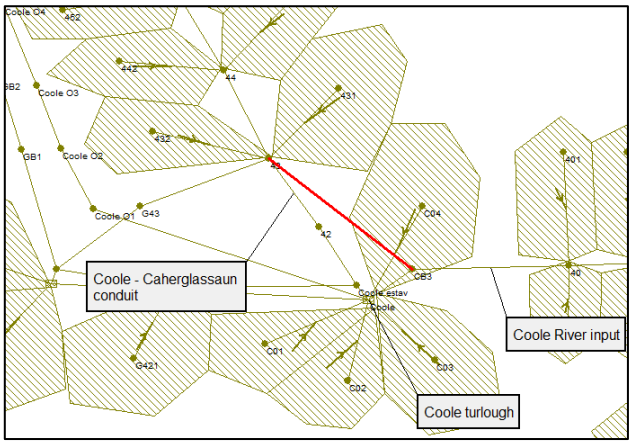

Figure 6.51: Model schematic (Coole bypass highlighted in red).

COOLE EPIKARST

The increased flow volume from the Beagh River led to overestimations of the volumes of the lower three turloughs, particularly Coole. Even with the updated stage-volume relationship, recession rate at high water levels was much too slow as there was only one outlet in its base for drainage (aside from an overflow surface outlet at 11m for extreme flooding which was seldom needed). As a high level epikarst system is known to exist in the Coole-Garryland region (Peach et al., 1998), it was conceived that Coole could partially drain via this epikarst system at higher levels. A series of multi-level conduits were applied to Coole between 6-9 mAOD (at 0.5m intervals) to represent an epiphreatic system similar to how epikarst operates within the region. In reality, the degree of this epiphreatic/epikarst drainage is likely to increase with elevation (weathering starts from the surface). However after a number of trial simulations, the most accurate recession curve was achieved when the set-up involved conduits reducing in diameter with increasing elevation (Figure 6.52). In order to keep the epikarst-drained water within the Gort Lowlands system, these epiphreatic channels were re-introduced to the conduit network downstream of Coole turlough. These conduits succeeded in reducing the recession curve of Coole turlough to a realistic level Figure 6.53.

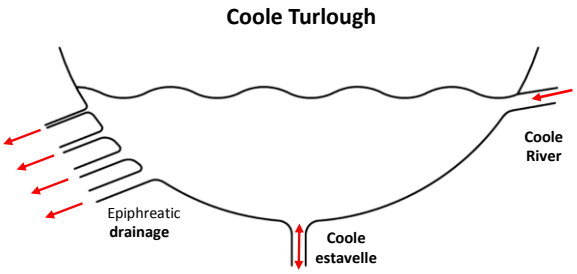

Figure 6.52: Coole turlough updated with epiphreatic drainage.

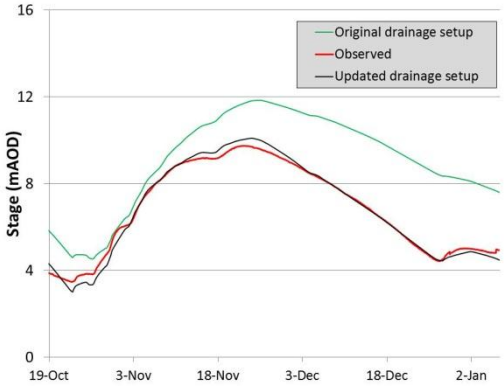

Figure 6.53: Flooding pattern (Coole).

COOLE – GARRYLAND EPIKARST LINK

As mentioned in Section 5.2, the relationship between Coole and Garryland is stage dependant. At low-medium water levels, the flooding pattern of Garryland tends to mirror Caherglassaun with water levels typically about 1m below those of Coole. When Garryland reaches 7-8 mAOD, the flooding pattern shifts to that of Coole. This behaviour suggests an epiphreatic fracture linkage between the turloughs at 7-8 mAOD. Setting up the model to behave in this manner involved two stages. Firstly, the underground conduit link between the turloughs was constricted to reduce the low-medium water levels of Garryland to a realistic level. Secondly, an upper level linkage was installed (Figure 6.54) joining the turloughs at 7 mAOD. This linkage ensured that Garryland and Coole flooding patterns balanced for high flood levels (Figure 6.55).

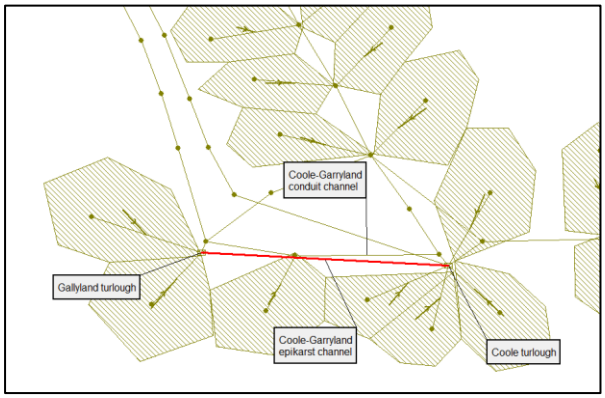

Figure 6.54: Model schematic (Coole-Garryland epikarst channel in red).

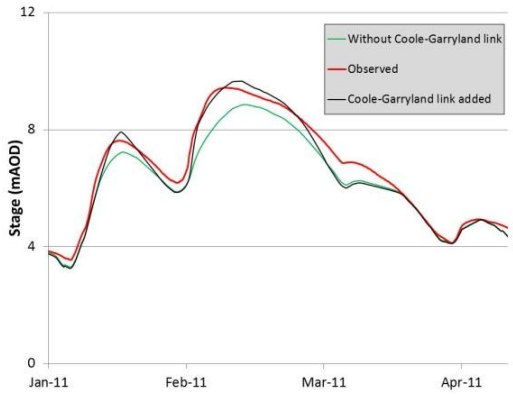

Figure 6.55: Flooding Patterns (Garryland).

NORTHERN FLOW ROUTE

The existence of a northern flow route was proposed by the Gort Flood Studies based on tracer tests and groundwater level fluctuation mapping. Groundwater level monitoring as part of this thesis has also suggested its presence (Section 5.5). As such, it was decided to include a northern flow route onto the model to make it more representative of the real system (Figure 6.56). A 0.8m conduit was added transmitting water from the Owenshree River directly towards an outlet (Kinvara East). As can be seen in Figure 6.57, the presence of a northern flow route reduced accuracy as the volume of water being transmitted to the upper two turloughs was diminished. The failure of the modelled northern flow route was two-fold. Firstly, the lack of any data for the 13.5 km distance between the Owenshree River and Kinvara was an issue. If the northern flow route was to be modelled, it would require significant details about the conduit system to determine if the water could drain freely or was being backed up by a separate network of turloughs (e.g. Lydacan turlough). Secondly, the model already struggled to make Blackrock peak high enough (as can be seen in Figure 6.57). Any further diminishing of the flow into the turlough would only decrease accuracy. Consequently, the Northern Flow Route was not included in the final calibration.

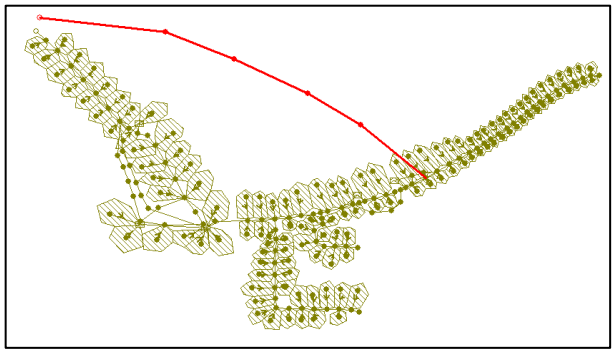

Figure 6.56: Model Schematic (northern flow route in red).

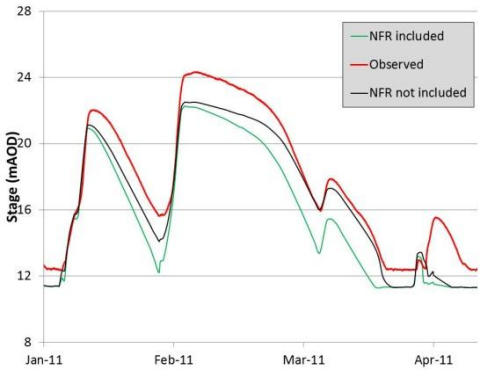

Figure 6.57: Flooding patterns (Blackrock).

The final calibrated model results for each turlough across a 3 year period (2010 to 2012) are displayed in Figures 6.58 and 6.59.

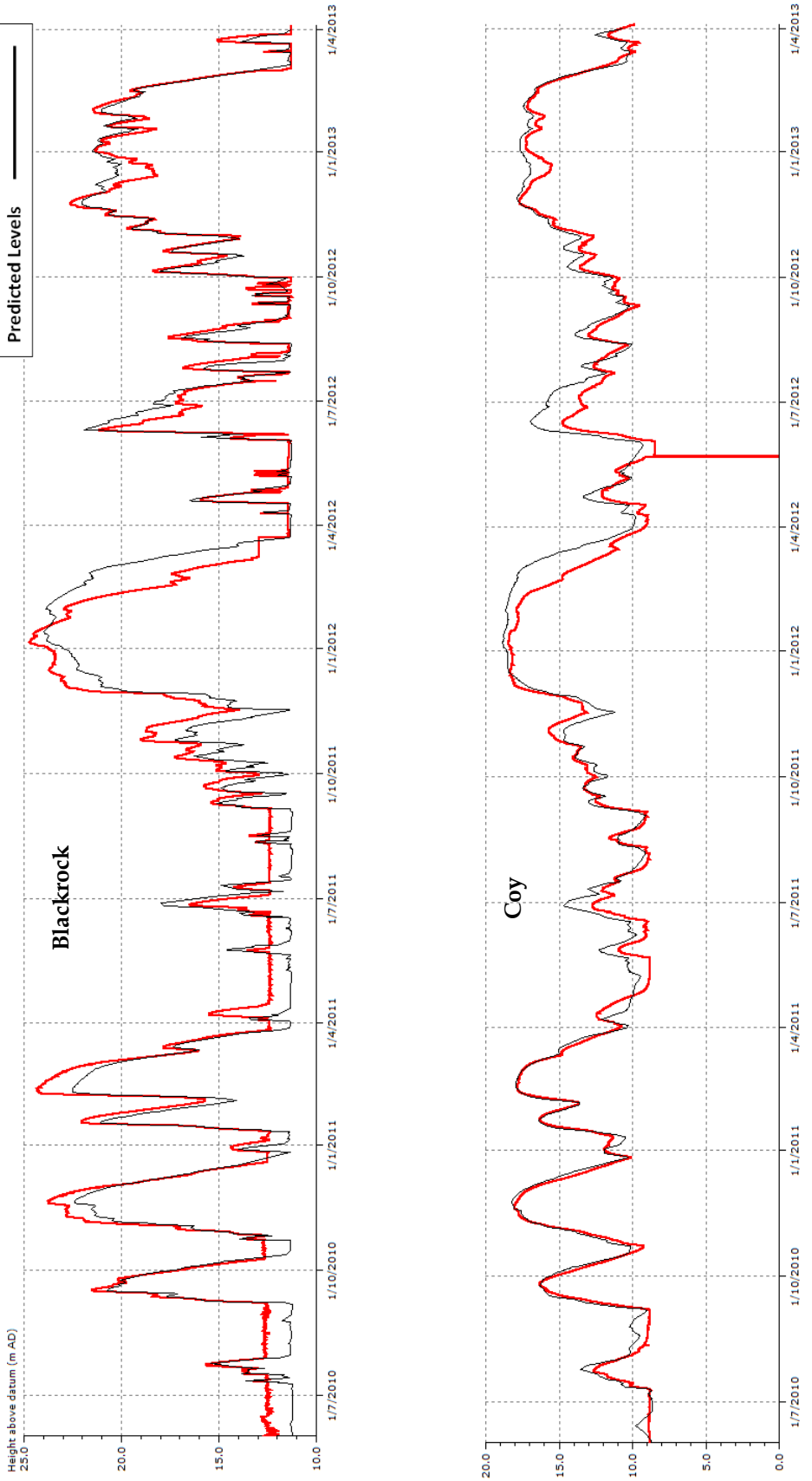

Figure 6.58: Blackrock and Coy final calibration. Note: the sudden drop of observed stage in Blackrock in April 2012 is due to diver repositioning (discussed in Section 5.2)

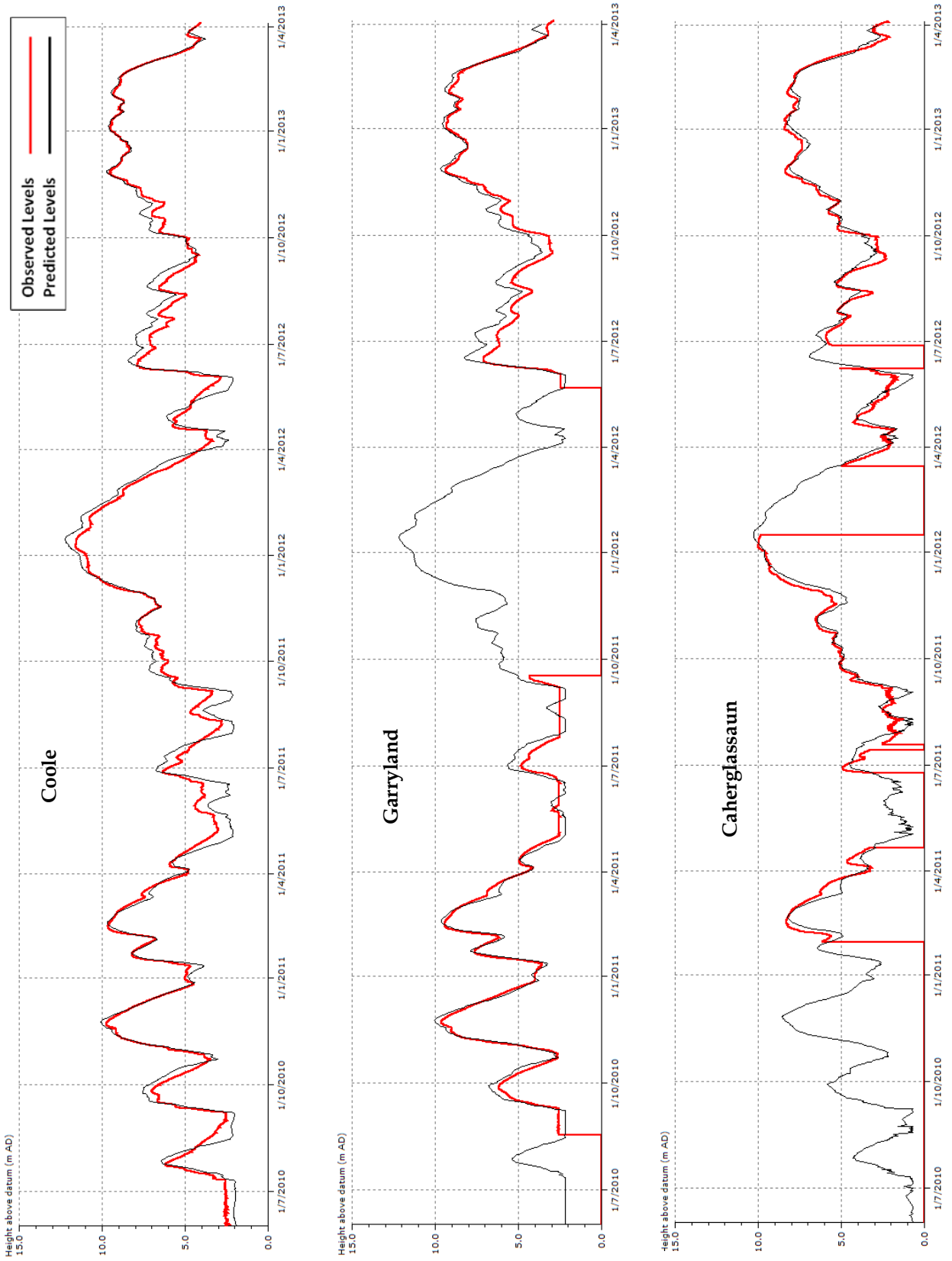

Figure 6.59: Coole, Garryland and Caherglassaun final calibration results.

The simulated water levels show good correlations with the measured water levels, particularly for the lower three turloughs. Model efficiency, E (goodness of fit – i.e. the Nash-Sutcliffe criterion) was calculated using Equation 5.1. Efficiency was determined for turlough water level and volume for the entire dataset (2010-2013) for Blackrock, Coy and Coole. For Garryland and Caherglassaun, partial datasets were used due to missing water level data. The results are presented below in Table 6.2.

Table 6.2: Efficiency of model results for turlough water level and volume data.

	Water Level	Volume
Blackrock	0.888	0.813
Coy	0.891	0.889
Coole	0.933	0.963
Garryland	0.961	0.974
Caherglassaun	0.963	0.962

The lower three turloughs calibrated very well with E values all above 0.93 for water level and above 0.96 for volume. The upper two turloughs did not calibrate as well with E values of 0.888 & 0.891 for water level and 0.813 & 0.889 for volume. The likely cause of the reduced accuracy of the upper two turloughs is due to the use of NAM for filling in gaps in the river flow dataset (Section 5.4.2). While the NAM model does provide a reasonable estimation of runoff within a catchment, it cannot match the accuracy of the river flow gauges. For example, NAM was used for a large portion of the 2011-2012 flooding season due to malfunctioning river gauge equipment. As can be seen in Figure 6.58, the simulated water levels of Blackrock and Coy for this period appear to be impacted negatively by this NAM usage. While the turloughs do reach the correct water level, both the peaks and recessions occur too late.

Another minor source of inaccuracy for Blackrock turlough is the incorrect base-level whereby the simulated water levels appear to drop another meter below the measured base-level of Blackrock. This is due to the diver platform being placed too high in the turlough. At these depths however, the effect that this error has on turlough volume is negligible.

For Coy, Garryland and Caherglassaun turloughs, the water level and volume E-values are quite similar. This is not the case for Blackrock and Coole. These differences are caused by the stage-volume curve. At high levels, a small error in water level results in a large error in volume. This

issue is particularly prevalent for Blackrock during the 2010-2011 flooding season where the model struggles to match the observed levels causing a moderate inaccuracy in water level but a large in inaccuracy in volume. For Coole turlough, the opposite is the case. High water levels are modelled better than low water levels resulting in the volume E-value being greater than the stage E-value.

When compared to the efficiency values for the model as calibrated by Gill et al. (2013a) (for stage only), the recalibrated model displays reduced accuracy for the upper two turloughs and increased accuracy for the lower three turloughs. However, due to the alterations made to the rating curves and stage-volume relationships, the two calibrations are not directly comparable. The recalibration has resulted in a slight reduction of stage accuracy for Blackrock and Coy but a significant increase in volume accuracy for all turloughs.

Similar to how NAM was used to fill in gaps in the river hydrographs, the calibrated turlough model was used to fill in gaps in the turlough datasets. This was important for Garryland and Caherglassaun turlough datasets as the divers suffered from equipment failure a number of times. These complete datasets could then be used for hydrochemical analysis. Also, the calibrated model provides a modelled outflow at Kinvara (KW) (Figure 6.60). This modelled outflow provides a very useful estimate for submarine groundwater discharges into Kinvara Bay over the study period (and is used throughout Chapter 7). Overall, the modelled outflow at Kinvara is 17% greater than the combined river input due to the contribution of rainfall on the diffuse/epikarst subcatchments.

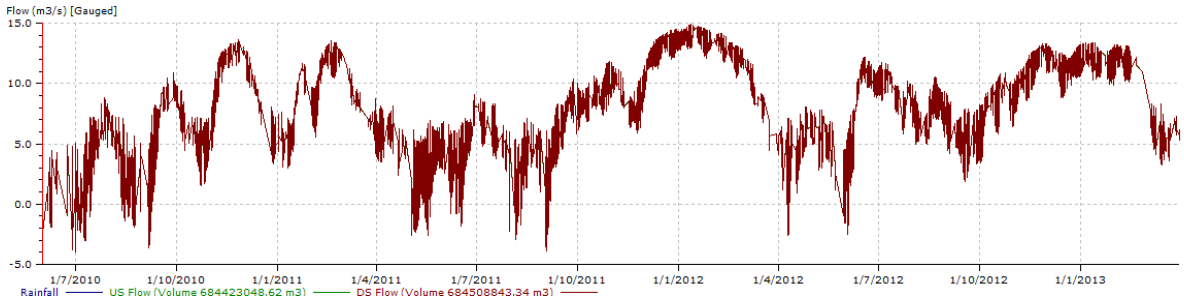

Figure 6.60: Modelled outflow at Kinvara (July 2010 – March 2013).

6.3.4 Model Analysis – Model Parameters

Similar to the conduit diameter sensitivity analysis in Section 6.3.3.1, the model was used to test the sensitivity of a variety of parameters such as roughness coefficient, conduit shape, subcatchment land use etc. The effect of changing these parameters was again assessed based on the changing

water levels of the turloughs. For consistency, the same analysis period as the conduit diameter analysis was used, 9th Sept 2010 – 20th Oct 2010.

6.3.4.1 Conduit Roughness

The effect of conduit roughness was investigated by altering the Colebrook-White roughness factor (ks=60) for all the conduits by ±10, 25, 50%. The results of this analysis on Blackrock turlough are shown in Figures 6.61 and 6.62 (all turloughs showed similar effects). The black dotted line represents the calibrated model and the coloured lines represent the altered roughness scenarios. The figures show that higher conduit roughness within the catchment leads to a small increase in turlough peak and a longer recession.

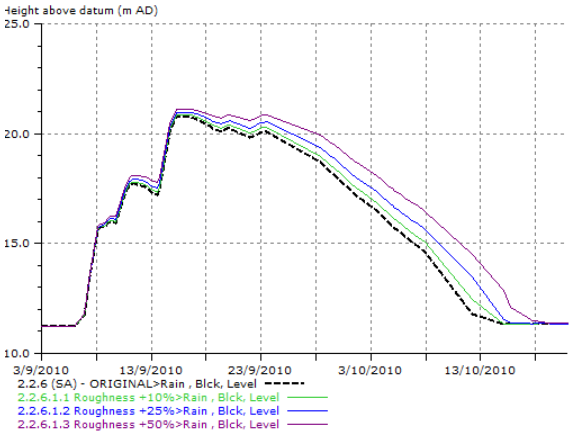

Figure 6.61: Increasing roughness (Blackrock).

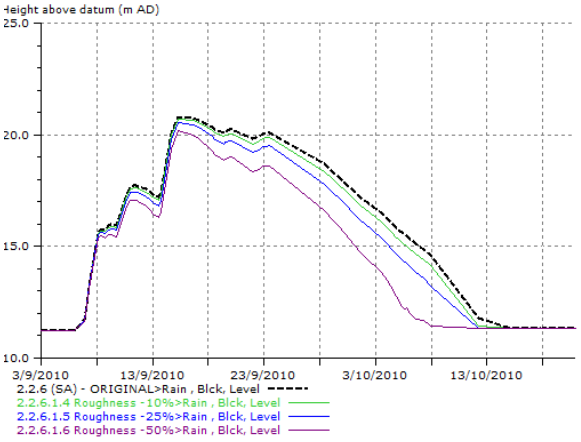

Figure 6.62: Decreasing roughness (Blackrock).

6.3.4.2 Conduit Shape

The calibrated model is based on conduits with circular cross section. The effect of changing these circular cross sections to elliptical cross sections was investigated as can be seen in Figure 6.63 (as many karstic conduits are really elliptical in shape). The ellipse was defined according to coordinate geometry (Equation 6.6) where a is the horizontal semi-axis and b is the vertical semi-axis and the origin is the ellipse centre point. The conduit areas were kept the same. In Figure 6.63, the green line represents an ellipse of height-width ratio 1:1.2 and the blue line represents a ratio of 1:1.7. Evidently, the Infoworks model predicts that the more elliptical a conduit is, the lower the turloughs rises. This is somewhat surprising considering that an elliptical conduit would have a higher surface area to volume ratio than a circular conduit and would thus be expected to provide slightly more friction (thus impeding drainage throughout the network).

$$\frac{x^2}{a^2}+\frac{y^2}{b^2}=1$$ *Equation 6.7*

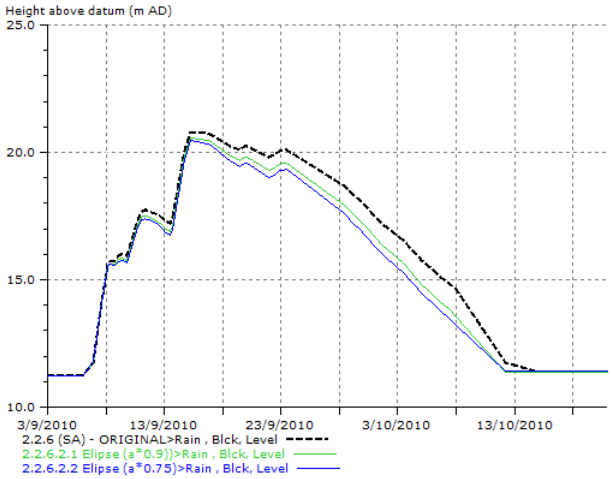

Figure 6.63: Elliptical vs. circular conduits (Blackrock).

6.3.4.3 Subcatchment Parameters:

A range of runoff and infiltration module parameters were altered to investigate which parameters are most influential on the subcatchment drainage. All parameters were adjusted by ±50%. See Table 6.3 for results.

Table 6.3: Subcatchment parameters analysis (continues over next two pages).

Parameter (original value)	Plot	Conclusion
Soil depth (1.5m)	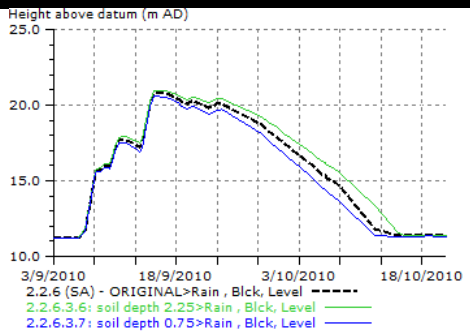	• Moderate effect
Percolation Coefficient (200) - A time coefficient, determined by calibration from existing data.	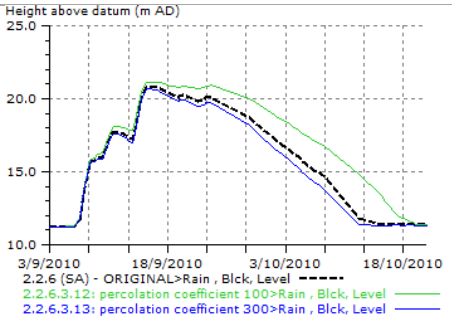	• Moderate effect for increase • Large effect for reduction

Baseflow Coefficient (2) - A time coefficient, determined by calibration from existing data.	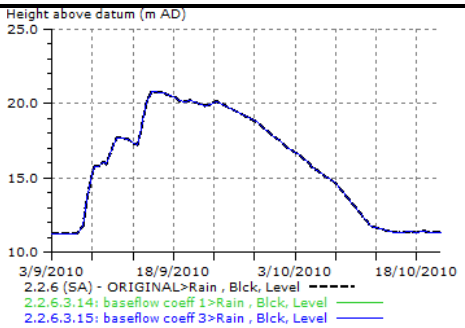	• No effect
Infiltration coefficient (30) - A time coefficient, determined by calibration from existing data.	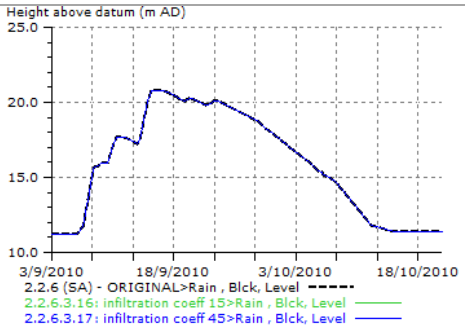	• No effect
Percolation threshold (0.9) - The percentage saturation level of the soil at which water starts to percolate downwards (only -50% analysis carried out, +50% was above limit)	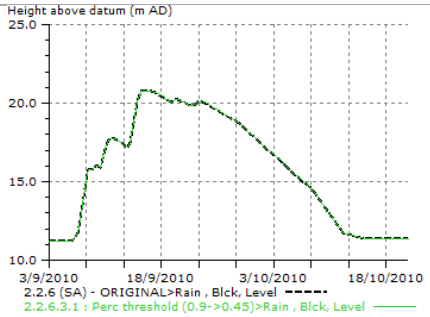	• No effect
Percolation % infiltrating (90) - The percentage of percolation flow that infiltrates directly into the drainage network. (only -50% analysis carried out, +50% was above limit)	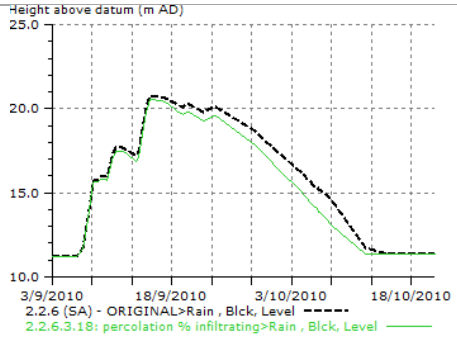	• Large effect
Porosity of soil (30)	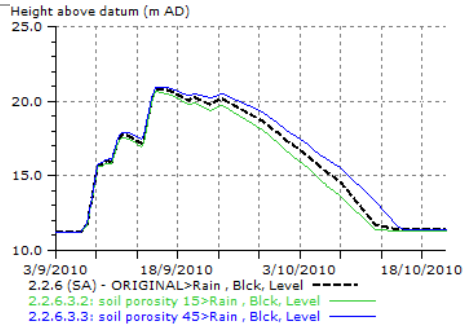	• Moderate effect

Porosity of ground (50)	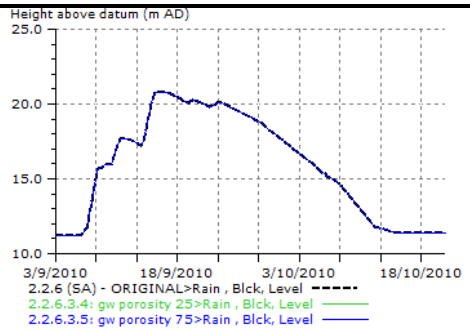	• No effect
Baseflow threshold level (-1) - The groundwater level at which secondary infiltration occurs	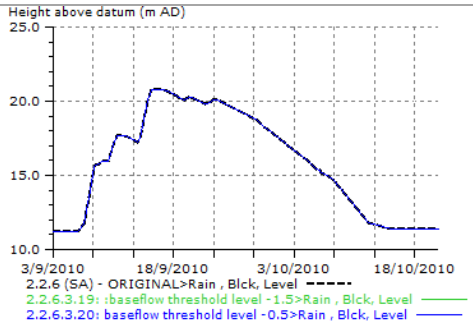	• No effect
Infiltration threshold level (1) - The level of the groundwater storage reservoir at which groundwater infiltration occurs	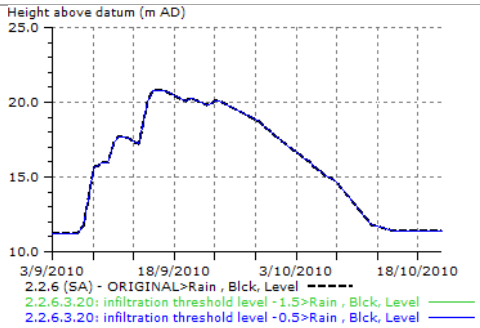	• No effect
Fixed runoff coefficient (0.05) - a coefficient determining proportion of runoff, i.e. a value of 0.1 indicates 10% runoff from the surface	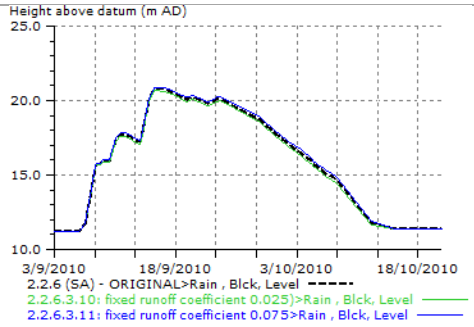	• Small effect
Runoff routing value (24)	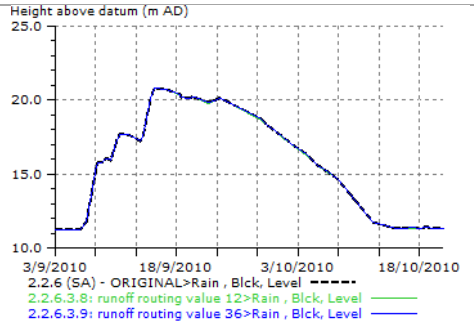	• No effect.

From these tests, it can be seen that the parameters relating to percolation and the soil reservoir are the most influential on the network.

6.3.4.4 Model analysis – Input Parameters (Sensitivity of Turloughs Input Data)

All climatic data (except for PET) that is used for simulation is inputted into the model as hourly timesteps. This provides the model with good temporal resolution and ensures the turlough flooding behaviour could be modelled as accurately as possible. In these tests, the temporal resolution of the inputs was reduced to investigate the sensitivity of the model to the input data.

Input data for river flows and rainfall was converted from one hour into one day, five day and ten day averages. These datasets were then inputted into the model and simulations carried out for the 2010-2011 flooding season. The results for Blackrock are shown in Figure 6.64 and for Coole in Figure 6.65.

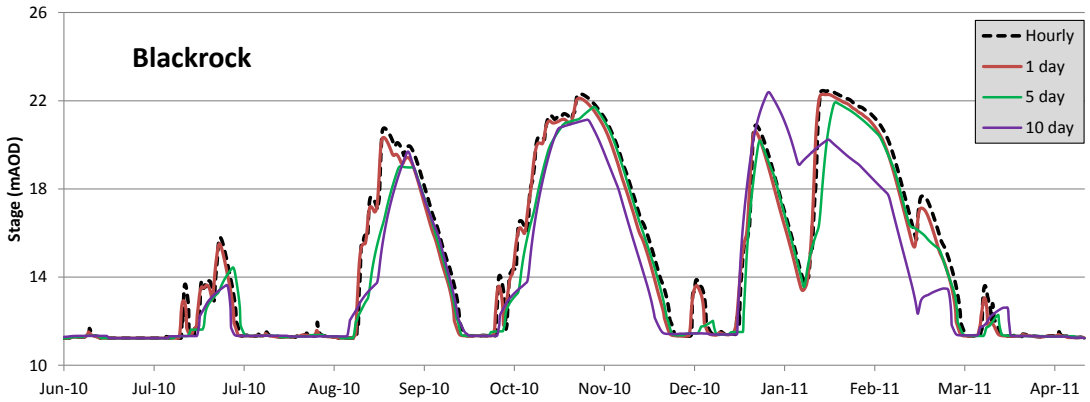

Figure 6.64: Input sensitivity analysis results (Blackrock).

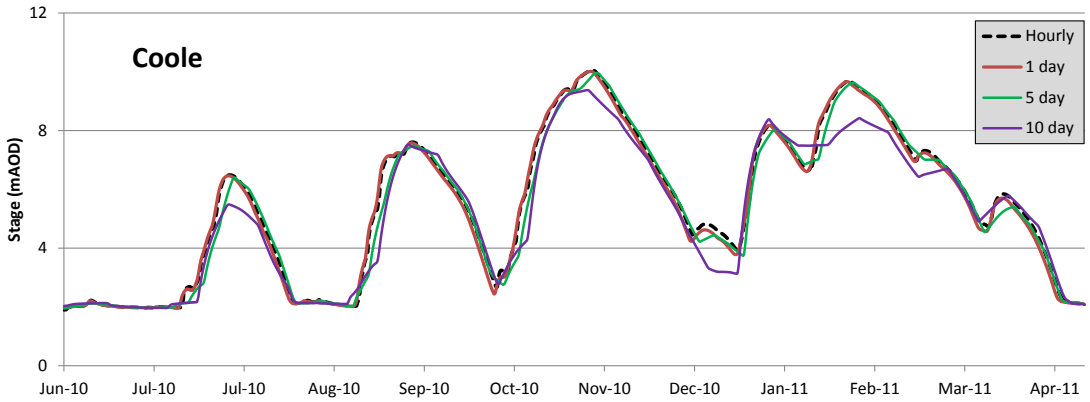

Figure 6.65: Input sensitivity analysis results (Coole).

For both Blackrock and Coole, the 1-day and 5-day average input datasets show little difference from the hourly input dataset. The difference is more pronounced for Blackrock turlough as it is fed directly by the Owenshree River resulting in rapid changes (the same difference is observed with Coy turlough). As Coole is fed by the Beagh River which has been attenuated by Lough Cutra, the effect of dampening the inputs is less significant with almost no discernible difference between the hourly and 1-day, 5-day inputs. A considerable change is caused by the 10-day averaged input data leading to poor accuracy for Coole and extremely poor accuracy for Blackrock.

In conclusion, it can be said all of the turloughs react minimally to inflow variation on a time scale below 24 hours and the lower three turloughs show little reaction to inflow variation on the scale of up to 5 days. All turloughs however are affected by variation within a 10-day time period.

6.4 Evaluating the Impact of Climate Change using the Pipe-Network Model.

Evidence of climate change is incontrovertible. Over the last fifty years, average global surface temperature has increased at a rate of 0.13°C per decade. This warming effect has led to changes in average air and ocean temperatures, widespread melting of snow and ice and rising global average sea level (IPCC, 2007). In this section, the impact of global warming on the flooding patterns of the Gort Lowlands is investigated by combining the pipe-network model with projected changes in climatological parameters, specifically rainfall and sea-level.

6.4.1 Global Trends

According to the Fourth Assessment Report (AR4), from the Intergovernmental Panel on Climate Change (IPCC), most of the warming observed since the mid-20th century is 'very-likely' (greater than 90% likelihood) due to the to increases in anthropogenic greenhouse gas (GHG) emissions (IPCC, 2007). There is 'high agreement and much evidence' that global GHG emissions will continue to grow over the next few decades based on current climate change policies and related sustainable development practices. However, future emissions cannot be predicted with confidence. In order to address this uncertainty, the IPCC published the Special Report on Emissions Scenarios (IPCC, 2000) which provides a number of alternative development pathways, covering a wide range of demographic, economic and technological driving forces resulting from GHG emissions. These scenarios can then be used to drive global climate models (GCM) in order to

predict future changes in global climate. Four 'scenario families' were developed and are displayed in Figure 6.66 below:

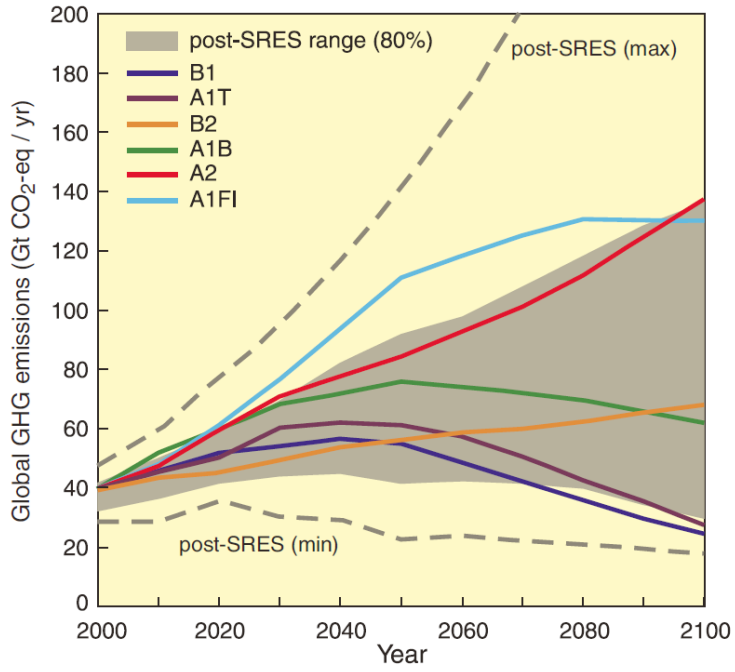

Figure 6.66: Projected global GHG emission scenarios until 2100 (IPCC, 2007).

- The A1 pathway assumes a world of very rapid growth, a global population that peaks in mid-century and rapid introduction of new and more efficient technologies. The pathway is sub-divided based on technological change into: A1FI (fossil intensive), A1T (non-fossil energy) and A1B (balance).
- The B1 pathway describes a convergent world with the same global population as A1, but with more rapid changes in economic structures toward a service and information economy.
- B2 describes a world with intermediate population and economic growth, emphasising local solutions to economic, social, and environmental sustainability.
- A2 describes a very heterogeneous world with high population growth, slow economic development and slow technological change.

Using these scenarios with GCMs, projections of future climate changes over the course of the 21st century have been made. Fealy and Sweeney (2008) summarise these changes as the following:

- Global average surface temperature is likely to increase by approximately 1.8°C to 4.0°C over the present century.

- Increased winter precipitation in mid to high latitude regions by the middle of the century with large year-to-year variations.
- An increase in maximum temperatures and frequency of hot days.
- Storm tracks are projected to migrate polewards resulting in changes in precipitation.
- The present day retreat of mountain glaciers is likely to continue. While Antarctica is likely to gain ice due to enhanced precipitation, Greenland is likely to lose mass due to a greater increase in run-off over precipitation increases.
- Global mean sea level is projected to rise by between 0.28 and 0.4 m.

6.4.2 Climate Change in Ireland

In Ireland, the effects of climate change have already been observed with mean annual temperatures in rising by 0.74°C over the past 100 years. The number of frost days has diminished and annual precipitation has increased on the north and west coasts with higher rainfall intensity and persistence (McElwain and Sweeney, 2007). The consequences of this increased rainfall intensity was seen already in the Gort Lowlands where there has been five major flooding events since 1989 where previously, similar events only occurred once every 30 years. McGrath et al. (2011) suggest that the recent flooding of November 2009 is 'likely to be linked to natural climate variability combined with a small expected increase in rainfall due to anthropogenically driven climate change'. Looking forward, climate models suggest that short duration extreme events will become more frequent in future and that Ireland will experience wetter winters and drier summers (McGrath et al., 2011).

A study on climate change in Ireland by the Environmental Protection Agency (2008) used empirical statistical downscaling to enable the use of GCMs on a regional scale. Two emission scenarios, A2 and B2, were modelled using three GCM's, namely, the HadCM3, the Canadian Centre for Climate Modelling and Analysis (CCCma) (CCCM2) and the Commonwealth Scientific and Industrial Research Organisation (CSIRO Mark 2). The results of this study were presented as individual results for each scenario and GCM but also as ensembles whereby the results of the three GMO's were averaged in order to try and account for different model and emissions uncertainties. Ensembles were calculated using a weighted mean based on the Impacts Relevant Climate Protection Index (IR-CPI) (Wilby and Harris, 2006) which weights each GCM based on its ability to reproduce the properties of the observed climate. The IR-CPI derived scores were then used to weight the relevant downscaled output from the different GCMs in order to produce an ensemble mean for both the A2 and B2 emissions separately and both emissions together (Environmental

Protection Agency, 2008). The 'both emissions together' mean can thus be used as a third emission scenario which is essentially a rough average of scenarios A2 and B2. Henceforth, in this chapter, this 3rd scenario shall be referred to as 'A2 & B2 ensemble' or just 'ensemble'. Results for temperature and precipitation were presented in terms of projected seasonal changes for the 2020's, the 2050's and the 2080's. See Table 6.4 below for precipitation results for scenarios A2, B2 and the A2 & B2 ensemble.

Table 6.4: Percentage changes in mean precipitation (Environmental Protection Agency, 2008).

	Winter	Spring	Summer	Autumn
A2				
2020	+2	-4	-7	-3
2050	+12	-8	-12	-4
2080	+19	-12	-23	-9
B2				
2020	+4	+3	0	-2
2050	+13	-6	-12	-2
2080	+12	-4	-14	-6
A2 & B2 Ensemble				
2020	+3	-1	-3.5	-2.5
2050	+12.5	-7	-12	-3
2080	+16	-8	-19	-7.5

6.4.3 Application of the Gort Lowlands Model

Using the climate change projections of the Environmental Protection Agency (EPA) (2008), an investigation can be carried out into how climate change could likely alter the flooding patterns in the Gort Lowlands. The EPA's projected seasonal changes in rainfall can be applied to a current rainfall dataset to produce hypothetical future rainfall datasets. Using these datasets, a comparison can be made between current flooding patterns and hypothetical future flooding patterns using the pipe network model. To apply the EPA projections, the pipe-network inputs were altered in the following manner:

RAINFALL

Rainfall input data was altered for each timestep by a factor related to the seasonal projected change (e.g. 2 mm of rainfall falling in winter becomes 2.38 mm in winter 2080 under scenario A2).

Rainfall datasets for the 2020's, 2050's and 2080's were produced for both Kilchreest and Francis Gap rain gauges using emission scenarios A2, B2 and the ensemble scenario.

RIVER FLOWS

Future river input data for the Owenshree and Ballycahalan Rivers was calculated using the NAM rainfall-runoff model based on the future rainfall datasets. However, input data for the Beagh River could not be calculated in this manner as the NAM model is not suitable due to the significant attenuation effect caused by Lough Cutra. Instead, the Beagh river flows were calculated using a reservoir routing calculation (Section 6.4.3.1) based on Owendalulleegh River flows.

As mentioned in Section 5.4.2, the Owendalulleegh River could not be calibrated using NAM and so another method to predict its altered river flows was necessary. As the catchment is located very close to the other two NAM calibrated catchments and comprises similar runoff characteristics (geology, slope, vegetation etc.), it was deemed valid to use the percentage alterations caused to these rivers and apply them to the Owendalulleegh River.

SEA-LEVEL

Projections of future changes in sea level were calculated as part of the fourth assessment report (IPCC, 2007) and are shown below in Figure 6.67. The IPCC projections for sea level are based on 1990 as the datum and as such, the sea level over the study period (2010-2013), according to the projections, is approximately +4 mm. Increases from this +4 mm value were therefore added to the Kinvara tidal data for input into the model Table 6.5.

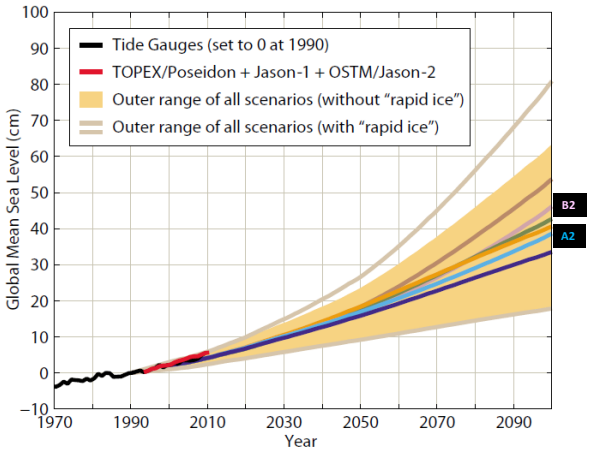

Figure 6.67: Global average projections for sea level rise (from Church et al. (2011)).

Table 6.5: Projected increases in global sea level (mm).

	A2	B2	Ensemble
Present	+4	+4	+4
2020	+7	+7	+7
2050	+13	+13	+13
2080	+32	+29	+30.5

6.4.3.1 Reservoir Routing – Lough Cutra

Lough Cutra (Figure 5.19) causes a considerable attenuated and lagged response to the peak flows from the Owendalulleegh River (Figure 5.20) due to the large area of the lake (3.9 km^2). Flows in the River Beagh rarely rise above 20 m^3/s whereas the Owendalulleegh River can reach flows over 70 m^3/s. Lough Cutra is also fed by a smaller river to the north, the Gorteenboy River which drains a catchment of approximately 8.2 km^2 in area (the Owendalulleegh catchment is 89.3 km^2 in size). As suggested by Gill (2010), this smaller catchment was accounted for using a factor based on the relative sizes of the catchments. Thus a factor of 0.09 (9%) was applied to Owendalulleegh flows in order to account for the extra volume although it is acknowledged that the relative timing of this flow into Lough Cutra may not be accurate.

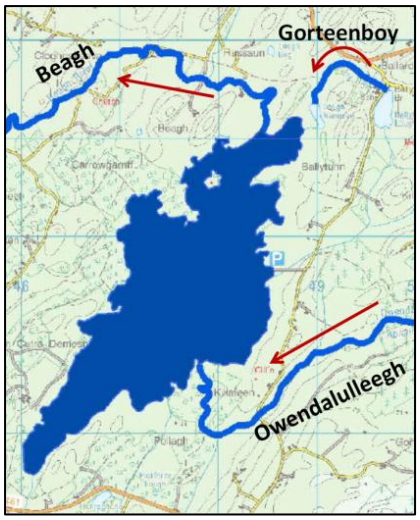

Figure 6.68: Lough Cutra.

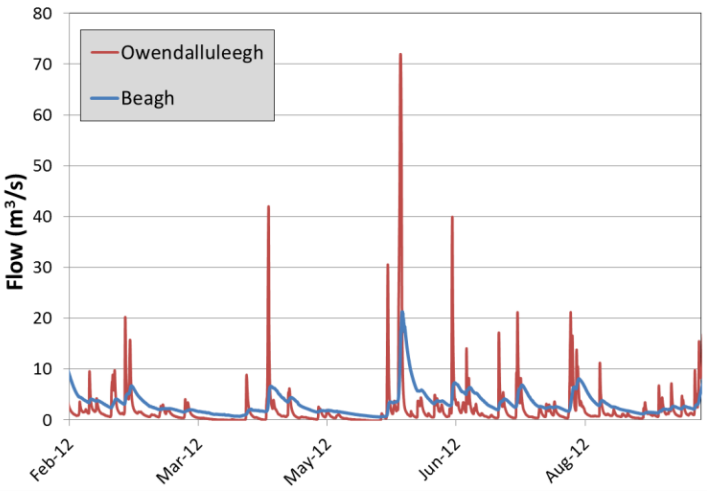

Figure 6.69: Owendalulleegh inflow and Beagh outflow from Lough Cutra.

A cumulative flow plot between the Owendalulleegh and Beagh rivers shows a difference in volume as can be seen in Figure 6.70. The un-factored input is shown as a red dotted line and the factored as a red solid line. It can be seen that even with the factored input the output is still considerably larger. This difference has a number of possible causes such as rainfall on the lake or an underestimation of the contribution of the Gorteenboy River but the most likely cause is inaccuracies is the rating curve for the Owendalulleegh River at medium-high flows.

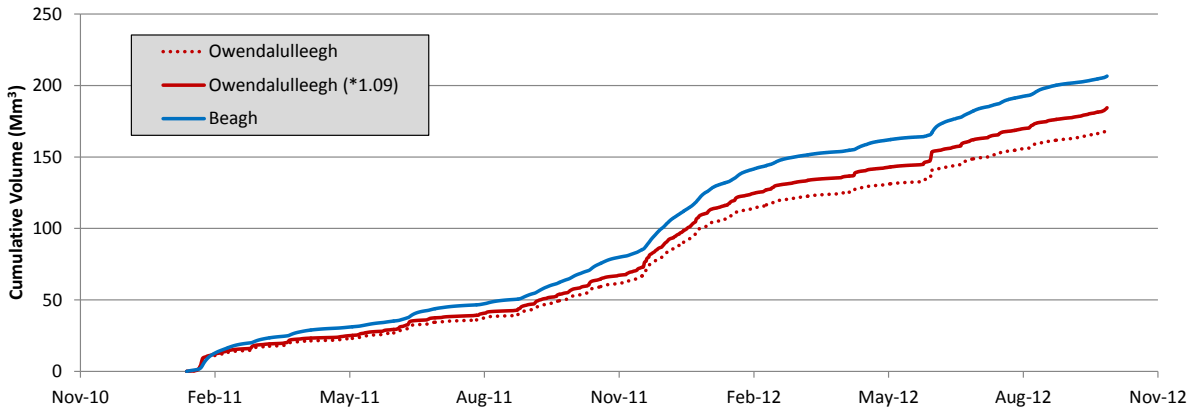

Figure 6.70: Cumulative inflow and outflow from Lough Cutra (2011-2012).

The reservoir (or level-pool) routing method was chosen to route the flows across Lough Cutra. The reservoir routing method is based on a combination of the continuity equation with a non-linear storage discharge equation (Shaw, 2011). For this, a stage-discharge and stage-storage relationship needed to be defined – the so-called auxiliary curve, which is a plot of G vs. Q_{out} according to the following relationships:

$$G_2 = G_1 + \frac{(Q_{in(1)} + Q_{in(2)})}{2} - Q_{out\,(1)} \qquad \textit{Equation 6.8}$$

$$Q_{out(2)} = x_2 G_2^2 + x_1 G_2 + x_0 \qquad \textit{Equation 6.9}$$

$$G_t = S_t + \frac{(Q_{out(t)})}{2} \qquad \textit{Equation 6.10}$$

where Q_{out} is outflow, Q_{in} is inflow, G represents the function: $[(S/\Delta t)+(O/2)]$, S is storage, Δt is the time interval for the routing period and x_0, x_1, x_2 represent the coefficients used for optimisation. The outflow (Q_{out}) at each time step is thus calculated sequentially through the data. The parameters were optimised using the Solver macro function in Excel in order to minimise the sum of the difference squared between the observed and simulated data at each time step. The final optimised parameters were:

$x_0 = 0.000001$

$x_1 = 0.0109$

$x_2 = 0$

In order to balance the total volume of the observed and predicted outflow results, a factor of 0.23 (23%) was added to the Owendalulleegh River flow data. This factor suggests an imbalance of 14%

(23%-9%) between the Owendalulleegh and Beagh flows. This imbalance is likely due to the contribution of rainfall to the lake and an underestimation of flow on the Owendalulleegh River. The final reservoir routing model showed a good match between predicted and observed flows in the Beagh River, as can be seen Figure 6.71.

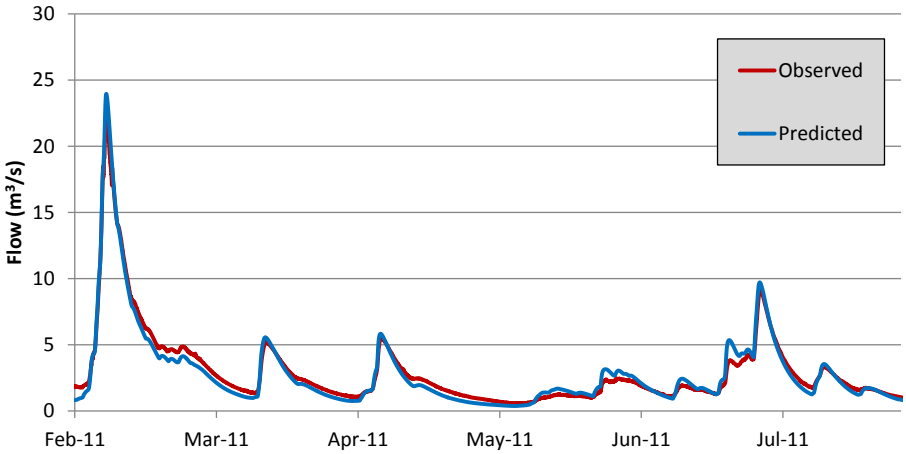

Figure 6.71: Reservoir routing results, Observed vs Predicted (2011).

6.4.4 Results

The choice of analysis period was limited to periods with good flow data from the three rivers involved. The flow records from the Owenshree and Ballycahalan Rivers were complete after being integrated with NAM predictions (Section 5.4.2) but the Owendalulleegh River had large gaps. As a result, analysis was limited to January 2011 – November 2012. This period was acceptable for analysis as it included one complete flooding season and numerous smaller floods.

The results of the analysis for emission scenarios A2 and B2 are shown in Figures 6.72 & 6.73 (see Appendix E for Ensemble results). The figures display the changing flooding patterns on each turlough as caused by the projected rainfall of the 2020's, 2050's and 2080's. The 'Present' line on the graph related to the rainfall datasets with no alterations from what occurred in reality. It should be noted that the 'Present' results are based on using NAM generated runoff rather than observed river flows for the Owenshree and Ballycahalan Rivers. This was done so as to give a clear comparison of the effects of the changing rainfall patterns, i.e. present NAM runoff is compared with future NAM runoff rather than present observed runoff compared to future NAM runoff. Using NAM data in this way resulted in a slight alteration of the flooding pattern for the upper two turloughs with slightly lower flood peaks. Changes to the flooding pattern of the lower three turloughs was negligible.

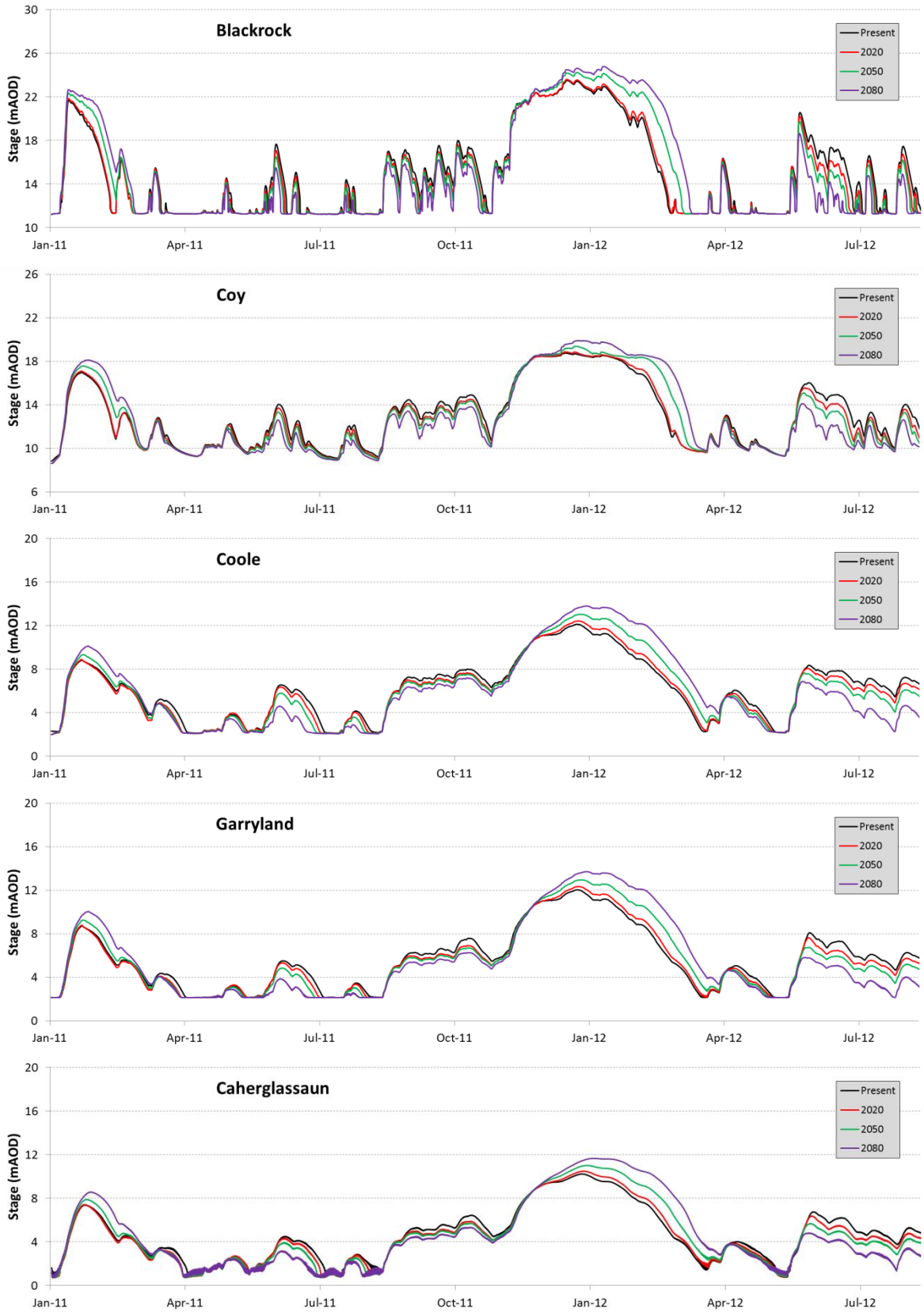

Figure 6.72: Turlough flooding patterns according to emission scenario A2.

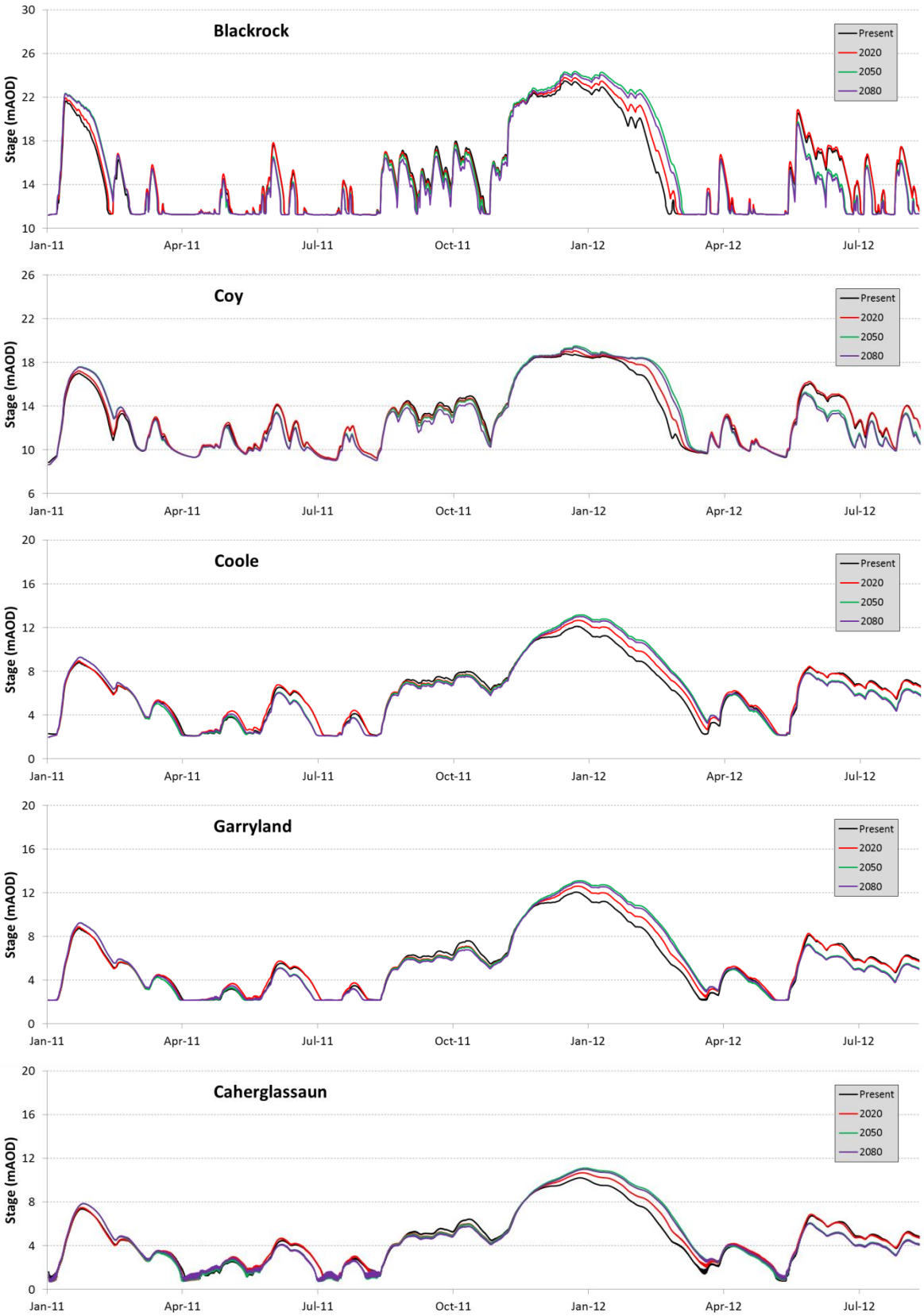

Figure 6.73: Turlough flooding patterns according to emission scenario B2.

As can be seen from the results, the reduced summer rainfall and increased winter rainfall from the climate change scenarios leads to significant alterations in the turlough flooding patterns over the 615 day period. The projected changes for stage volume and area are shown in Tables 6.6, 6.7 and 6.8.

Both simulated scenarios project a continuous increase in global GHG emissions over the next 100 years. Scenario A2 projects a steep rate of increased emissions for the first 30 years followed by a lower, but still significant, rate of increase up to 2100. Scenario B2 projects a more gradual increase with a slight reduction in rate after the 2060's (Figure 6.66). The variation between these emission scenarios leads to variation between projected rainfall patterns (Table 6.4) which in turn leads to variation between the turlough flooding patterns (Figures 6.72 & 6.73). Scenario A2 projects increased winter rainfall and decreased summer rainfall with time. This rainfall pattern is translated to the turloughs resulting in much higher water levels with longer recessions in winter and lower flood levels in summer. Scenario B2 projects less rainfall than scenario A2 with winter rainfall increasing for the 2020's and 2050's followed by a slight drop in winter rainfall in the 2080's. This drop in rainfall possibly reflects the drop is reduced rate of increase of GHG emissions after the 2060's for this scenario. This drop in rainfall translates to 2080's water levels peaking slightly below the 2050's water levels. The Ensemble scenario projects a rough average between the other two scenarios.

Overall, the effect of climate change tends to result in a net drop of annual river flow volumes despite increased winter flows. This effect can be seen in the cumulative plots of the Owenshree River as seen in Figure 6.74. The only scenario resulting in increased river flows is that of B2 for the 2020's. It should be noted however that these cumulative flow plots contain one and a half years data (two winters and one summer) and thus are biased towards winter conditions.

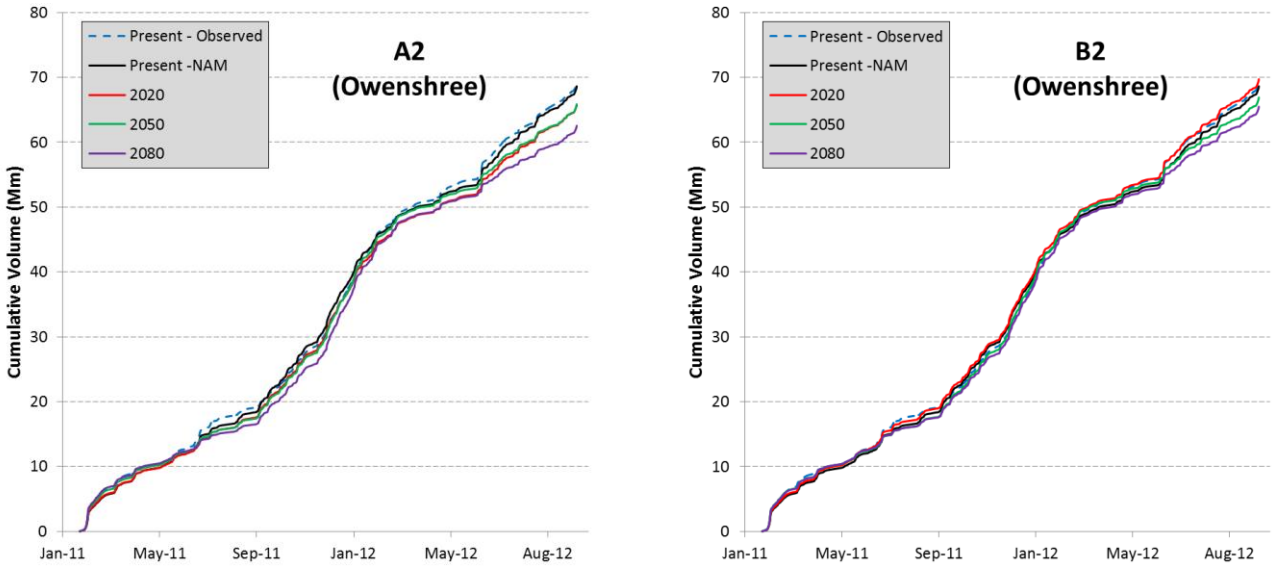

Figure 6.74: Cumulative flow plots for the Owenshree River for scenarios A2 and B2 for the period between Jan 2011 and October 2012.

Table 6.6: Maximum stage (m) predicted for emission scenarios A2, B2 and the Ensemble (A2 & B2) for the period between Jan 2011 and October 2012.

	Blackrock	Coy	Coole	Garryland	Caherglassaun
'Present'	23.5	18.8	12.1	12.1	10.2
A2					
2020	23.6	18.9	12.4	12.4	10.5
2050	24.2	19.4	13.0	13.0	11.0
2080	24.8	19.9	*	*	11.7
B2					
2020	23.8	19.1	12.7	12.6	10.7
2050	24.4	19.5	13.2	13.1	11.1
2080	24.2	19.4	13.0	13.0	11.0
A2 & B2					
2020	23.8	19.0	12.6	12.5	10.6
2050	24.3	19.5	13.1	13.0	11.1
2080	24.4	19.5	13.2	13.1	11.1

*above maximum surveyed level

Table 6.7: Maximum Volume (*1,000,000 m³) and %-increase from 'Present' maximum Volume for emission scenarios A2, B2 and the Ensemble (A2 & B2) for the period between Jan 2011 and October 2012.

	Blackrock		Coy		Coole		Garryland		Caherglassaun	
	Max	% increase	Max	% increase	Max	% increase	Max	% increase	Max	% increase
'Present'	3.466	-	1.818	-	15.371	-	1.931	-	3.064	-
A2										
2020	3.570	2.9	1.868	2.7	16.315	5.8	2.037	5.2	3.265	6.1
2050	4.349	20.3	2.147	15.3	18.373	16.3	2.263	14.7	3.709	17.4
2080	5.109	32.2	2.520	27.9	*	*	*	*	4.305	28.8
B2										
2020	3.823	9.3	1.952	6.8	17.123	10.2	2.127	2.1	3.438	3.4
2050	4.545	23.7	2.210	17.7	18.845	18.43	2.314	2.3	3.811	3.8
2080	4.285	19.1	2.124	14.4	18.314	16.1	2.257	2.3	3.710	3.7
A2 & B2										
2020	3.745	7.4	1.920	5.3	16.839	8.7	2.095	7.9	3.377	9.3
2050	4.448	22.1	2.174	16.4	18.578	17.3	2.285	15.5	3.753	18.4
2080	4.527	23.4	2.206	17.6	18.803	18.3	2.309	16.4	3.813	19.7

*above maximum surveyed level

Table 6.8: Maximum Area (ha) and %-increase from 'Present' maximum Area for emission scenarios A2, B2 and the Ensemble (A2 & B2) for the period between Jan 2011 and October 2012.

	Blackrock		Coy		Coole		Garryland		Caherglassaun	
	Max	% increase	Max	% increase	Max	% increase	Max	% increase	Max	% increase
'Present'	1,125	-	484	-	3,100	-	351	-	777	-
A2										
2020	1,147	1.9	501	3.4	3,218	3.7	359	2.2	808	3.9
2050	1,311	14.2	611	20.9	3,478	10.9	374	6.0	877	11.4
2080	1,434	21.6	894	45.9	*	*	*	*	965	19.5
B2										
2020	1205	6.7	527	0.0	3319	6.6	365	3.8	835	7.0
2050	1343	16.3	656	26.3	3533	12.3	377	6.8	892	13.0
2080	1299	13.5	598	19.1	3472	10.7	373	6.0	877	11.4
A2 & B2										
2020	1,186	5.2	517	6.5	3,283	5.6	363	3.2	826	5.9
2050	1,328	15.3	628	23.0	3,502	11.5	375	6.4	883	12.1
2080	1,340	16.1	653	26.0	3,528	12.1	376	6.7	893	13.0

*above maximum surveyed level

While scenario A2 results in the highest peak water levels of the turloughs during winter, the summer months see much less flooding resulting in a net increase in dry days for all five turloughs. This can be seen below in Table 6.9 (table limited to data from Jan 2011 to Jan 2012 in order to remove winter bias in results). For the 2080's, four of turloughs see over 25 extra dry days over the year (The lower results for Coy turlough are likely a result of poor simulation accuracy at low water levels for this turlough). Scenario B2 shows more varied results with less empty days in the 2020's and more in the 2050's and 2080's. Again, the Ensemble scenario produces a rough average between A2 and B2 scenarios, resulting mostly in increased empty days.

Table 6.9: Change in empty days for turloughs for emission scenarios A2, B2 and the Ensemble (A2 & B2) over the period Jan 2011 – Jan 2012.

	Blackrock	Coy	Coole	Garryland	Caherglassaun
A2					
2020	+9	+2	+5	+8	+8
2050	+11	+2	+19	+15	+15
2080	+29	+10	+33	+34	+26
B2					
2020	-3	+2	-16	-5	-12
2050	+7	+2	+9	+10	+9
2080	+12	+2	0	+7	+2
A2 & B2					
2020	+4	+2	-5	3	+2
2050	+11	+2	+16	+12	+12
2080	+23	+7	+20	+17	+14

This change in flooding patterns behaviour can be presented graphically using flood duration curves. Duration curves provide a way to represent the amount of time a given quantity is equalled or exceeded over a defined interval (Fetter, 2001). For example, in the context of turlough hydrology, a duration percentage value of 80% indicates that the turlough equals or exceeds the corresponding depth 80% of the time. Duration curves are useful for turloughs as they present a means of quantifying the flooding effect or disturbance experienced by ecological communities at any point within a turlough basin. Within any defined period, a flood duration gradient exists whereby elevations at the base of the turlough experience longer flood duration that those higher up the basin. The water level - duration curve quantifies this gradient. Flood duration curves were used for turloughs in this manner by Naughton (2011).

The procedure for generating a duration curve, as outlined by Fetter (2001), is as follows:

- The level data is first sorted in descending order, from highest to lowest
- A rank *m* is assigned to each value from 1 to *n*, *n* being the length of the data set.
- The probability *P* of a given level being equalled or exceeded within the period n is given by:

$$P = 100\frac{m}{n+1} \qquad \textit{Equation 6.11}$$

- A plot of probability P against stage (the so-called duration curve) shows the percentage of time each level is equalled or exceeded.

Flood duration curves of the turloughs for scenarios A2 and B2 are presented in Figure 6.75. In this figure, each sub-plot displays the projected changes in flood duration behaviour for a particular turlough, for a particular emission scenario (results for the ensemble scenario can be found in Appendix E). Looking at these plots, all turloughs show a similar trend whereby the duration at which turloughs have high water levels will increase while the duration at which turloughs have low-medium water levels will decrease. For instance, Blackrock turlough currently shows depths equal to or exceeding 8m for 20% and 4m for 40% of the analysis period. By 2080 (scenario A2), Blackrock would be expected to have higher water levels of almost 10m for 20% of the analysis period while water levels will drop to almost 3m for 40% of the analysis period. It should again be noted that poor simulation accuracy at low water levels hinders the accuracy of Coy turlough (in reality, Coy turlough spends more time at lower water levels, i.e. the duration curve should be shifted somewhat to the right hand side of the sub-plot).

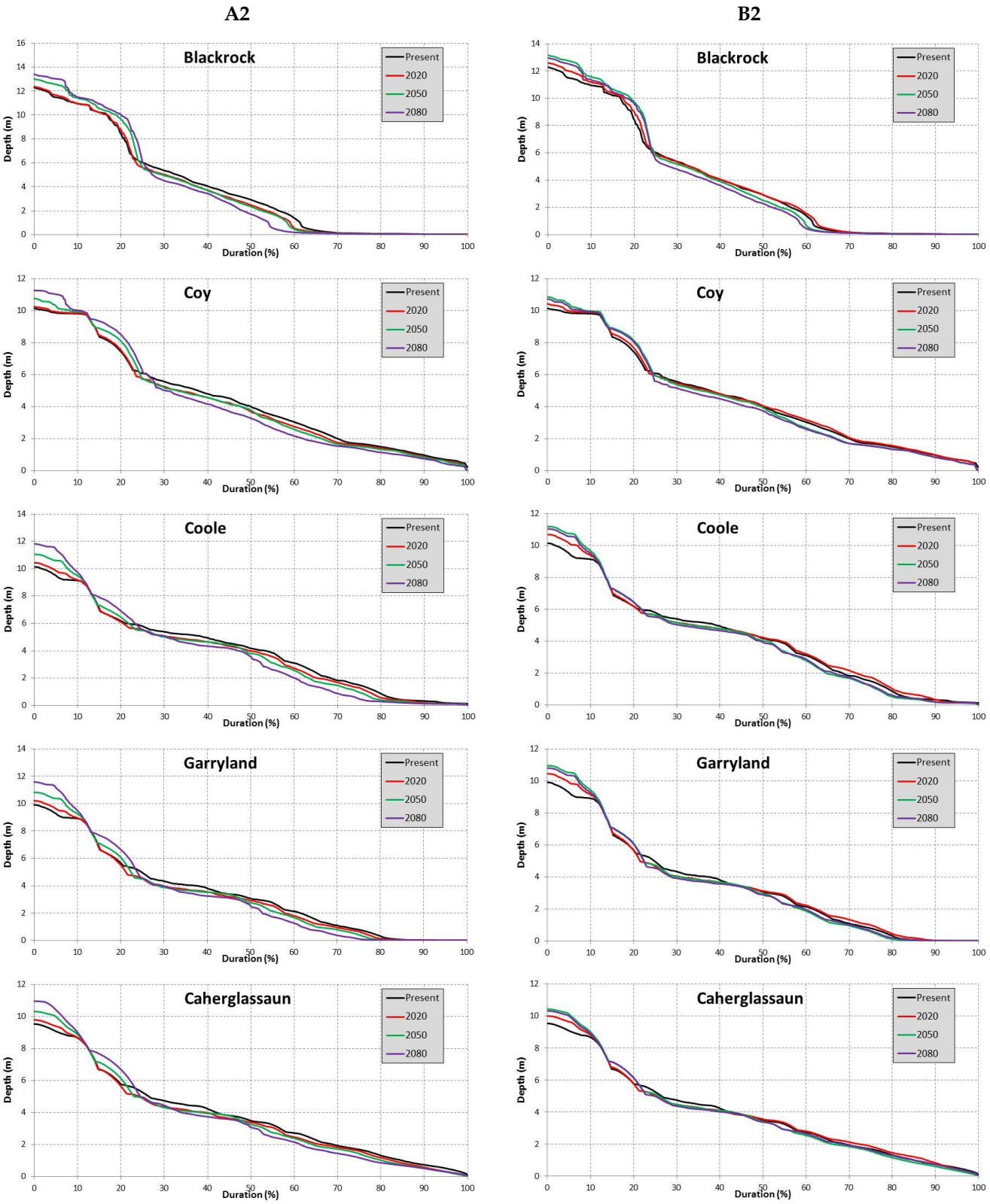

Figure 6.75: Flood duration curves for each turlough for scenarios A2 and B2 over the period Jan 2011 – Jan 2012.

The projected rise in turlough winter flood levels is likely to cause significant flooding issues within the catchment in future. The dataset used in this analysis describes what is considered to be a typical flooding season. For scenario A2, this dataset reaches near November 2009 flood levels by the 2050's, and by the 2080's the dataset has surpassed them. Regular flooding such as this would obviously cause severe damage to the region but would also damage the biodiversity of the turloughs as they would then likely be subject to drainage works which could alter their hydro-ecological characteristics permanently.

Another noticeable but less damaging effect caused by the projected climate change scenarios is the change in sea water level. The increase in sea-level would lead to an increased level of interaction with the catchment. This can be seen in Figures 6.72 and 6.73 which show increased tidal variation in Caherglassaun turlough at low water levels in the future, particularly 2080. In future years, salt-water intrusion will also occur further up the catchment. The extent of salt-water intrusion can be calculated using the velocity time series data from the outlet, i.e. using the negative outlet velocity values produced during high tide to calculate a distance travelled back up the system by a target particle. At present, the pipe-network model estimates a maximum penetration of salt-water up to 3.7 km into the catchment over the study period. This level of penetration rises to 4.6 km in the 2050's and 5.2 km in the 2080's (for both A2 and B2 scenarios). The impact of this salt-water intrusion is relatively minor compared to the likely flooding issues, but a number of residences extracting water from the karst aquifer could be affected.

As with climate change modelling in general, the use of the pipe-network model for simulating climate change scenarios is limited and brings with it a large degree of uncertainty. Consequently, the analysis carried out in this section can only be looked at as an illustration of possible impacts of climate change rather than a detailed analysis. The limitations involved in this analysis include:

- The analysis did not take into account the increased probability of once-off extreme weather events. Events such as severe flooding or heat waves are projected to occur with increased frequency as climate change occurs. Fealy and Sweeney (2008) suggest an increase in greatest 5-day rainfall values and an increase in 'heavy rainfall days' as well as increased 'longest dry periods'. These events would lead to an increase in extreme behaviour from the turloughs with increased flood levels a likely result. However, the sensitivity study in Section 6.3.4.4 suggests that, so long as the overall rain quantity does not change, the intensity should have only a minor effect on the turloughs (over a period of up to approximately 5 days).

- The projected changes in rainfall derived from the EPA (2008) report describe broad changes for the entire country of Ireland. Regional effects are not accounted for. In reality, the west of Ireland is likely to experience a greater proportion of winter runoff (Murphy and Charlton, 2008) causing increased flooding.

- The EPA study on which the rainfall data is based on the use of three global climate models (GCM's) downscaled to a regional level. This is a low number of GCM's compared to other climate change reports such as the ENSEMBLES report (Van der Linden and Mitchell, 2009) which used 12 GCM's to predict climate change for Europe. The EPA report was chosen however as it is specifically tailored to climate change in Ireland rather than Europe-wide.

The First Assessment Report, AR5, is scheduled for publication on the 30th September 2013 (i.e. the submittal date of this thesis). As such, climate change projections from this more recent report could not be included in this section.

6.5 Water Quality Modelling

Along with modelling the hydraulic processes of a pipe network, Infoworks *CS* also incorporates a water quality model which allows the modelling of sediment build-up in a network and the movement of sediment and pollutants through a drainage system during a rainfall event. This water quality model was used in order to evaluate the nutrient transport processes within the Gort Lowlands and the results are discussed in Section 7.4. In this section, just the model and its calculative processes are discussed.

The water quality model involves a separate calculation process which effectively occurs in parallel with the hydraulic modelling calculations. At each timestep, the output from the hydraulic model is used to calculate the associated output from the water quality model. Thus the water quality model receives feedback from the hydraulic model, but the hydraulic model receives no feedback from the water quality model (unless sediment build-up is included). Infoworks allows the modelling of up to nine different pollutants (e.g. Biochemical Oxygen Demand, Total Phosphorus etc.) with two different sediment fractions. Each pollutant can be modelled as being entirely dissolved or partially attached to sediment. The modelling of pollutants is fully conservative. There is no interaction between pollutants and their environment, nor between one pollutant and another.

Pollutants and sediments can enter a model from a number of sources:

- ***Wastewater and trade waste events***
  These sources describe the daily pattern of domestic waste or industrial waste from one or more subcatchment or industrial sources. For the Gort Lowlands model, these sources were ignored.

- ***Subcatchment contribution***
  The pollutant contribution from subcatchments is modelled using a specific *surface pollutant model*. This model calculates the build-up and wash-off of pollutants on catchment surfaces using a 'wash-off model' for sediment-attached pollutants and a 'gully-pot' model for dissolved pollutants.

- ***Point source***
  Point source pollutants are applied using an inputted time-series which is applied to a chosen node. For the Gort Lowlands model, the primary source of pollutants/nutrients derives from the rivers. As such, river nutrient concentrations are applied to the relevant nodes as point sources.

The surface pollutant model offers an ideal method for estimating the contribution of pollutants/nutrients to the pipe-network from the subcatchments. Unfortunately however, the surface pollutant model is only compatible for standard subcatchment-pipe links rather than the laterally-fed permeable pipe subcatchment links used in the Gort Lowlands model (used to represent Darcian flow in the epikarst). As a result, the modelling of nutrient input from the diffuse/epikarst component of the catchment was limited. Overall however, this issue was of minor importance as the primary goal of modelling the catchment was to investigate the nutrient transport through the active, i.e. mostly river (point source) fed, network. Ultimately, the nutrient contribution from diffuse flow into a number of turloughs was studied and calculations were carried out using a more manual approach (Section 7.4.2).

The water quality model carries out its calculations in three stages for each timestep.

1. The *Network Model* calculates the concentration of dissolved pollutants and suspended sediment at all nodes using the following conservation of mass equation:

$$\frac{dM_J}{dt} = \sum_i Q_i C_i + \frac{dM_{sJ}}{dt} - \sum_o Q_o C_o \qquad \textit{Equation 6.12}$$

where: M_J = Mass of suspended sediment or dissolved pollutant in node J (kg)
Q_i = Flow into node J from link i (m^3/s)
C_i = Concentration in the flow into node J from link i (kg/m^3)
M_{sJ} = Additional mass entering node J from external sources (kg)
Q_o = Flow from node J to link o (m^3/s)
C_o = Concentration in the flow from node J to link o (kg/m^3)

2. The *Conduit Model* calculates the concentration of dissolved pollutants and suspended sediment along each conduit. Similar to the hydraulic conduit model, a conduit is represented as a conceptual link of defined length between two nodes in the network. The governing equation describing the transport of the suspended sediment and dissolved pollutant (based on the conservation of mass) is the following:

$$\frac{dc}{dt} + u\frac{dc}{dx} = 0 \qquad \textit{Equation 6.13}$$

where: c = Concentration (kg/m^3)
u = Flow velocity (m/s)
t = Time (s)
x = The spatial co-ordinate (m)

However, for this equation to apply a number of assumptions must be made. Assumptions such as:

- Flow is one-dimensional in the conduit.
- Concentrations are fully mixed across the conduit section.
- Sediments and pollutants are transported along the conduit with the local mean velocity of the flow.
- Dispersion of the sediment and pollutant along the conduit is negligible.

3. The Conduit Model then calculates the erosion and deposition of sediment in each conduit using one of three erosion/deposition models (Ackers White model, Velikanov model, KUL model).

For water quality modelling of the Gort Lowlands network (Section 7.4), the analysis was focussed on transport of dissolved nutrients (Nitrate and Total Dissolved Phosphorus). Thus sediment concentration and its erosion/deposition capabilities were not included in the simulations.

Chapter 7

Hydrochemistry

7 HYDROCHEMISTRY

Between March 2010 and March 2013, monthly sampling was carried out across the catchment with 20-25 sites (see Figure 4.10 for locations) being regularly sampled for a range of hydrochemical parameters. Samples were taken from rivers, turloughs, springs and boreholes/wells and tested for alkalinity, pH, electrical conductivity, and nutrient concentrations (N and P). In this chapter, the findings of these hydrochemical tests are presented and discussed. In Section 7.1, the background information regarding land use and previous relevant studies is discussed. Section 7.2 presents results and analysis of the monthly sampling for alkalinity, pH and electrical conductivity as well as a number of sub-studies involving the use of CTD divers. In Section 7.3, the results of nutrient sampling are presented and analysed. In Section 7.4 the calibrated Infoworks model is used to shed light on the dynamics of nutrient transport within the turlough/conduit network. In Section 7.5, the results of these hydrochemical investigations are discussed in terms of catchment-wide behaviour and individual turlough behaviour. Finally, in Section 7.6, a turlough unconnected to the active network, Ballinduff, is briefly described in order to contrast the active conduit fed turloughs against a more epikarst/diffuse fed turlough.

7.1 Background

The water quality of the Gort Lowlands is characterised by the large component of allogenic recharge feeding the catchment from the Owenshree, Ballycahalan and Owendalulleegh Rivers. The river waters are distinguished by their low alkalinity, high iron and sediment concentrations (Southern Water Global, 1998) and high degree of colour (Cunha Pereira, 2011). Due to this allogenic recharge, the conduit-fed turloughs of the Gort Lowlands form a unique subset of highly coloured, low alkalinity turloughs when compared to more typical turloughs found around Ireland. The Gort Lowlands turloughs are also nitrogen (N) limited water bodies whereas other turloughs and permanent lakes tend to be phosphorus (P) limited (Cunha Pereira, 2011). Looking beyond the conduit network, the more epikarst/diffuse regions of the catchment consist of water more typical of limestone aquifers, rich in calcium (Ca^{2+}) and bicarbonate (HCO_3^-) (Einsiedl, 2012).

Recently, the Gort Lowlands has been subject to a number of hydrochemical studies. Gill (2010) and Cunha Pereira (2011) studied the changing concentrations of N and P within the Gort Lowland chain of turloughs in an effort to understand the source and pathway of the nutrients. Cunha Pereira (2011) concluded from the nutrient data that the turloughs act as *diffuse flow-through* systems rather than the *surcharge tank* systems as put forward by Gill (2010). This differing conceptualisation

is dealt with further in Sections 7.2.1.2, 7.3.1.2 and 7.5.2. The western portion of the Gort Lowlands has also been the subject of much recent hydrochemical research with a number of publications dealing with the salt-water/groundwater interactions occurring at the coastline (Einsiedl, 2012, Petrunic et al., 2012, Smith and Cave, 2012, Cave and Henry, 2011). Relevant findings from these studies shall be discussed throughout this chapter.

7.1.1 Turlough Spatial Homogeneity

As described in Section 4.3, turloughs were sampled by taking one sample from the main body of the lake. In order for this sample to be representative of the hydrochemistry, the turloughs are assumed to be homogeneous. This assumption is a considerable one considering that turlough characteristics include multiple inflows and outflows, rapidly changing water volumes, dynamic interactions between soil and water and often a complex morphology. In order to prove the assumption, surveys were carried out by both Cunha Pereira (2011) and Gill (2010) whereby turloughs were sampled at multiple locations and the spatial variation of their hydrochemistry was assessed.

The larger study was that of Cunha Pereira (2011) who sampled four turloughs (at four locations) at monthly intervals between December 2007 and May 2008 and tested samples for a range of hydrochemical parameters. Results showed a high degree of spatial homogeneity for most chemical variables such as total nitrogen (TN), total oxidised nitrogen (TON) and alkalinity within the turloughs. However, considerably more spatial variation was found for total phosphorus (TP) with points taken at the turloughs' water edge, (where Cunha Periera carried out his regular sampling) showing higher values than other points in the basin, especially during early and latter stages of flooding. Cunha Periera concluded that, in most cases, the large spatial differences are caused by accumulations of filamentous green algae near the shore during the later stages of flooding.

The study by Gill (2010) was smaller in scale, focusing on just one turlough for one day (29th May 2009), but critically, the study took samples at multiple depths providing a three dimensional profile. Samples were tested for P at nine locations within the body of the turlough and three locations along its edge. Results from the body of the turlough showed no particular spatial gradients across the area of the lake although a trend of decreasing P with increasing depth of water sample was observed. Gill (2010) suggested that this trend could be due to the warm weather conditions on the day of the survey causing the shallower water to release P into soluble form.

Similarly to Cunha Pereira (2011), samples recovered from the edge of the turlough showed increased concentrations of P.

The main conclusion that can be drawn from these surveys is that the turloughs can be assumed homogeneous for analysis purposes so long as the sample taken from the body of the turlough rather than the edge (i.e. within arms-length of dry land). However, the findings of a sub-study carried out as part of this thesis on Blackrock and Coy turloughs (see Section 7.2.3 later) calls into question the homogeneity of Blackrock turlough.

7.1.2 Land Use and Associated Nutrients/Contamination

The study by Cunha Pereira (2011) was part of the multidisciplinary National Parks and Wildlife (NPWS) project 'Assessing the Conservation Status of Turloughs' which studied 22 turloughs in Western Ireland. As such, Cunha Pereira's study encompassed four of the five turloughs studied by this thesis, these being Blackrock, Coy, Garryland and Caherglassaun. The findings of Cunha Pereira's thesis in relation to turlough catchment delineation and catchment land use are used in this chapter and are detailed below.

Turlough catchments (or Zones of Contributions – ZOCs) for the 22 catchments under study by the NPWS project were delineated based on known topographical and hydrological data (Owen Naughton, Paul Johnston, Catherine Coxon, David Drew, Sarah Kimberley and Caoimhe Hickey pers. Comm.). Due to the difficulty in delineating karst catchments, the resulting ZOC's for the 22 turloughs were only the best possible estimates given the available data with degrees of confidence ranging from 50 to 80%. However, due to the large proportion of easily delineated non-karst land within the Gort-Lowland turlough catchments, the confidence with these ZOCs is relatively high. The calculated ZOC's of the four Gort Lowland turloughs are presented below in Table 7.1.

Table 7.1: Total area of turlough ZOCs (Cunha Pereira, 2011).

Turlough ZOC	Area (km^2)
Blackrock	80.9
Coy	83.3
Garryland	393.0
Caherglassaun	398.0

The ZOCs for the Gort Lowland turloughs are considerably larger than the other 18 turloughs in the NPWS study with no other turlough ZOC being larger than 20 km². The ZOC for Coole turlough is not calculated but it can be inferred to be approximately 393 km² as it shares the same catchment as Garryland.

For land use data, Cunha Pereira (2011) extracted information from the Teagasc-EPA Soil and Sub-soil Mapping Project (Environmental Protection Agency, 2009) and the CORINE 2000 Project (Bossard et al., 2000) geo-referencing databases. While the CORINE database has an advantage in that it breaks grassland data into 'improved' and 'unimproved' pastures (useful for differentiating intensively and non-intensively managed grasslands), it does suffer from lower spatial resolution (25 ha unit sizes compared to the Teagasc-EPA databases at 1 ha resolution) as well as a lack of recent ground-truthing. The two datasets broadly agree with each other for the four Gort lowland turlough catchments, classifying them as primarily grassland (agricultural land) with sizeable forest and peat coverage. The land use categories and their respective areas (and % areas) for the Gort Lowlands are presented below in Table 7.2.

Table 7.2: Land use catagories areas within each turoughs ZOC extracted from the Teagasc-EPA database (Cunha Pereira, 2011).

	Rock		Bogs/Peat		Forest/Scrub		Water		Dry Grassland		Wet Grassland		Total Grassland		Other*	
Turlough	Area (Km²)	Area (%)	Area (Km²)	Area (%)	Area (Km²)	Area (%)	Area (Km²)	Area (%)	Area (Km²)	Area (%)	Area (Km²)	Area (%)	Area (Km²)	Area (%)	Area (Km²)	Area (%)
Blackrock	0.4	0.5	11.7	14.4	10.4	12.9	0	0	50.1	61.9	8.4	10.3	58.4	72.2	0	0
Coy	0.4	0.5	11.7	14	10.6	12.7	0.1	0.1	52.2	62.6	8.4	10.1	60.6	72.7	0	0
Garryland	22.7	5.8	73.3	18.6	86.1	21.9	7.2	1.8	180.1	45.8	23.2	5.9	203.3	51.7	0.7	0.2
Caherglassaun	22.7	5.7	73.3	18.4	86.1	21.6	7.4	1.9	184.6	46.4	23.2	5.8	207.8	52.2	0.7	0.2

*includes 'built land' and 'coastal complex'

What makes the Gort Lowland turloughs stand out from the other 18 turloughs in the NPWS study is the relatively high proportion of peat bog and forestry coverage. For Blackrock and Coy, bog and forest coverage takes up almost 30% of the catchment area while in Garryland and Caherglassaun (and Coole) catchments, it takes up over 40% of the area with the remainder consisting mostly of grassland. The other 18 studied turloughs typically consist of less that 5% bog and forest cover, instead being predominantly covered by grassland or open rock. The extensive bog and forestry coverage within the catchments provide the Gort Lowland turloughs with their characteristic high colour levels due to the leaching of humic substances from the bog/forest lands (Cunha Pereira, 2011). The forest/peat lands are also a key source of P due to the application of phosphatic fertiliser

which is critical to the survival of new plantations. These fertilisers contain significant concentrations of P. For example, the current recommended practice of the fertiliser *superphosphate* (used in areas of pH >6, such as the Slieve Aughtys) stipulates 42 kg/ha P can be applied (Renou-Wilson and Farrell, 2007). The loss of this P from the plantations can be significant depending on edaphic (soil related) characteristics, fertilisation variables and transport factors. Surface runoff is a very important pathway for P loss and is most prevalent after initial fertilisation due to the cambered surface and the absence of vegetation cover. Also, the drainage channels constructed in such commercial forestry plantations promote fast runoff. High precipitation following the application of fertiliser inevitably enhances the P loss (Renou-Wilson and Farrell, 2007). In terms of N, forestry tends to contribute relatively little. Indeed forestry is understood to yield the least amount of NO_3 to ground or surface waters compared to other typical agricultural land uses (Di and Cameron, 2002). The other major source of nutrients, both N and P, to the turlough ZOCs is the grassland areas where agriculture is widespread.

Over the last few decades, the use of inorganic fertilisers on agricultural lands has increased across the globe. This increased usage has had an impact on groundwater quality, particularly nitrate concentrations. The landspreading of organic material such as agricultural wastes (livestock manure or slurry, silage effluent, farm yard runoff) and agro-industrial wastes (dairy effluent, blood, offal) has also increased. The resulting water quality problems are felt across various aquifer/bedrock types throughout the world. Karst aquifers are particularly vulnerable due to their high permeability, often combined with thin soil cover (Coxon, 2011). Agricultural activities and their resulting nutrient concentrations are regulated in the government document 'European Communities Good Agricultural Practice for Protection of Waters Regulations 2010' (Stationery Office Dublin, 2010). This document presents concentrations for various agricultural activities such as the N and P concentrations in slurry or the annual nutrient excretion rates of livestock. For example, the document states that cattle excrete 65 kg of N and 10 kg of P per year with dairy cattle excreting up to 85 kg of N and 13 kg of P. The document also gives guidelines to the maximum permitted amount of applied fertilisation in terms of N and P concentrations from commercial fertilisers. Broadly speaking, agricultural soil effluents tend to be nitrogen intensive with high N:P ratios (>20 up to 250) whilst more concentrated sources such as fertilisers usually have lower ratios (<10) (Downing and McCauley, 1992). One of the largest non-agricultural sources of nutrient input is that of septic tank effluent (Coxon, 1999, Drew and Daly, 1993). The typical concentration of domestic wastewater effluent has been estimated as 50 mg/l TN (Environmental Protection Agency, 2000) and 5-20 mg/L TP (Environmental Protection Agency, 2009). The low N:P ratios typical of these point source effluents aid in the identification of turlough contamination as a

contaminated turlough would show significantly enriched levels of P with more minor enrichment of N (Cunha Pereira, 2011). Although excessive nutrient concentrations are harmful to catchments ecosystem, contributing to eutrophication of surface waters and subsequent degradation of water quality (Renou-Wilson and Farrell, 2007), it is contamination from faecal microbial organisms (bacteria, viruses or protozoans) that poses the greatest risk to the general population (Karst Working Group, 2000). Coxon and Drew (2000) point out that water supply schemes in karst regions may have more in common with surface water abstractions than with conventional groundwater sources in terms of management strategies.

Cunha Pereira (2011) also carried out an investigation into the relationship between land use and nutrients in turloughs. Significant positive correlations ($p<0.05$) were found between:

- Septic tank density and mean TN (but not TP).
- Agricultural land (CORINE) and mean TP and TN.
- Total pasture land (CORINE) and mean TP and TN.
- Unimproved pasture (CORINE) and mean TP and mean colour.
- Total grassland (Teagasc-EPA) and mean TN .
- Peat bogs (CORINE and Teagasc-EPA) and mean colour.

Most of these correlations showed low Spearman r values (most ≤0.6) with a wide spread of points in scatter plots. However, many of these plots displayed a 'triangular' shape with the widest spread of points at the highest percentages of land use (See Figure 7.1 for an example of this). This indicates that turloughs with a high percentage of agricultural land in their catchments span a wide range of nutrient concentrations. Cunha Pereira suggested that the upper margin of these 'triangular' plots may represent a maximum potential of nutrient release from the catchments.

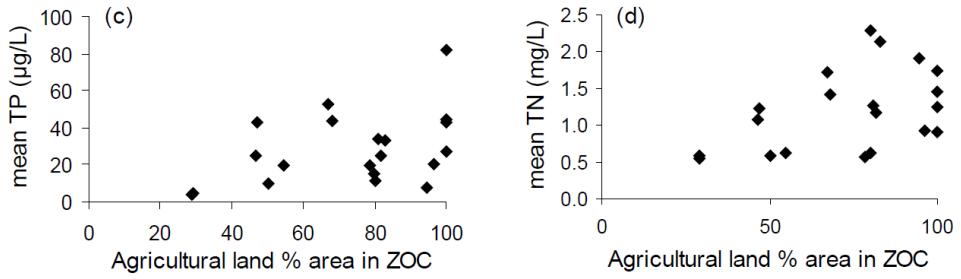

Figure 7.1: Scatter plots of total percentage area of grassland/agricultural land in turlough ZOCs and mean TP (c) and TN (d) per turlough (Cunha Pereira, 2011).

7.1.3 Previous Studies and Findings

As seen in previous sections, a number of hydrochemical studies have been carried out in the catchment already. The main hydrochemical findings from these studies are discussed below in terms of the surface water, the groundwater and the water outlet at Kinvara.

SURFACE WATER

One of the earliest hydrochemical studies of the region was carried out by Williams (1964) who observed the hardness of the water as it travelled from the Owendalulleegh River through Gort and out towards Kinvara. Williams noted that the water showed a steady increase in hardness (due to dissolution) once it had crossed onto the limestone bedrock. The hardness rose at a steady rate until reaching Polltoophill (Figure 3.7) where a jump in hardness occurred due to the influx of the harder Owenshree and Ballycahalan River waters. Beyond Coole, the rate of hardness increase slowed down. Williams determined that this slowing-down was due to reduced corrosion capacity as the water became saturated with calcium carbonate.

The most widespread hydrochemical study carried out in the Gort Lowlands was that of the Gort Flood Study (Southern Water Global, 1998). This study characterised the Gort Lowlands into seven different water 'types' based on alkalinity, iron chloride and nitrate (see Section 3.5.1.1). Using these water types, the study was able to describe the hydrological pathways in the region whereby Slieve Aughty river recharge (low alkalinity, high iron) flows down the catchment into the Coole-Garryland complex and mixes with groundwater from the southern Cloonteen catchment (with its higher alkalinity and lower iron concentrations). Turloughs not connected to the active conduit network tended to have higher alkalinities and lower iron concentrations as they received water from local direct recharge either from the limestone or from drift deposits. The study also looked at nutrient concentrations and found higher nitrate levels in turloughs that were more strongly grazed indicating a possible effect of manure deposition in the turloughs.

Nutrient concentrations and alkalinities in the turloughs have been measured more recently by Cunha Pereira et al. (2010) and to a lesser extent by Gill (2010). The results of Cunha Periera's studies are presented in Table 7.3. These results show similar values to those of Gill (2010). However, Gill also sampled Coole turlough which had concentrations ranging 0.7-1.25 mg/l for TN and 10-65 µg/l TP.

Table 7.3: Hydrochemical measurments of the Gort-Lowland turloughs (Cunha Pereira et al., 2010).

	TN (mg/l)		TP (µg/l)		TN:TP	Alkalinity (mg/l $CaCO_3$)	Trophic status (based on TP)
	Mean ±SD	*Range*	*Mean ±SD*	*Range*			
Blackrock	1.72±0.29	1.3-2.1	52±16	27.4-73.5	35	167	Eutrophic
Coy	1.41±0.26	1.1-1.9	43±16	24.7-61.9	36	143	Eutrophic
Garryland	1.08±0.42	0.6-1.8	11.7±31.4	11.7-31.4	46	122	Mesotrophic
Caherglassaun	1.22±.0.23	0.9-1.6	43±12	31.8-66.7	30	112	Eutrophic

GROUNDWATER

Recent studies on the groundwater in the region have been focussed around the coast (from downstream of Caherglassaun across to the North Burren) rather than the whole Gort Lowlands region. Petrunic et al. (2012) studied the major ion chemistry of the coastal area and found the groundwater to be Ca^{2+} and bicarbonate rich with varying but moderate NO_3 concentrations. However, a correlation was found between NO_3 and chloride (Cl) concentrations suggesting a common origin attributed to anthropogenic sources. Also, groundwater in the Gort Lowlands was found to have higher Mg concentrations than water in the nearby Burren, likely due to the presence of dolomite. Petrunic's findings suggest that the influence of saltwater intrusion on the groundwater geochemistry was limited to near the coast but the hydraulic connectivity of the groundwater system extends further inland (as can be seen from turlough water levels in dry periods).

Einsiedl (2012) carried out a study in the same coastal area using geochemistry and isotopes of dissolved sulphate ($\delta^{34}S$ and $\delta^{18}O$) and dissolved nitrate ($\delta^{15}N$ and $\delta^{18}O$) to shed light on the sea-water/groundwater interactions on the water quality of the region (and of Ireland's Atlantic coastal zone in general). Einsiedl found that geochemical conditions in the aquifer do not promote attenuation of NO_3 through denitrification. Also, Einsiedl calculated N loading to Kinvara Bay as 5 tons/day on average compared to an estimated input that derives from precipitation of approximately 25 tons/annum.

KINVARA

Kinvara Bay is protected as part of the Galway Bay Complex SAC/SPA (Special Area of Conservation and Special Protected Area for birdlife) due to the presence of several habitats and species listed in the EU Habitats Directive (EEC, 1992). The bay also includes some

commercial/licensed shellfish production zones approximately 2 to 3 km into the bay. The saltwater/groundwater interaction processes at Kinvara have been the subject of intense research in recent years with a number of studies producing estimates of flow rates and nutrient concentrations at the intertidal springs.

Cave and Henry (2011) used electrical conductivity measurements to estimate Submarine Groundwater Discharge (SGD) from the springs. Discharge calculations gave a wide range of flows between 4 and 198 m^3/s and an average flow of approximately 30 m^3/s. Combining the flow rate with measurements of TON taken during winter 05/06, average winter loading rates of TON ranged between 1666 kg/d to 26431 kg/d (depending on time period and choice of flow calculation limits).

Another study by Smith and Cave (2012) measured both TON and DIP (Dissolved Inorganic Phosphorus) at both springs in Kinvara (KE and KW) and also at springs in the neighbouring Aughinish Bay. Results showed that Kinvara is much more heavily influenced by fresh water input than Aughinish Bay and is a strong source of fixed nitrogen into Kinvara Bay. This is important as nitrogen tends to be the limiting nutrient in the marine environment rather than phosphorus which is generally the limiting nutrient in freshwater systems. TON concentrations from KE were measured at up to 1 mg/l while water from KW tended to have approximately half that concentration (similar to the results of Gill (2010)). Neither the Kinvara nor Aughinish springs, however, were considered as significant sources of DIP to their respective bays. Low concentrations of DIP compared to the DIP concentration in Galway Bay indicated that Kinvara may actually be a sink of DIP rather than a source (similar to the findings of Holman et al. (2010)).

As well as nutrient loading from the springs, Kinvara Bay is also subject to untreated wastewater discharge from a 300 mm diameter outfall pipe approximately 100m out into the bay. The outfall drains the town of Kinvara, an area of approximately 15 ha consisting primarily of combined collection systems (Galway County Council, 2009). Due to the lack of treatment, and the consequent organic enrichment and faecal contamination, the bay is at risk of losing its SAC conservation status. To combat this, a new waste water treatment plant with a new outfall further into the bay to promote dilution (Figure 7.2) has been proposed which would produce a treated effluent with significantly lower associated ecological impacts. At the time of printing this thesis, the treatment plant has not yet been installed.

Figure 7.2: Locations of current and proposed wastewater outfalls at Kinvara.

7.2 Alkalinity, pH, and Electrical Conductivity

In carbonate aquifers, alkalinity, pH and electrical-conductivity are invaluable hydrochemical parameters as they indicate the dissolutional behaviour of the water. Alkalinity is a measurement of the capacity of water to neutralise acids. In natural waters, alkalinity is primarily due to the salts of weak acids and strong bases. Although many materials such as borate, silicate and phosphate contribute to the alkalinity of water, the major proportion of the alkalinity of natural waters is caused by three major classes of materials: hydroxide (OH^-), carbonate (CO_3^{2-}) and bicarbonate (HCO_3^-). Bicarbonate represents the major form of alkalinity since it is formed in considerable amounts from the action of carbon dioxide upon the basic materials in soil. Hydroxide and carbonate are more associated with water of high pH value (>8.5 for carbonate and >10 for hydroxide) (Sawyer et al., 2003). In carbonate aquifers such as the Gort Lowlands, alkalinity predominantly results from the dissolution of calcium carbonate ($CaCO_3$) from limestone bedrock which is eroded during the natural processes of weathering. Some alkalinity also derives from the soil. Alkalinity is typically reported in the units *mg/l as* $CaCO_3$ or *meq/l*. In this thesis, the units *mg/l as* $CaCO_3$ are used.

Electrical conductivity (EC) is a measure of the ability of an aqueous solution to carry an electrical current. As the conductance of electrical current is facilitated by the charge on ions in solution, the conductivity of a solution is proportional to its ionic concentration. EC (measured in microsiemens, µS/cm) is thus often used as an index of total dissolved solids (TDS). In karst, the major cations present are typically calcium (Ca^{2+}) and magnesium (Mg^{2+}) and the major anion is bicarbonate

(HCO_3^-). Similar to alkalinity, the concentrations of these ions in natural waters (measured indirectly by an EC meter) give an indication of water mineralisation (and bedrock dissolution) as the water passes through a karstic aquifer. As referred to in Section 7.1.3, the ionic concentration in the Gort Lowlands have been studied previously by Petrunic et al. (2012) who plotted results on a piper diagram as seen in Figure 7.3.

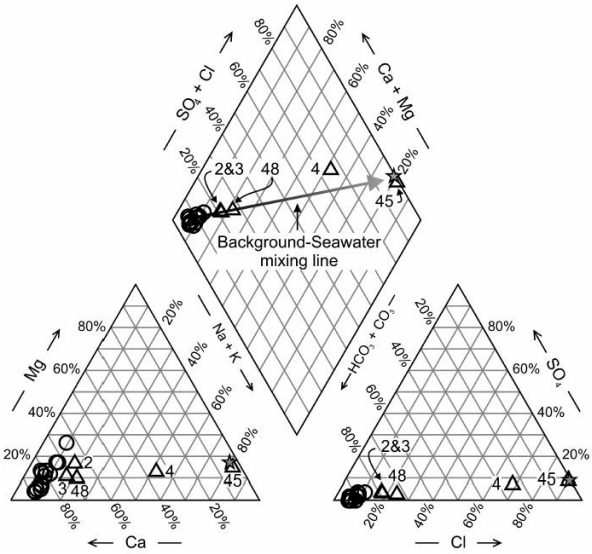

Figure 7.3: Piper diagram for groundwater samples taken near Kinvara (Petrunic et al., 2012).

In the Gort Lowlands, these hydrochemical parameters (alkalinity, pH, EC) are particularly beneficial due to the substantial input of under-saturated allogenic recharge. Using the distinct contrast between the low alkalinity/EC allogenic recharge and the saturated, high alkalinity/EC diffuse/epikarst recharge, insights can be made into the likely source of water within the catchment. In this Section, these parameters (alkalinity, pH, EC) are used in such a manner. In addition, a number of sub-studies were carried out using CTD divers in order to quantify diffuse recharge (Section 7.2.2), study the hydrochemistry of Blackrock and Coy turloughs in detail (Section 7.2.3) and quantify flow at Kinvara outlet (Section 7.2.4).

7.2.1 Results of Monthly Sampling

The results of alkalinity (i.e. bicarbonate concentration) for the rivers, turloughs, groundwater and Kinvara springs are presented in Table 7.4 and Figures 7.5, 7.7, 7.10 and 7.11. Plots of EC follow the pattern of alkalinity very closely and can be seen in Appendix G. Regression analysis of alkalinity and EC shows a significant correlation for all hydrological systems: rivers, turloughs, groundwater

and Kinvara (see Figure 7.4) with an overall R^2 value of 0.97 (for all systems combined). Due to this correlation, the discussion of hydrochemical results in this section is generally limited to alkalinity and pH as EC measurements can be assumed to follow the same trends.

Table 7.4: Ranges and mean values for alkalinity, EC and pH for rivers, turloughs, groundwater and Kinvara (grouped and individual).

	Alkalinity (mg/l $CaCO_3$)		EC (µS/cm)		pH	
	range	*mean*	*range*	*mean*	*range*	*mean*
Rivers	**1-246**	**48.5**	**24-481**	**136.4**	**5.13-8.4**	**7.2**
ORU	12-107	55.3	70-352	143.2	6.47-8.4	7.6
ORL	15-246	148.1	135-481	351.4	6.98-8.37	7.8
BRU	8-96	30.1	39-176	92.3	6.15-8.1	7.4
BRL	12-205	68.2	58-292	181.6	5.8-8.05	7.5
DRU	4-54	20.5	38-161	85.4	5.13-8.1	7.0
DRL	2-92	38.8	61-192	119.5	5.7-7.84	7.2
F	1-42	16.5	34-128	63.9	4.55-7.88	6.9
P	1-31	10.2	24-138	53.6	5.14-7.33	6.0
Turloughs	**42-239**	**131.8**	**152-497**	**291.2**	**6.61-9.38**	**7.8**
Blackrock	46-239	138.4	159-497	318.0	7.55-8.19	7.9
Coy	58-220	150.3	152-432	329.0	6.8-9.38	7.9
Coole	42-235	114.4	152-353	253.2	6.61-8.75	7.7
Garryland	77-170	134.6	155-396	293.4	6.7-8.5	7.8
Caherglassaun	77-235	121.3	189-267	268.0	6.67-8.52	7.8
Groundwater	**104-547**	**365.1**	**487-987**	**716.7**	**6.1-8.28**	**7.3**
BH3	135-547	387.8	487-987	768.1	6.91-7.9	7.3
BH5	246-508	307.7	553-701	612.5	7.15-8.22	7.6
BH7	308-420	366.9	659-878	778.8	6.88-7.65	7.2
BH10	104-458	357.0	516-803	690.4	6.89-7.74	7.3
BH11	269-362	313.6	593-690	632.9	6.1-7.72	7.3
BH12	123-439	375.5	686-871	752.8	6.85-7.8	7.3
BH14	162-458	375.5	535-851	737.0	6.85-8.28	7.4
BH15	369-481	425.7	710-813	755.9	6.88-7.48	7.1
BH16	316-462	376.0	654-790	721.7	6.85-7.6	7.2
Kinvara	**96-347**	**208.0**	**309-692**	**465.8**	**6.7-7.94**	**7.4**
KW	96-200	155.6	309-439	365.2	6-94-7.94	7.5
KE	150-347	260.4	381-692	559.4	6.7-7.79	7.4

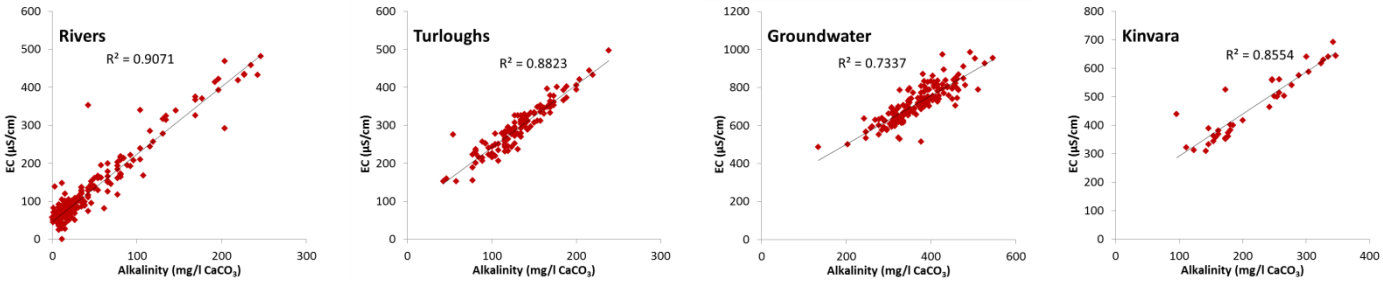

Figure 7.4: Alkalinity and EC correlation for each hydrological system (rivers, turloughs. groundwater and Kinvara).

7.2.1.1 Rivers

Time-series plots of river alkalinity measurements are presented in Figure 7.5. From these plots, it can be seen that of the three rivers, the Owenshree contains the highest levels of alkalinity while the Owendalulleegh shows the least. This trend is explained by the bedrock geology (Figure 3.4) as the different degrees of alkalinity concentrations mirror the amount of time the river spends travelling across the thin band of pure unbedded limestone which lies between the red sandstone of the Slieve Aughtys and the pure bedded limestone of the lowlands. The more time the river water has spent in contact with limestone, the more calcite will have been dissolved resulting in increased alkalinity, increased EC (mineralisation) and increased pH (i.e. a reduction in acidity and thus the solutional capacity of the water). For the same reasoning, the upper river site samples show smaller concentrations than the lower site samples. Runoff samples taken from the forest areas (F) and peat areas (P) of the Slieve Aughty Mountains inevitably show the lowest concentrations as they only contact the sandstone and have short residence times. A mean pH of 6 was observed for samples collected from the peat (site P) waters at the top of the Slieve Aughtys. This is the lowest pH recorded in the catchment and reflects the typical pH values found in peat bogs. Large variation in alkalinity can be seen between samples. This variation is primarily due to rainfall events flushing the system with low pH, non-mineralised rainwater (see Figure 7.19 for a good illustration of this effect). Another cause of variation could be the partial pressure of CO_2 (pCO_2) existing in the soils of the rivers catchment area. Variations of soil pCO_2 over the course of a year could cause variations in the rivers alkalinity, EC and pH (P-Y Jeannin, pers. Comm). Concentrations of alkalinity, EC and pH were all seen to decrease with increasing flow rates in the three rivers. As samples were only collected once a month, this concentration-flow relationship could only be broadly observed. In order to better quantify and understand this relationship, samples should ideally be sampled on an hourly or daily basis.

Figure 7.5: Time-series plots of alkalinity results for rivers. Dots represent individual samples and dashed lines are used to aid graphical interpretation.

7.2.1.2 Turloughs

As expected, alkalinity concentrations in the turloughs follow similar behaviour to that of the rivers, i.e. they tend show a reduction in alkalinity after a significant rainfall event. An example of this effect can be seen in Figure 7.6. Overall however, the behaviour of the turloughs is more complex, with a number of processes capable of affecting their $CaCO_3$ concentrations. These processes include river influx, varying water retention behaviours, diffuse input, carbonate precipitation and dissolution.

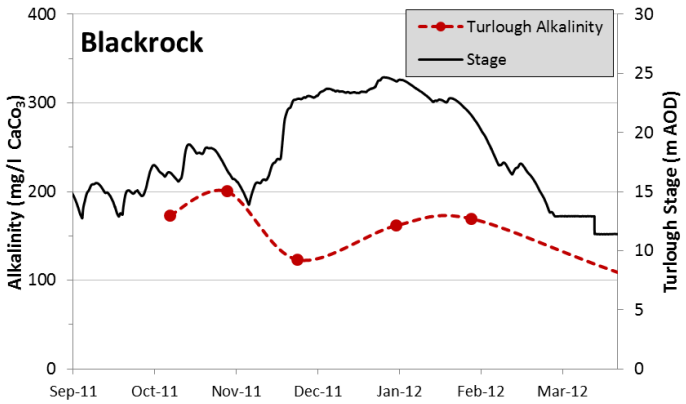

Figure 7.6: Blackrock turlough stage and alkalinity results (September-March 2012).

Blackrock and Coy turloughs have mean alkalinities of 138.4 and 150.3 mg/l $CaCO_3$ respectively, but with very different trends (as discussed later). These concentrations reflect the alkalinity of their primary source of water, the Owenshree River (ORL), which has a mean alkalinity of 148.1 mg/l $CaCO_3$. The alkalinities of Coole, Garryland and Caherglassaun turloughs are slightly lower (114.4, 134.6 and 121.3) reflecting the low concentrations of the Ballycahalan (68.2) and Owendalulleegh (38.8) rivers which also feed these turloughs. However, these turloughs have noticeably higher concentrations than would be expected from their combined river input. A weighted mean alkalinity based on their percentage flow contribution (Section 5.4.3.1) suggests an alkalinity of 71 mg/l $CaCO_3$ would be more likely from these turloughs. The reason for their increased alkalinity relative to what would be expected from the river inputs has four main factors. Firstly, these turloughs receive water from the more highly alkaline Cloonteen catchment to the south resulting in higher concentrations. Results suggest this influx is most significantly felt at Garryland turlough (similar to the findings of the Gort Flood Studies). Secondly, as the rivers (BRL and DRL) enter the limestone system undersaturated in dissolved calcium carbonate, their water is chemically aggressive and has a high dissolution potential. As a result, the water from these two rivers is likely to cause considerable solution of the limestone bedrock and increase their alkalinity as they flow towards Coole. Thirdly, as the river/conduit water moves through the catchment towards the lower three turloughs, it is being diluted by the addition of high-alkalinity diffuse/epikarst groundwater. Finally, the Coole-Garryland complex is known to have a large epikarst component. Any recharge from this epikarst would bring with it higher levels of alkalinity.

Time series plots of turlough alkalinities and turlough stages can be seen in Figure 7.7. For comparative purposes, these plots also include alkalinity measurements from the relevant feeding rivers. For Blackrock and Coy, data from the Owenshree River Lower is used whereas for the lower

three rivers, a weighted mean time series was calculated based on the overall %-contributions of each river (as calculated in Section 5.4.3.1). Looking at Figure 7.7, the turloughs show a considerable degree of variation. However, a particular trend can be seen whereby some turloughs experience a slow increase in alkalinity over the flooded period. This trend can be seen predominantly in Coy, Garryland and Caherglassaun turloughs over the 2011-2012 and 2012-2013 seasons. The trend can also be seen to a somewhat lesser degree in Coole turlough. For Blackrock turlough, this trend is not evident with the turlough sometimes experiencing considerable drops in alkalinity during a flooded period (highlighted with a purple circle in Figure 7.7). However it should be noted that identifying hydrochemical patterns within Blackrock turlough using monthly sampling is challenging due to the rapidity of its filling and emptying events (a higher resolution study of Blackrock and Coy turloughs was carried out over winter 2012-2013, discussed later in Section 7.2.3).

By comparing the hydrochemical behaviours of the turloughs to that of the rivers feeding them, an insight into their varying water retention characteristics can be gained. Coy, Garryland and Caherglassaun are estavelle-only fed turloughs (with a degree of isolation from the main karst flows through the system) and their hydrochemistry suggests that the low-alkalinity water brought in from the initial flooding event remains within the turloughs and slowly becomes enriched in bicarbonate, most likely due to gradual recharge from the epikarst (or possibly dissolution of the turloughs underlying bedrock). The turloughs show little interaction with the rivers once they are flooded and essentially behave like surcharge tanks as put forward by Gill et al. (2013a). An exception to this pattern can be seen in Garryland turlough during the 2011-2012 flooding season whereby the alkalinity dips as the turlough reaches its peak water level. This dip can be explained by the high-level hydrological connection between Coole and Garryland (mentioned in Section 5.2). At the highest water levels, the greatest mixing with Coole occurs, thus the alkalinity of Garryland at the time (64 mg/l $CaCO_3$) drops down closer to that of Coole (62 mg/l $CaCO_3$). Blackrock and Coole turloughs, on the other hand, are seen to be directly influenced by river concentrations, even during flooded periods. A good example of this can be seen highlighted by a blue circle over the Coole turlough plot in Figure 7.7 (see Section 7.2.3 for examples from Blackrock). This pattern suggests that these turlough can receive a significant amount of new low-alkalinity water from its surface input while draining away the older higher alkalinity water through its estavelle, i.e. the turlough acts as a *river flow-through* system (i.e. permits flow-through of river water, as opposed to the *diffuse flow-through* systems put forward by Cunha Pereira (2011) which permit flow-through of diffuse groundwater from the surrounding epikarst). For a simple graphical interpretation of the differences between *river flow-through*, *diffuse flow-through* and *surcharge tank* systems, see Figure 7.8.

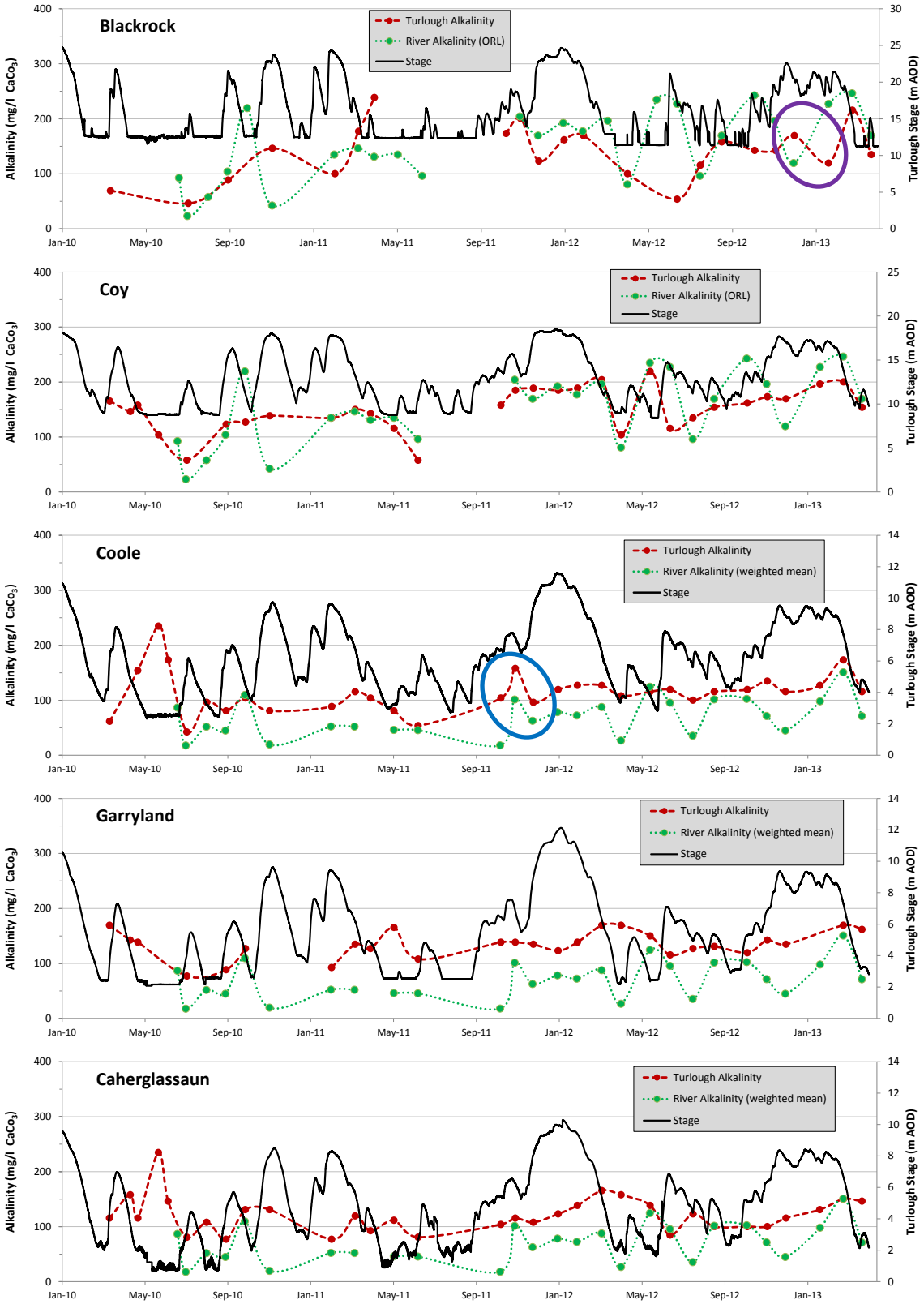

Figure 7.7: Time-series plots of alkalinity and turlough stage values. Highlighted circles represent drops in alkalinity following a period of flooding. Note: ORL refers to 'Owenshree River Lower'

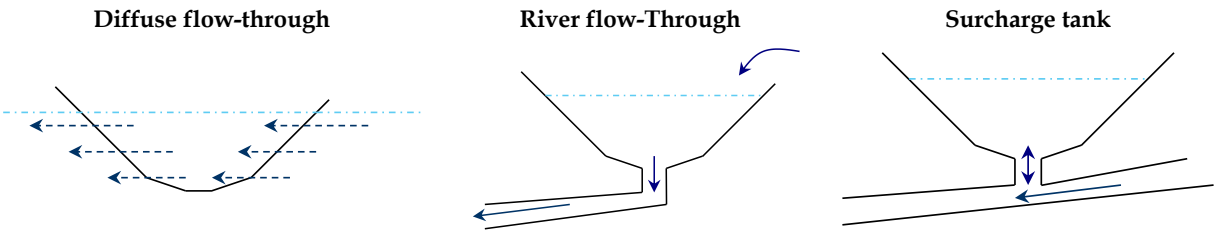

Figure 7.8: Conceptualisation of diffuse flow-through, river flow-through and surcharge tank turlough systems.

In Section 5.5 of this thesis, it was shown that a hydraulic gradient exists between a turlough and the epikarst catchment surrounding it. This hydraulic gradient is likely the cause of seepage from the epikarst into the turloughs and thus the enhancement of $CaCO_3$ concentrations within the turloughs. In an effort to quantify the amount of diffuse water entering the turloughs, a simple mass balance was carried out for a number of samples. The calculation entailed picking two samples which were collected during a period of recession (to rule out changes in alkalinity caused by influx from an estavelle). Using these sample concentrations, the volume of the turloughs and the mean concentration of groundwater (365.1 mg/l $CaCO_3$), the amount of groundwater required to raise the alkalinity by the measured amount could be calculated. Due to the variable flooding conditions over the study period, only a small number of samples met the recession requirement. See Figure 7.9 below for an example of a suitable pair of samples.

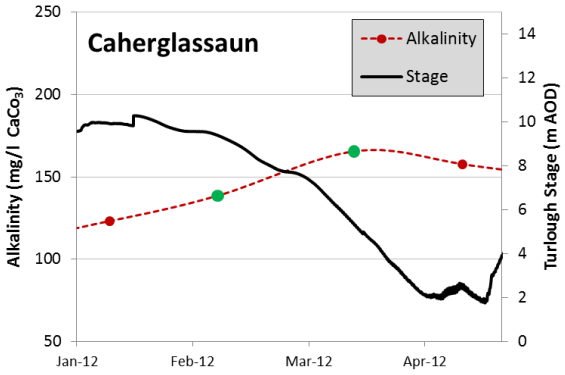

Figure 7.9: Suitable data points for calculating epikarst recharge (Spring 2012).

In this example, the quantity of diffuse recharge needed in order to raise the alkalinity of the turlough by the recorded amount would be 50900 m^3 over the 35 day period. In other terms, of the total volume of water that emptied from the turlough, 3% of that volume re-entered the turlough from the surrounding epikarst. Overall, diffuse recharge ranged between 1-13% of the volume lost during recession for Coy, Garryland and Caherglassaun turloughs.

This trend of increasing alkalinity over the flooding season is unusual for turloughs. Typical autogenically recharged turloughs tend to have much higher alkalinity levels due to the calcium carbonate ($CaCO_3$) rich waters that feed them. In turloughs such as these, the alkalinity does not increase over time (as they are saturated). Instead, alkalinity tends to decrease (as observed by Cunha Pereira (2011)). Coxon (1994a) suggested that losses in $CaCO_3$ from turloughs are due to the influx of water (saturated with CO_2), which comes into contact with the air and gradually loses its CO_2 to the atmosphere, primarily from physiochemical processes but also possibly biogenic processes. The loss of this CO_2 from the water results in the precipitation of $CaCO_3$ out of the water and onto the underlying soil. $CaCO_3$ precipitation/deposition within the Gort Lowlands network of turloughs was proved to be insignificant by Kimberley et al. (2012) who found only minor concentrations of $CaCO_3$ in the soil of these turloughs.

7.2.1.3 Groundwater

Results of groundwater alkalinity (and water level where applicable) can be seen in Figure 7.10. The groundwater alkalinity generally varies between 300 and 400 mg/l $CaCO_3$ with the exception of BH3 and BH14 which show much larger ranges. Mean groundwater alkalinity for the entire catchment was calculated as 365.1 mg/l $CaCO_3$.

The broad agreement and lack of variation between most groundwater samples indicates the presence of a large diffuse/epikarst type aquifer with low transmissivity (as discussed in Section 5.5). The variation in BH3 is in accordance with the findings of its groundwater level fluctuation data i.e. the well not only shows hydraulic connectivity with the nearby Owenshree River but a hydrochemical influence as well. However, the same could not be said for BH7 whose water level plot shows a degree of hydraulic connectivity but the plot of alkalinity shows very little hydrochemical variation (Figure 7.10). This suggests BH7 is distantly linked to the active conduit network, close enough to influence its water level but too far to receive water from the active network. BH14 on the other hand shows a degree of hydrochemical variation but minimal groundwater level fluctuation. The alkalinity in the well appears to dip during the summer months, being replenished the following autumn. This hydrochemical variation could be a result of the exposed nature of BH14 which is an open walk-in well. As the water lies in the well, it gradually loses its CO_2 to the atmosphere resulting in a reduction in bicarbonate concentration and thus alkalinity (Cunha Pereira, 2011). The fact that this behaviour occurs in BH14 indicates that the water in the well is not being replenished by newer ground water, i.e. there is no groundwater flow-through. This suggests that BH14 is part of a slightly confined system similar to a surcharge-type turlough.

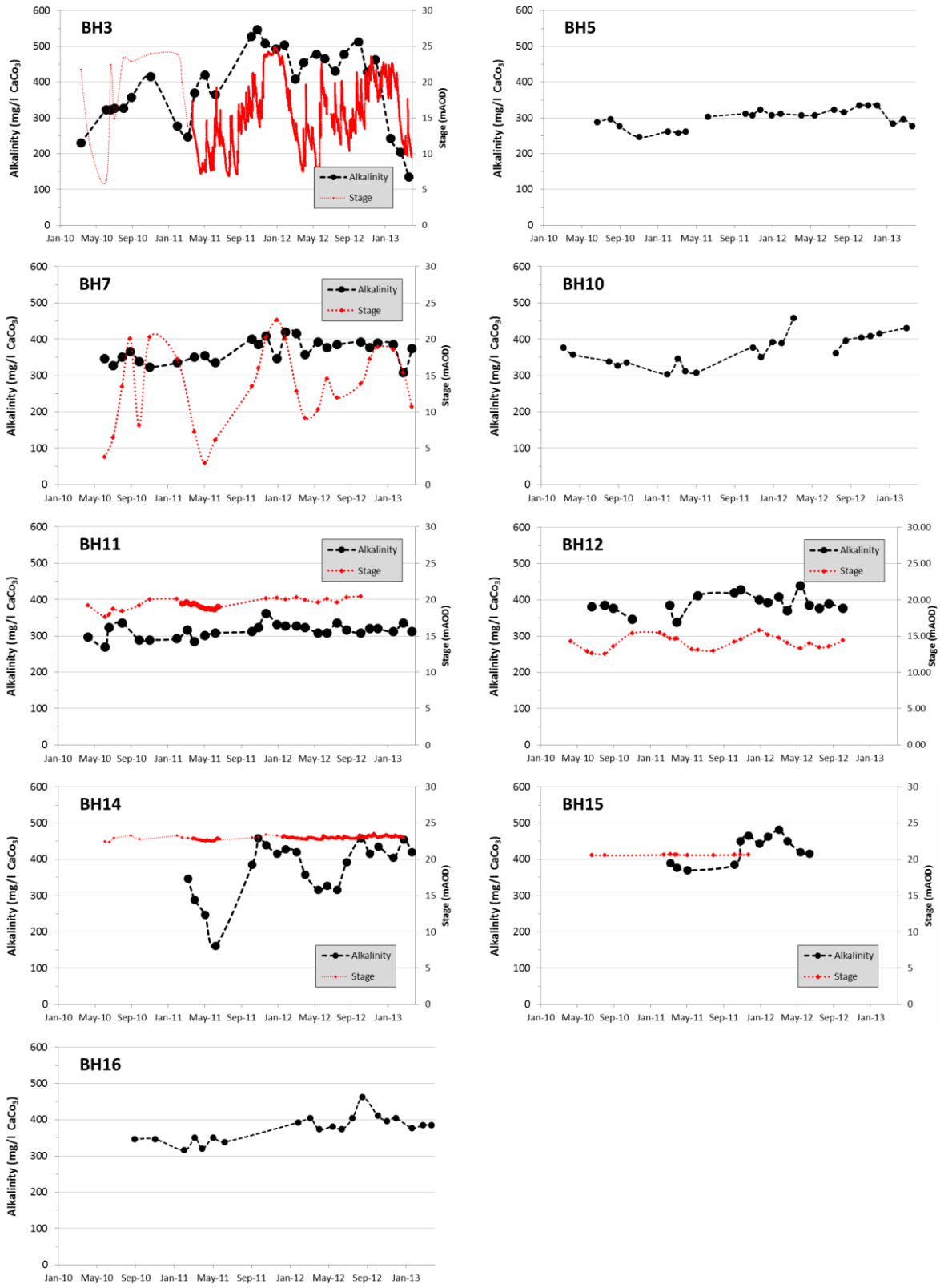

Figure 7.10: Alkalinity results for Boreholes/wells.

7.2.1.4 Kinvara

A time series plot of alkalinity for both Kinvara West (KW) and Kinvara East (KE) springs (along with the modelled outflow from the conduit network) is shown below in Figure 7.11. A distinct contrast can be seen between the springs with KE discharging water with significantly higher alkalinity than KW. The reasoning for this difference is well understood and has been reported on numerous occasions (Smith and Cave, 2012, Cave and Henry, 2011, Gill, 2010, Southern Water Global, 1998, Smyth, 1996, Drew and Daly, 1993). KW is the outlet for the shallow active conduit network with its relatively low levels of alkalinity while KE discharges water from a more diffuse/epikarst type deeper source with alkalinity levels more typical of autogenic bicarbonate-rich recharge. As well as diffuse/epikarst discharge, KE is also thought to be the outlet for the northern flow route as seen in Figure 3.6 (Southern Water Global, 1998). This northern flow route connection is evidenced somewhat by the fact that the mean alkalinity for KE (260.4 mg/l $CaCO_3$) is greater than KW (155.6 mg/l $CaCO_3$) but also considerably less than the mean groundwater alkalinity (365.1 mg/l $CaCO_3$). If KE was fed exclusively by slow moving epikarst recharge from the karst lowlands (i.e. autogenic recharge), the alkalinity would be expected to be more akin to the mean groundwater alkalinity. Instead, the mean alkalinity of KE is lower which suggests some dilution with low alkalinity water, most likely originating from the Slieve Aughtys. KE also maintains a strong flow all year round while discharge from KW varies over time (as can be seen by the modelled outflow in Figure 7.11).

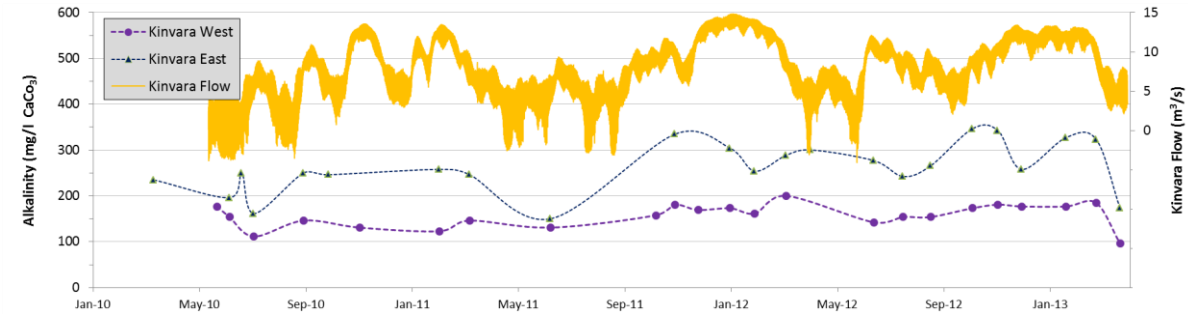

Figure 7.11: Alkalinity results from Kinvara springs with modelled discharge (yellow).

In Figure 7.11, the alkalinity at KW is noticeably less variable than KE. This is an interesting finding considering that KE is fed by a more diffuse slow-moving water source than KW and thus might be expected to show less variation. The cause of this contrasting variability is likely due to the influence of the turloughs on KW. The turloughs act to significantly attenuate (and mix) the flow of water through the active conduit network and thereby damp such water quality variations at the

spring whereas, in the more diffuse network feeding KE, the flow moves slower and in more of a plug flow manner which therefore reflects temporal variations more explicitly.

A comparison between the alkalinities of Caherglassaun and KW are shown below in Figure 7.12. In this plot, it can be seen that the Caherglassaun and KW follow very similar patterns over time. However concentrations in KW are enhanced. The mean concentration of KW is 155.6 mg/l $CaCO_3$ while the mean concentration of Caherglassaun is only 121.3 mg/l $CaCO_3$. Similar to the situation with Coole turlough, this increase in alkalinity suggests further bicarbonate enhancement through dissolution or the addition of water with higher alkalinity from a separate catchment. The latter reason is likely to be the predominant factor as tracer tests have proven a link from the Cloonteen catchment joining the active conduit network between Caherglassaun and Kinvara (Southern Water Global, 1998).

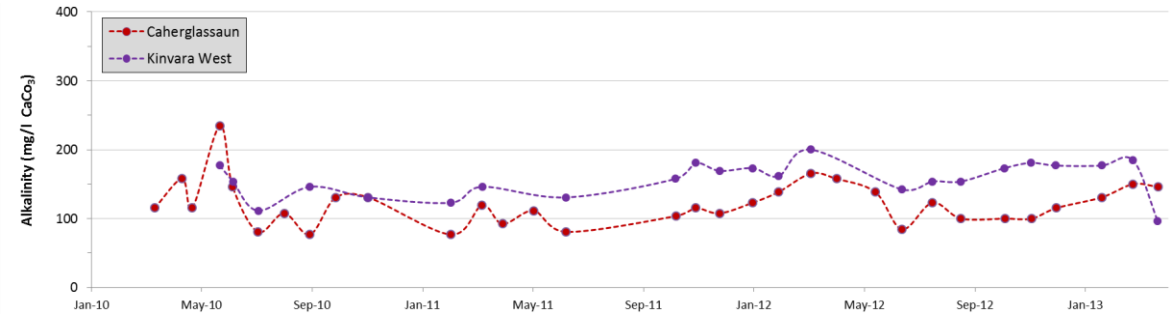

Figure 7.12: Alkalinity results from Kinvara West (KW) and Caherglassaun turlough.

Using the hydrological model, a mass balance can be carried out in order to quantify the amount of water required to enhance the alkalinity between Caherglassaun and KW to recorded level. This mass balance calculation is based on the assumption that external groundwater originates from high alkalinity sources with similar alkalinity values as the diffuse groundwater within the Gort Lowlands (350 - 400 mg/l $CaCO_3$). This assumption is a reasonable one considering that the two likely sources of external water are from the Cloonteen catchment and the north-east Burren, and both of these areas are known to have high alkalinity values typical of diffuse/epikarst water.

The hydrological model predicts that over a three year study period, the amount of water flowing from Caherglassaun to KW is approximately 680,470,000 m^3 whereas the amount of water discharging at KW is approximately 684,950,000 m^3. Thus the flow from Caherglassaun increases by 0.7% due to addition from the modelled epikarst within the Gort Lowlands. So supposing that this epikarst water (with alkalinity 365.1 mg/l $CaCO_3$) was the only source of additional water to KW,

the alkalinity would be expected to increase from 121.3 mg/l $CaCO_3$ at Caherglassaun to just 123 mg/l $CaCO_3$ at KW. This value is considerably lower than the recorded 155.6 mg/l $CaCO_3$ which suggests that there is a significant contribution of external water which is not accounted for by the model. The amount of additional water (with alkalinity between 350 and 400 mg/l $CaCO_3$) required to enhance KW to the recorded level would be between 96,000,000 and 121,900,000 m^3, i.e. an increase of 14–17.8%. Thus based on this mass balance calculation, the mean modelled outflow at Kinvara increases from 7.64 to approximately 8.7-9.0 m^3/s due to the addition of flow from external catchments such as Cloonteen or the north-east Burren.

7.2.2 Quantifying Diffuse Input using CTD Divers

The stretch of river between Kilchreest river gauge and Castle-Daly river gauge offers an opportune location for the quantification of diffuse input into the river. At the Kilchreest gauge, the Owenshree River runs off the Old Red Sandstone down onto the karst limestone where it runs for approximately 8 km before reaching the gauging station at Castle-Daly (Figure 7.13). The purpose of this sub-study was to measure the EC and flow at both gauges so as to quantify the increased levels of EC in the river on the premise that any increase would be associated with the diffuse recharge. Quantifying diffuse recharge to the river is beneficial to the conceptual understanding of the aquifer and also for verifying the accuracy of the pipe-network model.

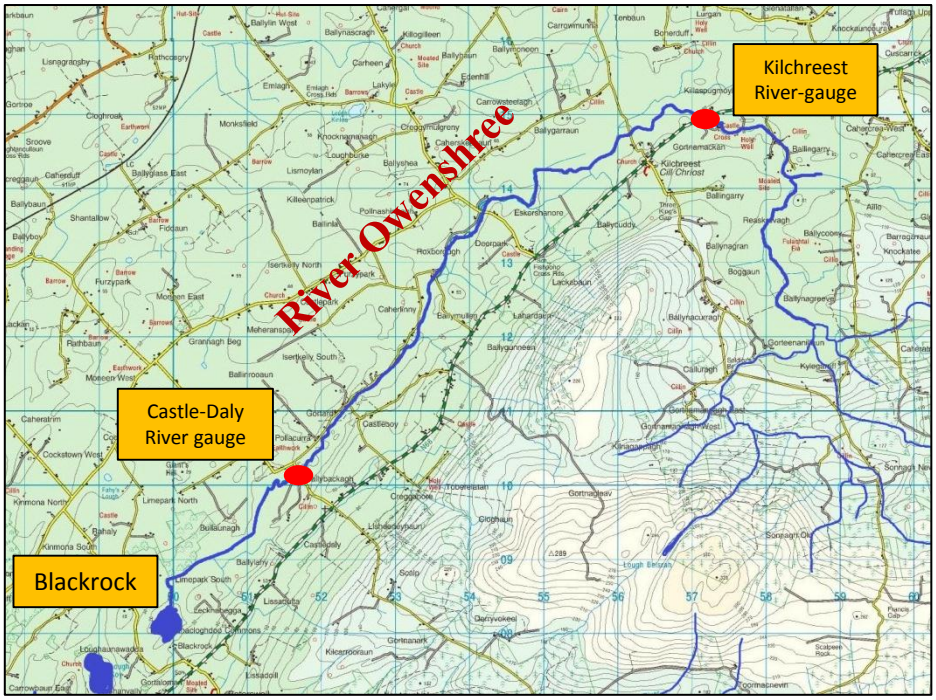

Figure 7.13: Owenshree River gauge locations.

The study was carried out over 52 days between the 15th of May and the 9th of July 2013. CTD divers were fixed in place at Kilchreest and Castle-Daly gauge locations and set to record at 10 minute intervals. The results from these CTD divers are shown below in Figures 7.14 & 7.15.

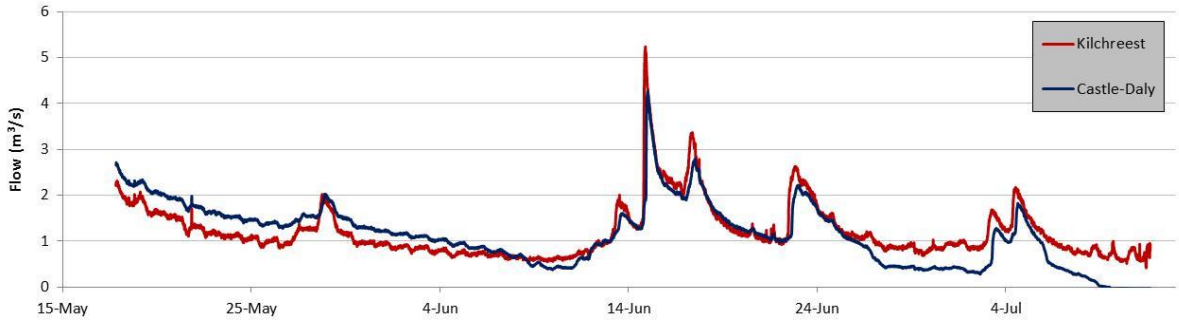

Figure 7.14: Flow data for Kilchreest and Castle-Daly gauging stations (May-July2013)

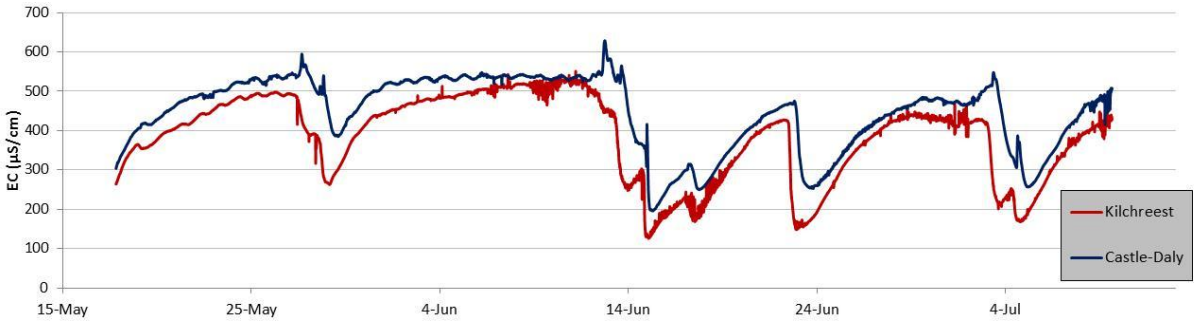

Figure 7.15: EC data for Kilchreest and Castle-Daly gauging stations (May-July 2013).

As can be seen from Figure 7.14, discharge was quite variable between the two gauging points. The downstream gauge at Castle-Daly can experience flow that is sometimes higher and sometimes lower than the upstream gauge at Kilchreest. This variation is due to two factors. Firstly, contribution from the surrounding epikarst (modelled as subcatchments in the Infoworks pipe network model) can increase flow between the two gauging stations. Secondly, water is known to be lost through a series of swallow holes in the base of the Owenshree River. It is suspected that the majority of this lost water travels through a conduit towards Blackrock. However, tracer tests have suggested another linkage bringing water directly towards Kinvara (Southern Water Global, 1998). In the early stages of this CTD study, Castle-Daly flow surpassed Kilchreest flow because contribution from the epikarst was greater than loss to the bedrock. This is likely due to consistent rainfall over 15 days prior to the start of this study which would have reduced the capacity of the underground conduit network and raised the water table of the surrounding epikarst to a level above the main line conduit, thus increasing diffuse recharge. A number of individual rainfall

events were seen during the period leading to peaks in river flow peaks but generally, the period was quite dry. This dryness severely reduced downstream flow as the river sank into the bedrock. By the end of the study, the river bed at Castle-Daly was completely dry (Figure 7.16) as the river sank into a swallow hole approximately 30m upstream of the gauging station.

Figure 7.16: Owenshree River dried up at Castle-Daly gauging station (9th July 2013).

EC data from the divers in Figure 7.15 shows a clear difference between the gauging stations with enhanced EC at the downstream gauge. This enhancement is due to contribution from the surrounding epikarst which Table 7.4 indicates has an EC value of 716 μS/cm (mean groundwater EC). Figure 7.15 also shows a consistent influx of higher EC water even during the later stages of the study when considerable amounts of water was being lost to bedrock. Also, clear indications of piston flow can be seen on three occasions at the Castle-Daly gauge with spikes in EC occurring directly before a corresponding drop (see Section 2.3.7 for a description of piston flow).

In order to quantify the amount of diffuse recharge entering the river, a hydrograph separation was carried out using end member mixing analysis (Shaw, 2011, Leibundgut et al., 2009). In this analysis, the total flow (Q_T) is split into 'event' water (Q_E) and 'pre-event' water (Q_P) as such:

$$Q_T = Q_E + Q_P \qquad \textit{Equation 8.1}$$

This can be split into:

$$Q_T{*}C_T = Q_E{*}C_E + Q_P{*}C_P \qquad \textit{Equation 8.2}$$

where C_T = flow concentration (measured), C_E = event water concentration (end member) and C_P = pre-event water concentration (end member)

so

$$Q_E = Q_T \frac{Q_T - Q_P}{Q_E - Q_P} \qquad \textit{Equation 8.3}$$

and

$$Q_P = Q_T + Q_E \qquad \textit{Equation 8.4}$$

For this study, the difference between upstream and downstream EC levels was being investigated so the inputted concentration (C_T) was the Castle-Daly EC value minus the Kilchreest EC value for each time-step i.e. the EC gained in the river between the gauging stations. As such, the 'event' water end member (C_E) was considered as the EC concentration of water in the river input without any changes or external inputs so $C_E = 0$ (if the flow was entirely from river input, there would be no change in EC between Kilchreest and Castle-Daly). The 'pre-event' end member was considered to be the EC value of water originating from the surrounding epikarst so $C_P = 716$.

Applying these values to the above equations results in the following plot, Figure 7.17, showing the total flow (Q_T), 'event'/river flow (Q_E) and 'pre-event'/diffuse flow (Q_P) for the river. The analysis suggests a low but consistent input from diffuse sources, typically below 10% of total flow but occasionally reaching above 40% following a heavy rainfall during the generally drier summer period, indicating the speed of the response from the local karst recharge contribution being slightly faster than the allogenic river contribution at the beginning. Overall, the average contribution from diffuse sources amounted to 8.7%.

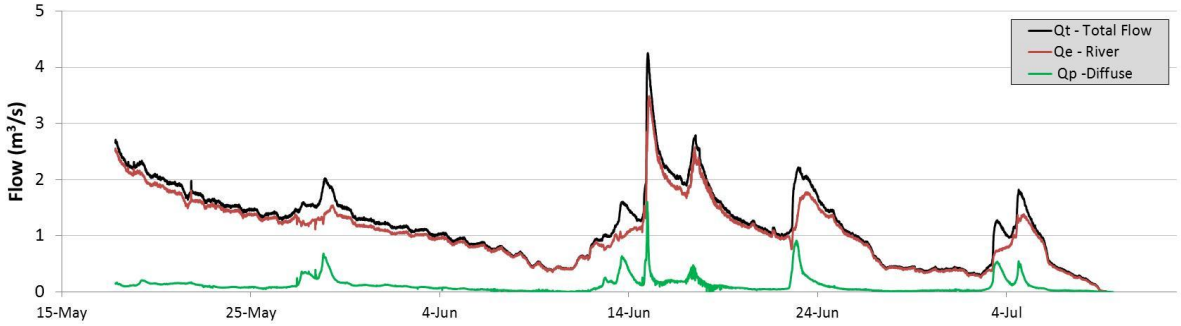

Figure 7.17: Hydrograph separation of Castle-Daly gauging station.

For the same section of river, the pipe-network model (see Chapter 6) estimated a diffuse contribution of 10%. This result was calculated by comparing the cumulative flows at the nodes which represented the locations of Kilchreest and Castle Daly. The Castle-Daly node experienced total flow volumes of 10% greater than the Kilchreest node. Also, in the model, the section of river is only represented by a single open-conduit on the surface, thus losses into the underlying conduit would not be accounted for. As a result, the flow at the Castle-Daly node is likely to be overestimated. This overestimation is reflected in the difference between modelled diffuse contribution (10%) and the measured diffuse contribution (8.7%). Overall however, this modelled-measured comparison seems to validate the accuracy of the diffuse component of the pipe-network model.

7.2.3 CTD Study of Blackrock and Coy turloughs

Although turloughs have been a source of much multi-disciplinary research for many years, hydrochemical sampling of the turloughs has been generally limited to once-off or monthly sampling. It was therefore the intention of this sub-study to carry out a high temporal-resolution, hydrochemical survey on two turloughs, Blackrock and Coy, using CTD divers.

The study was carried out over the 2012/2013 flooding season (October 2012 - February 2013) using 5 CTD divers. Two divers were placed in each turlough, one at the major spring/estavelle and one in the main 'body' of the turlough (for the purposes of this sub-study, the spring/estavelles of the turloughs will be termed as 'springs'). It should be noted however that these springs were only the *supposed* main springs of the turloughs. It is not yet fully understood if these springs are actually the most influential to the turloughs, particularly in Blackrock. Another diver was placed at the Owenshree River gauging station at Castle-Daly (See Figure 7.18 for an illustration of CTD diver locations within the turloughs). Using these divers, hydrochemical comparisons could be made between the water feeding the turloughs, the water filling/draining from the turloughs at the springs and the main body of water within the turloughs.

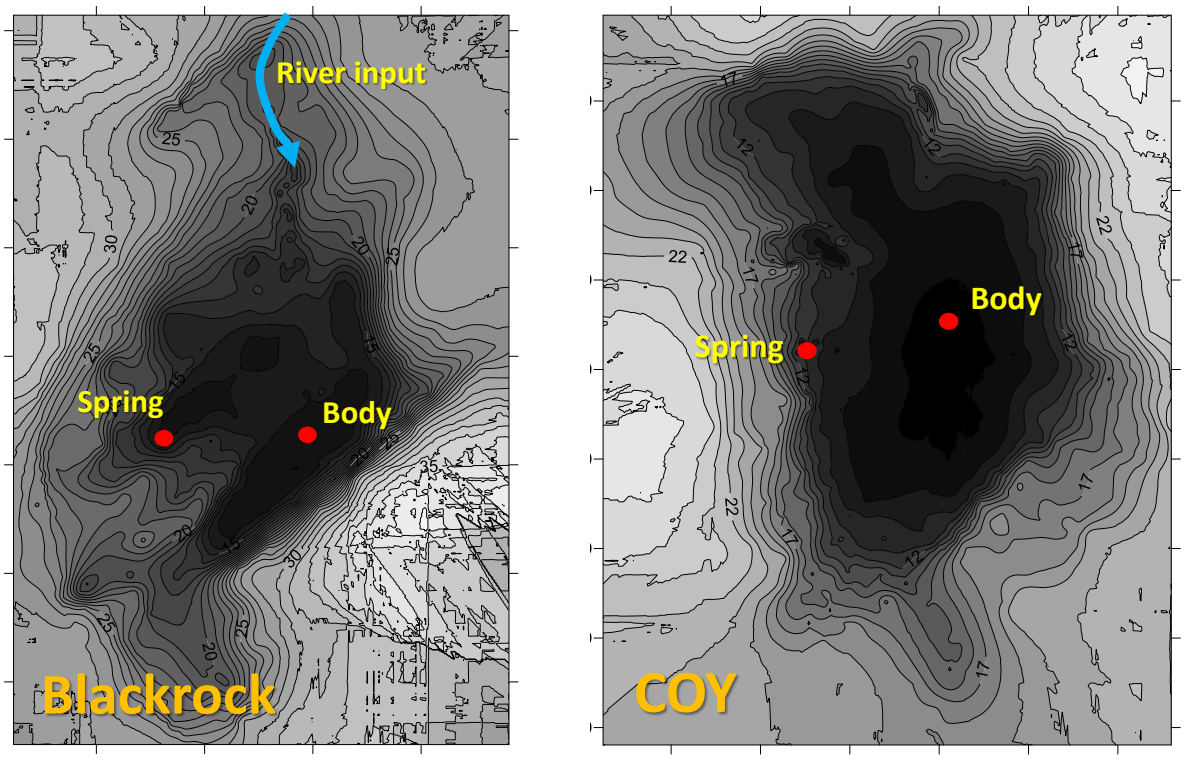

Figure 7.18: CTD diver locations in Blackrock and Coy turloughs.

EC results from the CTD divers are presented in Figures 7.19, 7.20 and 7.21, for temperature data from these divers, consult Appendix G. In Figure 7.19, flow and EC data for the Castle-Daly gauging station are presented. A clear trend can be seen whereby during (or soon after) a rainfall event, the EC in the river plummets due to the increased concentration of 'fresher', less mineralised rainwater in the river flow. Following such an event, the river EC levels slowly rise up until the next rainfall event.

In Blackrock turlough (Figure 7.20), EC appears to vary considerably over time with some clear differences between EC levels at the spring and in the main body of the turlough. Coy turlough, on the other hand, appears quite temporally and spatially stable with a number of distinct peaks but a general trend of increasing EC during the entire flooded period (similar to the results of monthly sampling). A number of strange peaks are recorded by the Coy-body CTD. These peaks are difficult to explain as they rise up to and over 600 µS/cm, i.e. higher than the highest recorded EC in the Owenshree River. Due to the extreme nature of these peaks, it is assumed that they are the result of equipment failure or interference. Results from these CTD's will be further discussed in terms of the Owenshree's influence on Blackrock and the influence of the Owenshree and Blackrock on Coy.

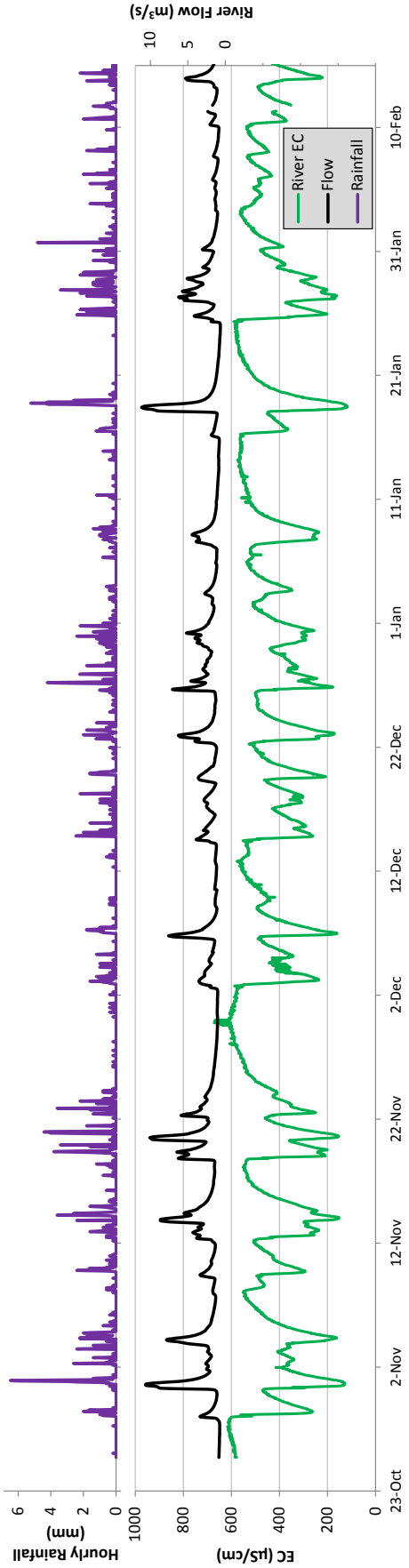

Figure 7.19: Flow and EC data from Castle-Daly River gauge (and precipitation).

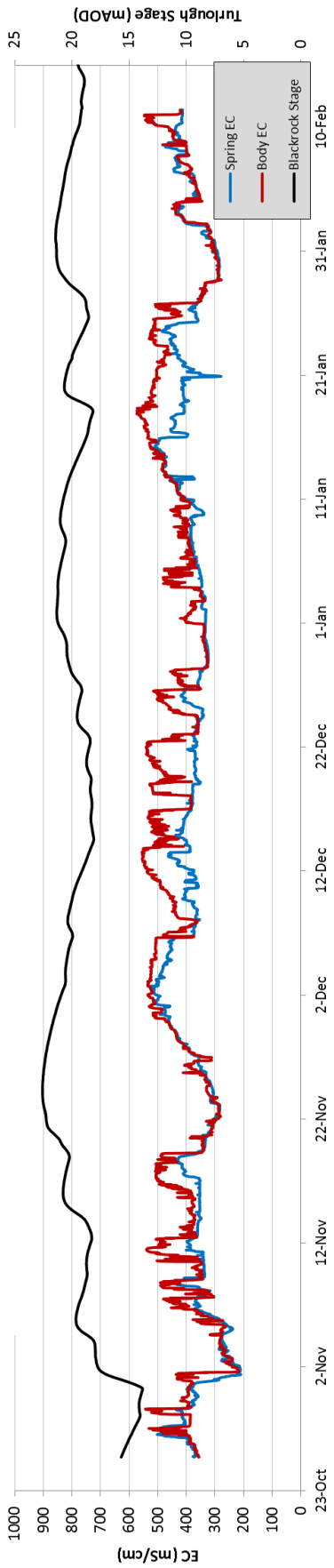

Figure 7.20: Stage and EC data from Blackrock turlough.

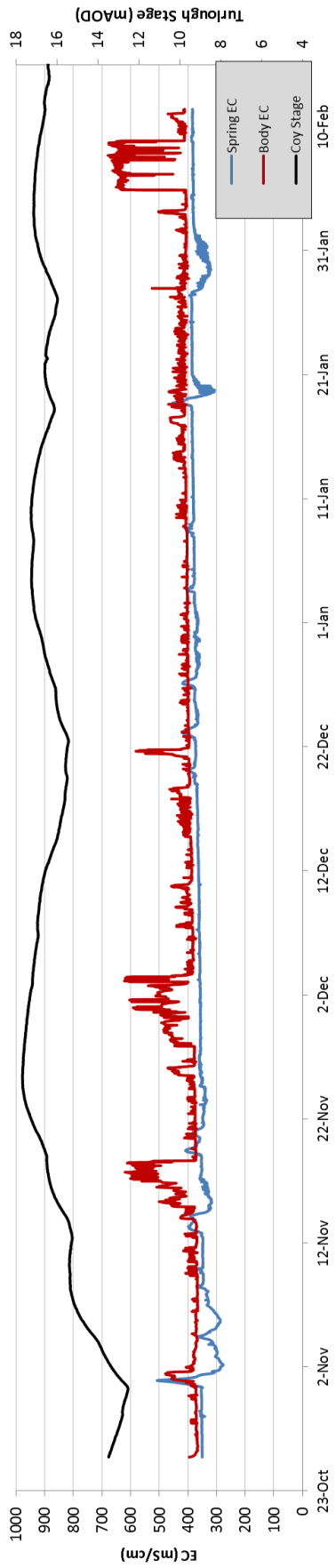

Figure 7.21: Stage and EC data from Coy turlough.

7.2.3.1 Blackrock.

Blackrock turlough displays a highly variable pattern which is influenced significantly by the Owenshree River. The influence of the river, however, is not straightforward. A quick change in river EC always provokes a response in the EC of the turlough. However, this response is not always the same. Generally, the EC measured at the body of the turlough varies in accordance with the river, rising and falling in sync with the EC observed at Castle-Daly gauging station. The spring, however, tends to have a more muted pattern, occasionally dropping in sync with the river during a flood but rarely increasing in sync with the river during a recession.

Flooding events in Blackrock tend to result in a homogeneous reaction across the turlough with the EC of both the spring and body dropping considerably. After such a flooding event, the turlough could remain homogeneous for a period of time (for an example, see Figure 7.22). Heterogeneity within the turlough tended to be introduced during a period of recession, particularly when lesser river surges have occurred during a large recession, for example, see Figure 7.23. In this figure, Blackrock is initially emptying and the EC concentration is rising homogeneously across the turlough due to the higher EC in the river (highlighted with a purple dotted circle). Then in early December a river surge occurs (orange circle). This surge is not enough to reverse the recession but it does cause the spring EC to start showing lower EC values than the body, indicating that the turlough is becoming less homogeneous. Following this EC split, another river surge occurs. After a brief rise in volume, the turlough recedes again but this time, the body of the turlough is in sync with the river EC rather than the spring (grey circle). The uniformity of river EC and body EC suggests that river water is being picked up by the body-CTD directly, i.e. there is no mixing occurring before water reaches the CTD. This indicates that the body-CTD is picking up river water discharging from a spring/estavelle in its vicinity. The spring-CTD, on the other hand, shows much less resemblance to the river, implying that the spring is not discharging. Considering that the turlough is in recession, it is likely that the spring is draining the turlough. This finding is significant as it suggests that Blackrock can be fed by a spring (estavelle) while in recession, i.e. water is coming in one estavelle and out another. From this point on, the turlough shows erratic and poorly mixed behaviour. Perhaps this altering homogeneous/heterogeneous recession behaviour could be due to the level of water. During recessions from a high level (21-22 mAOD, i.e. 9 - 10m depth), the turlough might remain homogeneous because the hydrostatic pressure of the turlough water prevents any influx from underground. At lower levels however, the pressure is less and so the springs/estavelles are able to discharge, causing heterogeneity within the turlough.

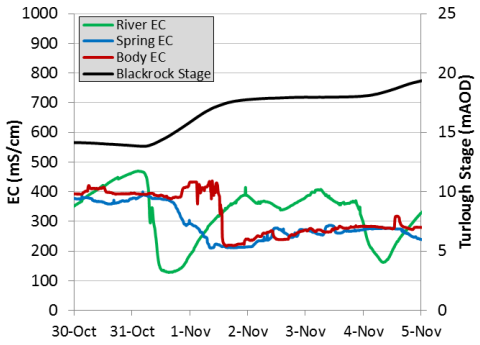

Figure 7.22: Spring and Body EC dropping during a flooding event.

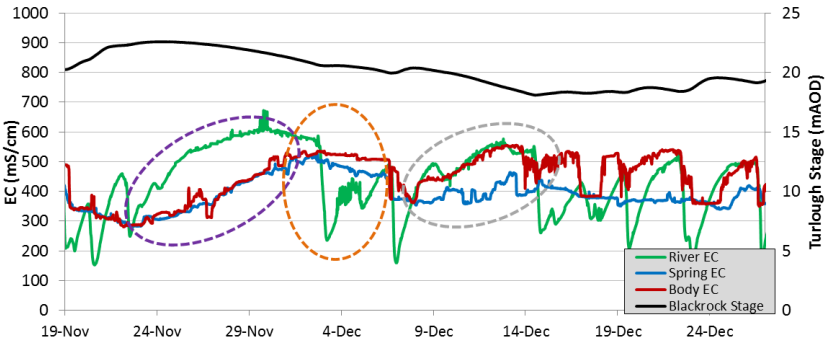

Figure 7.23: EC heterogeneity introduced during recession.

In Figure 7.23 it was seen that the discharge can occur from springs/estavelles near the body of Blackrock turlough while the turlough was in recession. This suggests that while the turlough is draining through the 'spring', it can also be filling (to a lesser degree) via the body. However, in Figure 7.24 it can be seen that the spring also discharges water on occasion. In this plot, a pulse of cold, low EC water was seen at the spring (highlighted by purple circles). This pulse occurred two and a half days after a river surge, possibly indicating that river water that became trapped within the conduit/fracture network under the turlough. As the turlough begins to recede, this water may have been released into the turlough as a rapid pulse. After this pulse, the body and spring EC's start to converge indicating the turlough is returning to a homogeneous conditions. Overall, the turlough shows a high degree of complexity, with no clear explanation for why a spring/estavelle discharges or drains at a particular time. Perhaps the mixed behaviour is due to the sheer amount of minor estavelles throughout the bed of the turlough. The complex nature of the underlying rock may result in these estavelles changing from filling to draining behaviour independent of one another (unless during high water levels, when no filling occurs from beneath).

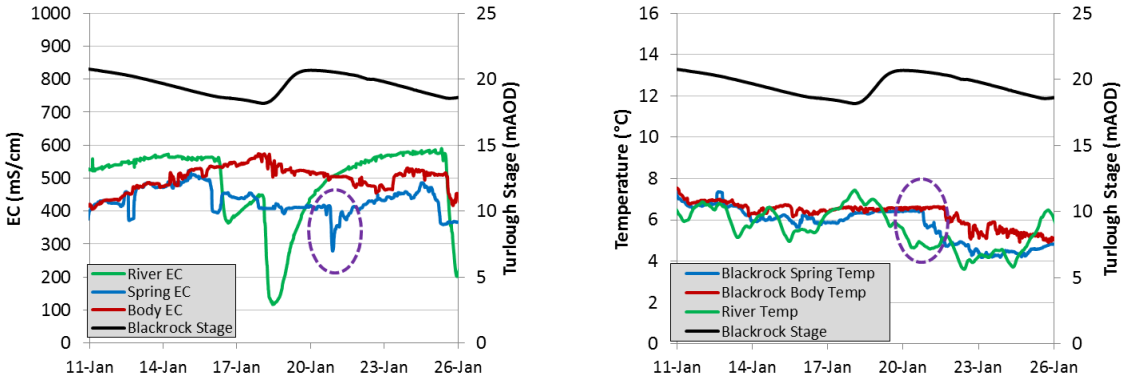

Figure 7.24: EC and Temperature drop at Blackrock Spring, January 2013.

This highly complex hydrological behaviour of Blackrock turlough is reflective of its underlying bedrock. An Electrical Resistivity Tomography study carried out by O'Connell et al. (2011) illustrates this complexity (Figure 7.25). O'Connell found a mixture of shallow karstified zones and a deep conduit karst zone. In Figure 7.25, the deep conduit zone can be seen crossing the turlough from the north-east to the south-west, passing underneath the location of the main spring. A shallow karst channel can be seen underlying the location of the body CTD. These two separate karst zones underneath Blackrock could provide an explanation for the variable EC behaviour. Perhaps during high water periods, hydrostatic pressure causes the turlough to drain into both the shallow and deep karst systems whereas during lower periods, the turlough drains into the deep conduit system but gains water from the shallow karst system.

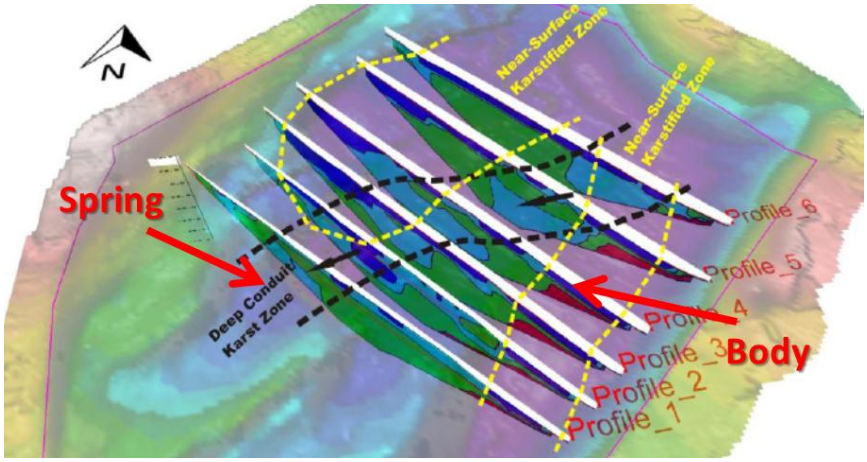

Figure 7.25: ERT study of Blackrock turlough (modified from O'Connell et al. (2011)).

From a water sampling point of view, the heterogeneity of Blackrock turlough is damaging to the concept of one sample being representative of the turloughs hydrochemistry. However, CTD data seems to show that water within the vicinity of the spring tends to be better mixed and less prone to variation than water from further out in the main body of the lake. As samples for this thesis were in fact recovered from near the spring (via kayak), the obtained hydrochemistry data is probably the closest approximation for the turlough's average chemical composition.

7.2.3.2 Coy

From Figure 7.21 it can be seen that Coy turlough experiences much less variation than Blackrock. This is not surprising considering the surcharge tank nature of Coy compared to the river flow-through nature of Blackrock. The predominant trend that can be seen from both the spring and body CTDs is the slow increase in EC over the flooded period. As discussed earlier in Section

7.2.1.2, this gradual increase is likely due to the steady contribution of highly mineralised water from the epikarst surrounding the turlough. However, a number of periods of lower EC water can be seen at the spring during periods of flooding. These low EC influxes (which also correspond with distinct changes in temperature) are clear indications of the turlough filling with Owenshree River water (which has either gone through or gone under Blackrock). Note, the slight offset between the spring and body is likely due to CTD calibration error.

Looking back at Figure 7.21, the cases of water influx at the spring appear to be straight forward, i.e. a filling period corresponds to a reduction in EC due to the influx of water. However, an anomaly occurs during the second large filling period (late December) where water at the spring does not drop in EC. Instead, three small rises in EC can be seen at the spring. See Figure 7.26 below for an illustration of a typical influx pattern (January 2013) and Figure 7.27 for the anomalous influx pattern (December 2012). In these figures, the left plot shows turlough stage and EC at the spring while the right plot shows the temperature readings from both the spring and the body of the turlough.

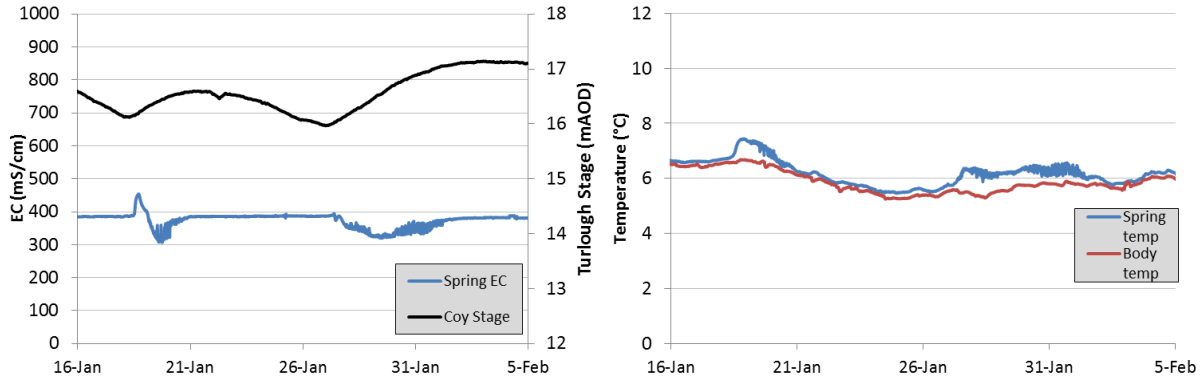

Figure 7.26: Typical influx pattern at Coy Spring (left – EC, right – temperature).

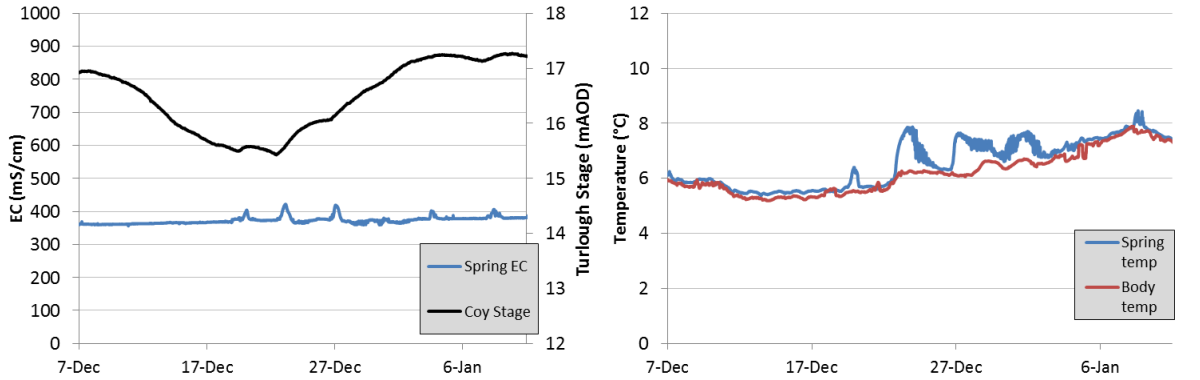

Figure 7.27: Anomalous influx pattern at Coy Spring (left – EC, right – temperature).

Figure 7.26 displays a typical pattern with reduction in EC caused by an influx of heavily rainfall diluted river water (piston flow is also observed during the first of the two influxes). The pattern is also reflected in the temperature measurements from the spring which show distinct increases in temperature compared to the body. The low EC of the water entering the turlough at this time (300-320 µS/cm) suggests a large contribution directly from the Owenshree River (whose EC drops down to 150 µS/cm) rather than from Blackrock turlough (EC between 400-500 µS/cm).

Figure 7.27 on the other hand does not show any reductions in EC during flooding which might indicate little activity at the spring. However the temperature data displays significant changes over the period signifying considerable influx. This influx must therefore originate from a location with a relatively high EC, i.e. capable of raising the EC of Coy from ≈370 µS/cm to ≈420 µS/cm. This indicates that the water does not come directly from the river as the river EC has dropped to ≈200 µS/cm nor does it come directly from Blackrock which has EC of ≈370 µS/cm. Looking at Figure 7.28, the EC of Coy can be seen reacting oppositely to the EC of the river, suggesting some piston flow behaviour in operation. Perhaps the surges in the Owenshree River caused some water which had been trapped underground (gradually increasing in EC due to dissolution) to be released into the turlough. Considering that the typical groundwater temperature is 11-12°C (from borehole diver measurements), any piston flow water would be expected to raise temperatures within the turlough, and indeed it does (Figure 7.27).

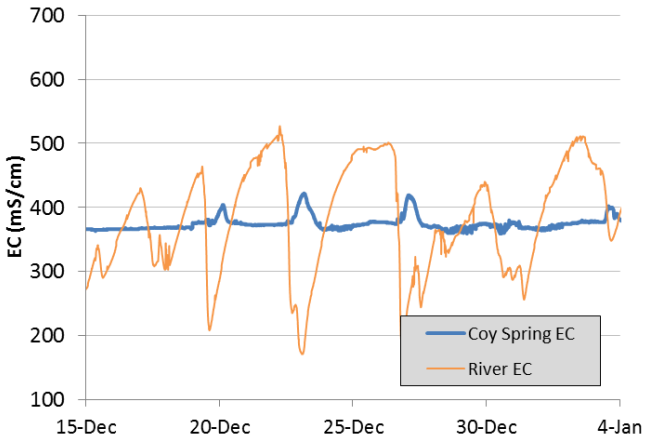

Figure 7.28: EC data from the Owenshree River and Coy turlough showing piston flow behaviour (December 2012).

Overall, Coy turlough appears remarkably well mixed. As such, the assumption of one sample being representative of the entire turlough could be deemed a reasonable one.

7.2.3.3 Conclusions

- Blackrock turlough has been shown to be a highly complex system, heavily influenced by its surface water input. The distribution of water in the turlough varies between homogeneous and heterogeneous, seemingly controlled by the level of water in the turlough. At higher levels, the turlough appears variable but well mixed, whereas at lower levels, and particularly during recession, water in the turlough behaves more erratically. This erratic behaviour at low levels is likely the result of a mixture of inflow and outflow occurring at the same time through separate karstified zones.

- In contrast, Coy turlough displays exceptionally well mixed behaviour. Influxes of river water (which has either bypassed or flown through Blackrock) can be seen at the spring as well as influxes of piston flow water (i.e. water which has been trapped underground for some time). However, after these influxes, the turlough returns to its well mixed state relatively quickly. The turlough also showed evidence of diffuse input over the flooded period as demonstrated by a slow, gradual increase in EC.

- This study proved to be a good demonstration of the contrasting behaviour of two turloughs which lie only 1 km apart. Due to financial constraints, only five CTD divers could be acquired. In any future study, the use of more CTD divers in Blackrock turlough would be extremely beneficial. Placement of CTD divers should also be carried out during dry periods so as to confidently place the CTD's close enough to the springs/estavelles. Also, further geophysical work could shed some more light on the hydrodynamics of the turloughs and the likely path (shallow or deep) taken by water from Blackrock to Coy.

7.2.4 CTD Study of Kinvara Bay

7.2.4.1 Introduction

As mentioned in Chapter 3, the intertidal nature of the Kinvara springs renders direct flow measurement impossible. Thus it was the intention of this sub-study to conceive of an alternative methodology which could be used to calculate the outflow at Kinvara for the purposes of validating the hydraulic model.

The technique chosen was to use CTD-divers in order to measure the altering salinity levels within the Bay. EC (mS/cm) can be converted into salinity (practical salinity units or 'psu') based on the formulation of Schemel (2001). Using this formulation, EC (mS/cm) is converted to salinity (psu) by an approximate factor of 0.61. In theory, for each tidal cycle, the input of freshwater at Kinvara should result in a slightly reduced salinity value for the bay. When the tide comes in, the freshwater at Kinvara is held back (in dry periods, the freshwater is even pushed back into the aquifer). Then when the tide goes out, the freshwater is released and should cause a measurable dip in salinity across the bay. Using survey data (LIDAR) of the bay, the volume of freshwater required to cause such a dip in salinity could be measured.

This method was used previously by Cave and Henry (2011). Specifically, Cave and Henry used the 'tidal prism' analysis technique to determine the fresh water input into the bay. The steps involved in this calculation are the following:

i. First, the salinity of water between each high and low tide was averaged. Then two different values of seawater salinity are used, to put an upper and lower limit of the amount of fresh water contained in the ebb.
ii. For the upper limit, the averaged salinity value is divided by a seawater salinity of 33.5 (average salinity of Galway Bay) to get the maximum proportion of fresh water contained in the ebb water.
iii. For the lower limit of the ebb fresh water volume, the averaged salinity of the ebb is divided by the maximum salinity measured on the previous flood tide (this allows for some ebb water being returned to the bay on the following flood tide).
iv. The height of low water in metres is subtracted from the height of high water for that tide, and the result multiplied by the surface area of the estuary, to get the total volume of water brought out on the ebb tide.
v. The total ebb tide volume is then multiplied by the freshwater proportion to get the volume of freshwater removed on each ebb tide (Cave and Henry, 2011).

Importantly, this technique is based on the assumption that the bay is well mixed. Using this technique, Cave and Henry estimated outflow of fresh water to be between 14 (lower limit) and 96 m^3/s (upper limit). These flows are noticeably higher than the outflow predicted from the hydrological model (5-15 m^3/s, see Figure 6.60)

7.2.4.2 Methodology

To carry out this study, a number of fieldtrips were conducted between May 2012 and February 2013 whereby CTDs were placed at various points within the bay to monitor salinity. CTDs were placed in three locations, the springs, the approximate midpoint of the bay and the outlet (marked as red dots in Figure 7.29). The CTDs were positioned on the base of the bay using a concrete platform and, in some cases, at a depth of approximately 1m within the water column, suspended from the buoy-platform rope (Figure 7.30). The CTD placed at the spring was positioned far enough out into the bay so as to pick up the combined flow from KW and KE springs (thus when the term 'spring' is used in this section, it is referring to the combined outflow of KW and KE). A salinity transect was also carried out to observe the mixing behaviour of the bay (marked as pink line in Figure 7.29).

Figure 7.29: CTD locations in Kinvara Bay.

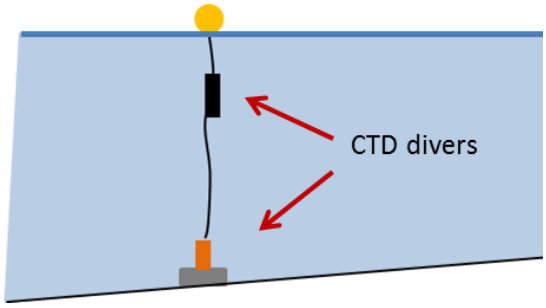

Figure 7.30: CTD positioning in the water.

7.2.4.3 Results

In Figure 7.31, the results from a CTD positioned at the spring (during mid-July) are shown. In this plot, it can be seen that the salinity shows dramatic shifts downward when the tide lowers to a certain degree, indicating that the CTD is in contact with freshwater. Then as the tide starts to rise

up again, the salinity shows a dramatic shift back up to a value more akin to saltwater. As time goes on, the tidal range is decreasing due to the approaching neap tide (period at which the difference between high and low tide is least). As a result of this decreasing range, a critical point is reached on July 12th when the tide does not drop sufficiently low enough to allow freshwater to contact the CTD. It should be noted that depth on these plots is based on chart datum rather than ordinance datum (chart datum is the datum used for nautical charts and oceanography).

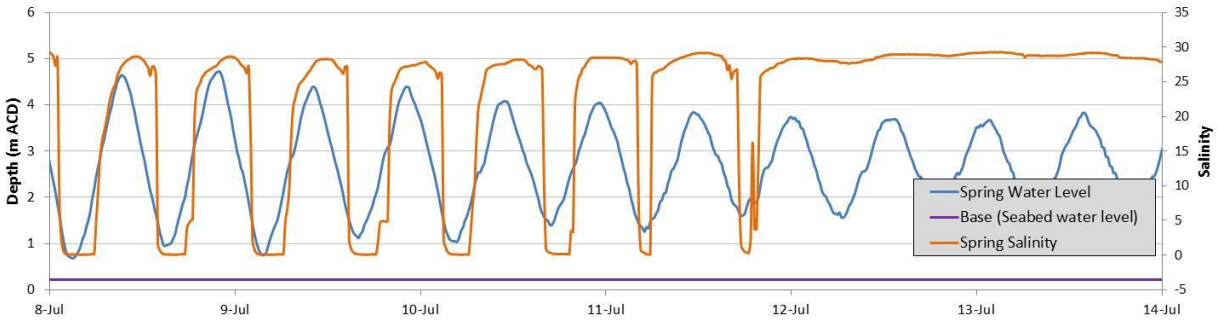

Figure 7.31: Data from the spring CTD (8th July – 14th July).

This behaviour suggests the existence of a sharp interface between saltwater and freshwater (freshwater sits on top of saltwater as it is less dense). This interface is displayed conceptually in Figure 7.32. Essentially, the fresh water sits on top of the salt water in the form of a wedge. Salt water wedges such as this are a well-known phenomenon which are more usually associated with estuaries (Partch and Smith, 1978) The presence of this wedge indicates limited saltwater-freshwater mixing is occurring near the spring.

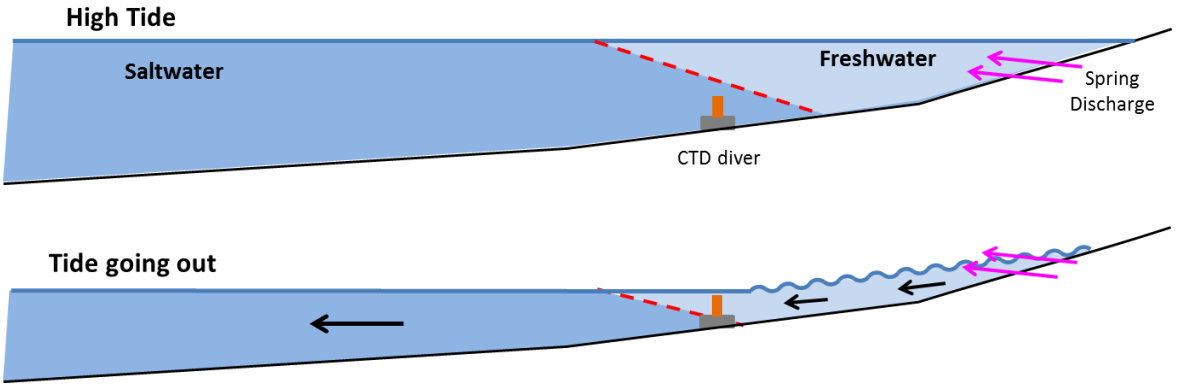

Figure 7.32: Conceptual interface between saltwater and freshwater at Kinvara spring.

This interface is less distinct in the water column at the midpoint CTD (as seen in Figure 7.33). This plot displays data from approximately 1m depth which was collected during early May. From the plot, it can be seen that the wedge is still present but the interface between freshwater and saltwater

has become wider and less distinct due to mixing processes. Spot samples taken during this sampling period, however, showed that pure freshwater was still present on the upper few centimetres of water. Thus at this location, the wedge is only present at the very top of the water column.

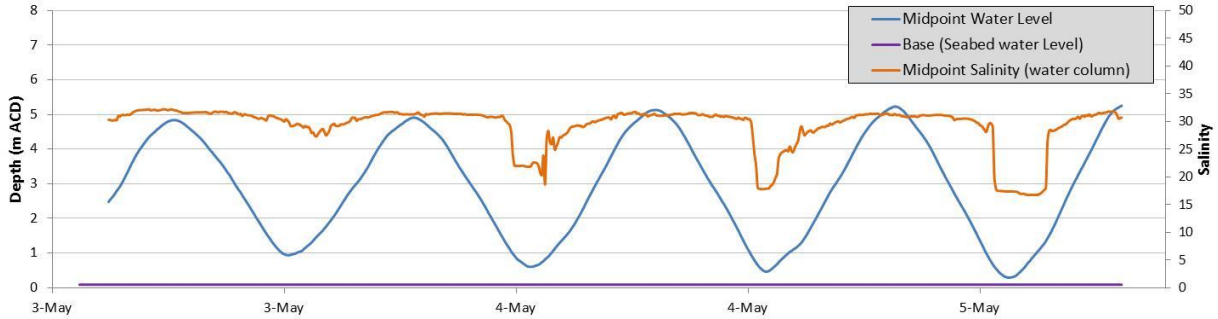

Figure 7.33: Data from the Midpoint CTD (3rd May – 5th May).

At the outlet, the interface is not evident within the water column, suggesting that the water is totally mixed at this point (solid orange line in Figure 7.34). However, curiously, the CTD positioned at the outlet base (dashed orange line in Figure 7.34), shows salinity approximately half that of the water column. This contrast between salinity at the outlet base and the outlet water column is difficult to explain. Perhaps the lower salinity at the outlet base is an indication that the CTD was placed within the vicinity of an unknown submerged spring. While the cause of this salinity behaviour is unknown, its occurrence suggests that water passing through Kinvara Bay outlet cannot be considered well mixed.

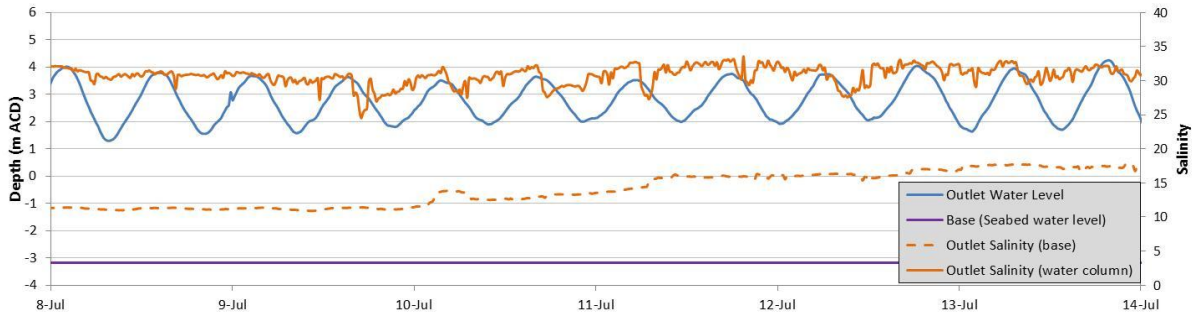

Figure 7.34: Data from the Outlet CTDs (water column – solid line, base – dashed line), 8th July – 14th July.

The salinity transect of the bay was carried out on the 11th of February 2013 and is presented in Figures 7.35 and 7.36. The salinity transect shown in these figures started at the bay outlet and

ended at Kinvara and was carried out as the tide was coming in. CTDs were rigidly suspended from the boat at depths 10 cm and 90 cm. In these figures, the plot of salinity values is overlaid on an aerial photo in order to show the changing salinity with distance moved across the bay. In Figure 7.35 it can be seen that a distinct layer of freshwater is present to a depth of at least 10 cm and extends out to the midpoint of the bay. In Figure 7.36, the deeper CTD picked up no such interface but did show a general trend of decreased salinity as the CTD approached Kinvara. These plots indicate that the conceptual wedge of freshwater is extremely shallow and can stretch far out into Kinvara Bay. Also, the saltwater layer lying beneath this wedge is not homogeneous and gradually increases in salinity with distance from the spring.

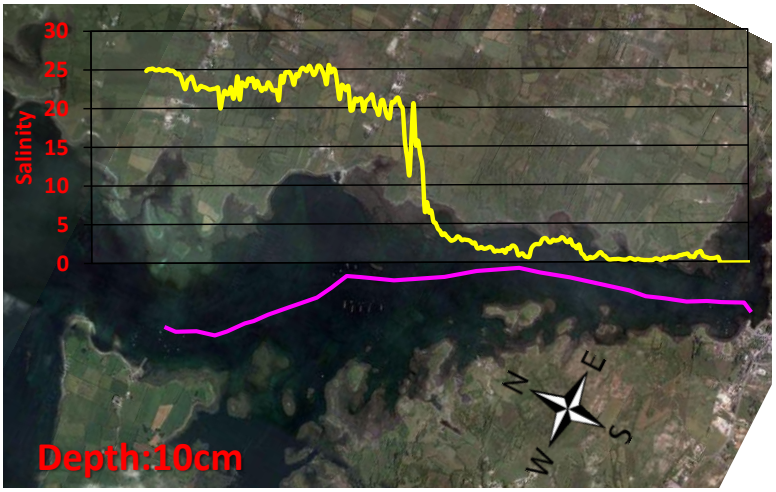

Figure 7.35: Salinity transect of Kinvara Bay at depth 10 cm. Pink line represents the path taken along the bay, yellow line represents the water's Salinity.

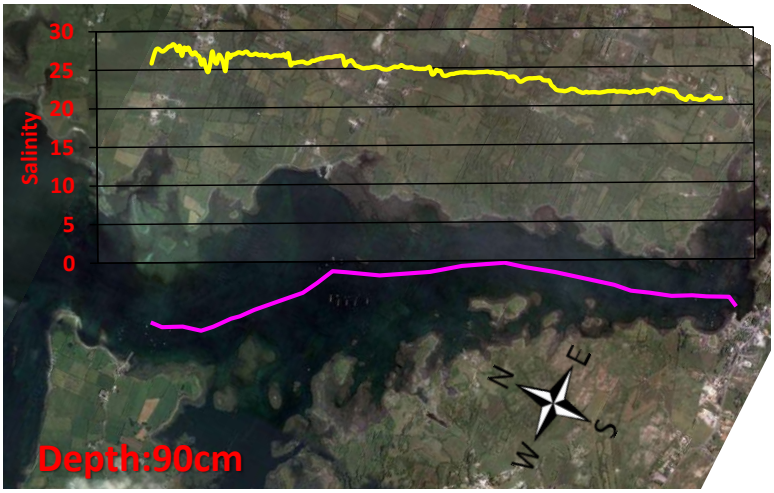

Figure 7.36: Salinity transect of Kinvara Bay at depth 90 cm. Pink line represents the path taken along the bay, yellow line represents the water's Salinity.

7.2.4.4 Analysis and Discussion

Based on the findings of the CTD divers, the assumption of homogeneity within the bay has been shown to be false. Instead, the freshwater has been observed to sit on top of the saltwater with a distinct interface. This wedge of freshwater has been seen to occur up to the midpoint of the bay. However at this distance from Kinvara, the freshwater-saltwater interface becomes less defined. Spot sampling (with a portable EC meter) has also shown the wedge to extend further out of the bay in the form of a thin film of freshwater sitting on the top few centimetres of the water column. Considering these factors (as well as the indication of unknown submarine discharges further out in the bay), the use of the tidal prism method (Section 7.2.4.1) for calculation of freshwater entering the bay becomes impractical which perhaps explains the relatively high outflow values of Cave and Henry (2011).

However, based on the concept of the freshwater wedge, another calculation technique could be proposed. As the tide comes in, the wedge is pushed backwards towards Kinvara and its volume expands due to the continuous discharge of freshwater from the springs. At low tide, this freshwater is then released into the bay, and onwards towards Galway Bay. From various fieldtrips, it has been seen that at low tide, the freshwater discharge at Kinvara is freely draining, similar to a typical surface water spring. Thus, focussing on the CTD located at the spring, the change in volume of the freshwater wedge between the start and end of a low tide period should give an indication of the amount of freshwater lost from the wedge (which should theoretically be similar to freshwater entering the wedge, i.e. spring discharge).

An example of such a low tide period is shown in Figure 7.37. In this Figure, a time series plot of depth and salinity for an individual tidal cycle is shown. Four specific points in time are chosen and are conceptualised with individual graphs. Point A shows the spring at high tide when the CTD is fully immersed in saltwater. Point B shows the point at which the interface passes across the CTD while the tide goes out. Point C shows the spring at low tide. At this point, it can be seen that the water level at the spring (blue line) does not drop as low as the water level at the outlet (green dotted line), this is due to the constant discharge from the spring. Point D shows the point at which the tide has turned and pushes the interface back across the CTD.

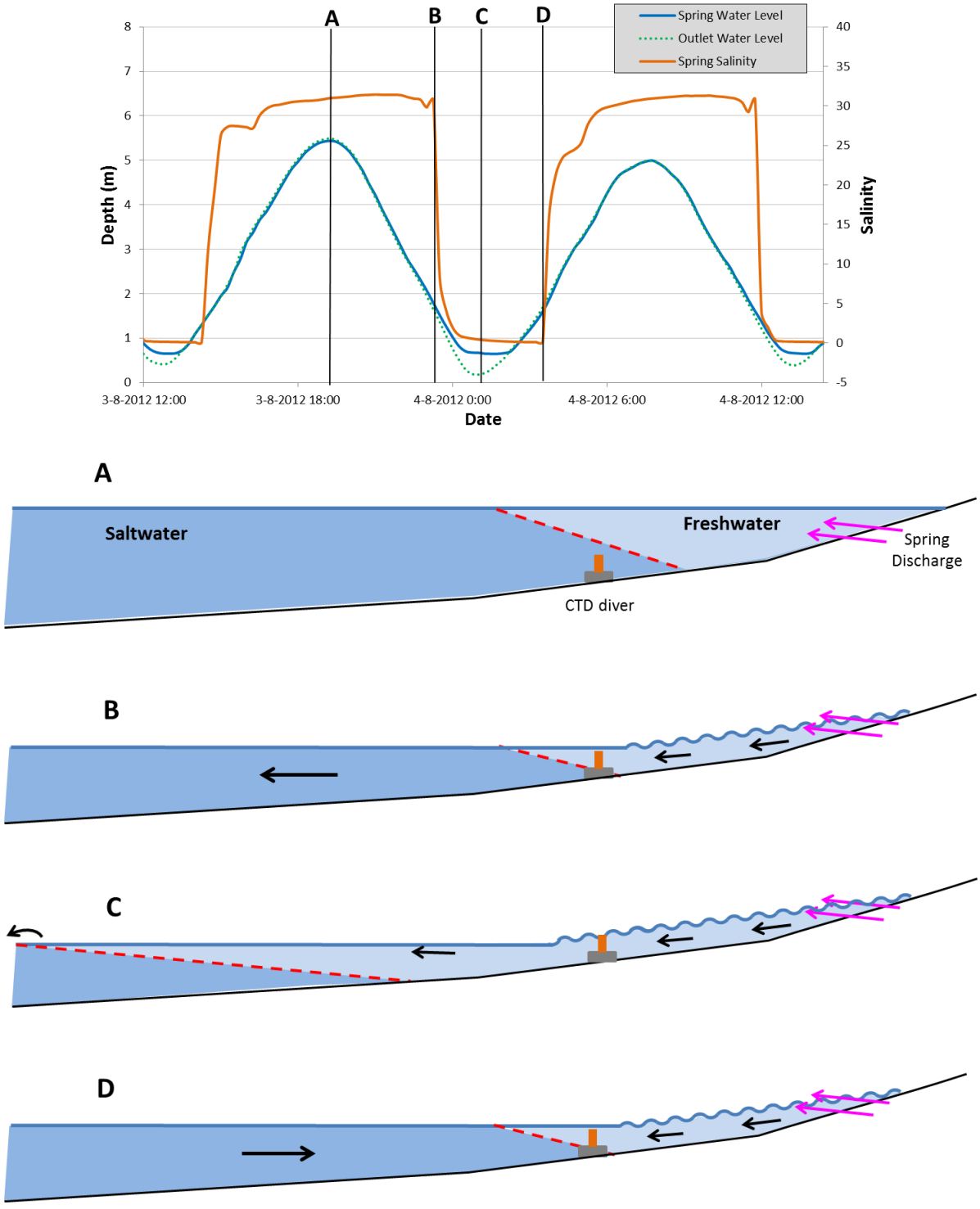

Figure 7.37: Freshwater wedge calculation showing time series plot (top) and conceptual plots for points A, B, C and D.

Using this conceptualisation, the change in wedge volume between points B and D should give an indication to the amount of freshwater lost from the wedge. This method requires the somewhat

flawed assumption that there is no mixing between the freshwater and saltwater zones and that each zone is homogeneous. Thus any result can only be viewed as a rough estimate. However, this estimate should be sufficient to determine which outflow prediction is more realistic - the hydraulic model (mean discharge from KW: 8.7 - 9 m^3/s) or Cave and Henry (2011) (14 - 96 m^3/s).

The volume of the wedges was calculated by combining, CTD depth data, Kinvara Bay survey data and an estimated wedge slope. The slope of this wedge was estimated based on the findings of multi-depth spot sampling. The volume of the wedge at points B and D were found to be 693,056 m^3 and 548,906 m^3. So the change in volume over the low tide period was 144,151 m^3. Thus, over the 4.5 hour period between points B and D, it would take an outflow of 8.9 m^3/s from the wedge to result in such a volume reduction. Over this same period, the Infoworks model predicts a mean outflow from KW of 8.09 m^3/s. This modelled discharge increases to approximately 9.4 m^3/s with the inclusion of external catchment water (Section 7.2.1.4) and 10.5 m^3/s with the inclusion of KE discharge (estimated later in Section 7.3.1.4). In contrast, a sample calculation of the Cave and Henrys method was carried out for the midpoint CTD (similar to where Cave and Henrys equipment was located) and estimated an outflow of between 84 and 93 m^3/s. Based on these results, it could be cautiously stated that the salt wedge technique is the superior calculation technique and validates the results of the hydraulic model. It should be noted however that the salt wedge method does not account for discharges into Kinvara Bay other than those from KW and KE springs. In reality, this discharge is further enhanced by various other freshwater springs (known or unknown) throughout the bay.

For a more confident result, the shape of the wedge and its mixing characteristics should be monitored in greater detail, over a range of tidal cycles. This would involve the use of multiple CTDs located throughout the bay at multiple depths so as to characterise the shape and dynamics of the wedge. Another alternative approach for studying the bay could be the use of high-resolution salinity data and information about the hydrodynamics within the bay (currents, mixing, additional springs, etc.) to develop a mixing model for the bay, for example, using Computational Fluid Dynamics (CFD). A study such as this would be useful for quantifying both flow and potentially nutrient inputs but is outside the scope of this thesis.

7.3 Nutrients

In non-carbonate aquifers, N and P are subject to separate transport dynamics. Nitrate is often found to be conservatively transported due to the high solubility and mobility characteristics while P is retained due to its affinity to particulate matter (Weiskel and Howes, 1992). In carbonate aquifers, however, the existence of point recharge makes it easier for N and P to gain access. Swallow holes provide direct access points to the aquifer, with little or no attenuation, so contaminants more frequently associated with surface waters, which would not normally enter by diffuse recharge (i.e. P), may enter karst conduits by point recharge bypassing the protective soil cover (Coxon, 2011). In principle, P can be transported in ecologically significant quantities across large distances in karstic systems (Cunha Pereira, 2011). A study carried out in Cregduff, Co. Mayo by Mellander et al. (2013) found that of the various karst features within the studied catchment, bedrock dolines were considered to be the most likely surface feature to transmit P due to the direct connection to the underlying material. P is also known to be removed from groundwater in limestone areas due to the formation of calcium-phosphate compounds (Cable et al., 2002). This has been observed in Kinvara by Smith and Cave (2012).

Evidence of non-conservative flow behaviour of P is seen in a study by Kilroy and Coxon (2005) who observed temporal changes in P in two limestone catchments in Western Ireland. In this study, P concentrations at springs were observed at levels greater than the 20 µg/l threshold for eutrophic conditions in Irish lakes (as well as the 35 µg/l OECD eutrophication threshold for rivers and lakes (OECD, 1982)). P concentrations were also seen increasing with increasing rainfall, likely due to the dislodging of loosely bound particulate P (PP) and dissolved organic P (DOP). Daily sampling demonstrated total phosphorus (TP) concentrations of up to 1814 µg/l indicating the vulnerability of karst aquifers to groundwater contamination (Kilroy and Coxon, 2005). This vulnerability is due to the shallow bedrock and rapid transport of water within karst aquifers providing contaminants with an ideal pathway. Drew and Daly (1993) point out that the Mid-Galway, South-Mayo, North-Clare region (which includes the Gort Lowlands) is likely the worst region in Ireland for groundwater contamination. The four main sources of groundwater pollution within the region are septic tank systems (with some only < 2m above fractured bedrock), farmyards, landspreading of organic wastes and sewage in sinking streams. A more recent study by Bartley et al. (2009) carried out in the Burren presented similar findings with point sources (such as animal feeding sites, surface water accessed by animals, or septic tanks) being designated as the main cause of occasional elevated phosphorus concentrations in groundwater. Due to the relatively unconstrained transport of nutrients in karst aquifers, contamination from these point sources is not limited to local areas

and can affect sensitive areas such as turloughs even at significant distances from the source (Cunha Pereira, 2011).

7.3.1 Results

Nitrate (NO_3), total nitrogen, (TN), total dissolved phosphorus (TDP) and total phosphorus (TP) were tested for. The sub-species of TN, Nitrite (NO_2) and ammonium (NH_4), were also tested for originally. However these parameters were often near-to or below detection limits and as such, their measurement was ceased in late 2010. Petrunic et al. (2012) suggest that the low concentrations of NO_2 and NH_4 in the region are likely due to their rapid conversion to NO_3. This would be expected in an oxygenated groundwater environment such as the Gort Lowlands. See Table 7.5 below for a brief overview of NO_2 and NH_4 results taken over the course of 2010. Highest levels of nitrite and lowest levels of ammonia were found in the rivers while lowest nitrite and highest ammonia was found in the groundwater. For a detailed look at the ranges and mean values of NO_3 TN, TDP, TP, see Table 7.6.

Table 7.5: Mean values for Nitrite (NO_2) and Ammonium (NH_4), 2010.

	NO_2 (mg/l)	NH_4 (mg/l)
Rivers	0.018	0.032
Turloughs	0.014	0.121
Groundwater	0.004	0.160
Kinvara	0.006	0.101

It should be noted that some test results showed clearly erroneous values. Causes of these errors included sample contamination or evaporation, poor chemical reagent preparation and poor spectrometer calibration. Results such as these were removed from the dataset.

Table 7.6: Ranges and mean values for Nitrate (NO3), Total Nitrogen (TN), Total Phosphorus (TP) and Total Dissolved Phosphorus (TDP) for Rivers, Turloughs, Groundwater and Kinvara (grouped and individual).

	TN (mg/l)		NO_3 (mg/l)		TP (µg/l)		TDP (µg/l)		TN:TP
	range	*mean*	*range*	*mean*	*range*	*mean*	*range*	*mean*	
Rivers	**0-3.9**	**1.01**	**0-3.1**	**0.71**	**3.7-120.8**	**26.01**	**0-67.6**	**18.39**	**39.0**
ORU	0.3-2.3	1.05	0-1.9	0.74	6.6-121	27.2	7-57.7	19.2	38.7
ORL	0.2-3.4	1.03	0.1-1.5	0.55	13.5-113	27.3	6.3-44.1	16.1	37.9
BRU	0-2.6	0.95	0-2.4	0.78	18.2-77.7	37.0	10.6-67.6	28.2	25.7
BRL	0-3.1	1.12	0.1-1.6	0.68	15.8-102	32.3	8.1-63.9	23.6	34.8
DRU	0.2-3.9	1.10	0.1-2.5	0.91	13.1-65.4	29.5	7.6-58.1	23.4	37.3
DRL	0.1-3.5	1.09	0.1-3.1	0.66	11.5-86.8	30.9	7-48.6	20.0	35.3
F	0-3.7	0.87	0-2.4	0.53	4.8-21.4	11.2	0-14	7.4	77.5
P	0.2-2.2	0.89	0-3	0.84	3.7-55	12.8	0-42	9.3	69.6
Turloughs	**0.1-4.3**	**1.12**	**0-2.4**	**0.66**	**13.8-115**	**33.70**	**6-61.4**	**21.19**	**33.2**
Blackrock	0.3-3	1.32	0.3-1.5	0.81	21.7-115	47.7	13.2-61.4	28.7	27.7
Coy	0.3-3	1.11	0-2	0.57	25-63.5	42.0	6-45.5	21.4	26.3
Coole	0.3-3.2	1.10	0.2-1.7	0.66	23.5-44.7	30.6	8.6-32.4	19.9	36.1
Garryland	0.3-2.7	0.95	0.1-1.7	0.60	13.8-34.4	21.0	5.3-25.2	15.7	45.4
Caherglassaun	0.1-4.3	1.11	0-2.4	0.65	18.9-36.3	27.2	8.2-28.4	20.2	40.7
Groundwater	**0.2-10.4**	**2.30**	**0-10.3**	**1.51**	**0-582**	**31.28**	**0-484.9**	**20.61**	**73.5**
BH3	0.4-3.9	2.45	0.1-3.6	1.60	3-50.8	13.4	0-34.9	7.6	182.3
BH5	0.3-3.1	1.39	0-1.4	0.48	9-582	72.0	4.5-484.9	51.6	19.3
BH7	0.4-10.4	3.31	0-10.3	2.79	7.1-53.1	14.7	4.8-14.4	7.7	225.6
BH10	0.1-4.2	2.17	0.1-2.6	1.52	0-12.6	5.1	0.6-9.9	3.5	422.3
BH11	0.2-2.4	1.24	0-2.9	0.69	5.4-128.8	32.9	3.7-21.2	7.2	37.8
BH12	0.3-5.2	2.95	0.2-3.8	1.97	7.5-46.7	19.1	1.6-28.7	6.9	154.1
BH14	1.1-5	2.91	0-3.4	1.75	33.2-82.2	52.9	30.6-64.5	42.1	55.0
BH15	0.2-3.1	1.31	0.1-1.9	0.68	30.9-80	51.9	29-57.5	41.6	25.2
BH16	0.3-5.5	2.96	0.2-4.3	2.15	11.1-38.8	19.4	8.5-33.5	17.4	152.5
Kinvara	**0.4-3.6**	**1.52**	**0.1-3.7**	**0.89**	**9.3-36.7**	**23.55**	**8.1-23**	**16.89**	**64.4**
KW	0.4-2.3	1.05	0.1-2.5	0.66	9.3-32.5	22.9	8.1-21.8	16.5	45.6
KE	0.6-3.6	1.99	0.1-3.7	1.12	19.2-36.7	24.2	8.2-23	17.3	82.3

7.3.1.1 Rivers

From Table 7.6 it can be seen that values for N in all rivers range between 0 and 3.9 mg/l with a mean of 1.01 mg/l. For P, values range between 0 and 120.8 µg/l with a mean value of 26 µg/l (Table 7.6). Nutrient concentrations in the rivers show a high degree of variation, although a mean concentration seasonal trend is apparent (Table 7.7). Mean concentrations for both N and P are highest in summer (similar to the findings of Drew and Daly (1993)) whereas lowest concentrations are in the winter for N and the spring for P. In terms of river flow, a minor but statistically significant relationship can be seen between river flow and P. No such relationship was found for N (See Figure 7.38 below for regression plots of flow vs. TN and TP for the Ballycahalan River).

Table 7.7: Mean Seasonal River Concentrations of TN, NO3, TP and TDP.

	Spring	Summer	Autumn	Winter
TN (mg/l)	1.04	1.49	1.10	0.78
NO_3 (mg/l)	0.62	0.93	0.70	0.64
TP (µg/l)	20.48	38.97	28.18	22.43
TDP (µg/l)	14.41	20.41	19.50	16.84

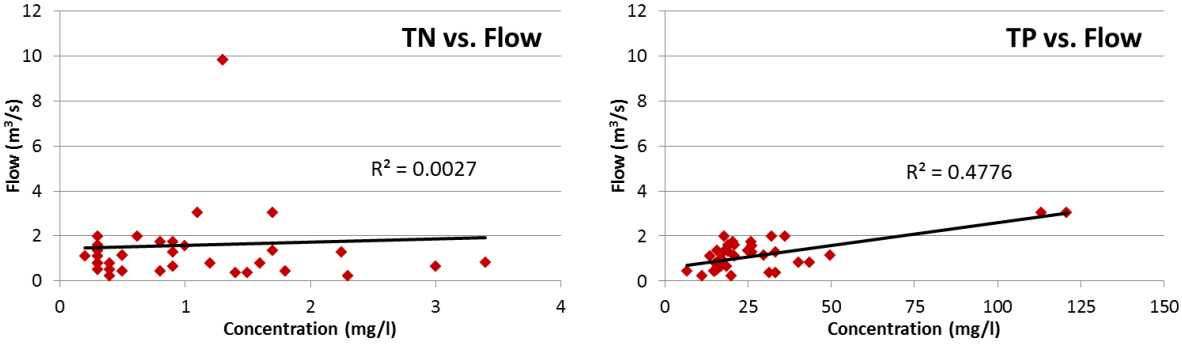

Figure 7.38: Regression plots of Flow vs TN and TP Concentrations (Owenshree River).

Nutrient results for the upper and lower sampling points on each river are shown in Figure 7.39 (TN and NO_3) and Figure 7.40 (TP and TDP). Overall, these time-series plots show that TP and TDP display similar levels of variation within the rivers whereas TN shows greater variation compared to NO_3. This suggests high variability from the organic component of TN, possibly as a result of agricultural runoff.

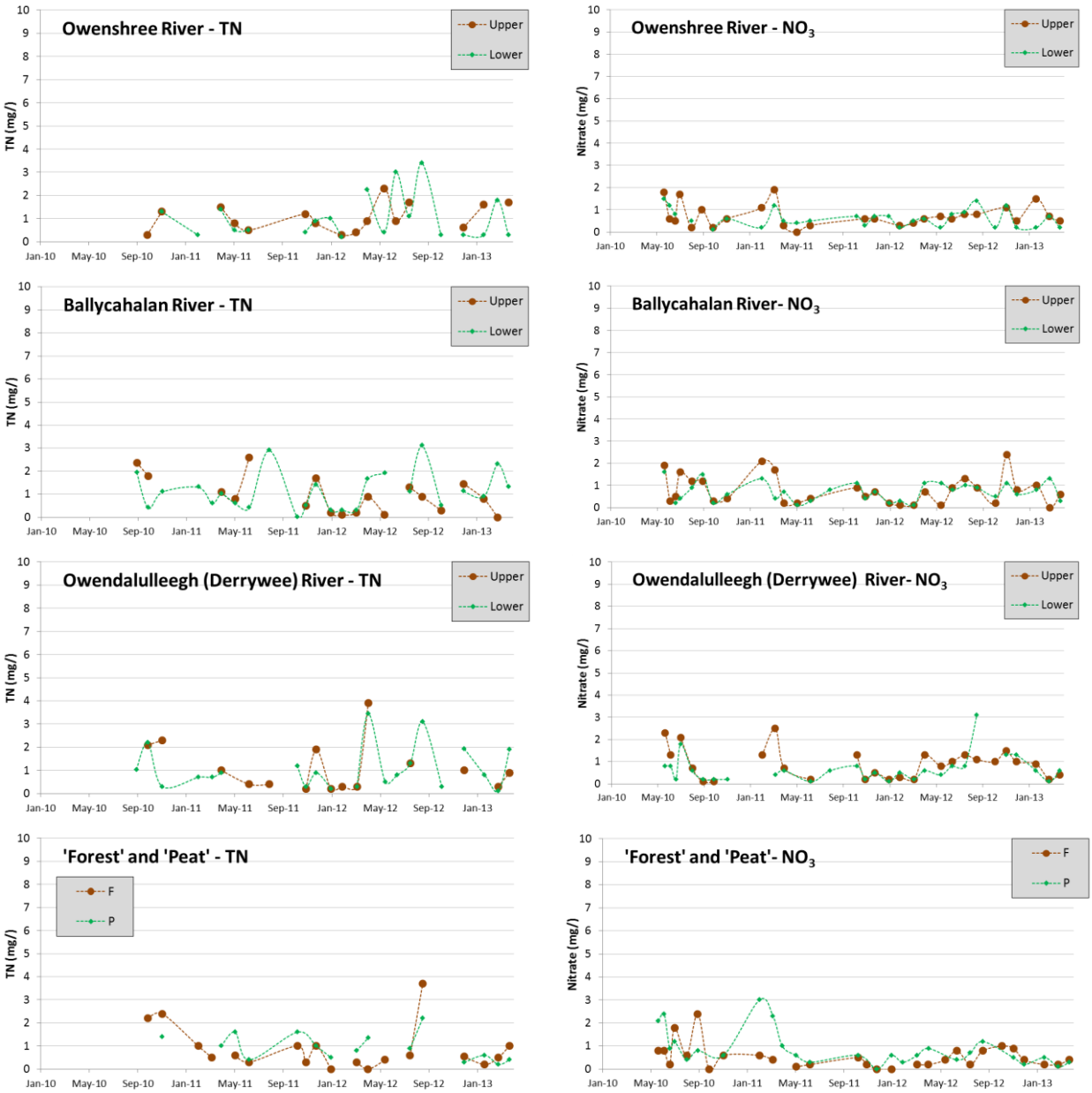

Figure 7.39: Time-series plots of Total Nitrogen (TN) and Nitrate (NO_3) results for rivers.

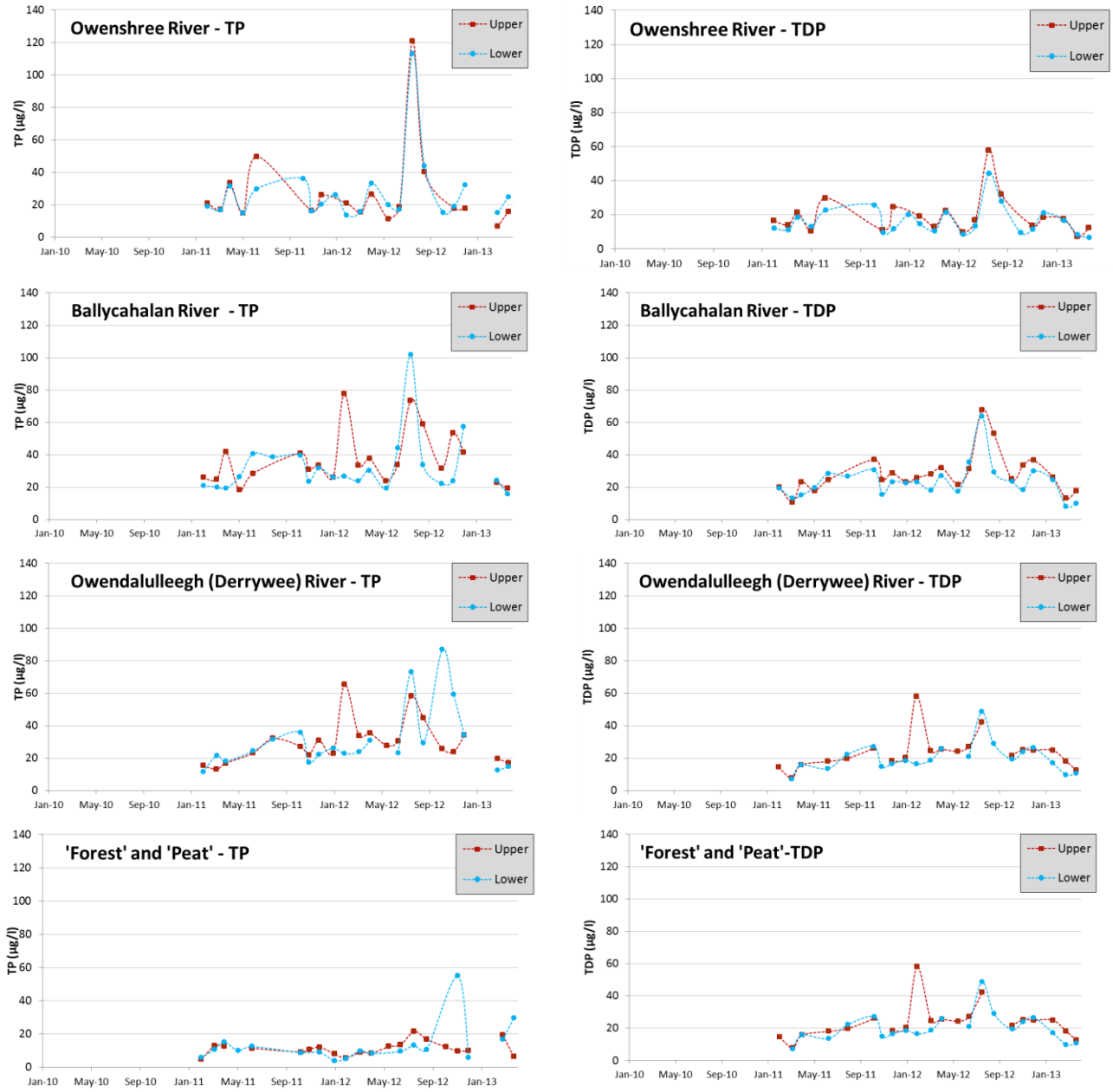

Figure 7.40: Time-series plots of Total Phosphorus (TP) and Total Dissolved Phosphorus (TDP) results for rivers.

Looking at the rivers individually, the contrasting source/transport dynamics between N and P are apparent. Mean values of N for each river are quite similar, ranging between 0.87 and 1.12 mg/l (TN) whereas for P, the rivers show a wide range of mean values between 11.2 and 37.0 µg/l (see Table 7.6). Highest mean values of P are found in both the Ballycahalan River sampling locations,

possibly reflecting the large amount of forestry in this catchment (forestry fertilisers tend to be highly phosphatic, see Section 7.1.2).

The lack of variation between all sampling locations for N, and the lack of variation between upper and lower river sampling locations for both N and P indicates that there is a minor but constant addition of nutrients to the rivers as they travel down through their catchments. In fact, the mean nutrient concentrations for all rivers still lie within the expected nutrient concentrations of rainfall (Beltman et al., 1993, Loehr, 1974). This might suggest that overall agriculture and forestry practices on the Slieve Aughty Mountains catchment add very little nutrients into the rivers or that the net attenuation processes leave only low levels of nutrients in the surface water. Care must be taken when interpreting these results however as samples were only taken monthly. Nutrient concentrations within the rivers could vary considerably between sampling events due to relatively fast moving plumes of point source pollution.

In July 2012, a peak in P (TP & TDP) can be seen in the three main rivers. This peak occurs during the typical forestry fertilisation season of April to August (Teagasc, 2013) and coincides with a period of heavy rainfall, thus suggesting contamination due to highly phosphatic fertiliser such as *superphosphate*. Kilroy and Coxon (2005) also suggest that a response such as this possibly reflects a hydrological switch where the catchments change from a soil moisture deficit to a soil moisture surplus situation.

Nutrient load quantities in the rivers can be calculated by combining the measured nutrient concentration data with the observed flow data. This technique is easily applicable to the Owenshree and Ballycahalan Rivers due to their complete flow records. For the Owendalulleegh River however, the poor river flow record (and poor NAM calibration) hinders this calculation. Instead, the mean flow for the Owendalulleegh was considered to be 81% that of the Beagh River (based on reservoir routing calculations, Section 6.4.3.1). This factored mean flow was then multiplied by the overall mean nutrient concentrations from the Owendalulleegh in order to give a rough estimate of mean nutrient loading. Mean daily loading rates (in kg/day) and loading rates per hectare (kg/day/ha) for the rivers are shown in Table 7.8. Looking at the loading rates per hectare, the catchments appear to show similar nutrient loading behaviour (although for more accurate calculation of loading rates in the rivers, regular short interval sampling would be required). For this study, only monthly sampling was possible. Consequently, the calculated loading rates can only be viewed as an indication of the loading rates rather than precise data.

Table 7.8: Mean Nutrient Loading Rates in Rivers (kg/day) and Loading Rates per Hectare (kg/day/ha).

	TN		NO_3		TP		TDP	
	(kg/day)	(kg/day/ha)	(kg/day)	(kg/day/ha)	(kg/day)	(kg/day/ha)	(kg/day)	(kg/day/ha)
Owenshree	117.9	0.034	70.05	0.020	3.11	0.0009	1.84	0.00053
Ballycahalan	122.1	0.026	73.95	0.016	3.51	0.0007	2.57	0.00054
Owendalulleegh	281.0	0.031	169.2	0.019	7.95	0.0009	5.15	0.00058
Total	**521.0**		**313.2**		**14.57**		**9.56**	

7.3.1.2 Turloughs

Mean turlough nutrient concentrations and ranges can be seen in Table 7.6. Mean TN and TP concentrations for the turloughs were calculated as 1.12 mg/l and 21.19 µg/l with highest concentrations recorded of 4.3 mg/l TN and 115.4 µg/l TP.

Generally, the upper two turloughs showed higher nutrient concentrations than the lower three turloughs. Also, the upper turloughs showed mean concentrations greater than those of the Owenshree River feeding them (except NO_3 in Coy). This suggests that the turloughs act as sources rather than sinks of nutrients. This increase in mean nutrient concentration is particularly evident for TP with Blackrock and Coy turloughs displaying mean TP concentrations exceeding those found in the Owenshree River by 75% and 65% respectively. For these turloughs, there are three main factors that are likely the cause of the increased nutrient concentrations. Firstly, both turloughs are actively grazed during the summer months. This would lead to increased nutrient concentrations at the onset of flooding due to manure deposition (grazing in turloughs has been proven to result in increased soil-P concentrations (Kimberley et al., 2012)). Secondly, nutrient concentrations within Blackrock are likely being enhanced by the presence of an abattoir on its south eastern edge. Nutrient enhancement from the abattoir could also have a knock on impact on Coy turlough as it is known to receive water from Blackrock (as seen in the Blackrock/Coy CTD study, Section 8.3.2). Thirdly, the elevated nutrient concentrations (particularly N) could indicate additional flows coming in from the nutrient enriched diffuse sources (see groundwater, Section 7.3.1.3). Another factor that should not be ignored is the temporal resolution of sampling. Monthly sampling of turloughs is adequate to characterise the system as water is typically retained in the turloughs for long periods. However, for the rivers, monthly sampling only offers a snapshot of concentrations at the time of sampling. Thus any potential plumes of point source contamination in the rivers could easily be missed by the river samples but would likely be accounted for in the

turlough samples. This issue could likely be a cause of the imbalanced river-turlough mean nutrient concentrations.

Mean nutrient concentrations in Coole, Garryland and Caherglassaun turloughs showed lower concentrations than Blackrock and Coy. Concentrations in these three turlough tended to reflect the concentrations of the rivers feeding them. For example, mean concentrations of TN and TP in Coole turlough lie within ±1% of their primary source of water, the Owendalulleegh (DRL). Nutrient concentrations in Caherglassaun show similar values to Coole indicating a direct relationship between these turloughs. However, Garryland turlough displays lower nutrient concentrations, most likely due to influx of water from the Cloonteen catchment to the south. These results are in accordance with the findings of Cunha Pereira (2011).

All five turloughs appear to show a relationship between mean N and P concentrations, i.e. if mean N is relatively high in one turlough, mean P is also shown to be high. This is not surprising considering that all potential sources of contamination such as agricultural wastes (Stationery Office Dublin, 2010) or septic tanks (Gray, 1995) contain both N and P. However, the ratio of N to P does alter depending on the source. Agricultural soil effluents, such as runoff from unfertilised fields, tend to have high N:P ratios (>20 up to 250) while more common point source effluents such as animal waste, slurry or septic tanks tend to have low N:P ratios (<10) (Downing and McCauley, 1992). Therefore a turlough contaminated by point source effluent would receive greater enrichment of P than of N. Taking this into account, the lower N:P ratios of Blackrock and Coy turloughs (Table 7.6) could indicate an higher degree of point source inputs into the Owenshree catchment than into the other two river catchments.

As discussed briefly in Section 3.4.4.2, a number of classification systems exist in order determine the trophic status of a lake. These methods typically involve the measurement of hydrochemical parameters such as TP, chlorophyll-*a* (chl-*a*) or transparency. Another method that can, and has, been used on surface water bodies such as turloughs is to catalogue plant life to determine Ellenburg-N indicator values (Tynan et al., 2007). In this thesis, the trophic classification scheme used is that of the International Eutrophication Programme (OECD, 1982) which established trophic status categories based on the levels of algal biomass or total phosphorus in lakes and rivers. The resulting trophic statuses of this classification system (OECD-fixed boundary method) based on the mean recorded P concentrations are presented in Table 7.9.

Table 7.9 Turlough Trophic Status based on P concentrations using OECD fixed boundary method (OECD, 1982).

Turlough	Trophic Status
Blackrock	Eutrophic
Coy	Eutrophic
Coole	Mesotrophic
Garryland	Mesotrophic
Caherglassaun	Mesotrophic

Most of these results are in accordance with the findings of Cunha Pereira (2011). However, Cunha Pereira determined Caherglassaun to be eutrophic rather than mesotrophic. Tynan et al. (2007), on the other hand, determined all five turloughs to be Eutrophic. It should be noted that Tynan's chosen classification scheme (using plant life) was based on a turlough trophic status range rather than an all-inclusive surface water body trophic range. As a result, Tynan's results were skewed towards higher values trophic statuses when compared to typical water bodies.

7.3.1.2.1 Nutrient Concentrations

Time series plots of nutrient concentrations are shown in Figures 7.41 and 7.42. These plots show nutrient concentrations and turlough volumes between January 2011 and March 2013. This dataset incorporates both the 2011/2012 and 2012/2013 flooding seasons and the final flooding event of the atypical 2010/2011 season. The previous isolated flooding events of the 2010/2011 season are omitted as their rapid filling and emptying behaviour makes them impractical to analyse using only monthly sampling data. Looking at the time series data in Figures 7.41 and 7.42, the nutrient data appears highly variable. However upon closer inspection a number of trends can be discerned:

- Turloughs that are grazed during dry periods tend to show peaks of P at the start of a flooding period. These peaks are in excess of the concentration in the water entering the turloughs from the rivers suggesting an internal source of nutrients within the turloughs, i.e. manure from animal grazing. This lines up with the findings of Kimberley et al. (2012) who found grazed turloughs to have higher soil P concentrations than ungrazed (whereas the opposite was true for N, suggesting grazing animals remove more N than they add). This trend is most obviously seen in Blackrock and Coy turloughs. Also, as Blackrock turlough is the highest turlough in the network and is primarily fed by a river, any contamination to this river would impact the turlough. An example of this can be seen in

July 2012 where Blackrock experiences a minor flood event but a major increase in P concentration (TP=115 µg/l) due to elevated P levels in the Owenshree River.

- During the flooded periods, there appears to be considerable variation in nutrient concentrations. However a general trend can be seen (especially for P) whereby the nutrient concentrations reduce over the course of the flooded season. This trend (similar to that found by Cunha Pereira (2011) can be seen in all turloughs to some extent, although it is not seen for every flooded period. The mechanisms for these losses are discussed further in Section 7.5.2.

- For Blackrock, Coy, Coole and Garryland turloughs, spikes in TN concentration are seen during relatively dry periods following a recession. These spikes are likely due to the increased sensitivity of the turloughs to their river inputs during dry periods. During these periods, the turloughs have less capacity to dilute any incoming nutrient plumes and so spikes in nutrient concentrations should be expected. Cunha Pereira (2011) observed similar spikes and suggested they were due to the possible release of nutrients and organic matter to the water column owing to the increased soil-water interactions. Another cause for these spikes could be linked to the high groundwater contribution at that time of year, i.e. the higher N in groundwater is being released into the turloughs as the water table drops. This effect can be seen April 2012 where the four turloughs mentioned see spikes in TN (in accordance with spikes of TN in the Owenshree and Owendalulleegh Rivers).

Looking at the data from these five turloughs, it appears that N shows slightly more erratic variability than P. This is in contrast to the results of Cunha Pereira (2011) who found P more erratic than N. This finding would therefore seem to corroborate with the spatial homogeneity study carried out by Cunha Pereira (Section 7.1.1) which suggested that sampling from the edge of a turlough is likely to cause inaccuracies in measured TP concentrations. It should be noted however that the monthly timestep is a limiting factor in this study. A shorter timestep would facilitate a more detailed analysis.

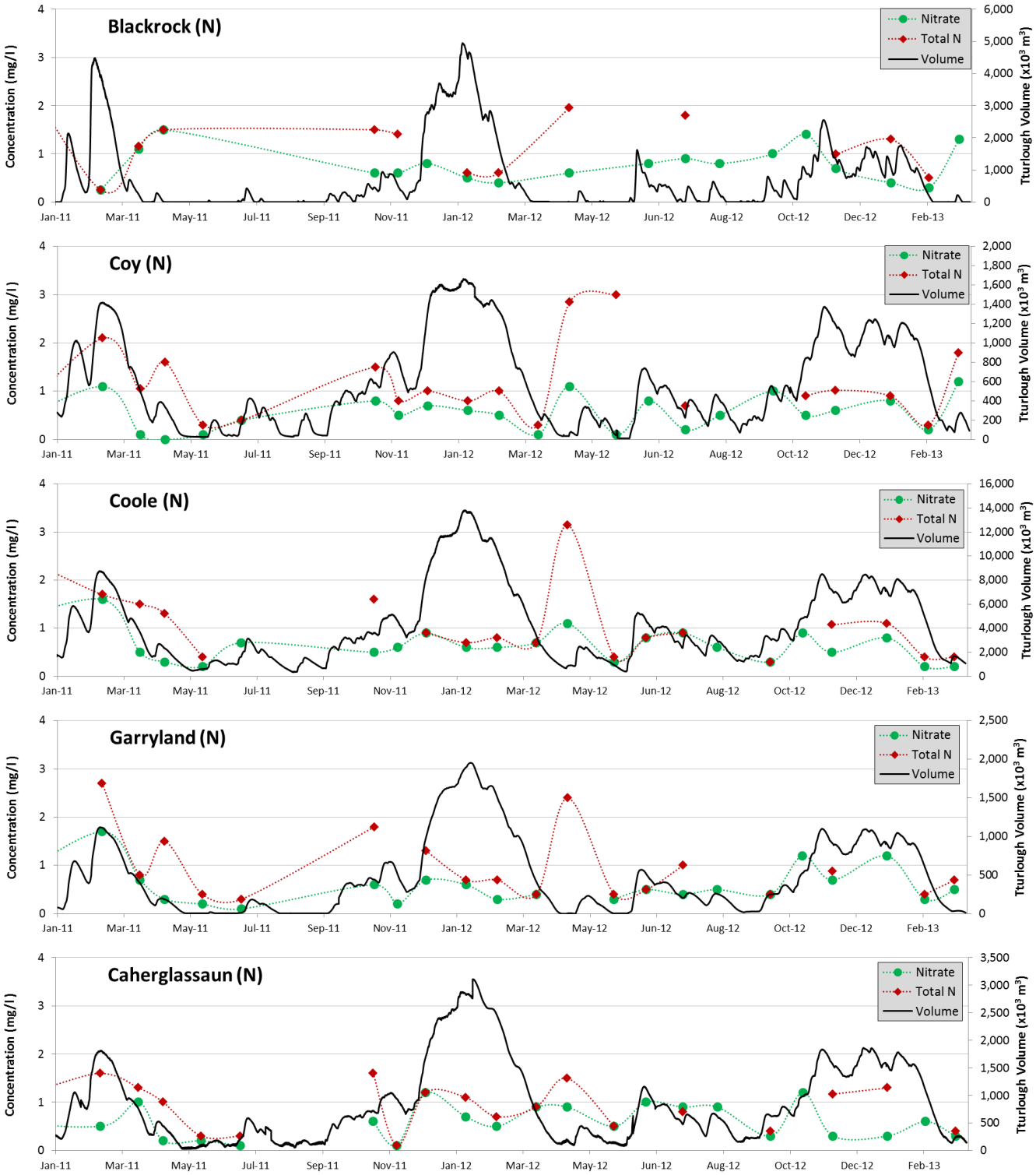

Figure 7.41: Time-series plots of Total Nitrogen (TN) and Nitrate (NO_3) concentrations for Blackrock, Coy, Coole. Garryland and Caherglassaun turloughs.

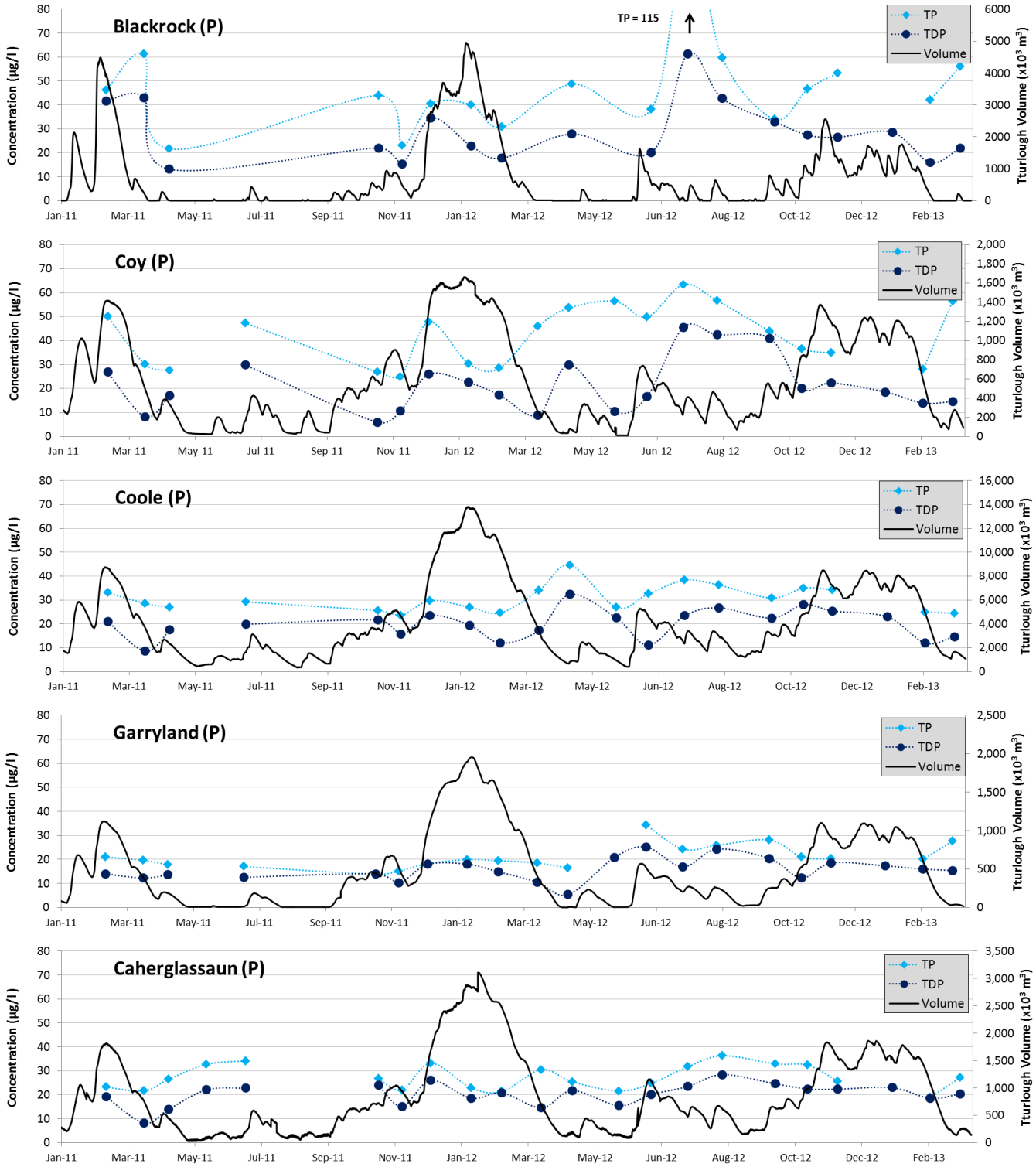

Figure 7.42: Time-series plots of Total Phosphorus (TP) and Total Dissolved Phosphorus (TDP) concentrations for Blackrock, Coy, Coole, Garryland and Caherglassaun turloughs.

7.3.1.2.2 Nutrient Loads

Nutrient loads in the turloughs can be calculated by combining the turlough volume data with the nutrient concentration data. Using this approach, some trends can be seen more clearly than with concentration data alone. When this approach is applied to the data of Cunha Pereira (2011) to the 22 turloughs under study for the 2006-2007 flooding season, a trend of decreasing N over the flooding season can be seen. The mass of N was seen peaking in early November when the turloughs had just filled, then could be seen steadily declining over the season even though the turlough water levels remained high. This behaviour is presented below in Figure 7.43 which shows the nutrient loading data of Ardkill turlough (from Cunha Pereira's dataset). This behaviour indicated some attenuation process and/or the dilution of the turloughs from the epikarst and was a key element in Cunha Pereira's conclusion that the turloughs were diffuse flow-through systems, i.e. nutrient concentrations were altering over time due to the constant through flow of water (rather than a surcharge tank system in which the nutrients should stay constant). However, under closer inspection of the Gort-Lowland network of turloughs, this flow through behaviour appears to be less prevalent (see Figure 7.44 for Caherglassaun N loads using Cunha Periera's dataset). P loads showed more erratic behaviour but this could be due to the un-representative sampling technique (as described in Section 7.1.1).

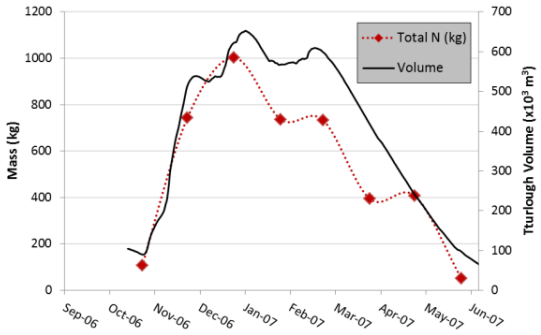

Figure 7.43 Nutrient Loading of Ardkill turlough 06-07 (data from Cunha Pereira (2011)).

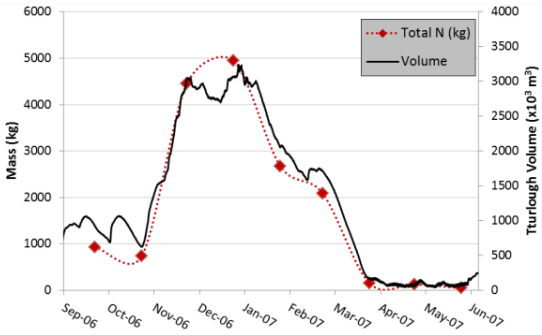

Figure 7.44: Nutrient Loading of Caherglassaun turlough 06-07 (data from Cunha Pereira (2011)).

Nutrient loads calculated using the 2010-2013 dataset from this thesis/study are shown in Figures 7.45 and 7.46. From these plots, a mixture of behaviours can be seen. The turloughs show evidence of surcharge tank behaviour but also some evidence of reducing nutrients over the flooding season. Also, P data appears to show some non-erratic behaviour with visible seasonal trends. The variability of nutrient loads within the turloughs is discussed further in Section 7.5.2.

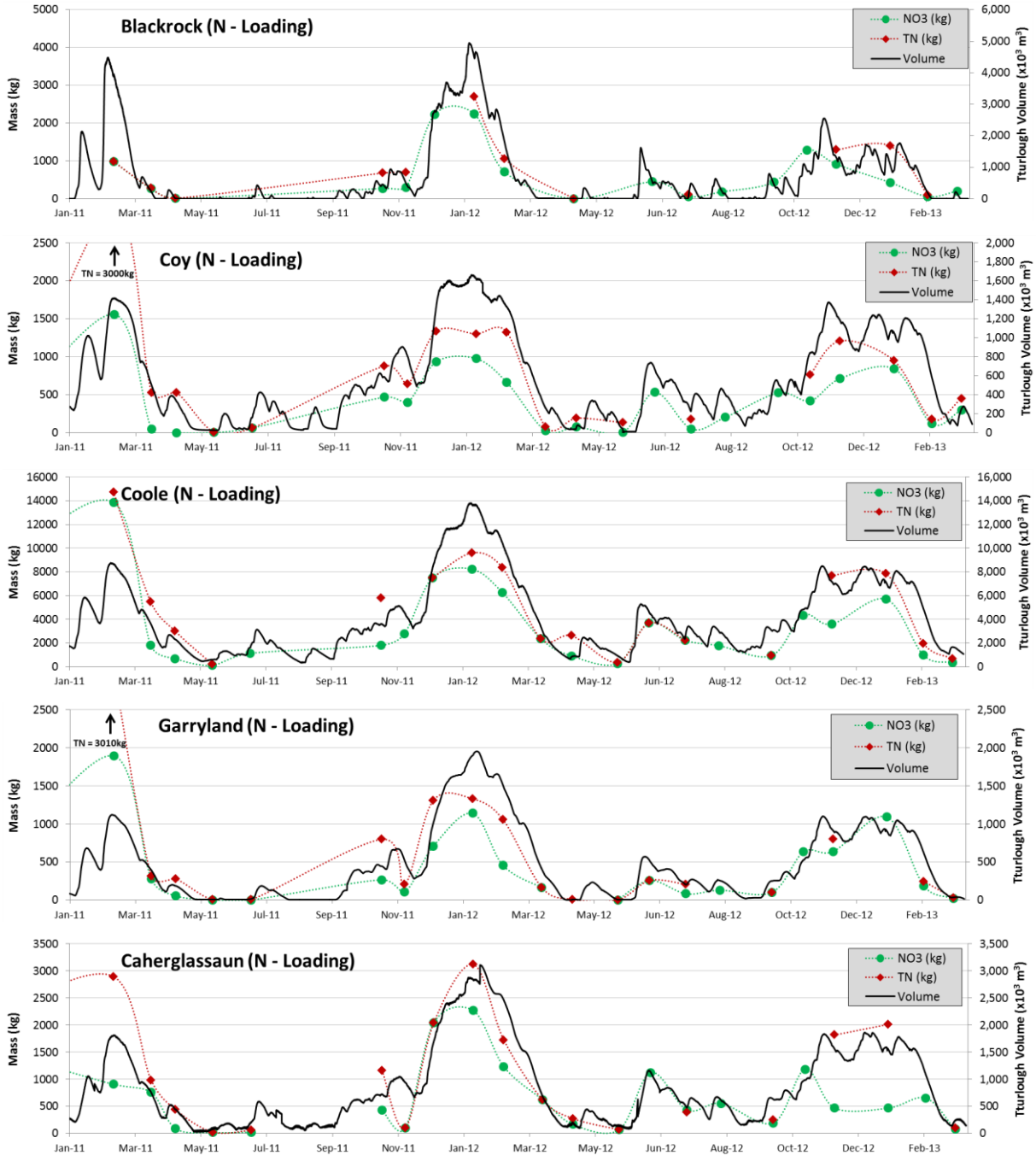

Figure 7.45: Time-series plots of Total Nitrogen (TN), Nitrate (NO_3) loads for Blackrock, Coy, Coole, Garryland and Caherglassaun turloughs.

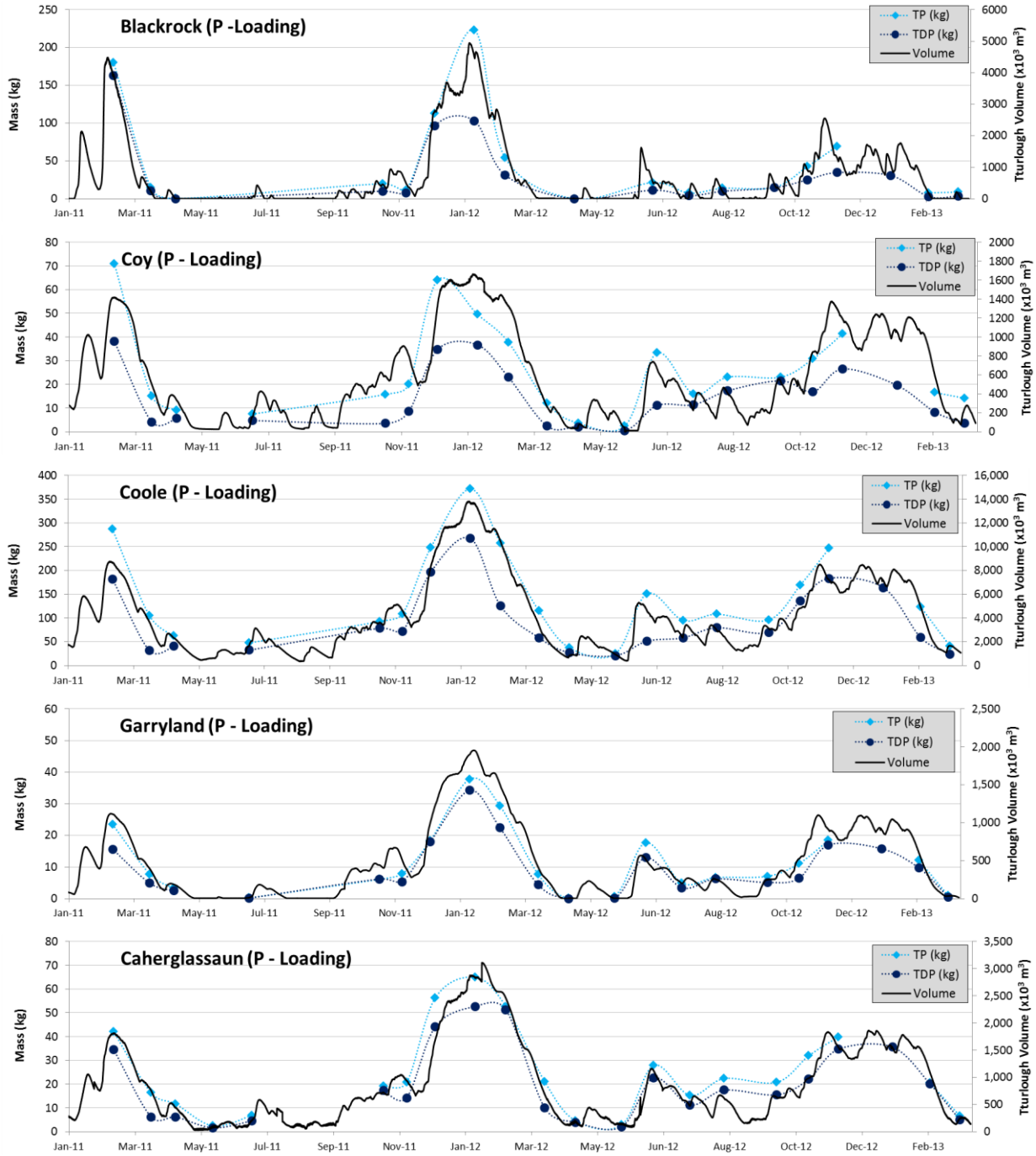

Figure 7.46: Time-series plots of Total Phosphorus (TP) and Total Dissolved Phosphorus (TDP) loads for Blackrock, Coy, Coole, Garryland and Caherglassaun turloughs.

Maximum nutrient loads recorded in the turloughs are presented in Table 7.10. From this table it can be seen that, predictably, Coole turlough records the highest nutrient loads with up to 14.7 tonnes of TN and 372 kg of TP calculated.

Table 7.10: Maximum nutrient loads recorded in the turloughs over the study period.

	TN (kg)	NO_3 (kg)	TP (kg)	TDP (kg)
Blackrock	3553	2525	233	163
Coy	2979	1560	71	38
Coole	14750	13883	372	268
Garryland	3011	1896	39	34.2
Caherglassaun	3121	2039	65	52.7

7.3.1.3 Groundwater

Time series plots of groundwater nutrient concentrations are shown in Figures 7.47 and 7.48. The plots show a wide range of groundwater nutrient behaviours across the catchment with no clear seasonal pattern. Mean concentrations across the catchment were recorded as 2.30 mg/l and 31.28 µg/l for TN and TP respectively (Table 7.6) Overall, groundwater showed mean N concentrations almost double those of surface water bodies while the overall mean P concentrations of the turloughs and groundwater were shown to be similar.

Upon closer inspection of the data, some seasonal changes are shown. In Table 7.11, mean groundwater concentrations are split into mean seasonal concentrations. From this table it can be seen that NO_3 concentrations are highest over the winter period as would be expected (although TN concentrations are highest during summer). In contrast, TP and TDP show roughly consistent concentrations for spring, summer and winter but show elevated concentrations during autumn.

Table 7.11: Mean Seasonal Groundwater Concentrations of TN, NO_3, TP and TDP.

	Spring	Summer	Autumn	Winter
TN (mg/l)	2.25	2.76	1.91	2.45
NO_3 (mg/l)	1.54	1.33	1.61	1.93
TP (µg/l)	30.73	28.40	41.06	33.08
TDP (µg/l)	16.53	17.31	32.14	19.48

Looking at the data in Table 7.6 and Figures 7.47 and 7.48, the different behaviour of N and P in groundwater becomes apparent. While N shows a wide range of recorded results (0.2-10.4 mg/l TN), the mean concentrations at each borehole across the catchment are within a similar range (between 1.2 and 3.3 mg/l). P on the other hand shows a greater range of measured results (0-582

µg/l TP) but more significantly, the mean concentrations at each borehole differ enormously (between 5.1 and 72 µg/l TP). This contrasting behaviour illustrates the differing mobility traits of N and P. N is shown to access the groundwater relatively easily and due to its mobility, it more or less equalises across the catchment. P on the other hand is much less mobile, only entering the groundwater in areas of extreme vulnerability (i.e. shallow and/or permeable subsoil protection). However, once P has entered the conduit system, it is known to be transported conservatively with negligible attenuation (Mellander et al., 2013, Kilroy and Coxon, 2005).

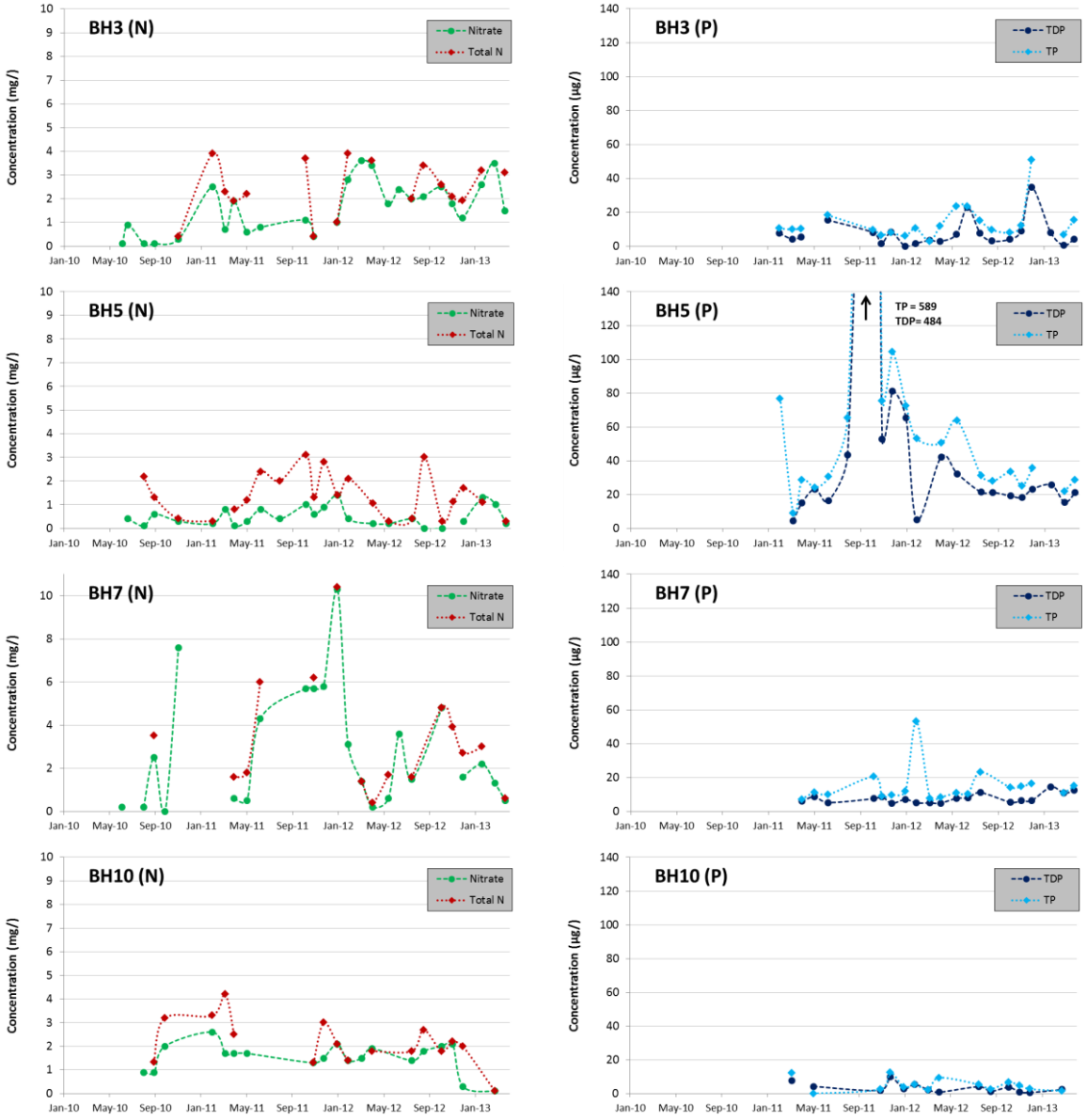

Figure 7.47: Time-series plots of Total Nitrogen (TN), Nitrate (NO_3), Total Phosphorus (TP) and Total Dissolved Phosphorus (TDP) results for BH3, BH5, BH7 and BH10.

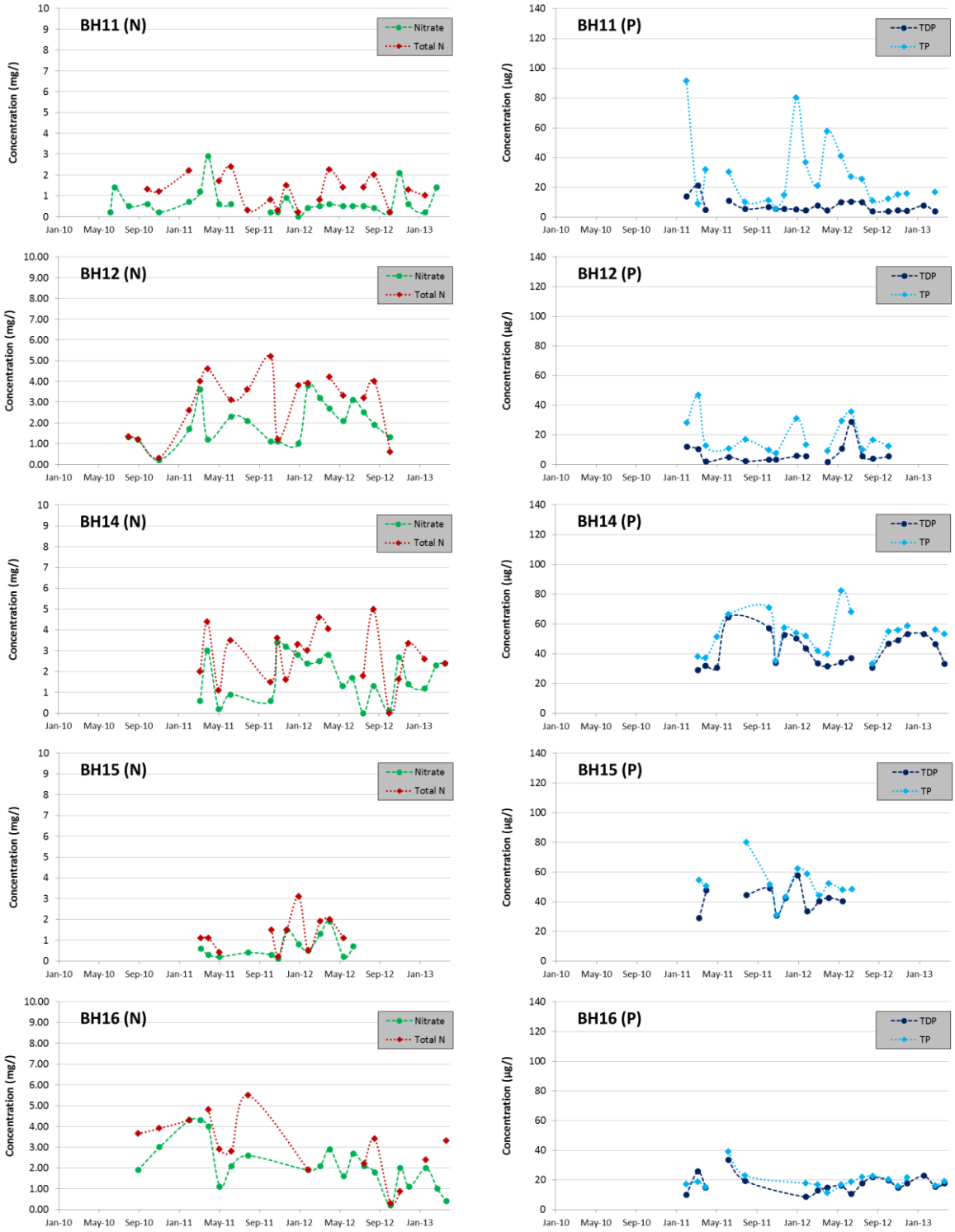

Figure 7.48: Time-series plots of Total Nitrogen (TN), Nitrate (NO_3), Total Phosphorus (TP) and Total Dissolved Phosphorus (TDP) results for BH11, BH12, BH14, BH15 and BH16.

The contrasting behaviour of N and P in groundwater is also evident when looking at the data for each borehole/well individually. Compared to the surface water systems which tend to show a relationship between mean N and mean P, the nutrient concentrations of individual borehole/wells have no such pattern. This behaviour could again be attributed to the poor mobility of P. Boreholes showing elevated concentrations of P but not N (e.g. BH5, Figure 7.47) indicate contamination from a low N:P ratio source (e.g. animal waste) reaching the groundwater in a highly vulnerable area. Boreholes with elevated N but not P on the other hand (e.g. BH7, Figure 7.47), indicate high levels of contamination but little penetration of P into the groundwater.

It should also be noted that any P that has made it into the diffuse/epikarst bedrock is likely affected by removal processes due to the formation on calcium-phosphate compounds (Cable et al., 2002).

7.3.1.4 Kinvara

Nutrient results for the springs at Kinvara are shown in Figure 7.49 (with modelled outflow added to the KW plots). Mean TN concentration for KW was measured as 1.05 mg/l while mean TN for KE was approximately double that of KW at 1.99 mg/l (similar to the findings of Smith and Cave (2012)). Little difference was observed for P between KW and KE with concentrations of 22.9 µg/l and 24.2 µg/l respectively (TP).

Mean concentrations of N at KW (1.05 mg/l TN) reflect the mean concentrations of the turloughs (1.12 mg/l TN) while the higher mean concentration of KE indicates the greater proportion of diffuse flow (with its higher TN) emerging at this spring. Concentrations of P at the springs are among the lowest mean concentrations found within the catchment suggesting the loss of P as water moves through the karst system. These mean concentrations are in accordance with the findings of Smith and Cave (2012) who suggest that Kinvara Bay is a source of N to the greater Galway Bay while it acts as a sink for P. The concentrations recorded at KW reflect the combined water from the Gort Lowlands and a contribution from external catchments. Thus the concentrations recorded at KW are not a perfect reflection of the Gort Lowlands system output. However, in Section 7.2.1.4 this additional contribution was estimated to be only 14-18%, thus the effect on nutrient concentrations should be minor.

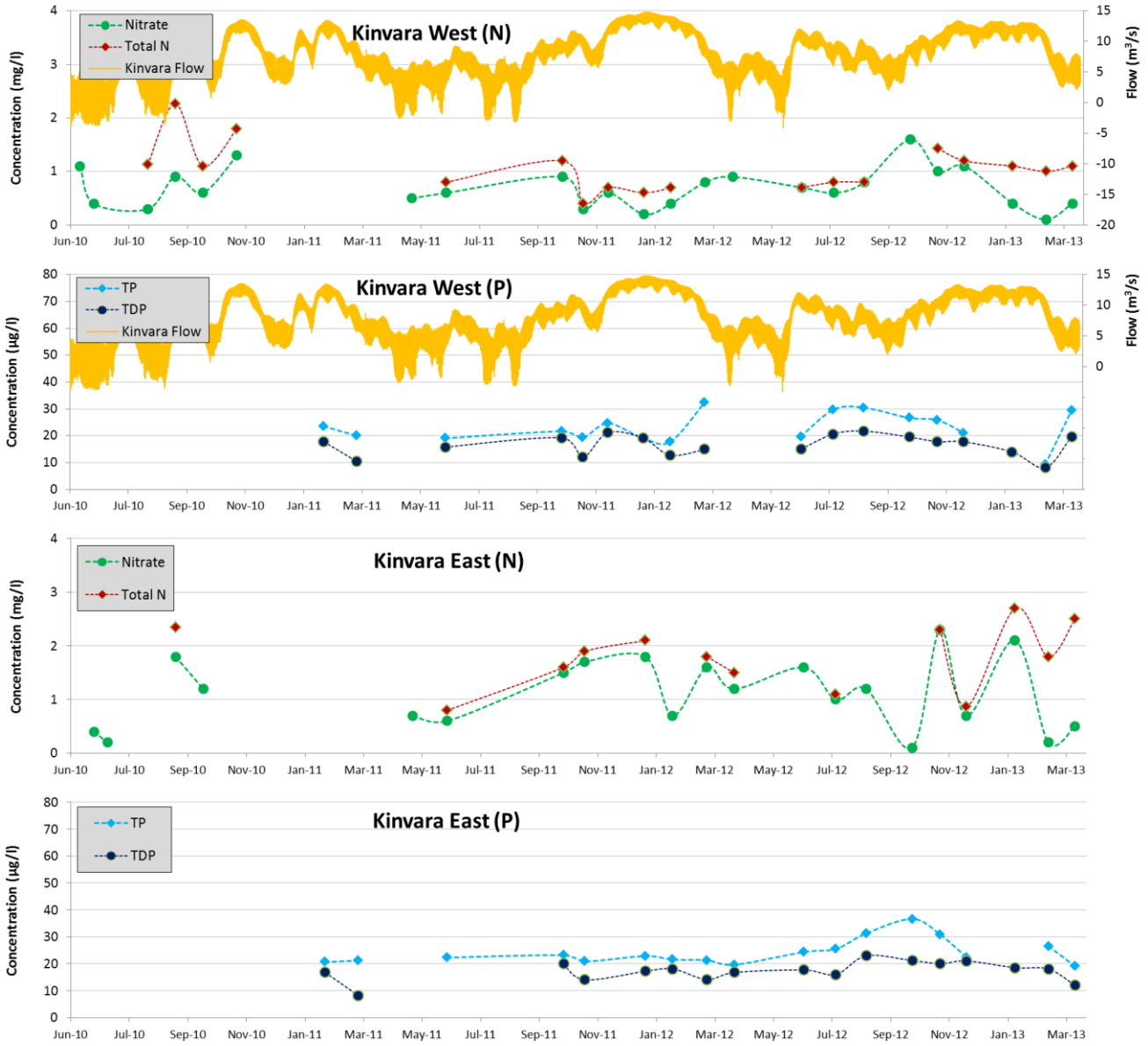

Figure 7.49: Time-series plots of Total Nitrogen (TN), Nitrate (NO_3), Total Phosphorus (TP) and Total Dissolved Phosphorus (TDP) results for KW and KE.

Similarly to the river data, nutrient loads leaving the Gort Lowlands system can be calculated by combining the outflow from KW (estimated using Infoworks model) with the appropriate nutrient concentration data. In order to calculate the loading correctly, mean daily flow from KW was determined so that the tidal affect was accounted for. The nutrient loads exiting the system along with the mean daily flow data from KW are shown in Figure 7.50. The average daily TN load was calculated as 690 kg/day with a measured range of 190-1922 kg/day. For TP, the average daily load was 15.15 kg/day with a measured range of 7.7-25.2 kg/day (a comparison between river input and KW output in the Gort Lowlands is discussed later in Section 7.5.1).

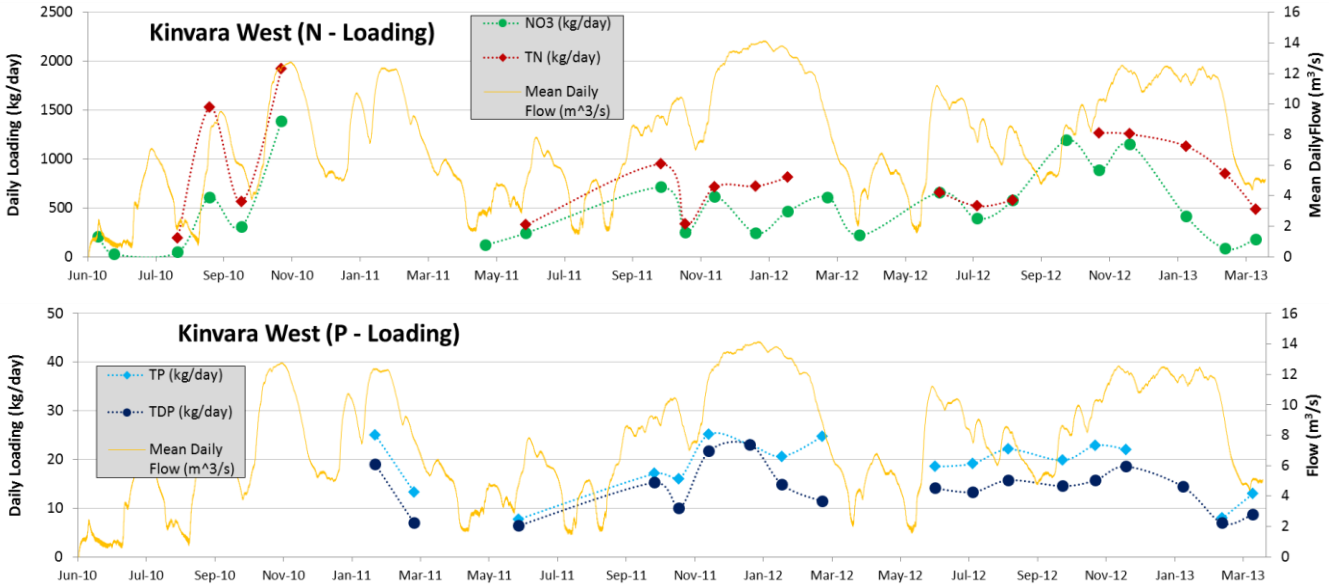

Figure 7.50: Daily Nutrient Loads exiting the system at KW (based on modelled outflow).

Using similar methodology, an approximation of the total flow leaving KW can be estimated, i.e. including the 14-18% external catchment water which was not accounted for by model. Thus to estimate the total KW nutrient load, the concentrations are multiplied by a factored flow. For the sake of this approximation, a factor of 1.16% is used (+16%). This results in an N output of approximately 800 kg/day and a P output of approximately 17.6 kg/day.

The approximation of nutrient loading into Kinvara can be expanded further with the inclusion of KE. Clearly however, the loading rate cannot be calculated in a straightforward manner as there is no flow data for KE. However, a rough approximation of flow can be made by taking the diffuse contribution at each timestep from the Infoworks model (i.e. outflow from the subcatchments) and dividing it by the total area of subcatchments. Thus a value of diffuse flow per unit area of karst is obtained. Considering that these model subcatchments are calibrated to the karst aquifer underlying the Gort Lowlands, their calibration should apply to the catchment feeding KE as much as it does KW (bedrock geology is the same for both catchments). Thus the 'diffuse flow per unit area' can be applied to the KE catchment in order to find a rough approximation of flow feeding KE which equates to 1.05 m^3/s (i.e. an increase of 10.6% on the total outflow from KW).

As part of the modelling component of the Gort Flood Studies Report, a catchment for KE was estimated as 8800 ha. Using this catchment size combined with the 'diffuse flow per unit area' and KE nutrient concentrations, loading rates from KE were calculated as 164 kg N/day and 2.2 kg

P/day. Thus the total nutrient load entering Kinvara Bay can be (roughly) approximated as 964 kg N/day and 19.8 kg P/day.

It should be noted that these values for N are considerably lower than those predicted by Cave and Henry (2011) who estimated average TON concentrations over winter 06/07 to be between 1660 and 26431 kg (depending on time period and choice of flow calculation limits). The cause of the disparity between Cave and Henry's results and the results of this thesis is due to the flow calculation. Cave and Henry estimated submarine groundwater discharge using the tidal prism method which calculated flow rates much greater than those predicted by the Infoworks model, i.e. their method estimated average flows (over winter 06-07) to be between 14 and 96 m^3/s whereas the average flow rate from KW (over the period 2010-2013) as estimated from this thesis is using the Infoworks model was 7.64 m^3/s (or 9.91 m^3/s when the contributions from other catchments and KE are included).

7.4 Nutrient Modelling

In this section, the Gort Lowlands pipe network model is used to investigate the transport of nutrients through the active conduit network and how the turloughs (storage ponds) react to nutrient influx. Two main studies were carried out. Firstly, a number of nutrient input scenarios were implemented so as to determine the differing nutrient retention behaviours of individual turloughs. Secondly, the proportion of nutrient loading originating from the diffuse/epikarst subcatchments as opposed to the active conduit system was investigated. The results of these simulations provide predictions of nutrient movement within the conduit network as conceptualised by the model, i.e. turloughs are a linked network of surcharge tanks rather than diffuse flow-through systems. The simulations were then compared to observed nutrient results in order to support the conceptualisation.

As discussed in Section 6.5, the Infoworks water quality model can only simulate conservative flow of pollutants/nutrients within the pipe-network. In many catchment types, this limitation would be a severe drawback to modelling. However, as mentioned is Section 7.3.1.3, nutrient transport through a highly karstified catchment such as the Gort Lowlands can be reasonably assumed to act conservatively (once the nutrients have entered the conduit system). In order to facilitate this conservative transport requirement, NO_3 and TDP were chosen to be modelled rather than TN and TP. These sub-components were chosen as they are more likely to follow conservative flow behaviour due to their absence of particulate matter. The conservative transport assumption essentially removes the differing mobility traits of the nutrients and thus the nutrients behave quite similarly. For this reason, simulation results tend to focus on one nutrient (P) rather than both nutrients as their behaviours will be identical. It should be noted that due to the inability of the Infoworks software to model nutrient transport through laterally-fed permeable pipes, the model needed to be recalibrated to allow for standard subcatchment-pipe links. Using the findings of the subcatchment parameters analysis (Section 6.3.4.3), standard links were added and the subcatchments were recalibrated so that their overall diffuse flow contribution was maintained over an annual cycle. Unfortunately, as a result of this recalibration, the rate of diffuse contribution was altered. This caused a minor knock on effect on some of the turlough flooding patterns.

7.4.1 Turlough Nutrient Retention.

In this section, a number of varying nutrient input scenarios shall be applied to the model in order to see the nutrient retention behaviour of each turlough for each input scenario. Due to the inability to model diffuse flow correctly, the nutrient contribution from diffuse/epikarst sources shall be

ignored for these simulations. As a result, the nutrient loads recorded within the turloughs were somewhat underestimated (for N more so than P). Results from these scenarios shall primarily be focussed on Blackrock and Coy turloughs as these two turloughs offer a prime example of river flow-through and surcharge tank behaviour. Also, these two turloughs are not influenced by external water sources nor are their inputs affected by attenuation processes, i.e. Lough Cutra's influence on the lower three turloughs. The input scenarios carried out are the following:

- **Scenario one**: Constant input (using mean observed nutrient concentrations).

- **Scenario two**: Modelling a contaminant plume at low water levels, based on the P plume recorded during July 2012 (Figure 7.40). As this scenario uses inputs which reflect the observed river behaviours, it offers an opportunity to compare observed and modelled output concentrations directly.

- **Scenario three**: Modelling a contaminant plume at high water levels.

- **Scenario four**: Modelling a contaminant plume at the onset of flooding.

7.4.1.1 Scenario One: Constant Input

In this scenario, the nutrient inputs were set as constant values based on the mean measured concentrations at the relevant river sites. So the inputs were 16.1, 23.61 and 20.0 µg/l for the Owenshree, Ballycahalan and Beagh Rivers respectively. Constant nutrient loading rates such as these are obviously unrealistic inputs and provide poor results in terms of nutrient variation but the overall nutrient loads reaching the turloughs should be reasonable. The results from these simulations can also be used as 'blanks' for future scenarios involving contamination plumes. See Figure 7.51 for the results of this simulation for TDP over the 2011-2012 flooding season (plots of the 2012-2013 flooding season can be seen in Appendix G). Modelled and observed data for all five turloughs is shown as well as KW (note: outflow from KW is presented as daily average values).

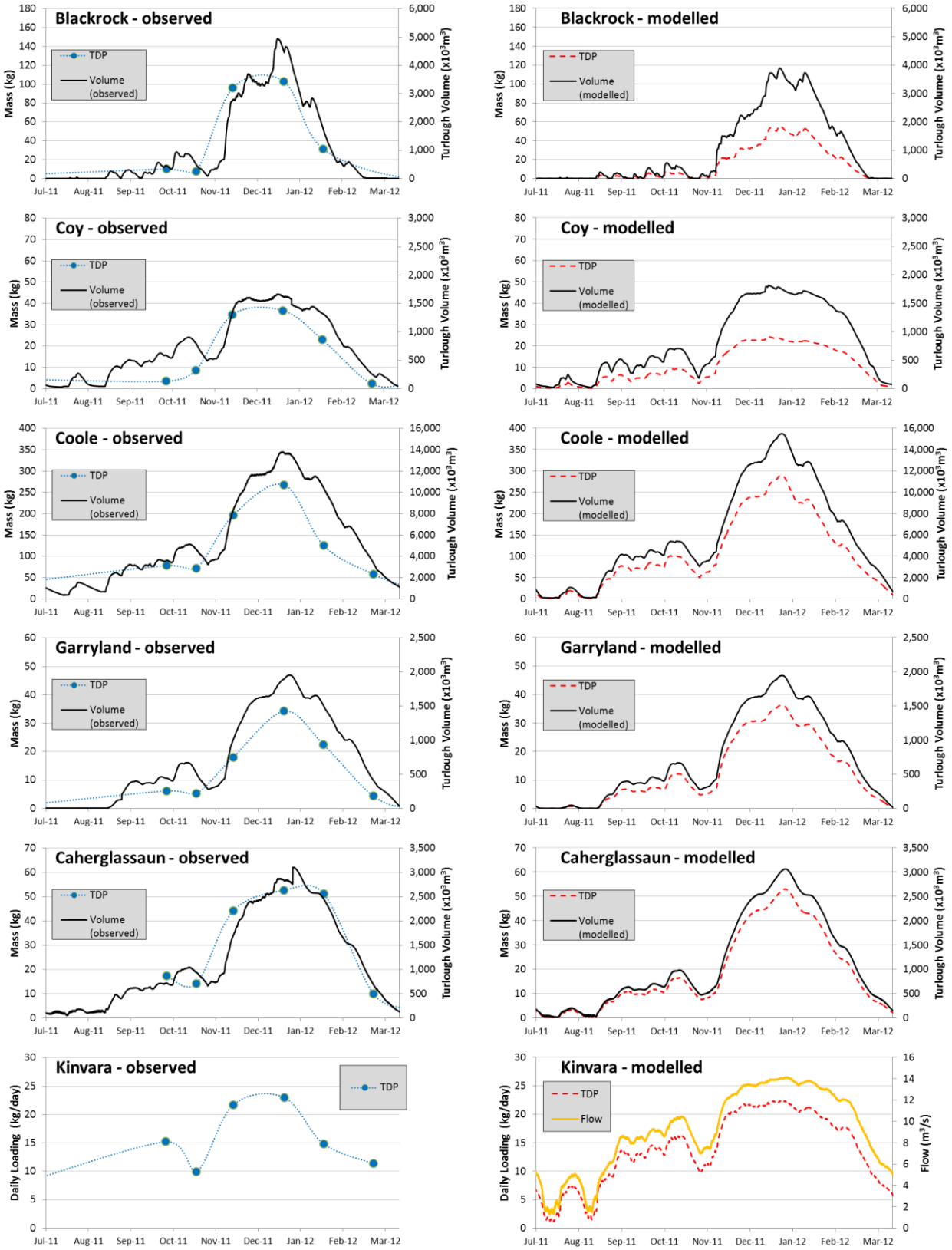

Figure 7.51: Observed and modelled results for P loading from scenario 1 (constant nutrient inputs).

From Figure 7.51 it can be seen that Blackrock and Coy turloughs are modelled quite poorly. Modelled nutrient loads fall considerably shorter than the quantities observed in the field. This lines up with the findings of Section 7.3.1.2 which suggest Blackrock (and indirectly Coy) act as sources of nutrients to the system (and that the river sampling suffered from poor temporal resolution, possibly resulting in underestimated mean concentrations). Results for the lower three turloughs prove to be more accurate, possibly as a result of the influx of low-nutrient external water from Cloonteen which would offset the model's diffuse-underestimation error. The modelled P load in Caherglassaun is underestimated. Again, this is likely due to the diffuse-underestimation error (which would affect Caherglassaun worst as it lies at the end of the turlough network). Results from Kinvara line up well with observed results which indicates that the diffuse-underestimation error is again offset by the influx of external water or the removal of P due to chemical processes (Cable et al., 2002).

7.4.1.2 Scenario Two: Modelling P Plume of July 2012 (Low water Level Period).

For this scenario, the real contamination event that occurred in July 2012 shall be modelled. This scenario serves two purposes. Firstly, it provides a comparison between observed and modelled concentration outputs. This comparison can be used to draw conclusions about whether the nutrients behave conservatively (as the model requires) or are affected no non-conservative effects such as transformations or losses. Secondly, the scenario shows the effect of a contamination event across the turloughs during a relatively low water level period.

The inputs for this scenario were designed based on the river hydrochemistry data taken during July 2012. Concentrations of P peaked in the three rivers suggesting some contamination, possibly from a phosphate-heavy forestry fertiliser. These peaks were applied to mean concentration dataset used for scenario one. For the Beagh input, the peak P pattern from the Owendalulleegh River was transferred through the reservoir routing model (Section 6.4.3.1) to account for the attenuation effect of Lough Cutra. The inputs can be seen below in Figure 7.52.

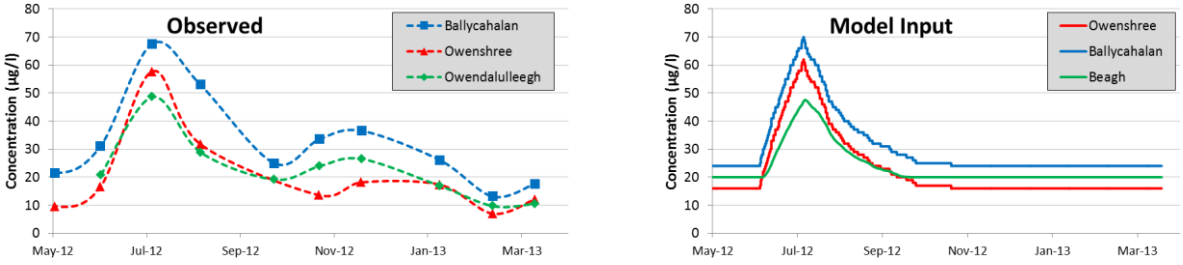

Figure 7.52: Observed and modelled P concentrations in the Owenshree, Ballycahalan and Owendalulleegh/Beagh Rivers (scenario 2).

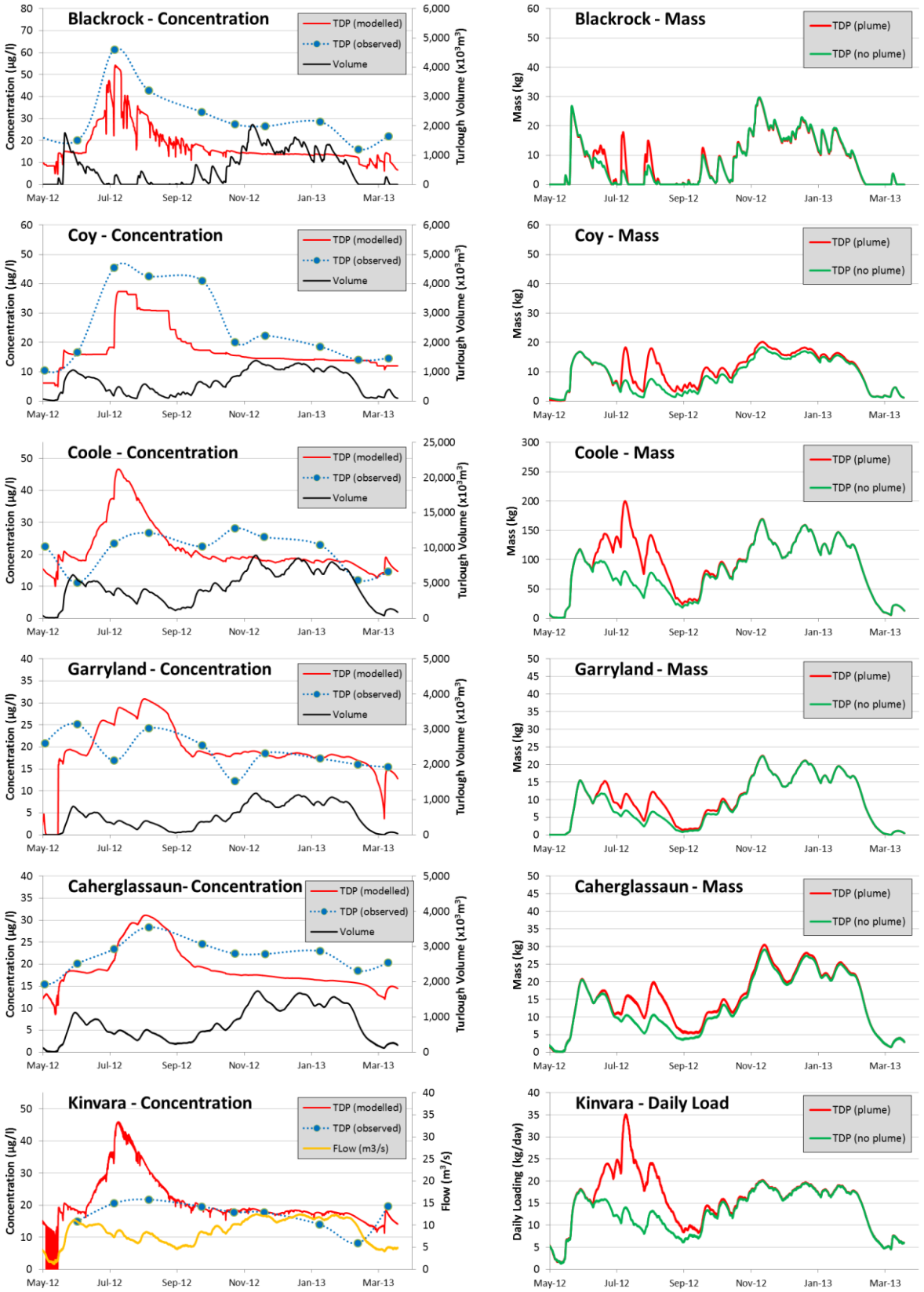

Figure 7.53: Model results for P loading from scenario 2 (modelling the P plume of July 2012)

Results of this simulation are shown in Figure 7.53. In this Figure, plots on the left show the observed (blue) and modelled (red) P concentrations, the turloughs volume (Black) and modelled outflow at Kinvara (Orange). Plots on the right show P-load from this scenario (red), and the P-load from scenario 1, i.e. the 'blank' (green).

Looking at Figure 7.53, results from Blackrock and Coy turloughs show underestimated concentrations of P (as expected) but their temporal patterns appear reasonably well modelled. Blackrock turlough experiences a peak in concentration quickly followed by a recession (with many sub-peaks and recessions due to the turlough emptying). Coy turlough shows a sharp (almost immediate) increase in concentration representing the influx of river water. This concentration then remains constant until the turlough is fed by more water, at which point the concentration drops. In terms of P-load, both turloughs show short-lived increases in load but these loads are quickly lost (especially for Blackrock) due to the turloughs draining. The contrast between modelled and observed results indicates that Blackrock and Coy are both subject to nutrient enhancement through non-conservative factors. Such factors could include N and P gain via the abattoir near Blackrock, P gain from grazing or N gain from diffuse input.

Coole turlough shows a similar modelled concentration pattern as Blackrock. This would be expected as both turloughs are primarily river fed. The turlough is receiving increased P-loads from all three rivers and as a result, the increase in nutrient load is considerable. However, again, the additional P-load only remains within the turlough until it drains halfway through the season. Garryland and Caherglassaun turloughs show similar but more muted P-loading to Coole. All three lower turloughs show modelled P concentrations exceeding observed concentrations. This indicates some nutrient loss mechanisms affecting these turloughs that were not accounted for by the model (nutrient loss mechanisms are discussed later in Section 7.5.2). At Kinvara, the modelled concentration peak and its associated increase in P-loading are plainly evident. The observed P concentrations are lower due to the nutrient loss processes in the turloughs but also a number of additional factors such as influx of separate catchment water and possible dilution in the large cave system known to exist behind Kinvara. The P-load (in kg/day) exiting the system at Kinvara is noticeably greater than Garryland and Caherglassaun turloughs for this simulation. This indicates that a significant proportion of the P-plume in the model bypassed under these turloughs and travelled directly towards Kinvara.

7.4.1.3 Scenario Three: P-Plume Occurs During a High Water-Level Period.

In this simulation, the P-plume is altered so that it occurs later in the flooding season (peaking in December). The purpose of this scenario is to observe the change in nutrient loading when the plume occurs during a high water-level period rather than a relatively low water-level period as seen in the previous scenario. As the river flow during this contamination period is higher, the concentration of the P-plume was reduced so as to keep the contaminant mass consistent. The inputted time series data is shown below in Figure 7.54. Simulation results are presented in Figure 7.55.

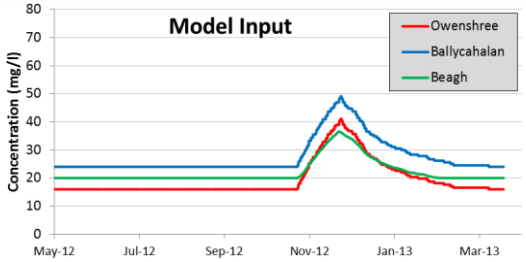

Figure 7.54: Modelled P concentration in the Owenshree, Ballycahalan and Beagh Rivers (scenario 3)

In this simulation, the most significant factor affecting the nutrient loadings of the upper two turloughs is the fact that Blackrock is flooded. This means Blackrock effectively acts as a damper to the system, slowing down the release of the Owenshree River P-plume. While the volume of water in Blackrock remains fairly consistent, the concentration of P can be seen changing over time (a peak followed by a recession). This implies that Blackrock is acting as a river flow-through system. The P-load can also be seen to follow this pattern. At the beginning of the flooded period, the P-load is almost double its corresponding 'blank' value while by the end of the period the majority of the P-plume has left the turlough. The behaviour of Coy, on the other hand, is strikingly different. P concentrations in Coy show no evidence of a sudden influx of P-enriched river water. Instead a gradual rise in concentration can be seen occurring across the entire flooding season until the turlough empties. This pattern of Blackrock concentration receding while Coy increases is similar to the findings of the physical model tracer studies (Section 6.2.6) which implied that the 'lower' turlough tracer (or nutrient) concentrations were being enhanced by water discharging from the 'upper' turlough. So overall, Coy turlough acts as a surcharge tank rather than flow-through system, i.e. once water enters the turlough, it remains there until drainage. However, it does appear to receive some input from Blackrock which alters its nutrient concentration and mass over time.

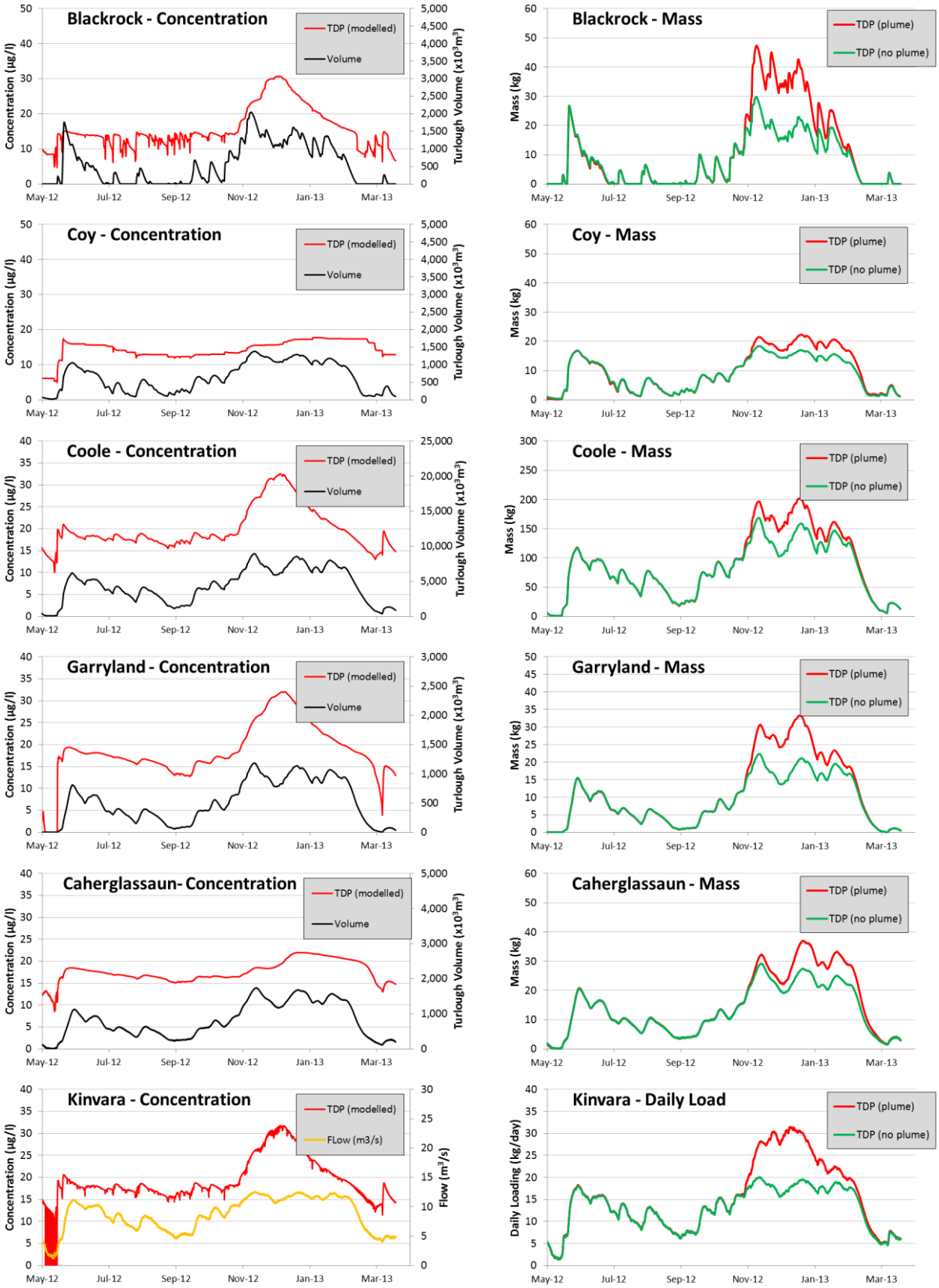

Figure 7.55: Model results for P loading scenario 3 (P-Plume occurs during a high water-level period)

Again, the concentration in Coole follows the same pattern as Blackrock - a peak followed by a recession. The behaviour of Garryland however has changed. In this scenario, the concentration of Garryland more closely reflects that of Coole. This is due to the hydraulic link between the turloughs which occurs when Garryland reaches a depth of approximately 7 - 8m of water (Section 5.2). Finally, the behaviour of Caherglassaun has altered similar to that of Coy, which matches the conceptual model of these two turloughs as slightly off-line surcharged tanks. The turlough now shows a gradual increase in concentration over the flooded period rather than a peak and recession.

7.4.1.4 Scenario 4: P Plume occurs at onset of flooding (Owenshree River)

The purpose of this scenario is to contrast the reaction of a flow-through system and a surcharge tank system to a P-plume which occurs at the onset of a large flooding event. As such, this scenario shall be focussed on Blackrock and Coy turloughs with the P-plume only occurring in in the Owenshree River. The main flooding event of the 2011-2012 flooding season was chosen for this simulation and the inputted P concentrations are shown below in Figure 7.56 (altered to keep mass consistent with other scenarios).

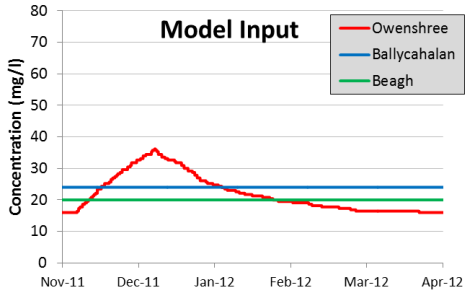

Figure 7.56: Model P concentration in the Owenshree, Ballycahalan and Beagh Rivers (scenario 4).

Results for Blackrock, Coy and Coole turloughs are shown in Figure 7.57 (For results of other turloughs, see Appendix G). In this figure, an extra plot is shown for each turlough (middle column). These plots show a comparison between P-load and turlough volume (similar to Figures 7.43 and 7.44).

Again, the concentration of Blackrock shows a peak-recession trend pattern. As a result, the P-load peaks before the water volume does and starts to recede earlier as well (middle column plot). For Coy turlough, the concentration can be seen to rise at the start of the flooding season, followed by a minor (and slow) drop in level until a constant concentration is reached. The slight reduction in

concentration is due to the presence of an overspill drainage link at 10m depth, i.e. as purer water surges into Coy via the estavelle, a proportion of water is draining out of the top of the turlough (but only at depths greater than 10 m). Coole can be seen to follow similar behaviour to Blackrock (as expected). However the effect on concentration and P-load has been significantly attenuated due to the upper two turloughs.

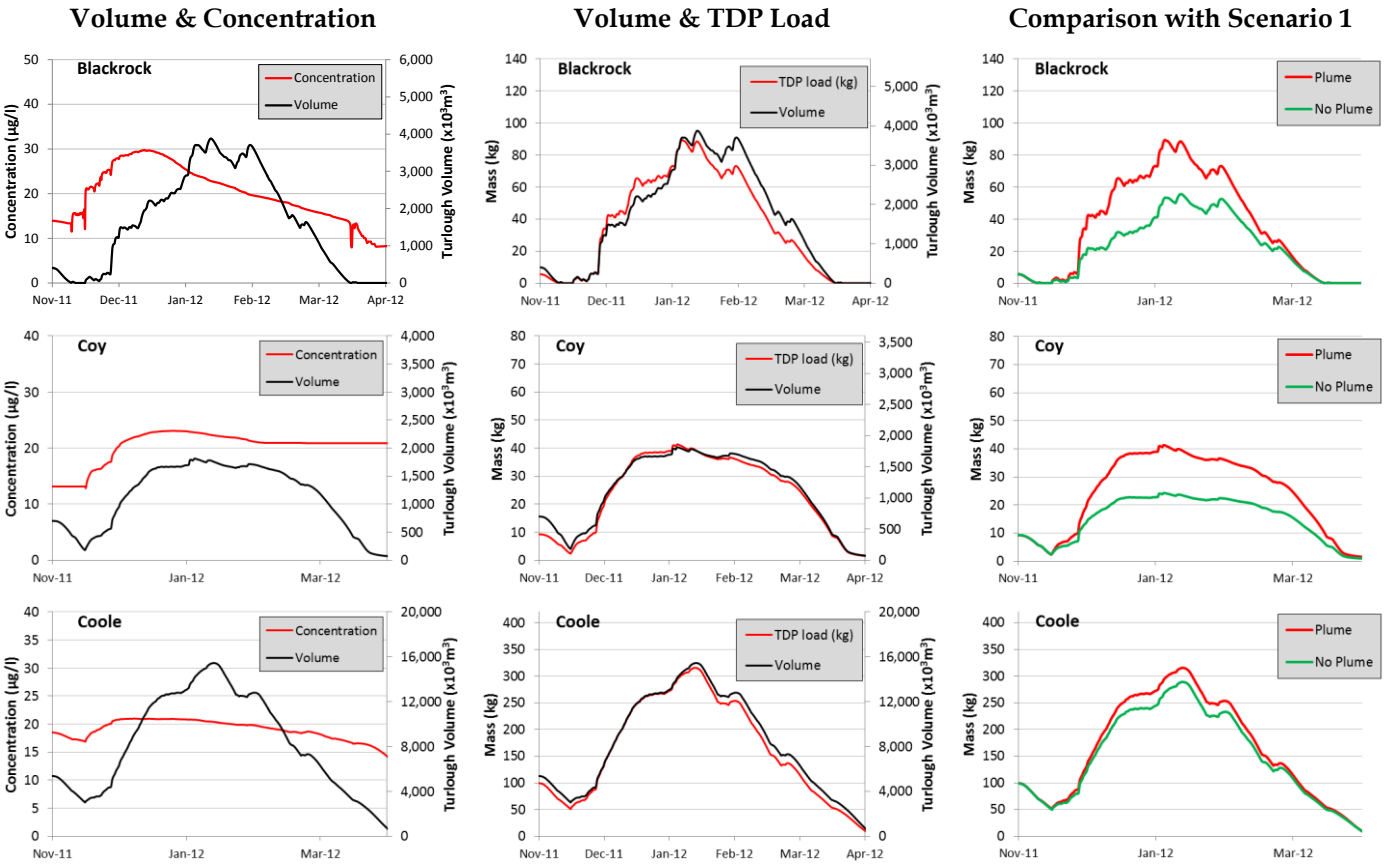

Figure 7.57: Model results from Scenario 4 (P plume occurs at onset of flooding).

Another simulation was also carried out whereby the P-plume occurred in the Beagh River (unlikely in reality due to attenuation from Lough Cutra). In this simulation, the turloughs behaved in a similar fashion, i.e. the river flow-through system (Coole) showed a peak-recession pattern while the surcharge tank system (Caherglassaun) showed an increase followed by a constant elevated P concentration. Results from this simulation can be seen in Appendix G).

7.4.2 Diffuse Contribution.

In this section, the contribution of diffuse flow (and its associated nutrient load) into the turloughs is investigated. As the water quality model was incapable of modelling diffuse flow, nutrient loading from the different sources was manually calculated. This involved combining the modelled diffuse flow from each subcatchment with the measured mean groundwater nutrient concentrations. Groundwater concentrations were then multiplied by subcatchment outflow at each timestep to provide a loading rate in kg/hour. Seasonal trends were applied to river and groundwater input concentrations using the mean seasonal concentrations as calculated previously (Table 7.7 and Table 7.11). For a particular turlough, its diffuse contribution was calculated by comparing the flow (and nutrient content) of its main feeding conduit with the contribution from all subcatchments upstream of that turlough.

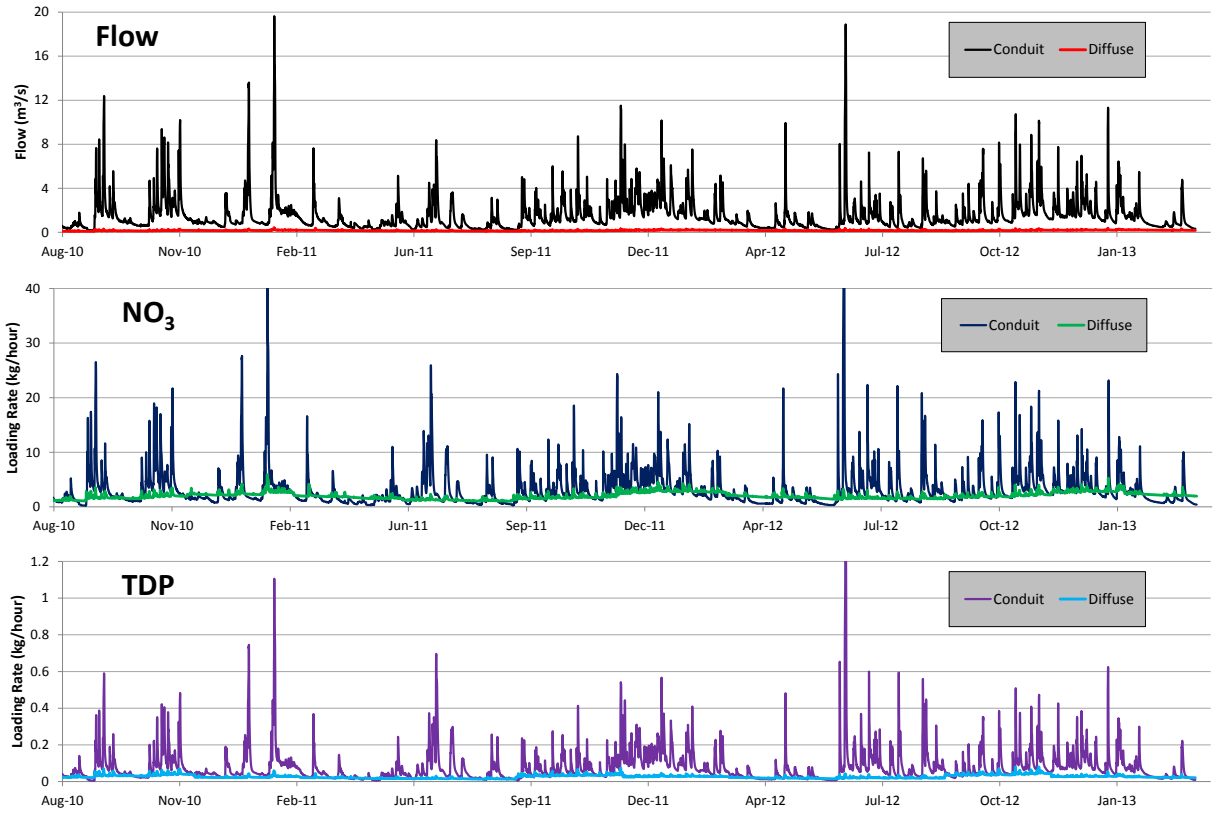

Figure 7.58: Blackrock turlough diffuse-conduit contribution comparison for Flow, NO_3 and TDP (August 2010 – March 2013).

See Figure 7.58 for results from the conduit feeding Blackrock turlough (August 2010 – March 2013). Plots of flow, NO_3 and TDP concentrations are presented. Over the analysis period, diffuse flow contribution amounted to 10% (of total flow) whereas NO_3 and TDP load contributions were

calculated as 38% and 24% respectively. It should be noted however that the TPD contribution is an estimate based on mean catchment TDP concentrations. In reality, groundwater TDP concentration across the catchment are so erratic that applying the mean catchment TDP concentration to a particular catchment sub-section is an imprecise methodology.

Results for the conduit feeding Coole are shown below in Figure 7.59. For Coole, diffuse contribution for flow, NO_3 and TDP amounted to 11%, 39% and 22% respectively. These plots indicate the diffuse contribution from the main conduit feeding Coole and do not account for any contribution of external catchment water. Plots of diffuse contribution for turloughs downstream of Coole are not presented as the models exclusion of external water hinders its accuracy.

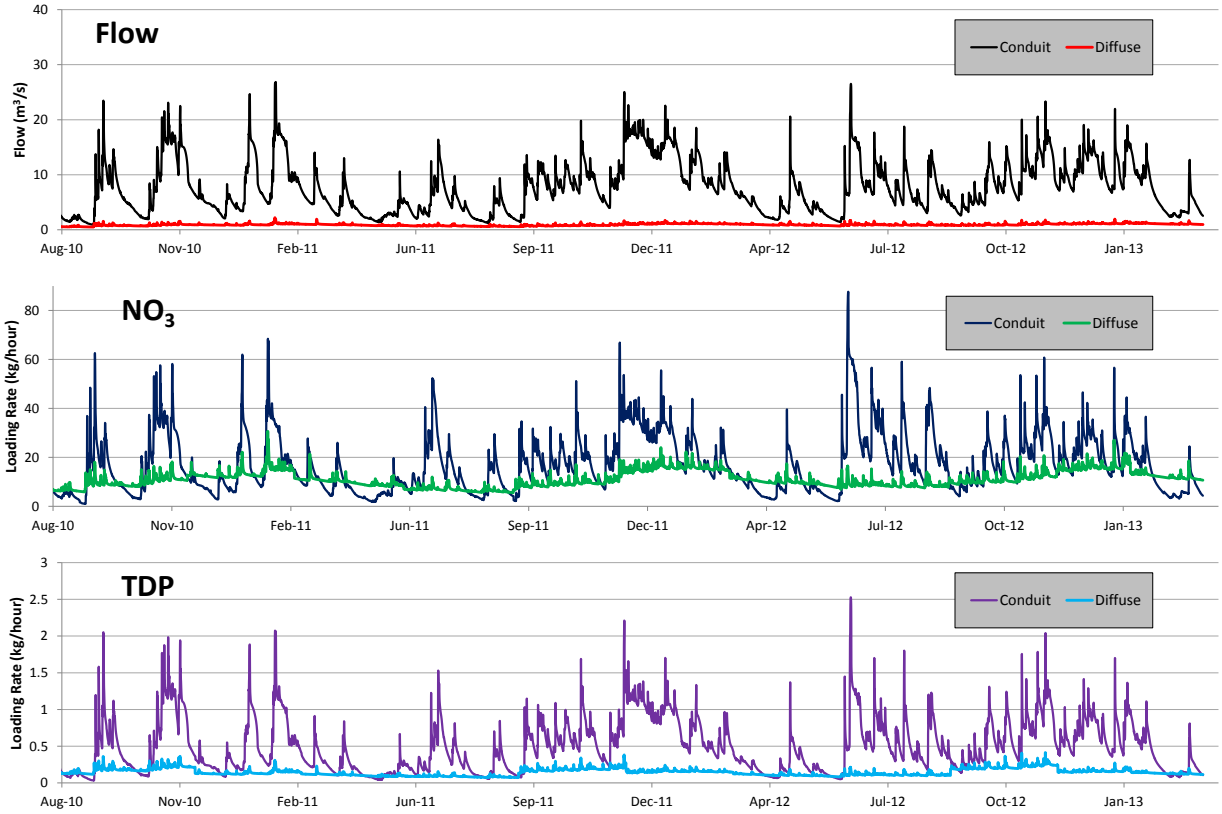

Figure 7.59: Coole turlough diffuse-conduit contribution comparison for Flow, NO3 and TDP (August 2010 – March 2013).

7.4.3 Water Quality Modelling - Discussion

Overall, water quality modelling proved a useful tool for the understanding and quantification of nutrient transport/retention within the conceptual model of the Gort Lowlands (assuming conservative nutrient transport).

The nature of each turlough (flow-through or surcharge tank) has been determined. Blackrock and Coole operate as river flow-through systems. Although it should be noted that these turloughs do experience a considerable degree of surcharge tank behaviour during flooded periods which slows down their flow-through nature. In comparison, many of the turloughs studied by Cunha Pereira (2011) display much clearer flow-through behaviour (faster peak and recession patterns) such as the northern Galway/Roscommon turloughs, Coolcam and Ardkill (Figure 7.43). However, this comparison is flawed as the flow-through nature of these turloughs (epikarst diffuse-fed) is hydrologically unrelated to those of the Gort Lowlands (river-fed).

Both Coy and Caherglassaun turloughs displayed similar behaviour, seemingly both acting as surcharge tank systems. This echoes the findings of Gill et al. (2013b) who, through the use of Fast Fourier transform time-series analysis, found identical periods and similar recession patterns for these two turloughs. Garryland turlough appears to operate as both systems, acting as a surcharge tank at low levels and a flow-through system at high levels (above 7-8 m).

In terms of different flooding/contamination scenarios, the flow-through turloughs showed similar contaminant patterns for all scenarios – a peak recession pattern with a considerable increase in nutrient load. Thus the effect caused by contamination could be deemed of relatively low sensitivity to water level in these turloughs. The water level in these flow-through systems does however have a large effect on the turloughs further downstream. At low water levels, these turloughs offer little storage and the contaminant quickly moves downstream and enters other turloughs. At high water levels, the contaminant is stored in the turlough and slowly released resulting in less loading of the downstream turloughs.

The surcharge tank systems, on the other hand, display varied behaviour depending on the flooding situation. At low water levels, the turloughs can be contaminated (due to poor storage in preceding turloughs) but the contamination is able to drain away. At high water levels, a contamination plume is unable to enter the turlough as easily and mostly passes underneath it. However, some slight enrichment can be seen over time, likely due to contamination draining out of an upstream system. At the onset of a large flooding event, the contaminant will easily enter the

turlough at a low water level but will remain in the turlough for the entirety of the flooded period (as no drainage is occurring at high water levels). While these flow-through/surcharge tank effects are a reasonable reflection of the hydrological set-up of the turloughs, the disparity between observed and modelled turlough concentrations indicate that some non-conservative nutrient mechanisms are at work. These nutrient losses/gains/transformations are discussed further in Section 7.5.2.

Results from the diffuse contribution analysis suggest a high degree of NO_3 contribution (just under 40%) from non-conduit/river sources and a moderate contribution of TDP (20-25%). These contributions explain to a certain extent the general underestimation of turlough nutrient loads in the previous turlough nutrient retention scenarios. If diffuse flow had been included in that analysis, the modelled results would likely have shown a degree of attenuation (increasing with proximity to the catchment end point at Kinvara).

For any future water quality modelling of this catchment, a number of recommendations can be made to improve accuracy. These are the following:

- As with all models, the quality of output depends on the quality of the input. For future studies, river hydrochemistry should be monitored with higher temporal accuracy (e.g. daily/weekly). Also, a sampling site should be set up on the Beagh River (rather than using data from the Owendalulleegh River).

- The contribution of water from the southern Cloonteen catchment should be quantified. This would provide details on the extent of dilution caused by the external water source.

- Further improvements to the accuracy of the hydraulic model would lead to even greater accuracy for water quality modelling as some features which are hydraulically non-significant can be very significant for water quality modelling (such as mixing inside the turloughs).

7.5 Discussion

In this section, the findings of Sections 7.2, 7.3, and 7.4 are discussed in terms of catchment-wide behaviour and individual turlough behaviour.

7.5.1 Hydrochemical behaviour across the catchment

Samples were collected over the entire length of the catchment, from the peaks of the Slieve Aughty Mountains to the final outfall at Kinvara. The results of these samples (particularly the overall mean values) enable the characterisation of the hydrological and hydrochemical characteristics of the water as it moves through the catchment.

The majority of water feeding the karst network originates from precipitation falling on the Slieve Aughty Mountains. As this water runs off the mountains via the three main rivers down towards the lowlands, it starts to pick up alkalinity through dissolution but experiences very little nutrient enhancement above that of the original rainfall. This lack of nutrient enhancement indicates only minor input from agricultural/forestry practices in the Slieve Aughty Mountains. However some enhancement of P is seen in the Ballycahalan River.

In the lowlands, the groundwater of the non-active diffuse portions of the limestone bedrock inevitably shows high levels of alkalinity with an average concentration of 365.1 mg/l $CaCO_3$. The primary land use in these lowlands is agriculture and as such, there are significant additional sources of N and P. The effect of these sources can be seen by the N concentration of groundwater which has a mean value (2.3 mg/l) of double that found in the active conduit/turlough network (1.12 mg/l). N is also well distributed across the catchment due to the high mobility and solubility of NO_3. Similar to N, the sources of P are widespread. However the ability of P to reach the groundwater is highly variable due to its poor mobility. As a result, concentrations of P in groundwater are highly erratic across the catchment. Water quality modelling estimated that the diffuse contribution of nutrient loads in the turloughs is approximately 40% for N and 20-25% for P.

In the conduit/turlough network, water enters at the top of the system in Blackrock turlough. The alkalinity of the turlough matches that of its feeding river but the measured nutrient concentrations in the turlough exceed those measured in the river, particularly P. This suggests an internal source of nutrients such as from grazing or the nearby abattoir. Otherwise, the imbalance could be due to the poor temporal resolution of the river data. However overall, the elevated concentrations in Blackrock turlough suggest it is a source of nutrients to the karst system. As the water moves through the conduit network from Blackrock through Coole towards Kinvara, the nutrients are transported conservatively with N retaining its concentration throughout while concentrations of P seem to drop en-route.

At Coole, the alkalinity and nutrient concentrations of the water reflect that of the combined flow from the three main rivers (with alkalinity suggesting some contribution from diffuse sources). Although Garryland turlough lies beside Coole and is known to be hydrologically connected (particularly at high water levels), it shows evidence of influx from the southern Cloonteen catchment. The influx of this high alkalinity (alk), low nutrient water from the south results in Garryland having the lowest nutrient concentrations of the five turloughs. From this point on, the hydrochemistry of the karst system becomes more complex due to the combined contributions of Cloonteen water (high alk, low N, low P) and diffuse input (high alk, high N, low P). So between the Coole-Garryland complex and Kinvara, N and P behave differently. The reduction in N from the Cloonteen water is essentially cancelled out by contribution of high N diffuse water and so the water at Kinvara is relatively unchanged (1.10 mg/l at Coole, 1.05 mg/l at KW). P, on the other hand, experiences a reduction due to dilution from the low P Cloonteen water and the low P diffuse recharge. Due to this dilution, mean P concentration drops from 30.6 µg/l to 22.9 µg/l between Coole and KW.

An alternative method of looking at nutrient dynamics throughout the catchment is to consider the changes between input (river) and output (KW) nutrient loads. The mean daily TN load entering the system through the rivers is approximately 590 kg. This value was calculated similar to the values in Table 7.8. However, instead of using the Owendalulleegh loading rate, a loading rate for Beagh River is estimated based on combining Beagh River flow with Owendalulleegh River nutrient concentrations. This estimate thus (dubiously) assumes negligible gains or losses of nutrients across Lough Cutra (in future studies, Beagh River should be sampled directly). The mean daily load exiting the system is estimated as 690 kg/day, as calculated with the aid of the Infoworks model. This indicates that even though the concentrations remain similar, there is a net gain of TN as water moves through the system. This net gain of N at Kinvara amounts to a 17% increase from that of the rivers. Considering that the overall diffuse input of N (as calculated in Section 7.4.2) was estimated as 40%, this suggests that the contribution of high-N diffuse water to the system is offset by losses, most likely within the turloughs (discussed in the following section). It should be noted that in reality, the outflow at Kinvara is further enhanced by the influx of water from separate catchments (as indicated by alkalinity results and tracer studies for the Gort Flood Studies Report).

Unlike TN, TP shows a slight reduction in daily loading rate between the rivers (16.46 kg/day) and Kinvara (15.15 kg/day) which indicates that a greater proportion of P is being lost from the system than is being gained. Again, these losses are most likely occurring within the turloughs and are discussed in the next section.

7.5.2 Hydrochemical Behaviour within turloughs

Hydrologically, turloughs fall under a spectrum of different types ranging from diffuse flow-through dominated to conduit dominated. Cunha Pereira (2011) suggested that the majority of turloughs fall under the diffuse flow-through category. The turloughs of the Gort Lowlands, however, predominantly fall under the conduit dominated category. These turloughs are known to operate as river flow-through systems (Blackrock and Coole), surcharge systems (Coy and Caherglassaun) and a mixed system (Garryland), all of which are heavily controlled by conduit type hydraulics. Conceptually, the flow-through turloughs reflect the hydrochemistry of their feeding rivers whereas the surcharge tank turloughs can be isolated from any nutrient input (depending on the flood conditions). In Section 7.4, the disparity between the conceptual model (which assumed conservative hydrochemical flow behaviour) and the observed behaviour of the turloughs was presented. In this section, the non-conservative hydrochemical effects are discussed.

7.5.2.1 Alkalinity, EC and pH

In terms of alkalinity, EC and pH, the turloughs behaved somewhat as would be expected from the conceptual model. Blackrock and Coole turloughs showed signs of flow-through behaviour as evidenced by quick drops in alkalinity during a flooded period. Coy and Caherglassaun, on the other hand, showed no such behaviour (as would be expected of a surcharge tank). Garryland also showed predominantly surcharge tank behaviour although, at high levels, the turlough appeared linked to Coole. The most noticeable trend, particularly for the surcharge tank turloughs, is the increase in alkalinity/EC across the flooding season. As mentioned in Section 7.2.1.2, this could be attributed to gradual recharge from the surrounding epikarst during recession due to a hydrological gradient between the turlough and its surrounding epikarst. This theory is contested however by the lack of a corresponding enhancement of N in the turloughs (from the N-rich diffuse water). However, as discussed in the next section, the lack of a corresponding N enhancement could be due to loss of N from the turlough through various reduction processes.

This trend of increasing alkalinity is unusual for turloughs. Looking at the data of Cunha Pereira (2011), out of the 22 turloughs he sampled, the only turloughs that showed alkalinity increasing over time were the three surcharge tank turloughs of the Gort Lowlands (Coy, Garryland and Caherglassaun). The reason this trend was not seen in the other turloughs is because their higher calcium carbonate concentration is in equilibrium with the surrounding bedrock, thus the addition of any diffuse/epikarst water would have no impact. It is this subsaturated nature of $CaCO_3$ in the Gort Lowland turloughs which provides another possible cause for their $CaCO_3$ enhancement:

dissolution of their underlying bedrock. This cause is likely to have a more minor influence, however, due to the large volumes of water involved and the presence of overlying till on the turlough beds which would disrupt the water-bedrock interaction.

7.5.2.2 Nitrogen

The typical pattern of N in turloughs was described by Cunha Pereira (2011) as peak N concentrations occurring in mid-winter (coinciding with peaks or near-peaks in water levels) followed by a reduction in concentrations (and load) throughout the spring and summer. This pattern is also reported in numerous permanent water bodies in Ireland such as Lough Bunny (Pybus et al., 2003) and Lough Carra (King and Champ, 2000) as well as in Scotland (Petry et al. (2002) and Wales (Reynolds et al. (1992). The trend is usually explained by reduced effective rainfall and increased plant and microbial N-uptake in the catchments during the growing season (late spring to early autumn) and the reverse process occurring in the late autumn and winter (Cunha Pereira, 2011, Kaste et al., 2003). This pattern would thus be expected of Blackrock and Coole turloughs (as they should reflect the N of the water feeding them), and indeed it is seen for the most part. Interestingly however, the trend can also be seen in Coy, Garryland and Caherglassaun turloughs for the 2011-2012 flooding season. This suggests that N is being lost from these turloughs by some reduction process.

In wetlands, particulate forms of nitrogen (organic and inorganic) are removed through settling and burial, whereas the removal of dissolved forms (inorganic only) is regulated by various biogeochemical reactions functioning in the soil and the overlying water column (Reddy and DeLaune, 2008). Losses of N from lakes are typically explained by three main processes: (a) net loss with outflowing water (i.e. flow-through), (b) permanent loss of inorganic and organic nitrogen-containing compounds to the sediments, and (c), reduction of NO_3 to N_2 by bacterial denitrification and subsequent return of N_2 to the atmosphere (Wetzel, 2001). These possesses are of additional importance within the Gort Lowland as the limiting nutrient in these turloughs has been shown to be N rather than P (Cunha Pereira et al., 2010). An additional complication for N cycling in turloughs is the shift from flooded and dry phases which result in fluctuation between aerobic and anaerobic soil conditions. In the following sub-sections, the primary effects likely to be causing N variation within the turloughs are discussed.

7.5.2.2.1 Net Loss with Outflowing Water.

Cunha Pereira (2011) concluded that the most plausible explanation for the decline of N concentration in his 22 turloughs was due to an equivalent decline in N concentrations from the inflowing water (i.e. declining losses from the catchments). These catchment losses were reflected in the turloughs due to their diffuse flow-through nature. This conceptualisation is plausible for the majority of Cunha Periera's turloughs as they are mainly epikarst fed systems rather than conduit and surcharge tank systems. Mass balance calculations carried out by Naughton (2011) showed that in order for dilution to be the main process responsible for lowering TN concentrations, an extremely high level of turnover is required during the recession period. Blackrock turlough was shown to need a turnover of 15% within a month while Lisduff turlough (in Co. Roscommon) needed up to 55% turnover. These calculations were also based on the unrealistic assumption that the diluting water would have negligible nutrient concentration. Based on these calculations, Naughton concluded that, while flow-through behaviour is occurring, other N reduction processes are also likely to be taking place.

This outflow/dilution concept is a suitable partial explanation for the behaviour of Blackrock and Coole turloughs which are closely related to their respective river inputs. See Figure 7.60 for an illustration of Blackrock NO_3 concentration reducing in response to reduced river NO_3. Similar behaviour can be seen for TDP (see Figure 7.61). This concept does not however explain the reduction of N in the surcharge tank turloughs. While these surcharge tank turloughs do experience some dilution from diffuse water (as shown by alkalinity measurements, Section 7.5.2.1), the incoming water would be more likely to increase N concentration rather than reduce it. Thus internal reduction processes must also be taking place within these turloughs.

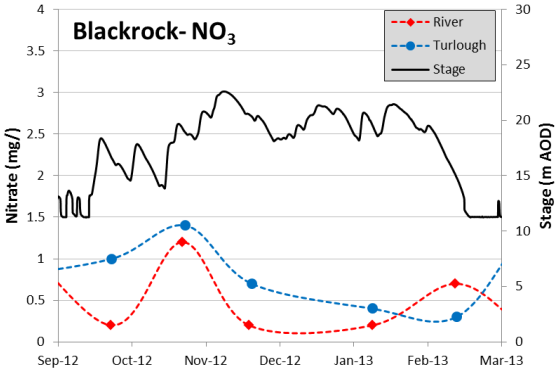

Figure 7.60: River-turlough NO_3 comparison, (Blackrock, 2012-2013 season).

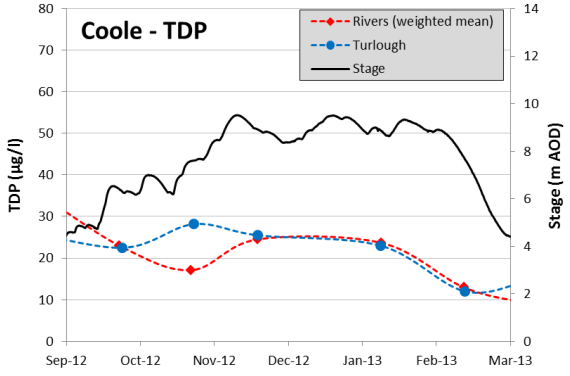

Figure 7.61: River-turlough TDP comparison, (Coole, 2012-2013 season).

7.5.2.2.2 Sediment and Soil Interaction.

In many permanent lakes, sedimentation can be a major source of N loss. Wetzel (2001) presents a number of nitrogen budgets calculated for various permanent lakes (e.g. Lake Mendotta, Wisconsin and Mirror Lake, New Hampshire). In these budgets, sedimentation accounted for approximately half of the entire N losses for the lakes. The losses occur because N is lost as a result of permanent internment of partially decomposed biota and inorganic and organic nitrogen compounds adsorbed to organic particulate matter in the sediments (Wetzel, 2001). However, it is primarily organic nitrogen that is lost to sediments as dissolved forms of N such as ammonium and nitrate are hardly adsorbed by sediment particles and do not normally precipitate to insoluble forms in the sediment (Scheffer, 1998). In the turloughs under study (and most turloughs in general), N is primarily found in an inorganic form. As such, the effect of sedimentation on the Gort Lowlands turloughs would be limited.

Although sedimentation of N in turloughs is minor, evidence for it has been seen. A study by Kimberley and Waldren (2012) showed evidence of N accumulation in turlough soils, particularly at lower elevations which are more often inundated with water. Kimberly also found a relationship between soil TN and organic matter content and concluded that the relatively higher TN concentrations within the lower turlough zones are likely the result of organic matter accumulation resulting from longer hydroperiods (periods of inundation). Overall however, Kimberly found very little relationship between soil N concentrations and turlough flooding behaviour (unlike for P, see Section 7.5.2.3.1). In a separate study, Kimberly concluded that results from the 22 NPWS-project turloughs indicated that land use, vegetation and soil depth are more important drivers of turlough soil TN than flooding factors (Kimberley et al., 2012). As such, sedimentation can be considered to have only a minor role in N loss from turloughs.

7.5.2.2.3 Denitrification

Denitrification is the process in which nitrate (NO_3) and nitrite (NO_2) are biochemically reduced into nitrogen gas (N_2) (with an associated oxidation of organic matter). The general sequence of denitrification is as follows:

$$NO_3^- \rightarrow NO_2^- \rightarrow N_2O \rightarrow N_2$$

This process can cause significant loss of N in lakes. For instance, a study by Jensen et al. (1991) carried out on a series of shallow Danish lakes found denitrification was the cause of 77% of total N

loss. For denitrification to take place, the key condition required is a lack of dissolved oxygen (DO), i.e. anoxic conditions. Due to this condition, denitrification is an unlikely cause of N loss in most turloughs as they tend to show DO levels near saturation (>10 mg/l) (Cunha Pereira, 2011). As most turloughs are shallow with average depths between 1 - 3m (Naughton, 2011), the DO levels can be assumed to remain high throughout the turlough water column.

The turloughs of the Gort Lowlands however are deeper, typically reaching depths greater than 10 m. These turloughs are also more eutrophic which would encourage a 'clinograde' oxygen profile whereby DO levels reduce with depth due to oxidative process. In lakes where this 'clinograde' oxygen profile occurs, oxygen consumption is most intense at the sediment-water interface, where the accumulation of organic matter and bacterial metabolism are greatest (Wetzel, 2001). Thus the sediment surface is the most important site for denitrification (Scheffer, 1998). Analysis of soil samples by Kimberley and Waldren (2012) found that elevated concentrations of available forms of N and P in the lower turlough zones may be the result of anaerobic conditions. Thus implying that denitrification can take place within the turloughs of the Gort Lowlands.

Considering the observed losses of TN, and particularly NO_3, in the turloughs (seen previously in Figures 7.43 and 7.44), denitrification is a plausible explanation for the N losses seen in the surcharge tank turloughs over the 2011-2012 flooded period. As this winter flooding season was the most 'normal' season, it offered the turloughs a degree of stability, i.e. the water remained stationary in the turloughs rather than constantly changing due to filling/emptying. Thus with this stability, and depth of water, the turloughs could form a clinograde oxygen profile which would promote denitrification at the base of the turloughs.

Reddy and DeLaune (2008) state that denitrification rates in lakes vary between 34 and 57 mg $N/m^2/day$. Looking at the example of Caherglassaun over the 2011-2012 flooding season, that would suggest a removal of 755–1266 kg N between sampling points A and B highlighted in Figure 7.62 (sampling points are one month apart).

The actual amount of N removed can be calculated as follows:

- N load at point A is 3121 kg (1.1 mg/l x 2,837,295 m^3). N load at point B is 1724 kg.
- Supposing that N was removed by outflow only, the concentration should stay at 1.1 mg/l while the volume reduces to 2,463,686 m^3. So the N load at point B would be 2710 kg.
- Thus 986 kg N (2710-1724) has been removed by non-conservative processes.

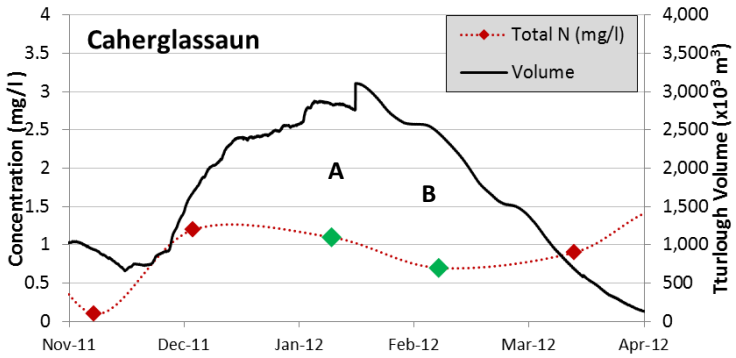

Figure 7.62: Denitrification example, Caherglassaun. Denitrification occurring between points A and B.

This value (986 kg) sits comfortably between the denitrification values as predicted for Caherglassaun (755–1266 kg N), based on the denitrification rates of Reddy and DeLaune (2008). As such, it can be concluded that denitrification is a very likely cause of N removal from the turloughs during flooded periods.

Daily N loading from the rivers has been calculated as 590 kg N/day (Section 7.5.1). Thus monthly N loading is approximately 17700 kg N, while monthly N loss from Caherglassaun was seen to be approximately 986 kg N. These values suggest that, during flooded periods, 4.8% of the N brought into the catchment from the rivers can be lost from Caherglassaun turlough alone. As such, the turloughs can be considered as considerable sinks of N (so long as the turloughs are deep enough and stable enough for denitrification to take place).

7.5.2.2.4 Vegetation, Algae and Grazing

Nitrogen is an essential nutrient for wetland vegetation and algae. As a result, plants and algae can assimilate ammonium, nitrate and in some cases, organic N. Sources of nitrogen to plants include external sources, mineralisation of organic nitrogen in the water and soil, and flux of ammonium from the soil to the water column (National Parks and Wildlife, in review). Assimilation by vegetation causes a net loss of nutrient from the water column (TN and NO_3 reduce) although the nutrients can later be released back into the water through decay. Uptake by algae however only reduces NO_3 as the N taken up by the algae should still be picked up. However this depends on the algae. Filamentous green algae are known to accumulate at the edges of turloughs, thus removing it from the body of the turlough. Unicellular algae, on the other hand, is well dispersed and should be picked up by a sample (Catherine Coxon, pers. Comm.). It should also be noted that algae can also lead to N gain in turloughs due to assimilation of atmospheric N_2 via biological fixation.

Overall, the effect of algae on the Gort Lowlands turloughs is thought to be minor as algae concentrations in these turloughs are known to be low, most likely to the highly coloured water quality in these turloughs and their depths (Cunha Pereira et al., 2010). The effect of vegetation on the turloughs of the Gort Lowlands has not been thoroughly investigated although low soil-N concentrations in these turloughs indicate only low levels of vegetation assimilation during flooded periods. In dry periods however, N is known to be lost from the turloughs due to herbage removal via grazing (Kimberley, 2008).

7.5.2.3 Phosphorus

P has been identified as a major limiting nutrient in turlough floodwaters. Although it should be noted that P shows less significance within the Gort Lowland turloughs due to their relatively high SRP (soluble reactive phosphorous) values (Cunha Pereira et al., 2010). The major source of P to the turloughs is from their river inputs. For the lower three turloughs, mean turlough P concentrations are a clear reflection of their river input. The upper two turloughs, however, show P levels in excess of their water source (Owenshree River) which suggests that these turloughs act as a source of P (or perhaps Blackrock is the source and Coy P concentrations are only elevated by influx of Blackrock outflow). The cause of this elevated P is likely due to grazing on both turloughs and the abattoir located next to Blackrock.

The broad trend seen in all five turloughs was that P concentrations reduced over time during flooded periods. For the flow-through turloughs, Blackrock and Coole this trend can be explained by the altering P concentration of its feeding water but the surcharge tank turloughs, the pattern indicates that P is being removed from the turlough over time. Unlike N, the P cycle in lakes has no gaseous loss mechanism, thus any P added to the surcharge tank turloughs remains within the system until drainage, but not necessarily the water column (Reddy and DeLaune, 2008). The main processes causing P loss are described in the following subsections.

7.5.2.3.1 Sediment and soil interaction.

P is much more easily adsorbed onto particles than N. As such, sediment interaction and subsequent accumulation and soil deposition are key mechanisms of P removal/transformation within a lake system. During eutrophic periods when nutrient concentrations are high, P will adsorb onto sediment (oxides of iron, aluminium, calcium). Later, when concentrations are reduced, P can be re-released back into the water column. This process is known as 'internal

loading' and causes a delay in the response of lake P to a reduction in external loading (N responds faster as it does not sorb as easily to particulate matter). If P has been sorbed onto particulate matter, it can settle and accumulate at the base of the turlough, thus reducing the total P (TP) concentration of the water column, i.e. the flux of particulate matter is generally from the water column to soil. Dissolved P, on the other hand, is typically found in higher concentrations in soil than the overlying water, thus the flux of dissolved P is generally from soil to overlying water. Overall however, the net P flux is typically from the water column to the soils or sediments (National Parks and Wildlife, in review). This was confirmed by Keane (2010) who found that turlough soils do not re-release significant P amounts back into the water column (although it should be noted that Keane's study did not involve any turloughs of the Gort Lowlands). The retention of inorganic P is regulated by various physiochemical properties including redox potential, iron, aluminium, pH, calcium content of soils, P loading and ambient P content of soils (Reddy and DeLaune, 2008). Turloughs with mineral soils (such as the Gort Lowlands turloughs) are more likely to accumulate P than turloughs with organic soils (Kimberley, 2008). As the P is retained in the soil, it can transfer from available P pools into much larger immobile P pools and thus keep accumulating in the soil, a well-documented phenomenon in ordinary agricultural soils (Catherine Coxon, pers. Comm.).

The pattern of reducing P within the turloughs of the Gort Lowlands could thus be partially due to adsorption of P from a dissolved form to a particulate form and subsequent sedimentation out of the water column into the soil. The relative depth of these turloughs also contribute to this process as the settled P passes a 'point of no return' where it is incapable of returning to the upper water levels (Scheffer, 1998). This 'point of no return' factor is less important in more typical, shallow turloughs (a possible explanation for why Cunha Pereira (2011) found less P loss pattern in many of his turloughs). The sedimentation process would result in a reduction of both TP and TDP species, as can be seen occurring in the turloughs. Indeed, this process is somewhat evidenced by (Kimberley and Waldren, 2012) who found elevated P concentrations in soil samples taken from the more saturated lower zones of turloughs. Kimberley et al. (2012) also found a positive correlation between soil P concentrations and the frequency of turlough flooding. Thus the turloughs of the Gort Lowlands, which flood relatively frequently, tend to have higher soil P concentrations. Catherine Coxon (pers. Comm.) however suggests that this correlation has less related to the flooding behaviour and more associated with the chemical signature of water which tends to fill the frequently flooded turloughs, i.e. frequently flooded turloughs tend to be conduit fed with larger nutrient producing catchments.

7.5.2.3.2 Vegetation, Algae and Grazing

Dissolved P in the water column can be taken up by algae or vegetation, and interchanges with organic P via microbes, discrete phosphate minerals, metal oxides and clay mineral surfaces (National Parks and Wildlife, in review). Microorganisms integrate dissolved P into cellular constituents, thus increasing the particulate P concentration in the water column. In lakes with high algal concentrations, P is mobilised from the sediment into the water column by the algae through various mechanisms. This results in reduced sediment P storage and greater P concentration in the water column. In the Gort Lowlands, low algal concentrations suggest that this process is not important to the turlough P cycle.

Similar to N, vegetation can assimilate P from the water column but much of the P is released back into the water column upon vegetative decomposition (above ground biomass portion returned to water, below ground biomass portion returned to soil). Again, very little research has been carried out regarding nutrient assimilation within the turloughs of the Gort Lowlands, and so the level of water-vegetation interaction within these turlough is unknown.

Grazing was shown to have a positive correlation with P concentrations in turlough soil, thus increasing the soluble forms which can be released upon inundation (Kimberley et al., 2012). It is likely the cause of the spikes in turlough P concentration seen at the onset of flooding. Its effects are particularly evident in Blackrock and Coy turloughs which shown P concentrations in excess of their feeding river.

7.5.2.3.3 Interaction with Calcium Carbonate

In carbonate aquifers, P is known to be lost from water due to the formation of calcium phosphate compounds (Cable et al., 2002). This process is unlikely to affect water within the conduit network or the turloughs. It is however likely to be an active process within the diffuse/epikarst portion of the catchment. Thus this process does not directly affect the turloughs but it does indirectly influence the turloughs as any water seeping into the turlough via groundwater is likely to have somewhat reduced concentrations of P.

7.5.2.4 Internal turlough Processes - Overview

Overall, the hydrological behaviour of the Gort Lowlands turloughs appears to be controlled by a number of mechanisms. Blackrock and Coole turloughs are both primarily influenced by their

riverine flow-through nature whereas within Coy, Garryland and Caherglassaun, other processes appear to be at work. Such processes include:

- Gradual influx of epikarst groundwater resulting in a gradual increase in Alkalinity.
- Denitrification resulting in N loss from the system.
- Sedimentation resulting in P loss from the water column.
- Vegetative assimilation resulting in loss of N and P from the water column.

7.6 Ballinduff

In this section, Ballinduff turlough is looked at briefly as it offers an interesting comparison (both hydrologically and hydrochemically) between conduit-fed turloughs and epikarst driven turloughs, particularly as it lies so near to the conduit fed turloughs under study in this thesis.

Ballinduff turlough is situated in a narrow limestone basin which lies 5 km north-east of Gort. See Figure 7.63 below for its mapped location and Figure 7.64 for aerial photos of the turlough during wet and dry periods. The turlough is quite shallow, rarely filling deeper than 4m and is protected as an SAC due to its unusual plant communities.

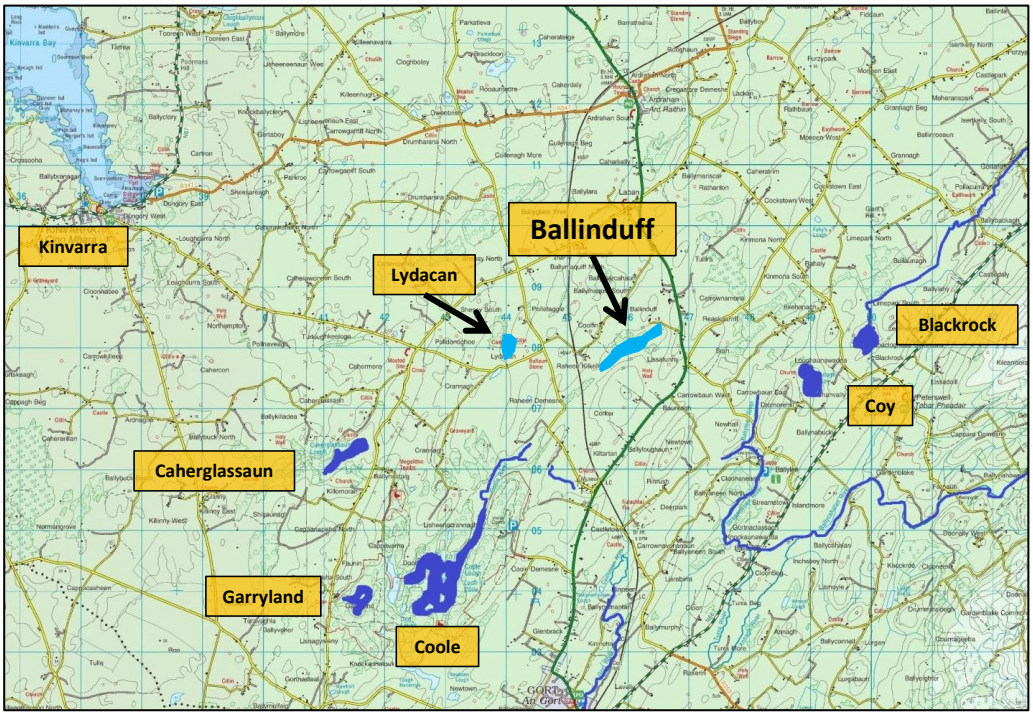

Figure 7.63: Ballinduff location map.

Figure 7.64: Ballinduff turlough, dry vs. wet.

Ballinduff turlough lies in an area of minor groundwater fluctuation, sandwiched between the main active conduit system to the south and the northern flow route to the north. Consequently, the turlough exhibits behaviour more typical of an epikarst/diffuse driven turlough. The turlough is discussed in terms of hydrological and hydrochemical behaviours below:

HYDROLOGICAL

The flooding pattern of Ballinduff operates at a much slower speed to that of the conduit-fed turloughs. Typically, the turlough only fills once and empties once per year. The flooding pattern of the turlough between December 2012 and July 2013 can be seen below in Figure 7.65 (with Garryland for comparison). As can be seen in the plot, Ballinduff shows just one long slow recession whereas Garryland turlough shows a faster recession with multiple minor flood events. This indicates that the drainage of Ballinduff turlough is much more constrained than for the relatively freely draining Garryland turlough.

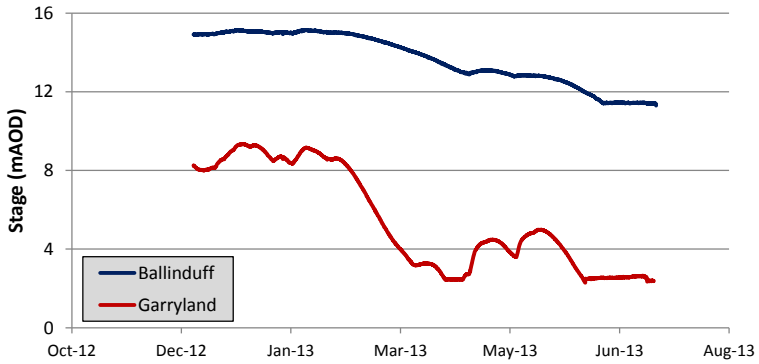

Figure 7.65: Hydrographs of Ballinduff and Garryland turloughs (December 2012 – July 2013).

HYDROCHEMICAL

Hydrochemical data for Ballinduff turlough is presented below in Table 7.12 along with the mean hydrochemical data for the conduit-fed turloughs (sampling carried out between December 2012 and April 2013). Looking at the data, Ballinduff appears much more akin to a typical autogenic-fed turlough such as those studied by Cunha Pereira (2011). Mean alkalinity is greater than twice that of the conduit fed turloughs (305.7 compared to 131.8 mg/l $CaCO_3$) which indicates that the turlough is fed by hard, calcium carbonate $CaCO_3$ rich waters, i.e. local autogenic sources (a similar comparison is seen with EC data). Due to the heavy $CaCO_3$ content of the lake and the relatively long periods of inundation, a thin layer of $CaCO_3$ can be seen deposited on vegetation after drainage (noticeable in the 'dry' aerial photo in from Figure 7.64).

The mean TN concentration of Ballinduff is seen to be higher than the conduit-fed turlough. Again, this indicates a higher contribution from slow moving, N-rich, diffuse water. P also shows a similar pattern with a mean P concentration closer to that of groundwater (31.28 µg/l) than to the conduit fed turloughs.

Table 7.12 Mean Hydrochemical values for Ballinduff turlough (and the conduit fed turloughs).

	TN	TP	Alkalinity	EC	pH
	(mg/l)	*(µg/l)*	*(mg/l CaCO3)*	*(µS/cm)*	
Ballinduff	1.37	30.3	305.7	611	7.9
Conduit-fed	1.12	33.7	131.8	291.2	7.8

Considering the hydrological and hydrochemical behaviour of Ballinduff turlough, it can be stated with confidence that the turlough is an epikarst/diffuse driven turlough fed by local rainfall. The turlough base-level is situated approximately 8m above the base-levels of the nearby Coole-Garryland complex turloughs. This relatively high hydrological-gradient could suggest a possible drainage route for Ballinduff towards Coole, especially considering the high degree of epikarst surrounding Coole turlough. Also, at high water levels, an overland flow route is known to exist between Ballinduff and Coole. Another possible drainage route for Ballinduff turlough is for the water to drain north-westwards, linking up with the northern flow route and discharging at Kinvara East. These differing theories on the turlough's likely drainage direction could be investigated by carrying out a simple tracer study at low water levels (not within the scope of this thesis).

Overall, Ballinduff turlough offers an interesting comparison with the conduit fed turloughs. The fact that various turloughs within the same catchment can operate so differently is an excellent example of the highly heterogeneous nature of a karst aquifer.

Chapter 8

Stable Isotopes of Water, ^{18}O and ^{2}H

8 STABLE ISOTOPES OF WATER, ^{18}O AND ^{2}H

Stable isotopes have long been used as a tool to characterise karstic systems. The close interaction between groundwater and surface-water in these systems makes them favourable for isotope analysis. In surface waters, the natural variations of stable isotopes can be considered as a tracer demonstrating the changes over time as surface water interacts with groundwater. Also, the isotopic composition of water may be altered by physical and geophysical processes such as evaporation and exchange. These processes can be observed using isotopes. In this study, the stable isotopes of water, ^{18}O and ^{2}H, were examined.

It should be noted that ^{13}C isotopes were also considered for analysis based on the principle that ^{13}C values become more enriched the longer water spends in contact with a carbonate aquifer. Thus, in theory, ^{13}C isotopes could be used to characterise where turlough water has originated, from diffuse/epikarst sources or directly from a river/conduit input. This technique has been used successfully in a number of previous studies on carbonate groundwater (Emblanch et al., 2003, Gonfiantini and Zuppi, 2003). However, the interaction of surface water and groundwater in the Gort Lowlands results in an insurmountable complication. As well as becoming enriched from bedrock contact, ^{13}C also experiences enrichment from exposure to the atmosphere. Thus any water sampled from a turlough could be enriched from either bedrock contact or atmospheric exposure, rendering the quantification of diffuse contribution impractical. However, a number of samples were collected. Results from these samples can be seen in Appendix F.

8.1 Background

A change in the ratio of isotopes in a particular phase is called fractionation. Fractionation occurs in any thermodynamic reaction due to the differences in the rates of reaction for different molecular species. Phase changes, evaporation, condensation, freezing, sublimation, melting and some chemical reactions are all causes of fractionation. A simple example of this is evaporation from a water body where the lighter isotopes of oxygen and hydrogen will preferentially evaporate leaving the water body enriched with heavier isotopes.

The study of environmental isotopes of water is based on the determination of the isotopic ratio between the more abundant isotope species (^{16}O, ^{1}H) and its lesser abundant isotope, (^{18}O, ^{2}H). So for ^{18}O, this ratio is denoted by R, such that:

$$R = \frac{^{18}O}{^{16}O} \qquad \textit{Equation 8.1}$$

This ratio is compared to the known standard Vienna Standard Mean Ocean Water (VSMOW) which has an absolute R value of (2005.2 ± 0.45)*10^{-6} for ^{18}O and (155.76 ±0.05)*10^{-6} for ^{2}H (Baertschi, 1976). Isotopic concentrations are reported in delta (δ) units which are parts per thousand (‰) deviations from the standard (VSMOW) and are given by:

$$\delta = \frac{R_{sample} - R_{standard}}{R_{Standard}} \qquad \textit{Equation 8.2}$$

Thus a positive δ value indicates enrichment of an isotope relative to VSMOW, while a negative value indicates depletion. By definition, the ocean has a $\delta^{18}O$ value of ≈0‰ and water from the hydrologic cycle ranges from -50 in arctic regions to +10 in arid regions (Leibundgut et al., 2009). As mentioned previously, the most important fractionation process is that between water and vapour. As water evaporates from the surface of a reservoir, the vapour leaving the surface is depleted in heavy isotopes (^{18}O, ^{2}H) as they have slightly lower saturation vapour pressures than the ordinary molecules (^{16}O, ^{1}H). This is known as kinetic isotope fractionation and leads to an overall enrichment in heavy isotope species in the remaining water.

Craig (1961) proposed that the relationship between the $^{2}\delta$ ($\delta^{2}H$) and $^{18}\delta$ ($\delta^{18}O$) values of precipitation from various parts of the world could be described by the equation:

$$^{2}\delta = 8\ ^{18}\delta + 10‰ \qquad \textit{Equation 8.3}$$

This relationship is known as the Global Meteoric Water Line (GMWL) and is characterised by a slope of 8 indicating that the equilibrium isotopic fraction of hydrogen differs from that of oxygen by about 8 times but maintains a fixed relationship. This relationship can be plotted graphically using a 'delta-plot' as shown in Figure 8.1. The intercept with the $^{2}\delta$ axis is known as the deuterium excess (d-excess or 'd') and was first proposed by Dansgaard (1964) in order to characterise the deuterium excess in global precipitation. The d-value is largely controlled by conditions of atmospheric humidity (*h*) during the vapour forming process, i.e. the greater the humidity, the lower the d-excess value. For example, under conditions of 100% humidity, water vapour is in isotopic equilibrium with seawater, and so any rainfall should plot on a line through the origin (seawater plots through the origin, by definition). When humidity is lower (e.g. h =50%), the

vapour is highly depleted and precipitation should plot above the GMWL. As the global average humidity of water vapour is approximately 85%, this produces a line that is displaced from seawater by +10‰ for $^{2}\delta$, hence the value of 10 for the d-excess of the GMWL (Clark and Fritz, 1997).

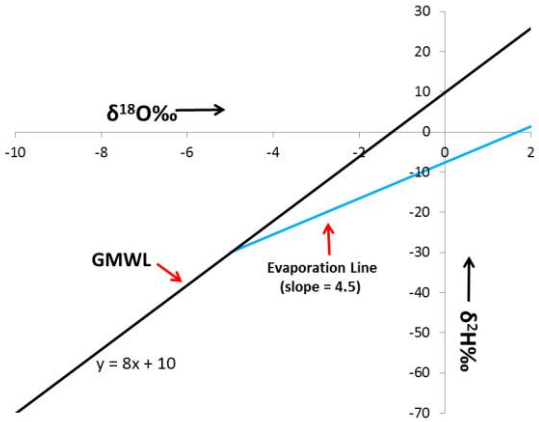

Figure 8.1: Delta plot ($^{18}\delta$ vs. $^{2}\delta$) showing GMWL and theoretical evaporation line (slope 4.5, *h*= 50%).

If water samples analysed for $\delta^{18}O$ and $\delta^{2}H$ are plotted against the GMWL (a delta-plot) and lie below the line (i.e. a relatively greater enrichment in $\delta^{18}O$ than for $\delta^{2}H$), this indicates the water has undergone evaporation (see Figure 8.1). This is because the evaporation is a non-equilibrium process (kinetic fractionation of $\delta^{18}O$ exceeds that of $\delta^{2}H$). Thus isotope fractionations are not necessarily related by a factor of 8. The slope of this evaporation line depends on atmospheric humidity - the lower the humidity, the lower the slope. For example, a humidity of 50% would produce a slope of 4.5 while a humidity of 95% would produce a slope of 6.8 (Gonfiantini, 1986). In Ireland, the average humidity is approximately 87% which suggests a slope between 5 and 6. The displacement of a sample along this evaporation line is dependent on the amount of evaporation (Darling et al., 2003). Also, the intersection of GMWL with the evaporation line represents the isotopic signature of the original non-evaporated rainfall.

At any specific location, the isotopic composition of rainfall can be different from the GMWL due to a number of factors. These factors can be both short-term and long-term in nature. Examples of short term effects include origin and rainout history of the air mass, temperature, rainfall intensity, cloud structure, whether the precipitation falls as rain or snow and the degree of evaporation during the descent of rain droplets to the ground (Gat, 2010). Factors such as these can cause rapid changes in the isotopic signature of rainfall for a particular region over a short space of time. For example, the Global Network for Isotopes in Precipitation (GNIP) station in Wallingford recorded

changes in $\delta^{18}O$ between -2‰ and -10‰ on successive days (Darling and Talbot, 2003). Long-term factors include the 'latitude effect' (the higher the latitude, the more seasonal the isotopic signature of rainfall becomes), the 'continental effect' (progressive $\delta^{18}O$ depletion in rainfall with increasing distance to the coast) and the 'altitude effect' (isotopes are more depleted at higher elevations). Overall, these factors cause the local meteoric water to deviate from the GMWL resulting in a Local Meteoric Water Line (LMWL). Around the globe, LMWLs show a wide range of deviation from the GMWL in terms of both d-excess and slope. For example, d-excess can be seen up to 22 around the eastern Mediterranean (Clark and Fritz, 1997) and down below -15 in Greenland (Mook, 2006) while in Tokyo, the LMWL slope is as low as 4.7 (Gat, 2010). LMWLs reflect the origin of water vapour and any subsequent modifications by secondary processes of re-evaporation and mixing (Clark and Fritz, 1997). As such, any detailed isotopic study should endeavour to define a LWML.

In the British Isles, evaporative effects on surface waters are relatively small (Darling and Talbot, 2003). As a result, there have been comparatively few isotopic studies carried out in Ireland. However, out of the few studies that have been undertaken, a number have included sampling from the Gort Lowlands (as mentioned in Section 2.4.5). Deifendorf and Patterson (2005) carried out a national survey during the summer of 2003. 144 lake and river locations in Ireland were sampled over a three week period to give a snapshot of stable isotope values for one season. Their study did not include turloughs as they were dry but did include a number of surface water bodies within the Gort Lowlands such as Lough Cutra and the Gort River. Bowen and Williams (1973) sampled the Gort Lowlands and the neighbouring River Fergus catchment for $\delta^{18}O$ and Tritium (^{3}H) values. Two reconnaissances were carried out in winter 1970 and spring 1971 in which 26 surface and groundwater locations were sampled. Their study showed how the groundwater variability within the catchment is heavily influenced by seasonal patterns. Another recent study by Einsiedl (2012), used a range of isotopes to characterise sea-water/groundwater interaction in Galway Bay. Einsield's samples were collected during summer 2008 and February 2009 from the Kinvara springs, 7 groundwater wells within the catchment (between Caherglassaun and Kinvara) and one turlough. See Table 8.1 for further details of these studies. It should also be noted that isotopic studies using radon and radium isotopes are on-going in Kinvara Bay. These studies are being carried out by Carlos Rocha (Trinity College Dublin) and have yet to be published.

A notable aspect of these previous studies is the brief sampling periods involved. The studies only sampled the catchment at one or two periods during the year. These brief sampling periods suited the aims and objectives of the studies but for a more complete understanding of the seasonal pattern and distribution of stable isotopes within the Gort Lowlands, a longer sampling period is

required. For this reason, the isotope study carried out as part of this thesis collected samples over a period of 2-3 years.

Table 8.1: Results from previous isotopic studies in the Gort Lowlands.

Study	Sampling period	Isotopic range (‰ TU) (TU = tritium units)		
Deifendorf and Patterson (2005)	Summer 2003	Surface water:	^{18}O:	-5.7 to -6.1
			^{2}H:	-39 to -41
Bowen and Williams (1973)	Winter 1970 and Spring 1971	Surface water:	^{18}O:	-3.9 to -6.25
		Ground-water:	^{18}O:	-5.7 to -7.2
			TU:	75 to 101
		Springs:	^{18}O:	-3.3 to -6.4
			TU:	79 to 92
Einsiedl (2012)	Summer 2008 and February 2009	Ground-water:	^{18}O:	-6.07 to -6.56
			^{2}H:	-36 to -38.9
		Turlough:	^{18}O:	-3.5%
			^{2}H:	-26

8.2 Isotopes in Precipitation

When studying groundwater or surface waters using stable isotopes, it is essential to have understanding of the concentrations and distribution of isotopes in the local precipitation. The stable isotope concentration of the meteoric water serves as an input signal to the system and a baseline for groundwaters (Clark and Fritz, 1997).

Unfortunately, regular sampling of rainfall proved impractical for this study due to the irregularity of site visits. Also, any samples recovered during a particular site visit could only be characteristic of the particular weather system on the day of sampling (rather than a broader average figure). However, the Met Éireann weather station in Valentia (located 175 km from the study catchment) has been part of the IAEA's GNIP (Global Network for Isotopes in Precipitation) network since the 1957 and has an excellent record of monthly meteoric isotope data for Ireland. The data is provided as monthly averages to account for short term variation (multiple samples collected over a month cumulated into a single bottle). See Figure 8.2 for the LMWL for Valentia based on data from 1990-2012.

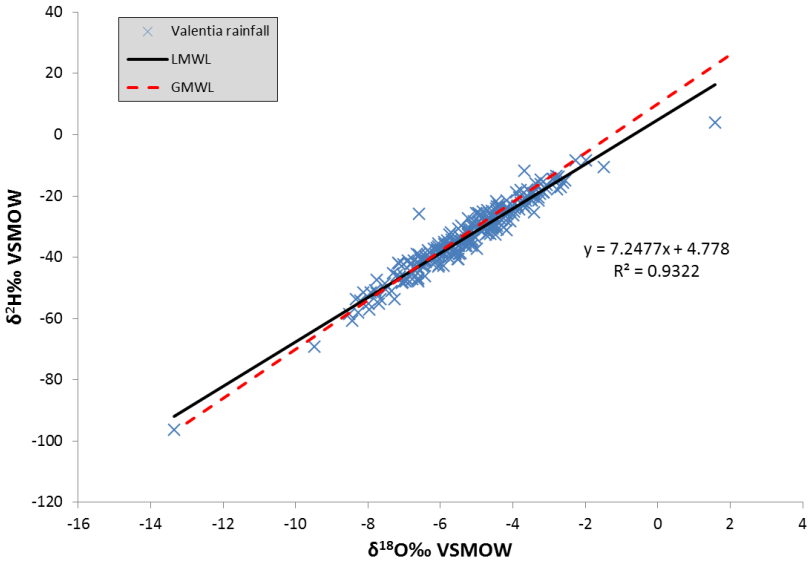

Figure 8.2: Valentia measurments and LMWL (1990-2012).

The LMWL for Valentia is $^{2}\delta = 7.25^{18}\delta + 4.8‰$. The slope, 7.25, is below the GMWL. However this is consistent with the slopes of other long-term stations in NW Europe (Darling and Talbot, 2003). The deviation of Valentia LWML from the GMWL is likely in-part due to its location along the coast of the North Atlantic. Samples collected from the station are liable to include some sea-spray that has mixed with the meteoric water. Sea water is isotopically heavier with δ-values of approximately 0‰ for $^{18}\delta$ and $^{2}\delta$. Consequently, any mixing of sea spray would result in a slight drop in d-excess from 10 towards 0.

Isotopic data from Valentia serves a useful purpose in observing variations in δ-values in time but cannot be relied upon as an accurate LWML for the Gort Lowlands. This was particularly evident as the Valentia LMWL lies significantly below the isotopic data from river samples from the catchment as shown in Figure 8.3. Efforts were taken to reduce the effect of sea spray (and evaporation) by removing Valentia samples that occurred during low rainfall. When samples below 100 mm per month were excluded, the LMWL became $^{2}\delta = 7.41^{18}\delta + 5.9‰$ and when samples below 200 mm per month were excluded, the LMWL became $^{2}\delta = 7.6^{18}\delta + 7.5‰$. These equations point to the LMWL approaching the GMWL ($^{2}\delta = 8^{18}\delta + 10‰$) as rainfall quantity is increased. This is expected as the quantity of rainfall dilutes any deviations caused by sea-spray, evaporation, etc. A similar trend is observed when Valentia data is split between winter (Oct-Mar) and summer (Apr-Sept) samples. Summer rainfall is characterised by isotopically heavier samples and a lower d-excess ($^{2}\delta = 7.21^{18}\delta + 3.6‰$) compared to winter samples ($^{2}\delta = 7.84^{18}\delta + 9.3‰$) which almost match

the GMWL. Nevertheless, the GMWL is still too low to characterise the relatively light $^{8}\delta$ values found in the Gort Lowlands (Figure 8.3).

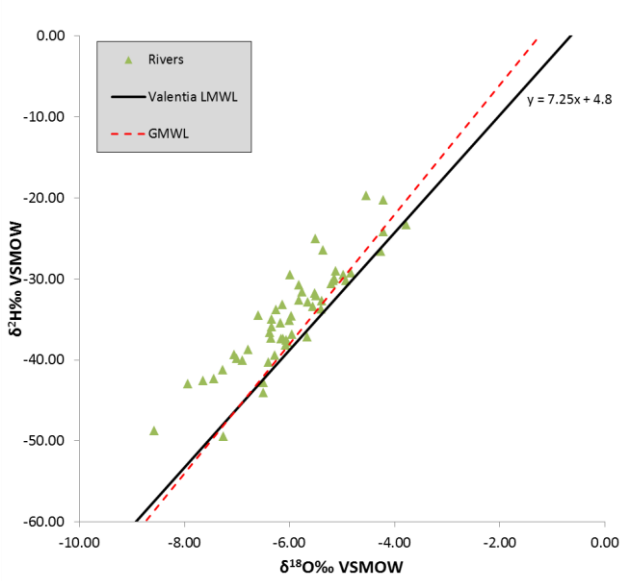

Figure 8.3: Gort Lowlands River data plotted with Valentia LMWL and GMWL.

The relative isotopic lightness of the Gort Lowlands compared Valentia has been observed before by Bowen and Williams (1973) and Einsiedl (2012). Both of these studies attribute the lightness to the greater quantity of light $^{18}\delta$ rainfall during the winter compared to the isotopically heavier $^{18}\delta$ rainfall during the summer. This imbalance in seasonal rainfall volumes results in a depleted mean $^{18}\delta$ value for the Gort Lowlands relative to Valentia. Einsiedl suggested a LMWL of $^{2}\delta = 8^{18}\delta + 13‰$. However, based on other NW Europe LMWLs, the suggested slope of 8 appears too high (LMWL slopes in NW Europe are typically around 6.5 - 7). Deifendorf and Patterson (2005) attribute the isotopic variation across Ireland to 'a combination of topographic and continental rain-out effects acting on moisture from predominantly west-to-southwesterly moisture sources' and estimate the Gort Lowlands to be 2‰ lighter than Valentia. Another factor that could be influencing the Gort Lowlands is the altitude effect. Darling and Talbot (2003) point out that, in the British Isles, for every 100m risen, $^{18}\delta$ drops by -0.3‰ in winter and -0.2‰ in summer. In the case of the Slieve Aughty Mountains which rise above 350 m, this effect could impart a difference of up to 1‰ for precipitation falling on the Slieve Aughtys (Valentia lies at only 25m above sea level).

As rainfall data for the catchment was unavailable, a best approximation of the LMWL could only be made using surface water data (as suggested by Rozanski et al. (2001)). The data chosen for this approximation was from sampling site 'Forest' (F) as samples from this site are essentially runoff

and show the least influence of evaporation from all surface water sites (as seen later in Table 8.2). As such, the site should provide the closest reflection of the isotopic signature of rainfall. Using runoff in this manner should also somewhat account for short term isotopic variations in rainfall as runoff consists of an accumulation of rainfall over a period of time unlike an instantaneous rainfall sample. Using this method, the best approximation for the LMWL is $^{2}\delta = 6.4^{18}\delta + 4.5‰$. In actuality, the LMWL slope is likely to be closer to 7 and the d-excess would likely fall between to 6 and 7 (Deifendorf and Patterson, 2005). Thus based on the findings of Darling and Talbot (2003), the LMWL of the Gort Lowlands could more accurately be estimated as $^{2}\delta = 6.9^{18}\delta + 7‰$ (see Figure 8.4). The isotopic lightness of the Gort Lowlands can be seen in Figure 8.5 which shows a time series of Valentia rainfall $^{18}\delta$ data along with samples from F. The graph shows the Forest samples have a vaguely similar pattern to the Valentia rainfall data but generally lie approximately 1-2‰ below it.

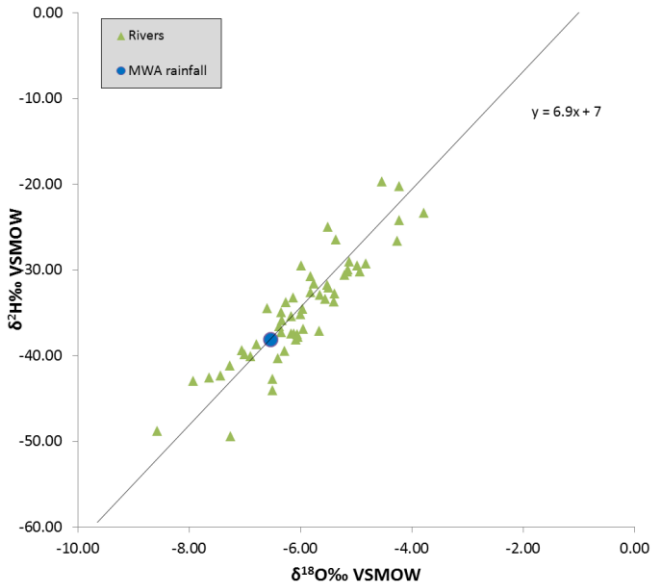

Figure 8.4: Gort Lowlands river data plotted with the approximate LMWL ($^{2}\delta = 6.9^{18}\delta + 7‰$).

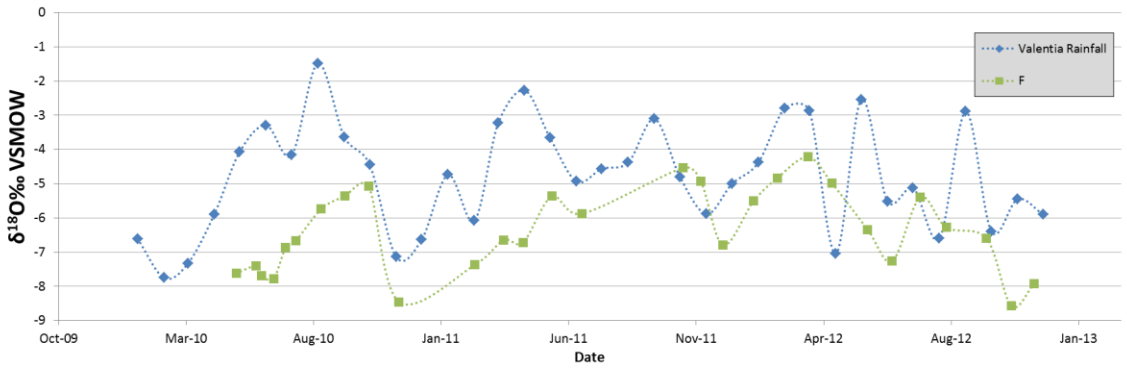

Figure 8.5: Valentia rainfall and forest (F) $^{18}\delta$ time series.

The mean weighted average (MWA) isotopic composition of rainfall provides a long term estimate of isotopic input into a system. Also, the MWA of rainfall should give a similar result to the average isotopic composition of groundwater (Darling et al., 2003). The MWA is a mean isotopic value, calculated based on monthly rainfall quantities and their relevant δ-values. The MWA isotopic composition of Valentia rainfall between 1990 and 2012 is $^{18}\delta$: -5.37, $^{2}\delta$: -33.76. In Figure 8.6 below, the average monthly precipitation and $^{18}\delta$ values for Valentia between 1990 and 2012 are presented. A clear seasonal trend is evident with $^{18}\delta$ values highest and rainfall lowest during the summer months. Seasonal trends such as this are typically based on a relationship between temperature, $^{18}\delta$, latitude and continentally. The fundamental relationship is that between temperature and $^{18}\delta$ which becomes more pronounced at higher latitudes and greater distance from the coast. So the latitude of Valentia encourages seasonality but the coastal location discourages it. It could thus be inferred that a more inland location such as the Slieve Aughtys would experience a greater seasonal effect than the Valentia rainfall.

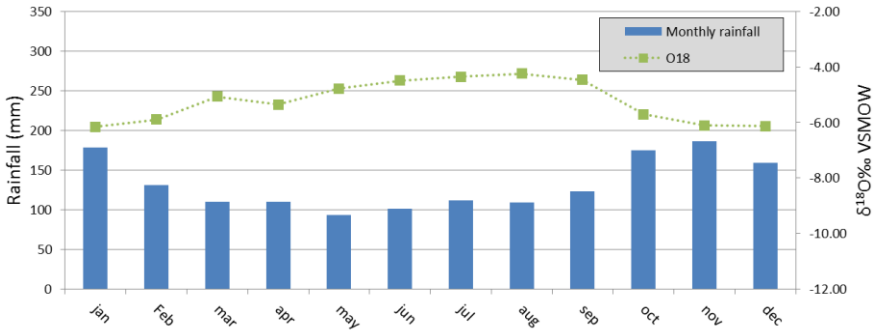

Figure 8.6: Average monthly precipitation and $^{18}\delta$ values for 1990-2012 at Valentia.

As discussed above, Valentia rainfall is not suitable for direct comparison with Gort-Lowland rainfall so the MWA for Valentia cannot be considered as an input into the Lowlands system under study. So to calculate a reasonable estimate of MWA rainfall, samples from F are used. Applying the mean weighted average rainfall from Kilchreest rain gauge to the samples from F gave an $^{18}\delta$ value of -6.54. This result is similar to average isotopic composition of groundwater, -6.57 (when evaporation-affected samples are removed, see Section 8.3.3). This correlation could be seen as partially validating the use of F as a substitute for rainfall. The position of the MWA rainfall along the LMWL is indicated by a blue dot on Figure 8.4.

The average monthly variation in precipitation (i.e. runoff sampled from 'F') for Gort Lowlands between 2010 and 2012 is shown in Figure 8.7. This data is in clear contrast to the Valentia long-term data shown in Figure 8.6 with lower rainfall during the early months of the year and heavier

rainfall during the summers (particularly June 2012). The $^{18}\delta$ values also show a contrast with long-term data with reduced $^{18}\delta$ levels during the summer. In tropical marine regions, this drop in $^{18}\delta$ could be assumed to be related to the rainfall amount. However in the case of the temperate Gort Lowlands, this relationship is minimal (R^2=0.1).

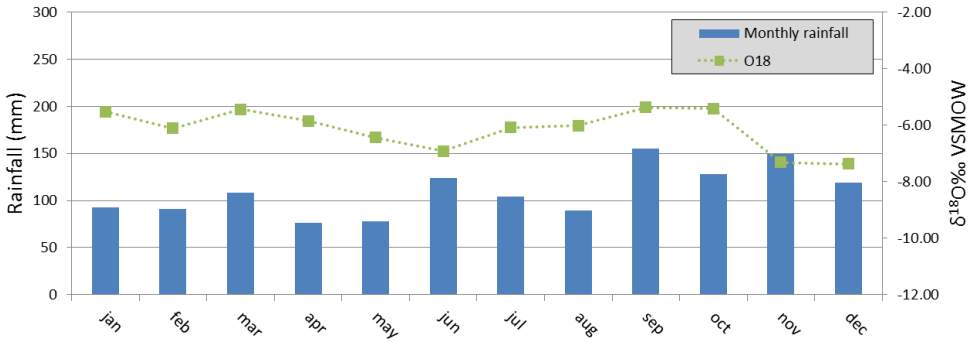

Figure 8.7: Average monthly precipitation and $^{18}\delta$ values for 2010-2012 in the Gort Lowlands.

8.3 Isotopes in Surface water and Groundwater

In this study, 521 samples in total were collected from surface and groundwater sources between March 2010 and December 2012. Of these samples, 347 were tested solely for $^{18}\delta$ and 174 samples were tested for both $^{18}\delta$ and $^{2}\delta$. The results of these tests are presented in Table 8.2

From this table it can be seen that groundwater shows the least influence from evaporation, rivers show minor evaporation and the turloughs show the most evaporation. This affect can be shown more clearly in a delta-plot as shown in Figure 8.8. In this plot, the effect of evaporation can be seen lowering the best-fit lines to slopes of 5.97, 4.27 and 3.9 for rivers, turloughs and Kinvara West respectively. Groundwater points were excluded from this plot as the small isotopic range for these samples hinders the application of a best-fit line. Samples from KE were excluded for this same reason (for more information on these samples, see Sections 8.3.3 and 8.3.4). It should be noted that these best-fit lines do not represent the 'evaporation line' for the system. These lines are instead the result of a best-fit regression line which encapsulates the evaporated and non-evaporated samples. Thus the slope of the line indicates the relative influence of evaporation but not the actual evaporation line slope. The best fit line for river samples show a slight degree of evaporation, deviating away from the LMWL, from a slope of 6.9 to 5.97. The turloughs, on the other hand, present a much lower slope of 4.27. This is due to the evaporation effects that can be seen on the turloughs, particularly when they are low. Each of these systems and their respective evaporative effects are discussed in their relevant sub-sections within this chapter. As mentioned previously,

the intersection of LMWL and evaporation line indicates the isotopic composition of the average rainfall input into the system. Figure 8.8 suggests an intersection at approximately -6.65, slightly lighter than the mean groundwater isotopic composition (perhaps suggesting a slight evaporative effect on groundwater).

Table 8.2: Minimum, maximum and mean values of $^{18}\delta$ and $^{2}\delta$ for rivers, turloughs, groundwater and Kinvara (grouped and individual).

	$\delta^{18}O$‰ VSMOW			$\delta^{2}H$‰ VSMOW		
	min	*max*	*mean*	*min*	*max*	*mean*
Rivers	**-8.63**	**-3.71**	**-6.04**	**-49.42**	**-19.70**	**-34.58**
ORU	-7.82	-4.80	-6.12	-	-	-
ORL	-8.02	-4.71	-6.28	-41.18	-31.56	-36.36
BRU	-7.83	-4.23	-5.97	-	-	-
BRL	-7.77	-3.78	-6.11	-42.75	-23.30	-33.85
DRU	-7.47	-4.02	-5.72	-	-	-
DRL	-7.81	-4.22	-6.04	-44.03	-24.18	-34.03
F	-8.57	-4.22	-6.37	-49.42	-19.70	-34.08
P	-8.63	-3.71	-5.75	-	-	-
Turloughs	**-8.22**	**-2.69**	**-5.92**	**-47.86**	**-27.81**	**-35.13**
Blackrock	-7.29	-4.47	-6.21	-47.86	-29.21	-36.83
Coy	-8.22	-2.69	-5.91	-42.41	-30.51	-36.12
Coole	-7.45	-4.36	-5.94	-41.52	-27.81	-34.64
Garryland	-7.15	-4.25	-5.72	-41.13	-28.37	-33.64
Caherglassaun	-7.55	-4.19	-5.84	-41.60	-28.39	-34.44
Groundwater	**-7.81**	**-5.23**	**-6.44**	**-45.03**	**-34.08**	**-39.61**
BH3	-7.81	-6.11	-6.95	-45.03	-39.05	-42.69
BH5	-6.58	-5.91	-6.29	-	-	-
BH7	-7.59	-6.26	-6.68	-42.78	-39.30	-40.87
BH10	-7.49	-5.68	-6.68	-	-	-
BH11	-6.80	-6.06	-6.27	-	-	-
BH12	-6.48	-5.23	-5.86	-	-	-
BH14	-6.87	-5.40	-5.94	-41.25	-34.08	-36.81
BH15	-6.98	-5.96	-6.49	-	-	-
BH16	-7.45	-6.08	-6.60	-38.78	-37.33	-38.08
Kinvara	**-8.47**	**-2.24**	**-5.98**	-	-	-
KW	-8.05	-2.24	-5.75	-40.35	-29.32	-35.07
KE	-8.47	-4.80	-6.20	-40.72	-33.41	-37.41

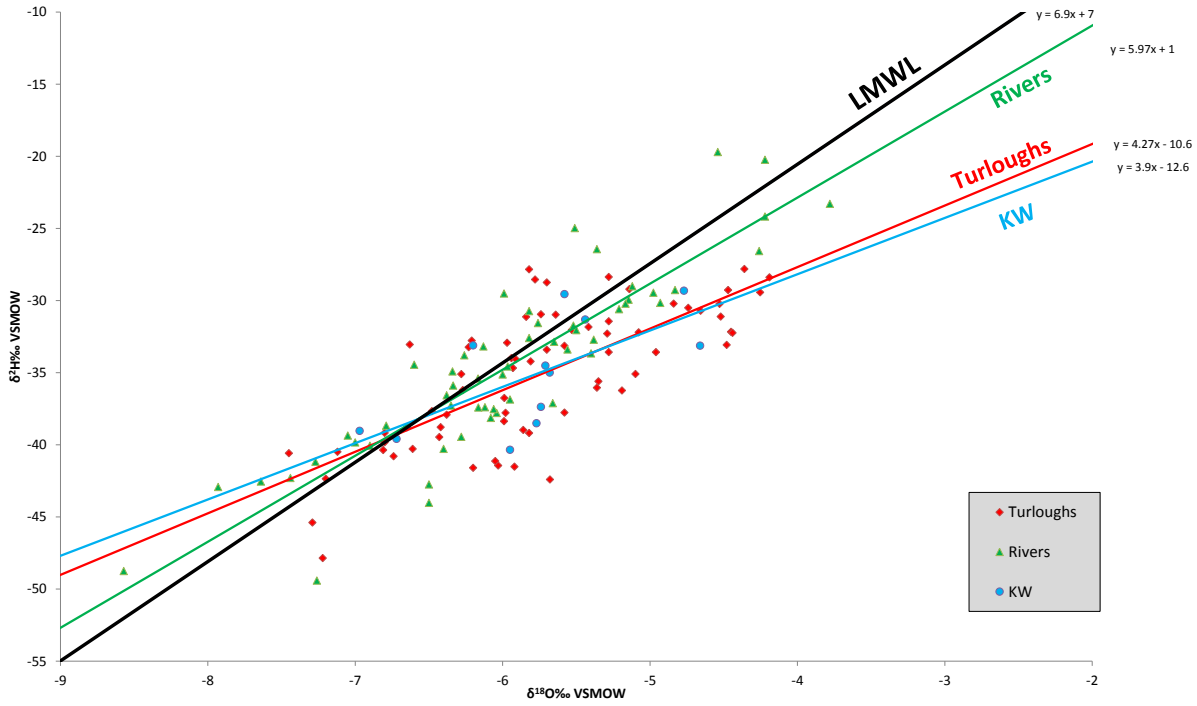

Figure 8.8: Delta-plot for all surface-water samples (segregated into rivers, turloughs and KW).

The slope of the evaporation line can be calculated theoretically using the equations and parameters as defined by Craig and Gordon (1965). In order to carry out this calculation, a range of isotopic and climactic parameters are required. Values for most of these parameters are known through field observation. However some parameters such as the isotopic composition of atmospheric moisture (δa) require the use of an assumption. The parameters required for this calculation are presented and discussed below (see Table 8.3 for their values):

- **T_o:** Lake surface temperature (based on data from Coy turlough diver).

- ***h*:** Relative humidity normalised to average lake-surface temperature (vapour pressure of the air divided by the saturation vapour pressure at the lake- surface temperature. Calculated using mean annual humidity data from Oranmore weather station and T_o.

- **$\alpha_{V/L}$:** Equilibrium isotope fractionation factor of water vapour relative to liquid. Specified as a function of temperature by Majoube (1971). (Available from Rozanski et al. (2001)).

- **$\varepsilon_{V/L}$:** Equilibrium fractionation factor, given as $\varepsilon_{V/L} = (\alpha_{V/L}-1)*1000$.
- **$\Delta\varepsilon$:** Kinetic fractionation factor, defined as $12.5(1-h)$ for $^{2}\delta$ and $12.5(1-h)$ for $^{18}\delta$.
- **ε:** Total fractionation factor, $\varepsilon = \varepsilon_{V/L} + \Delta\varepsilon$ or $\varepsilon = (\alpha_{V/L}-1)*1000 + \Delta\varepsilon$.
- **δ_p:** Isotopic composition of rainfall.
- **δ_a:** Isotopic composition of atmospheric moisture. For moderate climates, δ_a can be assumed to be in isotopic equilibrium with rainwater (Rozanski et al., 2001), thus $\delta_a = \delta_p - \varepsilon_{V/L}$.

Table 8.3: Variables used to calculate the theoretical evaporation slope.

Climatic Variables	Value	Isotopic Variable (units of ‰, except $\alpha_{V/L}$)	Value ($^{18}\delta$)	Value ($^{2}\delta$)
T_o (°C)	10.6	$\alpha_{V/L}$ (ratio)	0.989	0.912
h (ratio)	0.889	$\varepsilon_{V/L}$	10.6	88.03
		$\Delta\varepsilon$	1.58	1.39
		δ_p	-6.65	-38.8
		δ_a	-17.14	-126.2

With these variables determined, the evaporation slope is defined as

$$E_{slope} = \frac{h(\delta_a - \delta_I)_2 + \varepsilon_2}{h(\delta_a - \delta_I)_{18} + \varepsilon_{18}} \qquad \textit{Equation 8.4}$$

where subscripts '2'and '18' represent their respective isotope and δ_I represents the initial water composition. In this calculation, δ_I represents rainfall (δ_P). Using this equation, the slope of the evaporation line (E_{slope}) is given as 4.12. This slope is noticeably lower than the slope of 5-6 as predicted for Irish surface waters (based on the relatively high humidity of Ireland, Section 8.1). This difference is because the slopes predicted by Gonfiantini (1986) are deviations from the GMWL, not a LMWL. For instance, if the rainfall input into this equation ($^{18}\delta$: -6.65, $^{2}\delta$: -38.8) was shifted so that it lay on the GMWL ($^{18}\delta$: -6.65, $^{2}\delta$: -43.2), the calculated slope would be 5.5. However as the LMWL slope in the Gort Lowlands is approximately 6.9, the theoretical evaporation line

slope also drops, giving a value of 4.12. This slope is shown graphically in Figure 8.9 below (with $^{18}\delta$: -6.65, $^{2}\delta$: -38.8 as the intercept).

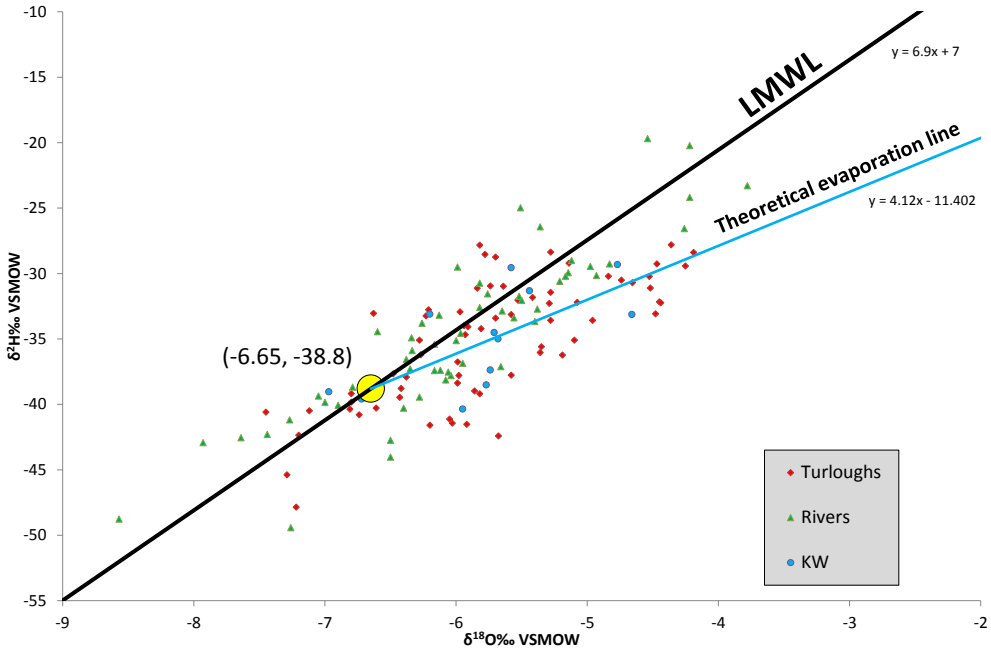

Figure 8.9: Delta-plot showing LMWL and theoretical evaporation line overlaid on isotopic data.

This theoretical evaporation line can be used as the basis for examining the effect of evaporation on surface water samples. The line is useful as the evaporation effect on samples is difficult to find due to the relatively low levels of evaporation and high variability around the LWML.

8.3.1 Rivers

All 8 river/surface-water sites were sampled for stable isotopes. The lower sections of each river (and 'F') were tested for $^{18}\delta$ and $^{2}\delta$ whereas the upper sections (and 'P') were only tested for $^{18}\delta$.

The three rivers being studied are relatively small/short rivers which are sampled close to the location of the originating rainfall. As a result, the isotopic composition of the river water is strongly influenced by that of precipitation. See Figure 8.10 for a time-series plot of $^{18}\delta$ values for all 8 river sites. From this graph, it is evident that all rivers follow a similar isotopic pattern and respond rapidly to changes in rainfall. This rapid response to rainfall is typical of small rivers as the surface runoff component of the flow is more direct and pronounced (Mook, 2006). Rivers with a greater base-flow component show much less variation. For example, Darling et al. (2003) present data from the River Thames which shows variation of less than 1‰ over a period of 8 months.

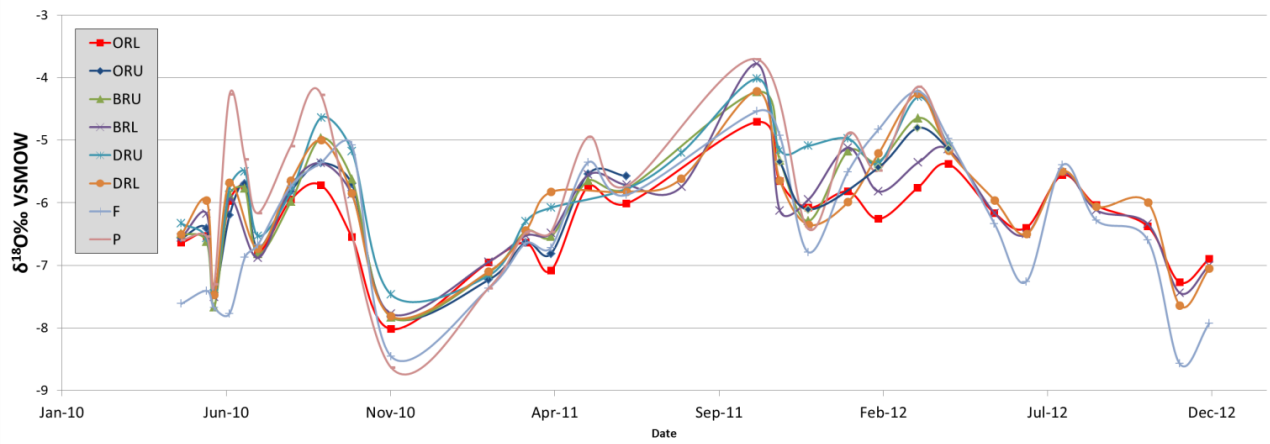

Figure 8.10: $^{18}\delta$ values for river samples (May 2010 – December 2012).

River δ-values ranged from -8.63 to -3.71 for $^{18}\delta$ and -49.42 to -19.7 for $^{2}\delta$ with mean concentrations for $^{18}\delta$ and $^{2}\delta$ of -6.04 and -34.58 respectively (Table 8.2). In Figure 8.10, it can be seen that the rivers display a degree of seasonality, typically showing isotopically lighter flows in winter and heavier flows in summer. The most isotopically depleted flows can be seen during winter 2010-2011 (-8.6). This is likely due to the contribution of snowmelt (snowfall is isotopically lighter than rainfall as the frozen water is unable to equilibrate with ambient moisture as the raindrops fall to the ground (Gat, 2010)). Winter 2012-2013 also shows some isotopically light flows whereas winter 2011-2012 does not. The two highest sampling locations, F and P, display greater extremes in variation than the other rivers. This behaviour is to be expected as these sampling locations are the most likely to reflect the isotopic signature of rainfall compared to the other sampling locations further downstream. This behaviour is more clearly seen in a comparison of delta plots, particularly between ORL and F (Figure 8.11).

It should be noted that the upstream samples tended to show higher (heavier) $^{18}\delta$ values than the downstream samples (as can be seen in Table 8.2). The average $^{18}\delta$ value for the lower sites was recorded as -6.2‰ whereas, upstream the average $^{18}\delta$ was seen to be -5.89‰. This contrast suggests some influence from the altitude effect (for every 100m risen, $^{18}\delta$ drops by -0.3‰ in winter and -0.2‰ in summer).

Looking at Figure 8.11, little evidence of evaporation can be seen from the rivers. Indeed the evaporative effect is very subtle, only dropping the best-fit line slope down from 6.9 (LMWL) to 5.97 (as seen in Figure 8.8). This is not surprising as the rivers are sampled quite near their source (within approximately 20 km) so there has been little opportunity for water to evaporate. Also, the

typical stream cross-section for these rivers is relatively deep which limits the potential for evaporation.

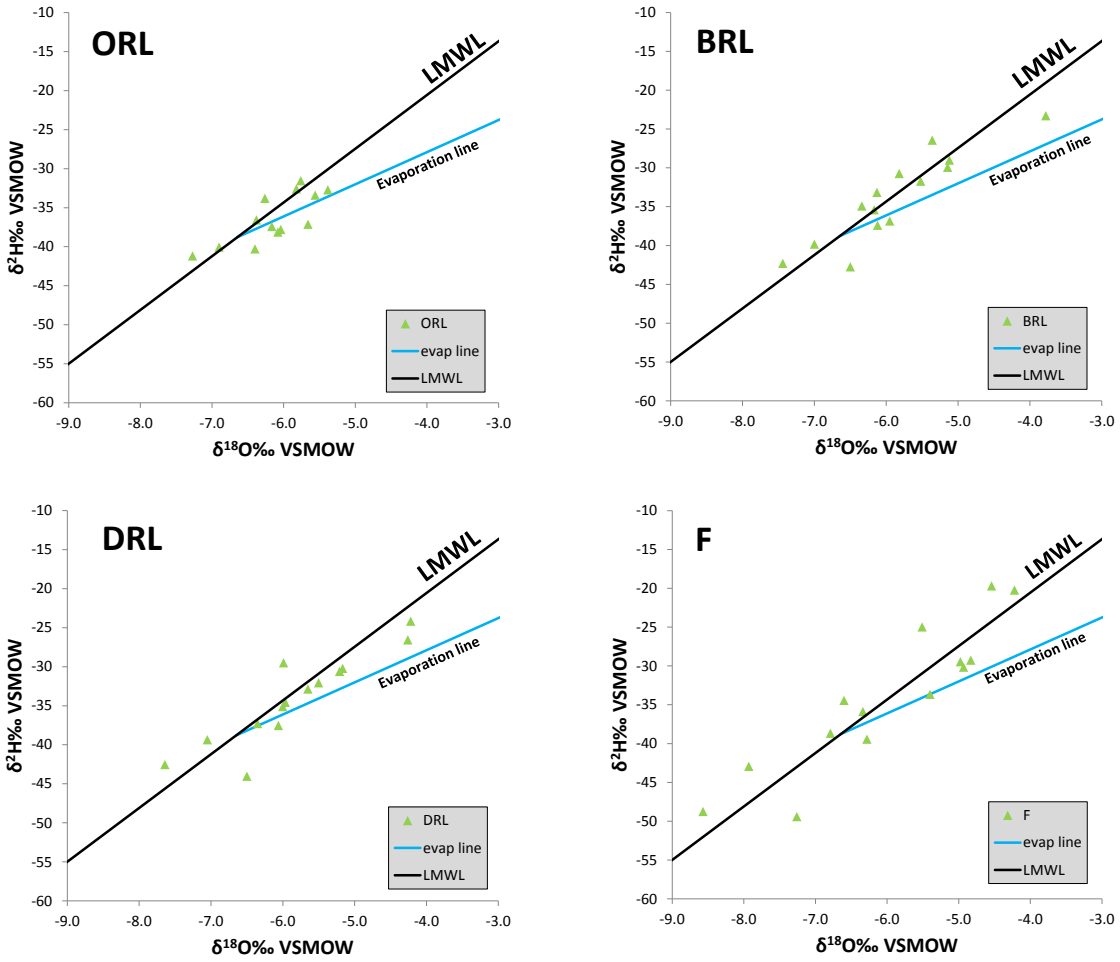

Figure 8.11: Delta plots for river sites ORL, BRL, DRL and F.

While evaporation was seen to have very little influence on the rivers' isotopic signatures, the rivers did appear to be influenced by weather patterns. This influence was evidenced by a number of unusual isotopic readings. In these instances, the unusual readings were found in all rivers on the same sampling date. For example, on the 20th of June 2012, each river displayed noticeably low d-excess values. These unusual readings can be seen in Figures 8.12 and 8.13. Figure 8.12 presents the delta plot for the rivers with the atypical values highlighted (colour coded by date). This data can be better presented using an $^{18}\delta$ vs. d-excess plot (Figure 8.13). In this plot, the unusual readings can be seen more clearly with points having a d-excess value greater than (e.g. 18/10/11) or less than (e.g. 20/6/12) what would be expected given their $^{18}\delta$ value. These deviations are the result of different weather systems occurring within the catchment producing rainfall that does not lie on

the LMWL (but lies on that particular weather system's LMWL). Although these samples appear to be uncharacteristic of the catchment and result in misleading isotopic signatures, they are included in the catchments LMWL so as to take account of all weather systems influencing the catchment. The influence of these different weather systems does however hinder the interpretation of evaporative effects (due to relatively scattered data points).

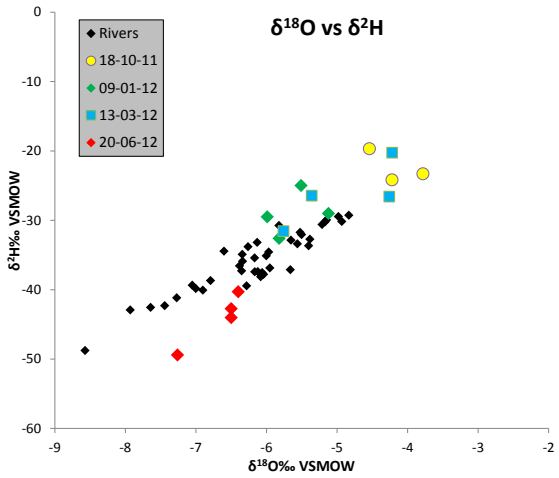

Figure 8.12: $^{18}\delta$ - $^{2}\delta$ plot showing all rivers with atypical readings highlighted.

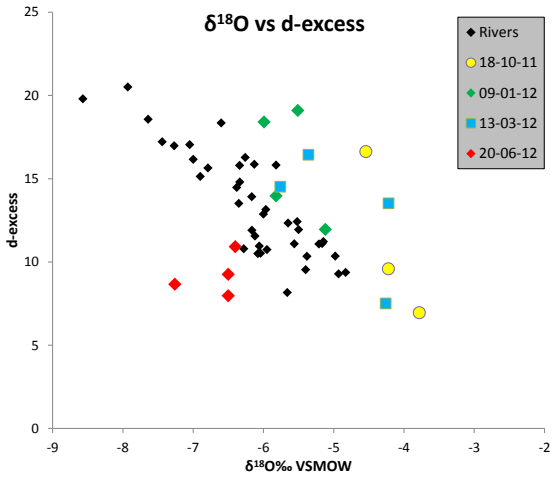

Figure 8.13: $^{18}\delta$ - d-excess plot showing all rivers with atypical readings highlighted.

8.3.2 Turloughs

For typical non-ephemeral lakes, the isotopic composition of the water is primarily determined by the river input and, to a lesser degree, by that of direct precipitation and the upwelling of groundwater (Mook, 2006). Further changes in the isotopic composition of the water are caused by evaporation. The Gort-Lowland turloughs act in a similar fashion. However in most cases the 'river' water reaches the turloughs via underground conduits rather than from the surface. In this section, the turlough variation is looked at first in terms of river input and secondly in terms of evaporation.

RIVER INPUT

Comparative plots of river and turlough $^{18}\delta$ values are presented in Figure 8.14. Similar to Section 7.2.1.2, Blackrock and Coy turloughs are compared to isotopic data from ORL whereas the lower three turloughs are compared to a weighted mean time-series (based on the overall contributions from each river, see Section 5.4.3.1).

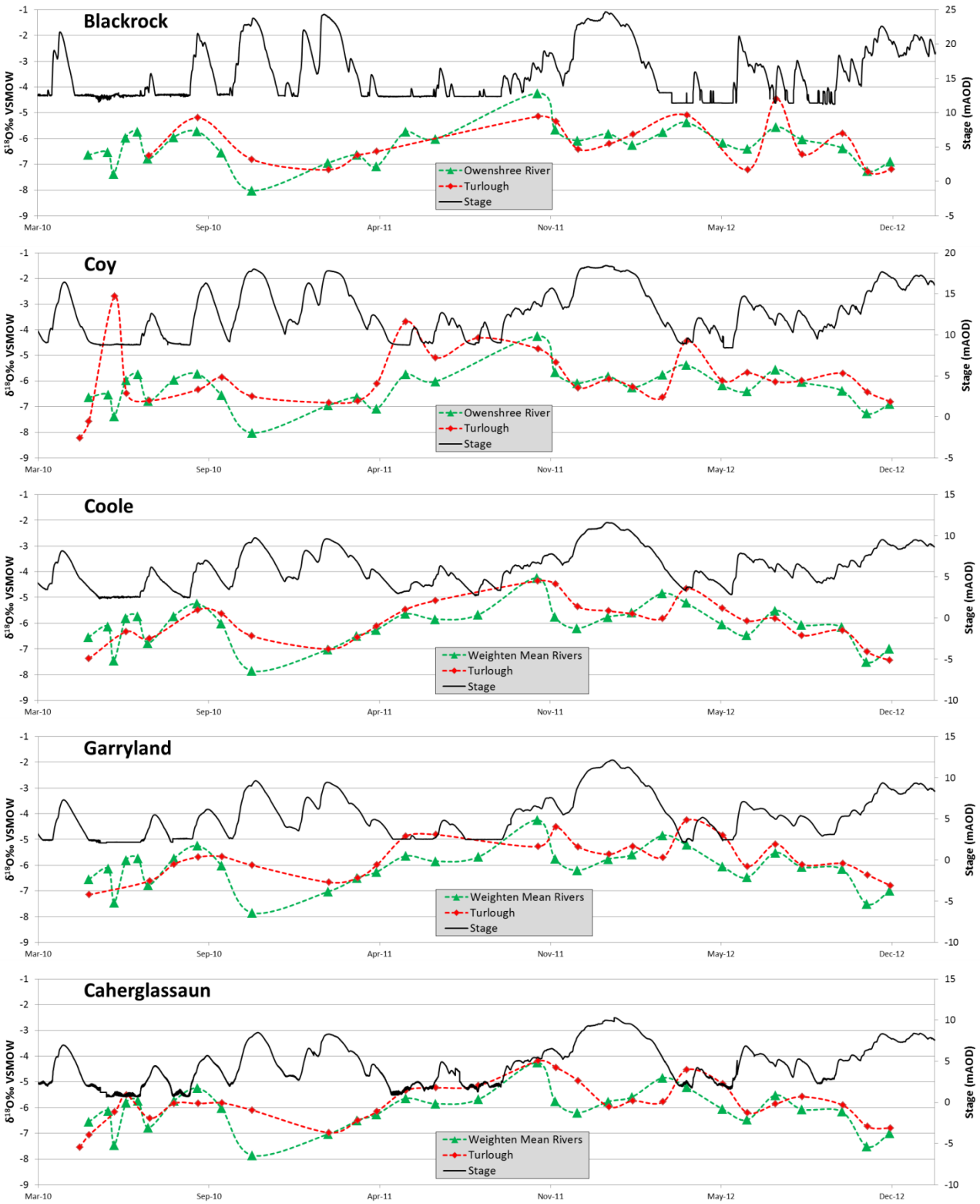

Figure 8.14:Time series plots of river and turlough isotopic compositions and turlough stage for Blackrock, Coy, Coole, Garryland and Caherglassaun turloughs.

From Figure 8.14, it can be seen that the turloughs broadly follow the patterns of the rivers feeding them. Accordingly, the turloughs tend to show isotopically lighter water during flooded periods and heavier water during emptier summer periods.

Blackrock turlough inevitably displays the closest relationship with the river water feeding it (and the least evaporation due to shortest retention time). The flow-through pattern in this turlough can most clearly be seen over the 2011-2012 winter period as evidenced by an inverted peak and recession pattern, i.e. the $^{18}\delta$ level drops at the onset of flooding and gradually rises. Coy turlough also shows a similar pattern to ORL. However the turlough $^{18}\delta$ levels show enrichment relative to the river during low water level periods, indicative of evaporation. Coy shows no peak-recession pattern such as in Blackrock. Instead the turlough appears to become slightly isotopically lighter over the flooded period. This lightening is likely due to the influx of isotopically depleted groundwater from the surrounding epikarst (as seen previously with alkalinity measurements, Section 7.2.1.2). The trend also indicates negligible evaporation over winter (as would be expected). The time series of Coy shows one incidence of extreme evaporation in June 2010 where an $^{18}\delta$ value of -2.69‰ was recorded. This anomaly is attributed to the extremely low water level of Coy and high summer temperatures. At such a low depth, the water in Coy becomes disconnected from the estavelle transforming the turlough into a shallow undrained pond, highly susceptible to evaporation.

The effect of isotope lightening over the flooding season is also seen in Coole and Garryland turloughs over the 2011-2012 winter season. Over this period, the turloughs appear to act oppositely to the combined river input. The rivers show a considerable initial drop followed by a gradual increase whereas the turloughs show gradual decreases over time until the water levels dissipate. Again, this trend suggests the influence of epikarst recharge but could also be due to attenuation and evaporation from Lough Cutra. It should be noted that, unlike the case of alkalinity where any input of groundwater results in a one-way change to a turlough (i.e. an increase because the groundwater alkalinity was always higher than that found in the turloughs), the influx of groundwater on $^{18}\delta$ values is more mixed (groundwater $^{18}\delta$ can be higher or lower than river/turlough $^{18}\delta$ depending on conditions). Indeed this mixed effect can be seen over the 2010-2011 season where the lower three turloughs dip to approximately -7‰ after filling. During the following recession, the contribution of slightly heavier groundwater (≈ -6.5 ‰) enriched the turloughs isotopic signature. The turloughs then appear to continue enriching past the groundwater signature, most likely due to evaporative effects taking hold as summer approaches. For the start of the 2012-2013 season, all turloughs show $^{18}\delta$ lightening over time. In this case, the

pattern is likely due to the high frequency of minor flooding events during the early part of this season. These minor filling events preserve a degree of river-turlough interaction (as can be seen from the data). Unfortunately, $^{18}\delta$ data was not collected for the more 'typically flooded' second half of this season. If it was, it is likely that the surcharge tank mechanisms would have been more obvious, i.e. no interaction with river and slight dilution from epikarst (as was seen from the alkalinity/EC results in Section 7.2.1.2).

EVAPORATION

As can be seen from the overall delta-plot (Figure 8.8), the turloughs show a considerable degree of evaporation, having a best-fit line of slope 4.27, just slightly higher than the theoretical evaporation line. The evaporation is evidenced mostly during the summer when turlough levels are low, temperatures are higher and humidity is lower. This can be seen in a net daily precipitation/evaporation below in Figure 8.15.

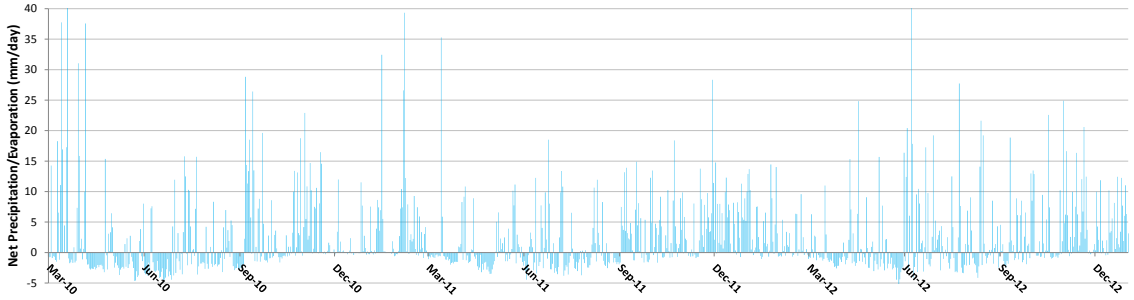

Figure 8.15: Net daily precipitation/evaporation (March 2010 – December 2012).

In order to determine the nature of evaporation from the turloughs, the samples affected by evaporation needed to be identified. This process was complicated however by the isotopically varying river inputs. So to identify samples affected by net-evaporation, a distinction needed to be made between varying river input effects and evaporation effects. This was carried out by comparing the isotopic signature in the river inputs and the turloughs for the same given day using a time series plot and delta plots. An example of this process is shown for Blackrock turlough in Figure 8.16. In this Figure, the river and turlough delta plots are compared and a number of points which show clear shifts to the right hand side of the LMWL are shown (Navy – 10th April, Yellow - 23rd July, Blue – 9th October). These points can then also be seen in the time series plot which shows these shifts more clearly. From this plot, it can be seen that these shifts typically occur when the turloughs are low.

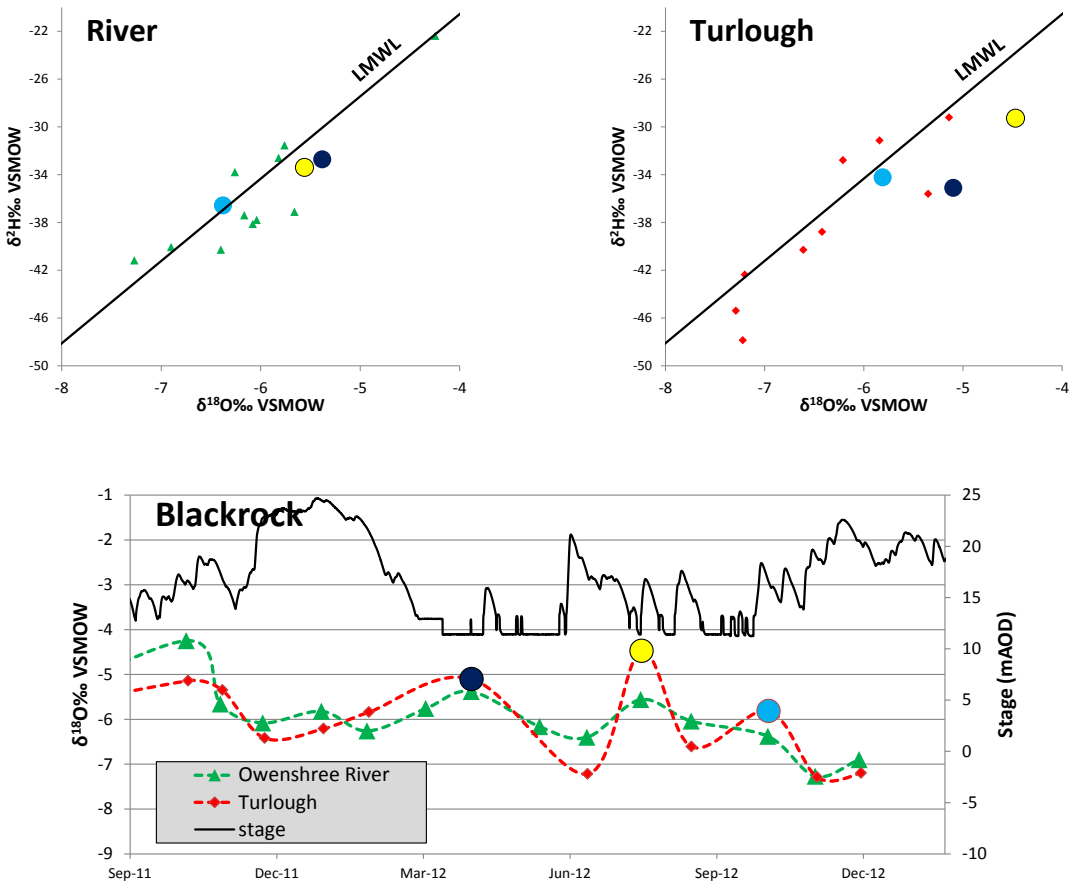

Figure 8.16: Comparison of turlough and river isotopic compositions using delta-plots and time series for the purpose of determining evaporation (Blackrock turlough, September-December 2012).

This technique was applied to each turlough and tended to show net-evaporation occurring on the same dates on each turlough throughout the study period. The results of this analysis can be seen in Figure 8.17. In these plots, the evaporation influenced samples can be seen clearly following the theoretical evaporation line. It should be noted that these plots are limited to data from October 2011 onwards as prior to this time, only $^{18}\delta$ was measured.

In these plots (Figure 8.17), little difference between each turlough can be seen in terms of evaporation with all turloughs experiencing an evaporative effect to roughly the same degree. Evaporation influenced samples tended to show $^{18}\delta$ values between -4 and -5‰ with an exception for Coy in summer 2010 during a period a very dry period (-2.7‰, seen in Figure 8.14). Overall, evaporative effects are seen in only a third of samples from the turloughs. This relatively low amount of influenced samples has two main causes: the climate of western Ireland and the nature

of turlough flooding. The climate of western Ireland is not conducive to high levels of evaporation. Deifendorf and Patterson (2005) suggest that the entire west coast of Ireland has nearly half the evapotranspiration of eastern Ireland. Net-evaporation appears to only occur during the summer and is quite sporadic (as shown in Figure 8.15). This, combined with the relatively quick-changing nature of turlough flood water, makes the turloughs unsuited for high levels of evaporation, i.e. any evaporative effect caused to a turlough during the summer can quickly be washed-away by the influx of new rainwater. In comparison, permanent lakes (in steady-state) would be much more susceptible to evaporation than turloughs. In Irish permanent lakes, isotopic enrichment could theoretically reach up to approximately 0-2‰ ($^{18}\delta$), although that would require a significant fraction of the lake volume to be evaporated (based on a humidity of 0.88 and using the graphs/calculations of Gonfiantini (1986)).

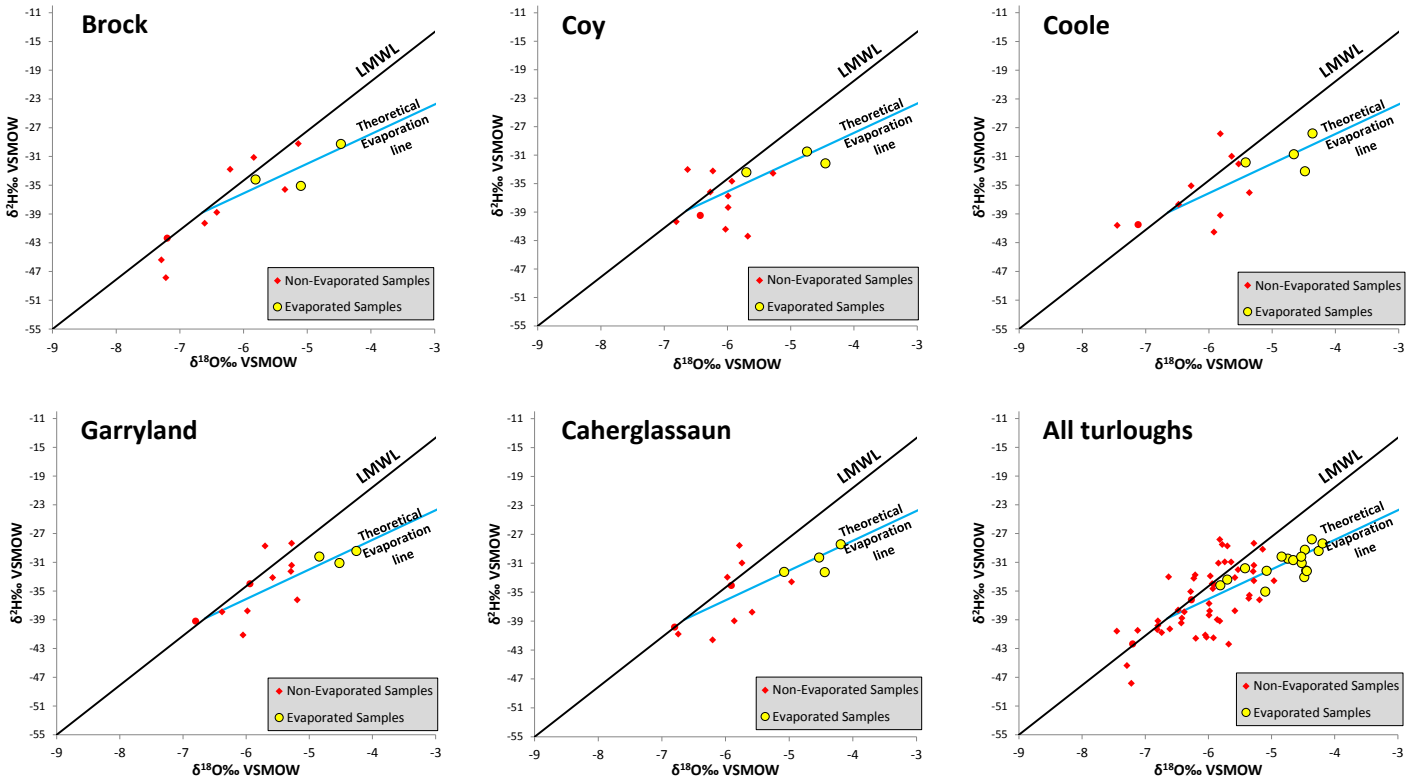

Figure 8.17: Delta plots showing evaporation influenced samples for each turlough individually and a group plot.

While Figure 8.17 indicates that the turloughs are affected by evaporation equally, some differences can be observed relating to the flooding/retention behaviour of the turloughs. The two turloughs with greatest range along the LMWL are Blackrock and Coole. They are also only turloughs which

show $^{18}\delta$ values below -7‰. This is due to their close relationship with the rivers feeding them. The other three turloughs on the other hand, show more damped behaviour with less range along the LMWL. This trend can also be seen in Table 8.2 where the two least enriched turloughs are Blackrock and Coole with mean $^{18}\delta$ values of -6.21 and -5.94 respectively. Overall it can be said that river input has greater degree of isotopic influence over the turloughs than evaporation.

8.3.3 Groundwater

As discussed previously, in temperate regions the isotopic composition of groundwater reflects the mean isotopic composition of precipitation. In the Gort Lowlands, the mean $^{18}\delta$ composition of rainfall was found to be -6.65‰ (based on the intersection of LMWL and evaporation line). Initially groundwater appears more enriched than the rainfall with an $^{18}\delta$ value of -6.42‰ (Table 8.2). However when evaporation influenced samples (from exposed wells, BH12 and BH14) are removed, this mean value becomes -6.57‰, only fractionally more enriched than the rainfall (and slightly lighter than -6‰, as predicted by Darling et al. (2003)). The delta-plot for groundwater taken from sites BH3, BH7, BH14 and BH16 is shown in Figure 8.18 (other sites were not sampled for $^{2}\delta$). In this plot, the data shows considerable variation and a bias towards the evaporation side of the LMWL. However these values lie within the variation shown by the other surface water data points (Figure 8.9).

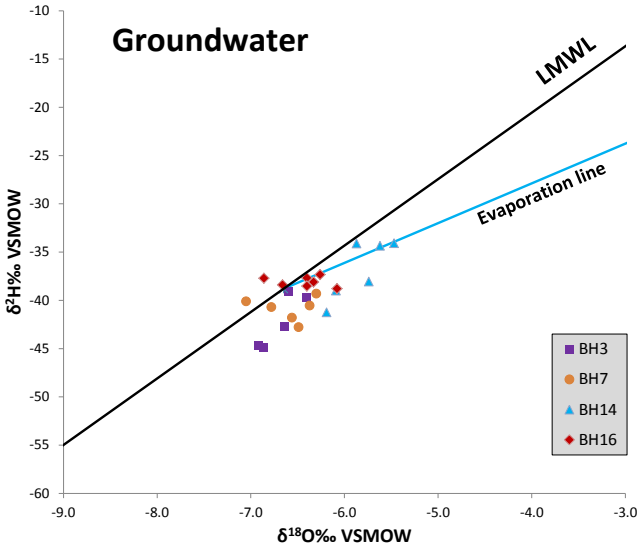

Figure 8.18: Delta plot of groundwater.

Unlike the chemical nature of groundwater which can be continuously altered by geochemical interactions with bedrock, the isotopic composition of groundwater should remain relatively

constant (unless temperatures rise above 60°C) (Gat, 2010). This lack of variation is evident in the Gort Lowlands and can be seen in time series plots of $^{18}\delta$ (Figure 8.19).

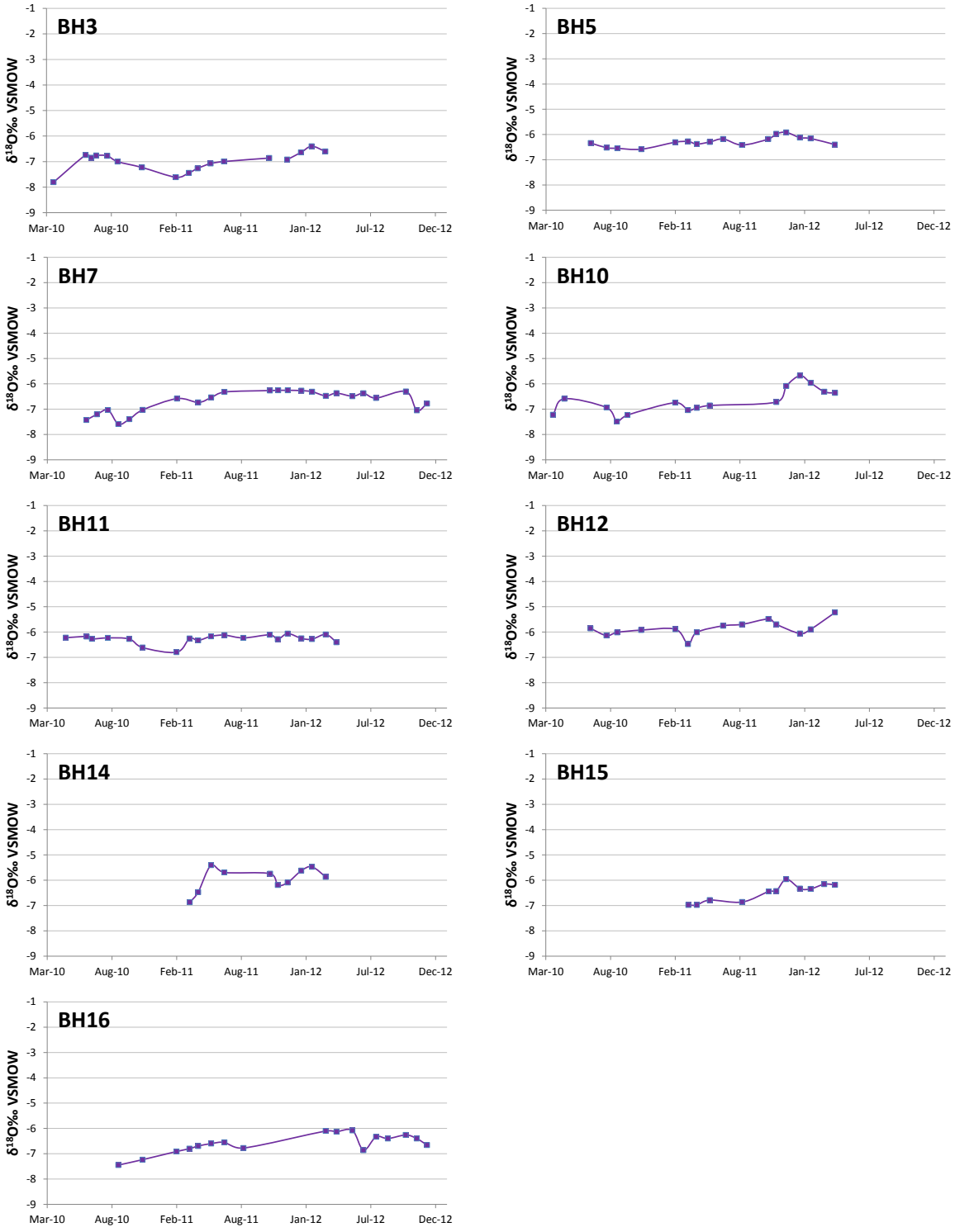

Figure 8.19: Time series plots of $^{18}\delta$ in groundwater.

These plots (Figure 8.19) show much less temporal variation than their relevant alkalinity (Figure 7.7) or nutrient plots (Figures 7.47 and 7.48). However, the sites do show a degree of spatial variability. For instance, water in BH3 appears quite isotopically light with a mean $^{18}\delta$ value of -6.95‰ whereas BH5 and BH11 show heavier mean $^{18}\delta$ values of approximately -6.3‰ (Table 8.2). This relative lightness of BH3 could possibly be explained by its proximity to the Slieve Aughtys which would result in isotopically lighter rainfall due to the altitude effect. Overall groundwater shows a slight seasonal effect with winter showing the heaviest mean $^{18}\delta$ value (-6.30‰) whereas mean $^{18}\delta$ values for the other seasons all lie between -6.48‰ and -6.55‰. This trend is in noticeable contrast to precipitation which tends to show lightest isotopic composition in winter. Although this contrast could possibly be due bias as far more samples were collected during winter than during summer.

No meaningful relationship was found between $^{18}\delta$ and depth of sample. However a slight pattern can be seen whereby only samples taken from depths less than 4m show $^{18}\delta$ values heavier than roughly -6‰ and only values deeper than 5m show $^{18}\delta$ values lighter than -7‰. This trend is illustrated below in Figure 8.20.

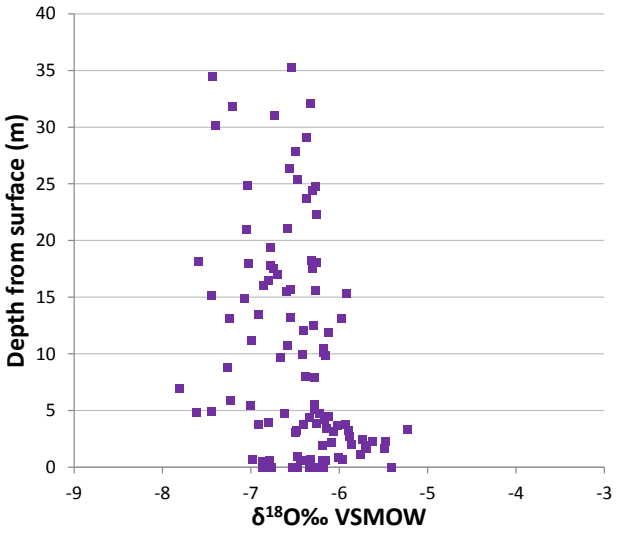

Figure 8.20: $^{18}\delta$ verses depth of sample from surface.

8.3.4 Kinvara

As Kinvara (KW) is the main outlet for the whole Gort Lowlands system, the isotopic composition of its water could be expected to match that of the catchment feeding it, and indeed it does. This close relationship can clearly be seen in a time series plot of Caherglassaun alongside KW (Figure

8.21). The temporal isotopic pattern of KW is essentially an extremely damped and attenuated version of the river isotopic time series shown in Figure 8.10 (which is itself, a damped time series of precipitation).

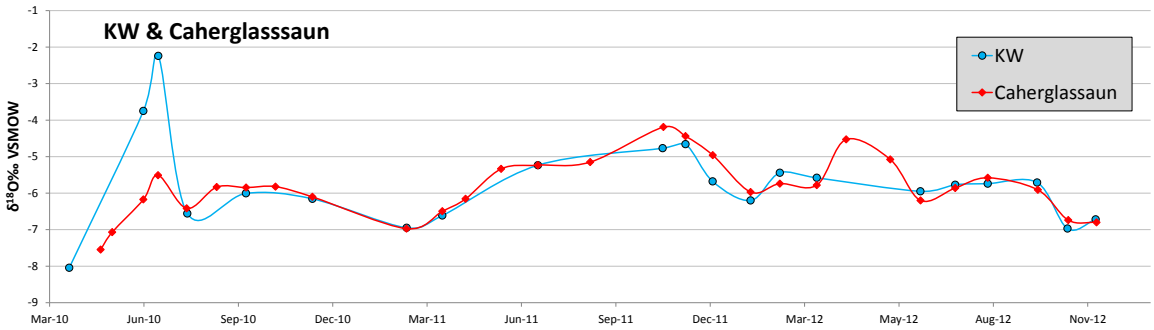

Figure 8.21: Time series plot of Caherglassaun and Kinvara West (KW).

It is interesting to note the difference between the Caherglassaun-KW $^{18}\delta$ plot (Figure 8.21) and the Caherglassaun-KW alkalinity plot (Figure 7.11). In the alkalinity plot, KW showed alkalinity values consistently higher than Caherglassaun (by approximately 30%) whereas in the $^{18}\delta$ plot, the values are more or less the same. This differing behaviour is further evidence of the contribution of diffuse groundwater and external catchment water between Caherglassaun and Kinvara. The additional water has an alkalinity much greater than that within the active conduit system but the $^{18}\delta$ is quite similar. Thus the alkalinity of the water changes but the isotopic signature does not.

This relationship with the turloughs can also be seen in the delta plot of KW in Figure 8.22 which shows KW samples typically lying along the LMWL. Similarly to groundwater, there is a slight bias towards the right hand side of the LMWL. The occurrence of this bias at Kinvara confirms the considerable contribution of groundwater/diffuse flow that the pipe-network has picked up on its path towards Kinvara. The mean $^{18}\delta$ value for KW is -5.75‰, which is in line with the values found at Caherglassaun (-5.75‰) and Garryland turloughs (-5.72‰). KE, on the other hand, shows a lighter mean $^{18}\delta$ value of -6.20‰ reflecting the greater component of isotopically lighter groundwater discharging from this spring. KE also shows a smaller range along the LMWL (Figure 8.22) which indicates how the spring is not influenced by the extremes of rainfall/surface water events to the same degree of KW.

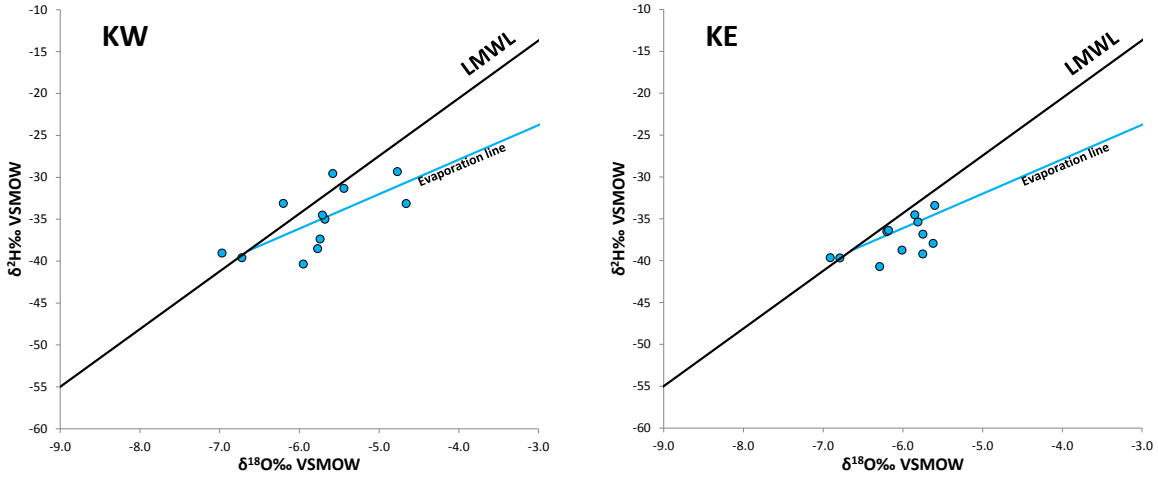

Figure 8.22: Delta plots of Kinvara West (KW) and Kinvara East (KE).

The relationship between KW and KE is further investigated in Figure 8.23. Similarly to the rivers, KW shows isotopically lighter water in winters 2010-2011 and 2012-2013 and a smaller dip in winter 2011-2012. KE appears lighter than KW for the most part and shows less variation, noticeably showing a much smaller and earlier dip than KW in winter 2011-2012.

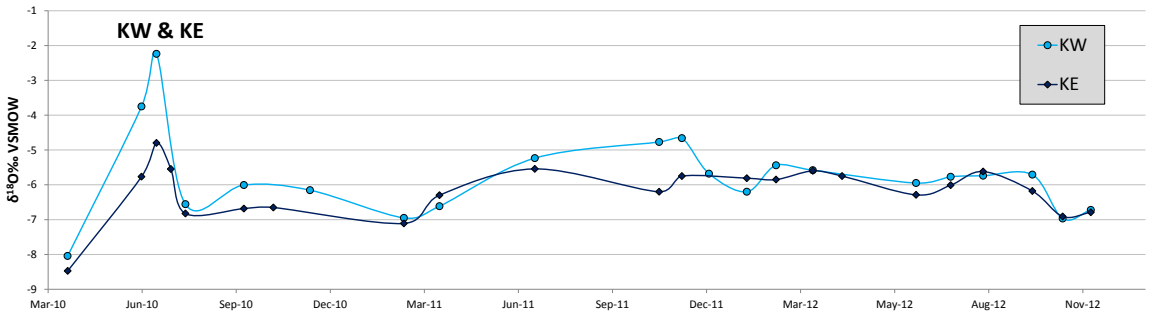

Figure 8.23: Time series plot of $^{18}\delta$ at Kinvara West (KW) and Kinvara East (KE).

The most striking aspect of the time series plot (Figure 8.23) is the extremely light water in March 2010 followed by extremely enriched water in June 2010. The light values in March can be attributed to the heavy flooding of the previous winter. The heavy flooding of 2009-2010 would have inundated the catchment with isotopically light winter rainfall. This rainfall could likely have been especially depleted in $^{18}\delta$ as the intensity of rainfall may have invoked the 'rainfall amount effect'. This effect involves rainfall becoming more depleted in $^{18}\delta$ as rainfall intensity increases. Convective storms in NW Europe have been seen to lighten the $^{18}\delta$ composition of water by up to 7‰ in one hour (Mook, 2006) (this effect was not demonstrated through the rest of the study period). Similarly, the peak values of June 2010 are also weather related. The peaks in KW and KE

are the result of both direct and indirect effects caused by the relatively dry weather over this period. As the weather was quite warm and dry, it led to some instances of heavy enrichment such as that seen Coy turlough. Thus the evaporation directly enriched the water. However, on a catchment scale, the enrichment was minor (the other three non-empty turloughs showed little enrichment). The other indirect but more significant reason for the peaks is due to the low discharge from KW during the dry period. The lack of water pumping out of KW enabled a greater degree of salt-water intrusion into the aquifer/conduit network (verified by the Infoworks model). Thus even though samples were taken of water flowing out of Kinvara, the discharging water would have been somewhat mixed with seawater. As seawater has an $^{18}\delta$ value of 0‰ (by definition), the contribution of seawater would have enriched the samples. Unfortunately, EC measurements were not taken at this time to verify this theory.

8.4 Discussion

This isotopic study offered a rare look into the behaviour of stable isotopes in an Irish catchment, particularly as the study incorporated almost three years of data. Compared to the more typical hydrochemical analysis methods of Chapter 7, isotope studies offer a set of parameters which operate differently. These parameters, $^{18}\delta$ and $^{2}\delta$, relate to the chemical composition of the water molecule itself rather than an external chemical signature. As such, the isotopic composition of water in the catchment does not alter due to processes such as water-rock interaction or pollution. The only process that can impart a measurable change to the isotopic composition of water (in this catchment) is evaporation. From this study, a number of findings and conclusions could be drawn about the catchment:

- The isotopic composition of rainfall in Western Ireland was shown to be relatively isotopically light, lighter than that of Valentia or the global average. The LMWL for the Gort Lowlands was estimated as $^{2}\delta = 6.9^{18}\delta + 7‰$, showing a lower slope and slightly higher d-excess than Valentia ($^{2}\delta = 7.25^{18}\delta + 4.8‰$). As such, any future isotopic studies in the region (or regions further from Valentia) should endeavour to determine their own LMWL rather than using the Valentia LMWL, as use of the Valentia LMWL may produce misleading results.

- The most depleted values of $^{18}\delta$ in the catchment were found in the groundwater, followed by the rivers and then the turloughs. $^{18}\delta$ values were seen to decrease as the water moved through the conduit network due to the frequent interaction with the atmosphere.

Looking at the turloughs in particular, isotopic behaviour was found to be in accordance with the findings of Chapter 7.

- All turloughs (not just the flow-through turloughs) showed a close relationship with the isotopic composition of rainfall and the rivers feeding them. Evaporation effects were only observed at low-water levels during the summer. Thus overall, evaporation had only a minor effect on turlough water volumes.

- Turloughs displayed similar flow-through and surcharge tank behaviour to that found in the previous chapter. However, this behaviour resulted in more mixed hydrochemical patterns due to isotopic composition of groundwater being either higher or lower than the turlough depending on conditions (unlike alkalinity in which the groundwater is always higher). As a result, the isotopic composition of the turloughs showed drifts upwards or downwards depending its original $^{18}\delta$ signature. Carrying out a mass balance calculation during a turlough recessions showed similar results to those carried out for alkalinity (discussed in Section 7.2.1.2). Of the volume of water lost during a recession, approximately 1-10% of that volume re-enters the turlough over the period of a month (based on a groundwater $^{18}\delta$ value of -6.57). Evaporative effects were also seen to become influential towards the end of a recession as summer approached.

- A sample taken from Ballinduff turlough (Section 7.6) in December 2012 had an isotopic value of $^{18}\delta$: -6.76, $^{2}\delta$: -39.31, lying directly on the LMWL and only slightly more depleted than the average groundwater value ($^{18}\delta$: -6.57). This value is in accordance with the concept that Ballinduff is a primarily groundwater fed turlough (rather than river/conduit fed).

Chapter 9

Conclusions

9 CONCLUSIONS

9.1 Conclusions

In this project, the hydrology and hydrochemistry of the Gort Lowlands catchment was investigated with the aid of a pipe-network model of the lowland karst conduit system. Analysis was carried out on a catchment-wide scale and at an individual turlough scale. This section discusses conclusions in terms of hydrological, modelling and hydrochemical findings. The various elements of this thesis and their inter-relationships are displayed as s synthetic sketch below in Figure 9.1.

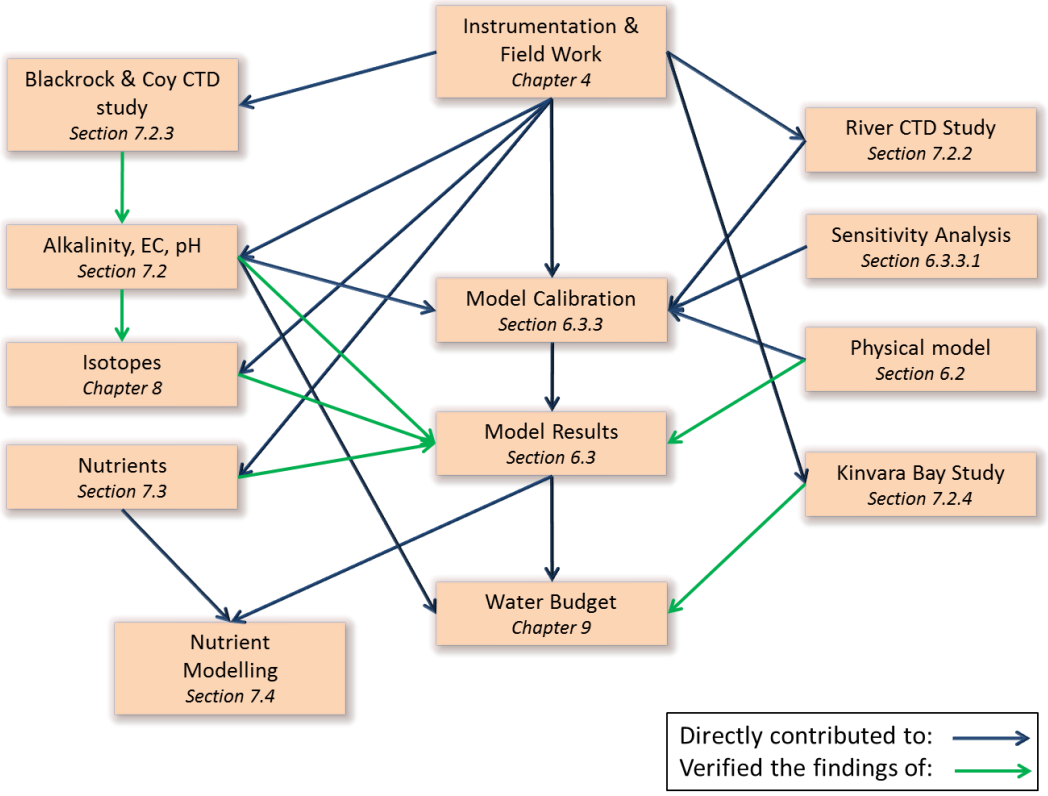

Figure 9.1: Synthetic sketch displaying the relationship between the various elements of this thesis.

HYDROLOGICAL

- The development of reliable rating curves was a key component to the understanding of the hydrological regime within the Gort Lowlands. With these improved rating curves in place, the inflows into the catchment and their associated loading rates could be

determined. The mean flow contribution into the karst lowland system from each river was calculated as 55.3%, 24% and 20.7% from the Beagh, Owenshree and Ballycahalan Rivers.

- Reservoir routing was successfully applied to Lough Cutra and found that outflow had, on average, 23% more flow than the inflow. This discrepancy is due to a number of factors including the influx of an additional minor river, direct rainfall onto the lake and suspected inaccuracies with the Owendalulleegh rating curve.

- Under most conditions, flooding starts to occur within Blackrock turlough when the flow within the Owenshree River exceeds approximately 1.23 m^3/s.

- Groundwater levels within the karst aquifer were found to be either responsive or non-responsive to changes in turlough flooding depending on vicinity to the turloughs or the active conduit network. Responsive boreholes/wells indicated a hydrologic (but not necessarily a hydrochemical) linkage to the active karst system. Non-responsive boreholes indicated a more epikarst/diffuse portion of the aquifer with very little association with the active conduit network. In some cases, a non-responsive borehole was found in close proximity to a turlough. As the water levels within the epikarst tended to lie above the turlough water levels, a hydraulic gradient was produced between a turlough and its surrounding epikarst, thus indicating a potential influx of groundwater into a turlough, particularly during a recession. This influx of epikarst water was confirmed with hydrochemical analysis.

- The rainfall-runoff modelling software, NAM, was successfully used to model the Owenshree and Ballycahalan catchments. The output of this data could then be used to fill gaps in the river flow datasets for these rivers.

MODELLING

With this improved knowledge of the catchment, the hydrological model of Gill et al. (2013a) could be recalibrated for better accuracy. Initially, a physical model was constructed in order to test a range of different conduit configuration scenarios both in terms of water levels and water mixing (using tracer). These tests found that the diameter of a turloughs 'throttle' is the most important factor controlling water levels. Tracer tests also revealed that water can transfer from one turlough to the other via the conduit linkage. A sensitivity analysis was then carried out on the numerical model in order to find out which model linkages held the most influence on turlough water levels.

Expectedly, it was found that the diameter of the conduit section directly downstream of a turlough had the greatest influence on that turloughs (and any other upstream turloughs) water level. Using the findings of these analyses (as well as a thorough investigation of previous tracer studies), the model was re-adjusted. The alterations to the model included:

- The use of more accurate river flow data.
- The application of more accurate turlough stage-volume curves.
- The addition of some new of conduit linkages (Blackrock River conduit links, Coole bypass and epikarst, Coole-Garryland epikarst linkage).

With these alterations, the estimation of water volumes was significantly more accurate for all five turloughs. Water level accuracy, on the other hand, was slightly reduced for Blackrock and Coy turloughs. Following the recalibration, the model was used for a number of purposes:

- After a successful simulation, a range of hydrologic data could be outputted. This was particularly useful for the outlet node as it gave an estimated time series for discharge at Kinvara. From this data, it could be seen that the mean flow at KW was 7.64 m^3/s (a result which was validated by a hydrochemical study of Kinvara Bay). This outflow is approximately 17% higher than the combined input from the three rivers. This increase is due to the contribution of rainfall on the epikarst which gradually feeds into the conduit network. This Kinvara flow data could then be used for hydrochemical analysis. Time series data was also used to fill in gaps in turlough stage data caused by equipment failure.

- Using the calibrated subcatchments from the model, the mean outflow from KE was calculated based on the premise that bedrock geology (and thus the model calibration) is similar for both KE and KW catchments. Outflow was estimated as 1.06 m^3/s (i.e. an increase of 10.6% on the total outflow from KW).

- The sensitivity of a number of model parameters was carried out. Findings included:
    - Increased conduit roughness led to increased turlough flooding.
    - Elliptical conduits led to reduced turlough flooding (unexpectedly).
    - Of the subcatchment parameters, the ones relating to percolation through the unsaturated zone proved to be most influential.

- All five turloughs show very little sensitivity to temporal input variation on the scale of 24 hours, i.e. any pattern of rainfall over 24 hours results in the same flooding pattern (so long as the quantity of rain is kept constant). For the lower three turloughs, little sensitivity can be picked up from the simulations for a period of up to five days.

- A selection of climate change scenarios were applied to the model in order to estimate future flooding patterns. Projections for the 2020's, 2050's and 2080's indicated that, in the future, turloughs shall generally be emptier for a greater proportion of the year. However, winter flooding shall be more severe. For instance, IPCC scenario A2 suggests that by 2080, a typical winter flood could reach the levels of the 1-in-500 year floods of November 2009.

HYDROCHEMICAL

Hydrochemical analysis sheds light on the distinctive allogenic recharge nature of the Gort Lowlands. This behaviour is particularly evident when observing the altering alkalinity concentrations (or EC) across the catchment. Some of the main findings from the alkalinity measurements were the following:

- The alkalinity of the turloughs was closely related to the alkalinity of their feeding rivers. Blackrock and Coy showed very similar concentrations to their feeding river whereas the lower three turloughs displayed higher alkalinity concentrations, most likely due to the contribution of high alkalinity water from the epikarst as water moved through the system. Using CTD divers, this epikarst contribution was estimated as adding 8.7% to the total flow (between Kilchreest and Blackrock turlough). For this same stretch of river, the model predicted 10% epikarst contribution. The contribution increases with distance along the conduit network (for example, the model predicts 11% contribution at Coole and 17% at Kinvara). Overall, alkalinity concentrations within the catchment and the turloughs confirmed the predictions of the hydraulic model.

- Blackrock and Coole turloughs both exhibit flow-through behaviour whereas Coy and Caherglassaun present surcharge tank behaviour. The behaviour of Garryland changes depending on water level; at lower water levels, it acts as a surcharge tank and at higher water levels, it hydraulically joins with Coole and acts more like a flow-through system. Alkalinity measurements also showed an influx of diffuse groundwater into the turloughs

over the flooding season. The volume of water entering the turloughs amounted to between 1 and 10% of the entire volume that drained from the turlough during a recession. The contrasting behaviour between a flow-through and surcharge tank turlough was shown in greater detail with the use of CTD divers in Blackrock and Coy turloughs. This sub-study illustrated the complex nature of turlough-groundwater interaction within Blackrock turlough (EC data suggests flooding and draining occurring at the same time) compared with the relatively simpler surcharge tank behaviour of Coy turlough.

- Combining alkalinity data with the hydrological model, a mass balance was carried out between Caherglassaun turlough and Kinvara West. This calculation found that flow at Kinvara West is enhanced by approximately 14-18% due to contribution from external catchments which are not included in the model.

Analysis of nutrient concentrations within the catchment presented the following findings:

- As water moves through the catchment, it becomes further enriched with N due to contribution from the N-enriched epikarst. As a result of this enrichment, the N load at Kinvara was shown to be approximately 17% higher than that of the combined river input into the system. This load is lower than would be expected (based on model results) due to N losses within the turloughs. The primary mechanism of N loss within the turloughs was determined to be denitrification.

- Unlike N, P loads decrease as water moves through the catchment. The P load discharging at Kinvara was found to be approximately 8% lower than the combined input from the rivers. This reduction is due to the minimal contribution of P from the epikarst and P losses from the turloughs. The primary mechanism of P loss within the turloughs was deemed to be sedimentation.

- Overall, the turloughs appear to act as nutrient sinks over the flooded period, particularly the surcharge tank turloughs. Blackrock and Coy turloughs, however, were found to be nutrient sources, primarily due to the presence of an abattoir at Blackrock (enhancing N and P) and a high degree of grazing during dry periods (enhancing P).

Isotopic analysis of the catchment revealed that the $^{18}\delta$ signature of water becomes slightly enriched as it moves through the catchment due to frequent interaction with the atmosphere (causing slight

evaporative effects). Overall however, the effect of evaporation within the catchment is quite minor. Within the turloughs, evaporation tends to only take place during the summer when the turlough water levels are low. Thus the evaporative effect on turlough water volumes is negligible. Also, isotopic patterns within the turloughs backed-up the findings of the alkalinity measurements which suggested some contribution to the turloughs from their surrounding epikarst over a flooded period. Overall however, the isotopic study proved to be only marginally beneficial to the findings of this thesis, providing little information which could not be determined using other (cheaper, less work intensive) hydrochemical parameters such as EC or Alkalinity. Isotopes can be extremely effective in some well-designed experiments (involving high evaporation rates) however their effectiveness is limited in such a regional study.

Combining the findings of the hydrological, modelling and hydrochemical studies, an approximate water budget can be made. This budget is shown schematically in Figure 9.2. In this figure, the relative contributions of water to the system and their approximate mean flows are presented. The three rivers can be seen to contribute 25%, 21% and 55% each. This total river flow is then supplemented by an additional 17% from diffuse flow as water moves through the system. Then as the water reaches KW, its flow has been further supplemented by an additional 14-18% (of the combined river and diffuse flow) from external catchments which were not included in the model. Then at Kinvara, the flow from KW is combined with the additional discharge from KE to give a total discharge into Kinvara Bay of approximately 9.7 – 10 m^3/s.

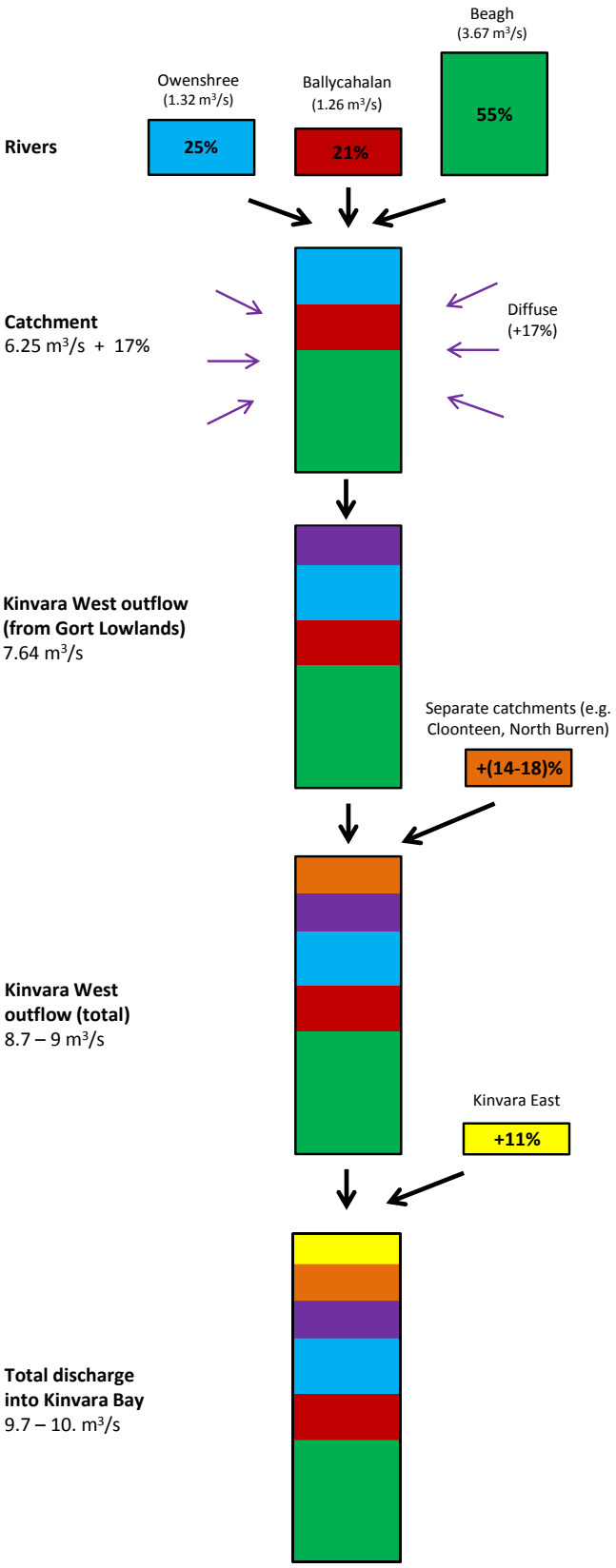

Figure 9.2: Gort Lowlands water budget schematic.

9.2 Recommendations for Further Research

HYDROLOGICAL MONITORING NETWORK

- For future studies within this catchment, an additional rain gauge should be installed within the Owendalulleegh River catchment. This would allow for more accurate rainfall-runoff modelling of the Owendalulleegh River.

- The river rating curves could be improved upon with the measurement of more high flow stage-discharge points, particularly for the Owendalulleegh River.

- A number of OPW river gauging stations are susceptible to data loss due to equipment failure. In future studies, it would be beneficial to install divers at these river stations to act as a back-up for the OPW gauges.

HYDROLOGICAL INVESTIGATIONS

- It has already been shown by O'Connell et al. (2011) that geophysical methods (electrical resistivity tomography) can be used within the Gort Lowlands to characterise the karst bedrock and identify underground conduit. Thus far, only a limited number of geophysical investigations have been carried out. Further investigations could involve:
    - Locating a conduit and tracing its path between turloughs. This would be particularly interesting between Blackrock and Coy turloughs as the connection between these turloughs proves to be the most difficult to model.
    - Attempting to identify the path and size of the northern flow route between Castle-Daly and Kinvara East (KE). A study such as this might start at Kinvara and work backwards as any hydraulic feature would be larger and more detectible at the downstream end.
    - Proving the existence of conduits feeding water directly from the Cloonteen catchment towards the western cave network (bypassing the turloughs). These conduits were suggested by the Gort Flood Studies Report (Southern Water Global, 1998).

- Aerial thermal imagery could be used during flooding periods to investigate which estavelles are most active within a turlough. Such a study would be hugely beneficial for the understanding of turloughs such as Blackrock which have multiple estavelles scattered

across their base. The best periods for such a study would be winter or summer as the lake temperature would show the greatest contrast to the groundwater temperature during these periods.

- Additional tracer studies could be carried out to further delineate hydrological linkages within the karst lowlands. Potential future tracer studies could involve:
    - Further investigation into where water in the northern portion of the lowlands drains to, i.e. whether it drains northwards towards the Dunkellin River catchments or towards Kinvara East (or possibly West).
    - Determining the path of water draining from Ballinduff turlough, i.e. whether it joins the northern flow route and ends up at Kinvara East or drains southwards and joins the active conduit network, ending up at Kinvara West. A similar study could be carried out for Lydacan turlough which lies in-between Ballinduff and Kinvara.
    - A tracer study of Blackrock and Coy turloughs (originally intended to be carried out as part of this thesis). For example, at the onset of a flooding event, tracer could be injected into the Owenshree River near Kilchreest. From this injection, a number of aspects of the turloughs' hydrology could be investigated:
        - The difference in tracer quantity within the river between Kilchreest and Blackrock inlet could provide an approximation of losses from the river to the conduit network.
        - The retention time of water within Blackrock turlough could be estimated.
        - What proportion of river water bypasses Blackrock and fills Coy.
        - How much water drains from Blackrock into Coy over the course of a flooded period.

      A tracer study such as this would require significant manpower, time and tracer quantity. The timing of the study would also be critical. Ideal hydrologic conditions for injection may only occur a few times a year.

MODELLING

- Further developments could be made to the hydraulic model to improve its accuracy. The most critical addition would be the inclusion of the Cloonteen catchment to the south. In order to facilitate this, the Cloonteen River would need to be gauged. Hawkhill and Newtown turloughs would also need to be monitored.

- Climate change modelling could be combined with the study of conduit dissolution rates. Thus it could be determined if the dissolution and expansion of the water carrying conduits could act in some way to mitigate the effects of climate change, i.e. as future flows within the conduits increase (during winter), so do the conduit sizes, thus diminishing the potential flood water volumes.

- Further work could be carried out in Kinvara in order to estimate the outflow of freshwater. This estimate could then be used to validate the hydraulic model.

- To improve the accuracy of the model for low flow scenarios, the calibration procedure for the model could be overhauled such that low flow scenarios are calibrated first, then higher flow scenarios are subsequently accounted for by adding upper level conduits. For an example of this technique, see Jeannin (2001).

HYDROCHEMISTRY

- In future, targeted sampling campaigns could be used rather than (or in addition to) continuous monthly sampling. Two or three concentrated sampling campaigns over some individual flooding periods may allow greater confidence in determining a turloughs nutrient flux. In addition to this, some high temporal resolution nutrient sampling of the rivers should be carried out at the onset of a flooding event, particularly for the Owenshree River. High resolution river data such as this would rule out the possibility of missing any nutrient peaks which could be measured in the turloughs but missed in the rivers. Thus, sampling resolution could be ruled out as a cause for imbalanced river-turlough nutrient concentrations.

- Further investigations should be carried out into the homogeneity of turloughs in terms of nutrients. However future studies should put more emphasis into the vertical profile of the turloughs, particularly within the surcharge tank turloughs. Such a study should include measurement of both N and P but also dissolved oxygen which would shed light on the potential for denitrification at depth within the turlough. Denitrification could also be investigated using stable nitrogen isotopes (^{15}N).

- In future, nutrient sampling should be carried out at both ends of Lough Cutra (Owendalulleegh and Beagh). This would allow for the analysis of nutrient gain or loss across Lough Cutra and provide a more accurate hydrochemical input for the hydrological model.

- Further study of the heterogeneity of Blackrock turlough could be carried out using a greater amount of CTD-divers. CTD-divers could also be attached to the rope between the buoy and the diver platform in order to get multiple depth profiles.

References

Adams, R. & Parkin, G. (2001). Development of a coupled surface-groundwater-pipe network model for the sustainable management of karstic groundwater. *8th Multidisciplinary Conference on Sinkholes and the Engineering and Environmental Impacts of Karst.* Louisville, Kentucky.

Adams, R. & Younger, P. L. (2001). A strategy for modelling ground water rebound in abandoned deep mine systems. *Ground Water,* 39**,** 249-261.

Aggarwal, P. K., Froehlich, K. & Gonfiantini, R. (2011). Contributions of the International Atomic Energy Agency to the development and practice of isotope hydrology. *Hydrogeology Journal,* 19**,** 5-8.

APHA (1999). *Standard Methods for Examination of Water & Wastewater*, American Public Health Association 20th Edition.

Atkinson, T. C. (1977). Diffuse flow and conduit flow in limestone terrain in the Mendip Hills, Somerset (Great Britain). *Journal of Hydrology,* 35**,** 93-110.

Atkinson, T. C., Smart, P. L. & Wigley, T. M. L. (1983). Climate and Natural Radon Levels in Castleguard Cave, Columbia Icefields, Alberta, Canada. *Arctic and Alpine Research,* 15**,** 487-502.

Atkinson, T. C., Smith, D. I., Lavis, J. J. & Whitaker, R. J. (1973). Experiments in tracing underground waters in limestones. *Journal of Hydrology,* 19**,** 323-349.

Baedke, S. J. & Krothe, N. C. 2000. Quantitative tracer test of the Beech Creek aquifer at the Ammunition Burning Grounds, Naval Surface Warfare Centre, Crane, Indiana. *In:* Sasowsky, I. D. & Wicks, C. M. (eds.) *Groundwater Flow and Contaminant Transport in Carbonate Aquifers.* Rotterdam: A.A. Balkema.

Baertschi, P. (1976). Absolute 18O content of Standard Mean Ocean Water. *Earth and Planetary Science Letters,* 31**,** 341-344.

Baldock, D. (1984). *Wetland drainage in Europe.*, London, Institute for European Environmental Policy.

Barnes, S. (1999). Karstic groundwater flow characteristics in the Cretaceous Chalk aquifer, Northern Ireland. *Quarterly Journal of Engineering Geology and Hydrogeology*, 32**,** 55-68.

Bartley, P., Moran, J. & Kuczynska, A. (2009). Risk of Nutrient Export Model. Final Report for the BurrenLIFE Project - Farming For Conservation in the Burren.

Bechtel, T. D., Bosch, F. P. & Gurk, M. 2007. Geophysical methods. *In:* Goldscheider, N. & Drew, D. (eds.) *Methods in Karst Hydrogeology.* London: Taylor & Francis.

Behrens, Beims, Dieter, Dietze, Eikmann, Grummt, Hanisch, Henseling, Käß, Kerndorff, Leibundgut, Müller, W., Rönnefahrt, Scharenberg, Schleyer, Schloz & Tilkes (2001). Toxicological and ecotoxicological assessment of water tracers. *Hydrogeology Journal,* 9**,** 321-325.

Beltman, B., Rouwenhorst, G., Whilde, A. & Cate, M. T. (1993). Chemical Composition of Rain in Western Ireland. *The Irish Naturalists' Journal,* 24**,** 267-274.

Benischke, R., Goldscheider, N. & Smart, C. 2007. Tracer techniques. *In:* Goldscheider, N. & Drew, D. (eds.) *Methods in karst hydrogeology.* London: Taylor & Francis.

Blackstock, T. H., Duigan, C. A., Stevens, D. P. & Yeo, M. J. M. (1993). Vegetation zonation and invertebrate fauna in Pant-y-Llyn, an unusual seasonal lake in South Wales, U.K. *Aquatic Conservation: Marine and Freshwater Ecosystems,* 3**,** 253-268.

Bonacci, O. (1993). Karst spring hydrographs as indicators of karst aquifers. *Hydrological Science,* 38**,** 51-62.

Bonacci, O. & Roje-Bonacci, T. (2000). Interpretation of groundwater level monitoring results in karst aquifers: examples from the Dinaric karst. *Hydrological Processes,* 14**,** 2423-2438.

Bossard, M., Feranec, J. & Otahel, J. (2000). CORINE land cover technical guide - Addendum 2000. European Environment Agency.

Boussinesq, J. (1904). Recherches theoretiques sur l'ecoulement des nappes d'eau infiltrees dans le sol et sur le debit des sources. *Journal de Mathematiques Pures et Appliquees,* 10**,** 5-78.

Bowen, R. & Williams, P. W. (1973). Geohydrologic Study of the Gort Lowland and Adjacent Areas of Western Ireland Using Environmental Isotopes. *Water Resources Research,* 9**,** 753-758.

Boycott, A., Bunce, C. & COwper, Q. (2011). Cave Notes: Co. Clare and Co. Galway, Ireland. *Proc. Univ. Bristol Spelaeol. Soc.,* 25**,** 233-248.

Burdon, D. J. & Papakis, N. (1961). Methods of investigating the groundwater resources of the parnassos-ghiona limestones. *Intern. Assoc. Sci. Hydrol. - Groundwater in Arid Zones,* 57**,** 143-159.

Butscher, C. & Huggenberger, P. (2007). Implications for karst hydrology from 3D geological modeling using the aquifer base gradient approach. *Journal of Hydrology,* 342**,** 184-198.

Cable, J. E., Riede Corbett, D. & Walsh, M. M. (2002). Phosphate Uptake in Coastal Limestone Aquifers: A Fresh Look At Wastewater Management. *Limnol Oceanogr Bull,* 11**,** 29-32.

Cave, R. R. & Henry, T. (2011). Intertidal and submarine groundwater discharge on the west coast of Ireland. *Estuarine, Coastal and Shelf Science,* 92**,** 415-423.

Chandler, D. G. & Bisogni Jr, J. J. (1999). The use of alkalinity as a conservative tracer in a study of near-surface hydrologic change in tropical karst. *Journal of Hydrology,* 216**,** 172-182.

Chapman, D. (1996). *Water quality assessments: A guide to the use of biota, sediments and water in environmental monitoring.*, UNESCO/WHO/UNEP.

Church, J. A., Gregory, J. M., White, N. J., Platten, S. M. & J.X., M. (2011). Understanding and projecting sea level change. *Oceanography,* 24**,** 130-143.

Clark, I. D. & Fritz, P. (1997). *Environmental Isotopes in Hydrogeology,* London, CRC Press.

Coxon, C. E. 1986. *A Study of the hydrology and geomorphology of turloughs.* Ph.D. (unpublished) Thesis, Department of Geography, Trinity College Dublin.

Coxon, C. E. (1987b). An examination of the characteristics of turloughs using multivariate statistical techniques. *Irish Geography,* 20**,** 24-42.

Coxon, C. E. (1994a). Carbonate Deposition in Turloughs (Seasonal Lakes) on the Western Limestone Lowlands of Ireland. I: Present day processes. *Irish Geography,* 27**,** 14-27.

Coxon, C. E. 1999. Agriculturally induced impacts. *In:* Drew, D. & Hotzl, H. (eds.) *Karst hydrogeology and human activities: impacts, consequences and implications.* Rotterdam, The Netherlands.: A.A. Blakema.

Coxon, C. E. 2011. Agriculture and Karst. *In:* Beynen, P. E. (ed.) *Karst Management.* Springer Science+Business Media.

Coxon, C. E. & Coxon, P. (1994b). Carbonate Deposition in Turloughs (Seasonal Lakes) on the Western Limestone Lowlands of Ireland. II: The Sedimentary Record. *Irish Geography,* 27**,** 28-35.

Coxon, C. E. & Drew, D. P. 2000. Interdependence of groundwater and surface water in lowland karst areas of western Ireland: management issues arising from water and contaminant transfers. . *In:* Robins, N. S. & Misstear, B. D. (eds.) *Groundwater in the celtic regions: Studies in Hard Rock and Quaternary Hydrology.* London, United Kingdom: The Geological Society of London.

Coxon, P., McMorrow, S., Coxon, C. E. & Nolan, T. 2005. Pollnahallia: A Tertiary palaeosurface and a glimpse of Ireland's pre-Pleistocene landscape. *In:* Coxon, P. (ed.) *The Quaternary of Central Western Ireland: Field Guide.* London: Quaternary Research Association.

Craig, H. (1961). Isotopic variations in meteoric waters. *Science,* 133**,** 1702-1703.

Craig, H. & Gordon, L. I. 1965. Deuterium and oxygen-18 variations in the ocean and marine atmosphere. *In:* Tongiorgi, E. (ed.) *Stable Isotopes in Oceanographic Studies and Paleo-Temperatures.* Pisa: Lab. Geol. Nucl.

Criss, R., Davisson, L., Surbeck, H. & Winston, W. 2007. Isotopic methods. *In:* Goldscheider, N. & Drew, D. (eds.) *Methods in karst hydrology.* London: Taylor & Francis.

Cunha Pereira, H. 2011. *Hydrochemistry and Algal Communities of Turloughs (Karst Seasonal Lakes).* PhD Thesis, Trinity College Dublin.

Cunha Pereira, H., Allott, N. & Coxon, C. E. (2010). Are seasonal lakes as productive as permanent lakes? A case study from Ireland. *Canadian Journal of Fisheries and Aquatic Sciences,* 67**,** 1291-1302.

Cunha Pereira, H., Allott, N., Coxon, C. E., Naughton, O., Johnston, P. & Gill, L. (2011). Phytoplankton of turloughs (seasonal karstic Irish lakes). *Journal of Plankton Research,* 33**,** 385-403.

Cvijic, J. (1924). The Evolution of Lapies: A Study in Karst Physiography. *Geographical Review,* 14**,** 26-49.

D'Arcy, G. H. 1983. *Post-drainage Assessments of Impacts on a Part of the River Clare Catchment, County Galway.* M.Sc. Thesis, Trinity College, Dublin.

Dansgaard, W. (1964). Stable isotopes in precipitation. *Tellus,* 16**,** 436-468.

Darcy, H. (1856). Les fontaines publiques de la Ville de Dijon. Dalmont, Paris, France.

Darling, W. G., Bath, A. H. & Talbot, J. C. (2003). The O and H stable isotope composition of freshwaters in the British Isles. 2. Surface waters and groundwater. *Hydrol. Earth Syst. Sci.,* 7**,** 183-195.

Darling, W. G. & Talbot, J. C. (2003). The O and H stable isotope composition of freshwaters in the British Isles. 1. Rainfall. *Hydrol. Earth Syst. Sci.,* 7**,** 163-181.

Deifendorf, A. F. & Patterson, W. P. (2005). Survey of stable isotope values in Irish surface waters. *Journal of Paleolimnology,* 34**,** 257-269.

Denić-Jukić, V. & Jukić, D. (2003). Composite transfer functions for karst aquifers. *Journal of Hydrology,* 274**,** 80-94.

Di, H. J. & Cameron, K. C. (2002). Nitrate leaching in temperate agroecosystems: sources, factors and mitigating strategies. *Nutrient Cycling in Agroecosystems,* 64**,** 237-256.

Doctor, D., Alexander, E., Petrič, M., Kogovšek, J., Urbanc, J., Lojen, S. & Stichler, W. (2006). Quantification of karst aquifer discharge components during storm events through end-member mixing analysis using natural chemistry and stable isotopes as tracers. *Hydrogeology Journal,* 14**,** 1171-1191.

Downing, J. A. & McCauley, E. (1992). The nitrogen:phosphorus relationship in lakes. *Limnology and Oceanography,* 37**,** 936-945.

Dreiss, S. J. (1982). Linear Kernels for karst aquifers. *Water Resources Research,* 18**,** 865-876.

Dreiss, S. J. (1989). Regional Scale Transport in a Karst Aquifer 1, Component Separation of Spring Flow Hydrographs. *Water Resources Research,* 25**,** 117-125.

Drew, D. P. Year. Hydrology of the north Co. Galway - south Co. Mayo lowland karst area, western Ireland. *In:* Proceedings of the 6th International Conference of Speleology, 1976 Prague. 57-61.

Drew, D. P. 1990. Hydrogeology of karstic terrains in Ireland. *In:* Back, W., Herman, J. & Paloc, H. (eds.) *Hydrogeology of selected karst regions (International Contributions to Hydrogeology).* International Association of Hydrogeologists.

Drew, D. P. 2003. The Hydrology of the Burren and of the Clare and Galway Lowlands. *In:* G.Mullan (ed.) *Caves of County Clare and South Galway.* Bristol, United Kingdom: University of Bristol Spelæological Society.

Drew, D. P. (2008). Hydrogeology of lowland karst in Ireland. *Quarterly Journal of Engineering Geology and Hydrogeology,* 41**,** 61-72.

Drew, D. P., Burke, A. M. & Daly, D. Year. Assessing the extent and degree of karstification in Ireland. *In:* Rozkowski, A., ed. International Conference on Karst Fractured Aquifers - Vulnerability and Sustainability, 1996 University of Silesia, Katowice-Ustron, Poland. 37-47.

Drew, D. P. & Daly, D. (1993). Groundwater and karstification in Mid-Galway, South Mayo and North Clare. *Report series 93/3.* Geological Survey of Ireland.

Drew, D. P., Doerfliger, N. & Formentin, K. 1997. The use of bacteriophages for multi-tracing in a lowland karst aquifer in western Ireland. *In:* Kranjc, A. (ed.) *Tracer Hydrology.* Rotterdam: Balkema.

Drew, D. P. & Jones, G. L. (2000). Post-Carboniferous pre-Quaternary karstification in Ireland. *Proceedings of the Geologists' Association,* 111**,** 345-353.

Dreybrodt, W. (1990). The Role of Dissolution Kinetics in the Development of Karst Aquifers in Limestone: A Model Simulation of Karst Evolution. *The Journal of Geology,* 98**,** 639-655.

Dreybrodt, W. (1992). Dynamics Of Karstification: A Model Applied To Hydraulic Structures In Karst Terranes. *Applied Hydrogeology,* 1**,** 20-32.

Dreybrodt, W. & Buhmann, D. (1991). A mass transfer model for dissolution and precipitation of calcite from solutions in turbulent motion. *Chemical Geology,* 90**,** 107-122.

Drogue, C. (1980). Essai d'identification d'un type de structure de magasins carbonates fissurées. Application à l'interprétation de certains aspects du fonctionnement hydrogéologique. . *Mémoires hors série Société Géologique de la France,* 11**,** 101-108.

EC (2000). Council Directive 2000/60/EC establishing a framework for Community action in the field of water policy. *Official Journal no. L 327/1, 22.12.2000*

EEC (1992). Council Directive 92/43/EEC on the conservation of natural habitats and of wild fauna and flora. Official Journal no. L 206, 27.7.92.

Einsiedl, F. (2005). Flow system dynamics and water storage of a fissured-porous karst aquifer characterized by artificial and environmental tracers. *Journal of Hydrology,* 312**,** 312-321.

Einsiedl, F. (2012). Sea-water/groundwater interactions along a small catchment of the European Atlantic coast. *Applied Geochemistry,* 27**,** 73-80.

Emblanch, C., Zuppi, G. M., Mudry, J., Blavoux, B. & Batiot, C. (2003). Carbon 13 of TDIC to quantify the role of the unsaturated zone: the example of the Vaucluse karst systems (Southeastern France). *Journal of Hydrology,* 279**,** 262-274.

EN ISO 748 (2007). Hydrometry - Measurment of liquid flow in open channels using current meters or floats.: International Organisation for Standardisation, Geneva.

Environmental Protection Agency (2000). Treatment systems for single houses - Wastewater treatment manual. Wexford, Ireland.: Enviromental Protection Agency.

Environmental Protection Agency (2004). Guidance on the assessment of pressures and impacts on groundwater dependant terrestrial ecosystems, Risk Assessment Sheet GWDTERA2a - Risk to turloughs from phosphate. *Water Framework Directive*

Pressures and Impacts Assessment Methodology, Guidance Document GW9. Working Group on Groundwater: Sub-commitee on Turloughs.

Environmental Protection Agency (2008). Climate Change - Refining the Impacts for Ireland. *STRIVE Report (2001-CD-C3-M1).* EPA, Co. Wexford, Ireland.

Environmental Protection Agency (2009). Teagasc-EPA soils and subsoils mapping project - Final Report. *In:* Fealy, R. & Green, S. (eds.). Dublin, Ireland.

Environmental Protection Agency (2011). Water Framework Directive Groundwater Monitoring Programme. Site Information: Kinvara Borehole.: Enviromental Protection Agency, Galway.

EU (1979). Directive on the Conservation of Wild Birds, European Economic Community Directive 79/409/EEC ('Birds Directive').

Ewen, J., Parkin, G. & O'connell, P. E. (2000). SHETRAN: a coupled surface/ subsurface modelling system for 3D water flow, sediment and contaminant transport in river basins. *ASCE J. Hydrol. Eng.,* , 5**,** 250-258.

Farmer, N. & Blew, D. (2010). Fluorescent dye Tracer Tests near the Malad Gorge State Park (Riddle well test). Idaho Department of Water Resources.

Fealy, R. & Sweeney, J. (2008). Climate Scenarios for Ireland. *Climate Change - Refining the Impacts for Ireland. STRIVE Report (2001-CD-C3-M1).* EPA, Co. Wexford, Ireland.

Fetter, C. W. (2001). *Applied Hydrogeology*, Prentice Hall.

Fiorillo, F. (2009). Spring hydrographs as indicators of droughts in a karst environment. *Journal of Hydrology,* 373**,** 290-301.

Fleury, P., Plagnes, V. & Bakalowicz, M. (2007). Modelling of the functioning of karst aquifers with a reservoir model: Application to Fontaine de Vaucluse (South of France). *Journal of Hydrology*, 435**,** 38-49.

Fontes, J. C., Boulange, B., Carmouze, J. P. & Florkowski, T. 1979. Preliminary oxygen-18 and deuterium study of the dynamics of Lake Titicaca. *Isotopes in Lake Studies.* Vienna: I.A.E.A.

Ford, D. C. & Williams, P. (2007). *Karst Hydrogeology and Geomorphology,* Chichester, John Wiley & Sons Ltd.

Gale, S. J. (1984). The hydraulics of conduit flow in carbonate aquifers. *Journal of Hydrology,* 70**,** 309-327.

Galway County Council (2009). Kinvara WWTP Discharge, Appropriate Assessement. Prepared by Ryan Hanley Consulting Engineers. .

Gat, J. R. (2010). *Isotope Hydrology: A study of the Water Cycle,* London, Imperial College Press.

Ghasemizadeh, R., Hellweger, F., Butscher, C., Padilla, I., Vesper, D., Field, M. S. & Alshawabkeh, A. (2012). Review: Groundwater flow and transport modeling of karst aquifers, with particular reference to the North Coast Limestone aquifer system of Puerto Rico. *Hydrogeology Journal,* 20**,** 1441-1461.

Gibson, J. J. (2002). Short-term evaporation and water budget comparisons in shallow Arctic lakes using non-steady isotope mass balance. *Journal of Hydrology,* 264**,** 242-261.

Gill, L. W. 2010. *Modelling a Network of Turloughs.* PhD Thesis, University of Dublin, Trinity College, Ireland.

Gill, L. W., Naughton, O. & Johnston, P. (2013a). Modelling a network of turloughs in lowland karst. *Water Resources Research,* 49**,** 3487-3503.

Gill, L. W., Naughton, O., Johnston, P. M., Basu, B. & Ghosh, B. (2013b). Characterisation of hydrogeological connections in a lowland karst network using time series analysis of water levels in ephemeral groundwater-fed lakes (turloughs). *Journal of Hydrology*.

Goldscheider, N. & Andreo, B. 2007. The geological and geomorphological framework. *In:* Goldscheider, N. & Drew, D. (eds.) *Methods in karst hydrogeology.* Taylor & Francis.

Goldscheider, N. & Drew, D. (2007). *Methods in karst hydrology,* London, Taylor & Francis Group.

Goldscheider, N., Meiman, J., Pronk, M. & Smart, C. (2008). Tracer tests in karst hydrogeology and speleology. *International Journal of Speleology,* 37**,** 27-40.

Gonfiantini, R. 1986. Environmental isotopes in lake studies. *In:* Fritz, P. & Fontes, J. C. (eds.) *Handbook of Environmental Isotope Geochemistry.* New York: Elsevier.

Gonfiantini, R. & Zuppi, G. M. (2003). Carbon isotope exchange rate of DIC in karst groundwater. *Chemical Geology,* 197**,** 319-336.

Goodwillie, R. (1992). Turloughs over 10 hectares: Vegetation survey and evaluation. Unpublished report for the National Parks and Wildlife Services, Office of Public Works, Dublin.

Goodwillie, R. (2001). Materials for an Action Plan for the priority habitat Turloughs. . *Draft Report for National Parks and Wildlife,* . Duchas, Dublin.

Goodwillie, R. 2003. Vegetation of turloughs. *In:* Otte, M. L. (ed.) *Wetlands of Ireland, Distribution, ecology, uses and economic value.* Dublin: University College Dublin Press.

Gray, N. (1995). Composition of septic tank effluent. *The Geological Survey Ireland groundwater newsletter,* 27**,** 8.

Greene, E. A., Shapiro, A. M. & Carter, J. M. (1999). Hydrogeologic characterization of the Minnelusa and Madison aquifers near Spearfish, South Dakota. . US Geol. Surv., Water Resour. Inv. Rept. 98-4156, 64.

Groves, C. G. 2007. Hydrological Methods. *In:* Goldscheider, N. & Drew, D. (eds.) *Methods in Karst Hydrogeology.* Taylor & Francis.

Groves, C. G. & Howard, A. D. (1994a). Early development of karst systems: Preferential flow path enlargement under laminar flow. *Water Resources Research,* 30**,** 2837–2846.

Groves, C. G. & Howard, A. D. (1994b). Minimum hydrochemical conditions allowing limestone cave development. *Water Resources Research,* 30**,** 607-615.

Grund, A. (1914). Der Geographische Zyklus im Karst. *Gesellschaft für Erdkunde,* 52**,** 621-640.

GSI (2011). Karst Database. Geological Survey of Ireland.

Gunn, J. (1983). Point-recharge of limestone aquifers — A model from New Zealand karst. *Journal of Hydrology,* 61**,** 19-29.

Gunn, J. (2006). Turloughs and Tiankengs: Distintive Doline Forms. *Speleogenesis and Evolution of Karst Aquifers,* 4**,** 1-4.

Gurrieri, J. T. & Furniss, G. (2004). Estimation of groundwater exchange in alpine lakes using non-steady mass-balance methods. *Journal of Hydrology,* 297**,** 187-208.

Harden, H. S., Chanton, J. P., Rose, J. B., John, D. E. & Hooks, M. E. (2003). Comparison of sulfur hexafluoride, fluorescein and rhodamine dyes and the bacteriophage PRD-1 in tracing subsurface flow. *Journal of Hydrology,* 277**,** 100-115.

Herak, M. & Stringfield, V. T. (1972). Karst, in Important Karst Regions of the Northern Hemisphere. *Elsevier, Amsterdam***,** 551 pp.

Hickey, C. (2010). The use of multiple techniques for conceptualisation of lowland karst, a case study from County Roscommon, Ireland. *Acta carsologica,* 39.

Holman, I. P., Howden, N. J. K., Bellamy, P., Willby, N., Whelan, M. J. & Rivas-Casado, M. (2010). An assessment of the risk to surface water ecosystems of groundwater P in the UK and Ireland. *Science of The Total Environment,* 408**,** 1847-1857.

Howard, A. D. & Groves, C. G. (1995). Early development of karst systems: 2. Turbulent flow. *Water Resources Research,* 31**,** 19-26.

Hunkeler, D. & Mudry, J. 2007. Hydrochemical methods. *In:* Goldscheider, N. & Drew, D. (eds.) *Methods in Karst Hydrology.* London: Taylor & Francis.

IPCC (2000). Special Report on Emissions Scenarios. *In:* Nakicenovic, N. & Swart, R. (eds.). Cambridge University Press, UK.

IPCC (2007). Climate Change 2007: Impacts, Adaptation and Vulnerability. Contribution of Working Group II to the Fourth Assessment Report of the Intergovernmental Panel on Climate Change. *In:* Parry M.L., Canziani, O. F., Palutikof, J. P., P.J., V. D. L. & Hanson, C. E. (eds.). Cambridge University Press, Cambridge, UK and New York, USA.

Jeannin, P. Y. (2001). Modeling Flow in Phreatic and Epiphreatic Karst Conduits in the Hölloch Cave (Muotatal, Switzerland). *Water Resources Research,* 37**,** 191-200.

Jennings, J. N. (1972). Karst. Cambridge, Mass: Massachusetts Institute of Technology Press.

Jennings O'Donovan & Partners (2010a). Assessment of the existing Kiltiernan/Ballinderreen Flood Relief Scheme. *Review of the South Galway Flood Studies Report.* Office of Public Works, Galway.

Jennings O'Donovan & Partners (2010b). Review of the recommendations & conclusions of the Mannin Cross, Kilchreest & Termon 2003 Flood alleviation schemes. *Review of the South Galway Flood Studies Report.* Office of Public Works, Galway.

Jennings O'Donovan & Partners (2011). Engineering Proposals for the Reinstatement of Culverts on the N18 and the Provision of New Culverts on Minor Roads at Kiltartan / Feasibility of an Overland Channel from Coole to Kinvarra:. *Review of the South Galway Flood Studies Report.* Office of Public Works, Galway.

Jensen, J. P., Kristensen, P. & Jeppesen, E. (1991). Relationships between N loading and in-lake N concentrations in shallow Danish lakes. *Verhandlungen Internationale Vereinigung Theoretisch Angewandte Limnologie,* 24**,** 201-204.

Johnston, P. & Peach, D. 1998. Groundwater modelling in the karst limestones of the Gort lowlands. Regional Lecture. In: Proceedings of the International Association of Hydrogeologists (Irish Group) 18th Annual Groundwater Seminar, Portlaoise, 21–22 April, 1998. IAH,Dublin.

Johnston, P. M. & Peach, D. Year. Hydrological modelling of the flows in the karst limestones of the Gort Lowlands. *In:* Proceedings of the Annual Irish Association of Hydrogeologists Symposium, 1999 Tullamore, Co. Offaly, Ireland.

Jukic, D. & Denic-Jukic, V. (2005). Nonlinear kernel functions for karst aquifers. *Journal of Hydrology,* 328**,** 360-374.

Karst Working Group (2000). *The Karst of Ireland: Limestone Landscapes, Caves and Groundwater Drainage Systems* Dublin, Geological Survey of Ireland.

Käss, W. (1998). *Tracing technique in geohydrology,* Rotterdam, Brookfield: Balkema.

Kaste, O., Stoddard, J. L. & Henriksen, A. (2003). Implication of lake water residence time on the classification of Norwegian surface water sites into progressive stages of nitrogen saturation. *Water Air and Soil Pollution,* 142.

Keane, A. 2010. *An assessment of the potential for P release from turlough soils.* MSc Thesis, University of Dublin, Trinity College, Ireland.

Keeler, R. R. & Zhang, Y. K. (1997). Modeling of groundwater flow in a fractured-karst aquifer in the Big Springs Basin, Iowa.: Geol. Soc. Am., Abs. Programs 29 (4), 25.

Kilchmann, S., Waber, H. N., Parriaux, A. & Bensimon, M. (2004). Natural tracers in recent groundwaters from different Alpine aquifers. *Hydrogeology Journal,* 12**,** 643-661.

Kilroy, G. & Coxon, C. E. (2005). Temporal variability of phosphorus fractions in Irish karst springs. *Environmental Geology,* 47**,** 421-430.

Kimberley, S. 2008. *Spatial and temporal fluxes of plant nutrients in turlough soils.* PhD Thesis, University of Dublin, Trinity College, Ireland.

Kimberley, S. & Coxon, C. (2013). Evaluating the Influence of Groundwater Pressures on Groundwater-Dependent Wetlands: Environmental Supporting Conditions for Groundwater-Dependent Terrestrial Ecosystems. *Strive Report (2011 -W-DS-5).* Environmental Protection Agency.

Kimberley, S., Naughton, O., Johnston, P., Gill, L. & Waldren, S. (2012). The influence of flood duration on the surface soil properties and grazing management of karst wetlands (turloughs) in Ireland. *Hydrobiologia,* 692**,** 29-40.

Kimberley, S. & Waldren, S. (2012). Examinations of turlough soil property spatial variation in a conservation assessment context. *Biology & Environment: Proceedings of the Royal Irish Academy,* 112B**,** 1-13.

Kinahan, G. H. (1865). Explanations to cover sheets 115-116. *Mem.Geol.Surv.Ireland*.

King, J. J. & Champ, W. S. T. (2000). Baseline water quality investigations on Lough Carra, Western Ireland, with reference to water chemistry, phytoplankton and aquatic plants. *Proceedings of the Royal Irish Academy - Biology and Environment,* 100B**,** 13-25.

Kiraly, L. 1975. Rapport sur l'etat actuel des connaissances dans le domaine des caracteres physiques des roches karstiques. *In:* Burger, A. & Dubertret, L. (eds.) *Hydrogeology of Karstic Terrains.* IAH, International Union of Geological Sciences, Series B, 3.

Kovacs, A. 2003. *Geometry and hydraulic parameters of karst aquifers: a hydrodynamic modeling approach.* PhD Thesis Thesis, Faculte des Sciences, Universite de Neuchatel

Kovács, A. & Perrochet, P. (2008). A quantitative approach to spring hydrograph decomposition. *Journal of Hydrology,* 352**,** 16-29.

Kovacs, A., Perrochet, P., Kiraly, L. & Jeannin, P. Y. (2005). A quantitative method for the characterisation of karst aquifers based on spring hydrograph analysis. *Journal of Hydrology,* 303**,** 152-164.

Kovacs, A. & Sauter, M. 2007. Modelling karst hydrodynamics. *In:* Goldscheider, N. & Drew, D. (eds.) *Methods in karst hydrogeology.* Taylor & Francis.

Kozlowski, A. & Warny, J. (2009). Baptism of Fire: Underwater Explorations beneath the Gort Lowlands. *Irish Speleology,* 18**,** 37-42.

Kresic, N. 2007. Hydraulic methods. *In:* Goldscheider, N. & Drew, D. (eds.) *Methods in Karst Hydrogeology.* Taylor & Francis.

Langmuir, D. (1997). *Aqueous Environmental Geochemistry,* Upper Saddle River, NJ, Prentice-Hall.

Lauritzen, S.-E., Abbott, J., Arnesen, R., Crossley, G., Grepperud, D., Ive, A. & Johnson, S. (1985). Morphology and hydraulics of an active phreatic conduit. *Cave Science,* 12.

Lee, Y. H. & Singh, V. P. (1999). Tank model using Kalman filter. *ASCE Journal of Hydrologic Engineering,* 4**,** 344-349.

LeGrand, H. E. & Stringfield, V. T. (1971). Development and distribution of permeability in carbonate aquifers. *Water Resour. Res.,* 7**,** 1284-1294.

LeGrand, H. E. & Stringfield, V. T. (1973). Karst hydrology -- A review. *Journal of Hydrology,* 20**,** 97-120.

Leibundgut, C., Maloszewski, P. & Kulls, C. (2009). *Tracers in Hydrology,* Chichester, John Wiley & Sons Ltd.

Liu, Z. & Dreybrodt, W. (1997). Dissolution kinetics of calcium carbonate minerals in H2O ・CO2 solutions in turbulent flow: The role of the diffusion boundary layer and the slow reaction H2O + CO2 → H+ + HCO3−. *Geochimica et Cosmochimica Acta,* 61**,** 2879-2889.

Loehr, R. C. (1974). Characteristics and Comparative Magnitude of Non-Point Sources. *Journal (Water Pollution Control Federation),* 46**,** 1849-1872.

Long, A. J. & Derickson, R. G. (1999). Linear systems analysis in a karst aquifer. *Journal of Hydrology,* 219**,** 206-217.

Long, A. J. & Putnam, L. D. (2004). Linear model describing three components of flow in karst aquifers using 18O data. *Journal of Hydrology,* 296**,** 254-270.

Long, J. C. S., Gilmour, P. & Witherspoon, P. A. (1985). A Model for Steady Fluid Flow in Random Three-Dimensional Networks of Disc-Shaped Fractures. *Water Resour. Res.,* 21**,** 1105-1115.

Longinelli, A., Stenni, B., Genoni, L., Flora, O., Defrancesco, C. & Pellegrini, G. (2008). A stable isotope study of the Garda lake, northern Italy: Its hydrological balance. *Journal of Hydrology,* 360**,** 103-116.

López-Chicano, M., Bouamama, M., Vallejos, A. & Pulido-Bosch, A. (2001). Factors which determine the hydrogeochemical behaviour of karstic springs. A case study from the Betic Cordilleras, Spain. *Applied Geochemistry,* 16**,** 1179-1192.

Lynn, D. E. & Waldren, S. (2001). Morphological Variation in Populations of Ranunculus repens from the Temporary Limestone Lakes (Turloughs) in the West of Ireland. *Annals of Botany,* 87**,** 9-17.

Mace, R. E. & Hovorka, S. D. 2000. Estimating porosity and permeability in a karstic aquifer using core plugs, well tests and outcrop measurements. *In:* Sasowsky, I., D (ed.) *Groundwater Flow and Contaminant Transport in Carbonate Aquifers.* Rotterdam: A.A. Balkema

Madden, B. & Heery, S. (1997). Wintering Waterfowl in South Galway Area. In: Southern Water Global and Jennings O'Donovan and partners (Eds.), An investigation into the Flooding Problems in the Gort–Ardrahan area of South Galway. Ecology Baseline, Vol. I. The Office of Public Works, Dublin, pp. 132–208.

Maillet, E. 1905. *Essais d'hydraulique souterraine et fluviale.* Thesis.

Maire, R. (1981). Inventory and general features of PNG karsts. . *Spelunca,* 3(Supplement)**,** 7-8.

Majoube, M. (1971). Fractionnement en oxygéne-18 et en deuterium entre l'eau et la vapeur. *J.Chim. Phys,* 68**,** 1423-1436.

Maurice, L., Atkinson, T. C., Williams, A. T., Barker, J. A. & Farrant, A. R. (2010). Catchment scale tracer testing from karstic features in a porous limestone. *Journal of Hydrology,* 389**,** 31-41.

McCormack, T. 2009. *Qunatifying Flow Pathways in Karstic Catchments.* Masters Thesis Thesis, Trinity College Dublin.

McElwain, L. & Sweeney, J. (2007). Key Meteorological Indicators of Climate Change in Ireland. *Environmental Research Centre Report*. Prepared for the Environmental Protection Agency by National University of Ireland, Maynooth.

McGrath, R. J., Fealy, R. & Sheridan, T. (2011). Recent Irish weather extremes and climate change. *9th, Scientific Statement.* . Royal Irish Academy, Dublin.

McGrath, R. J., Styles, P., Thomas, E. & Neale, S. (2002). Integrated high-resolution geophysical investigations as potential tools for water resource investigations in karst terrain. *Environmental Geology,* 42**,** 552-557.

Mellander, P., Jordan, P., Melland, A. R., Murphy, P. N. C., Wall, D. P., Mechan, S., Meehan, R., Kelly, C., Shine, O. & Shortle, G. (2013). Quantification of Phosphorus Transport from a Karstic Agricultural Watershed to Emerging Spring Water. *Environmental Science & Technology,* 47**,** 6111-6119.

Mochales, T., Casas, A. M., Pueyo, E. L., Pueyo, O., Roman, M. T., Pocovi, A., Soriano, M. A. & Anson, D. (2008). Detection of underground cavities by combining gravity, magnetic and ground penetrating radar surveys: a case study from the Zaragoza area, NE Spain. *Environmental Geology,* 53**,** 1067-1077.

Mohrlok, U. & Sauter, M. Year. Modelling groundwater flow in a karst terrane using discrete and double-continuum approaches; importance of spatial and temporal distribution of recharge. *In:* Proceedings of the12th International Speleological Congress, 1997. 167-170.

Monroe, W. H. U. S. (1970). A glossary of karst terminology. *Geol. Surv. Water-Supply Pap,* 1899-K**,** 26pp.

Mook, W. G. (2001). Environmental isotopes in the hydrological cycle - principles and applications: Volume 1: Introduction, IHP-V, Technical Documents in Hydrology, No 39, Vol 1. *IHP-V, Technical Documents in Hydrology, No 39, Vol 1*. Paris: UNESCO. .

Mook, W. G. (2006). *Introduction to Isotope Hydrology: Stable and Radioactive Isotopes of Hydrogen, Carbon, and Oxygen,* London, Taylor & Francis.

Moore, P. J., Martin, J. B. & Screaton, E. J. (2009). Geochemical and statistical evidence of recharge, mixing, and controls on spring discharge in an eogenetic karst aquifer. *Journal of Hydrology,* 376**,** 443-455.

Morales, T., Fdez. de Valderrama, I., Uriarte, J. A., Antigüedad, I. & Olazar, M. (2007). Predicting travel times and transport characterization in karst conduits by analyzing tracer-breakthrough curves. *Journal of Hydrology,* 334**,** 183-198.

Mullan, G. (2003). *Caves of County Clare and South Galway,* Bristol, United Kingdom, University of Bristol Spelæological Society.

Murphy, C. & Charlton, R. (2008). Climate Change and Water Resources. *Climate Change - Refining the Impacts for Ireland. STRIVE Report (2001-CD-C3-M1).* EPA, Co. Wexford, Ireland.

National Parks and Wildlife (2001a). Blackrock turlough (SAC) site synopsis.

National Parks and Wildlife (2001b). Caherglassaun turlough (SAC) site synopsis.

National Parks and Wildlife (2005). Lough Coy Conservation Plan.

National Parks and Wildlife (in review). *Turlough Project Final Report*.

Naughton, O. 2011. *The Hydrology and Hydroecology of Turloughs.* PhD Thesis, University of Dublin, Trinity College, Ireland.

Naughton, O., Johnston, P. M. & Gill, L. W. (2012). Groundwater flooding in Irish karst: The hydrological characterisation of ephemeral lakes (turloughs). *Journal of Hydrology,* 470–471**,** 82-97.

Neal, C., Hill, T., Hill, S. & Reynolds, B. (1997). Acid neutralization capacity measurements in surface and ground waters in the Upper River Severn, Plynlimon: from hydrograph splitting to water flow pathways. *Hydrol. Earth Syst. Sci.,* 1**,** 687-696.

Neuman, S. P. & De Marsily, G. (1976). Identification of linear systems response by parametric programming. *Water Resources Research,* 12**,** 253-262.

Ní Bhriain, B., Gormally, M. & Sheehy Skeffington, M. (2003). Changes in land use practices at two turloughs, on the east Burren limestones, Co. Galway, with reference to nature conservation *Biology and Environment Proceedings of the Royal Irish Academy,* 103B**,** 169-176.

Nielsen, R. & Hansen, E. (1973). Numerical simulation of the rainfall–runoff process on a daily basis. *Nordic Hydrology,* 4**,** 171-190.

Nugent, P. 2006. *Keynote talk at the Aughty People and Earth Day in Crusheen, 22nd April 2006* [Online]. Available: http://aughty.org/heritage.htm [Accessed 16th July 2012].

O'Connell, Y., Daly, E. & Henry, T. Year. Investigation of groundwater flow pathways in a Karst Aquifer using static & towed Electrical Resistivity Tomography Data. *In:* Irish Geological Research Meeting 2012 Cork, Ireland.

O'Connell, Y., Daly, E., Henry, T. & Rooney, S. (2011). A Geophysical Survey at Blackrock Turlough, Peterswell, Co. Galway. *Groundwater Newsletter (Geological Survey of Ireland),* 17-21.

O'Brien, R. J., Misstear, B. D., Gill, L. W., Deakin, J. L. & Flynn, R. (2013). Developing an integrated hydrograph separation and lumped modelling approach to quantifying hydrological pathways in Irish river catchments. *Journal of Hydrology,* 486**,** 259-270.

OECD (1982). Eutrophication of waters. Organisation for Economic Co-operation and Development (OECD), Paris, France.

Office of Public Works (2013). Assessment of Groundwater Flooding Risks Posed By Turloughs, Site Assessment Report - Gort Lowlands, Co. Galway. *In:* Naughton, O. (ed.). Galway: Office of Public Works.

Oron, A. P. & Berkowitz, B. (1998). Flow in rock fractures: the local cubic law assumption reexamined. *Water Resources Research,* 34**,** 2811 –2825.

Padilla, A. & Pulido-Bosch, A. (2008). Simple procedure to simulate karstic aquifers. *Hydrological Processes,* 22**,** 1876-1884.

Palmer, A. N. 1984. Geomorphic interpretation of karst features. *Groundwater as a Geomorphic Agent (ed. R.G. LaFleur).* London: Allen & Unwin.

Palmer, A. N. (1991). Origin and morphology of limestone caves. *Geological Society of America Bulletin,* 103**,** 1-21.

Partch, E. N. & Smith, J. D. (1978). Time dependent mixing in a salt wedge estuary. *Estuarine and Coastal Marine Science,* 6**,** 3-19.

Peach, D., Watson, S. & Carpenter, C. (1998). Flooding Problems in the Gort-Ardrahan Area of South Galway. Conceptual model of the Hydrogeological Regime. (Sub-report of the Gort Flood Studies Report).

Perrin, J., Jeannin, P.-Y. & Zwahlen, F. (2003). Epikarst storage in a karst aquifer: a conceptual model based on isotopic data, Milandre test site, Switzerland. *Journal of Hydrology,* 279**,** 106-124.

Perrin, J., Jeannin, P. Y. & Cornaton, F. (2007). The role of tributary mixing in chemical variations at a karst spring, Milandre, Switzerland. *Journal of Hydrology,* 332**,** 158-173.

Perriquet, M., Henry, T., Cave, R. R., Leonardi, V. & Jourde, H. Year. Hydrodynamics of a Coastal Karst Aquifer Affected by Saltwater Intrusion Under Climactic Influence, Co. Clare, Ireland. *In:* 22nd Salt Water Intrusion Meeting: Salt Water Intrusion in Aquifers: Challenges and Perspectives, 2012 Buzios, Brazil.

Peterson, E. W. & Wicks, C. M. (2006). Assessing the importance of conduit geometry and physical parameters in karst systems using the storm water management model (SWMM). *Journal of Hydrology,* 329**,** 294-305.

Petrunic, B. M., Duffy, G. P. & Einsiedl, F. (2012). Major ion chemistry in a coastal karstic groundwater resource located in Western Ireland. *Irish Journal of Earth Science.*

Petry, J., Soulsby, C., Malcolm, I. A. & Youngson, A. F. (2002). Hydrological controls on nutrient concentrations and fluxes in agricultural catchments. *Science of The Total Environment,* 294**,** 95-110.

Phillips, F. M., Person, M. A. & Muller, A. B. (1986). A numerical lumped-parameter model for simulating the isotopic evolution of closed-basin lakes. *Journal of Hydrology,* 85**,** 73-86.

Plummer, L. N. & Busenberg, E. (1982). The solubilities of calcite, aragonite and vaterite in CO2-H2O solutions between 0 and 90°C, and an evaluation of the aqueous model for the system CaCO3-CO2-H2O. *Geochimica et Cosmochimica Acta,* 46**,** 1011-1040.

Plummer, L. N., Wigley, T. M. L. & Parkhurst, D. L. (1978). The kinetics of calcite dissolution in CO 2 -water systems at 5 degrees to 60 degrees C and 0.0 to 1.0 atm CO 2. *American Journal of Science,* 278**,** 179-216.

Porst, G., Naughton, O., Gill, L., Johnston, P. & Irvine, K. (2012). Adaptation, phenology and disturbance of macroinvertebrates in temporary water bodies. *Hydrobiologia,* 696**,** 47-62.

Praeger, R. L. (1932). The flora of the turloughs: a preliminary note. *Proceedings of the Royal Irish Academy,* 41**,** 37-45.

Pybus, C., Pybus, M. J. & Ragneborn-Tough, L. (2003). Phytoplankton and Charophytes of Lough Bunny, Co. Clare. *Biology and Environment: Proceedings of the Royal Irish Academy,* 103B**,** 177-185.

Quinlan, J. F., Smart, C., Schindel, G. M., Alexander Jr., E. C., Edwards, K. J. & Smith, A. R. Year. Recommended administrative/regulatory definition of karst aquifer, principles of classificatino of carbonate aquifers, practical evaluation of vulnerability of karst aquifers, and determination of optimum sampling frequency at springs. *In:* Proceedings of the Third Conference on Hydrogeology, Ecology, Monitoring, and Management of Groundwater in Karst Terranes, 1991. 573-635.

Quinn, J. J., Tomasko, D. & Kuiper, J. A. (2006). Modeling complex flow in a karst aquifer. *Sedimentary Geology,* 184**,** 343-351.

Reddy, K. R. & DeLaune, W. H. (2008). *Biogeochemistry of Wetlands,* Academic Press Ltd.

Renou-Wilson, F. & Farrell, E. P. (2007). Phosphorus in surface runoff and soil water following fertilization of afforested cutaway peatlands. *Boreal Environment Research,* 12**,** 693-709.

Reynolds, B., Emmett, B. A. & Woods, C. (1992). Variations in streamwater nitrate concentrations and nitrogen budgets over 10 years in a headwater catchment in mid-Wales. *Journal of Hydrology,* 136**,** 155-175.

Reynolds, J. D. (1982). Ecology of Turloughs (Vanishing Lakes) in the Burren, Western Ireland. In: Transactions 14th International Congress of Game Biologists 14, pp. 183–188.

Reynolds, J. D. 1996. Turloughs, their significance and possibilities for conservation. . *In:* Reynolds, J. D. (ed.) *The conservation of Aquatic Systems.* Dublin: Royal Irish Academy.

Reynolds, J. D. (1997). Invertebrate surveys of S.E. Galway turloughs. Baseline Report. In: Southern Water Global and Jennings O'Donovan and Partners (Eds.), An Investigation of the Flooding Problems in the Gort–Ardrahan Area of South Galway. Ecology Baseline Study Vol. II. The Office of Public Works, Dublin. pp. 126–141.

Reynolds, J. D. & Marnell, F. (1999). New records of *Eurycercus glacialis* (Cladocera: Chydoridae) in turloughs in south-east Galway. *Irish Naturalists' Journal,* 26 177-180.

Robson, A. & Neal, C. (1990). Hydrograph separation using chemical techniques: An application to catchments in Mid-Wales. *Journal of Hydrology,* 116**,** 345-363.

Rodriguez, R. 1995. Mapping karst solution features by the integrated geophysical method. *In:* Beck, B. F. (ed.) *Karst geohazards.* Rotterdam: Balkema.

Rozanski, K., Froehlich, K. & Mook, W. G. (2001). *Environmental isotopes in the hydrological cycle - principles and applications: Volume 3: Surface Water, IHP-V, Technical Documents in Hydrology, No 39, Vol 3.,* Paris, UNESCO.

Russell, J. M. & Johnson, T. C. (2006). The Water Balance and Stable Isotope Hydrology of Lake Edward, Uganda-Congo. *Journal of Great Lakes Research,* 32**,** 77-90.

Ryan, M. & Meiman, J. (1996). An Examination of Short-Term Variations in Water Quality at a Karst Spring in Kentucky. *Ground Water,* 34**,** 23-30.

Sanford, W., Aeschbach-Hertig, W. & Herczeg, A. (2011). Preface: Insights from environmental tracers in groundwater systems. *Hydrogeology Journal,* 19**,** 1-3.

Sasowsky, I. D. 2000. Carbonate aquifers: a review of thoughts and methods. *In:* Sasowsky, I. D. & Wicks, C. M. (eds.) *Groundwater flow and Contaminant Transport in Carbonate Aquifers.* Rotterdam: A.A. Balkema.

Sauter, M. (1992). *Quantification and forecasting of regional groundwater flow and transport in a karst aquifer (Gallusquelle, Malm, SW. Germany),* Tubinger Geowissenschaftlichen Abhandlungen, Reihe C.13.

Sawada, A., Uchida, M., Shimo, M., Yamamoto, H., Takahara, H. & Doe, T. W. (2000). Non-sorbing tracer migration experiments in fractured rock at the Kamaishi Mine, Northeast Japan. *Engineering Geology,* 56**,** 75-96.

Sawyer, C., McCarty, P. & Parkin, G. (2003). *Chemistry for Environmental Engineering and Science,* McGraw Hill Professional.

Scanlon, B. R., Mace, R. E., Barrett, M. E. & Smith, B. (2003). Can we simulate regional groundwater flow in a karst system using equivalent porous media models? Case study, Barton Springs Edwards aquifer, USA. *Journal of Hydrology,* 276**,** 137-158.

Scheffer, M. (1998). *Ecology of Shallow Lakes.,* London, UK., Chapman & Hall.

Schemel, L. E. (2001). Simplified conversions between specific conductance and salinity units for use with data from monitoring stations. *IEP Newsletter,* 14**,** 17-18.

Shaw, E. M. (2011). *Hydrology in Practice (4th edition),* London, Chapman and Hall.

Sheehy Skeffington, M. & Gormally, M. (2007). Turloughs: A mosaic of biodiversity and management systems unique to Ireland. *Acta Carsologica,* 36**,** 217 - 222.

Sheehy Skeffington, M., Moran, J., O Connor, Á., Regan, E., Coxon, C. E., Scott, N. E. & Gormally, M. (2006). Turloughs - Ireland's unique wetland habitat. *Biological Conservation,* 133**,** 265-290.

Sheehy Skeffington, M. & Scott, N. E. (2008). Do turloughs occur in Slovenia? *Acta Carsologica,* 37(2-3)**,** 291-306.

Shuster, E. T. & White, W. B. (1971). Seasonal fluctuations in the chemistry of lime-stone springs: A possible means for characterizing carbonate aquifers. *Journal of Hydrology,* 14**,** 93-128.

Siemers, J. & Dreybrodt, W. (1998). Early development of karst aquifers on percolation networks of fractures in limestone. . *Water Resources Research,* a34**,** 409– 419.

Siggins, L. 2010. Cave diving duo plunge to new depths in epic 4km underwater adventure. *The Irish Times,* Sept 10, 2010.

Simms, M. J. (2001). *Exploring the Limestone Landscapes of the Buren and the Gort Lowlands: A guide for walkers, cyclists and motorists.,* Belfast, Burrenkarst.com.

Smart, C. & Simpson, B. (2002). Detection of fluorescent compounds in the environment using granular activated charcoal detectors. *Environmental Geology,* 42**,** 538-545.

Smart, C. C. (1988). Quantitative tracing of the Maligne karst system, Alberta, Canada. *Journal of Hydrology,* 98**,** 185-204.

Smith, A. M. & Cave, R. R. (2012). Influence of fresh water, nutrients and DOC in two submarine-groundwater-fed estuaries on the west of Ireland. *Science of The Total Environment,* 438**,** 260-270.

Smyth, T. (1996). A Case Study in the Gort-Ardrahan area of South Galway. Dublin: Office of Publin Works

Southern Water Global (1998). An investigation of the flooding problems in the Gort-Ardrahan area of South Galway. Final Report, April 1998. Produced by Southern Water Global and Jennings O`Donovan and Partners for the Office of Public Works, Dublin.

Springer, G. S. (2004). A pipe-based, first approach to modeling closed conduit flow in caves. *Journal of Hydrology,* 289**,** 178-189.

Stationery Office Dublin (2010). EU Statutory Instrument N. 610 - European Communities (Good Agricultural Practice for Protection of Waters) Regulations 2010. Stationery Office Dublin, Dublin Ireland.

Šumanovac, F. & Weisser, M. (2001). Evaluation of resistivity and seismic methods for hydrogeological mapping in karst terrains. *Journal of Applied Geophysics,* 47**,** 13-28.

Svensson, U. & Dreybrodt, W. (1992). Dissolution kinetics of natural calcite minerals in CO2-water systems approaching calcite equilibrium. *Chemical Geology,* 100**,** 129-145.

Teagasc. 2013. *Nutrient requirements in forestry* [Online]. Available: http://www.teagasc.ie/forestry/advice/nutrient_requirements.asp [Accessed 27th July 2013].

Teutsch, G. Year. An extended double-porosity concept as a practical modelling approach for a karstified terrain. Hydrogeol. Processes in Karst Terranes. *In:* Antalya Symp. And Field Seminar, Oct 1990, 1993. 281–292.

Teutsch, G. & Sauter, M. (1998). Distributed parameter modelling approaches in karst-hydrological investigations. *Bull. d'Hydrogeologie,* 16**,** 99-109.

Thrailkill, J. (1968). Chemical and Hydrologic Factors in the Excavation of Limestone Caves. *Geological Society of America Bulletin,* 79**,** 19-46.

Thrailkill, J. (1974). Pipe Flow Models of a Kentucky Limestone Aquifer. *Ground Water,* 12**,** 202-205.

Thrailkill, J., Sullivan, S. B. & Gouzie, D. R. (1991). Flow parameters in a shallow conduit-flow carbonate aquifer, Inner Bluegrass Karst Region, Kentucky, USA. *Journal of Hydrology,* 129**,** 87-108.

Tynan, S., Gill, M. & Johnston, P. M. (2007). Development of a Methodology for the Characterisation of a Karstic Groundwater Body with Particular Emphasis on the Linkage with Associated Ecosystems such as Turlough Ecosystems. Final Research Report to the Environmental Protection Agency (Project No. 2002-W-DS-08-M1). EPA, Johnstown Castle Estate, Wexford, Ireland.

Urban, J. & Rzonca, B. (2009). Karst systems analyzed using borehole logs — Devonian carbonates of the Świętokrzyskie (Holy Cross) Mountains, central Poland. *Geomorphology,* 112**,** 27-47.

Valdes, D., Dupont, J.-P., Massei, N., Laignel, B. & Rodet, J. (2006). Investigation of karst hydrodynamics and organization using autocorrelations and T-[Delta]C curves. *Journal of Hydrology,* 329**,** 432-443.

Van der Linden, P. & Mitchell, J. F. B. (2009). ENSEMBLES: Climate Change and its Impacts: Summary of research and results from the ENSEMBLES project. . Met Office Hadley Centre, FitzRoy Road, Exeter EX1 3PB, UK.

Visser, M., Moran, J., Regan, E., Gormally, M. & Skeffington, M. S. (2007). The Irish agri-environment: how turlough users and non-users view converging EU agendas of Natura and CAP. Land use Policy 24: 362–373.

Walsh, S. (2010). Report on Rainfall of November 2009. Met Eireann, Dublin, Ireland.

Weiskel, P. K. & Howes, B. L. (1992). Differential transport of sewage-derived nitrogen and phosphorus through a coastal watershed. *Environmental Science & Technology,* 26**,** 352-360.

Wetzel, R. G. (2001). *Limnology: Lake and River Ecosystems,* San Diego, CA, USA., Academic Press.

White, W. B. (1969). Conceptual Models for Carbonate Aquifers. *Ground Water,* 7**,** 15-21.

White, W. B. (1988). *Geomorphology and Hydrology of Karst Terrains,* Oxford University Press.

White, W. B. 1993. Analysis of karst aquifers. *In:* Alley, W. M. (ed.) *Regional Ground – Water Quality.* New York: Van Nostrand-Reinhold.

White, W. B. (2002). Karst hydrology: recent developments and open questions. *Engineering Geology,* 65**,** 85-105.

White, W. B. & White, E. L. (2005). Ground water flux distribution between matrix, fractures, and conduits: constraints on modeling. *Speleogenesis and Evolution of Karst Aquifers,* 3**,** 1-6.

Wilby, R. L. & Harris, I. (2006). A framework for assessing uncertainties in climate change impacts: low flow scenarios for the River Thames, UK. *Water Resources Research,* 42.

Williams, P. & Ford, D. C. (2006). Global distribution of carbonate rocks. *Zeitschrift für Geomorphologie N.F., Suppl.-Vol. 147, p. 1-2.*

Williams, P. W. (1964). Aspects of the Limestone Physiography of Parts of Counties Clare and Galway, Western Ireland. *Unpublished PhD Thesis.* University of Cambridge.

Williams, P. W. (1983). The role of the subcutaneous zone in karst hydrology. *Journal of Hydrology,* 61**,** 45-67.

Williams, P. W. (2008). The role of the epikarst in karst and cave hydrogeology: a review. *International Journal of Speleology,* 37**,** 1-10.

Wold, S., Esbensen, K. & Geladi, P. (1987). Principal component analysis. *Chemometrics and Intelligent Laboratory Systems,* 2 37-52.

Working Group on Groundwater (2005). Approach to Delineation of Groundwater Bodies, Guidance document no. GW2 . Working Group on Groundwater, . Environment Protection Agency, Dublin.

Worthington, S. R. H. 1991. *Karst Hydrogeology of the Canadian Rocky Mountains.* PhD thesis Thesis, McMaster University, Hamilton, Ontario.

Worthington, S. R. H. (1999). A comprehensive strategy for understanding flow in carbonate aquifer. *Speleogenesis and Evolution of Karst Aquifers,* 1**,** 1-8.

Worthington, S. R. H., Davies, G. J. & Quinlan, J. F. Year. Geochemistry of springs in temperate carbonate aquifers: recharge type explains most of the variation. . *In:* 5th Conference on Limestone Hydrology and Fissured Media, , 1992 Neuchatel, Switzerland. 341–347.

Worthington, S. R. H., Ford, D. C. & Beddows, P. A. 2000a. Porosity and Permeability Enhancement in Unconfined Carbonate Aquifers as a Result of Dissolution. *In:* A.V., K., Ford, D. C., Palmer, A. N. & Dreybrod, W. (eds.) *Speleogenesis; Evolution of Karst Aquifers.* Huntsville, AL.: National Speleological Society of America.

Worthington, S. R. H., Ford, D. C. & Davies, G. J. 2000b. Matrix, fracture and channel components of storage and flow in a Paleozoic aquifer. *In:* Sasowsky, I., D & Wicks, C. M. (eds.) *Groundwater Flow and Contaminant Transport in Carbonate Aquifers.* Rotterdam: A.A. Balkema.

Zibret, Z. & Simunic, Z. 1976. A rapid method for determining water budget of enclosed and flooded karst plains. *In:* Yevjevich, V. (ed.) *Karst Hydrology and Water Resources: Vol. 1 Karst Hydrology.* Colorado: Water Resources Publications.

Zimmerman, U. 1979. Determination by Stable Isotopes of Underground Inflow and Outflow and Evaporation of Young Artificial Groundwater Lakes. *Isotopes in Lake Studies.* Vienna: IAEA.

Zuber, A. & Motyka, J. (1998). Hydraulic parameters and solute velocities in triple-porosity karstic-fissured-porous carbonate aquifers: case studies in southern Poland. *Environmental Geology,* 34**,** 243-250.

Appendix A

Surveys and Maps

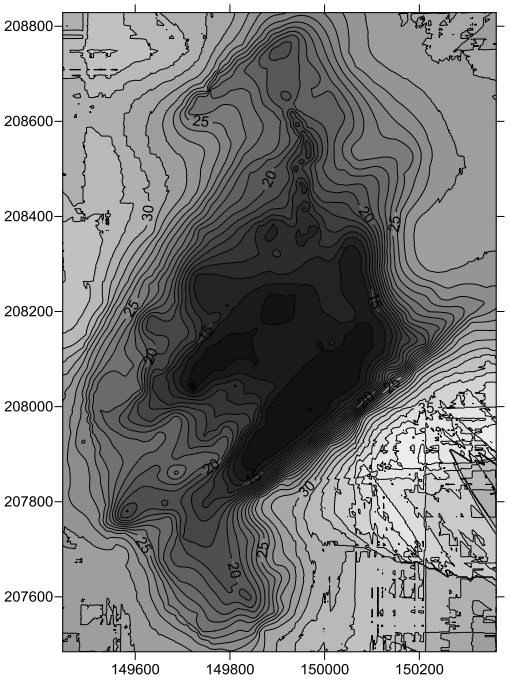

Figure A.1: Old Blackrock Survey

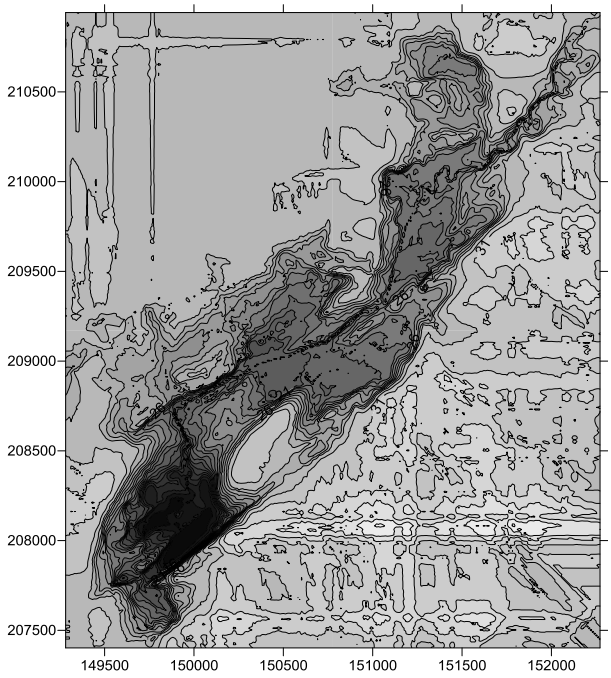

Figure A.2: New Blackrock Survey

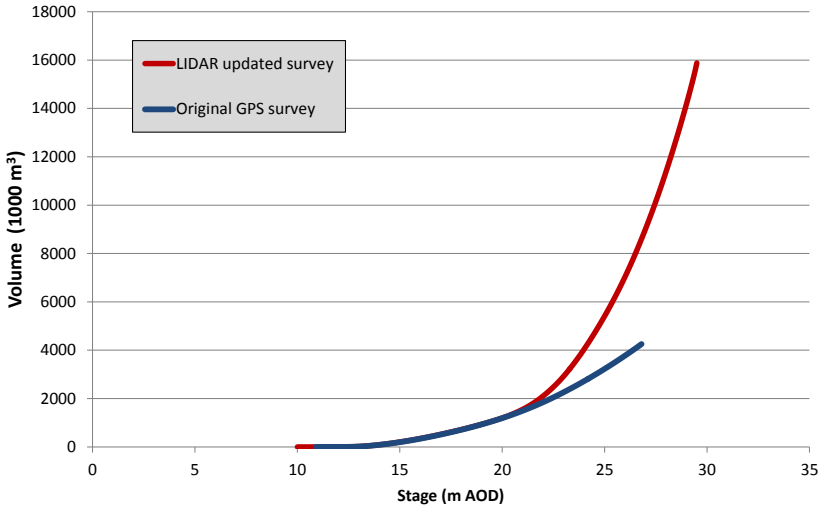

Figure A.3: Upgraded stage-volume curve for Blackrock turlough

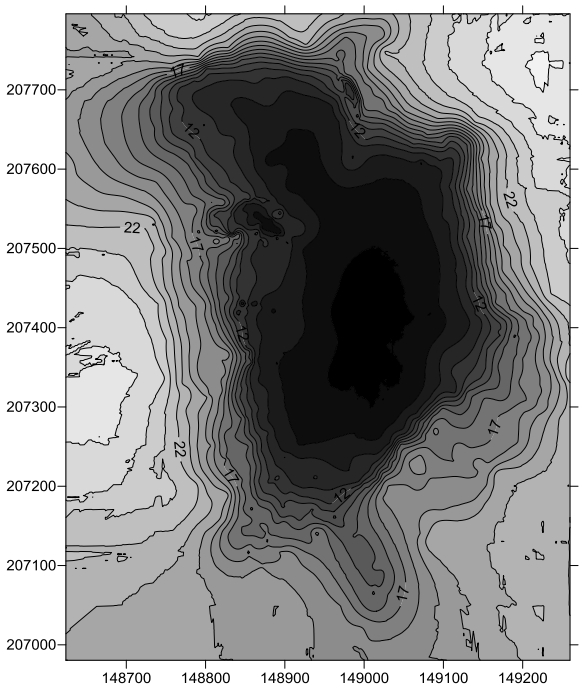

Figure A.4: Old Coy Survey

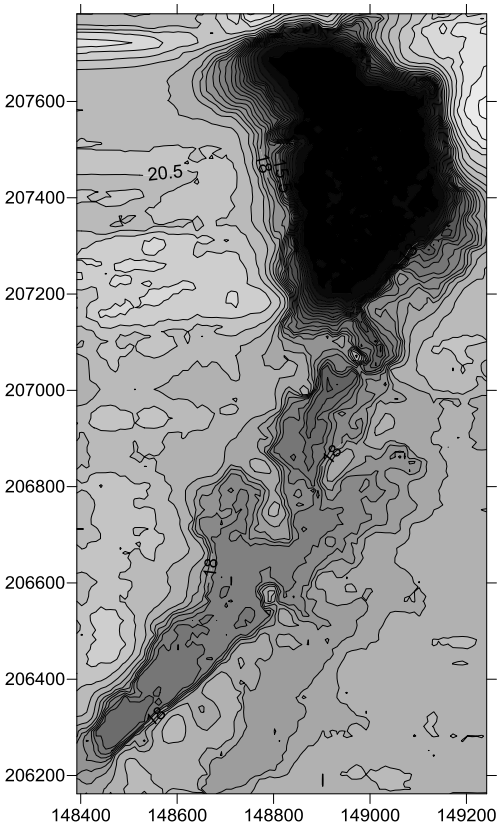

Figure A.5: New Coy Survey

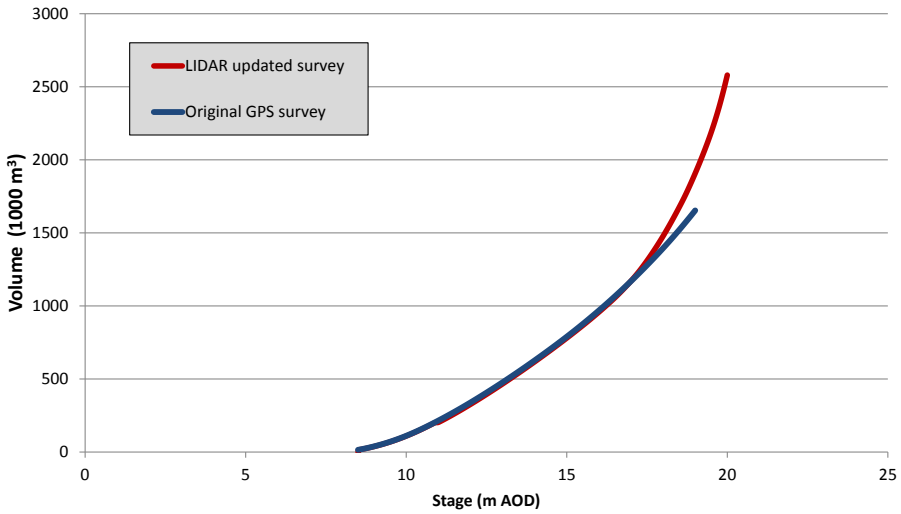

Figure A.6: Upgraded stage-volume curve for Coy turlough

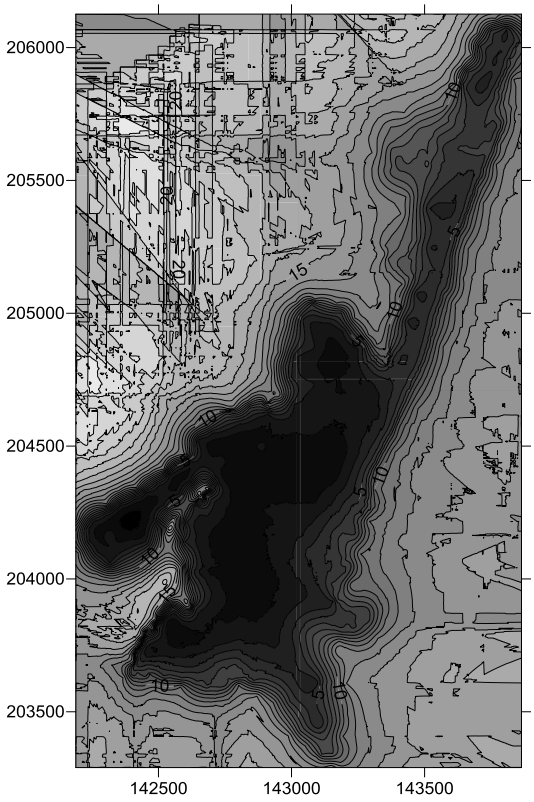

Figure A.7: Old Coole Survey

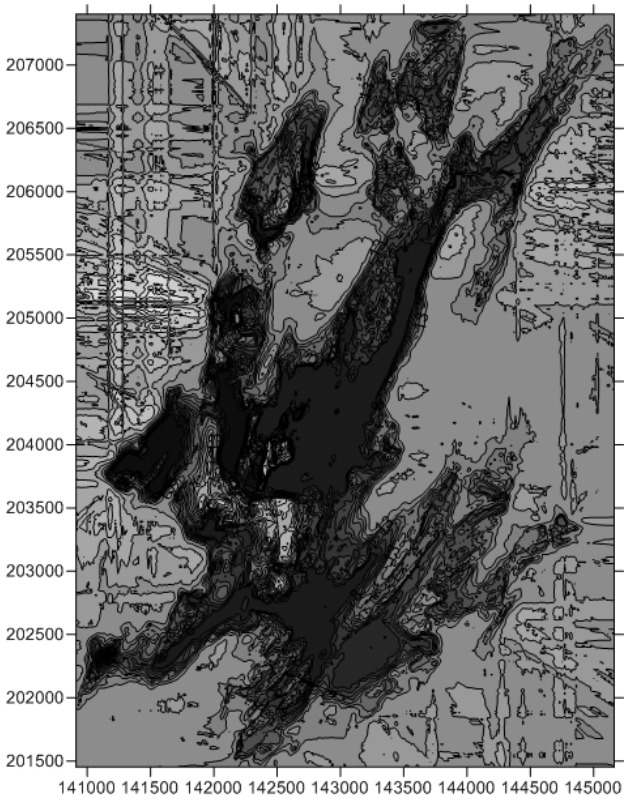

Figure A.8: New Coole Survey

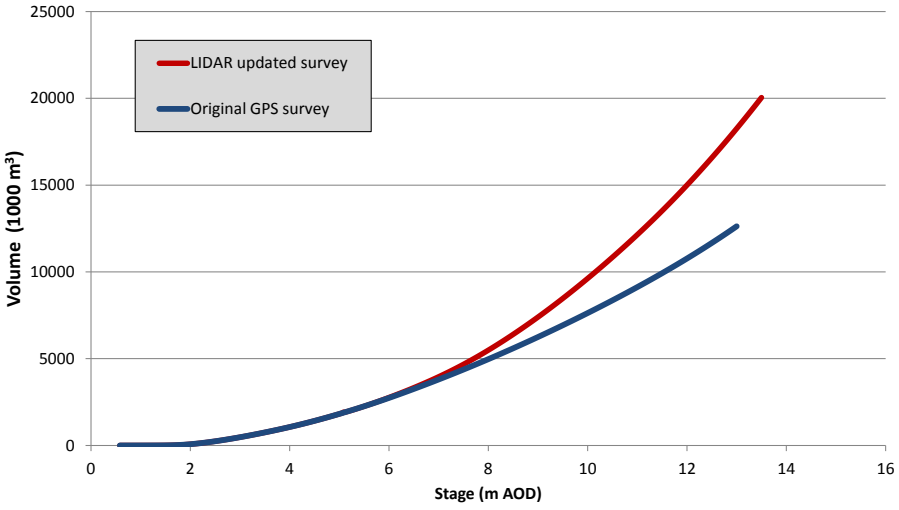

Figure A.9: Upgraded stage-volume curve for Blackrock turlough

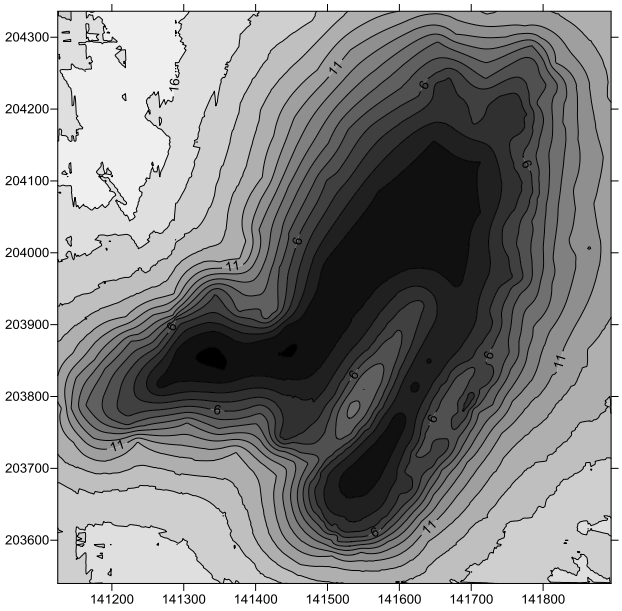

Figure A.10: Old Garryland Survey

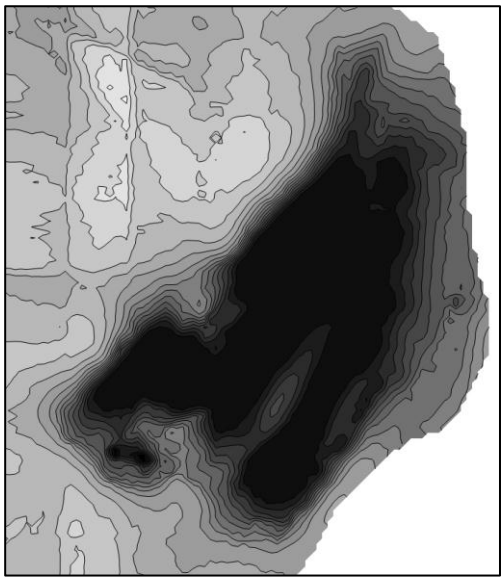

Figure A.11: New Garryland Survey

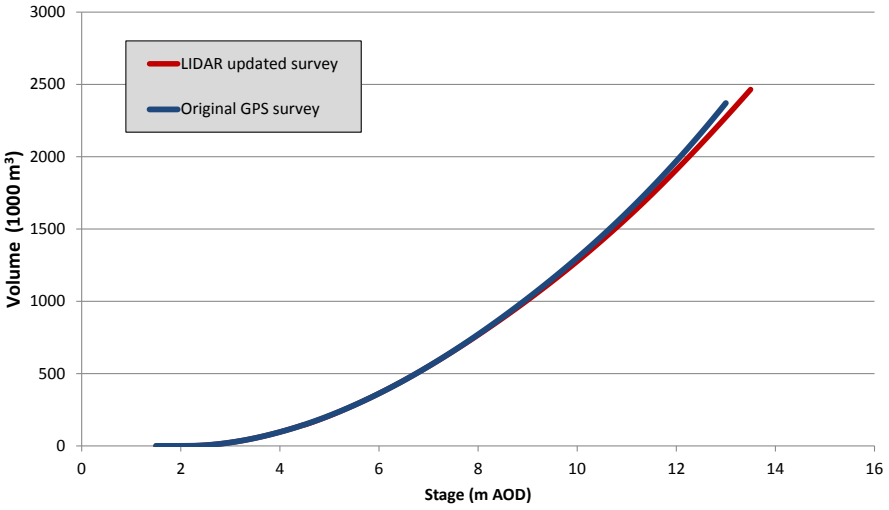

Figure A.12: Upgraded stage-volume curve for Garryland turlough

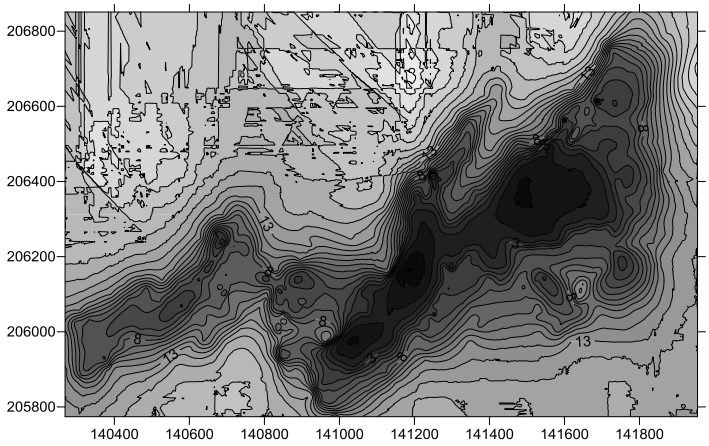

Figure A.13: Old Caherglassaun Survey

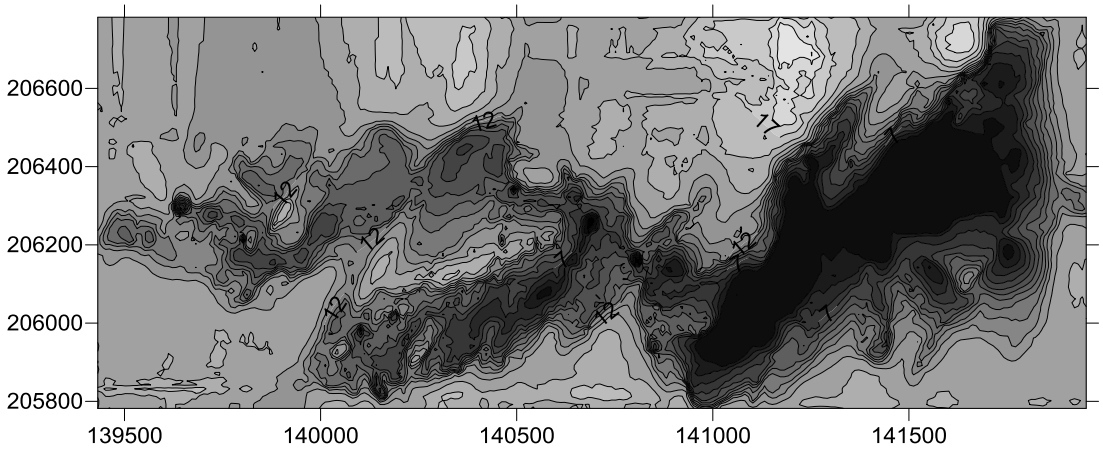

Figure A.14: New Caherglassaun Survey

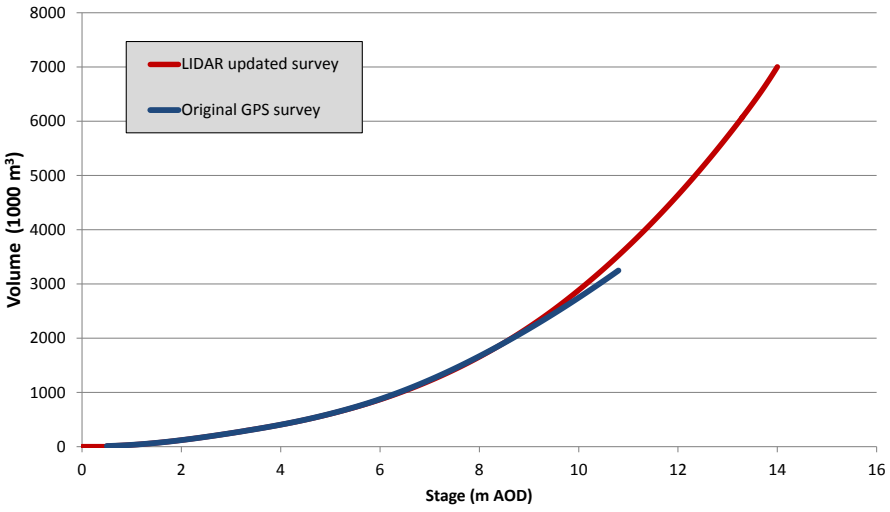

Figure A.15: Upgraded stage-volume curve for Caherglassaun turlough

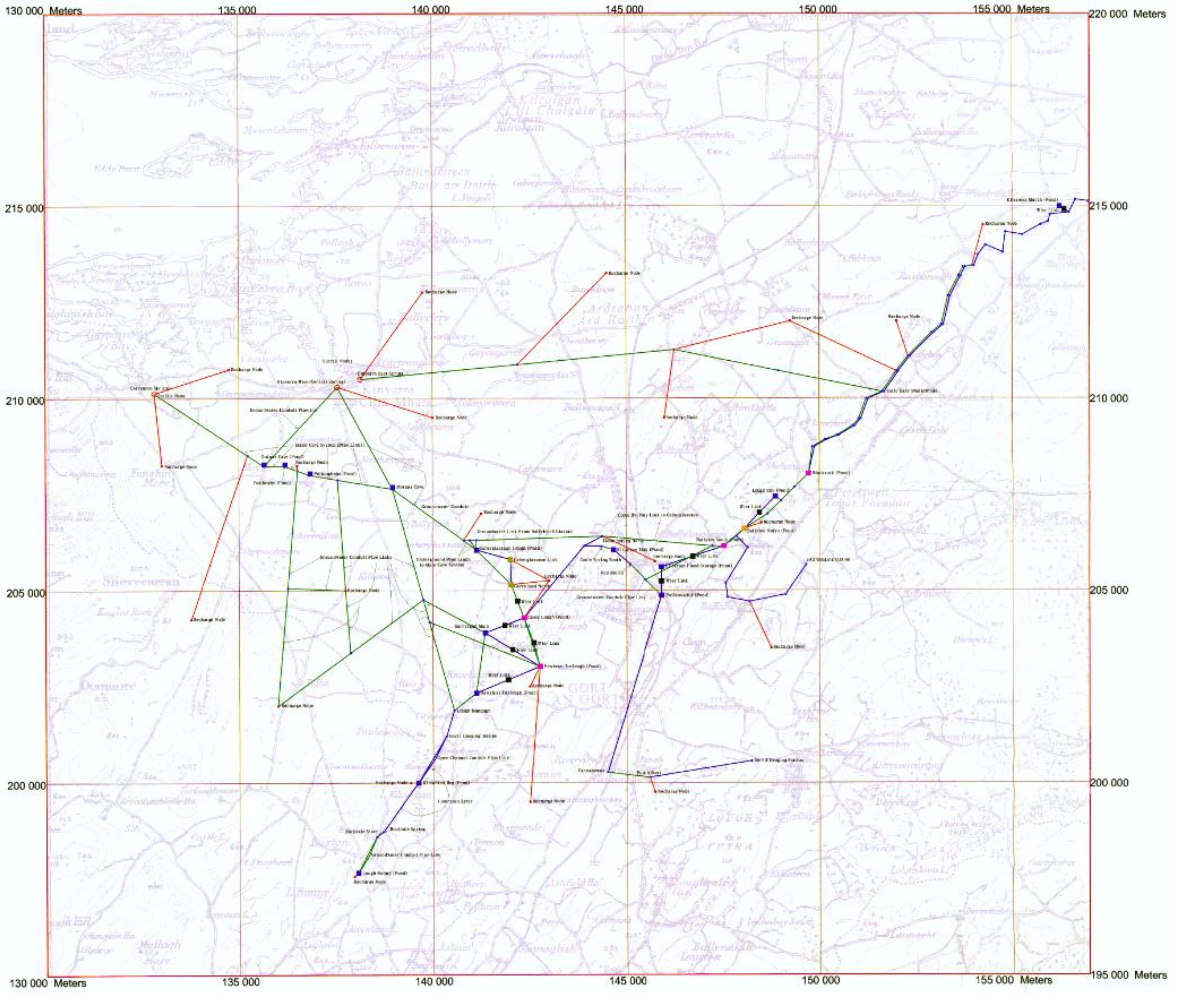

Figure A.16: Gort Flood Studies Conduit Network Conceptual Model

(Southern Water Global, 1998)

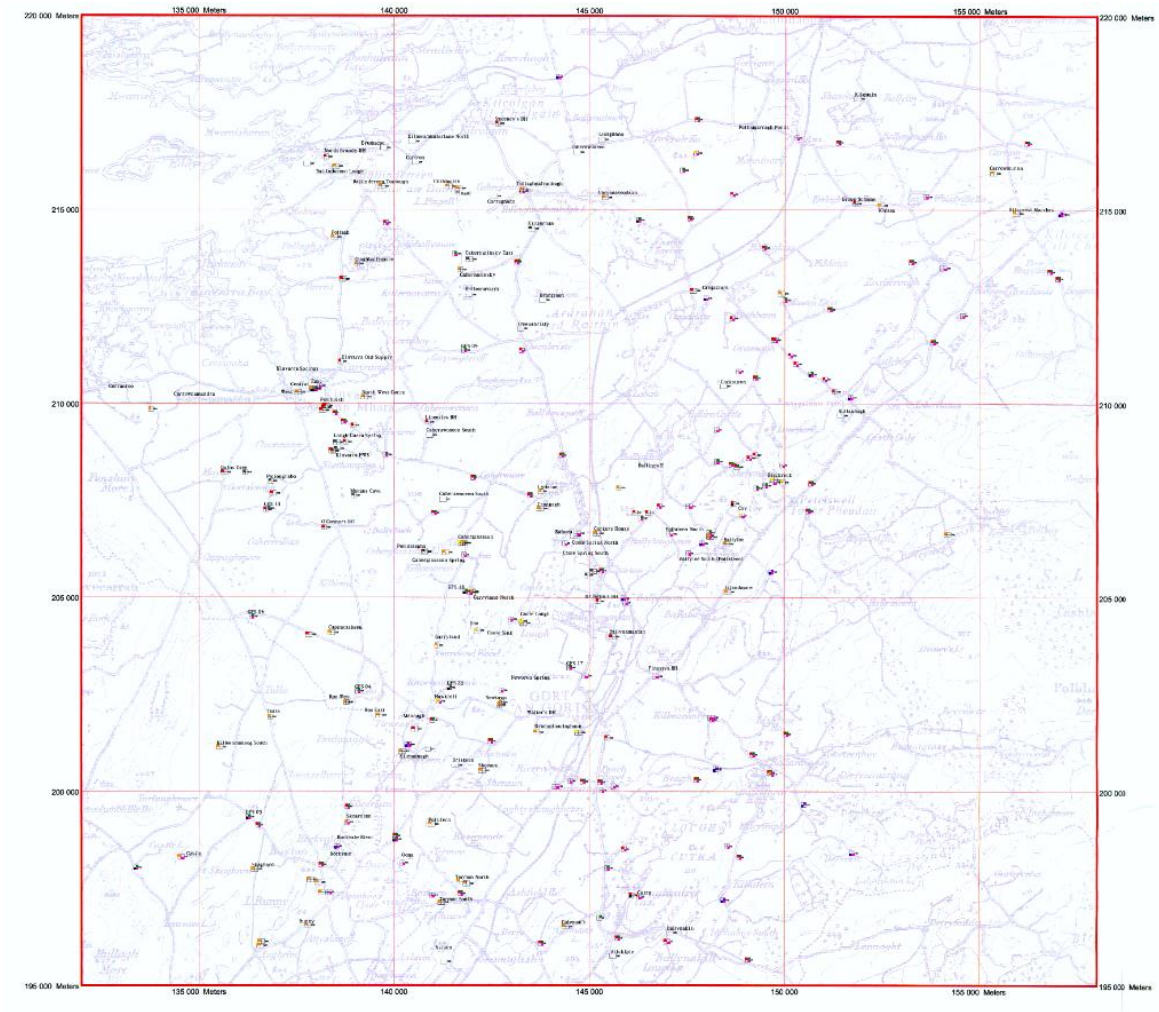

Figure A.16: Gort Flood Studies monitoring network locations (Southern Water Global, 1998)

Appendix B

Photos (November 2009 Floods)

Figure B.1: Floodwater crossing the N18 at Kiltartan

Figure B.2: Flooding on the N18 at Kiltartan (image taken from www.facebook.com/pages/South-Galway-Floods/199072411664)

Figure B.3: Flooding at Kiltartan (image taken from Jennings O'Donovan & Partners (2011))

Figure B.4: Flooding at Thoor Ballylee Castle (left image from image taken from Office of Public Works (2013), right image taken from www.facebook.com/pages/South-Galway-Floods/199072411664)

Figure B.5: Flooding at Blackrock turlough (viewed from the nearby abattoir to the south east)

Figure B.6: Flooding at Blackrock turlough (flooding the road south of the turlough)

The following set of images are screen-captures from OPW aerial imagery taken on the 26th of November, 2009. See Figure B.7 for image location and viewing angles.

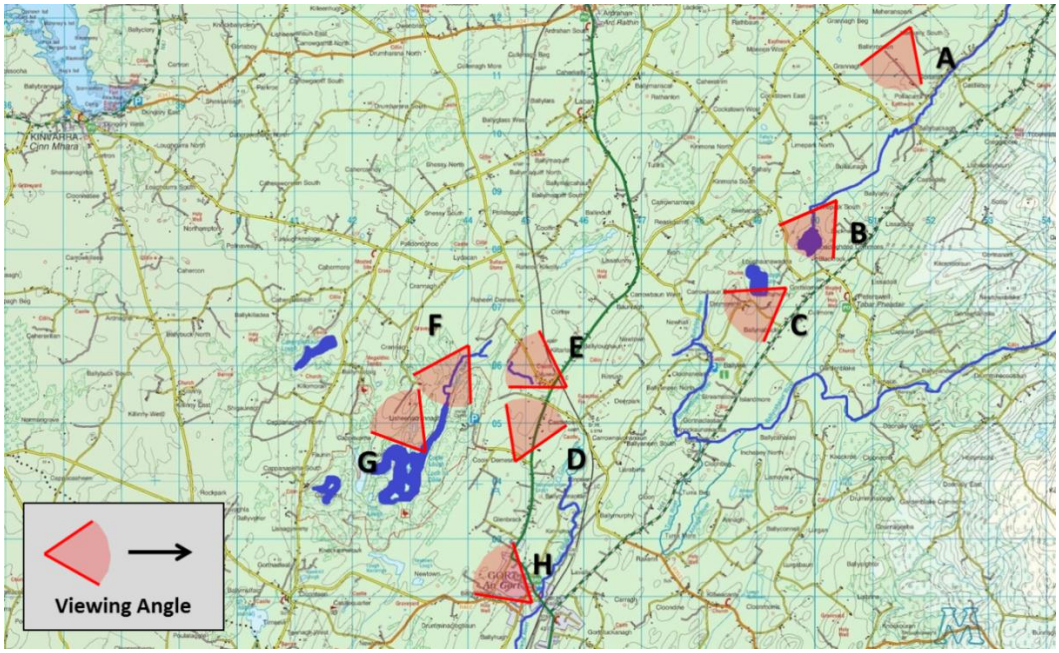

Figure B.7: Map showing image location and viewing angles of preceding images

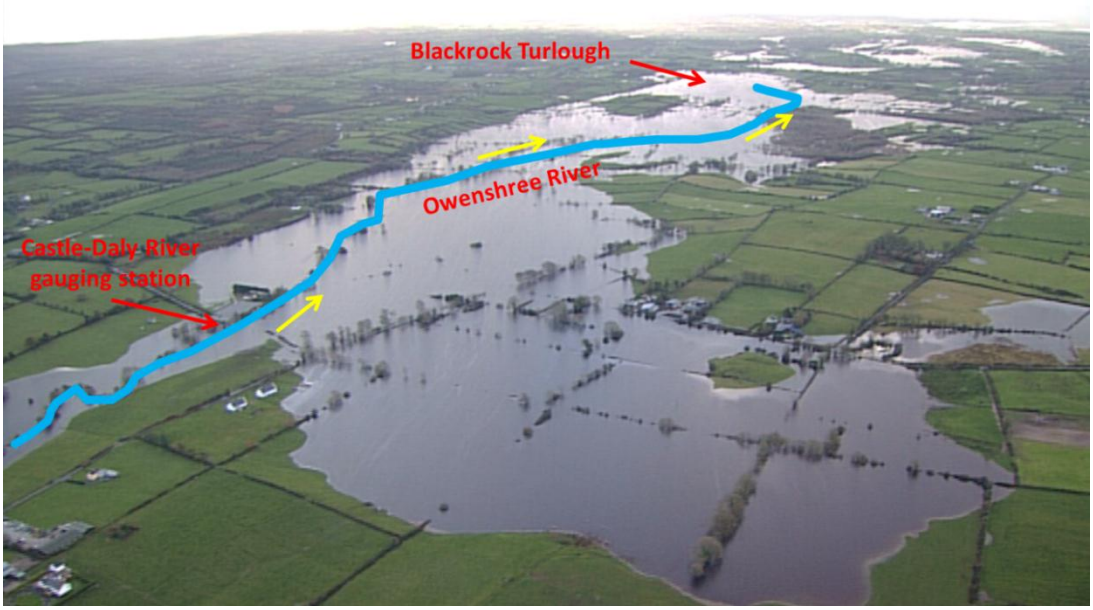

Figure B.8: Location A – Blackrock turlough. Image shows flooding extending northwards towards Castle-Daly River gauging station. (Owenshree River path highlighted in blue, flow direction shown in yellow)

Figure B.9: Location B – Blackrock and Coy turloughs.

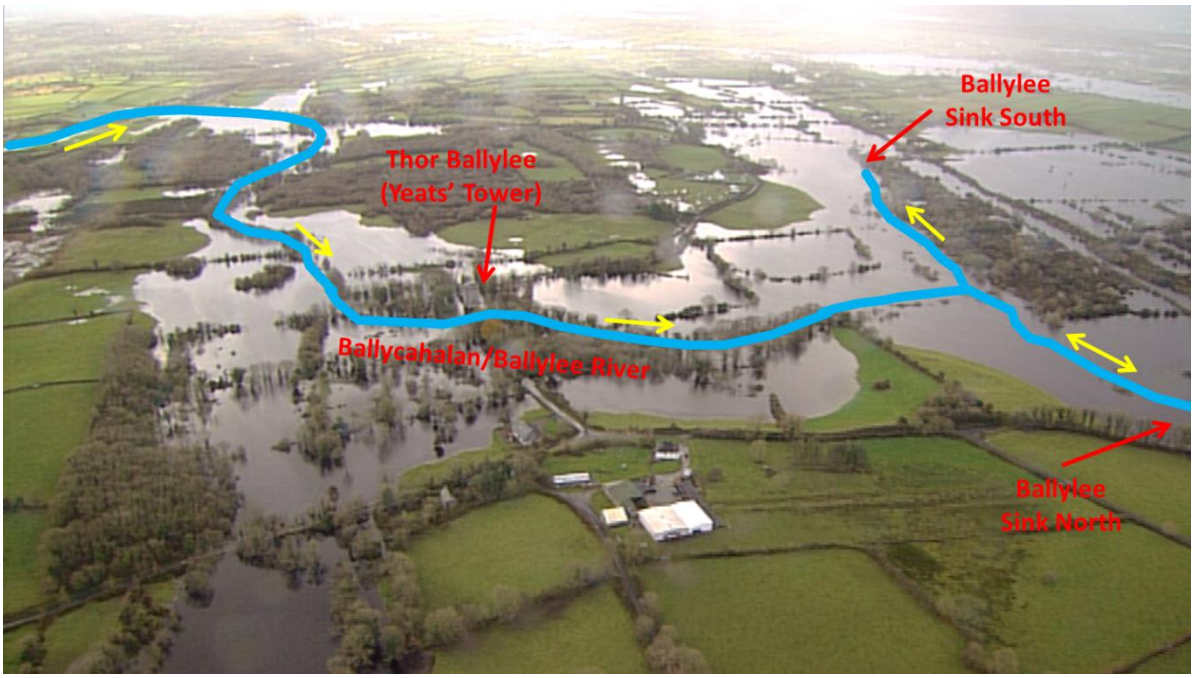

Figure B.10: Location C – Ballycahalan/Ballylee River (river path – blue, flow direction – yellow)

Figure B.11: Location D – Kiltartan. Image shows overland flow between Pollotoophill and Polldeelin (Overland flow direction shown in orange)

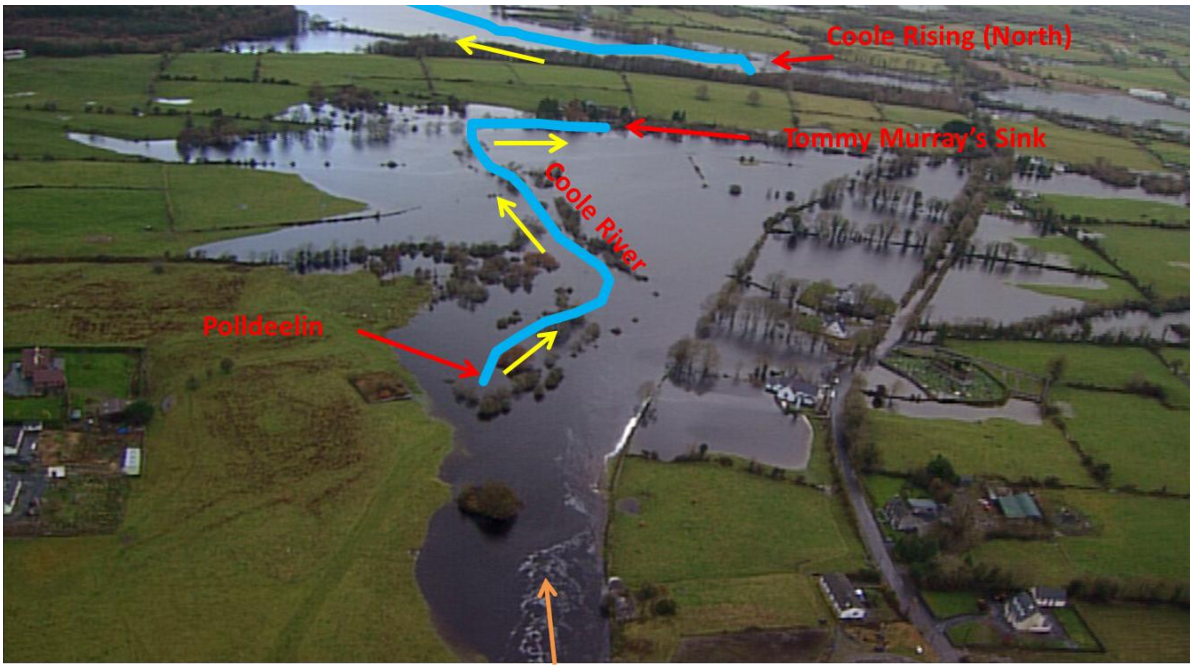

Figure B.12: Location E – Kiltartan. Image shows flooding at Coole River (river path – blue, flow direction – yellow, overland flow - orange)

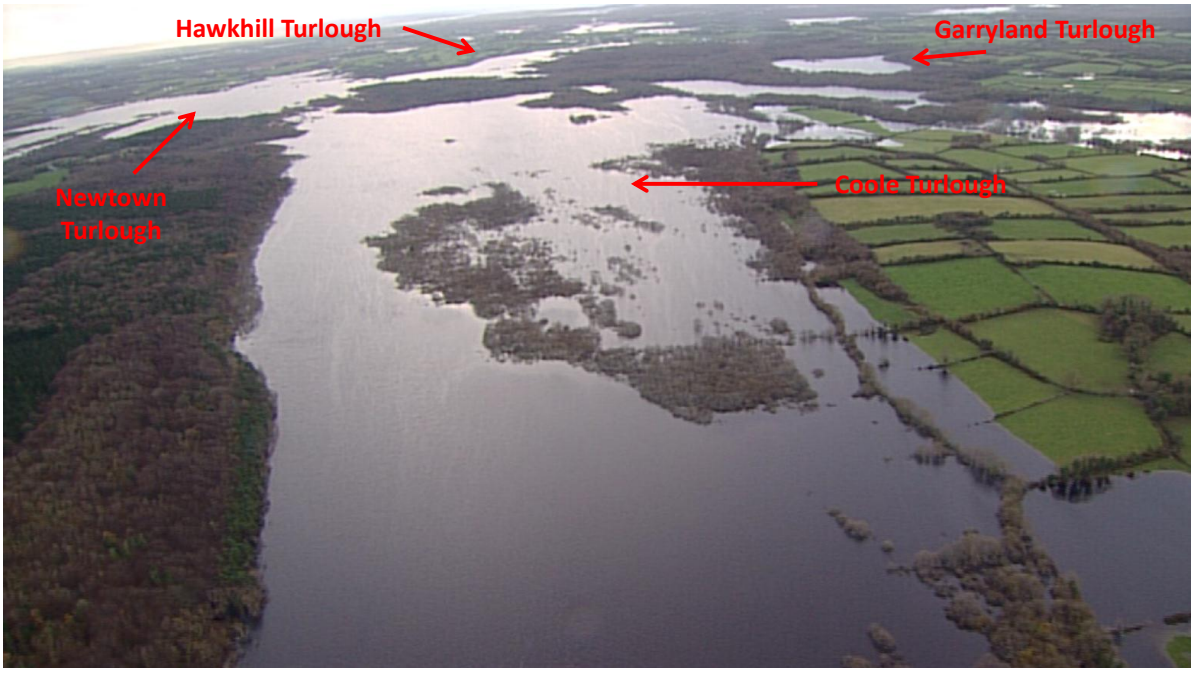

Figure B.13: Location F – Coole turlough and surrounding turloughs.

Figure B.14: Location G – Coole turlough and view towards Caherglassaun and Kinvara.

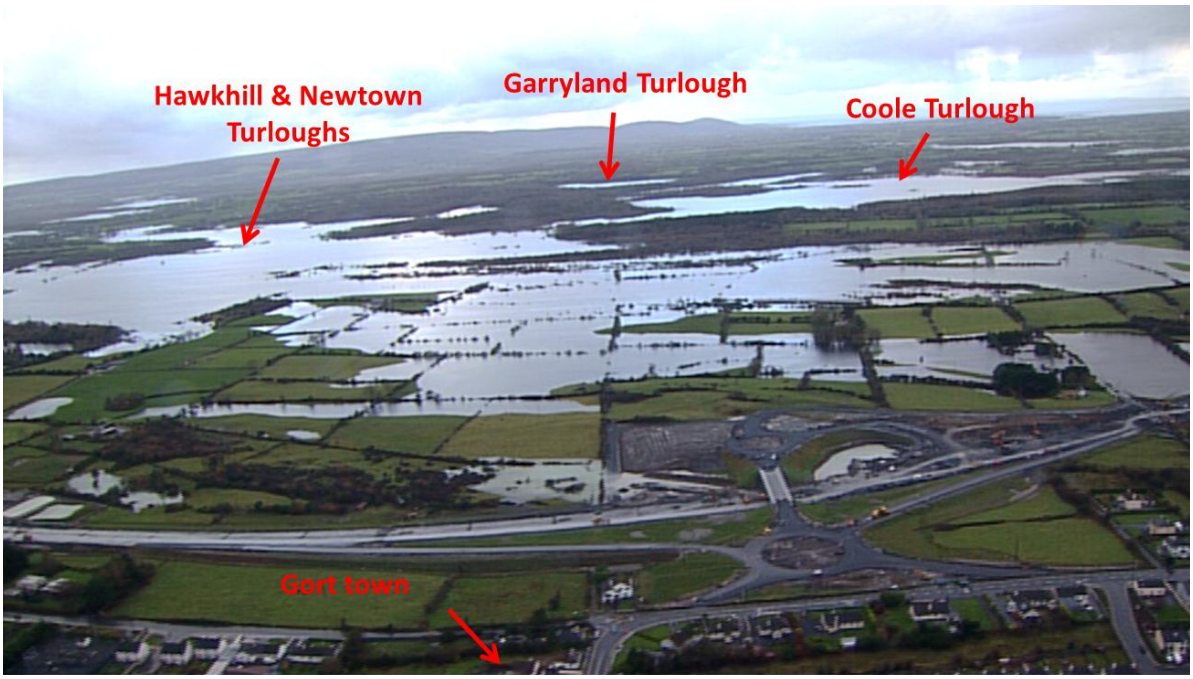

Figure B.15: Location H – Coole turlough (and surrounding turloughs) as viewed from Gort town.

Appendix C

Hydrological Data

Plots for BH5 and BH16 water levels.

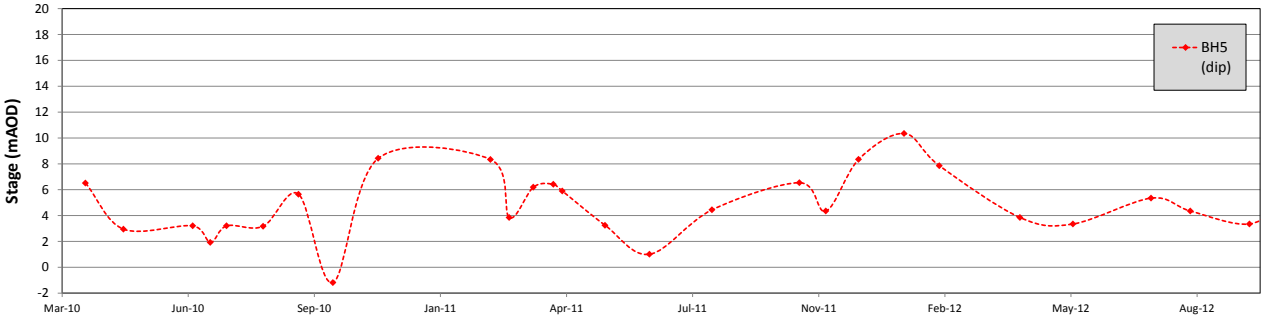

Figure C.1: BH5

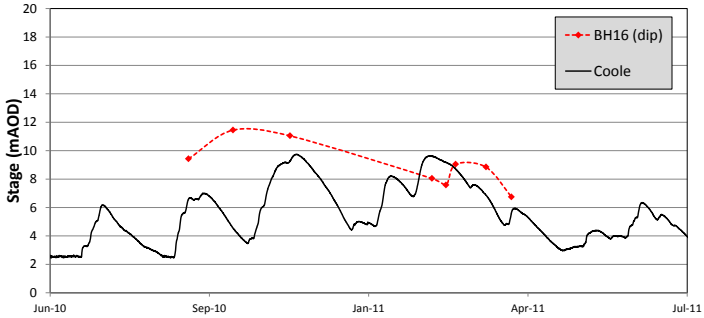

Figure C.2: BH16 and Coole

Appendix D

Sensitivity Analysis

Figure D.1: Conduit names and locations (for circular conduits)

Blackrock

Table D.1: Changes in max volume (1000 m³) of Blackrock turlough with altering conduit size (change in volume is positive unless indicated to be negative by a minus symbol).

	Increasing conduit size						Reducing conduit size				
Conduit name	105%	110%	125%	150%	175%	200%	95%	90%	75%	50%	25%
21.1	-9.824	-9.824	-9.824	-17.268	-20.088	-21.062	6.17	12.062	35.948	81.017	106.229
21.R	108.868	108.868	108.868	108.963	109.019	108.885	-73.221	-156.531	-506.13	-1672.91	-2125.59
22.1	-15.282	-15.282	-15.282	-45.251	-48.212	-49.783	9.219	19.1	53.38	99.442	122.888
23.1	-3.042	-3.042	-3.042	-6.685	-6.971	-6.96	2.973	6.376	25.368	68.663	101.158
24.1	-22.464	-22.464	-22.464	-46.493	-48.86	-49.78	17.818	42.492	192.279	1198.124	1860.449
25.1	-1.055	-1.055	-1.055	-1.812	-1.646	-1.174	1.025	2.261	10.941	100.491	379.997
25.2	-36.665	-36.665	-36.665	-62.716	-66.809	-68.901	30.832	70.773	268.935	890.676	1484.144
26.1	-6.107	-6.107	-6.107	-13.223	-14.504	-15.236	5.152	12.197	54.938	238.097	435.66
27.1	-7.691	-7.691	-7.691	-17.23	-18.906	-19.566	6.11	15.113	64.551	270.546	481.908
28.1	-0.786	-0.786	-0.786	-2.28	-2.522	-2.343	0.776	2.158	8.326	74.177	414.706
29.2	-1.079	-1.079	-1.079	-8.537	-15.363	-23.042	1.079	0.872	2.485	4.124	4.796
30.1	3.706	3.706	3.706	6.554	6.301	10.289	0.108	-0.034	-0.008	0.106	-0.102
31.1	-1.107	-1.107	-1.107	-3.699	-4.534	-6.596	0.625	1.581	8.519	89.906	798.909
32.1	-1.194	-1.194	-1.194	-3.586	-4.333	-5.997	0.575	1.766	8.611	96.781	821.27
33.1	-0.459	-0.459	-0.459	-0.905	-1.455	-0.807	0.265	0.307	1.099	12.216	371.466
34.1	-1.463	-1.463	-1.463	-3.37	-3.994	-4.179	0.882	2.394	11.471	101.186	1020.125
35.1	-9.261	-9.261	-9.261	-21.708	-23.918	-25.542	7.466	15.873	69.923	481.043	1273.001
36.1	-7.932	-7.932	-7.932	-18.925	-21.227	-22.463	5.817	14.499	61.418	440.081	1267.247
37.1	-9.633	-9.633	-9.633	-21.556	-23.679	-25.07	7.889	16.642	70.721	489.585	1275.881
38.1	-17.787	-17.787	-17.787	-40.993	-45.121	-47.556	13.724	32.199	151.986	796.865	1081.718
39.1	-14.766	-14.766	-14.766	-34.584	-41.019	-44.456	11.337	26.24	139.923	798.289	1078.938
42.1	0.064	0.064	0.064	-0.17	0.148	-0.118	-0.027	0.053	-0.035	-0.183	0.246
43.1	0.067	0.067	0.067	-0.115	-0.053	0.062	-0.066	0.116	-0.135	0.709	36.79
44.1	-0.148	-0.148	-0.148	-0.115	-0.045	-0.058	0.241	0.004	0.01	0.873	37.699
45.1	1.03	1.03	1.03	0.156	-0.091	-0.054	0.357	-0.149	-0.022	-0.422	34.711
46.1	-0.093	-0.093	-0.093	-0.061	0.019	-0.646	-0.091	0.335	0.222	0.023	21.428
47.1	0.298	0.298	0.298	0.051	0.015	-0.623	-0.019	-0.005	-0.074	-0.007	12.226
48.2	-0.08	-0.08	-0.08	-0.42	-0.224	-0.156	0.088	-0.099	-0.37	4.852	14.751
49.1	-0.011	-0.011	-0.011	-0.015	0.286	-0.429	0.211	0.289	-0.189	0.073	12.155
50.1	-0.063	-0.063	-0.063	0.436	0.039	-0.062	0.14	0.086	-0.139	0.274	15.025
51.1	-0.338	-0.338	-0.338	0.347	-0.393	-0.364	-0.013	-0.075	0.041	0.099	48.293
52.1	0.234	0.234	0.234	-0.332	-0.417	-0.403	0.31	-0.04	-0.128	-0.091	16.942
53.1	-0.007	-0.007	-0.007	-0.363	-0.453	-0.488	-0.089	0.085	-0.084	-0.04	17.389
54.1	-0.214	-0.214	-0.214	-0.4	-0.466	-0.234	0.264	-0.376	0.248	0.236	15.199
55.1	-0.395	-0.395	-0.395	-0.461	-0.424	-0.309	-0.108	0.064	-0.067	0.109	44.295
56.1	-0.187	-0.187	-0.187	-0.51	-0.517	-0.402	0.371	1.506	0.499	1.37	37.513
B7.1	1.682	1.682	1.682	8.098	10.172	12.647	-0.363	-0.424	-1.205	-58.764	-133.525
Blck.1	-173.89	-173.89	-173.89	-450.417	-498.209	-518.552	183.939	393.195	1122.696	1860.449	1860.449
Caherglassaun.1	-0.004	-0.004	-0.004	0.166	-0.051	-0.096	0.01	0.068	-0.033	0.227	-0.22
Coole.1	-0.556	-0.556	-0.556	-0.601	0.197	0.131	-0.091	-0.126	0.069	0.57	47.596
Coole.2	0	0	0	0	0	0	0	0	0	0	0
Coole_estav.1	-0.083	-0.083	-0.083	0.049	0.047	-0.169	0.197	0.262	-0.235	-0.094	-0.176
Coole_estav.2	-0.075	-0.075	-0.075	0.212	-0.201	-0.152	-0.291	0.029	0.144	0.054	0.335
Coole_O1.1	0	0	0	0	0	0	0	0	0	0	0
Coole_O2.1	0	0	0	0	0	0	0	0	0	0	0
Coole_O3.1	0	0	0	0	0	0	0	0	0	0	0
Coole_O4.1	0	0	0	0	0	0	0	0	0	0	0
Coole_O5.1	0	0	0	0	0	0	0	0	0	0	0
Coy.1	-1.821	-1.821	-1.821	-4.324	-4.763	-4.836	1.547	3.439	16.895	119.424	407.426
Coy.o	1.944	1.944	1.944	11.282	17.905	24.754	-0.813	-1.724	-4.119	-7.065	-7.868
G42.1	0.542	0.542	0.542	-0.003	-0.076	-0.018	0.085	0.163	0.11	-0.002	-0.008
G43.1	0.258	0.258	0.258	-0.165	-0.276	-0.22	0.029	0.435	-0.09	0.334	0.192
Garry_estav.1	-0.017	-0.017	-0.017	-0.084	0.193	-0.084	0.217	0.172	-0.13	0.138	0.032
Garry_estav.2	-0.069	-0.069	-0.069	-0.128	0.214	0.032	0.126	-0.052	0.309	0.182	-0.076
Garryland.1	-0.003	-0.003	-0.003	-0.118	-0.306	0.151	-0.094	0.014	0.11	0	-0.021
GB1.1	0.009	0.009	0.009	0.056	-0.016	0.008	0.095	0.024	0.245	-0.104	-0.092
GB2.1	0.016	0.016	0.016	-0.066	-0.097	0.007	0.128	0.059	0.186	0.036	-0.398
GB3.1	0.045	0.045	0.045	-0.039	0.037	0.046	0.397	0.029	-0.253	-0.224	0.07
GB4.1	-0.092	-0.092	-0.092	0.037	0.116	-0.55	0.004	0.049	0.09	0.079	0.062
P1.1	-36.173	-36.173	-36.173	-61.232	-64.62	-66.115	30.376	69.893	267.373	886.75	1484.66
P2.1	-36.132	-36.132	-36.132	-61.695	-65.288	-66.837	30.496	69.939	267.346	886.768	1483.983
P3.1	-36.124	-36.124	-36.124	-61.847	-65.619	-66.725	30.584	70.053	267.477	886.962	1482.877
X14.1	0.784	0.784	0.784	1.397	1.54	1.254	-0.767	-2.219	-12.003	-44.628	-59.184
X5.1	0.137	0.137	0.137	0.288	0.013	-0.246	0.031	-0.437	-2.557	-30.165	-48.648
X6.1	-0.142	-0.142	-0.142	0.225	-0.098	0.137	0.093	-0.338	-3.831	-32.743	-49.855

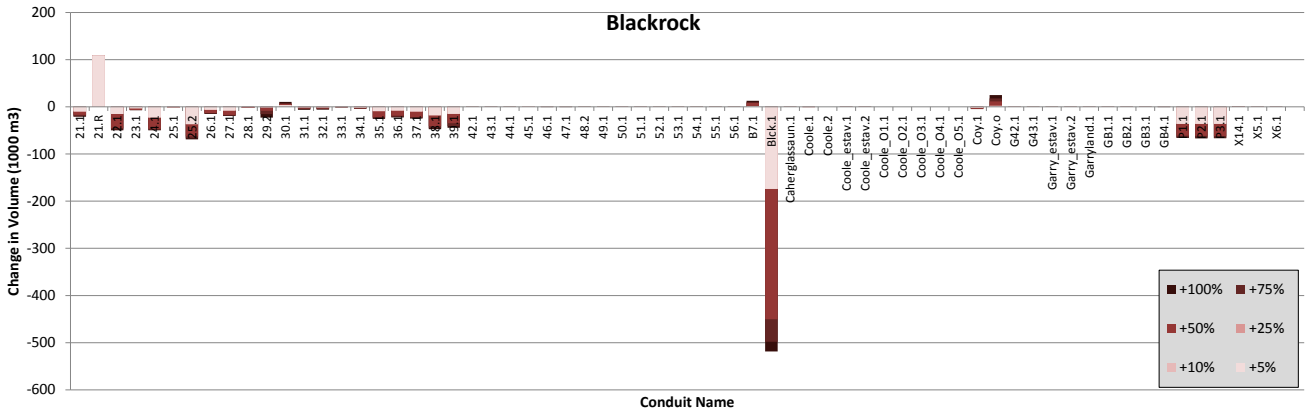

Figure D.2: Change in Blackrock volume when conduits expanded.

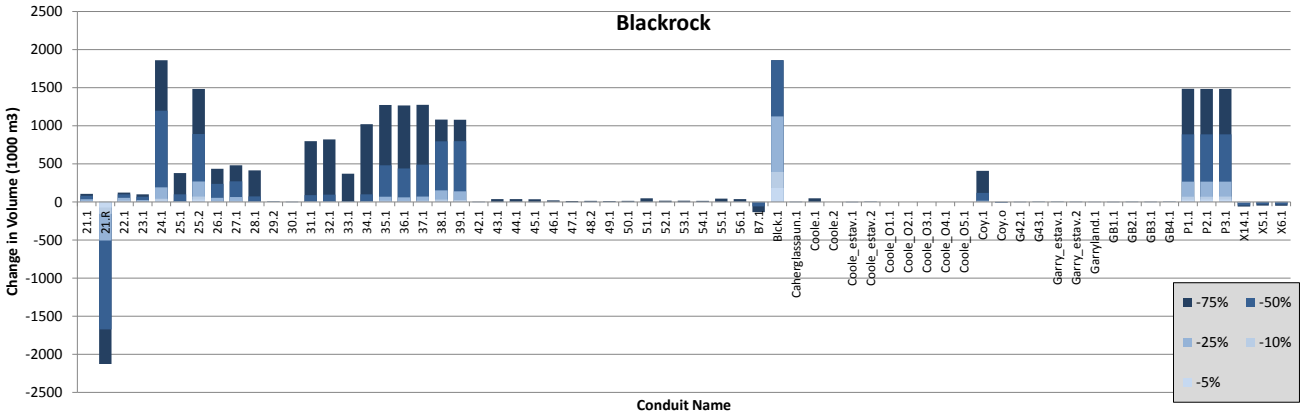

Figure D.3: Change in Blackrock volume when conduits reduced.

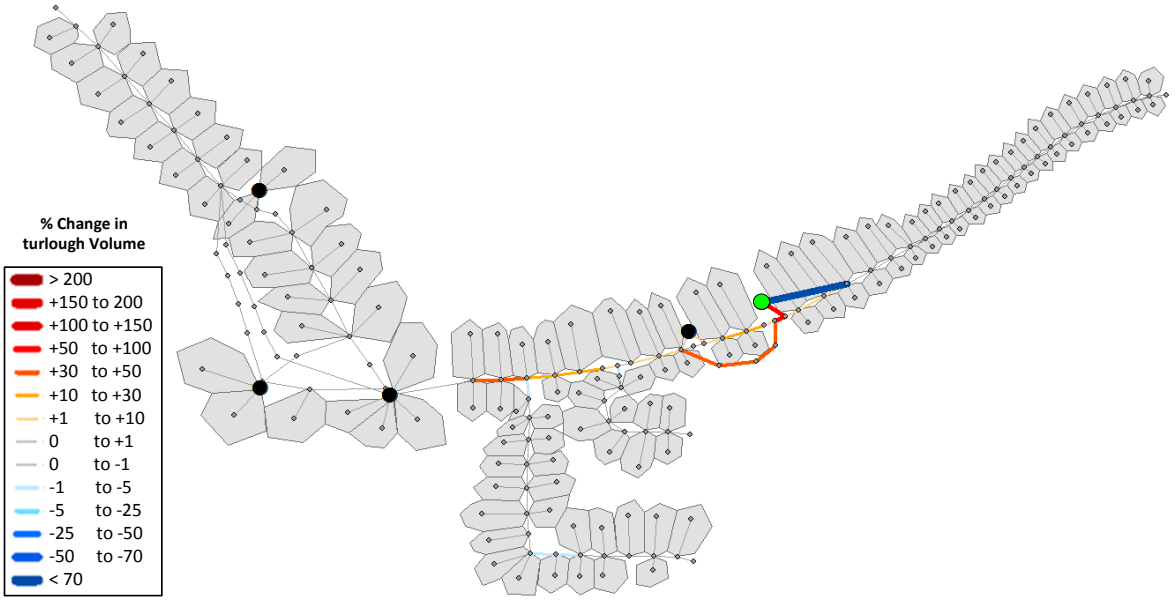

Figure D.4: Percentage changes in volume of Blackrock turlough from reducing size of individual conduits by 50%

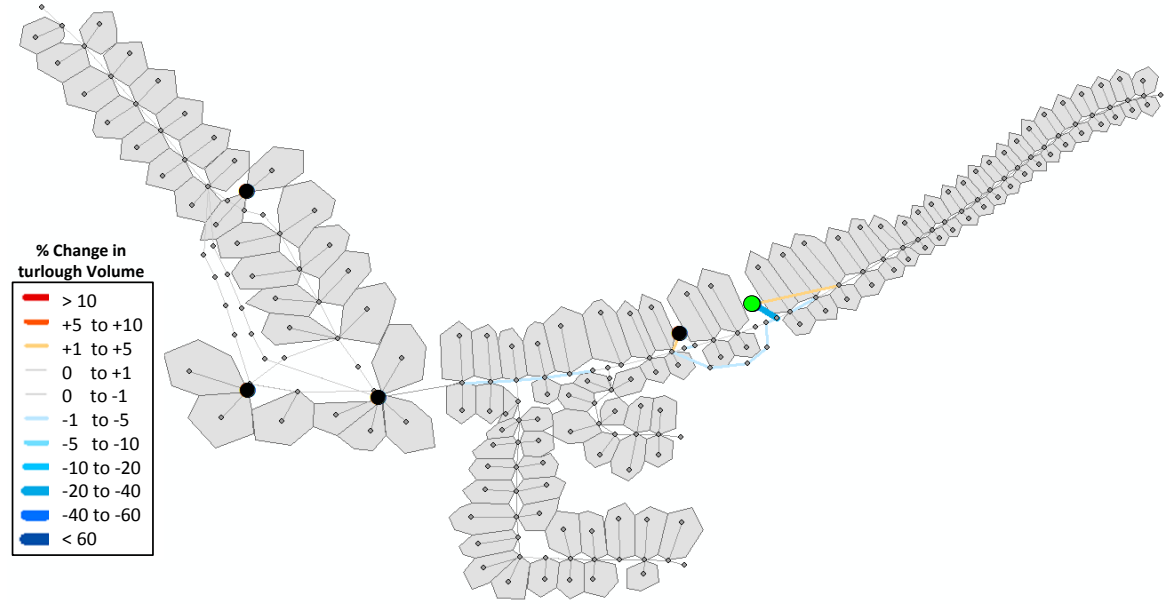

Figure D.5: Percentage changes in volume of Blackrock turlough from increasing size of individual conduits by 100%

Coy

Table D.2: Changes in max volume (1000 m³) of Coy turlough with altering conduit size (change in volume is positive unless indicated to be negative by a minus symbol).

	Increasing conduit size						Reducing conduit size				
Conduit name	105%	110%	125%	150%	175%	200%	95%	90%	75%	50%	25%
21.1	4.952	4.952	9.599	13.94	14.639	15.101	-3.351	-7.554	-22.986	-50.578	-65.255
21.R	21.273	21.273	21.017	20.837	20.747	20.736	-18.032	-39.891	-133.147	-528.605	-916.179
22.1	8.63	8.63	16.562	22.589	24.788	25.635	-5.106	-10.944	-30.604	-59.105	-72.175
23.1	1.85	1.85	3.238	4.292	4.587	4.669	-1.135	-2.799	-11.628	-51.168	-82.63
24.1	11.37	11.37	18.978	23.528	24.97	25.611	-9.194	-21.681	-95.314	-544.203	-973.657
25.1	3.109	3.109	5.502	7.157	7.85	8.393	-2.33	-5.689	-26.26	-159.948	-698.345
25.2	-62.333	-62.333	-105.937	-134.612	-144.959	-149.387	37.043	66.847	135.567	230.097	307.3
26.1	13.643	13.643	22.204	28.229	30.299	30.989	-11.091	-26.031	-93.547	-364.609	-861.216
27.1	15.39	15.39	25.201	32.266	34.514	35.425	-12.841	-29.546	-103.831	-404.761	-939.362
28.1	1.791	1.791	3.042	3.649	3.848	4.085	-1.299	-2.938	-15.073	-111.201	-682.576
29.2	-5.237	-5.237	-15.121	-35.913	-62.785	-94.473	2.641	4.307	9.539	14.782	16.927
30.1	4.358	4.358	4.138	7.298	6.049	9.076	0.075	-0.03	-0.031	0.044	-0.089
31.1	-1.252	-1.252	-2.344	-3.634	-4.163	-5.283	0.878	2.104	10.518	80.026	1006.376
32.1	-1.314	-1.314	-2.001	-3.423	-3.903	-4.841	0.786	2.153	10.298	81.128	1006.376
33.1	-0.379	-0.379	-0.56	-0.728	-0.922	-0.153	0.218	0.301	1.292	14.894	232.158
34.1	-0.77	-0.77	-1.755	-2.269	-2.561	-2.645	0.55	1.556	7.23	50.136	1006.376
35.1	-5.856	-5.856	-10.467	-13.553	-14.713	-15.528	4.678	9.938	37.232	287.685	1006.376
36.1	-5.005	-5.005	-8.705	-11.768	-13.174	-13.79	3.719	8.993	33.744	245.026	1006.376
37.1	-6.063	-6.063	-10.524	-13.482	-14.792	-15.571	4.848	10.237	37.283	315.231	1006.376
38.1	-12.488	-12.488	-21.861	-29.578	-32.823	-34.905	9.373	21.034	75.284	531.012	1006.376
39.1	-10.312	-10.312	-18.114	-25.166	-30.246	-32.828	7.443	16.758	69.284	530.272	1006.376
42.1	0.042	0.042	-0.062	-0.126	0.099	-0.072	-0.011	0.043	0.017	-0.214	-0.444
43.1	-0.002	-0.002	0.097	-0.201	-0.166	-0.105	0.014	0.115	-0.353	17.216	89.056
44.1	-0.115	-0.115	-0.221	-0.167	-0.131	-0.159	0.183	0.033	-0.289	17.864	89.554
45.1	0.489	0.489	0.059	-0.007	-0.115	-0.14	0.229	-0.045	-0.034	5.523	86.89
46.1	-0.042	-0.042	-0.045	-0.023	0.003	-0.365	-0.021	0.204	0.147	-0.543	73.967
47.1	0.158	0.158	0.001	0.037	0.053	-0.196	0.007	0.002	-0.015	-0.194	58.355
48.2	-0.244	-0.244	-0.278	-0.305	-0.251	-0.275	0.021	-0.481	2.74	55.028	66.405
49.1	-0.07	-0.07	-0.118	-0.202	0.008	-0.453	0.182	0.206	-0.503	12.493	66.329
50.1	-0.032	-0.032	0.161	0.504	-0.029	-0.065	0.111	0.112	-0.102	1.889	67.324
51.1	-0.197	-0.197	-0.037	0.164	-0.292	-0.276	0.003	0.001	0.028	1.808	89.416
52.1	0.12	0.12	-0.004	-0.24	-0.286	-0.283	0.201	0.007	-0.061	1.67	69.173
53.1	-0.066	-0.066	-0.23	-0.26	-0.296	-0.296	-0.008	0.093	0.002	1.682	71.521
54.1	-0.149	-0.149	-0.26	-0.266	-0.305	-0.211	0.198	-0.195	0.188	1.723	70.048
55.1	-0.269	-0.269	-0.271	-0.3	-0.281	-0.214	-0.023	0.063	0.02	0.855	87.875
56.1	-0.223	-0.223	-0.318	-0.354	-0.351	-0.321	0.348	1.046	0.48	0.616	66.702
B7.1	1.186	1.186	2.318	6.373	8.851	10.159	-0.114	-0.257	-0.635	-32.294	-71.687
Blck.1	88.581	88.581	134.074	156.525	162.821	165.085	-96.443	-198.617	-531.254	-871.11	-954.529
Caherglassaun.1	0.004	0.004	-0.005	0.116	-0.002	-0.026	0.018	0.044	-0.005	0.111	-0.091
Coole.1	-0.138	-0.138	-0.216	-0.143	0.117	0.131	-0.044	0.006	0.118	-0.183	94.121
Coole.2	0	0	0	0	0	0	0	0	0	0	0
Coole_estav.1	-0.041	-0.041	0.01	0.043	0.053	-0.14	0.122	0.157	-0.142	0.006	-0.115
Coole_estav.2	-0.045	-0.045	-0.198	0.062	-0.181	-0.17	-0.146	0.046	0.142	-0.189	-0.4
Coole_O1.1	0	0	0	0	0	0	0	0	0	0	0
Coole_O2.1	0	0	0	0	0	0	0	0	0	0	0
Coole_O3.1	0	0	0	0	0	0	0	0	0	0	0
Coole_O4.1	0	0	0	0	0	0	0	0	0	0	0
Coole_O5.1	0	0	0	0	0	0	0	0	0	0	0
Coy.1	4.096	4.096	6.921	8.594	9.083	9.34	-3.07	-7.499	-33.038	-190.461	-805.06
Coy.o	3.144	3.144	8.175	16.467	23.478	30.152	-1.373	-2.833	-6.521	-10.861	-12.502
G42.1	0.868	0.868	0.054	-0.028	0.019	-0.003	0.068	0.122	0.097	0.044	-0.029
G43.1	0.105	0.105	-0.049	-0.089	-0.203	-0.155	0.053	0.228	-0.019	0.236	0.145
Garry_estav.1	-0.003	-0.003	0.01	-0.052	0.142	-0.059	0.132	0.104	0.049	0.1	0.071
Garry_estav.2	-0.036	-0.036	0.166	-0.089	0.137	0.017	0.084	-0.02	0.193	0.173	-0.047
Garryland.1	0	0	-0.064	-0.062	-0.166	0.147	-0.041	0.003	0.08	0.027	0.008
GB1.1	0.006	0.006	-0.156	0.033	-0.001	0.013	0.064	0.026	0.18	-0.018	-0.041
GB2.1	0.02	0.02	0.132	-0.006	-0.074	0.022	0.099	0.062	0.132	0.069	-0.211
GB3.1	0.026	0.026	0.129	-0.026	0.028	0.028	0.221	0.039	-0.097	-0.006	0.068
GB4.1	-0.113	-0.113	-0.32	-0.192	-0.118	-0.375	-0.008	0.107	0.085	0.033	0.025
P1.1	-61.935	-61.935	-105.248	-133.383	-143.167	-147.175	36.789	66.606	135.309	229.911	307.655
P2.1	-61.957	-61.957	-105.339	-133.754	-143.722	-147.737	36.829	66.627	135.304	229.892	307.607
P3.1	-61.939	-61.939	-105.484	-134.451	-144.462	-147.624	36.857	66.646	135.316	229.892	307.576
X14.1	0.414	0.414	0.774	0.766	0.861	0.736	-0.348	-1.113	-7.073	-38.122	-52.018
X5.1	0.077	0.077	0.042	0.186	0.014	-0.139	0.049	-0.232	-1.08	-29.117	-45.894
X6.1	-0.064	-0.064	-0.01	0.145	-0.055	0.093	0.055	-0.213	-2.111	-31.746	-46.702

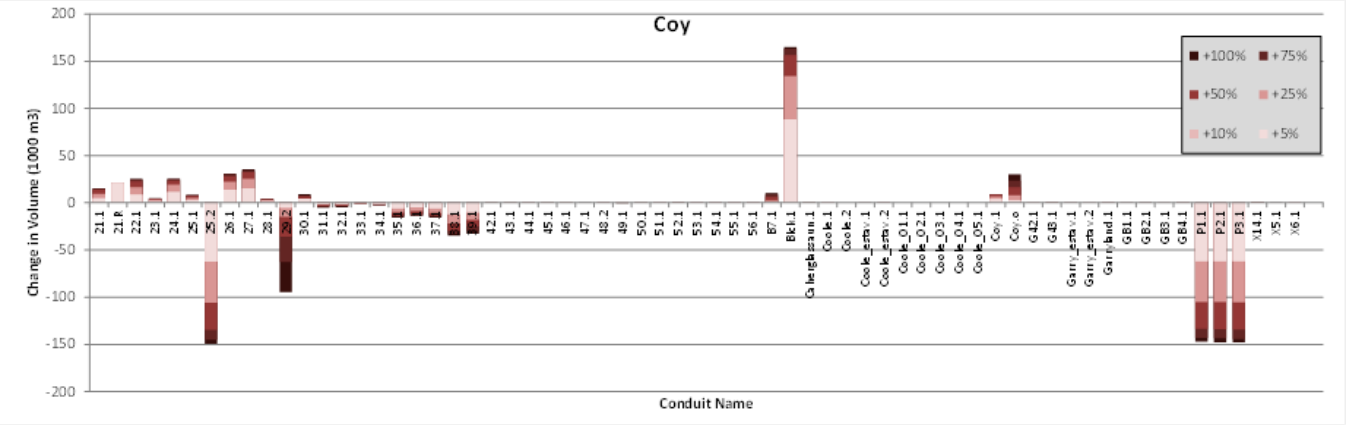

Figure D.6: Change in Coy volume when conduits expanded.

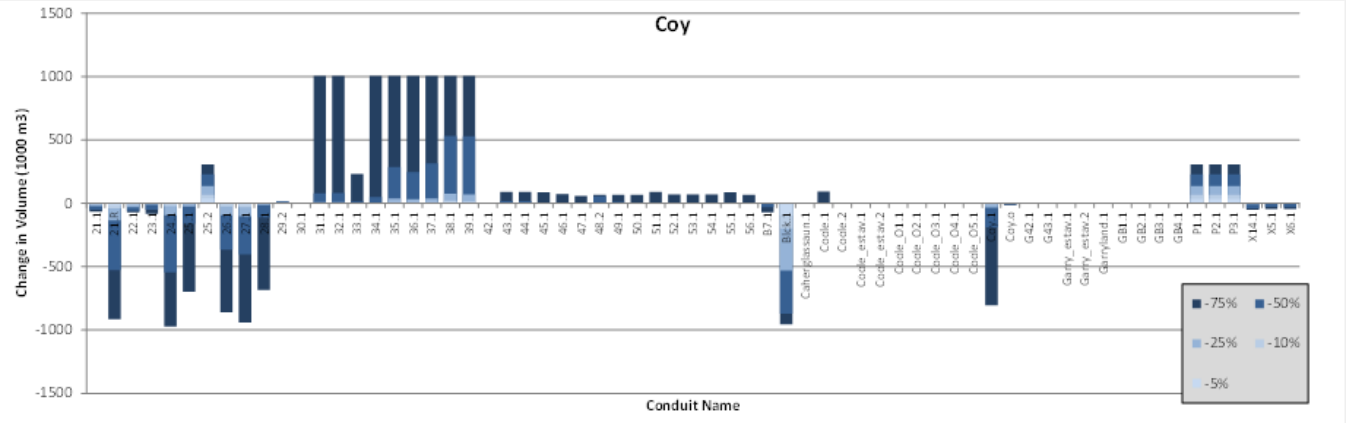

Figure D.7: Change in Coy volume when conduits reduced.

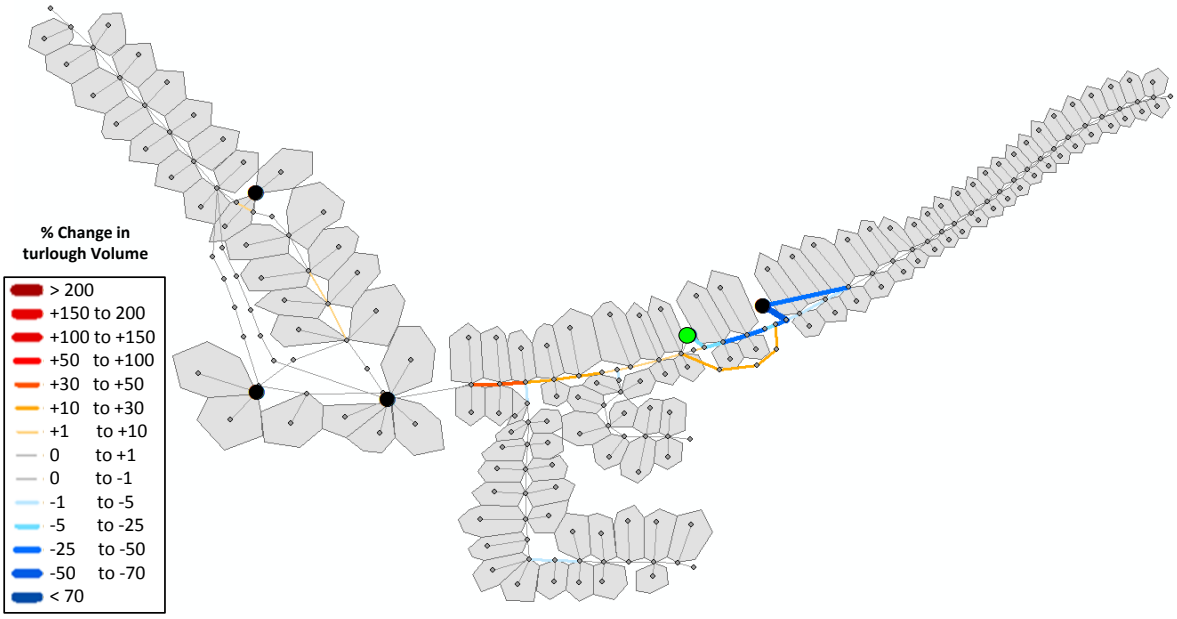

Figure D.8: Percentage changes in volume of Coy turlough from reducing size of individual conduits by 50%

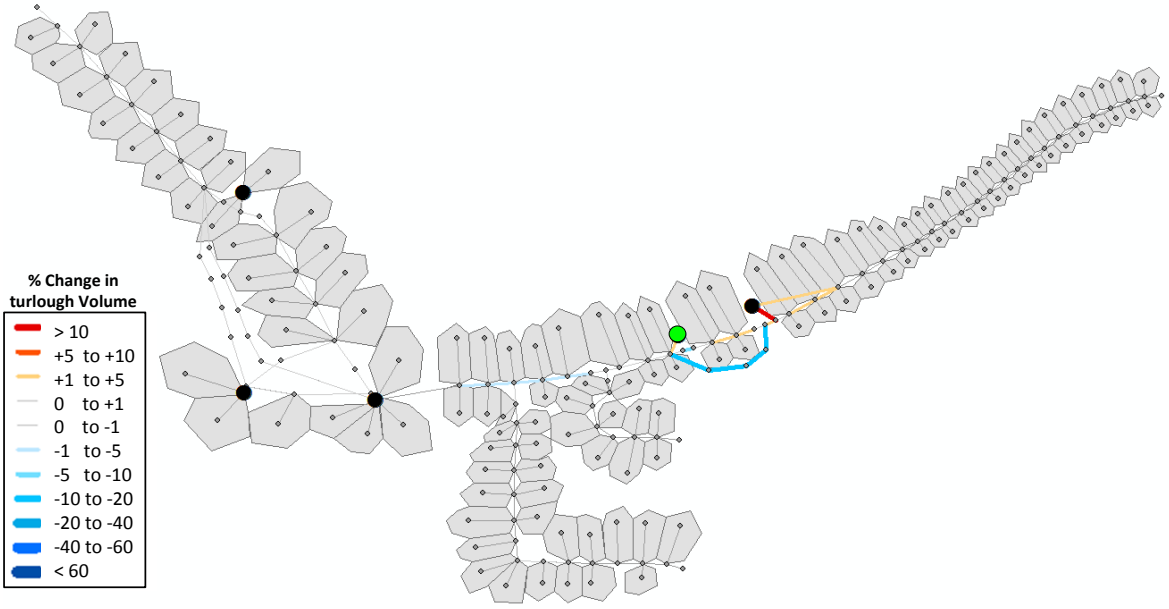

Figure D.9: Percentage changes in volume of Coy turlough from increasing size of individual conduits by 100%

Coole

Table D.3: Changes in max volume (1000 m³) of Coole turlough with altering conduit size (change in volume is positive unless indicated to be negative by a minus symbol).

	Increasing conduit size						Reducing conduit size				
Conduit name	105%	110%	125%	150%	175%	200%	95%	90%	75%	50%	25%
21.1	-0.637	-0.637	5.873	9.595	3.465	6.355	0.359	-2.115	-7.266	-32.287	-41.825
21.R	10.359	10.359	10.552	9.722	9.663	12.9	-3.659	-13.053	-73.391	-360.71	-946.367
22.1	8.466	8.466	15.142	16.551	20.795	20.841	-1.6	-4.67	-27.286	-45.308	-56.538
23.1	4.123	4.123	3.645	5.97	5.962	6.329	-0.32	-1.307	-8.365	-56.573	-76.832
24.1	9.602	9.602	14.088	17.885	16.74	19.262	-3.885	-8.032	-66.579	-390.211	-1202.546
25.1	0.47	0.47	-1.421	0.964	0.401	1.741	4.436	2.472	8.041	57.957	194.876
25.2	51.98	51.98	85.802	120.193	128.462	129.744	-45.505	-84.123	-250.332	-624.496	-961.353
26.1	-4.848	-4.848	-5.484	-6.503	-7.62	-11.031	3.732	8.616	33.41	118.684	212.935
27.1	-3.754	-3.754	-4.332	-7.949	-9.545	-10.465	4.134	10.709	34.317	132.79	231.396
28.1	3.406	3.406	2.893	2.149	-0.912	0.955	1.193	4.577	5.206	35.1	193.049
29.2	6.286	6.286	11.632	25.007	38.709	61.243	3.186	-6.379	-4.155	-7.234	-8.768
30.1	29.349	29.349	46.704	76.556	102.303	122.388	1.559	0.238	-0.068	2.941	-1.164
31.1	1.27	1.27	-1.542	-2.914	7.527	-0.417	-0.911	-0.929	-7.953	-109.742	-1012.563
32.1	-2.666	-2.666	9.85	-8.699	5.529	-1.007	-4.06	-1.273	-16.464	-115.851	-1045.334
33.1	-6.648	-6.648	-7.265	-6.046	-7.945	5.957	2.412	1.433	1.164	-22.405	-370.353
34.1	2.962	2.962	-2.145	-2.286	-2.242	-9.411	-8.349	-3.158	-25.792	-184.814	-1975.504
35.1	22.418	22.418	31.461	44.084	51.194	56.807	-8.242	-30.516	-118.645	-738.035	-3107.138
36.1	17.544	17.544	35.24	33.218	27.764	36.054	-16.142	-23.323	-98.464	-663.2	-3068.595
37.1	14.026	14.026	28.351	38.298	40.655	37.519	-6.253	-35.544	-122.401	-747.838	-3139.368
38.1	41.355	41.355	73.512	80.967	93.11	95.187	-34.031	-79.284	-325.948	-2209.126	-4174.576
39.1	31.998	31.998	60.46	80.229	77.698	88.793	-24.822	-69.597	-308.414	-2564.861	-4186.453
42.1	-10.717	-10.717	-26.644	-30.691	-27.105	-38.546	11.475	23.751	78.279	371.24	839.718
43.1	-67.402	-67.402	-120.781	-160.694	-170.751	-176.06	54.391	128.789	545.012	2958.679	6832.966
44.1	-69.783	-69.783	-127.343	-159.782	-170.558	-182.285	55.651	129.432	555.908	2988.03	6844.961
45.1	-33.812	-33.812	-65.629	-93.631	-100.658	-104.141	32.787	70.486	326.71	2201.372	6690.629
46.1	-15.338	-15.338	-24.448	-23.744	-25.846	-34.067	10.02	23.059	96.409	852.534	6010.959
47.1	-2.966	-2.966	-7.312	-9.812	-10.126	153.391	4.151	11.214	50.207	473.723	5139.956
48.2	-522.718	-522.718	-1056.682	-1486.124	-1657.149	-1716.279	320.022	669.626	1909.4	5005.625	5419.445
49.1	-92.688	-92.688	-168.771	-223.542	-233.7	-247.151	72.26	168.513	666.876	2963.978	5335.29
50.1	-22.571	-22.571	-41.433	-48.615	-57.233	-62.173	24.639	55.803	262.066	1730.647	5508.236
51.1	-28.964	-28.964	-40.495	-49.386	-67.458	-64.47	21.421	49.693	260.389	1732.931	5974.9
52.1	-20.622	-20.622	-42.213	-55.251	-60.258	-61.59	21.567	46.146	250.917	1725.805	5535.174
53.1	-24.227	-24.227	-42.035	-52.871	-64.016	-57.213	19.119	44.101	230.015	1720.05	5544.659
54.1	-28.53	-28.53	-40.213	-50.409	-54.617	-63.867	18.797	33.964	207.333	1702.355	5526.654
55.1	-23.622	-23.622	-35.199	-43.326	-54.495	-50.221	14.773	34.255	172.313	1560.22	5921.468
56.1	-10.971	-10.971	-15.383	-17.451	-19.497	-20.503	9.687	21.175	52.827	603.89	5272.866
B7.1	29.991	29.991	51.513	122.026	138.274	158.219	-2.825	-7.167	-5.657	-153.095	-1100.355
Blck.1	104.199	104.199	269.124	409.479	464.59	485.541	-68.943	-123.372	-363.212	-826.31	-1118.099
Caherglassaun.1	1.743	1.743	3.057	5.036	4.369	3.835	0.606	-5.792	0.126	4.577	144.936
Coole.1	-1.952	-1.952	16.389	72.79	-37.763	-3.671	14.233	29.73	127.265	1156.608	6721.875
Coole.2	0	0	0	0	0	0	0	0	0	0	0
Coole_estav.1	-3.943	-3.943	-6.184	-7.256	7.165	-22.254	7.425	10.637	25.798	156.317	334.474
Coole_estav.2	-34.1	-34.1	-77.718	-87.961	-105.444	-107.236	19.183	54.378	177.748	545.389	911.715
Coole_O1.1	0	0	0	0	0	0	0	0	0	0	0
Coole_O2.1	0	0	0	0	0	0	0	0	0	0	0
Coole_O3.1	0	0	0	0	0	0	0	0	0	0	0
Coole_O4.1	0	0	0	0	0	0	0	0	0	0	0
Coole_O5.1	0	0	0	0	0	0	0	0	0	0	0
Coy.1	0.46	0.46	1.412	0.931	-1.382	-0.219	3.381	0.611	10.287	62.315	218.016
Coy.o	0.352	0.352	1.476	3.566	6.612	7.892	3.072	-0.113	0.914	-5.255	0.372
G42.1	-2.118	-2.118	-12.046	-26.164	-19.126	-21.61	10.331	15.314	56.739	202.106	351.682
G43.1	-10.384	-10.384	-23.583	-34.845	-43.379	-54.564	10.169	20.47	52.976	122.755	169.967
Garry_estav.1	-2.224	-2.224	-3.191	-5.673	-3.045	-12.328	4.877	6.434	20.218	77.44	155.455
Garry_estav.2	-0.89	-0.89	1.509	-12.25	-0.961	-9.026	3.164	3.532	17.279	86.763	261.033
Garryland.1	1.312	1.312	-1.17	0.395	8.083	17.934	0.19	0.255	3.446	1.316	9.42
GB1.1	-0.852	-0.852	-2.302	-11.452	-3.509	-1.124	3.438	4.912	15.865	84.792	267.531
GB2.1	-1.244	-1.244	1.407	-1.447	-4.257	-2.576	4.25	5.782	13.638	86.065	261.731
GB3.1	-0.115	-0.115	0.082	-2.481	-1.144	-2.174	6.711	5.163	12.092	85.986	269.972
GB4.1	-76.133	-76.133	-199.83	-363.111	-483.023	-555.485	26.669	67.999	164.803	268.017	314.127
P1.1	51.9	51.9	87.591	115.666	132.257	134.305	-41.05	-92.415	-255.326	-627.04	-958.93
P2.1	52.003	52.003	92.916	117.434	130.547	133.892	-41.236	-86.877	-251.329	-627.351	-960.684
P3.1	54.116	54.116	92.634	123.018	127.661	135.644	-41.496	-86.233	-252.406	-628.812	-962.793
X14.1	8.386	8.386	13.031	13.332	15.599	14.954	-4.626	-15.005	-264.502	-1831.354	-2316.819
X5.1	0.915	0.915	2.58	4.67	1.156	-3.092	4.145	-4.782	-34.489	-1461.514	-2074.314
X6.1	-0.034	-0.034	1.098	2.359	-0.045	3.081	0.98	-4.884	-113.622	-1603.439	-2103.477

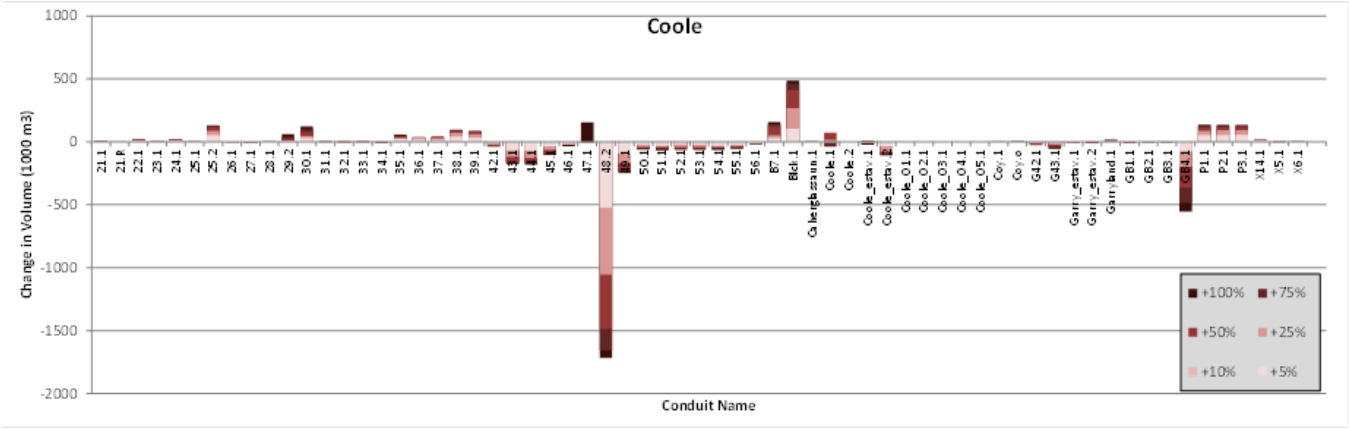

Figure D.10: Change in Coole volume when conduits expanded.

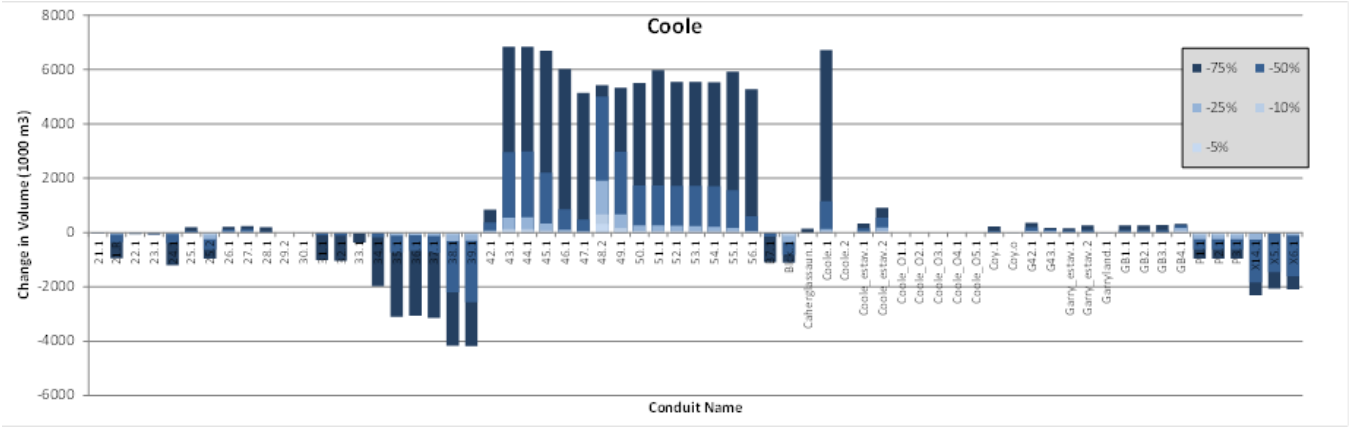

Figure D.11: Change in Coole volume when conduits reduced.

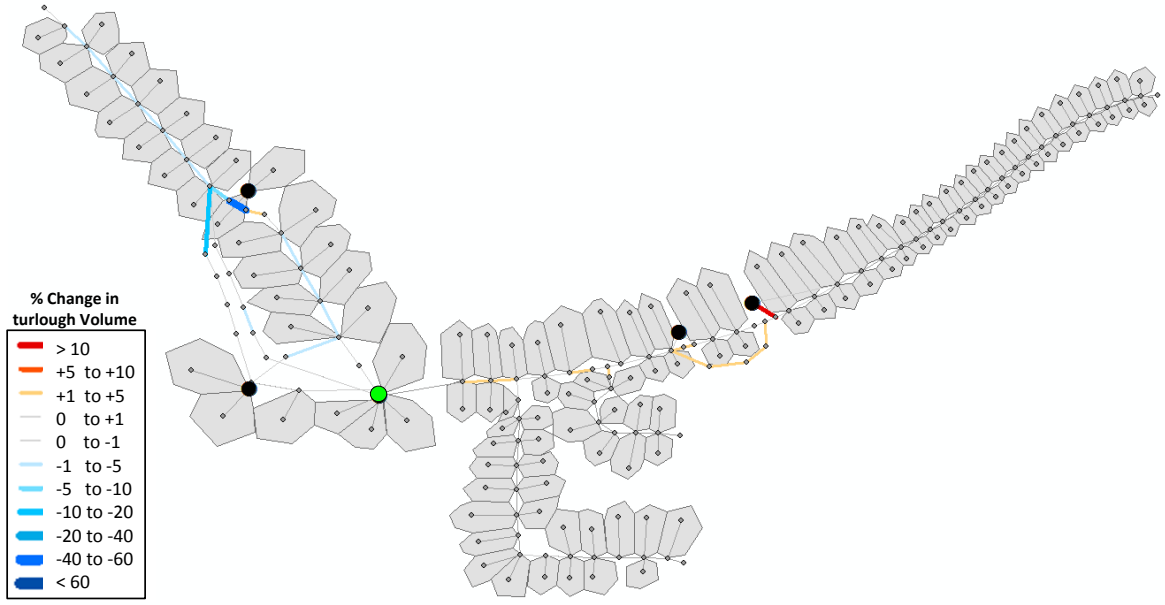

Figure D.12: Percentage changes in volume of Coole turlough from reducing size of individual conduits by 50%

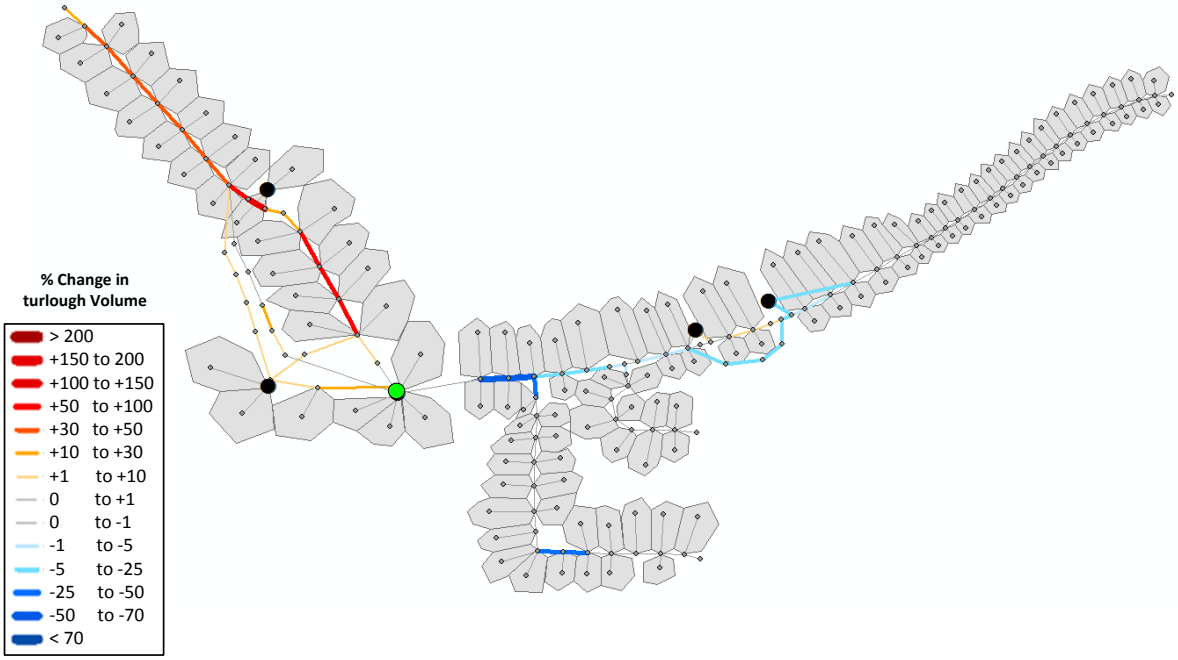

Figure D.13: Percentage changes in volume of Coole turlough from increasing size of individual conduits by 100%

Garryland

Table D.4: Changes in max volume (1000 m³) of Garryland turlough with altering conduit size (change in volume is positive unless indicated to be negative by a minus symbol).

	Increasing conduit size						Reducing conduit size				
Conduit name	105%	110%	125%	150%	175%	200%	95%	90%	75%	50%	25%
21.1	-0.122	-0.122	1.046	1.714	0.608	1.128	0.068	-0.373	-1.284	-5.763	-7.456
21.R	1.842	1.842	1.879	1.729	1.719	2.295	-0.641	-2.31	-13.037	-63.709	-165.309
22.1	1.516	1.516	2.71	2.956	3.718	3.726	-0.284	-0.831	-4.88	-8.088	-10.089
23.1	0.741	0.741	0.653	1.071	1.068	1.135	-0.055	-0.233	-1.497	-10.121	-13.716
24.1	1.718	1.718	2.515	3.192	2.986	3.439	-0.69	-1.423	-11.858	-68.917	-208.417
25.1	0.084	0.084	-0.259	0.171	0.069	0.31	0.8	0.445	1.456	10.45	34.976
25.2	9.334	9.334	15.518	21.764	23.276	23.516	-8.099	-14.942	-44.459	-110.308	-167.703
26.1	-0.877	-0.877	-0.996	-1.187	-1.394	-2.011	0.674	1.558	6.034	21.315	38.272
27.1	-0.682	-0.682	-0.794	-1.457	-1.724	-1.878	0.747	1.938	6.203	23.863	41.597
28.1	0.613	0.613	0.52	0.386	-0.166	0.171	0.215	0.825	0.942	6.351	34.675
29.2	1.123	1.123	2.069	4.44	6.92	11.016	0.578	-1.141	-0.73	-1.274	-1.546
30.1	5.172	5.172	8.219	13.515	18.115	21.647	0.282	0.044	-0.009	0.532	-0.205
31.1	0.217	0.217	-0.302	-0.558	1.314	-0.124	-0.16	-0.157	-1.389	-19.467	-176.688
32.1	-0.49	-0.49	1.752	-1.605	0.943	-0.235	-0.726	-0.218	-2.919	-20.53	-182.219
33.1	-1.192	-1.192	-1.302	-1.083	-1.426	1.035	0.436	0.262	0.218	-3.98	-65.582
34.1	0.497	0.497	-0.38	-0.403	-0.398	-1.691	-1.503	-0.566	-4.636	-32.761	-294.139
35.1	4.022	4.022	5.61	7.861	9.105	10.082	-1.482	-5.483	-21.209	-129.028	-501.638
36.1	3.164	3.164	6.306	5.925	4.943	6.425	-2.904	-4.192	-17.665	-116.124	-496.367
37.1	2.512	2.512	5.078	6.865	7.28	6.696	-1.122	-6.395	-21.859	-130.91	-505.984
38.1	7.394	7.394	13.173	14.59	16.77	17.143	-6.113	-14.197	-57.394	-336.625	-606.728
39.1	5.747	5.747	10.844	14.376	14.01	16.014	-4.461	-12.501	-54.295	-423.821	-606.842
42.1	-0.882	-0.882	-2.919	-3.084	-2.237	-4.222	1.289	2.478	7.158	36.71	83.86
43.1	-12.724	-12.724	-22.741	-30.168	-32.065	-33.052	10.28	24.545	105.304	591.854	1433.204
44.1	-13.142	-13.142	-23.904	-29.992	-32.014	-34.144	10.502	24.649	107.282	597.758	1435.865
45.1	-6.397	-6.397	-12.345	-17.518	-18.829	-19.475	6.153	13.321	62.543	435.187	1401.01
46.1	-2.847	-2.847	-4.551	-4.466	-4.858	-6.346	1.872	4.313	18.223	164.83	1247.615
47.1	-0.578	-0.578	-1.396	-1.87	-1.936	27.609	0.782	2.104	9.446	90.933	1072.157
48.2	-97.723	-97.723	-194.317	-267.762	-296.179	-308.412	61.893	130.277	382.836	1027.849	1113.346
49.1	-17.488	-17.488	-31.753	-41.963	-43.942	-46.378	13.805	32.41	129.686	599.672	1095.308
50.1	-4.315	-4.315	-7.882	-9.295	-10.853	-11.754	4.654	10.685	50.879	345.613	1136.827
51.1	-5.453	-5.453	-7.696	-9.396	-12.673	-12.151	4.062	9.524	50.586	345.988	1660.207
52.1	-3.94	-3.94	-7.986	-10.429	-11.364	-11.619	4.073	8.82	48.829	344.516	1142.568
53.1	-4.575	-4.575	-7.936	-9.981	-12.018	-10.816	3.619	8.39	44.671	343.272	1144.643
54.1	-5.338	-5.338	-7.587	-9.518	-10.313	-11.994	3.547	6.516	40.148	339.643	1140.625
55.1	-4.424	-4.424	-6.636	-8.183	-10.225	-9.478	2.799	6.5	33.215	310.206	1660.207
56.1	-2.021	-2.021	-2.847	-3.243	-3.623	-3.81	1.781	3.903	9.978	117.557	1085.469
B7.1	5.333	5.333	9.127	21.75	24.608	28.072	-0.518	-1.279	-1.006	-27.372	-190.678
Blck.1	19.113	19.113	48.94	74.326	84.331	88.138	-12.284	-21.923	-64.155	-144.662	-194.342
Caherglassaun.1	0.337	0.337	0.599	0.974	0.866	0.773	0.099	-1.062	0.112	1.708	28.16
Coole.1	5.101	5.101	12.7	25.94	6.716	13.422	-1.628	-4.409	-22.042	-178.506	-599.382
Coole.2	0	0	0	0	0	0	0	0	0	0	0
Coole_estav.1	1.464	1.464	2.744	3.659	6.666	1.484	-0.323	-1.931	-11.458	-50.087	-90.324
Coole_estav.2	-3.123	-3.123	-8.244	-7.981	-10.334	-10.314	1.435	5.449	17.621	55.079	92.19
Coole_O1.1	0	0	0	0	0	0	0	0	0	0	0
Coole_O2.1	0	0	0	0	0	0	0	0	0	0	0
Coole_O3.1	0	0	0	0	0	0	0	0	0	0	0
Coole_O4.1	0	0	0	0	0	0	0	0	0	0	0
Coole_O5.1	0	0	0	0	0	0	0	0	0	0	0
Coy.1	0.081	0.081	0.245	0.163	-0.252	-0.044	0.61	0.111	1.866	11.254	39.163
Coy.o	0.059	0.059	0.256	0.623	1.161	1.38	0.555	-0.019	0.171	-0.936	0.08
G42.1	4.057	4.057	5.837	5.635	7.753	7.636	-1.425	-4.656	-18.682	-63.905	-93.146
G43.1	-5.146	-5.146	-11.224	-16.682	-19.697	-22.341	3.672	7.459	19.137	38.753	49.875
Garry_estav.1	-0.964	-0.964	-1.59	-2.338	-1.973	-3.686	1.294	2.115	7.344	26.524	46.711
Garry_estav.2	-0.187	-0.187	0.222	-2.269	-0.241	-1.696	0.592	0.688	3.354	17.44	53.124
Garryland.1	0.235	0.235	-0.21	0.07	1.455	3.232	0.033	0.045	0.616	0.181	-5.953
GB1.1	-0.182	-0.182	-0.463	-2.127	-0.7	-0.272	0.641	0.934	3.099	17.086	54.306
GB2.1	-0.253	-0.253	0.203	-0.323	-0.834	-0.534	0.788	1.093	2.698	17.313	53.251
GB3.1	-0.049	-0.049	-0.036	-0.51	-0.273	-0.46	1.23	0.982	2.418	17.292	54.751
GB4.1	-15.203	-15.203	-39.582	-72.038	-95.546	-109.622	5.547	13.749	33.333	54.38	63.795
P1.1	9.321	9.321	15.84	20.953	23.959	24.338	-7.288	-16.42	-45.345	-110.755	-167.293
P2.1	9.339	9.339	16.793	21.27	23.651	24.263	-7.32	-15.427	-44.638	-110.812	-167.582
P3.1	9.717	9.717	16.742	22.273	23.143	24.582	-7.366	-15.31	-44.83	-111.057	-167.97
X14.1	1.513	1.513	2.35	2.404	2.812	2.694	-0.838	-2.713	-46.458	-312.108	-388.648
X5.1	0.165	0.165	0.465	0.841	0.209	-0.557	0.746	-0.865	-5.467	-250.326	-351.134
X6.1	-0.006	-0.006	0.197	0.424	-0.009	0.554	0.175	-0.88	-19.557	-273.457	-355.697

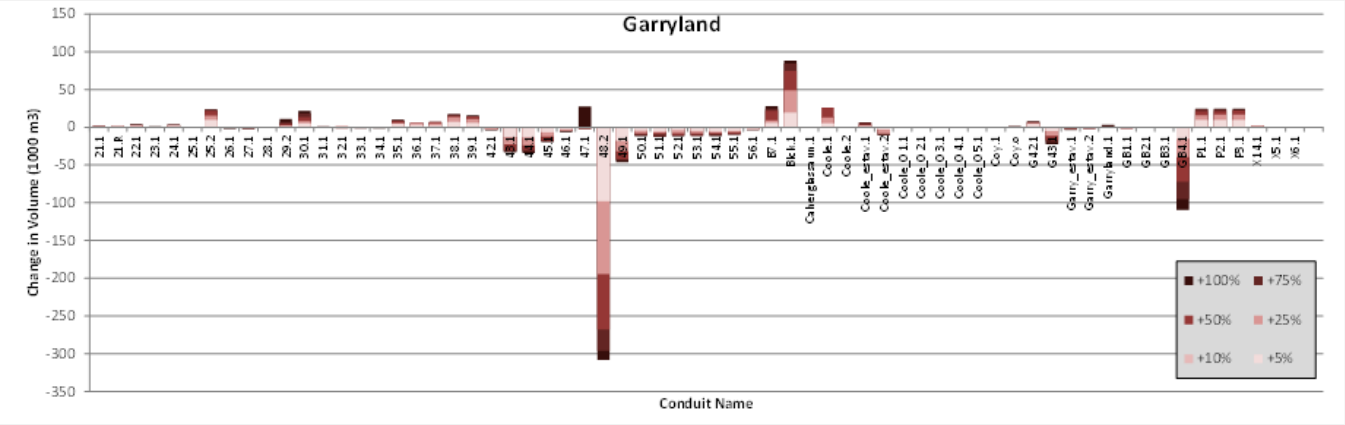

Figure D.14: Change in Garryland volume when conduits expanded.

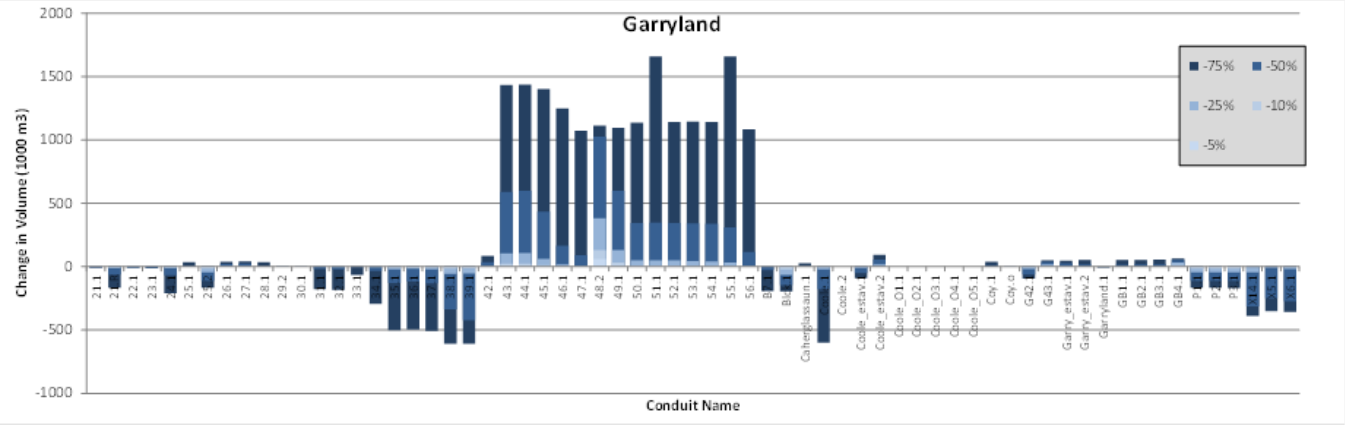

Figure D.15: Change in Garryland volume when conduits reduced.

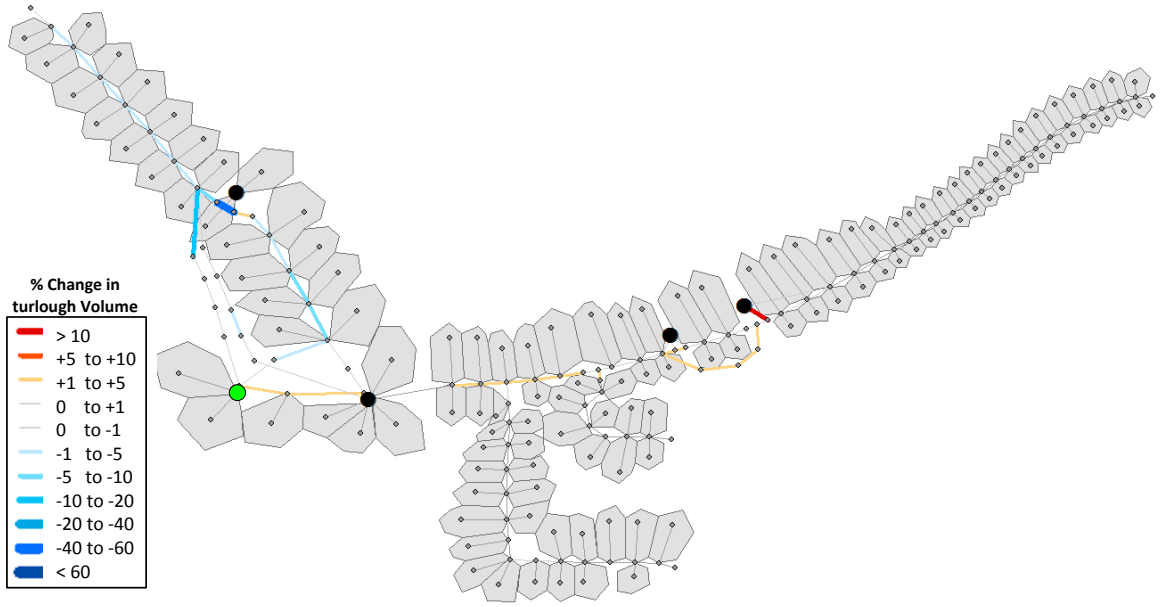

Figure D.16: Percentage changes in volume of Garryland turlough from reducing size of individual conduits by 50%

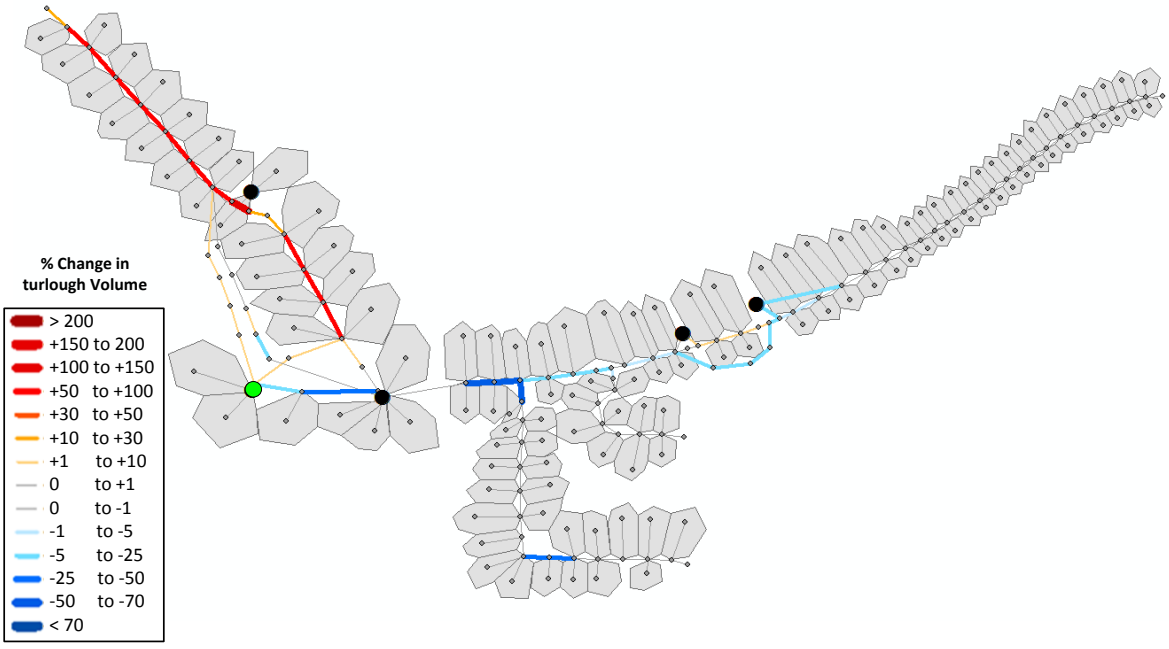

Figure D.17: Percentage changes in volume of Garryland turlough from increasing size of individual conduits by 100%

Caherglassaun

Table D.5: Changes in max volume (1000 m³) of Caherglassaun turlough with altering conduit size (change in volume is positive unless indicated to be negative by a minus symbol).

	Increasing conduit size						Reducing conduit size				
Conduit name	105%	110%	125%	150%	175%	200%	95%	90%	75%	50%	25%
21.1	-0.137	-0.137	1.232	2.023	0.742	1.347	0.072	-0.449	-1.533	-6.793	-8.761
21.R	2.169	2.169	2.218	2.042	2.034	2.666	-0.767	-2.736	-15.359	-73.886	-186.171
22.1	1.774	1.774	3.172	3.477	4.37	4.383	-0.339	-0.979	-5.693	-9.457	-11.798
23.1	0.864	0.864	0.76	1.246	1.239	1.32	-0.058	-0.276	-1.745	-11.763	-15.979
24.1	2.015	2.015	2.948	3.744	3.523	4.052	-0.817	-1.686	-13.908	-79.843	-233.267
25.1	0.104	0.104	-0.298	0.211	0.091	0.374	0.923	0.501	1.654	11.945	40.956
25.2	11.068	11.068	18.302	25.621	27.394	27.673	-9.658	-17.424	-51.054	-126.096	-189.721
26.1	-0.984	-0.984	-1.055	-1.18	-1.389	-2.093	0.764	1.77	6.849	24.709	44.852
27.1	-0.752	-0.752	-0.776	-1.416	-1.715	-1.886	0.843	2.203	7.008	27.659	48.764
28.1	0.711	0.711	0.609	0.453	-0.187	0.206	0.247	0.95	1.064	7.147	40.486
29.2	1.328	1.328	2.468	5.302	8.225	13.007	0.661	-1.344	-0.892	-1.547	-1.88
30.1	5.442	5.442	8.571	14.287	19.373	23.025	0.329	0.054	-0.008	0.614	-0.23
31.1	0.236	0.236	-0.376	-0.663	1.508	-0.163	-0.193	-0.19	-1.655	-22.552	-199.001
32.1	-0.573	-0.573	2.016	-1.889	1.034	-0.297	-0.844	-0.256	-3.408	-23.706	-204.937
33.1	-1.349	-1.349	-1.462	-1.204	-1.603	1.045	0.507	0.312	0.269	-4.63	-75.728
34.1	0.401	0.401	-0.408	-0.417	-0.416	-1.916	-1.733	-0.636	-5.292	-37.467	-365.769
35.1	4.573	4.573	6.226	8.756	10.047	11.039	-1.691	-6.26	-24.527	-142.987	-556.714
36.1	3.68	3.68	7.101	6.612	5.516	7.202	-3.335	-4.786	-20.586	-129.197	-550.542
37.1	2.825	2.825	5.725	7.791	8.247	7.511	-1.254	-7.315	-25.287	-144.398	-562.66
38.1	8.26	8.26	14.862	16.889	19.389	19.841	-6.989	-16.231	-64.994	-402.711	-752.268
39.1	6.556	6.556	12.286	16.191	16.178	18.511	-5.113	-14.349	-61.453	-462.796	-759.84
42.1	3.553	3.553	4.798	7.046	8.903	6.914	-1.921	-5.048	-24.135	-97.953	-207.179
43.1	21.811	21.811	38.372	48.196	52.53	53.991	-16.053	-37.511	-157.516	-574.266	-768.663
44.1	21.339	21.339	36.938	48.482	52.668	52.623	-15.836	-37.462	-156.253	-574.079	-780.097
45.1	12.025	12.025	19.855	23.248	24.984	25.521	-7.958	-20.381	-88.94	-474.108	-768.177
46.1	2.027	2.027	4.072	6.78	7.228	5.823	-2.011	-4.985	-26.027	-219.3	-720.457
47.1	2.129	2.129	3.291	4.116	4.513	39.598	-1.275	-2.767	-13.691	-127.427	-475.025
48.2	-191.435	-191.435	-354.628	-464.064	-503.566	-520.133	134.983	297.492	956.502	2365.118	2365.118
49.1	-37.048	-37.048	-65.982	-85.357	-90.47	-94.022	28.991	68.362	294.978	1500.738	2365.118
50.1	-9.271	-9.271	-16.486	-20.152	-22.552	-23.955	9.056	21.659	105.726	820.794	2365.118
51.1	-10.353	-10.353	-15.908	-19.749	-24.196	-23.978	8.108	19.57	105.52	820.911	2365.118
52.1	-8.371	-8.371	-15.848	-20.46	-22.241	-22.9	7.86	17.984	102.892	817.419	2365.118
53.1	-8.855	-8.855	-15.395	-19.464	-22.482	-21.486	7.088	16.804	93.33	813.785	2365.118
54.1	-9.487	-9.487	-14.576	-18.444	-20.045	-22.34	6.77	13.965	82.581	805.06	2365.118
55.1	-7.915	-7.915	-12.571	-15.758	-18.672	-18.137	5.479	12.906	66.656	728.61	2365.118
56.1	-3.122	-3.122	-4.659	-5.516	-6.124	-6.432	2.69	6.035	19.017	248.403	2365.118
B7.1	5.833	5.833	9.798	23.907	26.84	30.181	-0.643	-1.427	-1.11	-31.602	-212.203
Blck.1	23.036	23.036	58.968	89.263	101.188	105.723	-14.423	-25.962	-74.43	-164.118	-217.885
Caherglassaun.1	1.116	1.116	1.991	2.806	2.828	2.773	-0.428	-2.507	-5.3	-24.841	-269.768
Coole.1	5.645	5.645	14.263	29.572	7.122	14.888	-1.688	-4.84	-24.56	-192.318	-712.758
Coole.2	0	0	0	0	0	0	0	0	0	0	0
Coole_estav.1	0.174	0.174	0.467	0.743	3.941	-2.154	0.777	0.408	-2.64	-12.963	-42.675
Coole_estav.2	9.475	9.475	15.092	24.131	24.572	25.975	-7.22	-13.617	-47.331	-135.252	-217.673
Coole_O1.1	0	0	0	0	0	0	0	0	0	0	0
Coole_O2.1	0	0	0	0	0	0	0	0	0	0	0
Coole_O3.1	0	0	0	0	0	0	0	0	0	0	0
Coole_O4.1	0	0	0	0	0	0	0	0	0	0	0
Coole_O5.1	0	0	0	0	0	0	0	0	0	0	0
Coy.1	0.103	0.103	0.269	0.205	-0.271	-0.033	0.7	0.104	2.1	12.764	45.827
Coy.o	0.065	0.065	0.298	0.744	1.443	1.859	0.642	-0.03	0.192	-1.097	0.078
G42.1	1.41	1.41	1.105	-0.814	1.025	0.65	0.619	-0.396	-3.075	-20.224	-45.655
G43.1	5.83	5.83	11.105	15.433	16.325	15.08	-2.811	-6.232	-19.58	-42.117	-56.2
Garry_estav.1	0.974	0.974	1.902	2.143	2.956	1.112	-0.062	-1.175	-6.122	-27.63	-53.184
Garry_estav.2	-0.154	-0.154	0.351	-2.503	-0.149	-1.832	0.642	0.692	3.409	16.729	50.81
Garryland.1	0.267	0.267	-0.241	0.082	1.689	3.765	0.038	0.05	0.719	0.265	-0.9
GB1.1	-0.155	-0.155	-0.437	-2.344	-0.681	-0.177	0.699	0.966	3.118	16.314	52.183
GB2.1	-0.238	-0.238	0.326	-0.249	-0.831	-0.486	0.871	1.162	2.655	16.573	50.96
GB3.1	-0.002	-0.002	0.05	-0.469	-0.183	-0.392	1.382	1.033	2.326	16.519	52.703
GB4.1	-14.606	-14.606	-38.282	-67.964	-89.768	-102.922	4.963	12.965	31.753	52.286	61.537
P1.1	11.057	11.057	18.682	24.663	28.197	28.639	-8.678	-19.104	-52.061	-126.623	-189.277
P2.1	11.077	11.077	19.8	25.038	27.831	28.55	-8.708	-17.963	-51.249	-126.696	-189.561
P3.1	11.521	11.521	19.738	26.234	27.237	28.916	-8.756	-17.821	-51.475	-126.928	-190.112
X14.1	1.742	1.742	2.693	2.737	3.197	3.046	-0.97	-3.141	-51.901	-346.833	-445.652
X5.1	0.189	0.189	0.531	0.963	0.23	-0.661	0.868	-0.997	-4.258	-278.292	-407.582
X6.1	-0.006	-0.006	0.228	0.497	-0.005	0.644	0.2	-1.012	-20.674	-303.321	-412.166

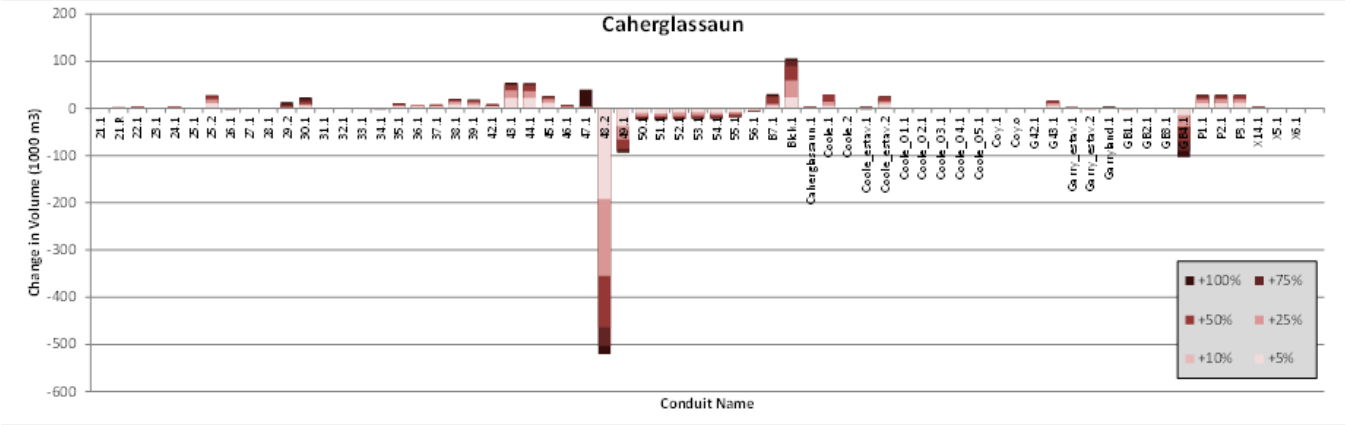

Figure D.18: Change in Caherglassaun volume when conduits expanded.

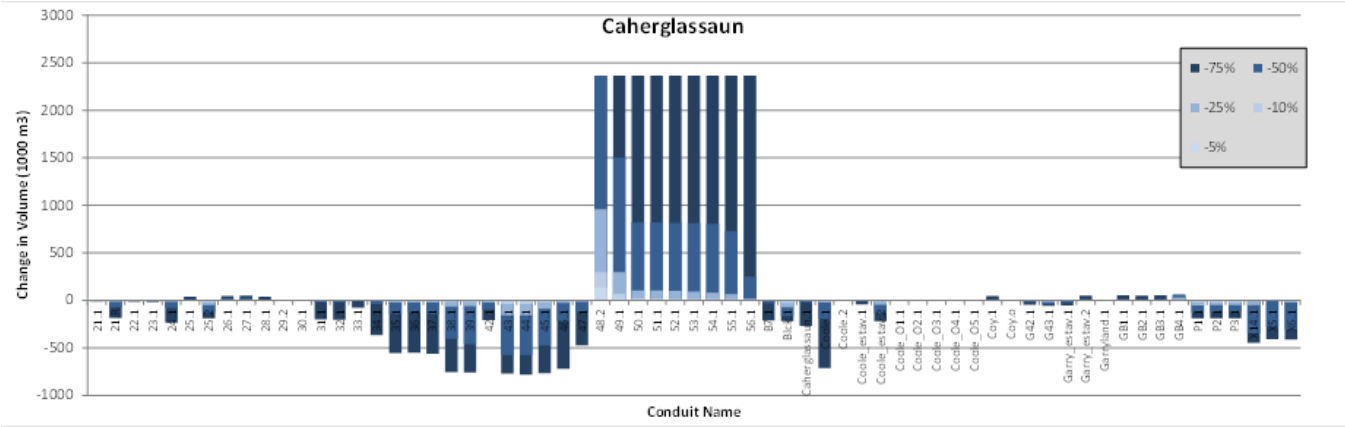

Figure D.19: Change in Caherglassaun volume when conduits reduced.

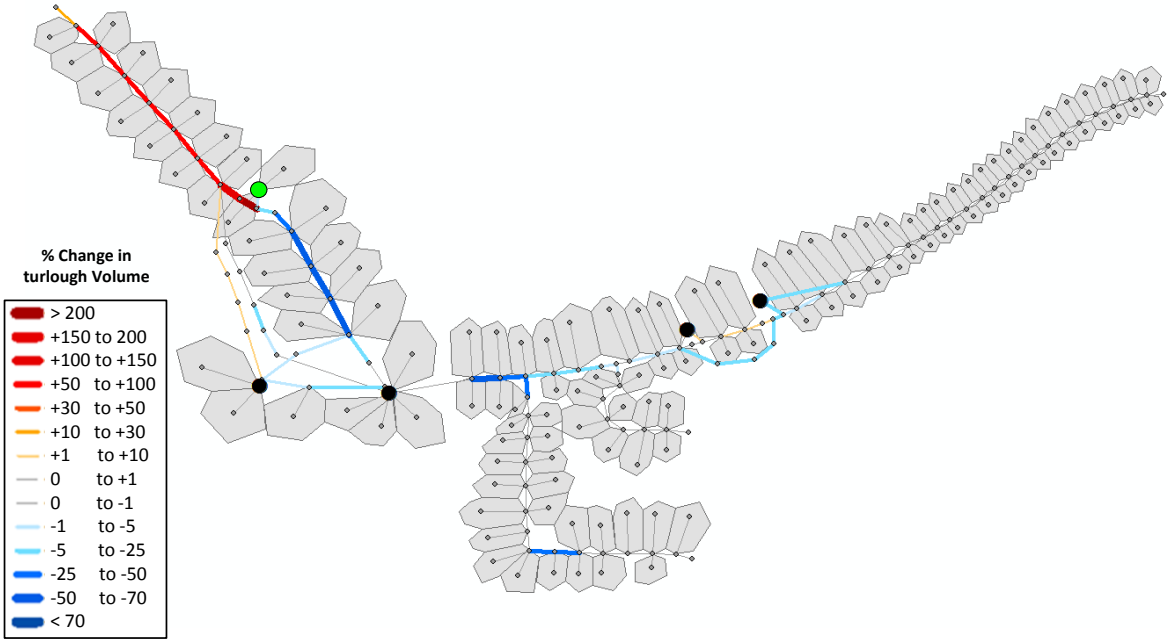

Figure D.20: Percentage changes in volume of Caherglassaun turlough from reducing size of individual conduits by 50%

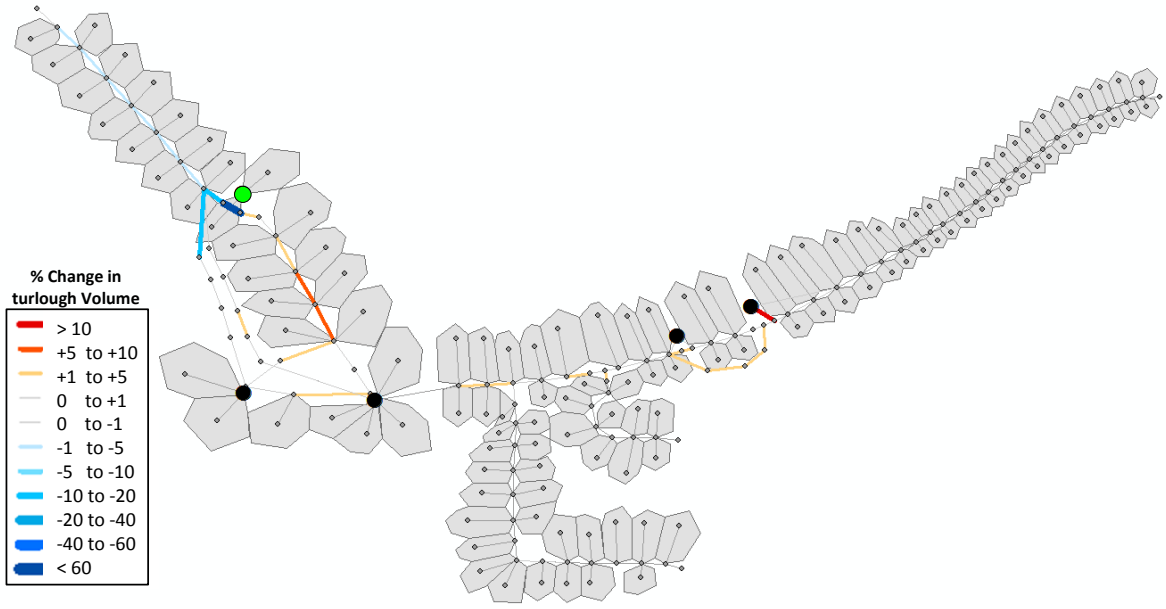

Figure D.21: Percentage changes in volume of Caherglassaun turlough from increasing size of individual conduits by 100%

Appendix E

Climate Change Data

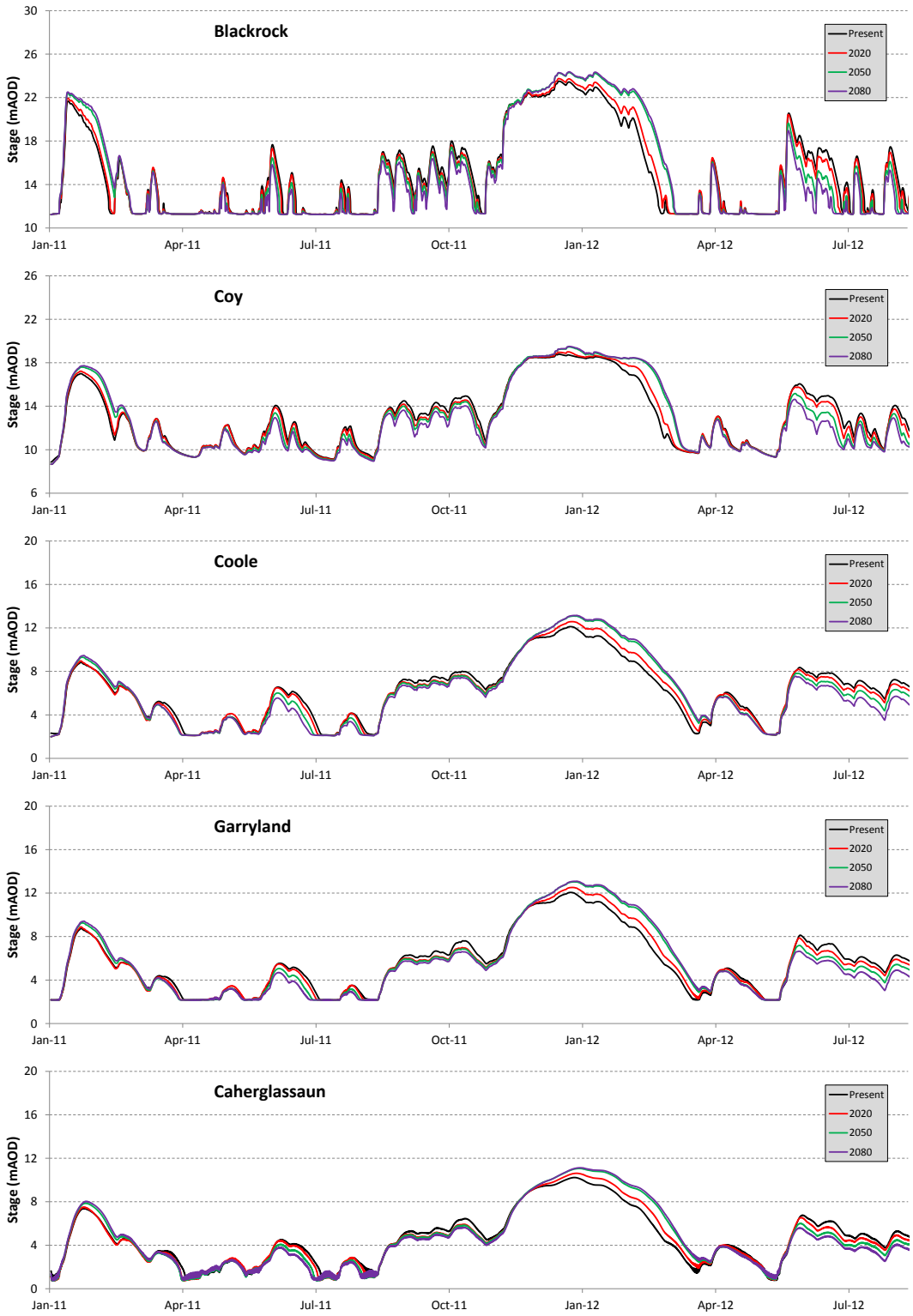

Figure E.1: Turlough flooding patterns according to emsemble emission scenario.

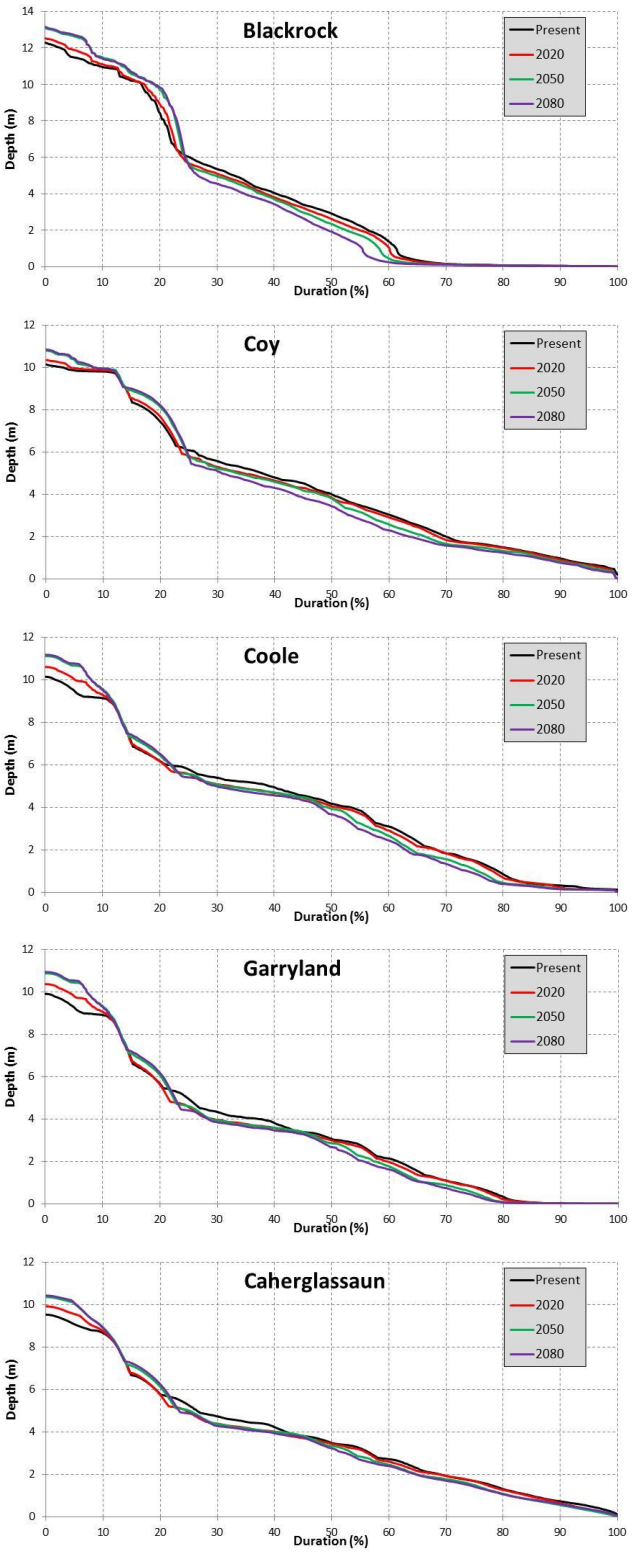

Figure E.2: Turlough flood duration curves according to emsemble emission scenario over the period Jan 2011 – Jan 2012.

Appendix F

Hydrochemistry Results - Tables

BH3

Pollacurra

Date/time	Depth (m)	Head (mAOD)	Nitrate (mg/l)	Nitrite (mg/l)	Total N (mg/l)	Ammonia (mg/l)	ph	Total Phosphorus (µg/l)	Total Dissolved Phosphorus (µg/l)	Alkalinity (mg/l as CaCO3)	EC (µS/cm)	$\delta^{18}O$ VSMOW ‰	$\delta^{2}H$ VSMOW ‰	$\delta^{13}C$ VPDB ‰	Comment
31-03-10 12:00	6.97	21.78								120		-7.81			
30-04-10 10:45	17.49	11.26													
23-06-10 15:00	22.5	6.25	0.1	<0.02		0.09				168		-6.74			
08-07-10 16:15	6.37	22.38	0.9	<0.02		0.14	6.94			168	537	-6.85			
21-07-10 10:45	13.87	14.88		<0.02		0.35	7			170	530	-6.76			
19-08-10 12:40	5.4	23.35	0.1	0.01		0.09				170	644	-6.77		-12.18454	
15-09-10 13:50	5.87	22.88	0.1	<0.02		0.37	7.46			186	670	-7.00		-13.59517	
18-11-10 11:30	4.81	23.94	0.3	0.01	0.4	0.03	7.21			216		-7.23		-11.25303	
15-02-11 13:10	4.89	23.86	2.5		3.9			10.50	7.64	144	633	-7.61			
02-03-11 17:35	8.83	19.92													
21-03-11 13:00	14.86	13.89	0.7		2.3		7.88	9.81	4.10	128	567	-7.44			
06-04-11 11:15	11.15	17.60													
13-04-11 12:45	16.04	12.71	1.9		1.9			10.35	5.49	192	744	-7.26			
17-05-11 12:00	21.18	7.57	0.6		2.2		7.5			210	862	-7.07			
01-06-11 15:50	18.98	9.77													
21-06-11 10:45	17.80	10.95	0.8				7.31	18.27	15.41	190		-7.00			
18-10-11 12:50	11.77	16.98	1.1		3.7		7.33	9.49	7.92	274	927	-6.86	-44.89		
08-11-11 11:45	12.16	16.59	0.4		0.4		7.03	6.45	1.45	284	955	-6.11	-45.03		
04-12-11 12:10								7.86	8.20	264		-6.92	-44.70		
09-01-12 12:15			1		1		7.03	5.96	0.00	256	987	-6.64	-42.75		
06-02-12 13:10			2.8		3.9		7.18	10.46	1.63	262	954	-6.40	-39.70		
13-03-12 10:55			3.6				7.2	2.98	3.38	212	829	-6.60	-39.05		
10-04-12 11:15			3.4		3.6		6.96	11.89	2.88	236	840				
22-05-12 11:00			1.8				7.4	23.49	6.98	248	848				
20-06-12 10:30			2.4				7.61	23.62	22.83	242	868				
23-07-12 10:20	13.96	14.79	2		2		6.98	15.24	7.82	224	895				
23-08-12 10:10			2.1		3.4		6.91	9.70	3.04	248	910				
09-10-12 12:10			2.5		2.6		7.482	7.86	4.10	266	789				
07-11-12 12:10			1.8		2.1		6.96	12.04	8.98	222	975				
04-12-12 11:40			1.2		1.93		7.15	50.76	34.88	240	846				
23-01-13 13:30			2.6		3.2		7.51		8.13	126	637				
26-02-13 10:00			3.5				7.35	6.61	0.48	106	501				
25-03-13 10:35			1.5		3.1		7.9	15.39	3.97	70	487				

BH5

Kiltartan

Date/time	Depth (m)	Head (mAOD)	Nitrate (mg/l)	Nitrite (mg/l)	Total N (mg/l)	Ammonia (mg/l)	ph	Total Phosphorus (µg/l)	Total Dissolved Phosphorus (µg/l)	Alkalinity (mg/l as CaCO3)	EC (µS/cm)	$\delta^{18}O$ VSMOW ‰	$\delta^{2}H$ VSMOW ‰	$\delta^{13}C$ VPDB ‰	Comment
31-03-10 13:45	9.84	6.51													
30-04-10 16:15	13.4	2.95													
24-06-10 14:30	13.14	3.21													
08-07-10 12:30	14.43	1.92	0.4	0.02		0.01	7.39			150	628	-6.34			
21-07-10 10:10	13.14	3.21													
19-08-10 10:30	13.18	3.17	1	<0.02	2.18	0.01				154	581	-6.52		-8.046434	
16-09-10 13:20	10.70	5.65	0.6	<0.02	1.31	0.01	7.94			144	553	-6.55			
13-10-10 19:00	17.53	-1.18													
18-11-10 16:45	7.92	8.43	0.3	0.01	0.4	0.01	7.64			128	566	-6.58		-8.855291	
15-02-11 17:50	8.01	8.34	0.2		0.3		8.22	76.80		136	596	-6.30			
02-03-11 14:40	12.50	3.85													
21-03-11 17:00	10.15	6.20	0.8				7.97	8.99	4.51	134	589	-6.27			
06-04-11 15:00	9.93	6.42													
13-04-11 15:45	10.45	5.90	0.1		0.8			28.54	15.20	136	595	-6.38			
17-05-11 14:00	13.10	3.25	0.3		1.2		7.76	24.11	23.28		631	-6.30			
21-06-11 19:20	15.34	1.01	0.8		2.4		7.72	30.48	16.23	158		-6.18			
10-08-11 10:50	11.90	4.45	0.4		2		7.83	65.49	43.56		654	-6.42			
18-10-11 17:50	9.81	6.54	1		3.1		7.59	581.95	484.93	162	634	-6.18			
08-11-11 16:40	12.00	4.35	0.6		1.3		7.44	75.38	52.75	160	619	-5.97			
04-12-11 16:30	8.00	8.35	0.9		2.8		7.31	104.33	81.07	168	701	-5.91			
09-01-12 16:40	6.00	10.35	1.4		1.4		7.5	72.59	65.43	160	594	-6.12			
06-02-12 17:15	8.50	7.85	0.4		2.1		7.58	53.08	5.08	162	673	-6.16			
10-04-12 14:45	12.50	3.85	0.2		1.05		7.33	50.39	42.20	160	595	-6.40			
22-05-12 15:15	13.00	3.35	0.2		0.3		7.74	63.78	32.31	160	610				
23-07-12 14:20	11	5.35	0.4		0.4		7.4	31.32	21.43	168	621				
23-08-12 17:50	12.00	4.35	0		3		7.32	28.01	21.35	164	597				
09-10-12 16:30	13.00	3.35	0		0.3		7.967	33.35	19.14	174	615				
07-11-12 16:20	11.00	5.35			1.12		7.22	25.09	18.18	174	667				
04-12-12 15:30	9.00	7.35	0.3		1.7		7.15	35.71	23.17	174	626				
23-01-13 11:10	8.50	7.85	1.3		1.1		7.45		25.68	148	577				
26-02-13 11:00	11.00	5.35	1				7.46	21.93	15.42	154	577				
25-03-13 14:40	11.00	5.35	0.2		0.3		7.66	28.72	21.10	144	602				

BH7

Grannagh

Date/time	Depth (m)	Head (mAOD)	Nitrate (mg/l)	Nitrite (mg/l)	Total N (mg/l)	Ammonia (mg/l)	ph	Total Phosphorus (µg/l)	Total Dissolved Phosphorus (µg/l)	Alkalinity (mg/l as CaCO3)	EC (µS/cm)	δ^{18}O VSMOW ‰	δ^{2}H VSMOW ‰	δ^{13}C VPDB ‰	Comment
23-06-10 15:50	34.46	3.80	0.2	<0.02		<0.05				180		-7.43			
21-07-10 11:15	31.8	6.46		<0.02		0.27	7.26			170	788	-7.20			
19-08-10 12:10	24.82	13.44	0.2	0.03		0.01				182	796	-7.03		-14.97827	
15-09-10 16:10	18.17	20.09	2.5	<0.02	3.51	0.01	7.54			190	659	-7.59		-17.60353	
14-10-10 15:45	30.15	8.11	0	0		0	7.38			176	101	-7.39		-15.35135	
18-11-10 11:45	18	20.26	7.6	0.01		0.03	7.16			168	693	-7.03		-12.60358	
16-02-11 11:10	21.04	17.221								174	5890	-6.58			Extremly high EC
13-04-11 13:00	30.99	7.27	0.6		1.6			7.11	5.90	182	738	-6.73			
17-05-11 12:20	35.3	2.96	0.5		1.8		7.48	11.16	8.73	184	742	-6.54			
21-06-11 11:20	32.1	6.16	4.3		6		7.6	9.92	5.23	174		-6.32			
18-10-11 13:15	24.76	13.50	5.7				7.34	20.45	7.53	208	833	-6.27			
09-11-11 13:50	22.28	15.98	5.7		6.2		7.12	9.08	8.68	200	807	-6.26			
04-12-11 12:45	18.03	20.23	5.8				7.12	9.74	4.78	212	813	-6.26			
09-01-12 12:45	15.6	22.66	10.3		10.4		7.35	11.99	7.09	180	787	-6.27			
06-02-12 13:30	18.24	20.02	3.1				7.11	53.08	5.08	218	87.8	-6.31			
13-03-12 11:15	25.4	12.86	1.4		1.4		7.32	7.77	4.97	216	836	-6.47			
10-04-12 11:50	29.12	9.14	0.2		0.4		6.98	8.41	4.92	186	772	-6.37			
22-05-12 11:30	27.88	10.38	0.6		1.7		7.25	10.82	7.75	204	829	-6.49	-42.78		
20-06-12 11:40	23.7	14.56	3.6				7.36	10.29	7.94	196	774	-6.37	-40.55		
23-07-12 10:50	26.35	11.91	1.5		1.6		7.06	23.07	11.12	200	834	-6.56	-41.80		
09-10-12 18:00	24.4	13.86	4.8		4.8		7.653	14.13	5.36	204	790	-6.30	-39.30		
07-11-12 12:25	21	17.26			3.92		6.98	14.73	6.29	196	808	-7.05	-40.11		
04-12-12 11:55	19.35	18.91	1.6		2.71		6.88	16.49	6.46	202	792	-6.78	-40.70		
23-01-13 13:45	19.7	18.56	2.2		3		7.04		14.40	200	779				
26-02-13 10:10	22.9	15.36	1.3				7.02	10.82	10.82	160	665				
25-03-13 10:55	27.57	10.69	0.5		0.6		7.32	15.01	12.35	194	721				

BH10

Ballyaneen South

Date/time	Depth (m)	Head (mAOD)	Nitrate (mg/l)	Nitrite (mg/l)	Total N (mg/l)	Ammonia (mg/l)	ph	Total Phosphorus (µg/l)	Total Dissolved Phosphorus (µg/l)	Alkalinity (mg/l as CaCO3)	EC (µS/cm)	δ^{18}O VSMOW ‰	δ^{2}H VSMOW ‰	δ^{13}C VPDB ‰	Comment
31-03-10 18:45	29	10.65								196		-7.22			
30-04-10 18:00	>13	<26.65								186		-6.59			
19-08-10 14:00	-		0.9	<0.02		0.02				176	671	-6.94			
15-09-10 18:30	-		0.9	<0.02	1.34	0	7.58			170	638	-7.49			
13-10-10 18:30	-		2.00	0	3.2	0.01	7.56			174	707	-7.23			
15-02-11 18:10	-		2.60		3.3		7.74			158	609	-6.74			
21-03-11 16:20			1.70		4.2		7.39	12.26	7.77	180	687	-7.04			
13-04-11 18:00			1.7		2.5					162	661	-6.95			
17-05-11 17:15			1.7				7.48	0.00	4.28	160	690	-6.85			
08-11-11 17:20			1.3		1.3		7.18	2.63	1.97	196	516	-6.72			
04-12-11 17:10			1.5		3		7.1	12.65	9.91	182	671	-6.09			
09-01-12 17:30			2.1		2.1		7.12	3.70	2.95	204	710	-5.68			
06-02-12 18:30			1.4		1.4		7.23	5.47	5.47	202	725	-5.96			
13-03-12 19:00			1.5				7.36	2.18	2.18	238	704	-6.31			
10-04-12 18:15			1.9		1.8		7.1	9.43	0.83		650	-6.36			
23-07-12 18:00			1.4		1.8		7.33	5.35	4.11	188	688				
23-08-12 18:40			1.8		2.7		7.04	2.63	1.38	206	702				
09-10-12 18:30			2		1.8		7.626	6.61	3.68	210	733				
07-11-12 18:00			2.1		2.2		6.89	4.76	0.92	212	803				
04-12-12 17:10			0.3		2		6.99	2.70	0.61	216	782				
26-02-13 17:20			0.1		0.1		7.03	1.63	2.39	224	770				

BH11

Bunragh

Date/time	Depth (m)	Head (mAOD)	Nitrate (mg/l)	Nitrite (mg/l)	Total N (mg/l)	Ammonia (mg/l)	ph	Total Phosphorus (µg/l)	Total Dissolved Phosphorus (µg/l)	Alkalinity (mg/l as CaCO3)	EC (µS/cm)	δ^{18}O VSMOW ‰	δ^{2}H VSMOW ‰	δ^{13}C VPDB ‰	Comment
30-04-10 16:45	4.7	19.20								154		-6.22			
24-06-10 17:30	6.31	17.59	0.2	<0.02		0.53				140		-6.18			
08-07-10 12:00	5.97	17.93	1.40	0.01		0.07	7.04			168	631	-6.27			
21-07-10 14:40	5.19	18.71													
19-08-10 11:45	5.5	18.40	0.5	<0.02		0.02				174	656	-6.23			
14-10-10 14:20	4.70	19.20	0.6	<0.02	1.3	0.44	7.53			150	631	-6.27			
18-11-10 17:00	3.89	20.01	0.2	<0.02	1.2	0.02	7.35			150	593	-6.61			
15-02-11 16:55	3.81	20.09	0.7		2.2		7.72	91.59	13.68	152	625	-6.80			
02-03-11 16:00	4.40	19.50													
21-03-11 18:00	4.20	19.70	1.2				7.34	8.99	21.23	164	635	-6.25			
06-04-11 13:50	4.51	19.39													
13-04-11 16:55			2.9					31.77	4.69	148	640	-6.33			
17-05-11 13:10			0.6		1.7		7.48			156	662	-6.17			
01-06-11 15:15	5.11	18.79													
21-06-11 20:00			0.6		2.4		7.61	30.08	10.93	160		-6.12			
10-08-11 10:20					0.3		7.37	9.88	5.38		669	-6.23			
18-10-11 18:20			0.2		0.8		7.42	11.25	6.75	162	613	-6.11			
08-11-11 15:30			0.2		0.3		7.32	5.39	5.39	168	628	-6.28			
04-12-11 16:00	3.73	20.17	0.9		1.5		7.22	14.70	5.46	188	690	-6.06			
09-01-12 16:00	3.7	20.20	0		0.2		7.23	80.11	5.21	172	614	-6.25			
06-02-12 16:15	3.9	20.00	0.4				7.27	36.57	4.32	170	641	-6.28			
13-03-12 13:45	3.6	20.30	0.5		0.8		7.36	20.93	7.77	170	641	-6.09			
10-04-12 14:10	3.95	19.95	0.6		2.25		7.09	57.76	4.52	168	619	-6.41			
22-05-12 14:50	4.27	19.63	0.5		1.4		7.48	40.76	10.05	160	594				
20-06-12 12:00	3.8	20.10	0.5				7.49	27.14	10.29	160	601				
23-07-12 13:40	4.3	19.60	0.5		1.4		7.34	25.55	9.88	174	651				
23-08-12 14:00	3.6	20.30	0.4		2		7.09	10.74	3.87	164	612				
09-10-12 15:30	3.47	20.43	0.2		0.2		6.637	12.25	3.68	160	595				
07-11-12 15:50			2.1				7.07	15.11	4.37	166	660				
04-12-12 15:45			0.6		1.29		6.1	15.65	4.16	166	646				
23-01-13 11:55	3.4		0.2		1		7.31		7.71	162	622				
26-02-13 10:50	3.4		1.4				7.01	16.76	3.74	174	662				
25-03-13 15:00			0.4		0.45		7.42	128.84	5.49	162	625				

BH12

Crannagh

Date/time	Depth (m)	Head (mAOD)	Nitrate (mg/l)	Nitrite (mg/l)	Total N (mg/l)	Ammonia (mg/l)	ph	Total Phosphorus (µg/l)	Total Dissolved Phosphorus (µg/l)	Alkalinity (mg/l as CaCO3)	EC (µS/cm)	δ^{18}O VSMOW ‰	δ^{2}H VSMOW ‰	δ^{13}C VPDB ‰	Comment
08-07-10 11:30	3.7	12.60		0.01		0.71	6.85			198	871	-5.86			
19-08-10 10:00	3.73	12.57	1.30	0.01	1.34	0.06				200	701	-6.14			
16-09-10 9:20	2.74	13.56	1.20	<0.02	1.14	0.66	7.57			196	686	-6.01			
18-11-10 16:20	0.89	15.41	0.2	0.01	0.3	0.02	7.35			180	713	-5.92			
16-02-11 10:30	0.82	15.48	1.70		2.6		7.74	27.99	11.77		752	-5.89			
02-03-11 15:00	1.12	15.18													
21-03-11 17:30	1.60	14.70	3.60		4		7.13	46.72	10.22	200	780	-6.48			
06-04-11 15:20	1.67	14.63													
13-04-11 16:00	1.60	14.70	1.2		4.6			12.37	1.86	176	700	-6.01			
01-06-11 15:00	3.12	13.18													
21-06-11 18:45	3.20	13.10	2.3		3.1		7.37	10.53	4.82	214		-5.75			
10-08-11 11:15	3.30	13.00	2.1		3.6		7.25	16.54	2.05		797	-5.70			
18-10-11 17:10	2.08	14.22	1.1		5.2		7.37	9.49	3.22	218	786	-5.48			
08-11-11 15:50	1.72	14.58	1.1		1.2		7.28	7.50	3.03	222	795	-5.69			
09-01-12 16:45	0.50	15.80	1		3.8		7.26	30.81	5.59	208	745	-6.06			
06-02-12 17:30	1.10	15.20	3.8		3.9		7.41	13.15	5.47	204	754	-5.89			
13-03-12 17:30	1.56	14.74	3.2				7.51			212					
10-04-12 15:10	2.25	14.05	2.7		4.2		6.95	9.02	1.65	192	719	-5.23			
22-05-12 15:50	3.00	13.30	2.1		3.3		7.21	29.24	10.44	228	808				
20-06-12 12:45	2.30	14.00	3.1				7.31	35.38	28.71	200	744				
23-07-12 13:40	2.85	13.45	2.5		3.2		7.25	9.88	5.35	196	749				
23-08-12 17:25	2.73	13.57	1.9		4		7.06	16.36	3.87	202	741				
09-10-12 16:00	1.90	14.40	1.3		0.6		7.797	12.04	5.36	196	709				

BH14

Skehanagh

Date/time	Depth (m)	Head (mAOD)	Nitrate (mg/l)	Nitrite (mg/l)	Total N (mg/l)	Ammonia (mg/l)	ph	Total Phosphorus (µg/l)	Total Dissolved Phosphorus (µg/l)	Alkalinity (mg/l as CaCO3)	EC (µS/cm)	δ^{18}O VSMOW ‰	δ^{2}H VSMOW ‰	δ^{13}C VPDB ‰	Comment
23-06-10 17:15	2.73	22.43													
08-07-10 15:15	2.8	22.36													
22-07-10 11:50	2.27	22.89													
16-09-10 10:40	1.91	23.25													
14-10-10 15:10	2.40	22.76													
15-02-11 15:50	1.90	23.26													
02-03-11 16:50	2.16	23.00													
22-03-11 14:15	2.26	22.90	0.6		2		7.65	37.95	28.98	180	729	-6.87			
13-04-11 14:00	2.22	22.94	3		4.4			37.03	31.77	150	629	-6.47			
17-05-11 12:10			0.2		1.1		8.28	51.17	30.56	128	535	-5.40			
01-06-11 15:50	2.50	22.66													
21-06-11 11:40			0.9		3.5		8.21	66.33	64.49	84		-5.69			
19-10-11 14:50	2.19	22.97	0.6		1.5		7.34	70.97	57.13	200	727	-5.74	-38.06		
08-11-11 12:15	2.12	23.04	3.4		3.6		7.16	35.12	33.81	238	851	-6.19	-41.25		
04-12-11 13:20	1.73	23.43	3.2		1.6		7.03	57.46	52.33	228	802	-6.09	-39.00		
09-01-12 13:10	1.93	23.23	2.8		3.3		7	53.77	50.19	216	800	-5.62	-34.35		
06-02-12 13:50			2.4		3		7.09	51.93	43.48	222	817	-5.47	-34.08		
13-03-12 11:55			2.5		4.6		7.62	41.68	33.30	218	794	-5.87	-34.12		
10-04-12 13:00	2.40	22.76	2.8		4.05		7.59	39.74	31.55	186	678				
22-05-12 12:20			1.3				7.39	82.21	34.23	164	625				
20-06-12 10:50			1.7				7.65	67.91	36.94	170	631				
23-07-12 11:10			0		1.8		7.35			164	606				
23-08-12 11:05			1.3		5		7.39	33.21	30.71	204	720				
09-10-12 12:45			0.1		-		7.625	54.66	46.72	238	821				
07-11-12 13:25			2.7		1.62		6.85	55.58	48.87	216	814				
05-12-12 12:25			1.4		3.35		7.15	58.70	53.26	226	839				
23-01-13 12:45			1.2		2.6		7.1		53.26	210	757				
26-02-13 17:10			2.3				7.26	56.03	46.45	236	807				
25-03-13 16:00			2.4		2.4		7.56	53.08	33.29	218	757				

BH15

Near Coy turlough

Date/time	Depth (m)	Head (mAOD)	Nitrate (mg/l)	Nitrite (mg/l)	Total N (mg/l)	Ammonia (mg/l)	ph	Total Phosphorus (µg/l)	Total Dissolved Phosphorus (µg/l)	Alkalinity (mg/l as CaCO3)	EC (µS/cm)	δ^{18}O VSMOW ‰	δ^{2}H VSMOW ‰	δ^{13}C VPDB ‰	Comment
08-07-10 14:40	0.63	20.59													
19-08-10 14:15	0.68	20.54													
02-03-11 12:00	0.61	20.61													
22-03-11 13:40	0.51	20.71	0.6		1.1		7.15	54.27	28.98	202	724	-6.98			
06-04-11 12:30	0.60	20.62													
13-04-11 14:45	0.61	20.61	0.3		1.1			50.57	47.74	196	710	-6.98			
17-05-11 17:00	0.63	20.59	0.2		0.4		7.48			192	710	-6.78			
10-08-11 16:30	0.64	20.58	0.4				7.37	79.98	44.34		746	-6.86			
19-10-11 15:20	0.61	20.61	0.3		1.5		7.23	51.39	49.04	200	778	-6.44			
08-11-11 12:40	0.60	20.62	0.1		0.2		6.88	30.91	30.65	234	794	-6.43			
04-12-11 13:40	0.59	20.63	1.5		1.5		6.95	43.26	42.41	242	788	-5.96			
09-01-12 13:45	0.59	20.63	0.8		3.1		6.97	62.05	57.53	230	758	-6.33			
06-02-12 14:15	-		0.5		0.5		6.94	58.46	33.50	240	797	-6.34			
13-03-12 12:15			1.3		1.9		7.07	44.07	40.08	250	813	-6.16			
10-04-12 18:45			1.9		2		6.91	52.03	42.61	234	741	-6.18			
22-05-12 13:10			0.2		1.1		7.31	48.05	40.37	218	741				
20-06-12 11:20			0.7				7.3	48.31		216	727				

BH16

Near Coole

Date/time	Depth (m)	Head (mAOD)	Nitrate (mg/l)	Nitrite (mg/l)	Total N (mg/l)	Ammonia (mg/l)	ph	Total Phosphorus (µg/l)	Total Dissolved Phosphorus (µg/l)	Alkalinity (mg/l as CaCO3)	EC (µS/cm)	δ^{18}O VSMOW ‰	δ^{2}H VSMOW ‰	δ^{13}C VPDB ‰	Comment
15-09-10 20:00	15.12	9.42	1.90	<0.02	3.65	0.54	7.6			180	654	-7.45			
13-10-10 19:15	13.10	11.44													
18-11-10 14:00	13.50	11.04	3.00	<0.02	3.9	0.04	7.19			180	680	-7.23			
15-02-11 17:15	16.50	8.04	4.30		4.3		7.6	16.86	9.86	164	675	-6.91			
24-02-11 13:00	16.97	7.57													
02-03-11 13:45	15.50	9.04													
21-03-11 16:00	15.70	8.84	4.30		4.8		7.19	18.78	25.61	182	690	-6.80			
06-04-11 14:45	17.80	6.74			2.9										
13-04-11 15:15			4		2.8			15.20	14.79	166	683	-6.70			
17-05-11 17:00			1.1		5.5		7.39			182	722	-6.60			
21-06-11 16:05			2.1		1.9		7.4	38.83	33.54	176		-6.55			
10-08-11 13:45			2.6				7.17	22.80	19.28		755	-6.77			
06-02-12 18:00			1.9				7.09	17.76	8.54	204	728				
13-03-12 14:10			2.1				7.16	16.54	12.95	210	742	-6.10			
10-04-12 17:50			2.9				6.92	11.07	14.76	194	713	-6.13			
22-05-12 18:20			1.6		2.2		7.25	16.58	16.19	198	722	-6.08	-38.78		
20-06-12 14:55			2.7		3.4		7.39	18.52	10.68	194	702	-6.86	-37.71		
23-07-12 17:35			2.1		0.3		7.15	21.84	17.72	210	746	-6.33	-38.11		
23-08-12 18:20			1.8		0.87		6.9	22.60	21.77	240	744	-6.40	-37.68		
09-10-12 15:20			<1.0				7.525	20.40	19.56	214	752	-6.26	-37.33		
07-11-12 17:30			2		2.4		6.85	15.88	14.73	206	790	-6.40	-38.53		
04-12-12 16:45			1.1				7.21	21.50	17.74	210	745	-6.66	-38.40		
23-01-13 11:20			2		3.3		7.1		22.76	196	732				
26-02-13 14:20			1				6.94	16.19	15.42	200	723				
25-03-13 14:00			0.4		3.3		7.32	18.82	17.68	200	736				

BH17

Near Coy turlough

Date/time	Depth (m)	Head (mAOD)	Nitrate (mg/l)	Nitrite (mg/l)	Total N (mg/l)	Ammonia (mg/l)	ph	Total Phosphorus (µg/l)	Total Dissolved Phosphorus (µg/l)	Alkalinity (mg/l as CaCO3)	EC (µS/cm)	δ^{18}O VSMOW ‰	δ^{2}H VSMOW ‰	δ^{13}C VPDB ‰	Comment
13-10-10 16:50	9.68	11.24													
18-11-10 17:25	3.80	17.12													
15-02-11 16:15	3.06	17.86	6.10				7.34	29.47	14.32	7.2	647	-6.66			
24-02-11 14:15	3.24	17.68													
02-03-11 16:30	3.66	17.26													
22-03-11 13:00	7.86	13.06	4.80				7.25	65.28	9.81	160	695	-6.91			
06-04-11 12:45	8.00	12.92													
13-04-11 14:20	8.87	12.05	1.50		4.8			48.35	17.22	140	631	-6.50			
01-06-11 15:50	10.84	10.08													
21-06-11 13:30	10.17	10.75	0.6		1.9		7.43	79.97	25.19	152		-6.481			

BH19

Near Coole(nra)

Date/time	Depth (m)	Head (mAOD)	Nitrate (mg/l)	Nitrite (mg/l)	Total N (mg/l)	Ammonia (mg/l)	ph	Total Phosphorus (µg/l)	Total Dissolved Phosphorus (µg/l)	Alkalinity (mg/l as CaCO3)	EC (µS/cm)	δ^{18}O VSMOW ‰	δ^{2}H VSMOW ‰	δ^{13}C VPDB ‰	Comment
24-02-11 13:10	8.40	18.22													
03-03-11 13:50	8.67	17.95													
21-03-11 16:15	8.80	17.82													
06-04-11 14:20	9.05	17.57													
17-05-11 17:00	9.15	17.47													
01-06-11 14:15	9.26	17.36													
18-10-11 19:00	8.72	17.90													
08-11-11 17:15	8.66	17.96													
10-01-12 9:40	8.19	18.43													
06-02-12 18:00	8.47	18.15													
13-03-12 14:20	8.99	17.63													
10-04-12 17:55	9.08	17.54													
22-05-12 18:20	9.30	17.32													
20-06-12 14:55	8.83	17.79													
23-07-12 17:40	9.10	17.52													
23-08-12 18:20	8.84	17.78													
09-10-12 15:15	8.63	17.99													
07-11-12 17:20	8.54	18.08													
04-12-12 16:50	8.72	17.90													
23-01-13 11:20	8.75	17.87													
26-02-13 14:20	8.80	17.82													
25-03-13 14:00	9.17	17.45													

BH20

Kiltartan (nra)

Date/time	Depth (m)	Head (mAOD)	Nitrate (mg/l)	Nitrite (mg/l)	Total N (mg/l)	Ammonia (mg/l)	ph	Total Phosphorus (µg/l)	Total Dissolved Phosphorus (µg/l)	Alkalinity (mg/l as CaCO3)	EC (µS/cm)	δ^{18}O VSMOW ‰	δ^{2}H VSMOW ‰	δ^{13}C VPDB ‰	Comment
03-02-11 14:40	12.11	10.77													
21-03-11 16:45	12.60	10.28													
06-04-11 15:00	12.67	10.21													
13-04-11 15:40	12.50	10.38													
17-05-11 15:50	12.93	9.95													
01-06-11 15:15	12.98	9.90													
21-06-11 19:10	12.87	10.01													
18-10-11 17:40	12.50	10.38													
08-11-11 16:20	12.38	10.50													
06-02-12 17:10	11.40	11.48													
13-03-12 17:40	12.67	10.21													
10-04-12 14:35	12.83	10.05													
22-05-12 15:10	12.90	9.98													
20-06-12 13:10	12.56	10.32													
23-07-12 12:10	12.73	10.15													
23-08-12 17:40	12.56	10.32													
09-10-12 16:20	12.42	10.46													
07-11-12 16:15	12.00	10.88													
04-12-12 15:15	12.17	10.71													
23-01-13 11:10	11.99	10.89													
26-02-13 11:00	12.50	10.38													
25-03-13 14:45	12.80	10.08													

BH21

Kiltartan (along N18)

Date/time	Depth (m)	Head (mAOD)	Nitrate (mg/l)	Nitrite (mg/l)	Total N (mg/l)	Ammonia (mg/l)	ph	Total Phosphorus (µg/l)	Total Dissolved Phosphorus (µg/l)	Alkalinity (mg/l as CaCO3)	EC (µS/cm)	δ^{18}O VSMOW ‰	δ^{2}H VSMOW ‰	δ^{13}C VPDB ‰	Comment
21-03-11 16:35	3.52	14.71													
06-04-11 14:45	3.56	14.67													
13-04-11 15:20	3.51	14.72													
17-05-11 16:15	3.67	14.56													
21-06-11 19:40	3.81	14.42													
08-11-11 16:50	3.88	14.35													
04-12-11 17:00	3.82	14.41													
10-01-12 9:30	3.82	14.41													

T1

Blackrock

Date/time	Depth (m)	Head (mAOD)	Nitrate (mg/l)	Nitrite (mg/l)	Total N (mg/l)	Ammonia (mg/l)	ph	Total Phosphorus (µg/l)	Total Dissolved Phosphorus (µg/l)	Alkalinity (mg/l as CaCO3)	EC (µS/cm)	δ^{18}O VSMOW ‰	δ^{2}H VSMOW ‰	δ^{13}C VPDB ‰	Comment
31-03-10 19:45										36					
21-07-10 11:45				0.02		0.04	8.08			24	159	-6.67			
16-09-10 11:00			1.4	0.01	1.97	0.01	7.92			46	206	-5.20			
18-11-10 17:45				0.02	3	0.02	7.8			76	333	-6.81			
16-02-11 13:10			0.25		0.25		7.91	46.12	41.66	52	243	-7.21			
22-03-11 8:15			1.1		1.15		8.19	61.34	43.05	92	400	-6.66			
13-04-11 19:45			1.5		1.5			21.67	13.18	124	497	-6.51			
19-10-11 14:15			0.6		1.5		7.88	43.95	22.02	90	377	-5.14	-29.21		
09-11-11 13:15			0.6		1.4		7.87	23.02	15.26	104	405	-5.35	-35.60		
05-12-11 13:00			0.8				7.55	40.53	34.54	64	276	-6.42	-38.78		
10-01-12 16:00			0.5		0.6		7.97	40.00	22.90	84	345	-6.21	-32.78		
07-02-12 12:45			0.4		0.6		7.8	30.81	17.76	88	378	-5.84	-31.13		
10-04-12 12:40			0.6		1.95		7.71	48.75	27.86	52	218	-5.10	-35.10		
20-06-12 15:35			0.8				7.88	38.12	20.09	28	275	-7.22	-47.86		
23-07-12 18:55			0.9		1.8		8.04	115.43	61.42	60	250	-4.47	-29.27		
23-08-12 10:40			0.8				7.8	59.84	42.78	82	311	-6.61	-40.29		
09-10-12 17:10			1				8.079	34.00	33.00	74	288	-5.81	-34.22		
08-11-12 13:05			1.4				7.71	46.57	27.39	74	324	-7.29	-45.39		
05-12-12 12:50			0.7		0.994		7.82	53.26	26.52	88	347	-7.20	-42.36		
23-01-13 13:00			0.4		1.3		7.78		28.61	62	294				
26-02-13 16:40			0.3		0.5		7.89	42.00	16.00	112	444				
25-03-13 16:20			1.3				7.89	56.13	21.86	70	309				

T2

Coy

Date/time	Depth (m)	Head (mAOD)	Nitrate (mg/l)	Nitrite (mg/l)	Total N (mg/l)	Ammonia (mg/l)	ph	Total Phosphorus (µg/l)	Total Dissolved Phosphorus (µg/l)	Alkalinity (mg/l as CaCO3)	EC (µS/cm)	δ^{18}O VSMOW ‰	δ^{2}H VSMOW ‰	δ^{13}C VPDB ‰	Comment
31-03-10 19:00										86					
30-04-10 18:30										76		-8.22			
11-05-10 11:15										82		-7.58			
10-06-10 14:15			0.8	0.015		0.14				54		-2.69			
21-07-10 12:45				0.02		0.22	6.8			30	152.6	-6.77			
16-09-10 11:40			1.1	<0.02	1.2	0.01	7.94			64	279	-6.33			
14-10-10 12:00			0.25	0.03	0.25	0.52	7.94			66	326	-5.86			
18-11-10 17:35			0.25	0.01	0.25	0.03	7.73			72	329	-6.60			
16-02-11 12:35			1.1		2.1		7.99	50.09	26.88	70	314	-6.85			
22-03-11 9:00			0.1		1.05		8.32	30.20	8.18	78	334	-6.77			
13-04-11 19:25			0		1.6			27.73	17.22	74	312	-6.11			
17-05-11 18:15			0.1		0.3		9.38			60	269	-3.68			
21-06-11 12:40			0.4		0.4		7.9	47.39	29.87	30		-5.09			
19-10-11 13:20			0.8		1.5		8	26.91	5.96	82	344	-4.74	-30.51		
09-11-11 12:30			0.5		0.8		7.9	24.99	10.66	96	365	-5.28	-33.58		
05-12-11 12:10			0.7		1		7.74	47.88	25.99	98	372	-6.27	-36.21		
10-01-12 13:15			0.6		0.8		7.92	30.43	22.52	96	392	-5.93	-34.68		
07-02-12 12:00			0.5		1		7.91	28.51	17.37	98	402	-6.23	-33.24		
13-03-12 12:30			0.1		0.3		7.56	45.87	8.96	106	421	-6.63	-33.05		
10-04-12 18:30			1.1		2.85		7.75	53.67	29.91	54	248	-4.45	-32.17		
22-05-12 13:55			0.1		3		8.23	56.49	10.44	114	432	-5.99	-36.76		
20-06-12 15:15			0.8				7.9	49.88	16.56	60	231	-5.68	-42.41		
23-07-12 18:30			0.2		0.7		7.98	63.48	45.55	70	292	-6.03	-41.44		
23-08-12 11:40			0.5				7.71	56.72	42.57	80	312	-5.99	-38.37		
10-10-12 12:00			1				8.011	44.00	41.00	84	330	-5.70	-33.41		
08-11-12 12:25			0.5		0.907		7.59	36.59	20.10	90	361	-6.43	-39.47		
05-12-12 11:20			0.6		1.02		7.72	34.88	22.34	88	357	-6.81	-40.37		
23-01-13 12:35			1.1		0.9		7.86		18.58	102					
26-02-13 16:10			0.2		0.3		7.92	28.00	14.00	104	393				
25-03-13 15:50			1.2		1.8		8.01	56.51	14.63	80	348				

T3

Coole

Date/time	Depth (m)	Head (mAOD)	Nitrate (mg/l)	Nitrite (mg/l)	Total N (mg/l)	Ammonia (mg/l)	ph	Total Phosphorus (µg/l)	Total Dissolved Phosphorus (µg/l)	Alkalinity (mg/l as CaCO3)	EC (µS/cm)	δ^{18}O VSMOW ‰	δ^{2}H VSMOW ‰	δ^{13}C VPDB ‰	Comment
31-03-10 18:00							6.61			32					
11-05-10 14:00										80		-7.39			
10-06-10 13:15			1	0.02		0.07	7.99			122					
24-06-10 13:15			0.5	0		0.17	7.81			90		-6.34			
21-07-10 14:00				0.02		0.17	7.71			22	152.6	-6.60			
19-08-10 11:15			0.5	0.02		<0.05	7.67			50	240				
16-09-10 10:10			0.7	<0.02	1.15	0.01	7.95			42	200	-5.49			
14-10-10 11:15				0.02	1.6	0.39				54	219	-5.64			
18-11-10 14:30			1.1	0.01	2.5	0.01	8.75			42	225	-6.50			
16-02-11 11:45			1.6		1.7		7.89	33.08	20.99	46	256	-7.01			
22-03-11 9:50			0.5		1.5		7.88	28.57	8.58	60	277	-6.55			
13-04-11 17:30			0.3		1.3		7.59	26.92	17.62	54	277	-6.12			
17-05-11 16:30			0.2		0.4		7.54			42	237	-5.47			
21-06-11 16:30			0.7				7.2	29.26	19.89	28		-5.13			
19-10-11 11:50			0.5		1.6		7.64	25.54	21.63	54	249	-4.36	-27.81		
09-11-11 11:45			0.6				7.53	23.55	15.65	82	335	-4.48	-33.08		
05-12-11 11:25			0.9		0.9		7.59	29.75	23.59	50	223	-5.36	-36.04		
10-01-12 10:10			0.6		0.7		8.11	27.04	19.51	62	284	-5.53	-32.04		
07-02-12 10:00			0.6		0.8		7.46	24.67	12.00	66	307	-5.64	-30.98		
13-03-12 14:30			0.7		0.7		7.63	34.10	17.34	66	289	-5.82	-27.84		
10-04-12 17:20			1.1		3.15		7.81	44.66	32.37	56	206	-4.66	-30.71		
22-05-12 17:40			0.3		0.4		7.856	26.94	22.53	60	264	-5.42	-31.84		
20-06-12 14:35			0.8				7.46	32.63	11.07	62	232	-5.92	-41.52		
23-07-12 17:10			0.9		0.9		7.56	38.33	23.49	52	218	-5.82	-39.19		
23-08-12 14:30			0.6				7.63	36.33	26.76	60	242	-6.48	-37.67		
10-10-12 11:10			0.3		0.3		7.59	30.84	22.49	62	263	-6.28	-35.10		
08-11-12 11:50			0.9				7.87	35.06	28.16	70	269	-7.12	-40.49		
04-12-12 16:10			0.5		1.07		7.56	34.25	25.47	60	258	-7.45	-40.59		
23-01-13 11:35			0.8		1.1		7.63		22.97	66	252				
26-02-13 14:00			0.2		0.4		7.59	25.00	12.00	90	353				
25-03-13 13:30			0.2		0.4		7.87	24.53	14.63	60	256				

T4

Garryland

Date/time	Depth (m)	Head (mAOD)	Nitrate (mg/l)	Nitrite (mg/l)	Total N (mg/l)	Ammonia (mg/l)	ph	Total Phosphorus (µg/l)	Total Dissolved Phosphorus (µg/l)	Alkalinity (mg/l as CaCO3)	EC (µS/cm)	δ^{18}O VSMOW ‰	δ^{2}H VSMOW ‰	δ^{13}C VPDB ‰	Comment
31-03-10 15:40										88					
30-04-10 14:30										74					
11-05-10 15:15										72		-7.15			
21-07-10 16:20				0.01		0.29	6.7			40	154.6	-6.61			
16-09-10 8:30			0.6	<0.02	1.11	0.03	7.97			46	214	-5.69			
14-10-10 10:30			1.1	0.01	1.3	0.31	7.89			66	295	-5.67			
18-11-10 15:10			0.7	0.01		0	7.64				243	-6.01			
16-02-11 8:45			1.7		2.7		7.82	20.99	14.00	48	252	-6.67			
22-03-11 10:45			0.7		0.8		7.86	19.60	12.26	70	325	-6.50			
13-04-11 17:00			0.3		1.5			17.83	13.58	66	281	-5.99			
17-05-11 15:00			0.2		0.4		8.5			86	396	-4.88			
21-06-11 17:00			0.1		0.3		8.15	17.04	12.56	56		-4.81			
19-10-11 11:00			0.6		1.8		7.67	13.80	13.99	72	298	-5.28	-28.37		
09-11-11 9:30			0.2				7.53	15.13	10.26	72	320	-4.52	-31.11		
05-12-11 10:30			0.7		1.3		7.58	18.29	17.95	70	303	-5.29	-32.29		
10-01-12 11:45			0.6		0.7		7.8	19.89	18.01	64	284	-5.58	-33.14		
07-02-12 8:45			0.3		0.7		7.75	19.48	14.88	72	308	-5.28	-31.44		
13-03-12 16:20			0.4		0.4		7.9	18.54	10.56	88	363	-5.70	-28.75		
10-04-12 16:45					2.4		8.1	16.39	5.33	88	352	-4.25	-29.43		
22-05-12 17:00			0.3		0.4		8.39		20.80	78	307	-4.84	-30.21		
20-06-12 14:05			0.5				7.48	34.40	25.18	60	246	-6.05	-41.13		
23-07-12 16:25			0.4		1		7.72	24.31	16.89	66	272	-5.19	-36.24		
23-08-12 15:45			0.5				7.67	25.93	24.26	68		-5.98	-37.79		
10-10-12 10:00			0.4		0.4		7.842	28.13	20.40	62	245	-5.94	-33.99		
08-11-12 10:15			1.2				7.51	21.06	12.24	74	310	-6.38	-37.92		
05-12-12 10:00			0.7		0.875		7.55	20.25	18.58	70	279	-6.80	-39.18		
23-01-13 10:20			1.2				7.71		17.32		317				
26-02-13 12:50			0.3		0.4		7.66	20.00	16.00	88	332				
25-03-13 13:00			0.5		0.7		7.87	27.58	15.39	84	344				

T5

Caherglassaun

Date/time	Depth (m)	Head (mAOD)	Nitrate (mg/l)	Nitrite (mg/l)	Total N (mg/l)	Ammonia (mg/l)	ph	Total Phosphorus (µg/l)	Total Dissolved Phosphorus (µg/l)	Alkalinity (mg/l as CaCO3)	EC (µS/cm)	δ^{18}O VSMOW ‰	δ^{2}H VSMOW ‰	δ^{13}C VPDB ‰	Comment
31-03-10 16:30										60					
30-04-10 15:15										82		-7.55			
11-05-10 16:15										60		-7.07			
10-06-10 11:10			0.35	0.065		0.1				122		-6.17			
24-06-10 10:45			0.3	0.01		<0.05				76		-5.51			
21-07-10 17:15				0.01		0.4	6.67			42	232	-6.42			
19-08-10 9:05			0.6	0.01	0.78	0.01				56	251	-5.83			
16-09-10 9:00			0.5	<0.02		0.01	7.99			40	189	-5.85			
14-10-10 9:30			2.4	0.01	4.3	0.23	7.96			68	325	-5.82			
18-11-10 15:25			0.8	0.01	1.4	0.02	7.7			68	236	-6.10			
16-02-11 8:45			0.5		1.6		7.81	23.22	19.09	40	223	-6.97			
22-03-11 11:20			1		1.3		7.91	21.64	8.18	62	295	-6.50			
13-04-11 16:20			0.2		1			26.52	13.98	48	252	-6.16			
17-05-11 15:25			0.2		0.3		8.52	32.74	22.07	58	279	-5.34			
21-06-11 17:40			0.1		0.3		8.19	34.15	22.75	42		-5.23			
10-08-11 12:15												-5.15			
19-10-11 10:00			0.6		1.6		7.69	26.72	23.98	249	249	-4.19	-28.39		
09-11-11 10:05			0.1		0.1		7.58	21.97	15.13	283	283	-4.44	-32.24		
05-12-11 10:00			1.2		1.2		7.61	33.17	25.99	234	234	-4.96	-33.58		
10-01-12 10:50			0.7		1.1		7.8	22.90	18.57	287	287	-5.97	-32.93		
07-02-12 9:30			0.5		0.7		7.74	21.40	20.83	307	307	-5.74	-30.96		
13-03-12 16:50			0.9		0.9		7.96	30.51	14.55	348	348	-5.78	-28.54		
10-04-12 16:15			0.9		1.5		8.04	25.40	21.72	352	352	-4.53	-30.23		
22-05-12 16:10			0.5		0.5		8.43	21.57	15.43	301	301	-5.08	-32.21		
20-06-12 13:25			1				7.63	24.79	20.09	216	216	-6.20	-41.60		
23-07-12 15:45			0.9		0.8		7.69	31.73	23.49	242	242	-5.86	-38.98		
23-08-12 16:20			0.9				7.66	36.33	28.42	216	216	-5.58	-37.77		
10-10-12 10:30			0.3		0.4		7.845	32.93	24.57	226	226	-5.91	-34.07		
08-11-12 10:50			1.2				7.15	32.37	22.40	243	243	-6.74	-40.80		
05-12-12 10:30			0.3		1.17		7.57	25.68	22.34	277	277	-6.80	-39.83		
23-01-13 10:00			0.3		1.3		7.57		22.97	278	278				
26-02-13 13:20			0.6				7.7	18.87	18.48	330	330				
25-03-13 12:30			0.3		0.4		8.02	27.19	20.34	296	296				

T6

Ballinduff

Date/time	Depth (m)	Head (mAOD)	Nitrate (mg/l)	Nitrite (mg/l)	Total N (mg/l)	Ammonia (mg/l)	ph	Total Phosphorus (µg/l)	Total Dissolved Phosphorus (µg/l)	Alkalinity (mg/l as CaCO3)	EC (µS/cm)	δ^{18}O VSMOW ‰	δ^{2}H VSMOW ‰	δ^{13}C VPDB ‰	Comment
05-12-12 11:40			0.1		0.87		7.79	0.02	0.01	0	174	638	-6.76		-39.31
12-12-12 12:10										0	148	625			
23-01-13 12:05			1.2		0.9		7.89		0.01	0	184	652			
26-02-13 10:30			9		1.7		7.91	0.01	0.01	0	168	613			
25-03-13 15:20			0.6		1.8		8.02	0.06	0.02	0	120	527.000			

KW

Kinvarra West

Date/time	Depth (m)	Head (mAOD)	Nitrate (mg/l)	Nitrite (mg/l)	Total N (mg/l)	Ammonia (mg/l)	ph	Total Phosphorus (µg/l)	Total Dissolved Phosphorus (µg/l)	Alkalinity (mg/l as CaCO3)	EC (µS/cm)	δ^{18}O VSMOW ‰	δ^{2}H VSMOW ‰	δ^{13}C VPDB ‰	Comment
31-03-10 17:20												-8.05			
10-06-10 10:15			1.1	0.01	0	<0.05				92		-3.75			
24-06-10 17:20			0.4	<0.02	0	0.05				80		-2.24			
22-07-10 9:15				<0.02		0.35	7.32			58	321	-6.56			
19-08-10 8:15											8140				salt water
16-09-10 7:45			0.9	<0.02	2.27	0.01	7.76			76	333	-6.01			
14-10-10 14:30											5410				salt water
18-11-10 15:55			1.3	0.02	1.8	0.02	7.5			68		-6.15			
16-02-11 11:30							7.79	23.54	17.81	64	312	-6.95			
22-03-11 12:05							7.66	20.01	10.42	76	389	-6.61			
17-05-11 13:30											6490				salt water
21-06-11 16:10			0.6		0.8		7.94	19.08	15.82	68		-5.23			
18-10-11 15:25			0.9		1.2		7.54	21.63	19.28	82	358	-4.77	-29.32		
09-11-11 10:40			0.3		0.4		7.35	19.34	11.97	94	383	-4.66	-33.13		
05-12-11 9:10			0.6		0.7		7.28	24.62	21.20	88		-5.68	-35.00		
10-01-12 12:25			0.2		0.6		7.52	19.14	19.14	90	352	-6.20	-33.11		
07-02-12 11:15			0.4		0.7		7.49	17.76	12.76	84	368	-5.44	-31.32		
13-03-12 15:40			0.8				7.78	32.50	14.95	104	417	-5.58	-29.56		
10-04-12 15:30											2500				salt water
20-06-12 12:25			0.7				7.7	19.70	14.99	74	309	-5.95	-40.35		
23-07-12 15:00			0.6		0.8		7.28	29.67	20.60	80	362	-5.77	-38.51		
23-08-12 16:40			0.8		0.8		7.3	30.50	21.77	80	343	-5.74	-37.37		
09-10-12 19:00			1.6				7.701	26.66	19.56	90	355	-5.71	-34.51		
07-11-12 17:00			1		1.43		6.94	25.85	17.80	94	401	-6.97	-39.04		
04-12-12 14:45			1.1		1.2		7.33	21.08	17.74	92	360	-6.72	-39.59		
23-01-13 9:30			0.4		1.1		7.53		13.98	92	373				
26-02-13 11:40			0.1		1		7.58	9.29	8.14	96	399				
25-03-13 11:20			0.4		1.1		7.32	29.48	19.58	50	439				

KE

Kinvarra East

Date/time	Depth (m)	Head (mAOD)	Nitrate (mg/l)	Nitrite (mg/l)	Total N (mg/l)	Ammonia (mg/l)	ph	Total Phosphorus (µg/l)	Total Dissolved Phosphorus (µg/l)	Alkalinity (mg/l as CaCO3)	EC (µS/cm)	δ^{18}O VSMOW ‰	δ^{2}H VSMOW ‰	δ^{13}C VPDB ‰	Comment
31-03-10 17:30										122		-8.475			
10-06-10 10:10												-5.766			
24-06-10 17:30			0.4	<0.02	7.91	<0.05				102		-4.798			
08-07-10 10:50			0.2	0.01		<0.05	6.7			130		-5.547			
22-07-10 9:25				0.01		0.28	7.68			84	381	-6.826			
19-08-10 8:15											8140				salt water
16-09-10 7:45			1.8	<0.02	2.35	0	7.58			130	501	-6.683			
14-10-10 14:20			1.2	0		0.41	7.54			128	561	-6.65			
16-02-11 10:05							7.79	20.68	16.86	134	560	-7.11			
22-03-11 12:20							7.37	21.23	8.18	128	558	-6.30			
17-05-11 13:35											3000				salt water
21-06-11 16:15			0.6		0.8		7.65	22.34		78		-5.54			
18-10-11 15:30			1.5		1.6		7.29	23.19	20.06		595	-6.20	-36.52		
09-11-11 10:50			1.7		1.9		7.15	20.92	14.08	174	640	-5.75	-39.20		
10-01-12 12:35			1.8		2.1		7.2	22.90	17.25	158	587	-5.81	-35.38		
07-02-12 11:25			0.7				7.39	21.60	18.14	132	500	-5.85	-34.52		
13-03-12 15:50			1.6		1.8		7.59	21.33	14.15	150	575	-5.60	-33.41		
10-04-12 15:40			1.2		1.5		7.21	19.67	16.80	156	640	-5.75	-36.85		
20-06-12 12:30			1.6				7.51	24.40	17.74	144	541	-6.29	-40.72		
23-07-12 15:10			1		1.1		7.11	25.55	16.07	126	463	-6.01	-38.74		
23-08-12 16:50			1.2				7.08	31.34	23.01	138	502	-5.62	-37.94		
09-10-12 19:10			0.1				7.475	36.69	21.23	180	644	-6.18	-36.38		
07-11-12 17:00			2.3		2.3		7.54	30.84	20.10	178	692	-6.91	-39.64		
04-12-12 14:50			0.7		0.868		7.15	22.34	21.08	134	513	-6.79	-39.68		
23-01-13 9:30			2.1		2.7		7.14		18.58	170	630				
26-02-13 11:45			0.2		1.8		7.21	26.53	18.10	168	617				
25-03-13 11:25			0.5		2.5		7.68	19.20	11.97	90	524				

OR-U

Owenshree river (upper)

Date/time	Depth (m)	Head (mAOD)	Nitrate (mg/l)	Nitrite (mg/l)	Total N (mg/l)	Ammonia (mg/l)	ph	Total Phosphorus (µg/l)	Total Dissolved Phosphorus (µg/l)	Alkalinity (mg/l as CaCO3)	EC (µS/cm)	δ^{18}O VSMOW ‰	δ^{2}H VSMOW ‰	δ^{13}C VPDB ‰	Comment
11-05-10												-6.567			
03-06-10				0.21		38						-6.414			
10-06-10			1.8	0.03		0.1						-7.442			
24-06-10			0.6	0.01		0.02						-6.203			
08-07-10			0.5	0.02		0.03						-5.699			
20-07-10			1.7	0.01		<0.05				24		-6.727			
19-08-10			0.2	0.01		0.15				56		-5.817			
15-09-10 14:00			1	<0.02		0.02	7.7			24	94.3	-5.37			
13-10-10 15:20			0.2	0.01	0.3	0.04	8.36			42	214	-5.70			
18-11-10 10:20			0.6	0.01	1.3	0.02	6.47			6	87.8	-7.82			
15-02-11 11:30			1.1				7.9	20.99	16.22	18	97.6	-7.23			
21-03-11 11:00			1.9				7.81	17.15	13.89	18	108	-6.64			
13-04-11 11:30			0.3		1.5			33.39	21.26	16	101.2	-6.81			
17-05-11 10:50			0		0.8		8.4	14.79	10.38	40	117	-5.54			
21-06-11 8:50			0.3		0.5		7.87	49.63	29.67	16		-5.57			
08-11-11 9:50			0.6		1.2		7.59	16.44	11.05	56	167	-5.35			
04-12-11 10:10			0.6		0.8		7.37	25.99	24.28	22	352	-6.11			
06-02-12 10:50			0.3		0.3		7.49	20.83	18.91	18	124	-5.44			
13-03-12 9:00			0.4		0.4		7.87	15.35	12.95	34	153	-4.80			
10-04-12 9:10			0.6		0.9		7.17	26.22	22.13	12	78.6	-5.14			
22-05-12 9:25			0.7		2.3		8.23	11.20	9.67	54	210				
20-06-12 9:30			0.6				7.34	18.52	16.56	40	160				
23-07-12 9:00			0.8		1.7		7.25	120.79	57.71	12	70.4				
23-08-12 8:50			0.8				7.67	40.07	31.75	34	125				
07-11-12 10:15			1.1				7.36	17.80	13.58	26	139				
04-12-12 10:10			0.5		0.62		7.83	17.74	18.16	20	90				
23-01-13 14:30			1.5		1.6		7.71		17.32	34	149.3				
26-02-13 8:50			0.7				7.74	6.61	6.99	42	208				
25-03-13 9:10			0.5		1.7		7.47	15.77	12.16	26	161				

OR-L

Owenshree river (lower)

Date/time	Depth (m)	Head (mAOD)	Nitrate (mg/l)	Nitrite (mg/l)	Total N (mg/l)	Ammonia (mg/l)	ph	Total Phosphorus (µg/l)	Total Dissolved Phosphorus (µg/l)	Alkalinity (mg/l as CaCO3)	EC (µS/cm)	δ^{18}O VSMOW ‰	δ^{2}H VSMOW ‰	δ^{13}C VPDB ‰	Comment
11-05-10												-6.639			
03-06-10				0.21		35						-6.530			
10-06-10			1.5	0.03		0.01						-7.380			
24-06-10			1.2	0.02		0.01						-5.975			
08-07-10			0.8	0.05		0				48		-5.732			
20-07-10				0.02		0.12				12		-6.780			
19-08-10			0.5	0.02		0.12				30		-5.949			
15-09-10 12:45				<0.02		0.01	7.6			54	340	-5.72			
13-10-10 15:00			0.1	0		0.01	8.37			114	418	-6.55			
18-11-10 10:05			0.6	0.01	1.3	0.03	7.23			22	135.1	-8.02			
15-02-11 11:00			0.2		0.3		8.01	19.09	11.77	70	324	-6.95			
21-03-11 10:30			1.2				7.94	16.74	11.03	76	339	-6.64			
13-04-11 11:15			0.5		1.4			31.37	18.43	68	316	-7.08			
17-05-11 10:30			0.4		0.5		8.22	14.89	12.97	70	314	-5.74			
21-06-11 8:30			0.5		0.5		8.1	29.67	22.34	50		-6.01			
18-10-11 10:40			0.7				7.58	36.12	25.54		245	-4.71			
08-11-11 9:30			0.3		0.4		7.95	15.92	9.34	106	468	-5.66	-37.12		
04-12-11 9:45			0.7		0.9		6.98	20.34	11.45	88	366	-6.08	-38.14		
09-01-12 10:10			0.7		1		7.93	26.10	19.89	100	413	-5.82	-32.60		
06-02-12 10:30			0.2		0.2		7.96	13.53	14.30	92	370	-6.26	-33.80		
13-03-12 8:30			0.5				7.98	15.75	10.36	102	392	-5.76	-31.56		
10-04-12 8:50			0.6		2.25		7.38	33.19	21.31	42	169.8	-5.38	-32.72		
22-05-12 8:50			0.2		0.4		8.23	20.03	8.32	122	458	-6.16	-37.42		
20-06-12 9:10			0.8				7.79	16.95	13.23	118	432	-6.40	-40.29		
23-07-12 8:40			0.9		1.1		7.56	113.16	44.10	50	207	-5.56	-33.39		
23-08-12 8:30			1.4		3.4		7.82	43.61	27.59	88	326	-6.04	-37.80		
09-10-12 10:30			0.2		0.3		8.091	15.17	9.33	126	432	-6.38	-36.57		
07-11-12 9:30			1.2				7.79	18.95	11.28	102	422	-7.27	-41.18		
04-12-12 9:50			0.2		0.3		7.66	32.16	20.88	62	257	-6.90	-40.07		
23-01-13 16:35			0.2		0.3		7.98		16.49	118	434				
26-02-13 8:30			0.7		1.8		7.99	15.04	8.14	128	481				
25-03-13 8:45			0.2		0.3		7.95	24.91	6.26	88	375				

BR-U

Ballycahalan river (upper)

Date/time	Depth (m)	Head (mAOD)	Nitrate (mg/l)	Nitrite (mg/l)	Total N (mg/l)	Ammonia (mg/l)	ph	Total Phosphorus (µg/l)	Total Dissolved Phosphorus (µg/l)	Alkalinity (mg/l as CaCO3)	EC (µS/cm)	δ^{18}O VSMOW ‰	δ^{2}H VSMOW ‰	δ^{13}C VPDB ‰	Comment
11-05-10												-6.491			
03-06-10				0.21		35						-6.622			
10-06-10			1.9	0.03		0.01						-7.666			
24-06-10			0.3	0.01		<0.05						-5.867			
08-07-10			0.5	0.01		<0.05				50		-5.772			
20-07-10			1.6	0.01		<0.05				4		-6.816			
19-08-10			1.2	0.03		0.09				16		-5.984			
15-09-10 15:20			1.2	0.01	2.37	0	7.3			10	53	-4.97			
13-10-10 16:15			0.3	0.02	1.8	0.01	7.9			34	177.5	-5.62			
18-11-10 11:10			0.4	0.02		0.04	6.15			8	75.7	-7.83			
15-02-11 12:40			2.1				7.16	25.92	20.04	8	60.6	-7.12			
21-03-11 12:20			1.7				8.06	24.90	10.62	12	73	-6.46			
13-04-11 12:15			0.2		1.1			41.75	23.08	10	77.3	-6.54			
17-05-11 11:40			0.2		0.8		8.1	18.22	17.62	14	96.3	-5.65			
21-06-11 10:10			0.4		2.6		7.6	28.45	24.37	12		-5.78			
18-10-11 12:00			0.9				7.65	40.82	36.90	6	73.3	-4.23			
08-11-11 11:00			0.5		0.5		7.48	30.78	24.34	18	99	-5.33			
04-12-11 11:30			0.7		1.7		6.8	33.52	28.55	6	61	-6.29			
09-01-12 11:40			0.2		0.2		7.64	26.10	23.09	8	100.5	-5.18			
06-02-12 11:50			0.1		0.1		7.23	77.66	25.82	6	80.8	-5.34			
13-03-12 10:20			0.1		0.2		8.01	33.30	28.11	18	98.9	-4.65			
10-04-12 10:30			0.7		0.9		6.74	37.69	31.96	10	66.1	-5.08			
22-05-12 10:20			0.1		0.1		8.03	23.87	21.57	42	164				
20-06-12 10:10			0.9				8.03	33.81	31.06	18	84.9				
23-07-12 10:00			1.3		1.3		6.19	73.38	67.60	6	38.7				
23-08-12 9:40			0.9		0.9		7.61	58.80	52.97	22	109.6				
09-10-12 11:40			0.2		0.3		7.383	31.68	24.99	14	84.7				
07-11-12 11:30			2.4				6.8	53.47	33.53	8	71				
04-12-12 11:10			0.8		1.45		6.79	41.56	36.55	6	-				
23-01-13 14:00			1		0.8		7.61		26.10	14	91.5				
26-02-13 9:30			0		0		7.76	22.70	13.12	42	172				
25-03-13 10:05			0.6				7.57	19.20	17.68	16	112.5				

BR-L

Ballycahalan river (lower)

Date/time	Depth (m)	Head (mAOD)	Nitrate (mg/l)	Nitrite (mg/l)	Total N (mg/l)	Ammonia (mg/l)	ph	Total Phosphorus (µg/l)	Total Dissolved Phosphorus (µg/l)	Alkalinity (mg/l as CaCO3)	EC (µS/cm)	δ^{18}O VSMOW ‰	δ^{2}H VSMOW ‰	δ^{13}C VPDB ‰	Comment
11-05-10												-6.559			
03-06-10				0.21		40						-6.174			
10-06-10			1.6	0.03		0						-7.507			
24-06-10				0.01		<0.05						-5.940			
08-07-10			0.2	0.02		0.06				64					
20-07-10			0.4	0.01		0				10		-6.883			
19-08-10			0.9	0.04		0.03				18		-5.730			
15-09-10 15:20			1.5	<0.02	1.94	0.02	7.64			24	134	-5.366			
13-10-10 17:05			0.2	0.01	0.4	0.03	8.05			60	285	-5.87			
18-11-10 12:10			0.6	0.02	1.1	0.02	5.8			8	97.3	-7.77			
15-02-11 12:40			1.3		1.3		7.25	20.99	19.40	24	144.2	-6.95			
21-03-11 14:10			0.4		0.6		7.81	20.01	13.07	6	147	-6.53			
13-04-11 13:45			0.7		1			19.24	15.20	48	221	-6.49			
17-05-11 17:45			0.1		0.6		7.95	26.46	19.65	34	165.1	-5.55			
21-06-11 14:00			0.3		0.4		7.56	40.67	28.45	20		-5.72			
10-08-11 15:45			0.8		2.9		7.42	38.47	26.72	14	107.7	-5.74			
18-10-11 14:30			1.1		0		7.49	39.64	30.63	54	239	-3.78	-23.30		
08-11-11 13:00			0.4		0.5		6.96	23.55	15.39	24	152	-6.13	-33.18		
04-12-11 14:40			0.7		1.4		7.48	31.80	23.25	34	199.6	-5.95	-36.86		
09-01-12 14:20			0.2		0.3		7.44	25.91	22.52	28	166.6	-5.12	-29.01		
06-02-12 14:50			0.3		0.3		7.77	26.59	23.13	40	202	-5.82	-30.74		
13-03-12 12:50			0.1				6.96	23.73	18.14	16	106.1	-5.36	-26.44		
10-04-12 1:30			1.1		1.65		7.99	30.32	27.04	68	277	-5.15	-29.94		
22-05-12 14:10			1.1		1.9		8.04	19.26	17.34	46	194.2	-6.17	-35.41		
20-06-12 16:00			0.8				6.94	44.00	35.38	10	58.1	-6.50	-42.75		
23-07-12 11:50			1		1.1		7.66	101.82	63.89	60	244	-5.52	-31.74		
23-08-12 12:10			0.9		3.1		7.724	33.83	29.26	44	213	-6.12	-37.40		
09-10-12 13:05			0.5		0.5		7.32	22.07	23.32	40	193	-6.34	-34.92		
07-11-12 13:50			1.1				7.15	23.94	18.37	20	98.2	-7.44	-42.30		
04-12-12 13:00			0.6		1.12		7.68	57.44	29.86	42	218	-7.00	-39.84		
23-01-13 14:45			0.8		0.9		7.81		24.43	106	292				
26-02-13 15:45			1.3		2.3		7.74	24.23	8.14	30	193.8				
25-03-13 16:45			0.3		1.3		7.74	15.77	9.87	30	193.8				

DR-U

Derrywee river (upper)

Date/time	Depth (m)	Head (mAOD)	Nitrate (mg/l)	Nitrite (mg/l)	Total N (mg/l)	Ammonia (mg/l)	ph	Total Phosphorus (µg/l)	Total Dissolved Phosphorus (µg/l)	Alkalinity (mg/l as CaCO3)	EC (µS/cm)	δ^{18}O VSMOW ‰	δ^{2}H VSMOW ‰	δ^{13}C VPDB ‰	Comment
11-05-10												-6.332			
03-06-10				0.22		35						-6.563			
10-06-10			2.3	0.03		<0.05						-7.450			
24-06-10			1.3	0.01		<0.05						-5.759			
08-07-10				0.05		<0.05						-5.499			
20-07-10			2.1	0.01		<0.05				14		-6.530			
19-08-10			0.7	0.03		0.08				6		-5.827			
15-09-10 17:10			0.1	0.01		0.01				12		-4.64			
13-10-10 17:40			0.1	0.02	2.1	0.09	5.83			8	56	-5.18			
18-11-10 12:40				0.02	2.3	0.02	8.1			28	161	-7.47			
15-02-11 15:00			1.3				5.13	15.43	14.32	6	88.1	-7.16			
21-03-11 12:20			2.5				6.56	13.07	7.56	6	56.2	-6.30			
13-04-11 18:25			0.7		1		7.86	16.82	15.60	8	70	-6.08			
21-06-11 15:00			0.2		0.4			23.15	17.86	10	89	-5.78			
10-08-11 15:00					0.4		7.63	32.01	19.67	6		-5.20			
18-10-11 15:10			1.3				6.33	27.11	25.94	2	72.8	-4.02			
08-11-11 14:20			0.2		0.2		7.14	21.71		10	94	-5.16			
04-12-11 15:00			0.5		1.9		5.25	30.78	18.46	8	57	-5.09			
09-01-12 14:50			0.2		0.2		6.48	22.90	20.27	4	91.8	-4.97			
06-02-12 15:30			0.3		0.3		7.08	65.37	58.08	4	77.2	-5.37			
13-03-12 18:10			0.2				7.82	33.70	24.52	8	86.7	-4.31			
10-04-12 18:40			1.3		3.9		6.95	35.24	25.40	10	77.2	-5.10			
22-05-12 19:10			0.8				7.99	27.71	24.25	28	129				
20-06-12 16:30			1				7.79	30.48	27.14	8	69.1				
23-07-12 12:25			1.3		1.3		6.16	58.12	42.04	6	38				
23-08-12 12:50			1.1				7.57	44.65		20	88				
09-10-12 14:10			1				7.29	25.83	21.65	12	72.9				
07-11-12 14:45			1.5				7.18	23.94	25.09	12	70				
04-12-12 13:30			1		1		6.7	34.04	24.85	14	50.4				
23-01-13 15:15			0.9				7.44		24.85	14	75.6				
26-02-13 14:40			0.2		0.3		7.55	19.63	18.10	18	137				
25-03-13 17:15			0.4		0.9		7.07	16.92	12.35	6	104.1				

DR-L

Derrywee river (lower)

Date/time	Depth (m)	Head (mAOD)	Nitrate (mg/l)	Nitrite (mg/l)	Total N (mg/l)	Ammonia (mg/l)	ph	Total Phosphorus (µg/l)	Total Dissolved Phosphorus (µg/l)	Alkalinity (mg/l as CaCO3)	EC (µS/cm)	δ^{18}O VSMOW ‰	δ^{2}H VSMOW ‰	δ^{13}C VPDB ‰	Comment
11-05-10												-6.507			
03-06-10				0.21		36						-5.961			
10-06-10			0.8	0.06		0.02						-7.477			
24-06-10			0.8	0.01		0						-5.683			
08-07-10			0.2	0.05		<0.05				38					
20-07-10			1.8	0.01		<0.05				8		-6.734			
19-08-10			0.6	0.02		0.05				30		-5.648			
15-09-10 17:35			0.2	0.01	1.04	0	7.23			10	84.2	-5.00			
13-10-10 18:10			0.2	0.01	2.2	0.27	7.75			32	80.7	-5.85			
18-11-10 13:10			0.2	0.02	0.3	0.02	5.7			6	77.6	-7.81			
15-02-11 15:30					0.7		6.7	11.45		10	94.9	-7.10			
21-03-11 15:30			0.4		0.7		7.64	21.64	6.95	14	107	-6.44			
13-04-11 18:50			0.6		0.9			18.03	15.60	28	166	-5.83			
21-06-11 15:35			0.1				7.47	24.37	13.38	14		-5.83			
10-08-11 15:20			0.6				7.76	31.42	22.02		138	-5.61			
18-10-11 15:40			0.8		1.2		6.62	35.73	27.11	12	92.5	-4.22	-24.18		
08-11-11 14:50			0.2		0.3		7.33	17.23	14.60	30	162	-5.65	-32.87		
04-12-11 15:30			0.5		0.9		6.32	22.23	16.41	12	101	-6.35	-37.29		
09-01-12 15:30			0.1		0.2		7.11	25.91	18.38	18	136.4	-5.99	-29.51		
06-02-12 16:00			0.5				7.06	22.75	16.22	18	118.9	-5.21	-30.60		
13-03-12 18:30			0.2		0.3		7.07	23.73	18.54	24	137.5	-4.26	-26.57		
10-04-12 19:10			0.6		3.45		6.86	30.73	25.81	0.8	81.6	-5.17	-30.22		
22-05-12 19:40			0.4		0.5		7.84			40	184	-5.97	-34.57		
20-06-12 16:50			0.8		0.8		7.67	23.22	20.87	22	115.6	-6.50	-44.03		
23-07-12 13:00			0.8		1.3		7.01	72.96	48.64	8	61.2	-5.50	-32.06		
23-08-12 13:15			3.1		3.1		7.46	29.26	28.84	36	144.8	-6.06	-37.53		
09-10-12 14:45					0.3		7.546	86.83	19.14	26	133.4	-6.00	-35.13		
07-11-12 15:00			1.3				7.13	59.23	23.94	8	119	-7.64	-42.55		
04-12-12 14:00			1.3		1.93		7	34.04	26.52	8	74	-7.05	-39.36		
23-01-13 15:40			0.6		0.8		7.42		16.91	26	136.4				
26-02-13 15:20			0.1		0.1		7.49	12.36	9.67	48	192				
25-03-13 17:40			0.6		1.9		7.09	14.63	10.44	18	129.3				

F

Forest

Date/time	Depth (m)	Head (mAOD)	Nitrate (mg/l)	Nitrite (mg/l)	Total N (mg/l)	Ammonia (mg/l)	ph	Total Phosphorus (µg/l)	Total Dissolved Phosphorus (µg/l)	Alkalinity (mg/l as CaCO3)	EC (µS/cm)	δ^{18}O VSMOW ‰	δ^{2}H VSMOW ‰	δ^{13}C VPDB ‰	Comment
11-05-10												-7.614			
03-06-10				0.22								-7.407			
10-06-10			0.8	0.02		<0.05						-7.680			
24-06-10			0.8	0.01		<0.05						-7.772			
08-07-10			0.2	<0.02		0.01				4		-6.873			
20-07-10			1.8	0.01		<0.05				1		-6.667			
19-08-10			0.6	0.02		0.05				16		-5.736			
15-09-10 14:20			2.4	0.03		0.02	4.55			0	57.8	-5.36			
13-10-10 15:45			0	0	2.2	0.27	7.75			10	80.7	-5.08			
18-11-10 10:30			0.6	0.01	2.4	0.04	6.17			6	57.1	-8.45			
15-02-11 11:50			0.6		1		7.32	4.78	0.00	4	42	-7.37			
21-03-11 11:15			0.4		0.5		6.34	12.66	4.10	4	48	-6.65			
13-04-11 11:45								12.37	7.92			-6.72			
17-05-11 11:10			0.1		0.6		7.88		9.13	2	51.8	-5.36			
21-06-11 9:20			0.2		0.3		6.3	11.34	13.38	6		-5.88			
18-10-11 11:15			0.5		1		6.69	9.10	9.49	4	67.2	-4.54	-19.70		
08-11-11 10:20			0.2		0.3		6.64	10.66	8.29	8	66	-4.93	-30.16		
04-12-11 10:30			0		1		6.44	11.96	10.08	6	54	-6.79	-38.68		
09-01-12 10:45			0		0		6.76	7.84	4.83	4	83.9	-5.51	-24.98		
06-02-12 11:00							6.73	5.47	5.47	6	60	-4.83	-29.27		
13-03-12 9:30			0.2		0.3		7.56	8.96	6.57	14	67.8	-4.22	-20.24		
10-04-12 9:30			0.2		0		6.75	8.41	5.95	0.4	50.6	-4.98	-29.46		
22-05-12 9:45			0.4		0.4		7.64	12.35	10.44	20	90.4	-6.34	-35.89		
20-06-12 9:45			0.8				7.6	13.42	10.68	12	57.1	-7.26	-49.42		
23-07-12 9:15			0.2		0.6		6.95	21.43	14.00	8	40.8	-5.40	-33.67		
23-08-12 9:10			0.8		3.7		7.32	16.77		22	74	-6.28	-39.45		
09-10-12 11:00			1				7.302	12.04	7.86	10	60.7	-6.60	-34.45		
07-11-12 10:30			0.9				6.7	9.74	8.98	12	56.9	-8.57	-48.76		
04-12-12 10:25			0.4		0.539		6.77	9.80	9.38	4	34.7	-7.93	-42.93		
23-01-13 14:20			0.2		0.2		7.19		8.55	10	55.8				
26-02-13 9:00			0.2		0.5		7.19	19.25	1.25	22	128				
25-03-13 9:30			0.4		1		6.96	6.26	6.26	16	83.5				

P

Peat

Date/time	Depth (m)	Head (mAOD)	Nitrate (mg/l)	Nitrite (mg/l)	Total N (mg/l)	Ammonia (mg/l)	ph	Total Phosphorus (µg/l)	Total Dissolved Phosphorus (µg/l)	Alkalinity (mg/l as CaCO3)	EC (µS/cm)	δ^{18}O VSMOW ‰	δ^{2}H VSMOW ‰	δ^{13}C VPDB ‰	Comment
11-05-10												-6.596			
03-06-10				0.24								-6.537			
10-06-10			2.1	0.06		<0.05						-7.305			
24-06-10			2.4	0.03		<0.05						-4.269			
08-07-10			0.9	0.01		<0.05				4		-5.311			
20-07-10			1.2	0.01		<0.05				2		-6.164			
19-08-10			0.4	0.02		0.05				10		-5.094			
15-09-10 14:45			0.8	0		0.01	5.67			4	24.6	-4.27			
18-11-10 10:45			0.6	0.01	1.4	0.03	5.14			4	53.5	-8.63			
15-02-11 12:05			3				6.5	5.73	5.41	2	60.3	-7.37			
21-03-11 11:40			2.3				5.51	10.62	0.43	4	40	-6.47			
13-04-11 12:00			1		1			15.20	3.07	4	37.7	-6.47			
17-05-11 11:15			0.6		0.4		5.45	9.94	6.85	2	48.3	-4.95			
21-06-11 9:40			0.3		0.4		5.39	12.36	7.88	8		-5.73			
18-10-11 11:40			0.6		1.6		5.57	8.71	4.79	2	48.3	-3.71			
04-12-11 10:50			0		1		5.69	8.88	0.00	4	40	-6.42			
09-01-12 11:05			0.6		0.5		5.22	3.70	2.58	2	70.5	-4.89			
06-02-12 11:20			0.3				5.59	5.08	4.70	4	43.5	-5.48			
13-03-12 9:45			0.6		0.8		5.7	9.76	3.78	6	43.1	-4.15			
10-04-12 10:00			0.9		1.35		5.58	8.20	7.38	0.4	44	-5.16			
20-06-12 9:50			0.4				6.74	9.50	4.02	6	28.5				
23-07-12 9:30			0.7		0.9		5.94	13.18	8.64	4	24.2				
23-08-12 9:25			1.2		2.2		5.85	10.53	5.95	8	27				
07-11-12 11:15			0.5				6.72	55.01	41.96	0.7	70				
04-12-12 10:50			0.2		0.292		7.33	5.62	3.53	10	49.7				
23-01-13 14:10			0.5		0.6		7.04		35.29	10	75.6				
26-02-13 9:10			0.1		0.2		7.33	16.57	13.89	16	138				
25-03-13 9:45			0.3		0.4		6.88	29.48	26.05	10	104.5				

Appendix G

Hydrochemistry Results - Figures

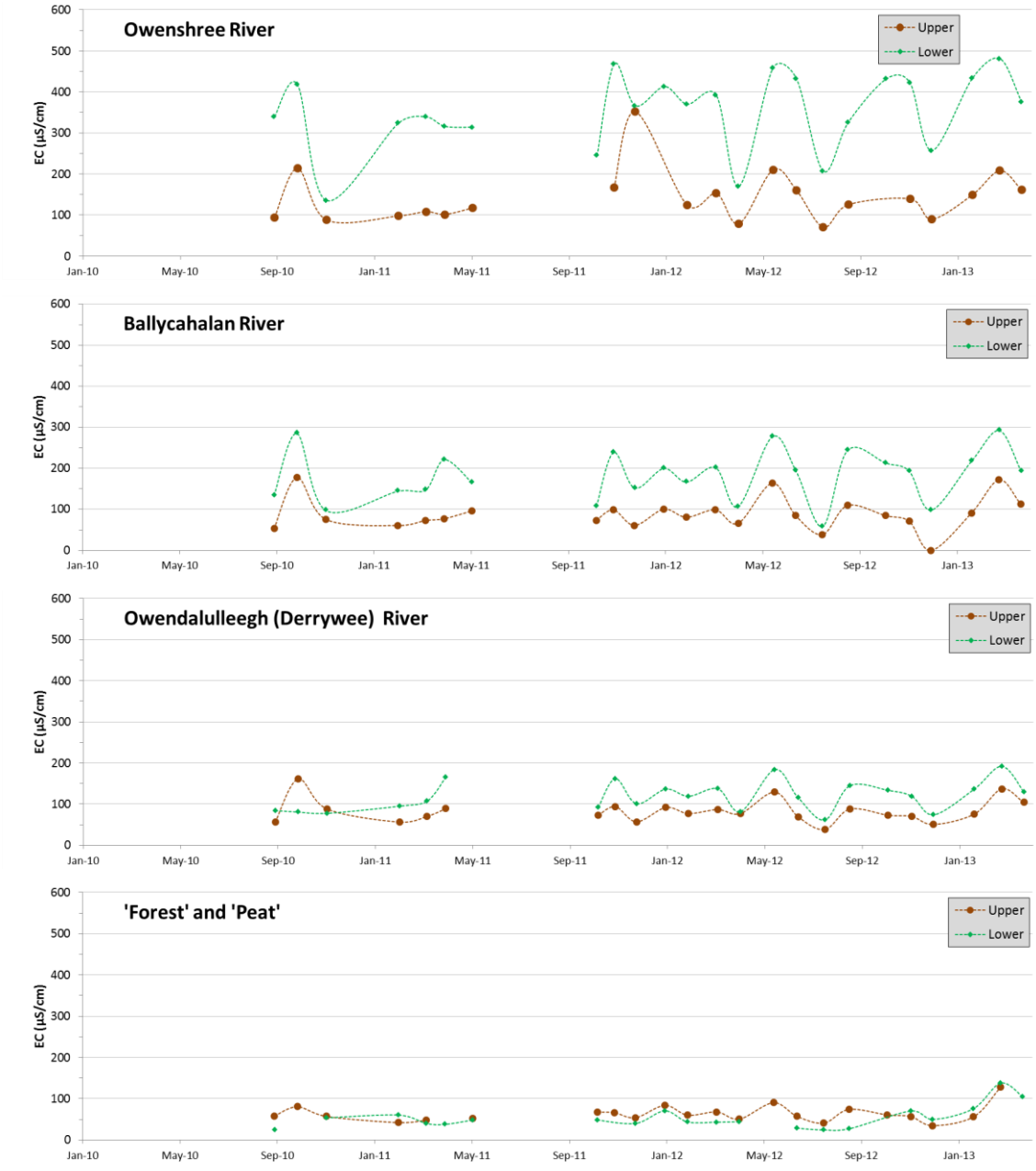

Figure G.1: River EC results

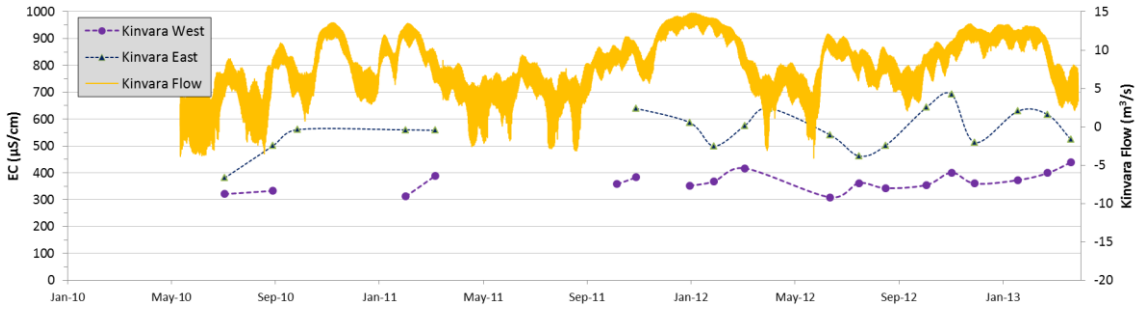

Figure G.2: Kinvara EC results

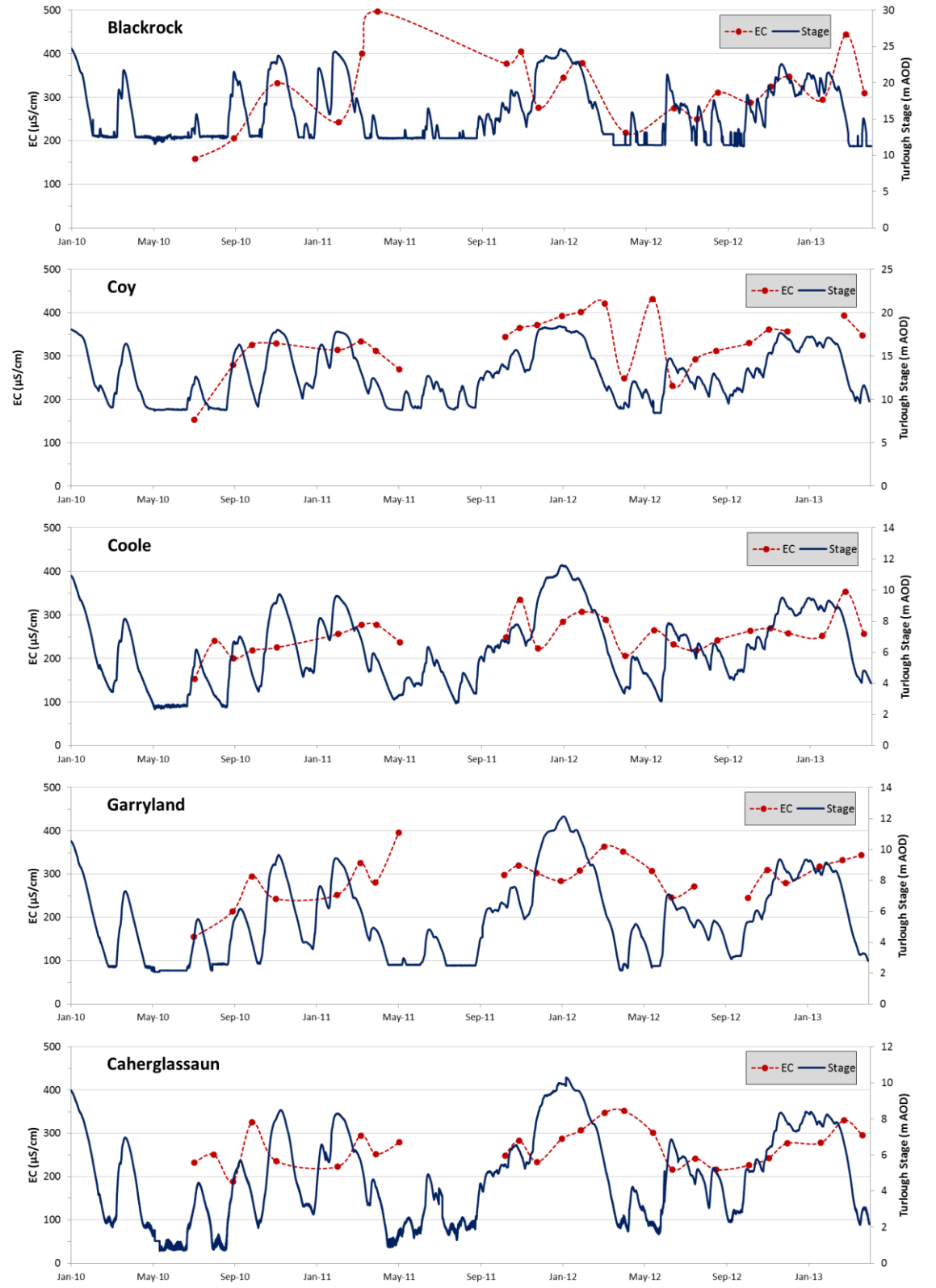

Figure G.3: Turlough EC results

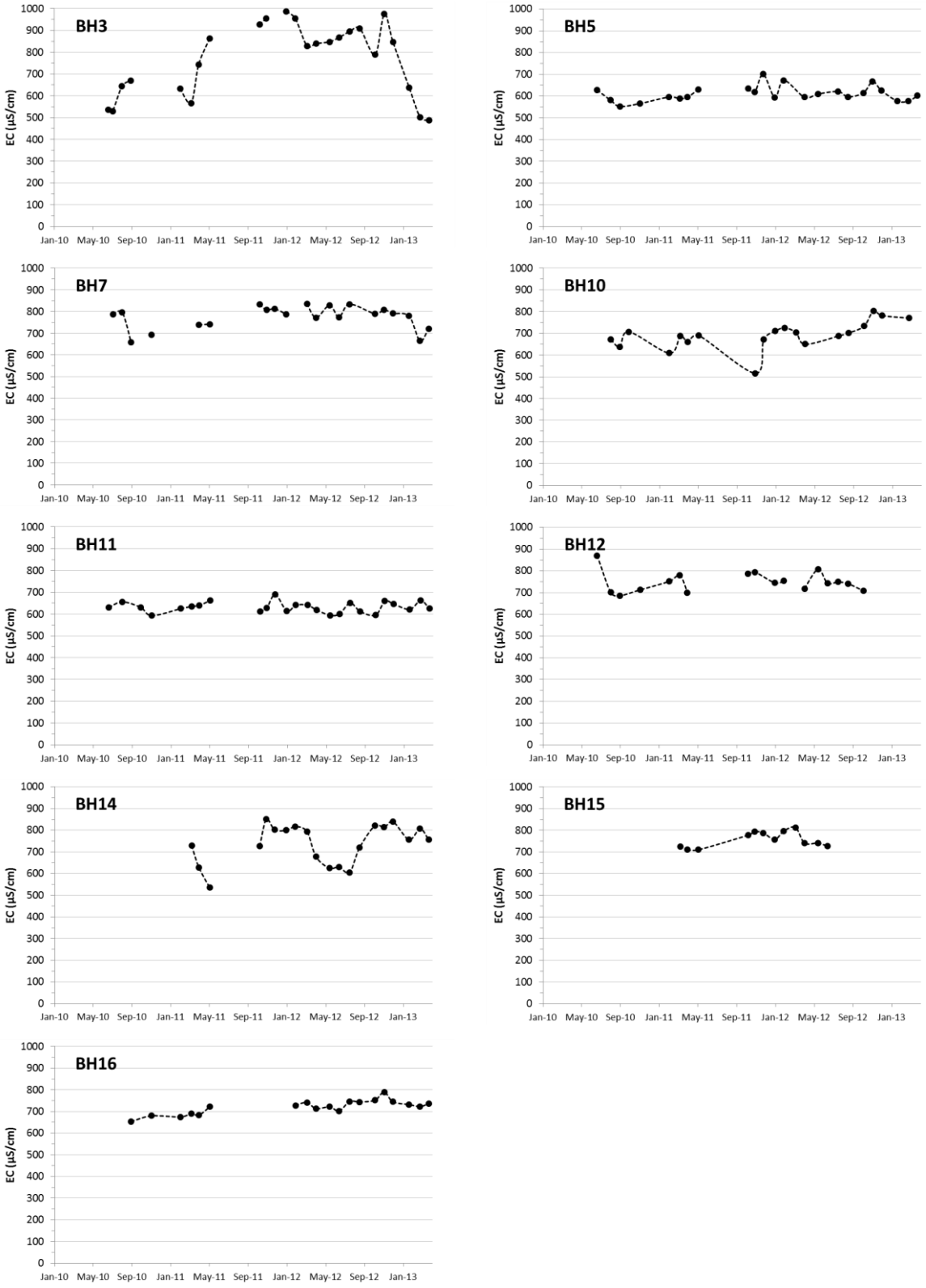

Figure G.4: Groundwater EC results

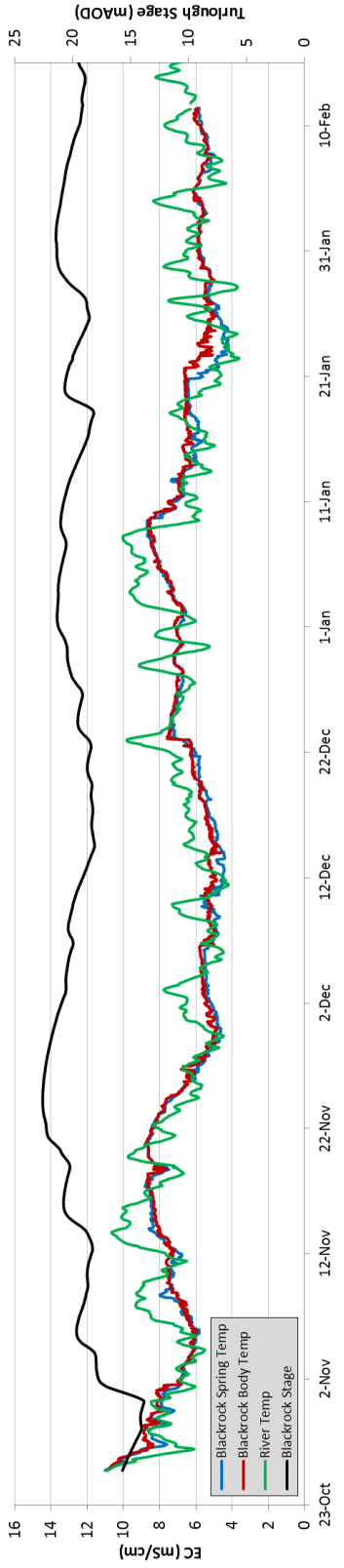

Figure G.5: Blackrock Temperature data (CTD study)

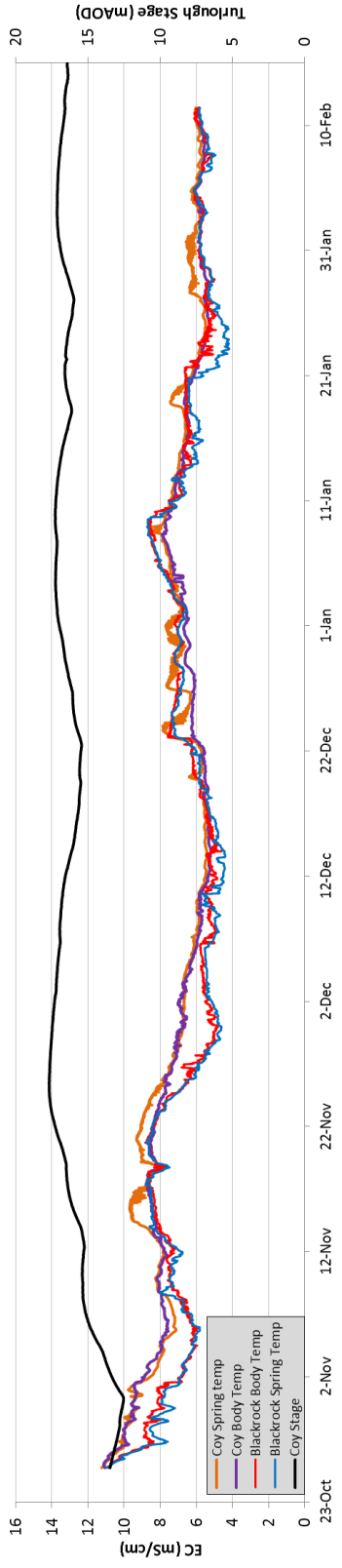

Figure G.6: Coy (and Blackrock) Temperature data (CTD study)

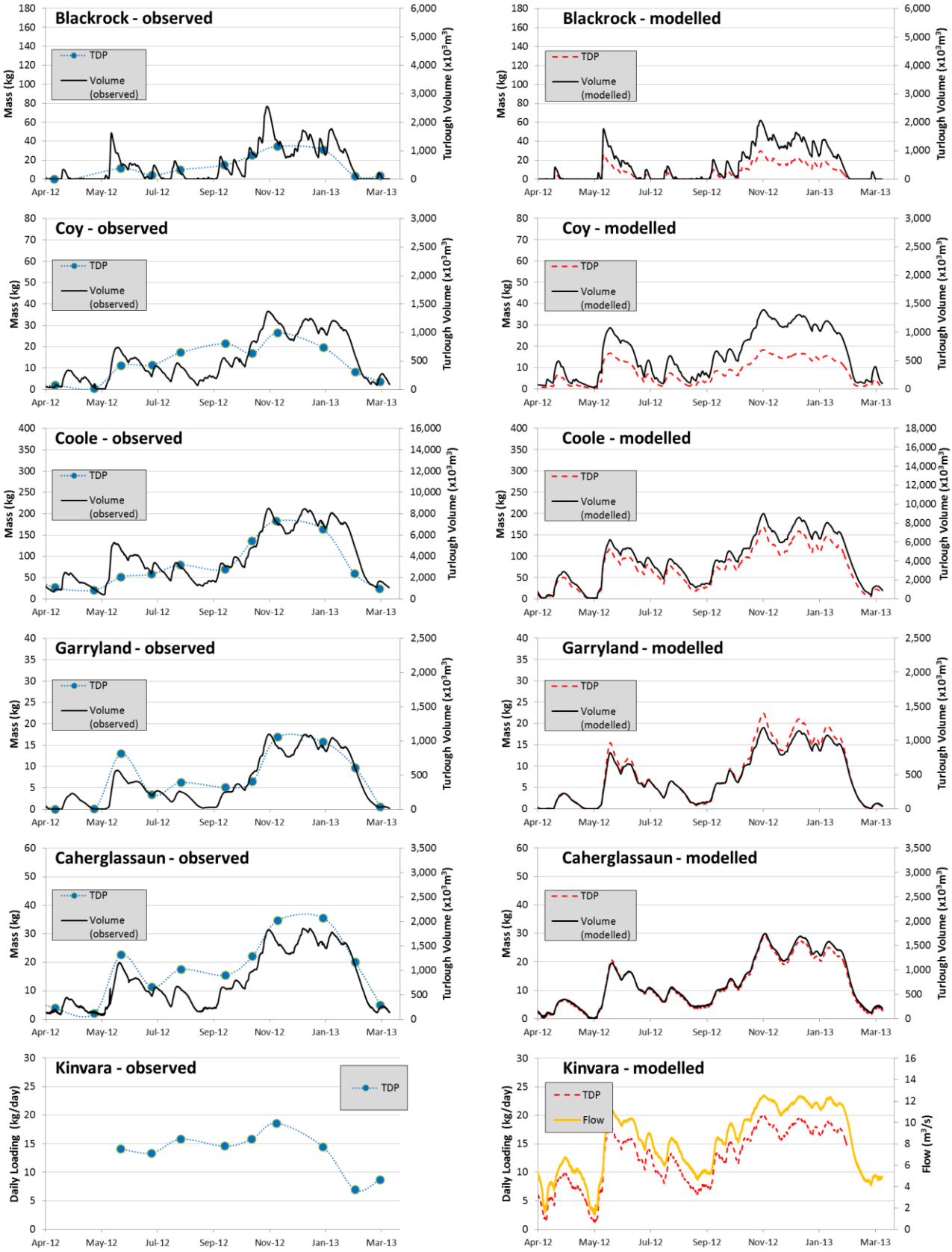

Figure G.7: Observed and modelled results for P loading from Scenario 1 (2012-2013)

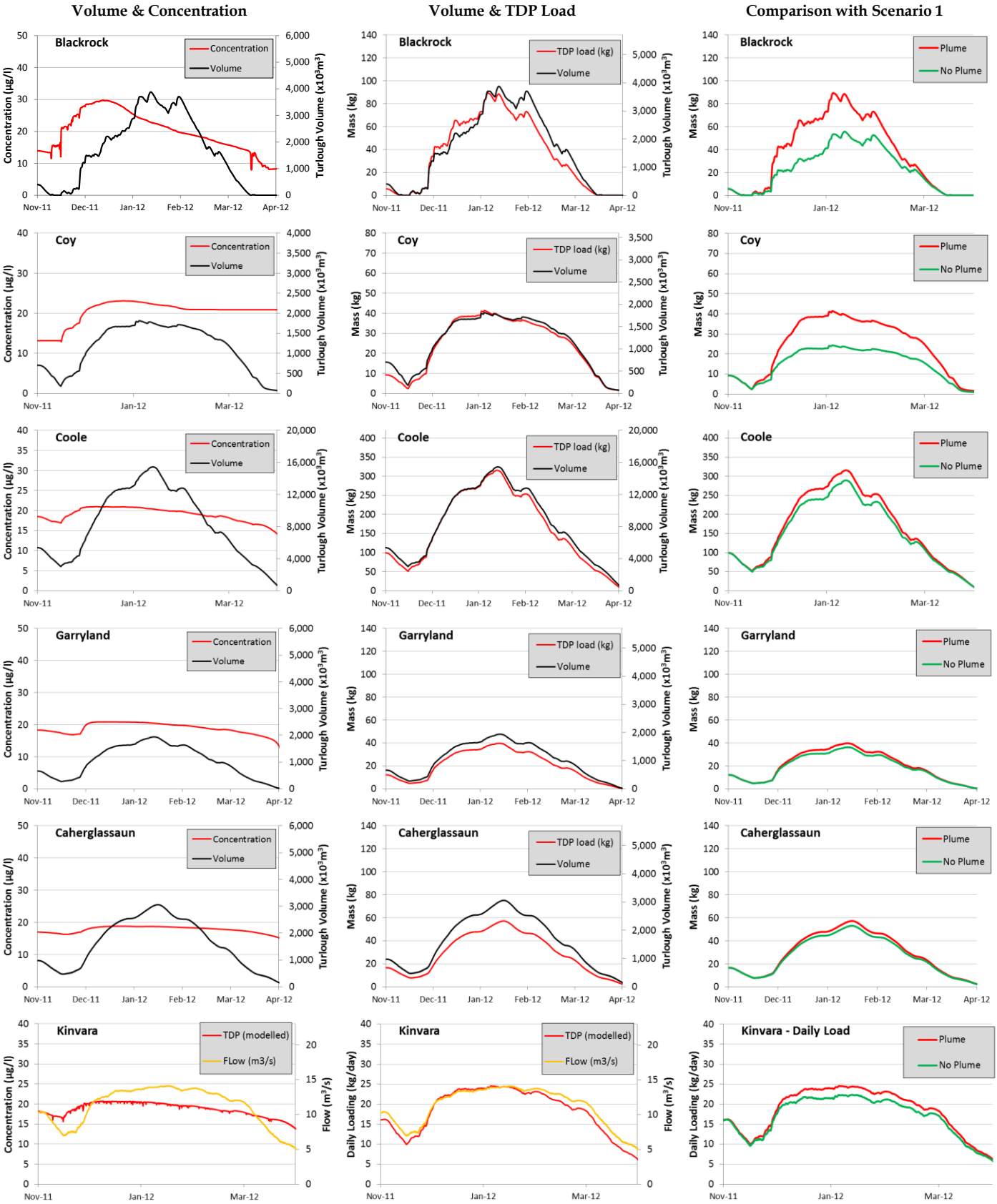

Figure G.8: Full Results for Scenario G4

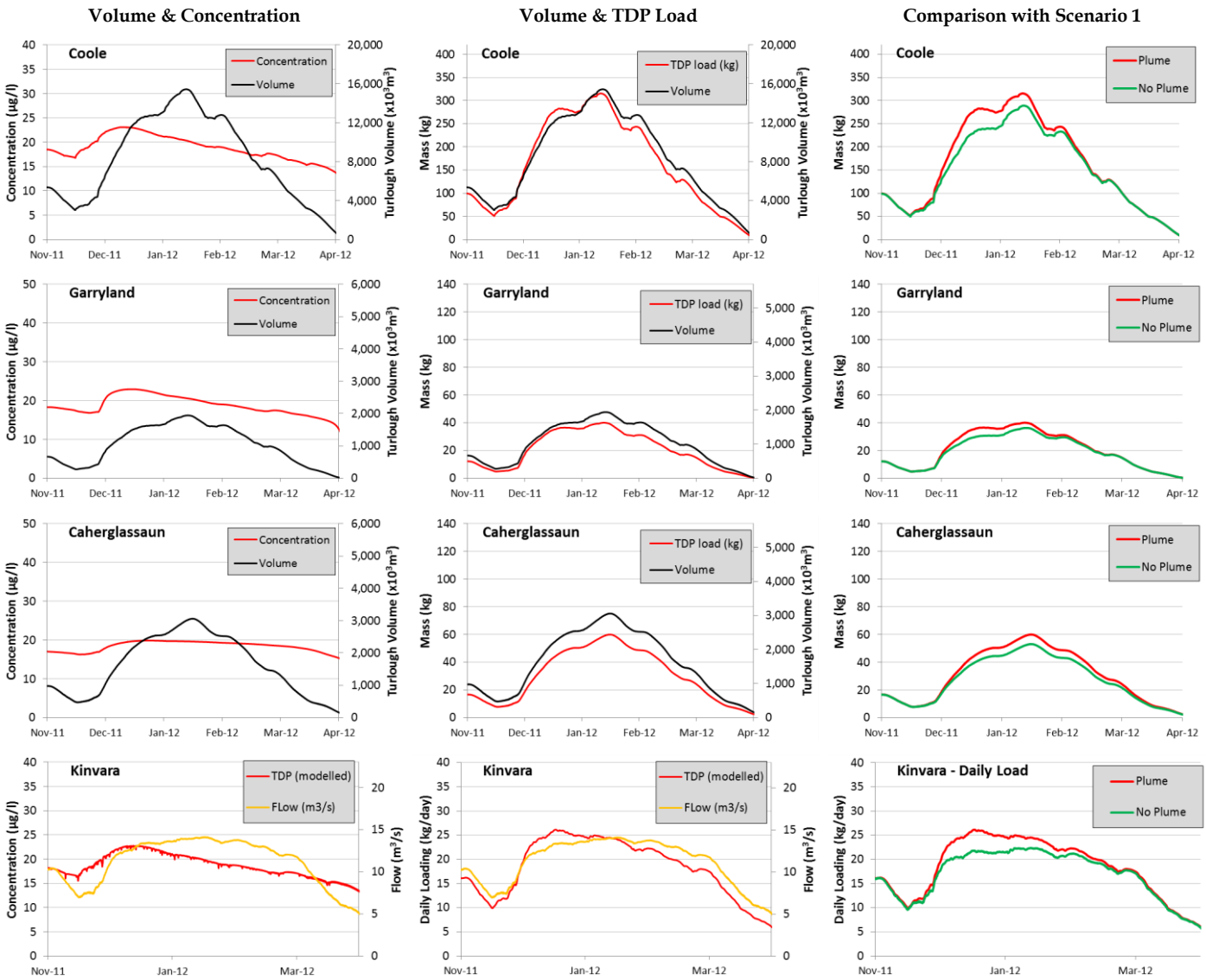

Figure G.9: Alteration of Scenario 4 – P-Plume occurs in Beagh River.